VOLUME 1 OF 2.

REFERENCE ONLY

UNIVERSITY OF LONDON THESIS

Degree MD Year 2005 Name of Author ALLESTON, J.M.

Molecular Targeting in Inflammatory Bowel Disease

An investigation to identify novel chemokine targets for the potential development of new therapeutic agents for inflammatory bowel disease

Volume 1

A thesis submitted for the degree of Doctor of Medicine

Dr Joanne Mary Puleston MBBS MRCP

The Royal Free Hospital School of Medicine

University of London

2005

Supervisors: Professor Roy Pounder and Dr Adam Platt

ProQuest LLC
789 East Eisenhower Parkway
P.O. Box 1346
Ann Arbor, MI 48106-1346

Abstract

Purpose

Inflammatory bowel disease is characterised by intense mucosal recruitment of activated leukocytes. As chemokines determine inflammatory leukocyte recruitment and retention, the expression of the entire chemokine family within colonic mucosa from IBD patients was compared to non-inflamed and inflamed controls.

Methods

A microarray of cDNAs, representing the entire chemokine superfamily and their cognate receptors, was hybridised with probes derived from colonoscopic biopsies. While expression levels of individual chemokines and their receptors have been measured in colon tissue previously, no one has attempted to analyse transcription levels of the entire chemokine superfamily in parallel. The array levels were correlated with histopathological inflammatory scores and expression of their cognate receptors by quantitative PCR and immunohistochemistry. Flow cytometry was performed on mucosally-derived colonic cells. Caco-2, HT29, T84, primary colonic epithelium and keratinocyte cell lines were stimulated with combinations of IL-1β, TNF-α, and LPS, and analysed using the same microarray.

Results

Expression of a distinct subset of chemokines, consisting of CXCL's 1-3 and 8 and CCL20, was up regulated in active colonic IBD, compared to non-inflamed areas or tissue from controls. This expression pattern correlated with histopathological inflammatory scores. Increased expression of their cognate receptors, CXCR1, CXCR2 and CCR6, was confirmed by quantitative PCR and immunohistochemistry. Flow cytometric revealed an increase of CCL20 expression on epithelial cells in IBD specimens, particularly in severe disease. An identical chemokine response was induced in Caco-2 cells by stimulation with IL-1β, but not TNF-α. By contrast, IL-1β and TNF-α were synergistic in HT29 and keratinocytes.

Conclusion

IL-1β and TNF-α appear to be the pivotal mediators of a coordinated epithelial chemokine response that dominates the mucosal environment in ulcerative colitis. These data suggest several new therapeutic targets for IBD, as well as identifying a previously unrecognised coordinated epithelial chemokine response.

Acknowledgements

My sincere thanks go to my supervisors, Professor Roy Pounder and Dr Adam Platt. I am grateful for a rewarding time of research, working as part of such an enthusiastic and inspirational team. Thank you for all the encouragement, guidance and patience.

Thank you to Simon Murch, not only for your imaginative, insightful contribution, but also for your warm welcome into the Department of Paediatric Gastroenterology. I am grateful to all the members of this department, for your help and friendship, in particular to Paul Ashwood, Stephanie Auld, Alan Phillips and Franco Torrente.

I would also like to thank the entire Department of Adult Gastroenterology, for a thoroughly enjoyable time at the Royal Free Hospital. It was a joy to work in such a friendly, cohesive unit. Thanks to Ashley Brown and Mark Hamilton for advice on write-up, and thank you to Professor Gazzard, Catherine Dunbar, Ann-Marie Brandom and my mother for proof-reading the manuscript, and for the constructive criticism.

Thank you to Rosalind Sim and John Auld from the Department of Pathology, for training me in the techniques of immunohistochemistry, and for making the time truly enjoyable. Thank you to Richard Morris for statistical assistance, and to Simon Thomas for Mac back up.

I am grateful to Celltech for sponsoring much of this work, especially to Richard Gellinas and his team of collaborators in Seattle, Washington. Thank you also to Shavy Makh, Celltech Slough for guidance in cell culture experimentation.

The magnitude and complexity of the universe mirrored by the unfathomable intricacies of molecular biology speak of hands of the one whose depth of beauty lies beyond all definition or comprehension. Were a man to study a cell for a lifetime, he would merely be as a child learning to read for the first time. Before the creator of all that I see and understand, and all that I do not, I bow down.

Index of Contents

Volume 1

Abstract 2

Acknowledgements 3

List of tables 10

List of photographic material 13

List of Abbreviations 14

Statement of problem and challenge underlying this research 16

Chapter 1: Introduction

1.1 **Incidence of IBD** 18

1.2 **Aetiology of IBD** 18

1.3 **Immune pathology in IBD** 20

1.4 **Chemokine overview** 25

1.5 **Cellular control by chemokines** 29

1.6 **Chemokines in disease** 35

1.7 **CCL20, CCR6 and β defensin** 37

1.8 **Other chemokines and chemokine receptors** 40

1.9 **Intestinal immunomodulatory cytokines** 43

1.10 **Regulation of chemokine production** 46

1.11 **Molecular targeting in IBD** 48

1.12 **Outline of MD thesis** 55

1.13 **Microarray technology** 56

Chapter 2: Materials and Methods

2.1 **Materials and buffers**

2.1.1 **Materials** 60

2.1.2 **Buffers** 62

2.2 **Methods**

2.2.1 **Patient inclusion, sample collection and preservation** 63

2.2.2 **Total cellular RNA preparation, cDNA probe synthesis, microarray hybridisation and RT-PCR** 63

2.2.2.1 Microarray construction 63

2.2.2.2 Preparation of total cellular RNA from colonic biopsies and cultured cell lines 64

2.2.2.3 RNA quantification 64

2.2.2.4 cDNA probe synthesis 65

2.2.2.5 Microarray hybridisation and analysis 65

2.2.2.6 Real-time quantitative RT-PCR 68

2.2.3 **Histopathological assessment of colonic tissue** 68

2.2.4 Immunohistochemical localisation and quantification of chemokines using immunoperoxidase technique 70
2.2.4.1 The technique of immunohistochemistry 70
2.2.4.2 Preparation of sections and pre-treatment methods 70
2.2.4.3 Primary antibody application 71
2.2.4.4 Secondary antibody application 71
2.2.4.5 Application of DAB 71
2.2.5 Analysis of cell lines 71
2.2.5.1 Cell propagation 71
2.2.5.2 Cell count and viability assessment 72
2.2.5.3 Cell stimulation 72
2.2.6 Quantitative determination of chemokine protein concentrations in cell culture supernatants 73
2.2.6.1 The technique of ELISA 73
2.2.6.2 ELISA procedure 73
2.2.6.3 Optical densometry 74
2.2.7 Flow cytometric analysis of colonic biopsies 75
2.2.8 Stimulation of colonic epithelium in colonic biopsies 75
2.2.9 Primary colonic epithelial culture and stimulation 76
2.2.9.1 Epithelial cell separation 76
2.2.9.2 Epithelial cell propagation 76
2.2.9.3 Cell count and viability assessment 76
2.2.9.4 Cell pellet formation 76
2.2.9.5 RNA extraction 76
2.2.9.6 Microarray hybridisation and analysis 76

Chapter 3: Quantification of chemokine RNA in colonic tissue

3.1 Introduction 78
3.2 Microarray hybridisation analysis of total cellular RNA obtained from colonic tissue
3.2.1 Sample preparation 78
3.2.2 Array results 78
3.2.3 Discussion 126
3.3 Real time quantitative PCR (RT-PCR) on colonic tissue
3.3.1 Background 128
3.3.2 RT-PCR technique 128
3.3.3 Results 128
3.3.4 Discussion 156
3.4 Discussion 157

Chapter 4: Immunohistochemical localisation and quantification of CCR6, CCL20, CXCL1 and CXCL2, using the immunoperoxidase technique

4.1 Background 162

4.2 Immunohistochemical localisation and quantification of CCL20 using the immunoperoxidase technique 162

4.2.1 Optimisation of pre-treatment method using appendix sections 162

4.2.2 Titration of primary antibody and finalisation of optimal pre-treatment method, using appendix and colonic surgical sections 162

4.2.2 Use of established immunohistochemical technique on colonic biopsy sections 163

4.2.3 Titration of link antibody using colonic biopsy sections, and finalisation of pre-treatment method 164

4.2.4 Immunohistochemical localisation and scoring of CCL20 on colonic biopsy sections 164

4.3 Immunohistochemical localisation and quantification of CCR6 using the immunoperoxidase technique 176

4.3.1 Optimisation of pre-treatment method using appendix sections 176

4.3.2 Titration of primary antibody using appendix sections 176

4.3.3 Use of established immunohistochemical technique on colonic sections 176

4.3.4 Titration of link antibody using colonic sections, and finalisation of pre-treatment method 177

4.3.5 Immunohistochemical localisation and scoring of CCR6 on colonic biopsies 177

4.4 Immunohistochemical localisation and quantification of CXCR1 using the immunoperoxidase technique 190

4.4.1 Optimisation of pre-treatment method using surgical colonic sections 190

4.4.2 Titration of primary antibodies using colonic biopsy sections 190

4.4.3 Further titration of link antibodies using colonic biopsy sections 190

4.4.4 Immunohistochemical localisation and scoring of CXCR1 on colonic biopsies 191

4.5 Immunohistochemical localisation and quantification of CXCR2 using the immunoperoxidase technique 204

4.5.1 Optimisation of pre-treatment method using surgically-obtained colonic and appendix sections 204

4.5.2 Titration of primary antibodies using colonic biopsy sections 204

4.5.3 Immunohistochemical localisation and scoring of CXCR2 on colonic biopsies 205

4.6 Discussion 218

Chapter 5: Coordinate chemokine response in stimulated human colon cancer cells

5.1 Introduction 221

5.2 Coordinate chemokine response in stimulated Caco-2 cells 222

5.2.1 Caco-2 cell count and viability assessment 222

5.2.2 RNA gel electrophoresis 223

5.2.3 Microarray results 224

5.2.4 Quantitative determination of chemokine protein concentrations in stimulated Caco-2 cell supernatants 233

5.2.4.1 Quantitative determination of CCL20 protein concentration in Caco-2 cell supernatant 233

5.2.4.2 Quantitative determination of CXCL8 protein concentration in Caco-2 cell supernatant 236

5.2.4.3 Quantitative determination of CXCL1 protein concentration in Caco-2 cell supernatant 239

5.2.4.4 Quantitative determination of CCL5 protein concentration in Caco-2 cell supernatant 242

5.3 Coordinate chemokine response in stimulated HT29 cells 246

5.3.1 HT29 cell count and viability assessment 246

5.3.2 RNA assay 246

5.3.3 Microarray results 247

5.3.4 RT-PCR results 249

5.4 Coordinate chemokine response in stimulated primary colonic epithelial cells 252

5.4.1 Primary colonic epithelial microarray results 252

5.5 Coordinate chemokine response in stimulated keratinocytes cells and primary lung epithelial cells 254

5.6 Discussion 256

Chapter 6: Flow cytometric analysis on mucosally derived cells

6.1 Background 259

6.2 Results 259

6.3 Discussion 259

Chapter 7: Immunohistochemical localisation and quantification of CCL20 and CCR6 in necrotising enterocolitis, using the immunoperoxidase technique

7.1 Background 262

7.2 H&E and immunohistochemical staining of NEC and control tissue to investigate potential immune-neural interactions 262

7.3 Immunohistochemical staining of NEC and control tissue for CCL20 and CCR6 to investigate potential immune-neural interactions 263

7.4 Discussion 263

Chapter 8: Discussion and conclusion

8.1 Discussion 274

8.2 Conclusion 282

References 283

Appendix (CD-ROM and volume 2)

Appendix 1 Ethics statement and permission

1.1 Statements concerning ethical approval

1.2 Study 1 ethical approval

1.3 Study 2b ethical approval

1.4 Study 2c ethical approval

1.5 Study 2b ethics application (CD-ROM)

1.6 Study 2c ethics application (CD-ROM)

Appendix 2 Colonoscopy study 1: A research study to evaluate and compare RNA samples derived from colonoscopy biopsies from volunteers without inflammatory bowel disease and patients with Crohn's disease and ulcerative colitis

2.1 Study protocol

2.2 Patient information sheets and consent form

2.3 Patient details

2.4 Array data

Appendix 3 Rectal biopsy study 2b: A research study to evaluate and compare RNA samples derived from rigid sigmoidoscopic biopsies from healthy subjects, patients with IBD and patients with infective diarrhoea

3.1 Study protocol

3.2 Patient information sheets and consent form

3.3 Patient details

3.4 Array data (infectious colitis)

3.5 Array data (cultured primary epithelial samples)

Appendix 4 Colonic resection study 2c: A research study to evaluate and compare RNA samples derived from resected bowel specimens from patients with Crohn's disease, ulcerative colitis, or other bowel diseases

4.1 Study protocol

4.2 Patient information sheets and consent form

4.3 Patient details

4.4 Array data (IBD and normal control tissue results)

4.5 Array data (inflammatory tissue results)

Appendix 5 Array data from Caco-2 and HT29 cell lines

5.1 Array data from Caco-2 cell line

5.2 Array data from HT29 cell line

Appendix 6 Details of collaborators and work performed

Appendix 7 Publications and poster presentations

List of tables

Table 1.1: Chemokines, chemokine receptors and their alias names.

Table 2.1: Panel of housekeeping genes included in the microarray.

Table 2.2: Histopathology scoring method used on colonic tissue.

Table 2.1: Stimulation solutions applied to Caco-2 cells.

Table 3.1: Clinical details and corresponding semi-quantified RNA concentration (ng/μl) from samples included in graph and figure 3.1, assessed using the Agilent system.

Table 3.2: Categories of level of gene expression, obtained from the semi-quantitative assessment of the microarray obtained from colonic tissue (strong/low/nil).

Table 3.3: Relative expression levels of CCR6, CXCL1, CXCL2, CXCL3, CCL20 and actin, obtained by semi-quantitative assessment of the microarray result from colonic biopsy tissue, with inflammatory scores.

Table 3.4: Relative expression levels of CCR7, CCL19, CCL21, CXCL13 and CXCR5, obtained by semi-quantitative assessment of the microarray result from colonic biopsy tissue, with inflammatory scores.

Table 3.5: Relative expression levels of CCR6, CXCL1, CXCL2, CXCL3, CCL20 and actin, obtained by semi-quantitative assessment of the microarray result from surgically obtained colonic tissue, with inflammatory scores.

Table 3.6: Relative expression levels of CCR7, CXCR5, CXCL13 and CCL19 obtained by semi-quantitative assessment of the microarray result from surgically obtained colonic tissue, with inflammatory scores.

Table 3.7: Relative expression levels of CXCL8, CXCL9, CXCL10, CXCL11, CCL5 and CCR5 obtained by semi-quantitative assessment of the microarray result from surgically obtained colonic tissue, with inflammatory scores.

Table 3.8: Relative expression levels of CCL2, CCL24, CXCR1, CXCR2, CXCR3, CCR3 and CCL3 obtained by semi-quantitative assessment of the microarray result from surgically obtained colonic tissue, with inflammatory scores.

Table 3.8: Relative expression levels of CXCR1, CXCR2, CXCL1, CXCL3, CXCL8, CCL20 and CCR6 in colonic biopsy tissue obtained by quantitative PCR, expressed as fold-up-regulation to an average of all uninvolved IBD samples analysed.

Table 3.10: Taqman quantitative PCR analysis data of chemokine expression of CXCL1, 9, 10, 11, CCL3 and CCL5 from full thickness colonic tissue with inflammatory score.

Table 3.11: Taqman quantitative PCR analysis data of chemokines CCL20 and 24, chemokine receptor expression of CCR3, CCR5, CXCR3 from full thickness colonic tissue with inflammatory scores A+C.

Table 4.1: List of sections, pre-treatments methods, primary antibody dilutions and blocking agents used in immunoperoxidase immunohistochemical optimisation for CCL20, as outlined in 4.2.2.

Table 4.2: CCL20 immunohistochemistry scores for the colonic biopsy series, inflammatory scores and gene expression levels as determined by TaqMan real-time quantitative PCR values.

Table 4.3: List of initial and repeat semi-quantitative immunohistochemistry scores for CCL20, to demonstrate reproducibility of scoring method.

Table 4.4: Values for statistical validation of CCL20 immunohistochemistry scores.

Table 4.5: CCR6 immunohistochemistry semi-quantitative assessment scores for the colonic biopsy series, with histopathological inflammatory scores and gene expression levels as determined by taqman real-time quantitative RT-PCR values.

Table 4.6: List of initial and repeat semi-quantitative immunohistochemistry scores for CCR6, to demonstrate reproducibility of scoring method.

Table 4.7: Statistical validation table of CCR6 semi-quantitative immunohistochemistry scores.

Table 4.8: CXCR1 immunohistochemistry semi-quantitative assessment scores for the colonic biopsy series, with histopathological inflammatory scores, CXCR1 gene array expression levels and CXCL1 taqman real-time quantitative RT-PCR values.

Table 4.9: List of initial and repeat semi-quantitative immunohistochemistry scores for CXCR1, to demonstrate reproducibility of scoring method.

Table 4.10: Values for statistical validation of CXCR1 immunohistochemistry scores.

Table 4.11: CXCR2 immunohistochemistry semi-quantitative assessment scores for the colonic biopsy series, with histopathological inflammatory scores, CXCR2 gene expression levels and CXCR2 TaqMan real-time quantitative RT-PCR values.

Table 4.12: List of initial and repeat semi-quantitative immunohistochemistry scores for CXCR2, to demonstrate reproducibility of scoring method.

Table 4.13: Statistical validation table of CXCR1 semi-quantitative immunohistochemistry scores.

Table 5.1: 2-hour normalised chemokine expression levels of CXCL1, 2, 3, 8, 10, CCL20 and actin from microarray analysis for Caco-2 cells stimulated with nil/IL-1β/ TNF-α/IL-1β + TNF-α/IL-1β +TSA/IL-1β + TNF-α + benzamide/TSA/LPS.

Table 5.2: 18-hour normalised chemokine expression levels of CXCL1, 2, 3, 8, 10, CCL20, and actin from microarray analysis for Caco-2 cells stimulated with nil/IL-1β/ TNF-α/IL-1β + TNF-αIL-1β +TSA/IL-1β + TNF-α + benzamide/TSA/LPS.

Table 5.3: Quantitative ELISA values for CCL20 protein concentration in Caco-2 cell supernatants, following stimulation of cells with combinations of IL-1β, TNF-α, LPS, TSA and benzamide for 2, 4 and 18 hours.

Table 5.4: Quantitative ELISA values for CXCL8 protein concentration in Caco-2 cell supernatants after stimulation of cells with combinations of IL-1β, TNF-α, LPS, TSA and benzamide for 2, 4 and 18 hours.

Table 5.5: Quantitative ELISA values for CXCL1 protein concentration in Caco-2 cell supernatants after stimulation of cells with combinations of IL-1β, TNF-α, LPS, TSA and benzamide for 2, 4 and 18 hours.

Table 5.6: Quantitative ELISA values for CCL5 protein concentration in Caco-2 cell supernatants after stimulation of cells with combinations of IL-1β, TNF-α, LPS, TSA and benzamide for 2, 4 and 18 hours.

Table 5.7: Details of stimulatory conditions used in HT29 cell culture, corresponding with semi-quantified RNA concentrations (ng/μl) obtained via the Agilent bioanalyser.

Table 5.8: 2-hour normalised chemokine expression levels of CXCL1, CXCL2, CXCL3, CXCL8, CXCL10, CCL20, Actin from microarray analysis for HT29 cells stimulated with nil/IL-1β/ TNF-α/IL-1β + TNF-α/LPS.

Table 5.9: Normalised fold-up regulation RT-PCR values for CXCL1, CXCL3, CXCL8 and CCL20, expression in HT29.

Table 5.10: 2-hour and 4-hour normalised CXCL1, CXCL2, CXCL3, CXCL8, CXCL10, CCL20, actin expression levels from microarray analysis of primary colonic epithelial cells stimulated with nil/IL-1β/ TNF-α/IL-1β + TNF-α/LPS.

Table 5.11: 2-hour normalised CXCL's1-3, CXCL8, CXCL10, CCL20, actin expression levels from microarray analysis of keratinocytes stimulated with nil/IL-1β/ TNF-α/IL-1β + TNF-α/LPS.

Table 7.1: CCL20 immunohistochemical scores of NEC and control samples.

Table 7.2: CCR6 immunohistochemical scores of NEC and control samples.

List of photographic material

Figure 3.2: Hierarchical clustering of gene expression data from colonic biopsy tissue.

Figure 4.1: Colonic immunohistochemical staining for $CCL20^+$ cells using the immunoperoxidase technique.

Figure 4.2: Colonic immunohistochemical staining of $CCR6^+$ cells using the immunoperoxidase technique.

Figure 4.3: Colonic immunohistochemical staining of $CXCR1^+$ cells using the immunoperoxidase technique.

Figsre 4.4: Colonic immunohistochemical staining of $CXCR2^+$ cells in a control sections, using the immunoperoxidase technique.

Figure 5.1: Agarose gel electrophoresis for RNA extracted from Caco-2 cells. The 18 and 28S ribosomal bands are indicated.

Figure 5.2: Hybridised genes for Caco-2 analysis, detected by radio labelling, with arrows demonstrating the spots corresponding to CCL20 pre- and post-stimulation with combinations of IL-1β, TNF-α and LPS.

Figure 5.3: Hierarchical cluster of Caco-2 expression data at 2 hours.

Figure 7.1: Histological examination of H&E stained bowel sections, demonstrating a lymphocyte infiltrate in myenteric plexus in NEC.

Figure 7.2: Immunohistochemical staining of neural fibrillary protein demonstrating normal innervation in a control patient.

Figure 7.3: Immunohistochemical staining demonstrating neural disruption strongly associated with myenteric plexus abnormalities.

Figure 7.4: Immunohistochemical straining demonstrating constitutive CCR6 and CCL20 expression in NEC.

Abbreviations

ANCA	Anti-neutrophil cytoplasmic antibodies
APC	Antigen presenting cell
CD	Crohn's disease
cDNA	Complementary deoxyribonucleic acid
CLA	Cutaneous lymphocyte antigen
CNS	Central nervous system
CRP	C-reactive protein
EDTA	Ethylene diamine tetraacetic acid
ELISA	Enzyme-Linked Immunosorbent Assay
FACS	Fluorescence activated sorter analysis
FCS	Foetal calf serum
GFAP	Glial fibrillary acidic protein
GRK	G-protein receptor kinase
G-CSF	Granulocyte colony-stimulating factor
GM-CSF	Granulocyte-macrophage colony-stimulating factor
H&E	Haematoxylin and eosin stain
Hb	Haemoglobin
HDAC	Histone deacetylase co repressor protein
HEV	High endothelial venule
IBD	Inflammatory bowel disease
IC	Inflammatory control
ICAM	Intracellular adhesion molecule
ICE	IL-1β converting enzyme
IFN	Interferon
(IRF)-3	Interferon regulatory factor
IL-1	Interleukin-1
IL-1ra	Interleukin-1 receptor antagonist
iNOS	nitric oxide synthase
LC	Langerhans cells
LPS	Lipopolysaccharide
MAdCAM-1	Mucosal addressin cell adhesion molecule-1
MALT	Mucosal associated lymphoid tissue
M cells	Membranous epithelial cells
MHC	Major histocompatability complex
MMPS	Matrix metalloproteinases
MS	Multiple sclerosis
NC	Normal control
NEC	Necrotising enterocolitis
NF-κB	Nuclear factor-κB
NK cell	Natural killer cell
NO	Nitric oxide

NSE	Neuron specific enolase
NGFR	Nerve growth factor
NFP	Neural fibrillary protein
PARP	Poly (ADP-ribose) polymerase
PBS	Phosphate buffered solution
RT-PCR	Reverse transcriptase polymerase chain reaction
RNA	Ribonucleic acid
TBS	Tris buffered saline
TGF-β	Transforming growth factor-β
TIMP	Tissue inhibitors of metalloproteinases
TNF	Tumour necrosis factor
TSA	Trichostatin A
UC	Ulcerative colitis
VCAM-1	Vascular cellular adhesion molecule-1
WCC	White cell count

Statement of problem and challenge underlying this research thesis

The chronic inflammatory bowel diseases (IBD) include Crohn's disease (CD) and ulcerative colitis (UC). CD is characterised by patchy, granulomatous transmural ulceration of the gastrointestinal tract. It occurs at any location in the bowel, most frequently at the terminal ileum. The chronic inflammation of UC is superficial to the muscularis mucosae, extending variable distances from the rectum proximally around the colon.

Current therapies offered for CD and UC are frequently inadequate at controlling these diseases, and the associated side effects limit their application. If the disease becomes intractable, surgical intervention is sometimes required, and there is a significant risk of malignancy (Bernstein et al, 2001), (Rhodes et al, 2002), (Sharan et al, 2002). These diseases are therefore common and important conditions for which the identification of precise immune targets could lead to more specific therapy, with enhanced therapeutic benefit and fewer associated side effects.

This MD sets to answer the following questions:

1 Which chemokines and their receptors are central to the disease processes in IBD?
2 Expression patterns of individual chemokines have been previously investigated, but is there a particular coordinate response to inflammatory stimuli in IBD?
3 What is the effect of pro-inflammatory cytokines on the chemokines identified?
4 What is the potential for therapeutic intervention at a chemokine/chemokine receptor/pro-inflammatory cytokine level in IBD?

Details of collaborators and their contribution to this research are detailed in appendix 6.

Chapter 1

Introduction

1.1 Incidence of IBD

1.2 Aetiology of IBD

1.3 Immune pathology in IBD

1.4 Chemokine overview

1.5 Cellular control by chemokines

1.6 Chemokines in disease

1.7 CCL20, CCR6 and β defensin

1.8 Other chemokines and chemokine receptors

1.9 Intestinal immunomodulatory cytokines

1.10 Regulation of chemokine production

1.11 Molecular targeting in IBD

1.12 Outline of MD thesis

1.13 Microarray technology

1.1 Incidence of IBD

CD and UC are amongst the most common immune-mediated disorders in developed-world countries. There has been an unexplained rising incidence of IBD over the last century, most notably in Northern Europe and North America (Hildebrand et al, 1994), (Montgomery et al, 1998). The incidence has begun to stabilise at a high rate in most developed countries, and continues to rise in regions where IBD had been less common (Loftus et al, 2002). The prevalence rates in survey of the UK are 3.3 per 1,000 by age 26, and 5.1 per 1,000 by age 43 (Montgomery et al, 1998), (Thompson et al, 2000).

1.2 Aetiology of IBD

The cause of IBD is unknown, although environmental and genetic factors are both implicated in a multifactorial manner. The most popular current theory implicates a T lymphocyte disorder in genetically susceptible individuals as a result of a breakdown of regular constraints in the mucosal immune responses to enteric bacteria (Shanahan, 2002). A genetic component is likely as IBD case clustering is common within families and there is increased concordance in monozygotic compared to dizygotic twins, particularly with regard to CD (Binder et al, 1996), (Thompson et al, 1996), (Tysk et al, 1998), (Orholm et al, 2000). Furthermore, age of onset and phenotype correlate within monozygotic twins (Rampton et al, 1986). Early linkage study of the familial clustering indicated that chromosomes 3, 7, 12 and 16 contain potential candidate genes for IBD (Hugot et al, 1996). Subsequently, two groups identified a frameshift variant and missense mutation of the CARD15 gene located on chromosome 16, conferring susceptibility to CD overlapping with the IBD1 locus (Hugot et al, 2001), (Ogura et al, 2001). It is now thought that this gene accounts for 20% of the genetic susceptibility in CD, although the insertion mutation in the CARD15 gene does not confer susceptibility to UC (Hampe et al, 2001), (Hugot et al, 2003). Certain CARD15 allelic variants are increased in Ashkenazi Jews which may explain the high incidence of CD in this group (Bonen et al, 2003). However, the discovery of CARD15 merely contributes one more piece of the jigsaw puzzle, as CARD15 variants do not account for all of CD (Shanahan, 2002), and furthermore, patients with Blau syndrome (missense mutations in nucleotide binding domain of CARD15) do not exhibit IBD (Miceli-Richard, 2001). Other regions of linkage have been implicated in IBD include 12q13, MHC on chromosome 6p23 and chromosome 14q11-12 (Watts et al, 2002).

CARD15 proteins are intracellular receptors for various pathogen-associated molecular patterns in the gastrointestinal tract (Bonen et al, 2003). Colonic involvement in active CD is associated with increased CARD15 gene expression in macrophages and intestinal epithelial cells (Berrebiet et al, 2003). Following pathogen detection, the transcription factor NF-κB is activated, which modulates the innate immune response (Duerr, 2002), (Hugot et al, 2003).

Infection is likely to be an important factor, due to the interaction between bacterial peptides and the mucosa (Martin et al, 2000), (Leiper et al, 2001). A variety of causal infections have been proposed, such as *Mycobacterium para tuberculosis*, which causes granulomatous bowel disease in cattle (Hampson et al, 1989), (Sanderson et al, 1992), (Ryan et al, 2004).

One popular hypothesis implicates defects in epithelial barrier function and/or immunoregulation leading to an immune response that is triggered by antigenic components of normal flora (Basset et al, 2002). Consistent with this is evidence from transgenic mice lacking IL-2 or IL-10, who develop colitis only in a non-sterile environment (Kuhn et al, 1993), (Sadlack et al, 1993). Furthermore, patients with IBD have increased levels of IgG to enteric flora during active disease (Macpherson et al, 1996).

Genetic polymorphism causing aberrant expression of regulatory proteins such as IL-1 receptor antagonist (IL-1ra) may be of aetiological importance in IBD although data have been conflicting (Louis et al, 1996), (Hacker et al, 1997), (Mwantembe et al, 2001).

An environmental aspect to the aetiology of IBD is suggested by marked geographical variation, with migrating populations adopting the incidence of IBD of their destination, for example, Asian immigrants to the UK (Feehally et al, 1993).

A number of case reports indicate long-term remission in IBD following autologous bone marrow transplantation which suggests that the primary defect may be immunological, although it is not thought to be primarily autoimmune (Kashyap et al, 1998), (Lopez-Cubero et al, 1998), (Talbot et al, 1998). This transplantation phenomenon could merely represent a 're-setting' of a previously hyper-stimulated system, with the immuno-pathogenesis occurring as a secondary event.

Intestinal ischaemia and vasculitis occur in IBD, although whether this is a cause or effect phenomenon is unclear. Associated arterio-venous thrombosis may be critical to its pathogenesis. Resin cast studies of mesenteric vasculature from resected intestinal CD sections led one group to propose a primary vasculitic model for IBD. They observed that mucosal ulceration concorded with infarction at the muscularis propria level (Wakefield et al, 1989). This same group also postulated that the measles virus could be an aetiological agent in IBD, via a vasculitic process, as viral genomic products were detected in mucosal biopsies from patients with active IBD (Lewin et al, 1995). However, these findings have not been re-produced, and the theory remains controversial. Further evidence for a vasculitic process comes from the association of anti-neutrophil cytoplasmic antibodies (ANCA) with IBD (Cambridge et al, 1992). This antibody is also found in association with Wegener's granulomatous vasculitis. Thrombocytosis and increased platelet aggregation in response to IL-1 and IL-8 are part of the inflammatory response and are thought to be part of the vasculitic process (Collins et al, 1994), (Schaufelberger et al, 1994). This may contribute to the systemic thromboembolism and mucosal inflammation in IBD (Collins et al, 1994).

The relative significance of mucins in IBD has not as yet been characterised. Mucins are constituents of the semi-permeable barrier mucous between the lumen and the epithelium. They determine the thickness and properties of mucous, which is a crucial part of the immunological defense system of the gastrointestinal tract. There is alteration in both secretory and membrane bound mucins in IBD, which may be of aetiological importance (Shirazi et al, 2000), (Einerhand et al, 2002).

Dietary factors such as sugar intake have been suggested as risk factors for IBD, but data are at present conflicting (Krishnan et al, 2002). High intakes of mono- and polyunsaturated fat and vitamin B6 may enhance the risk of developing UC (Geerling et al, 2000). Food additives such as fluoride, titanium dioxide and alumino-silicates have been proposed to be of importance in this multifactorial model for IBD (Powell et al, 2000). Smoking is associated with increased CD activity and relapse, and conversely, smoking cessation is associated with the onset of UC (Calkins, 1989). This is thought to be an immunomodulatory effect, altering pro-inflammatory cytokines and leukocyte adhesion to endothelial cells, in addition to effecting intestinal motility (Finnie et al, 1996), (Bhatti et al, 1997), (Benoni et al, 1998).

1.3 Immune pathology in IBD

Inflammatory infiltrate in IBD

IBD is characterised by a destructive host inflammatory response directed in part against the mucosal epithelium. There is intense leukocyte recruitment and retention within the lesions. Characteristic tissue damage occurs through a final pathway of pro-thrombotic mechanisms and proteolytic degradation of the extracellular matrix (MacDonald et al, 1994).

The dense leukocytic infiltrate that occurs in IBD includes activated cells from both the innate and adaptive (acquired) immune systems. These two components work in co-operation, with chemokines functioning as a vital constituent of signalling between them. The innate system provides the initial line of defence, and includes phagocytes (macrophages and neutrophils) in addition to specialised granulocytes (eosinophils and basophils), necessary to engulf small pathogens and contain larger parasites (Matsukawa et al, 2000), (Luster 2002). The adaptive response involves both T and B cells, and is characterised by specificity and long-lasting memory (Luster 2002).

The intensity of the inflammatory response is determined by the local expression of growth factors and pro-inflammatory cytokines within the mucosa, and by coordinated mechanisms of cellular recruitment (Kunkel et al, 2002). The location of and interaction between immuno-competent cells is critical to any appropriate immune response (Kunkel et al, 2002). As such, control of leukocyte trafficking is key. It is chemokines, their receptors and vascular adhesion molecules that determine the extent, type and duration of cellular infiltration, by controlling the migratory paths of dendritic cells, and lymphocytes both in homeostasis and inflammation. This implicates their immunological centrality (Sallusto et al, 1998)[1]. However, it has not been established which chemokines are contingent, nor which members of the chemokine and chemokine receptor superfamily are specifically involved in chronic colonic inflammation in IBD. Their identification could potentially lead to the discovery of novel therapeutic targets for IBD therapy. In addition, research into these diseases is likely to aid the immunological characterisation of other epithelial organs, as UC and CD are notable exemplars of human chronic inflammatory disease. The gastrointestinal tract is particularly conducive to investigative study owing to the accessibility of the mucosal tissue. It is the largest part of the immune system, and consists of organised lymphoid tissues including Peyer's patches, intraepithelial

lymphocytes and scattered cell components such as lymphocytes and plasma cells in the lamina propria (Mowat et al, 1997).

Epithelial involvement in immunity

The intestinal epithelium is vital not only as a barrier, but also in the primary recognition of pathogenic organisms and the subsequent recruitment of inflammatory cells to the mucosa (Van Deventer et al, 1997). Intestinal integrity and permeability is of fundamental importance in intestinal immunity, and is governed by intercellular tight junctions. These are made up of highly regulated complex proteins, such as zonula occludens, which maintain the seal between adjacent cells (Fiocchi, 1997). Pro-inflammatory cytokines and infectious agents modulate such inter-cellular interactions. For example, interferon-γ (IFN-γ) can down-regulate zonula occludens, causing a significant decrease in trans-epithelial resistance, with a deficient control of antigen transit leading to uncontrolled gastrointestinal inflammation (Shao et al, 2001). Regulatory T cells are not only involved in suppression of the inflammatory response, but are also thought to aid preservation of tight junctional complex integrity (Shao et al, 2001). Patients with IBD have increased flux of antigen across both inflamed and non-inflamed mucosal areas, with abrogation of tolerance to luminal flora (Shao et al, 2001). This loss of mucosal integrity may lead to the ingress of luminal antigens into the lamina propria, and thus augment the inflammatory response (Williams et al, 2000).

The direct contact of the large surface area with the intestinal milieu renders it particularly susceptible to inflammation, with exposure to antigenic, mitogenic, mutagenic and toxic stimuli. This necessitates flexibility within the immune system, which occurs partly by adaptability of chemokines and their receptor expression by epithelial cells. These cells therefore develop characteristics usually attributable to classical inflammatory cell types in addition to their normal absorptive and secretary functions. Chemokines secreted by human intestinal epithelial cells signal to neutrophils, macrophages and lymphocytes, vital for the inflammatory response. This contributes to the integrated, tightly regulated multicellular response whereby the target cells contribute to inflammation (Yang et al, 1997).

The highly specialised membranous epithelial cells (M cells) are important in mucosal immunity, and exist only in conjunction with lymphoid aggregates. These cells take up particulate antigen and transport adherent macromolecules efficiently. The antigen is carried to the underlying sub-epithelial dome, where mature dendritic cells phagocytose and process the antigen and migrate to T cell-rich interfollicular regions for antigen-presentation to naïve lymphocytes (Sarsfield et al, 1996), (Cook et al, 2000). In contrast, intestinal epithelial cells have processing and presentation pathways, with classical MHC I and II and non-classical MHC 1b pathways in addition to organism specific routes of invasion. Epithelial toll like receptors (TLRs) and CARD15 are crucial in the communication of pathogen recognition to effect an appropriate chemokine response, via transcription factor activation including NF-κB (Aderem et al, 2000). The cellular response and chemokine induction depends on the type of pathogen (Kawai et al, 2001). LPS in conjunction with LPS-binding protein binds to CD14 surface receptor on macrophages and monocytes, which subsequently activates TLR4 to initiate chemokine and

cytokine release, including TNF-α, IL-6 and IL-1β (Kawai et al, 2001). Experimentally, agonists to TLR2 and TLR4 induce chemokine levels (Jones et al, 2001). The multitude of pathways through these cells reflects the diversity of antigen the gastrointestinal tract is exposed to daily (Shao et al, 2001). Although intestinal epithelial cells are not true phagocytes, they ingest soluble antigen by fluid phase pinocytosis, and are able to present antigen. These cells may also be able to take up antigen via receptor mediated endocytosis, though *in vivo* data is lacking (Shao et al, 2001).

In the normal state, the gastrointestinal tract contains abundant leukocytes in intra-epithelial and sub-epithelial compartments, rendering it in a state of 'physiological inflammation' (Monteleone et al, 2002). The effector cells include neutrophils, macrophages and cytotoxic T lymphocytes. These constitute the main aggressors acting either directly by physical contact, or indirectly through the release of soluble factors such as reactive oxygen species and nitrogen metabolites, cytotoxic proteins, lytic enzymes and cytokines. The reactive behaviour of the immune cells governed in part by the cytokine milieu, underlie the symptoms and structural changes in IBD, for example pain, dysmotility, fibrosis, stricturing, fistula formation and neoplastic transformation (Panja et al, 1998).

Recruitment of specific leukocyte subpopulations into gastrointestinal tissue occurs via high endothelial venules (HEVs), which constitute the specialised endothelial post capillary mucosal microcirculation. They are the main entry point into peripheral lymph nodes for lymphocytes (Fiocchi et al, 1997). Chemokines and adhesion molecules control this leukocyte recruitment in two stages. Firstly, they control extravasation from blood into lymph nodes, Peyer's patches or inflamed tissue; a step also dependent on selectins and integrins (Sallusto et al, 2000). Only four chemokines have thus far been shown to functionally arrest circulating leukocytes under physiological conditions: CCL21 (which arrests lymphocytes), CXCL1, CCL2 and CCL5 (which arrests monocytes). No chemokines have as yet been shown to arrest neutrophils under inflammatory conditions (Ley, 2003).

Selectins are present on, and mediate the initial interactions between endothelial cells and leukocytes. They are lectin-like adhesion molecules, comprised of transmembrane glycoprotein receptors (Juliano, 2002). The expression and function of selectin is highly regulated, enabling appropriate leukocytic recruitment. Of the subtypes E-, L- and P-selectin, L-selectin is predominant, and is expressed by most leukocytes, including naïve T cells, B circulating monocytes and neutrophils (Patel et al, 2002). Selectin is made and transported to the cell surface within four hours of IL-1 and TNF release from activated macrophages. The interaction between leukocyte L-selectin and P/E-selectin on endothelial cells causes the cells to roll along the endothelial lining at decreased velocity. Leukocyte tethering, rolling, activation and subsequent adhesion are essential for cellular recruitment. Progression from rolling to cessation is currently thought to occur within a few seconds of an initial rolling contact, although there is some evidence to indicate that activation of rolling leukocytes by chemoattractants can be gradual (Kunkel et al, 2000).

Following the rolling contact, progression ceases via integrins (Campbell et al, 1998). Integrins are transmembrane glycoproteins on the surface of most leukocytes that mediate adhesion among cells as well as within the extracellular matrix (Sims et al, 2002). Integrins pre-exist in predominantly inactive states on circulating immune cells and are activated *in situ* following encounter with endothelial displayed chemokines or ligands to specific G protein-couples receptors on the leukocyte surface (Alon et al, 2003). Integrins consist of one of 18α and 8β subunits (Juliano, 2002). β2 integrin is thought to be of particular importance, interacting with the endothelial cell intercellular adhesion molecule (ICAM-1). The α4 integrin is expressed on almost all lymphocytes, and exists in combination with a β1 or β7 subunit, which interacts primarily with the endothelial ligands vascular cellular adhesion molecule-1 (VCAM-1) and mucosal addressin cell adhesion molecule-1 (MAdCAM-1) respectively. The α4β1-integrin is important in inflammatory recruitment of leukocytes and in other sitations that require cell adhesion to the vascular endothelium (Chigaev et al, 2003). The avidity of the cells expressing the α4β1-integrin can be rapidly changed by chemokines (Chigaev et al, 2003). The α4β7-integrin interaction with MAdCAM-1 is crucial to the leukocyte gastrointestinal mucosal homing (Sandborn et al, 2002). MAdCAM-1 contains several structural motifs that are homologous with ICAM-1, VCAM-1, and IgA1, although also contains a unique mucin-like domain not shared by these molecules. It is expressed on the lamina propria venules and Peyer's patch HEVs, in the marginal zone of the spleen and in areas of chronic inflammation. L-selectin may also interact with MAdCAM-1 in the gastrointestinal tract. MAdCAM-1 expression is stimulated by TNF-α in HEVs via NF-κB translocation (Oshima et al, 2001).

Human intestinal micro vascular endothelial cells derived from IBD mucosa display enhanced adhesiveness for leukocytes compared with those derived from normal mucosa, in addition to enhanced vascular permeability (Gautman et al, 2001). This adhesion is modulated by pro-inflammatory cytokines such as monocyte/macrophage-derived TNF-α, which induce endothelial cells to produce IL-1, which in turn increases polymorphonuclear and monocyte cellular adhesion to the vascular endothelium. These interactions determine leukocyte infiltration and are pivotal in tissue damage (Fiocchi, 1997). Understanding such interactions could aid future development of therapeutic targets (Fiocchi, 1997).

The second stage in leukocyte trafficking involves cellular transmigration into the site of inflammation. Following extravasation from the blood, leukocytes pry apart the inter-endothelial cell connections and migrate into the site of inflammation under the control of chemokines and their receptors with 'multistep navigation' (Foxman et al, 1997). This requires sequential ligand-induced desensitisation mediated by specific GRK kinases that phosphorylate the engaged receptor (Premont et al, 1995), (Daaka et al, 1998). Thus, in conjunction with adhesion molecules, chemokines control the recruitment of specific leukocyte sub-populations to sites of tissue damage.

Oxygen and nitrogen reactive metabolites in IBD

Immune activation in IBD results in a sustained overproduction of reactive metabolites of oxygen and nitrogen, and there is over expression of the inducible form of nitric oxide synthase (iNOS)

(Grisham et al, 2002), (Pavlick et al, 2002). The oxidative injury correlates with disease severity, and it is thought that oxidative induced cytoskeletal disruption is a prerequisite to tissue damage (Keshavarzian et al, 2003). However, colonic oxidant levels have also been found to be elevated in normal mucosa of affected patients, indicating that an oxidative imbalance does not necessarily lead to tissue injury, nor is not entirely consequential to tissue injury (Keshavarzian et al, 2003). A number of studies have demonstrated that reactive oxygen NO species may promote gastrointestinal inflammation, although other studies do not support this. Furthermore, there is some evidence to suggest that some of the reactive oxygen species may play a protective role in IBD, and other evidence to implicate an imbalance of these reactive metabolites to be a contributory factor to some of the intestinal damage that occurs in IBD (Pavlick et al, 2002), (Kruidenier et al, 2003). There therefore remains a lack of clarity as to the relative importance of the enhanced production of reactive oxygen species and iNOS-derived nitric oxide (NO). Antioxidant agents may be of therapeutic benefit in IBD, and further research is required (Langmead et al, 2002). The antioxidant effects of aminosalicylates may constitute at least part of their therapeutic action.

Mucosal lymphoid tissue

Mucosal lymphoid tissue in the gastrointestinal tract provides immunological tolerance to dietary antigens and immunity to pathogens (Sarsfield et al, 1996). This ability to differentiate between pathogens and non pathogens is a crucial characteristic of the immune system. Lymphocytes activated in Peyer's patches tend to recirculate, or return to intestinal mucosa, facilitating re-encounter with the same antigen originally presented to them in the Peyer's patch (Cook et al, 2000).

Other intestinal cell types

The immunological significance of other intestinal cell types, including fibroblasts and myofibroblasts is yet to be defined. These cells may be pivotal in the chronicity of IBD, or may merely represent cells that undergo 'bystander damage' (Fiocchi, 1997). Intestinal sub-epithelial myofibroblasts are present close to the basal surface of epithelial cell. They have an important role in wound healing and fibrosis, and enhance epithelial cell migration via secreted bioactive transforming growth factor (TGF)-β (Fiocchi 1997), (Beltinger et al, 1999). Bacterial components directly activate intestinal myofibroblasts expressing TLRs. This may be crucial to the innate response by sensing and responding to bacterial products that have penetrated into the subepithelial compartment (Otte et al, 2003).

The role of the enteric nervous system in the control of inflammation has not yet been elucidated. It has been postulated to mediate broad modulatory activities in acute and chronic inflammation, with its extensive rich network of enteric fibres and neurotransmitters (Fiocchi, 1997). The enteric glial cell network has tropic and protective functions towards enteric neurons, functionally equivalent to astrocytes (Cabarrocas et al, 2003). Similar to the astrocytic regulation of the blood brain barrier, glial cells are thought to regulate mucosal and vascular permeability in the gastrointestinal tract, in addition to tissue integrity. Disruption of the glial network may be important in the pathogenesis of CD (Cabarrocas et al, 2003). Targeted deletion of enteric glial

cells in transgenic mice has yielded pathological changes similar to necrotising enterocolitis (NEC) and early CD, possibly implicating the significance of the enteric system in the pathogenesis of bowel disease (Bush et al, 1998). This is poignant as NEC shares some mechanistic and phenotypic similarities with IBD (Bush, 2002).

Extracellular matrix

All interactions between immune and non-immune cells in the gastrointestinal tract occur in the midst of a complex mixture of proteins including fibronectin, collagen, laminin, thrombospondin, tenascin, enactin, and proteoglycans. These proteins constitute two main domains; the compact laminar structure termed the basement membrane, and a diffuse network surrounding lymphoid, mesenchymal, vascular and nerve cells (Fiocchi, 1997). The extracellular matrix is important in regulating the number, location and activation of leukocytes, so is a vital non-immune constituent of the immune system. Interaction between the extracellular matrix and immune cells occurs via matrix metalloproteinases (MMPs) which are a homologous family of zinc dependent peptidases produced by T cells and macrophages whose enzymic activity is directed against components of the extracellular matrix (Fiocchi, 1997). They play a central role in tissue remodelling (Stamenkovic, 2003). The enzymic and corresponding mRNA levels are increased in and correlate with inflammation in IBD suggesting that matrix metalloproteinases may play an important role in gastrointestinal inflammation (Pender et al, 1997), (Heuschkel et al, 2000). An imbalance between these enzymes and their natural inhibitor may be central to degradation. For example MMP3 is markedly up-regulated in ulcerated tissue, although the tissue inhibitors of metalloproteinases (TIMP1) remains unchanged (Heuschkel et al, 2000).

1.4 Chemokine overview

Chemokines are essentially chemo-attractive cytokines produced by immune and non-immune cells, including epithelial cells (Papadakis et al, 2000), (Hoover et al, 2002), (Standyk, 2002). They are small (8-14kDa), structurally related, mostly basic that bind heparin and are stored in secretary granules to be mobilised as required (Rollins et al, 1997), (Sallusto et al, 2000). In the cytotoxic granules of cytotoxic T lymphocytes, chemokines are stored together with proteoglycans and perforin in a form that is particularly effective in inhibiting HIV infection (Sallusto et al, 2000). Following stimulation with histamine or thrombin, the contents of these granules are transferred to the cell surface, allowing rapid leukocytic recruitment without the need for protein synthesis (Sallusto et al, 2000). Most are secreted, and tend to remain relatively local (Standyk, 2002). They form stable gradients as they are positively charged, so bind to sulphated proteoglycans in the extracellular matrix or on the cell surface (Webb et al, 1993). Their effects are transduced following ligation of one or more of nineteen specific G-protein coupled receptors, expressed predominantly on leukocytes. Appropriate immobilisation is important for the control of immunological effect (Sallusto et al, 2000). A few chemokines, such as fractalkine are expressed on the cell surface (Olson et al, 2002).

Chemokine function

Chemokines are of fundamental importance in the control of leukocyte trafficking and recruitment. For example, CCL21 production is both required and sufficient for β2-integrin

activities upon rolling T cells in peripheral lymph node HEVs (Stein et al, 2000). They work co-operatively, sometimes with directionally opposing gradients, such as occurs with monocytes, driven out from blood vessels into tissue (Ogilvie et al, 2003). Chemokines also modulate haemopoeisis, angiogenesis and tissue repair, and inhibit HIV infection (Baggiolini et al, 1998), (Sallusto et al, 1998)[2]. Furthermore, they are important in dendritic cell maturation, T and B cell development, and in Th1 and Th2 responses (Rossi et al, 2000). In addition to their immunological centrality, chemokines have also been implicated in cancer and autoimmune diseases (Ajuebor et al, 2002)[2].

Chemokine up regulation occurs in response to pro-inflammatory cytokines and to enteric pathogens directly, including bacteria, bacterial products, and chemical stimuli (Panja et al, 1998). For example, butyrate regulates expression of CXCL2, CXCL3 and CXCL8 in intestinal epithelial cells. This is a short chain fatty acid derived from the fermentation of non-absorbed carbohydrate by intestinal bacteria (Huang et al, 1997), (Fusunyan et al, 1998).

Chemokine classification

More than 50 chemokines have been identified, each with a specific pattern of cellular chemotaxis (Ono et al, 2003). The development of bioinformatics (computer-assisted sequence analysis) on expressed sequence tag databases has allowed the expansion of chemokine identification. Chemokines are ideal for such analysis owing to their small size, abundant expression and because they are secreted proteins (Zlotnik et al, 2000), (Yoshie et al, 2001).

Chemokines are categorised into four distinct families CXC (α group), CC (β group), CX_3C (δ group), and C (γ group), and differentiated structurally according to the number and spacing of the amino-terminal cysteines (Rossi et al, 2000), (Sallusto et al, 2000), (Zlotnik et al, 2000). CC chemokines have two adjacent amino-terminal cysteines, whereas CXC chemokines possess an intervening amino acid between the two amino-terminal cysteines (Rollins et al, 1997), (Baggiolini et al, 1997). Two disulphide bonds are formed between the first and third Cys and between the second and fourth Cys. Lymphactin is the exception to the four Cys rule, and has only two Cys residues, so it retains a functional structure with only one disulphide bond (Rossi et al, 2000). The chemokines and their pseudonyms are listed in table 1.1.

Table 1.1: Chemokines, chemokine receptors and their alias names

Chemokine	Alias names	Receptor
CXC group		
CXCL1	GRO1 (growth regulated protein), GROα, MGSA (melanoma growth stimulatory activity), SCYB1, NAP-3	CXCR1, CXCR2
CXCL2	GRO2, GROβ, MIP2α, SCYB2	CXCR2
CXCL3	GRO3, GROγ, MIP2β, SCYB3	CXCR2
CXCL4	PF4, Platelet Factor-4, SCYB4	Unknown
CXCL5	SCYB5, ENA-78, SCYB5	CXCR2
CXCL6	SCYB6, GCP-2, SCYB6	CXCR1, CXCR2
CXCL7	PPBP, (PBP>CTAP-III>β-TG>NAP-2), SCYB7, low-affinity platelet factor 4	CXCR2
CXCL8	IL-8, SCYB8, MDNCF, NAP-1, LYNAP, NAF, GCP-1	CXCR1, CXCR2
CXCL9	MIG (monocyte induced by IFγ), SCYB9	CXCR2, CXCR3
CXCL10	INP10, γ IP10, SCYB10	CXCR2 CXCR3
CXCL11	I-TAC (IFN-α inducible T cell α chemoattractant), β-R1, IP9, H174, SCYB11	CXCR2 CXCR3
CXCL12	SDF-1α, SDF-β, PBSF, SCYB12, TPAR1, TLSF	CXCR4
CXCL13	BCA-1, BLC, SCYB13	CXCR5
CXCL14	BRAK, bolekine, SCYB14	Unknown
CXCL15	Lungkine	Unknown
CXCL16	Small inducible cytokine B6	CXCR6
CC group		
CCL1	SCYA1, I-309, TCA-3	CCR8
CCL2	SCYA2, MCP-1 (monocyte chemotactic protein), MCAF, HC11	CCR2
CCL3	SCYA3, MIP-1α, MIP-1αS, LD78α, GOS19-1, PAT 464.1, TY-5, SISα	CCR1, CCR5
CCL4	SCYA4, MIP-1β, ACT-2, PAT744, H400 SIS-γ, LAG-I, HC21, G-26, MAD-5	CCR5
CCL5	SCYA5, SIS-δ, RANTES (regulated upon activation, normal thymus expressed and secreted)	CCR1, CCR3, CCR5
CCL6	C-10, MRP-2	CCR1, CCR2, CCR3
CCL7	SCYA7, MCP3 (monocyte chemotactic protein), NC28, FIC	CCR1, CCR2, CCR3
CCL8	SCYA8, MCP-2, HC14	CCR2, CCR3
CCL9		CCR1
CCL10		CCR1
CCL11	SCYA11, Eotaxin	CCR3
CCL12	SCYA12, MCP-3	CCR2
CCL13	SCYA13, MCP-4, CK β 10, NCC-1	CCR2, CCR3
CCL14	SCYA14, CC-1, HCC-1, NCC-2, CK β1, CCCK-1/CCCK-3, MCIF, MIP1δ	CCR1
CCL15	SCYA15, HCC-2, leukotactin-1 (Lkn-1) MIP5, CC-2, NCC-3	CCR1, CCR3
CCL16	SCYA16, HCC4, LEC, NCC-4, LMC monotactin-1 (Mtn-1), LCC-1, ILINCK	CCR1
CCL17	SCYA17, TARC (thymus and activation-regulated chemokine), STCP-1	CCR4
CCL18	SCYA18, DC-CK-1, PARC, MIP-4 AMAC-1, CK β 7	Unknown
CCL19	SCYA19, MIP-3α, ELC, exodus-3, CK β 7	CCR7
CCL20	SCYA20, MIP-3α (macrophage inflammatory protein-2α), LARC (liver and activation-regulated chemokine), exodus-1, CK α 7	CCR6
CCL21	SCYA21, 6Ckine, SLC, exodus-2, TCA4, CK β 9	CCR7
CCL22	SCYA22, MDC, STCP-1	CCR4

CCL23	SCYA23, MPIF-1, MIP-3, CK β 8-1	CCR1
CCL24	SCYA24, MPIF-2, eotaxin-2, CK β 6	CCR3
CCL25	SCYA25, TECK, CK β15	CCR9
CCL26	SCYA26, Eotaxin-3, MIP-4 α	CCR9 (GPR9-6)
CCL27	SCYA27, Eskine, CTACK, ILC, skinkine	Unknown
CCL28	Novel CK - ligand for CCR10	CCR10
C group		
XCL1	SCYC1, lymphotactin α, SCM-1α, ATAC	XCR1
XCL2	SCYC2, lymphotactin β, SCM-1β, ATAC	XCR1
CX_3C group		
CX_3CL1	SCDY1, Fractalkine, CX3X ligand	CX3CR1

Chemokine receptor	**Alias names**	**Ligand**	**Chromosome**
CCR1	CC CKR1, HM145, MIP-1α/R, MIP-1α/RANTES	CCL2 (with low affinity insufficient to signal) 3, 4, 5, 7, 8, 13, 14 (potent agonists for CCR1), 15, 16, 23	3
CCR2	CC CKR2A, CC CKR2B, MCP-1RA, MCP-1RB	CCL2, 7, 8, 13	3
CCR3	CC CKR3, CMKBR3, CKR-3	CCL5, 7,11	3
CCR4	CC CKR4, K5-5	CCL17, 22 (highly potent agonists with high receptor affinity)	3
CCR5	CC CKR5, CMKBR5, ChemR13	CCL 3, 4, 5, 8	3
CCR6	DRY6, CKR-L3, GPR-CY4, STRL22	CCL20	6
CCR7	EB1, BLR2	CCL19, 21	17
CCR8	ChemR1, TER-1, GPR-CY6, CKRL1	CCL21	3
CCR9	GPR-9-6	CCL25	3
CCR10	GPR2	CCL27, 28	17
CXCR1	IL-8R1(type A), Type 1 IL-8R	CXCL8	2
CXCR2	IL-8R2(type B), Type 2 IL-8R	CXCL1, 2, 3, 5, 6, 8, 9, 10, 11	8
CXCR3	IP10/MIGR, MIG, I-TAC	CXCL9, 10	8
CXCR4	LESTR, HUMSTER, HM89 LESTR, NPYRL, LCR1, Fusin	CXCL12	2
CXCR5	BLR1, MDR15	CXCL13	11
CXCR6	Bonzo, TYMSTER, STRL33		3
CX_3CR1	V28, CMKBRL1, GPR13	CX3CL1	3
XC1	GPR5	XCL1, 2	3

Human chemokine binding proteins

Receptor	**Alias**	**Ligands**	**Chromosome**
DARC	Duffy antigen	CCL2, 5 CXCL1, 8	1
CCX, CKR	CCR10, PPR1	CCL19, 21, 25	
D6	CCR10, JAB61	CCL2, 4, 5, 7, 8	3

(Horuk, 2001), (Zlotnik et al, 2000)

Distinct patterns of chemokine expression have been seen in different diseases, with CXC chemokines largely involved in recruitment of neutrophils and monocytes and CC chemokine are more strongly implicated in lymphocyte and dendritic cell recruitment (Papadakis et al, 2000), (Zlotnik et al, 2000). The C family of chemokines exert their actions on T lymphocytes and NK cells. The CX_3C chemokine fractalkine is active on T lymphocytes, NK cells, monocytes and neutrophils (Ajuebor et al, 2002)[1].

Chemokines may also be categorised into 'inflammatory' and 'lymphoid' groups. Inflammatory chemokines are produced by several cell types at high levels, including endothelial, epithelial, stromal cells and leukocytes, and are important in acute and chronic inflammation. This group includes CXCL8, CXCL10, CCL2, CCL4, CCL5 and CCL11, which are largely involved in recruitment of neutrophils and macrophages, and are induced by inflammatory stimuli such as LPS, IL-1β or TNF-α. The production of these chemokines varies according to the type of inflammation, for example CCL11 is found at high levels in the lung undergoing allergic inflammation (Sallusto et al, 2000). Lymphoid chemokines are produced within lymphoid tissue and maintain homeostatic leukocyte traffic and cell compartmentalisation within these organs. This group includes the CC chemokines. Some chemokines function as inflammatory or lymphoid chemokines depending on the environment. For example, CCL22 functions as an inflammatory chemokine when it is produced in the inflamed lung but can also contribute to the regulation of intercellular interactions in the secondary lymphoid organs (Sallusto et al, 2000).

The majority of chemokines are produced in a variety of tissues and locations, although some remain restricted to a particular tissue, such as CCL25 which is only produced in the thymus and intestine (Sallusto et al, 2000).

Chemokine receptors

Chemokines are biologically active via binding to cell surface receptors. Expression frequently varies according to the stage of celleular activation and differentiation (Ono et al, 2003). Various chemokine receptors have been cloned so far, including six CXC, ten CC, one CX_3C and two C receptors (Horuk, 2001). In many cases chemokine receptors are promiscuous, binding several chemokines within a single class with high affinity. CCR6 is an exception, with only two known ligands: CCL20 and β-defensin (Perez-Canadillas et al, 2001). CXCR1-5 bind CXC chemokines, CCR1-9 bind CC chemokines, XCR1 binds the C chemokine, lymphactin, and CXCR1 binds the CX_3C chemokines such as fractalkine (Rossi et al, 2000), (Horuk, 2001). These are members of superfamily of serpentine proteins that signal through G-protein coupled, seven-transmembrane receptors. Chemokine binding to a cognate receptor causes conformational changes in the chemokine, enabling N-terminal initiation of a signalling cascade of intracellular events that lead to biological action (Fernandez et al, 2002). There is a dissociation of the receptor associated G proteins into α and βγ subunits, which activates a variety of effector enzymes, including phospholipases, leading to inosital phosphate production, an increase in intracellular calcium and activation of protein kinases (Horuk, 2001). This signal transduction causes activation of chemotaxis by modulating actin-dependent cellular processes, up regulation of adhesion proteins, in addition to a variety of functions in leukocytes (Horuk, 2001).

1.5 Cellular control by chemokines

Dendritic cells

Dendritic cells are bone marrow derived antigen-presenting cells that are widely distributed throughout lymphoid and non-lymphoid tissues, although in relatively small numbers (Cravens et al, 2002). They prime or tolerise T lymphocytes thus initiating or inhibiting immune responses,

migrating to secondary lymphoid organs to present antigen to T lymphocytes in the T-zones (McColl, 2002). Recruitment of these cells from the bone marrow to the site of injury or infection is determined both by chemokines produced in a time specific manner, and by the ability of these cells to respond via their chemokine receptors at different stages of maturation (Luster 2002), (McColl, 2002). Dysregulation of dendritic cell migration is thought to contribute to the dendritic cell accumulation in the lesions of autoimmune disorders (Cravens et al, 2002).

The receptors CXCR1, CXCR2, CCR1, CCR2 and CCR5, CCR6 are present on immature dendritic cells and their precursors monocytes. These receptors account for the extravasation and migration of these cells into inflamed tissues. CXCR1 and CXCR2 probably account for the arrest of rolling monocytes (Sallusto et al, 1994). CCR6 expression is restricted to immature dendritic cells, explaining their strong response to its cognate ligand CCL20 which is highly expressed by intestinal epithelial cells in low basal levels, contrasted with high levels after stimulation (Carramolino et al, 1999), (Kucharzik et al, 2002), (Vanbervliet et al, 2002). Dendritic cells respond to various pathogen-associated molecular patterns such as LPS, bacterial lipoproteins, peptidoglycan and CpG dinucleotides via their several different receptor types. These include CD14, scavenger receptors and TLR2, 3, 4, 5, 6, 9 (Luster, 2002). Stimulation of these receptors induces dendritic maturation, which is characterised by the production of pro-inflammatory cytokines, up regulation of co-stimulatory molecules and altered expression of chemokine receptors (Olson et al, 2002). A 'chemokine gradient' enables the immature dendritic cells to encounter stimuli such as IL-1, TNF-α and LPS that facilitate maturation (Sallusto et la, 1994), (Randolph et al, 1998), (Cella et al, 1999). In contrast, IL-10 causes a down-regulation of antigen presenting cell function of many dendritic cells (Macdonald et al, 1999).

Following stimulation, dendritic cells initially produce large amounts of CCL3, CCL4 and CXCL8 for a short period of time. CCL2 and CCL5 are also produced, but in a steadier fashion (Olson et al, 2002). This pattern of expression enhances and sustains the recruitment of immature dendritic cells and other inflammatory cells. Pro-inflammatory cytokines secreted by activated macrophages bind to dendritic cell receptors and mediate cessation of phagocytosis and departure from the tissue to the nearest lymph node via the lymphatic system (Olson et al, 2002). This process is accompanied by a marked change in chemokine receptor expression, contributing to maturation. In the maturing dendritic cell, there is a rapid down-regulation of receptors that respond to inflammatory chemokines (i.e. CCR1, CCR5, CCR6), a loss in their responsiveness for the chemokine ligands for those receptors (CCL3, CCL4, CCL5, CCL20) and an up regulation of lymphoid chemokines such as CXCR4, CCR4 and CCR7 (Sallusto et al, 2000), (Skelton et al, 2003). This enables responsiveness to the chemokines CCL12, CCL17, CCL19, CCL21 and CXCL13 (Dieu et al, 1998), (Sallusto et al, 1998)[3], (Izadpanah et al, 2001), (Luster 2002). The CCR7-binding chemokines CCL19 and CCL21, and the CXCR5-binding chemokine CXCL13 are the primary mediators of dendritic cells and lymphocytes into secondary lymphoid tissue (Lindhout et al, 1999), (Reif et al, 2002). CCR7 ligands have a key role in the accumulation of antigen-loaded mature dendritic cells in T cell rich areas of draining lymph nodes (Sallusto et al, 1994), (Caux et al, 2002).

In the regional lymph nodes, dendritic cells are the primary cells responsible for activating naïve T and B cells, which then return to the site of inflammation and are also involved in the re-stimulation of experienced T-cells in the tissue. The interaction between dendritic cells and lymphocytes has a key role in linking innate and adaptive responses (Luster et al, 2002). T cell proliferation induced by dendritic cells yields either a Th1 or Th2 response depending on the cytokine environment and length of time of stimulation (MacDonald et al, 1999), (Sallusto et al, 2000).

T cell changes during inflammation:

Within 6 hours of inflammatory stimulation of T cell receptors, a transient switch in chemokine receptor expression occurs. There is a down-regulation of T-cell expression of CCR1, CCR2, CCR3, CCR5, CCR6, CXCR3, and an up regulation of CCR4, CCR7, CCR8 and CXCR5. The up regulation of CCR7 enables T cell migration to draining lymph nodes, with relocation of the cells to the sites where the receptors correspond to the newly expressed ligands, i.e. CCL19, CCL21 (CCR7 ligands), CXCL13, CCL1, CCL17 (Sallusto et al, 2000), (Stein et al, 2000). CCL21 is expressed in HEV, which facilitates cellular migration. In the regional lymph nodes, the naïve T cells are stimulated by antigen presenting cells.

The balance between Th1 and Th2 cells and between pro-inflammatory and anti-inflammatory cytokines is maintained by chemokines (Siveke et al, 1998). Th1 T cells secrete IFN-γ and IL-2, which up-regulates the Th1-attracting chemokines CCL3, CCL4 and CCL5 (Siveke et al, 1998), (Pavlick et al, 2002). CCL3 and CCL4 also induce the influx of NK cells, macrophages and immature dendritic cells. NK cells are an important source of IF-γ. IF-γ also induces expression of the T-cell recruiting chemokines CXCL9 and CXCL10 (Luster, 2002). CXCL10 is also induced directly by viruses and bacterial products, and thus may play an early role in T and NK cell recruitment into tissue (Luster, 2002). This is antagonised by Th2 attracting chemokines and IL-4. The receptors preferentially expressed by Th1 cells include CXCR3, CCR1 and CCR5 (Campbell et al, 2000). The expression of CCR1 and CCR5 explains Th1 co-localisation with macrophages and neutrophils in delayed type hypersensitivity lesions (Homey et al, 1999). Both Th1 and Th2 cells secrete CCL2 and CXCL12 (Sieveke et al, 1998). TNF-α is associated with Th1 and Th2 responses, and stimulates both types (Sallusto et al, 2000).

Examples of Th1-mediated diseases include rheumatoid arthritis and MS (Balashov et al, 1999), (Nanki et al, 2000). Nearly all T cells in the MS lesions express CCR5 and CXCR3, although usually only 5-15% of peripheral blood T cells have this phenotype. Production of IFN-γ, a cytokine that is a hallmark of Th1 type immune responses, is important to the pathogenesis of this disease. Increased production of IFN-γ precedes clinical attacks and injection of MS patients with recombinant IFN-γ induces exacerbations of the disease (Balashov et al, 1999), (Qin et al, 1997). Skin homing T cells are mainly Th1. It has been postulated that CD is a Th1-mediated response and UC a Th2-mediated response, based on the respective cytokine profiles in the gut, differentiating them immunologically (Scheerens et al, 2001), (Siegmund, 2002), (Weigmann et al, 2002).

Th2 cells secrete IL-4, 5, 9, 10 and 13, which probably stimulates the effector function of eosinophils and basophils, in addition to enhancing CCL11 and CCL22 production, thus amplifying and modulating the inflammatory reaction (Sallusto et al, 2000), (Montelone et al, 2002), (Pavlick et al, 2002), (Weigmann et al, 2002). This is counter-acted by IFN-γ production. Th2 cells express CCR4 (receptor for CCL17, CCL20 and CCL22), also expressed on basophils (Nagata et al, 1999), CCR8 (receptor for CCL1 and CCL21) (Nagata et al, 1999), CCR3 (receptor for CCL11, produced abundantly in mucosal tissues undergoing allergic inflammation) and CCR5. CCR5 is produced at lower levels on Th2 cells compared to Th1 cells. Eosinophils and basophils both express CCR3, which facilitates their co-localisation at sites of CCL11 production (Sallusto et al, 2000).

Th2 cells are important in atopic and allergic disease processes, contrasting with Th1 cell mediated delayed type hypersensitivity reactions such as contact allergic responses (Homey et al, 1999). CCR4 and CCR8 are examples of potential Th2 targets for therapeutic intervention, although the pathophysiological role in these diseases needs to be further investigated.

Memory T cells

A fraction of the activated T lymphocytes become memory cells that migrate throughout the peripheral tissues and possess rapid effector function. They undergo clonal expansion in lymph nodes. Memory T cells efficiently interact with E-/P-selectin and VCAM-1. They also express multiple chemokine receptors including CCR4 and CCR6. CCR6 may aid cellular migration in response to CCL20 both in the skin and gastrointestinal tract (Sallusto et al, 2000).

There are 2 types of memory T cells. Both types are more sensitive to T cell receptor stimulation than naïve T cells, and consequently stimulate dendritic cells more efficiently to produce IL-12. The first group constitutes a rapid effector group that can be rapidly recruited to inflamed peripheral tissues, where they perform delayed type hypersensitivity or cytotoxic functions, required to rapidly contain invasive pathogens. These cells lack CCR7, express low levels of L-selectin, high levels of integrins, and produce effector cytokines IFN-γ and IL-4. The second group of memory T cells constitute a lymph-node-homing, non-polarised phenotype. These express CCR7 and express high levels of L-selectin. They do not produce effector cytokines, and represent a pool that stimulate dendritic cells generate new waves of effector cells (Sallusto et al, 2000).

A subset of memory T cells preferentially migrates to gut or skin. Those that home to skin possess 'cutaneous lymphocyte associated antigen' (CLA), which binds E-selectin on endothelial cells of inflamed skin. CLA constitutes a carbohydrate modification of P-selectin glycoprotein ligand-1. CLA^+ memory T cells preferentially express CCR4, and inflamed dermal blood vessels express one of its ligands, CCL17. Together CLA, CCR4 and CCL17 may contribute to specific memory T cells trafficking to inflamed skin (Fitzhugh et al, 2000), (Sallusto et al, 2000), (Reiss et al, 2001), (Kunkel et al, 2002). In addition to its extravasation role through cutaneous vessels, CCR4 may also drive migration within other tissue types, for example lung and liver, where CCL17 is produced. CCL17, expressed by cutaneous although not intestinal endothelium,

induces integrin-dependent firm adhesion of CLA^+ T cells, consistent with its role in the extravasation process.

B cells

Chemokine expression determines the fate of developing B cell populations and directs their maturation in the bone marrow to the periphery (Bowman et al, 2000). CXCR4 has a role in B cell lymphopoiesis (Sallusto et al, 2000). CXCR5 is a selective and efficacious chemoattractant for circulating naïve B lymphocytes (Carlsen et al, 2002). CXCL12 is expressed constitutively in bone marrow-derived stromal cells and promotes proliferation of B progenitors (Sallusto et al, 2000).

T and B cell interaction in lymph nodes

Interaction between T and B cells is vital for immunological effect. Fluorescent labelling has demonstrated that upon stimulation the cells move from their designated areas to the boundary zone between the T and B zones, allowing immunological co-operation between these cells. A switch in chemokine receptor expression is likely to be the controlling migratory factor. The CXCR5 +ve T cells that localise to B cell follicles are functionally described as 'follicular B helper T cells', as they are required for efficient B cell help within the lymphoid follicle (Carlsen et al, 2002). Antigen-stimulated T cells down regulate CCR7 and upregulate the B cell area receptors CXCR5 and CCR4, thus move towards the B zone. The reciprocal changes occur in the B zone, with increased expression of CCR7 by antigen-engaged B cells, which is the receptor for the T-zone chemokines CCL19 and CCL21. This facilitates B cells migrate towards the T-zone (Reif et al, 2002), (Sallusto et al, 2000).

NK cells

NK cells participate in innate and adaptive immune responses to obligate pathogens and malignant tumours. Activated NK cells produce XCL1, CCL1, CCL3, CCL4, CCL5, CCL22 and CXCL8 (Robertson, 2002). CCL3, CCL4 and CCL5 from NK cells can inhibit *in vitro* replication of HIV. The numbers of NK cells are increased in CD, unlike in UC (Van Tol et al, 1992).

Neutrophils

Neutrophils are an important constituent of innate immunity, with their series of effector functions. They are extremely motile and migrate through tissues with relative ease (Zhelev et al, 2002). In addition to their defensive functions, neutrophils secrete a number of cytokines including CCL4, CCL14, CCL19, CCL20, CXCL1, CXCL8, CXCL9, CXCL10, and CXCL11 (Scapini et al, 2001). In addition, neutrophils can be induced by cytokines to express CCR6 and migrate in response to CCL20 (Schutyser et al, 2000). CCL19 and CCL20 production is induced by either LPS or TNF-α (Scapini et al, 2001). CXCL8 leads to neutrophil recruitment (Murphy, 1997), (Carlsen et al, 2002). Neutrophilic infiltration and accumulation is a prominent feature in the local inflammatory response in UC (Carlson et al, 2002). Like T lymphocytes, neutrophils roll along HEV walls during inflammation. Neutrophil activation is required to generate $\beta 2$ integrin bonds with the endothelium that stop their progression. Unlike naïve T cells, neutrophils are not only activated by ligation of G-protein coupled receptors with chemokines and other

chemoattractants but also receive signals from engagement of adhesion molecules including the selectins and β2 integrins (Ley, 2002).

Macrophages

Macrophages are important in the host's immunological and inflammatory responses. There are numerous macrophages in the normal intestinal mucosa, where they represent the major antigen presenting cells, capable of determining the type of T cell responses that develop in response to luminal antigens. The population of these cells is increased in IBD, and they are phenotypically different from those found in normal intestine, which cannot be easily induced to mediate acute inflammatory responses. Macrophages play a role in mediating the chronic mucosal inflammation, secreting IL-1, IL-6, IL-8, IL-12, IL-18, and TNF-β, which are important in the inflammatory responses in IBD. They also release metabolites of oxygen and nitrogen and proteases that degrade the extracellular matrix. Finally, macrophages appear to be important during resolution of inflammation and repair of the intestinal mucosa that occurs during disease remission (Mahida, 2000), (Murch, 1998).

Eosinophils

Eosinophils may be functionally involved in the pathophysiology of IBD, although data is lacking. CCL11 is a potent chemokine with selective chemotactic activity for eosinophils (Sullivan et al, 1999). CCL20 is also chemotactic to eosinophils. The levels of expression are higher in IBD, particularly CD, negatively correlating with peripheral eosinophil count (Mir et al, 2002). CCL5, CCL7, CCL12 and CCL22 are associated with eosinophil recruitment to the lung, and neutralisation of these chemokines modulates T lymphocyte recruitment (Homey et al, 1999). Chemokine receptor usage by eosinophils is a key area of research in diseases such as asthma, in which eosinophils are selectively recruited to the inflammatory site with associated degranulation. CCR3 is important for eosinophilic response, so is another potential target for therapeutic antagonism (Heath et al, 1997), (Xanthou et al, 2003). Receptor antagonists may prevent eosinophil entry and degranulation and rat monoclonal antibodies specific for CCR3 have been developed (Heath et al, 1997), (Grimaldi et al, 1999).

Mast cells

Mast cells are important as sentinel cells in host defence against bacterial infection (Lin et al, 2003). Although they are potent producers of many biologic active mediators, such as cytokines and chemokines, their precise biologic functions remain undefined. Most of their effectiveness is thought to depend on the recruitment of other immune cells, for example by production of inflammatory mediators such as histamine, proteinases, arachidonic acid metabolites and cytokines (Lin et al, 2003), (Ruschpler et al, 2003). They are thought to be involved in the induction and maintenance of a variety of severe allergic and autoimmune diseases (Stassen et al, 2002). Their relevance in IBD is unclear.

Basophils

CC chemokines receptors are present on basophils and have been implicated in the pathogenesis of IBD and a number of allergic inflammatory dermatitis (Power et al, 1995).

Platelets

In addition to their homeostatic mechanisms, platelets are also involved in protection against pathogens by means of phagocytosis. Furthermore, activation of platelets leads to release of CCCL3, CCL5, CCL7, CCL17, CXCL1, CXCL5 and CXCL8, which attract leukocytes and other platelets (Gear et al, 2003). CXCL12, CCL17 and CCL22 are rapid activators of platelet aggregation and adhesion after their binding to platelet CXCR4 and CCR4. CXCL12 is primarily secreted by endothelial cells. CCL17 and CCL22 are secreted by macrophages and monocytes.

1.6 Chemokines in disease

Aberrant expression of chemokines and their receptors play causative roles in the pathophysiology of numerous inflammatory and autoimmune diseases including multiple sclerosis (MS), rheumatoid arthritis, atherosclerosis, asthma and organ transplant rejection (Horuk, 2001), (Ajuebor et al, 2002)[2], (Rajarathnam 2002). In these diseases, a differential pattern of chemokine induction is observed.

Rheumatoid arthritis

Experimentally, mouse models for rheumatoid arthritis administered with CCR1/CCR2/CCR5 receptor antagonists or CCL5/CXCL8 antibodies exhibit reduced swelling, tissue destruction and pannus formation. CXCR2 knockout studies in mice are associated with lower levels of neutrophil infiltration (Ajuebor et al, 2002)[2].

Multiple sclerosis

Chemokines and matrix metalloproteinases play key roles in leukocyte migration across the blood-brain barrier in infectious and inflammatory diseases. The pattern of chemokine receptor expression patterns reflects disease activity and stage in MS (Sellebjerg et al, 2003). Chemokine research in MS has been focused on animal models with targeted gene deletion exhibiting autoimmune encephalomyelitis. Mice lacking CCR1 or CCR2 are protected from this disease. Administration of antibodies to CXCL10 to such mice with this pathology causes improvement (Ajubor et al, 2002)[1].

Atopic dermatitis

The CCL11/CCR3 ligand/receptor interaction is thought to relate to tissue damage in the initial phase of atopic dermatitis. CCR3 antagonists may be effective therapeutically, and may be utilised for an 'atopy patch test' (Homey et al, 1999).

Helicobacter pylori infection

Helicobacter pylori-mediated gastritis is associated with increased expression of CXCL5, CXCL8, CXCL10 and CXCL13. Ulceration is associated with increased expression of CXCL8 and CCL3. Eradication of *Helicobacter pylori* causes a reduction of chemokine levels (Ajuebor et al, 2002)[1].

Hepatic disease

Hepatic and serum levels of the neutrophil chemoattractant CXCL8 are increased in hepatitis. Hepatic CCL2, CCL7 and CCL8 are elevated in primary biliary cirrhosis and fulminant hepatic

failure. There are increased levels of CXCL9 and 10 in chronic hepatitis C, which are thought to be chemoattractants for T lymphocytes. The use of neutralising antibodies in animal models has demonstrated that CCL3 and CCL5 contribute to T cell recruitment and hepatic injury during T cell recruitment and hepatic injury during graft versus host disease. CXCR2 and CXCL2 have a hepato-protective effect, enhancing liver regeneration (Ajuebor et al, 2002)[1].

CCR6 is over expressed in small liver metastases of colon, thyroid and ovarian carcinomas compared to normal liver. As human liver constitutively expresses CCL20, it may select $CCR6^{+}$ cancer cells. Chemotaxis is thought to be crucial to the formation of liver metastases via up regulation of MMP-9, and inhibition of CCR6 may therefore be effective in prevention (Dellacasagrande et al, 2003), (Campbell et al, 2003).

HIV

Chemokine receptors are necessary for HIV infection and are potential therapeutic targets for treatment (Proudfoot et al, 2002). CCR5 and CXCR4 are the major co-receptors for macrophage tropic and T-cell line tropic viral isolates respectively (Hieshima et al, 2002). Patients lacking CCR5 are resistant to HIV infection (Proudfoot et al, 2002).

Neural disease

Chemokines and their receptors are constitutively expressed in the central nervous system (CNS) by many cell types including neurons and glial cells. In addition to their involvement in neuroinflammation, they are involved in neurodevelopment, and neurophysiologial signalling (Bajetto et al, 2002), (Cho et al, 2002), (Ragozzino, 2002).

Sarcoidosis

CCL19 is implicated in T lymphocyte recruitment in sarcoidodis. It is associated with disease progression and is down-regulated following treatment (Gibejova et al, 2003).

Coeliac disease

In coeliac disease, large numbers of $CCR9^{+}$ lymphocytes are recruited to the small intestinal mucosa, but not to the colonic mucosa, reflecting small bowel regional expression of CCL25 by small bowel enterocytes (Kunkel et al, 2000).

IBD

Chemokines have been implicated in the pathogenesis of IBD (Papadakis, 2004). There is increased expression of the neutrophil attracting CXC chemokines CXCL5 and CXCL8, and the CC chemokines CCL2 and CCL5 in IBD (Ajuebor et al, 2002)[1], (Dwinell et al, 2003). CXCL8 has been identified in infiltrating mononuclear cells, macrophages and neutrophils, whereas CXCL5 co-localises to the intestinal epithelial cells of these patients. CCL2 mRNA protein has been localised to macrophages, smooth muscle cells and endothelial cells, CCL5 mRNA in intraepithelial lymphocytes and in the sub epithelial lamina propria and CCL7 mRNA is found in epithelial cells. Immunohistochemical analysis indicates high intestinal levels of the chemokine receptors CXCR3, CXCR4, CCR3 and CCR5 in CD (Scheerens et al, 2001). Increased

enterocyte CCL20 production has been demonstrated in IBD, which may play an important role in lymphocytic recruitment to and activation in the colonic epithelium in IBD (Kwon et al, 2002).

1.7 CCL20/CCR6/β defensin

The CCR6/CCL20 chemokine receptor/ligand pair is an important constituent of mucosal and epidermal immunity. CCR6 receptor has only two cognate ligands: CCL20 (a CC chemokine) and β-defensin, contrasting with the other promiscuous chemokine receptors that bind multiple ligands (Baba et al, 1997), (Perez-Canadillas et al, 2001).

Structure

Nuclear magnetic resonance spectroscopy has demonstrated that CCL20 exhibits the same monomeric structure as the other chemokines: a three-stranded β-sheet and an overlying α-helix. The monomeric structure of CCR6 includes a disulphide bond between the first and second extracellular loops that confines a helical bundle together with the N-terminus adjacent to the third extracellular loop, creating the structural organisation critical for ligand binding and, therefore, receptor signalling (Ai et al, 2002). Receptor selectivity probably arises from the rigid conformation of the N-terminal dicyclohexylcarbodimide motif as well as the groove between the N-loop and the β2β3 hairpin, which is significantly narrower in CCL20 than in other chemokines (Perez-Candillas et al, 2001).

Gene location

The gene coding CCL20 is located at 2q33-q37 unlike the locus for other chemokine genes at 17q11.2. The gene for CCR6 is located on chromosome 6q27, unlike all the other mapped β-chemokine receptor genes that are clustered on 3p21.3 (Samson et al, 1996), (Siveke et al, 1998).

Location/cellular expression and function

CCL20 is a potent chemokine whose major function is to stimulate CCR6 expressing chemoattractant cells (Dieu-Nosjean et al, 2000). Both CCL20 and CCR6 are highly expressed in the gastrointestinal epithelium, liver, lung and tonsillar crypts (at the site of antigen entry). This chemokine/receptor pair has a particularly important role at skin and mucosal surfaces both in health and inflammation (Schutyser et al, 2003).

At a cellular level, CCL20 is produced by activated monocytes, endothelial cells, dendritic cells, fibroblasts and T cells. CCR6 is expressed by immature dendritic cells and almost all memory T cells that express α4β7 characteristic of mucosal homing and most mature, naïve and memory B cells capable of responding to antigen challenge, NK cells, Langerhan's cells (LC) (Liao et al, 1999), (Nakayama et al, 2001), (Ebert et al, 2002), (Schutyser et al, 2003). Naïve T cells do not express CCR6; this is acquired during activation (Cook et al, 2000). Both CCR6 and CCL20 efficiently attract B cells particularly IgD-memory B cells (Krzysiek et al, 2000), (Liao et al, 2002). CCR6 expression is down regulated after B cell antigen receptor triggering and remains absent during differentiation into Ig-secreting plasma cells, whereas it is reacquired at the stage of post-germinal centre memory B cells. Therefore, within the B-cell compartment, the expression of CCR6 is restricted to functionally mature cells capable of responding to antigen challenge. This

is consistent with a role in antigen-driven B cell differentiation and B-lineage maturation (Krzysiek et al, 2000).

Within the gastrointestinal tract, this chemokine/receptor pair is particularly located in Peyer's patches, where CCL20 induces local migration of dendritic cell subsets expressing CCR6 (Dieu et al, 1998), (Tanaka et al, 1999), (Iwasaki et al, 2000). Gene expression studies have confirmed that CCR6 and CCL20 are expressed in separate but adjacent cell populations within Peyer's patches. The interaction between CCL20 and CCR6 is also critical factor in the ability of memory T cells to firmly adhere to ICAM-1 on endothelial cells; a prerequisite for extravasation (Ebert et al, 2002). This chemokine-ligand pair is therefore important for antigen presentation and for the development of a host adaptive immune response (Liao et al, 1999), (Homey et al, 2000).

The regulation and expression of CCL20 is part of the epidermal and epithelial immune armamentarium to external assault, with up regulation in response to barrier disruption such as occurs in inflammatory disorders (Cook et al, 2000). This chemokine/receptor pair is part of host defence to counteract potential antigenic invasion (Homey et al, 2000), (Schmuth et al, 2002). The constitutive and regulated expression of CCL20 by epithelium is consistent with a role for CCL20 in mucosal adaptive immune response within the gastrointestinal tract (Izadpanah et al, 2001). In mouse knockout studies the absence of CCR6 results in less severe intestinal pathology in animals with chemical induced colitis (Varona et al, 2003). In addition, low basal levels of CCL20 have been detected in dermal blood vessels and epidermis of non-inflamed skin (Charbonnier et al, 1999), which may enhance T cell recruitment to the skin and epidermis for immune surveillance under non-inflammatory conditions (Fitzhugh et al, 2000).

Amongst all chemokines tested, CCL20 appears to be the most potent chemokine inducing the migration of LC and their precursors, which represent a unique population of dendritic cells colonising the epithelium (Dieu-Nosjean et al, 2000). This suggests that CCL20 plays a key role in the control of LC recruitment to inflamed epithelial surfaces and in the regulation of epithelial immunity. In response to inflammatory stimuli, intestinal cells also develop the capacity to chemo attract dendritic cells and memory T cells in close proximity to the single layer of intestinal epithelium that separates the intestinal lumen from the host's internal milieu via CCR6 receptor expression (Izadpanah et al, 2001), (Kaser et al, 2004).

After binding of CCL20 to dendritic cells, the expression of CCR6 is down regulated and CCR7 is up regulated. The up regulation of CCR7 causes dendritic cell migration to the lymph nodes in response to a CCL19/CCL21 chemokine gradient, where these cells present antigen to $CD8^+$ T cells (Olson et al, 2002)[2], (Muller et al, 2003). Thus, CCL20 can bridge the innate and adaptive immune response. Mouse knockout studies have also demonstrated that CCR6 is required for the localisation of immature dendritic cells to the sub-epithelial zone, although is not required for development of any major leukocyte populations, including dendritic cells. Mice with targeted disruption of CCR6 demonstrate deficiencies in Peyer's patch organogenesis (Cook et al, 2000). These mice show impairment of mucosal responses to both oral antigen and enteric pathogens, and additionally demonstrated cutaneous hypersensitivity reactions, while maintaining normal

systemic responses. There are altered responses in contact and delayed-type hypersensitivity models of inflammation. $CCR6^{-/-}$ mice developed more severe inflammation than wild-type animals with 2,4-dinitrofluorbenzene-induced contact hypersensitivity. Conversely, delayed-type hypersensitivity is absent (Varona et al, 2001). These studies indicate a defect in the activation/or migration of the $CD4^{+}$T-cell subsets that down-regulate or elicit the inflammation responses, respectively. Mice knockout studies have also demonstrated that CCR6 is required for normal allergen-induced eosinophil accumulation and for production of IL-5 and IgE (Cook et al, 2000), (Lukacs et al, 2001), (Varona et al, 2001).

CCL20, like many other chemokine, has antimicrobial effects on a wide variety of pathogens. This is probably related to a topological formation of a large, positively charged electrostatic patch on the surface of the molecule (Yang et al, 2003).

The antimicrobial peptide β-defensin (hBD-2) is a small polypeptide that contributes to host defence, and whose overall amino acid sequence shows homology to CCL20. It is able to recruit dendritic and T cells by interacting with CCR6. There is an up-regulated expression of this by human epithelial cells *in vitro* and *in vivo* in response to pro-inflammatory cytokine stimulation or bacterial infection.

Induction

The induction of CCL20 by TNF-α and/or IL-1β varies according to the cell type. These pro-inflammatory cytokines are released following physical injury or infection. IL-1, TNF or enteric pathogens induce CCL20 expression within 30 minutes, via an NF-κB site upstream of the promoter region (Fujiie et al, 2001), (Izadpanah et al, 2001), (Sugita et al, 2002). *In situ* hybridisation work has demonstrated a strong mucosal epithelial induction by systemic treatment with LPS (Tanaka et al, 1999), (Tohyama et al, 2001). In contrast, synergy between IL-1β and TNF-α is required for CCL20 induction in kidney and skin epithelial cell lines (Dieu-Nosjean et al, 2000), (Nakayama et al, 2001).

Disease

As previously outlined, CCL20/CCR6 are of immunological significance in colitis. There is an up regulation of CCL20 in intestinal and skin inflammation, for example in inflamed crypt epithelium in appendicitis, and epidermal keratinocytes in atopic dermatitis and psoriasis (Nakayama et al, 2001). This implicates CCL20 in such inflammatory processes (Dieu et al, 1998), (Tanaka et al, 1999). Psoriasis is characterised by a marked inflammatory infiltrate and hyperproliferation of keratinocytes, with an up regulation of CCR6 and CCL20 within skin lesions. The infiltrate is composed of T-cells, predominantly of the memory phenotype, neutrophils, lining macrophages, and increased numbers of dendritic cells. Skin-homing CLA^{+} T cells are responsible for the development of the lesions through the activation of keratinocytes in association with a consistent pool of maturing LC concentrated around vessels, further implicating an active role of CCL20 in LC trafficking (Dieu-Nosjean et al, 2000).

Most tumour cell lines of epithelial origin, for example renal and colonic adenocarcinomas, express CCL20. In such malignancies, the alteration that occurs in dendritic cell

development/maturation prevents their T cell stimulatory function, which suggests that tumours of epithelial origin producing CCL20 can attract LC cell precursors and divert their function to escape immune surveillance and reach a state of tolerance (Dieu-Nosjean et al, 2000).

CCL20 produced by peripheral dendritic cells and/or macrophages after necro-inflammatory response leads to the recruitment of activated T cells to the liver. This may be pivotal to the local immune response amplification that occurs in various liver diseases.

There is an increased production of CCL20 in rheumatoid arthritis with the accumulation of CCR6-expressing mononuclear cells in addition to synovial fibroblasts. *In vitro* cultured fibroblasts have also been shown to produce CCL20 in response to IL-1β and TNF-α (Matsui et al, 2001).

1.8 Other chemokines and chemokine receptors

CXCR1, CXCR2, CXCL8

Both CXCR1 and CXCR2 share a high degree of homology (Horuk, 2001). CXCR1 and CXCR2 have several cognate ligands in common, including CXCL1, CXCL6 and CXCL8. In addition, CXCR2 binds CXCL2, CXCL3, CXCL5, CXCL9, CXCL10 and CXCL11 (Horuk et al, 2001), (Schraufstatter et al, 2001). The absence of CXCR2 in knockout mice protects them from septic injury, probably by diminishing inflammatory cell recruitment (Ness et al, 2003). One of the cognate ligands for CXCR1 and CXCR2, CXCL8 is a neutrophil and dendritic cell chemoattractant. Neutrophil chemotaxis is mediated primarily through CXCR1 (Schraufstatter et al, 2001). CXCL8 was the first chemokine to be discovered in 1987 (Ajuebor et al, 2002)[1], (Bajetto et al, 2002). CXCL8 also activates neutrophils to degranulate and cause tissue damage (Dinarello, 2000)[2]. The local expression level of CXCL8 correlates with inflammation in IBD, suggesting that this chemokine may have an important role in mediating the immune response in the gastrointestinal tract (Ajuebor et al, 2002)[1], (Banks et al, 2003). CXCL8 is also produced by neurons, various cancer cells, colonic epithelial cells and endothelial cells (Williams et al, 2000), (Schraufstatter et al, 2001).

There is increased expression of CXCR1 in inflamed compared to non-inflamed areas, with strong up regulation in the mucosal epithelium of morphologically damaged surface epithelium, including in UC (Williams et al, 2000). The increased expression of this receptor probably accounts for the initial inflammatory destructive changes seen in UC, with an epithelial neutrophilic infiltrate. The significance of CXCR2 in the intestinal tract has not been defined (Williams et al, 2000).

The chemokine CXCL1 plays a major role in inflammation, tumourigenesis and wound healing (Dhawan et al, 2002). It is constitutively expressed at high levels during inflammation and progression of melanocytes into malignant melanoma (Nirodi et al, 2001). The CXCL1 gene is controlled by a promoter containing four cis-acting immediately upstream to the NF-κB binding sequence. The nuclear DNA-binding protein poly (ADP-ribose) polymerase (PARP) is thought to be a co-activator of CXCL1 transcription (Nirodi et al, 2001). PARP catalyes the transfer of long, branched ADP-ribose chains to either itself or different classes of target proteins involved in

chromatin decondensation, DNA replication, DNA repair, and gene expression (Nirodi et al, 2001). This proposed role of PARP is supported by findings that 3-aminobanzamide, an inhibitor of PARP-specific ADP-ribosylation, inhibits CXCL1 promoter activity and reduces levels of CXCL1 mRNA in a dose-dependent manner (Nirodi et al, 2001). CXCL1 and CXCL2, like CXCL8 are chemotactic for neutrophils. These chemokines are only expressed by the epithelium following stimulation with pro-inflammatory cytokines or LPS (Ohtsuka et al, 2001).

CCR1

Knockout studies indicate that this is a vital chemokine receptor, crucial to host defense. Research has demonstrated that an altered Th1/Th2 cytokine balance occurs in these mice. CCR1 is also vital in trafficking and proliferation of leukocytes of myeloid progenitor cells, and neutrophil migration in response to CCL3. CCR1 is expressed by monocytes, dendritic cells, eosinophils, and lymphocytes but not in neutrophils unless induced by specific cytokines. (Horuk, 2001).

CCR2

CCR2 is a major regulator of macrophage trafficking, and plays a role in the pathogenesis of MS (Horuk, 2001).

CCR3

CCR3 is primarily expressed by eosinophils, in which it has an important role (Horuk, 2001).

CCR4

CCR4 is a selective marker for Th2 T lymphocytes and is up regulated by T cell receptor activation. It is thought to be involved in the pathogenesis of liver injury (Horuk, 2001).

CCR5

CCR5 is thought to play role in the control of granulocytic lineage proliferation or differentiation. It also functions as a co-receptor for HIV-1, for which it is a major entry point (Horuk, 2001). CCR5 variants have been postulated to influence the inflammatory response (Hull et al, 2003).

CCR7

This chemokine receptor is expressed by Th2 cells, and is thought to have a role in allergic inflammation (Horuk, 2001). It is involved in the organisation of secondary lymphoid tissue and is expressed during chronic inflammation. The two cognate ligands for CCR7 are CCL19 and CCL21. The expression of CCL21 during chronic hepatitis C is implicated in T-lymphocyte recruitment that occurs in this disease, and in the organisation of inflammatory lymphoid tissue. CCL21 is thought to promote fibrogenesis within inflamed areas via activation of CCR7 on hepatic stellate cells (Bonacchi et al, 2003). In the periphery, mature naïve B and T cells utilize CCR7, CXCR5 and CXCR5 to recirculate through specialised microenvironments within the secondary lymphoid tissues. Effector and memory lymphocytes express a variety of adhesion molecules and chemokine receptors that enable functionality within microenvironments and non-lymphoid tissues inaccessible to naïve cells (Campbell et al, 2003).

CCR8

CCR8 is highly expressed in the thymus and spleen, and is hardly detected in the peripheral blood lymphocytes. Its precise biological role is unknown, although its expression in Th2 cells suggests a possible role in allergic inflammation. It is also thought to be of significance in HIV infection (Horuk, 2001).

CCR9

The two cognate ligands for CCR9 are CCL25 (secreted only by small intestinal cells), and MAdCAM-1 (Horuk, 2001). CCR9 is likely to be important in the functionally specialised immune system in different areas of the gastrointestinal tract. It is highly expressed in all $CD4^+$ and $CD8^+$ T lymphocytes in the small intestine, although only a small subset of lymphocytes in the colon is $CCR9^+$ (Kunkel et al, 2002). Lymphocytes from other tissues, including tonsils, lung and skin do not express CCR9. Both immature and mature thymocytes express CCR9, suggesting a role in T cell development in the thymus (Rossi et al, 2000), (Horuk, 2001). Although CCR9 is highly expressed in the thymus, it is minimally expressed in lymph nodes and the spleen.

CCR10

The CCL27/CCR10 pair is thought to play a role in both skin homeostasis and may have a role in the inflammatory response. CCR10 is highly expressed in the small intestine and testis, and at lower levels in other tissues (Horuk, 2001).

CXCR3

CXCR3 is crucial in T cell activation and recruitment, and is implicated in allograph destruction (Horuk, 2001).

CXCR4

CXCR4 is ubiquitously expressed by a wide variety of cell types, including most haematopoietic cells. CXCR4 and the ligand CXCL12 play a central role in the migration of haematopoietic stem cells (Campbell et al, 2003). CXCR4 is also involved in the retention of neutrophils within the bone marrow and in the homing of senescent neutrophils back to the bone marrow. As neutrophils age, the expression of CXCR4 is upregulated (Martin et al, 2003). CXCR4 is also highly expressed on vascular endothelial cells, neurons, microglia and astrocytes. It is involved in the embryological development of neuronal networks in the central nervous system and in blood vessel development in the gastrointestinal tract (Horuk, 2001).

CXCR5

CXCR5 is chemotactic for human B lymphocytes. Deletion of the gene for CXCR5 yields mice with abnormal primary follicles and germinal centre of the spleen and Peyer's patches, reflecting the inability of B lymphocytes to migrate into B cell areas. CXCR5 is also a marker for memory T cells (Horuk, 2001).

1.9 Intestinal immunomodulatory cytokines

Cytokines are regulatory proteins crucial for inter-leukocyte communication, classified according to biological activity (Dinarello, 2000). They are primarily located in the lamina propria and are mainly released from activated T and B lymphocytes and macrophages to stimulate immune effector cells. The pro-inflammatory cytokines include IL1, TNF and IL-6, which are contingent to amplification of immunologic and inflammatory processes, particularly in IBD and rheumatoid arthritis (Elliot et al, 2001), (Panja et al, 1998). Their levels are increased in the serum, biopsy tissue culture, and in isolated lymphocytes from IBD patients with levels predictive for acute relapses (Panja et al, 1998), (Schreiber et al, 1999), (Woywodt et al, 1999). Furthermore, patients in clinical remission who are at high risk of relapse can be identified by an increased capacity of intestinal lamina propria cells to secrete TNF-α and IL-1β (Shreiber et al 1998)[2]. There are some inconsistencies in the TNF data, however as some research has indicated that although concentrations of IL-1β and IL-6 correlate with inflammation in biopsy cultures, levels of TNF do not (Reimund et al, 1996).

Contra-inflammatory cytokines such as IL-4, IL-10 and IL-13 suppress genes for pro-inflammatory cytokines and chemokines, thereby balancing the pro-inflammatory responses to limit inflammation (Schreiber, 1998), (Dinarello, 2000). This balance is altered in IBD.

IL-1

IL-1 plays a key role in inflammation, signaling via transcription factors such as NF-κB (Bocker et al, 2000). IL-1 is produced early in inflammation, and induces the production of many other cytokines, amplifying their pro-inflammatory action (Cominelli et al, 1990). Tissue levels of IL-1 have been found to correlate with the degree of tissue inflammation. IL-1β levels are increased in colonic circular muscles of patients with UC, which may contribute to motor dysfunction (Vrees et al, 2002).

There is an evidence that IL-1β gene polymorphisms participate in the determination of the severity and course of IBD although data are not consistently confirmatory (Hacker et al, 1997), (Nemetz et al, 1999), (Mwantembe et al, 2001).

There are two forms of IL-1: IL-1α and β. Both are potent cytokines whose biological activities are indistinguishable (Dinarello, 1997). IL-1α and IL-1β bind to the same IL-1 receptor on various cell types, even though they are distantly related at the primary sequence level (Benjamin et al, 1990). Differential expression varies at a cellular level, for example IL-1β is produced by epithelial cells.

The pro-inflammatory potential of IL-1 is tightly controlled by endogenous inhibitors such as IL-1 receptor antagonist (IL-1ra), and soluble IL-1 receptors to prevent an acute or chronic overproduction of pro-inflammatory cytokines, leading to fatal consequences, as seen in septic shock. IL-1ra has specific purely antagonistic properties against IL-1 receptors, acting as an anti-inflammatory cytokine without causing signal transduction (Cominelli et al, 1997). In IBD, plasma IL-1ra levels correlate with disease activity in addition to laboratory parameters such as C-reactive protein and leukocyte count (Kuboyama, 1998). Measurement of IL-1ra levels may

be used as an indicator of disease activity (Propst et al, 1995). Mice deficient in IL-1ra develop spontaneous rheumatoid arthritis and lethal arteritis, with reduction in disease severity with administration of IL-1ra. A mucosal imbalance between IL-1 and IL-1ra has been proposed as a potential key immunopathology in IBD (Andus et al, 1997), (Dionne et al, 1998), (Stokkers et al, 1998). Study of animal models of intestinal inflammation has indicated that tissue IL-1ra:IL-1 ratio closely correlate with inflammation (Cominelli et al, 1996). One study indicated a slight association of IL-1ra polymorphism with UC, although other studies have not confirmed this (Hacker et al, 1998), (Carter et al, 2001).

Platelets express surface receptors for IL-1 and IL-18, which are significantly increased in IBD. This is thought to relate to the platelet aggregation in IBD, possibly implicating the functional importance of platelets in inflammation (Schaufelberger et al, 1994).

TNF-α

Monocytes, macrophages and T cells produce TNF-α. It can effect the proliferation, differentiation and function of virtually every cell type (Baert et al, 1999). In addition, TNF-α stimulates IL-1 and IL-6 production, expression of adhesion molecules, pro-coagulant activity, endothelial activation and fibroblast proliferation (Baert et al, 1999). Biological effects include cachexia, shock, cytotoxicity and a stimulation of the acute phase response (Baert et al, 1999). It has multiple effector functions, including induction of neutrophil accumulation, granuloma formation, up regulation of adhesion molecules on endothelial cells, pro-coagulant effects and induction of increased intestinal permeability. TNF-α is considered to be centrally involved in the inflammatory process that occurs in IBD in particular CD, as it is a typical Th1 cytokine (Baert et al, 1999), (Shreiber et al, 1999). Serum and stool TNF-α levels correlate with inflammation in patients with active CD (Baert et al, 1999). Blockade of TNF-α has prevented granuloma formation *in vitro* (Baert et al, 1999). There are two TNF receptors, TNFR1 and TNFR2. TNFR1 mediates the majority of biological activities (Sugita et al, 2002).

IL-4

IL-4 is a T-cell derived anti-inflammatory cytokine that inhibits IL-1β and TNF-α production *in vitro* by human monocytes. It also induces IL-1ra. However, there is also evidence that a down-regulation may be beneficial in inflammation (Baert et al, 1999).

IL-10

This anti-inflammatory cytokine inhibits various cell types, including macrophages and dendritic cells (Boone et al, 2003). It down-regulates cytokine production, for example it has a direct inhibitory effect on T cell production of IL-2 and TNF-α (Macdonald et al, 1999). IL-10 also has a major role in the regulatory balance of cytokines controlling mucosal tolerance (Braat et al, 2003). The mechanism of IL-10 inflammatory inhibition is poorly understood. It binds to a recently described receptor IL-10 that is composed of and α and β subunits (Boone et al, 2003).

A relative IL-10 deficiency in patients with UC is thought to contribute to persistent inflammatory changes (Ishizuka et al, 2001). *In vitro* data from cultured epithelial and blood mononuclear cells from patients with active IBD have demonstrated that IL-10 causes an inhibition of IL-1β and

TNF-α, and augmentation of IL-1ra production. Conversely, neutralisation of endogenous IL-10 enhances both TNF-α and IL-1β production and inhibits IL-1ra production, so the administration of IL-10 may be useful therapeutically (Shirachi, 1998). Animal mouse models have demonstrated that topical enema application of IL-10 induces a down-regulation of pro-inflammatory cytokines systemically and locally (Schreiber et al, 1995). Results from clinical trials have so far have been disappointing, although this may relate to the lack of effective mucosal delivery (Braat et al, 2003).

IL-6

IL-6 is a multifunctional pro-inflammatory cytokine that regulates the immune response, haematopoiesis, the acute phase response, and inflammation (Hirano, 1998), (Ishihara et al, 2002)[1]. It has a crucial role in wound healing, probably by regulating leukocytic infiltration, angiogenesis and collagen accumulation (Lin et al, 2003). When its activity as a pro-inflammatory cytokine persists, the acute inflammation becomes chronic, with inflammatory cell infiltration leading to further IL-6 production. It is thought to play an important role in IBD via activation of NF-κB in the intestinal epithelium (Wang et al, 2003). Serum IL-6 concentrations are higher in patients with CD than in UC and healthy controls, with levels correlating with the inflammatory activity (Ishihara et al, 2002)[1]. High levels are associated with a high frequency of relapse, and over expression of IL-6 may be pathogenic in IBD (Jones et al, 1993), (Jones et al, 1994), (Van Kemseke et al, 2000), (Ishihara et al, 2002)[2].

Trans signalling is thought to contribute to chronic intestinal inflammation, whereby IL-6 binds to cells lacking its receptor by formation of a complex with the soluble IL-1 receptor, which can activate T cells. This is a further potential target for antibody development for therapeutic application (Atreya et al, 2000).

IL-2

IL-2 is vital in modulating the immune response. It is an essential T cell growth factor required for division of antigen-activated T cells. IL-1 induces IL-2 receptors. Patients with CD have increased expression of IL-2 receptors in the blood (Choy et al, 1990).

IL-12

IL-12 is involved in the regulation, differentiation and activation of helper T cells, and is pivotal in a Th1 response (Sandborn et al, 2002).

IL-17

IL-17 is a T cell-specific cytokine released by Th1 and Th2 subsets of $CD4^+$ cells, and is a potent mediator of inflammatory responses. Receptors for IL-17 are widely distributed on various cell types (Hata et al, 2002).

IL-18

IL-18 induces IFN-γ production and Th1 responses (Dinarello, 2000)[1]. It mainly exists in activated macrophages and epithelial cells, and shares biological activity with IL-12 (Sandborn et

al, 2002). The IL-18 precursor must be activated by IL-1 converting enzyme (ICE, caspase-1) to yield the active cytokine (Siegmund, 2002). IL-18 is up-regulated in intestinal mucosal cells of patients with IBD (Sandborn et al, 2002). It is neutralised by IL-18 binding protein, which is a naturally occurring secreted protein. This may be a suitable target for therapeutic manipulation (Dinarello, 2000)[2]. Neutralisation of IL-18 reduces arthritis, lung injury and IBD in animal models.

TGF-β

The transmembrane protein transforming growth factor β (TGF-β) plays a major role in the epithelial inflammatory response. This cytokine is present on the cell surface and/or as a secreted polypeptide in an inactive form. Following activation by binding to extracellular matrix proteins, it influences gene transcription and translation of formed mRNA. Locally it acts as a pro-inflammatory agent, but systemically it is a potent immunosuppressive. TGF-β also inhibits the uncontrolled proliferation of epithelial, endothelial, and haematopoietic cells. Furthermore it is a growth factor for most epithelial cells, and affects remodelling phases of wound healing by stimulation of extracellular matrix synthesis. It is therefore important in tissue regeneration, remodelling and fibrosis (Marek et al, 2002). It stimulates immature dendritic cells resulting in an increased expression of a number of chemokines and their receptors, including CCR6 plus increased chemotaxis to its ligand. Conversely, there is a down regulation of CCR6 expression by mature dendritic cells, and thus reduction in chemotactic response (Sato et al, 2000). Defects in TGF-β signalling pathways are linked to carcinogenesis, atherogenesis, fibrosis and autoimmunity. An imbalance of biologically active TGF-β is thought to be pathogenic in IBD. Its expression is highest at sites of antigenic stimulation i.e. within the villi not the crypts, thus deprivation of normal TGF-β may increase susceptibility to IBD (Marek et al, 2002).

1.10 Regulation of chemokine production

The NF-κB protein family is a group of inducible transcription factors that regulate key genes important in immunity, inflammation and cellular proliferation (Sugita et al, 2002). Although there are many different cytokines with varying effector responses, NF-κB is the one common transcriptional activator that exists in virtually all cell types, and is viewed as the central mediator of the immune response. It is necessary for an adequate immune response. Target genes include those encoding the IL-1 receptor, IL-2, IL-12 and TNF-α, transcription factors, adhesion molecules, inducible nitric oxide synthase and acute phase proteins (Ghosh et al, 1998), (Neurath et al, 1998), (Hong et al, 2001), (Dijkstra et al, 2002), (Gan et al, 2002), (Li et al, 2002)[1]. Examples of intestinal epithelial cell NF-κB chemokine gene targets include CCL20, CXCL1 and CXCL8 (Izadpanah et al, 2001). NF-κB also functions as a central regulator of stress responses, including physical and oxidative stress and exposure to certain chemicals. Furthermore, it blocks cell apoptosis in several cell types. *In vitro,* IL-10 and steroids down-regulate NF-κB thereby inhibiting its driven transcription control of pro-inflammatory cytokines (Schreiber, 1998)[2].

Binding of NF-κB to specific DNA sequences located in gene promoter regions is crucial for the functional regulation of transcription. Binding sites are located in promoter regions of most pro-inflammatory cytokines (Schreiber, 1998)[2].

NF-κB is central to the epithelial inflammatory response in the gastrointestinal tract following activation with pro-inflammatory cytokines, or to enteric pathogens. It is crucial for the initiation of mucosal innate immune responses via TLRs and CARD15 and subsequent acute mucosal inflammatory responses. CARD15 is activated by components of the bacterial wall and induce activation of NF-κB (Hugot et al, 2003). NF-κB levels are increased in intestinal biopsies of patients with active CD (Schreiber, 1998)[2].

There are five known members of the NF-κB/Rel family: p65 (RelA), c-Rel, RelB, p50 (NF-κB1) and p52 (NF-κB2). NF-κB subunits are able to homo-/heterodimerize through the Rel homology domain, forming transcription factor complexes with a wide range of DNA-binding and activation potentials (Ashburner et al, 2001). NF-κB dimers containing p65 have the most profound pro-inflammatory activity. For example, p65 over expression increases CCL20 mRNA both directly and via a reduction in TNF (Sugita et al, 2002). p50 is either inactive or involved in blocking NF-κB sites against p65 dimers (Schreiber, 1998)[2].

NF-κB exists in the cytoplasm of mononuclear phagocytes in an inactive form, bound to the inhibitor IκB. This inhibitor is one of the NF-κB regulators (Ashburner et al, 2001). Activation requires the activity of Iκκ, a kinase complex that contains two catalytic subunits, Iκκα and Iκκβ, and a regulatory subunit Iκκ-γ. Activating stimuli including inflammatory cytokines, bacterial LPS, viruses, oxidative stress, UV light and a variety of mitogens leads to phosphorylation of IκB by Iκκ, with rapid proteolytic dissociation of the complex (Schreiber, 1998)[2], (Ashburner, 2001), (Hong, 2001), (Dijkstra et al, 2002). NF-κB is finally activated by further phosphorylation of p65, RelB and c-Rel (Li et al 2002)[1]. The cleaved, phosphorylated NF-κB translocates to the nucleus where it up regulates transcription of specific genes. NF-κB activity does therefore not require *de novo* protein synthesis, so rapid signal transduction is possible (Ghosh et al, 1998). In some tumours, there is constitutive activation of the kinases that modulate IκB kinase (Iκκ), leading to constitutive activation NF-κB with dysregulation of transcription genes coding for cytokines, chemokines, adhesion factors and inhibitors of apoptosis (Richmond, 2002).

The interaction between the p65 subunit and histone deacetylase co repressor proteins 1 and 2 constitutes another means of NF-κB regulation (Ashburner et al, 2001). Acetylation of the histone tails induces transcription through chromatin remodelling, with decondensation of the chromatin in the region of the promoters. Such disruption of the core particle is a prerequisite for transcription. Histone deacetylation, stimulated by IL-1β, reduces transcription, and thus represses NF-κB-regulated genes (Asburner et al, 2001). The activity of histone deacetylase co-repressor proteins is reduced by trichostatin A (TSA), which subsequently increases histone acetylation and TNF-α induced CXCL8 expression (Fusunyan et al, 1999). Like TSA, butyrate modifies the chromatin structure through inhibition of histone deacetylation thereby reversibly altering gene and chemokine expression (Pender et al, 2000).

A further regulator of transcription is poly (ADP-ribose) polymerase (PARP), a nuclear DNA binding protein, which may be involved in promoter specific transcription of chemokines. PARP causes an enhancement of NF-κB-mediated transcription (Virag et al, 2002). It functions as a DNA nick-sensor enzyme. Following binding to DNA breaks, activated PARP cleaves NAD^+ into ADP-ribose and nicotinamide. It polymerises ADP-ribose, catalysing the transfer of long branched ADP-ribose chains to itself or different classes of target proteins involved in chromatin decondensation, DNA replication, DNA repair and gene expression, including histones, transcription factors and PARP itself. Poly(ADP-ribosylation) contributes to DNA repair and to the maintenance of genomic stability. However, oxidative stress causes over activation of this polymerase, with consumption of NAD^+ and consequently ATP, leading to cell dysfunction or necrosis. PARP is activated during early stages of apoptosis in many cell types (Shiokawa et al, 1997). This cellular suicide mechanism has been implicated in many disease processes, and may well be important in the pathogenesis of IBD (Shiokawa et al, 1997), (Nirodi et al, 2001), (Virag et al, 2002). 3-aminobenzamide acts as an inhibitor of PARP-specific ADP-ribosylation, and inhibits CXCL1 promoter activity and reduces levels of CXCL1 mRNA (Shiokawa et al, 1997), (Nirodi et al, 2001).

1.11 Molecular targeting in IBD

Progress in the development of new therapeutic agents has been relatively slow over the last decade. The only biologic compounds of proven efficacy in CD are monoclonal antibodies to TNF (infliximab and CDP571), and to the leukocyte adhesion molecule α4 integrin (natalizumab) (Sandborn et al, 2002)[1]. However, many novel targets have been identified for potential therapeutic manipulation in IBD, and consequently several significant trials should emerge in the coming years.

Pro-inflammatory cytokines

Theoretically, blockade of the pro-inflammatory cytokines IL-1, IL-6, IL-8, TNF-α, IL-12 may be of therapeutic benefit. Reducing the biological activities of IL-1 and TNF has been attempted by several different, but highly specific strategies, which involve neutralising antibodies, soluble receptors, receptor antagonism, and inhibition of proteases that convert inactive precursors to active, mature molecules. The anti-TNF agent infliximab is a humanised chimeric monoclonal antibody of the IgG1 subclass (Zboril, 2002). This was shown to be effective in at least two thirds of patients with steroid-dependent chronic active CD, reducing the clinical signs, symptoms and histological disease activity (Baert et al, 1999). Additional benefit of this drug may be derived from the associated reduction in other pro-inflammatory mediators such as IL-6. Within 6 hours of infliximab therapy, IL-6 levels are normalised, with reduced levels of cytokine inhibitors such as soluble p75, p55 and IL-1ra (Charles et al, 1999). The use of infliximab as a therapeutic agent has been limited by toxicity for example acute and delayed sensitivity reactions following formation of human anti-chimeric antibodies (D'Haens et al, 2001), (Bauditz et al, 2002). The fully humanised CDP571 genetically engineered IgG4 monoclonal TNF-α antibody is less immunogenic. This was constructed by grafting the complementarity-determining region of a mouse anti-human TNF-α monoclonal antibody into a human IgG4

antibody framework. It is thought to be effective by neutralising soluble and transmembrane TNF. It is not effective in unselected patients with active CD and has been withdrawn from development, although it may be effective in patients with elevated C-reactive protein (Sandborn et al, 2003). A further biologic anti-TNF product CDP870 is to be assessed in phase III trials following good results with phase II trials with a good drug safety-profile (Choy et al, 2002), (Rose-John et al, 2003), (Sandborn et al, 2003).

The two cell surface TNF receptors, p55 and p75 constitute a further area of potential therapeutic manipulation. Soluble, truncated versions of these are present in body fluids, consisting only of the extracellular, ligand binding domain. They are thought to be involved in the regulation of TNF-activity (Sandborn et al, 2002). Onercept is a genetically engineered recombinant human TNF-receptor p55 monomer (Sandborn et al, 2002). Initial assessment of this drug indicates it has satisfactory safety and pharmacokinetic characteristics, and may be a suitable TNF-α antagonist for clinical anti-inflammation, although further studies are required to assess effectiveness (Trinchard-Lugan et al, 2001), (Sandborn et al, 2003). Etanercept is a genetically engineered fusion protein consisting of two identical chains of recombinant human p75 monomer fused with the Fc domain of human IgG1 (Sandborn et al, 2002), which is designed to neutralise soluble TNF receptors. Although this is safe, a placebo-controlled study failed to demonstrate any benefit (Sandborn et al, 2003).

Thalidomide is a small molecule that degrades TNF and IL-12 mRNA, thereby inhibiting their synthesis (Sandborn et al, 2002). Initial data has indicated that this is an effective short-term treatment for symptomatic IBD (Bariol et al, 2002). Multi-centre placebo controlled phase II trials are ongoing (Cellgene). Another TNF-blocking small molecule under evaluation is CNI-1493 (Sandborn et al, 2002).

IL-2 receptor antagonists have been used in double blind, placebo-controlled trials. Pilot studies of the IL-2 receptor antibody dacclizumab in refractory UC have demonstrated a benefit, although further evaluation is necessary (Van Assche et al, 2000). The chimeric antibody to IL-2, basiliximab appears to be effective at inducing remission in steroid-resistant UC (Creed et al, 2003).

The therapeutic potential of IL-1ra administration in IBD has been considered. After the cloning of IL-1 in 1990 and subsequent production of recombinant protein, much interest was generated in the use of recombinant IL-1ra as an anti-inflammatory drug. It was shown to reduce inflammation in animal models (Cominelli et al, 1990), and reduce mortality of patients with septic shock in phase II trials. However this benefit was not confirmed by a phase III trial. Therapeutic IL-1 receptor blockade in IBD has not been discounted, and modulation of the IL-1-ra/IL-1 balance may be of therapeutic benefit (Cominelli et al, 1997). The benefit of prednisolone may result from an alteration of this ratio, with a decrease in IL-1 receptor antagonist release (Shigematsu, 1998). One group demonstrated that IL-1 receptor antagonism inhibits IL-1β-augmented IL-1α and TNF-α release by mononuclear cells from patients with IBD (Shigematsu, 1998).

Antibodies to IL-1β, termed CDP-484 are being assessed in pre-clinical trials by Celltech, for potential therapeutic benefit in rheumatoid arthritis. This high affinity PEGylated antibody fragment may well be of clinical benefit in IBD.

The ICE protease cleaves the precursors of IL-1β and IL-18 into active cytokines (Siegmund et al, 2001), (Siegmund, 2002). Several ICE inhibitors are available for experimental use *in vivo* and *in vitro*. Phase I trials of the orally active ICE inhibitor Pralnacasan have demonstrated successful IL-1β inhibition and a good safety profile. Phase II trials are ongoing in rheumatoid arthritis (Siegmund, 2002).

Animal model studies have demonstrated that administration of IL-12 can prevent or reduce intestinal inflammation (Neurath et al, 1995). A phase II dose-finding trial with high affinity antibodies to this cytokine is underway (Sandborn et al, 2002).

Phase II studies are also underway to assess the use of anti-IFN-γ therapy in patients with CD. Animal models have indicated that this to be less effective than anti-IL-12 antibodies (Sandborn et al, 2002). Lidocaine and related local anaesthetics are effective in UC, probably from direct effects on epithelial cells to inhibit the secretion of pro-inflammatory cytokines (Lahav et al, 2002), although clinical trials are needed.

Antibodies to IL-18 have been reproduced, although their benefit in IBD has not yet been assessed (Sandborn et al, 2002).

Anti-inflammatory cytokines

Augmentation of the anti-cytokine IL-10 offers an alternative approach to therapy, with suppression of pro-inflammatory cytokine expression by macrophages, dendritic cells and neutrophils. In addition, it also suppresses enzymes of the cyclooxygenase pathway (Mahler et al, 2002). Several large multicentre trials treating patients with mild/moderate or therapy-refractory CD indicate that although it is was found to be safe and well tolerated, the clinical improvement was not significant (Herfarth et al, 2002). The failure of these trials may have resulted from incorrect dosing, mode of administration, or from usage in the wrong patient cohort or alternatively from the already augmented IL-10 levels in IBD. Further studies are ongoing. Genetic engineering of T cells has been considered as a means to deliver IL-10 as an immunotherapeutic agent (Madsen, 2002). The use of genetically engineered *Lactococcus* bacteria that delivers IL-10 to the colon is currently being assessed (Steidler et al, 2000).

IL-11 is an anti-inflammatory mesenchymally-derived chemokine that has been administered in recombinant form as a weekly subcutaneous dose in mild-moderately active CD. It is safe and clinically effective, although only in an undefined subset. Further trials are required (Sanborn et al, 2002).

Pro-inflammatory signalling

Control of pro-inflammatory signalling molecules, such as NF-κB is a further strategic area of potential targeting in the treatment of IBD (Schreiber, 1998)[2]. Steroid-induced healing of colonic

inflammation is associated with the disappearance of NF-κB from nuclear extracts which is supportive of this strategy (Ardite et al, 1998). Sulphasalazine and mesalamine are non-selective inhibitors of NF-κB (Sandborn et al, 2002). There are no human studies of selective NF-κB inhibitors with IBD (Sandborn et al, 2002). Animal models have demonstrated that p65 anti-sense oligonucleotide blocks NF-κB, but has unproven benefit in IBD. However, *in vitro* studies have demonstrated a reduction in IL-1, IL-6 and TNF production from macrophages extracted from patients with active CD following NF-κB blockade (Neurath et al, 1998). As the level of reactive oxygen species is thought to regulate NF-κB, antioxidants may inhibit phosphorylation of IκB upon TNF stimulation (Li et al, 2002). The therapeutic efficacy of 5-aminosalycilic acid in IBD may be related to its anti-oxidant properties (Simmonds et al, 1999).

Adhesion molecules

Alteration of adhesion molecules such as ICAM-1 is likely to affect lymphocyte trafficking, so they are potential targets for therapeutic benefit. Natalizumab is a recombinant IgG4 humanised monoclonal antibody to the α4 integrin. Phase II trials have indicated that this is well tolerated, and moderately effective in active CD (Gordon et al, 2001), and phase III trials are currently underway. Furthermore, large placebo-controlled, dose finding, trials are ongoing with LDP-02, a recombinant IgG1 humanised monoclonal antibody against α4β7.

Preliminary results have shown that the anti-ICAM antisense oligonucleotide ISIS 2302 (anti-ICAM) is effective in CD refractory to steroids (Heresbach et al, 1999). This is a 20 base phosphorothionate oligodeoxy-nucleotide designed to hybridise to a sequence in the 3' untranslated region of the human ICAM-1 message. The heterodimer formed is enzymatically cleaved, reducing the ICAM-1 expression (Sandborn et al, 2002).

Metalloproteinase enzymes

The development of specific MMP inhibitors could impact the natural history of IBD. In UC and CD, the imbalance between MMPs and TIMP favours degradation and may be significant in the pathogenesis of IBD. Enhanced production of MMP3 correlates well with IL-1β, IL-6, TNF-α and IL-10 (Louis et al, 2000). MMP enzymes are activated by T cells, and are inhibited by IL-10 (Pender et al, 1997). IL-10 therapy could theoretically be of benefit via its effect on MMP enzymes. One inhibitor of MMP is Marimastat, which reduces the gastrointestinal inflammation in animal models though has not been subject to clinical trials (Sykes et al, 1999).

Eicoasanoids

The pathogenic importance of eicoasanoids in IBD is unclear. Mucosal production of prostaglandins, thromboxanes and prostacyclins are elevated in IBD, but research has not clarified their pathogenic role (Rampton et al, 1980), (Ligumsky, et al, 1981), (Gertner et al, 1994).

Animal studies have indicated that suppression of cyclooxygenase-2 can result in exacerbation of inflammation-associated colonic injury (Reuter et al, 1996). However, the use of COX-2 inhibitors has not been adequately assessed in IBD; whether they will prove beneficial is not yet

known (McCartney et al, 1999). Ridogrel, an inhibitor of thomboxane-mediated platelet aggregation has been shown to be of no therapeutic benefit in IBD (Carty et al, 2001).

Others

A phase II trial of a monoclonal antibody to CD40L is underway in patients with CD. This co-stimulatory molecule is induced by antigen recognition of T cells (Sandborn et al, 2002). Studies assessing the benefit of antibodies to the CD4 markers of helper T cells are also ongoing (Sandborn et al, 2002).

Other biologic compounds for which there is insufficient evidence to judge efficacy for IBD include: IF-α, IF-β1a, granulocyte colony stimulating factor, (G-CSF), granulocyte macrophage colony stimulating factor (GM-CSF), epidermal growth factor, keratinocyte growth factor 2 (repifermin), human growth hormone and TGFβ (Sandborn et al, 2002). Following the identification of T-bet in the regulation of T cell-mediated colitis, specific targeting of this pathway may lead to clinical improvement in IBD, and other Th1 T lymphocyte-associated diseases (Neurath et al, 2002).

Heparin is possibly effective in UC (Evans et al, 1997), although this may relate to an as yet undefined immunomodulation rather than anticoagulation effect as warfarin has no clinical impact in IBD (Gaffney et al, 1995).

Chemokines

As chemokines are involved in pathological processes in addition to physiological, their receptors are potential targets for therapeutic intervention. This is likely to alter cellular infiltration and modulate the inflammatory response, which has been accomplished for many years using such drugs as corticosteroids and cyclosporin A (Ina et al, 2002), (Yang et al, 2002). However as these drugs are associated with numerous side effects, more specific less toxic agents are required. The blockade of a single chemokine receptor may theoretically provide the specific targeted therapy required.

There are six broad methods of reducing chemokine receptor stimulation. The first employs the use of monoclonal antibodies against chemokines or their receptors. Such antibodies have already been developed against certain chemokine receptors, and some also have additional receptor antagonistic properties (Heath et al, 1997), (Wu et al, 1997), (Grimaldi et al, 1999), (Onuffer et al, 2002). Neutralising antibodies to CCL3 have been demonstrated to inhibit type 1-hypersensitivity reactions *in vivo* (Ono et al, 2003). CAT231 is a genetically engineered antibody by Cambridge antibody Technology Plc with specificity for CCL11 (Ono et al, 2003).

The second method involves the use of specific receptor antagonists; a strategy used by herpes and pox viruses. The *Molluscum contagiosum* virus expresses an antagonist for several CC and CXC chemokines (Sallusto et al, 2000). Modification of the N-terminus of chemokines generates ligands that are effective antagonists, for example, N-terminal modifications of CCL5 results in powerful inhibitors of CCR5 and other chemokine receptors (Gong et al, 1996), (Simmons et al, 1997), (Mack et al, 1998). Antagonists against multiple rather than single chemokine receptors

may be more effective than inhibitors of specific chemokines for controlling cell migration and inflammation. For example, in one early study the NH2-terminal residues were found to partly determine the receptor specificity of CCL5, and deletions within his region permitted binding to multiple CC chemokine receptors (Gong et al, 1996).

The third method of receptor intervention involves the use of small organic molecules. These have been used to disrupt the ligand-binding to G protein-coupled receptors (Murakami et al, 1997), (Schols et al, 1997), (Onuffer et al, 2002). Chemokines bind their receptors with nanomolar affinity, and successful design of a small molecule antagonist should bind the receptor with an equivalent specificity and affinity (Rajarathnam et al, 2002). Such molecular receptor antagonists have been identified that are selective for CXCR2, CXCR4, CCR1 and CCR5. T22 synthesised peptide blocks CXCR4, inhibiting T cell-tropic HIV-1 entry into target cells (Murakami et al, 1997). There is evidence that inhibition of CCR6 may be effective in the treatment of contact dermatitis, liver disease and allergic pulmonary lung disease (Lukacs et al, 2001), (Shimizu et al, 2001).

The fourth method of receptor intervention involves internalisation of receptor and inhibition of receptor cycling, for example CCR5, the principal co-receptor for M-tropic HIV-1 strains (Mack et al, 1998).

The fifth method incorporates a primary reduction of chemokine expression, for example by use of leflunomide and methotrexate (Ho et al, 2003).

The final method involves the use of gene therapy, which has yet to be explored in IBD. As CXCR2 agonists are beneficial in tissue repair, particularly in hepatic diseases, gene therapy using adenoviral vectors to deliver CXCL2 cDNA to sites of inflammation is now being studied. Early results indicate a reduction in hepatic injury (Bone–Larsen et al, 2000), (Ajuebor et al, 2002)[2].

CXCL8 was one of the first chemokines to be considered as a potential target for therapeutic benefit because of its powerful effects on neutrophilic infiltration. However, the development of an effective agent was hampered by the lack of specificity of its cognate receptors, CXCR1 and CXCR2. These receptors differ in their selectivity for other chemokines as well as in their regulation and signal transduction (Murphy, 1997). A phase II clinical trial of humanised CXCL8 antibody ABX-IL-8 for use in treatment of rheumatoid arthritis is ongoing (Abgenix Inc, California, USA), (Ajuebor et al, 2002)[1].

Chemokines are being studied for their potential usage in promoting the regression or even eradication of tumour mass, by inducing the migration of T cells, NK cells, dendritic cells and/or macrophages. They can act as autocrine and paracrine growth factors, and can induce angiogenesis or angiostasis, regulate metastasis and have a role in the host's immune response against tumour cells. Although many chemokines have anti-tumour activity, including CCL1, CCL2, CCL5, CCL7, CCL16, CXCL9 and CXCL10, chemokines used in isolation seem to have limited anti-tumour efficacy (Rossi et al, 2000). The main current area of research is the usage

of chemokines as chemoattractants (e.g. CCL19, CCL21, CXCL9, CXCL10, CXCL12 and XCL1) combined with cytokines (IL-2, IL-12, and GM-CSF, which stimulate T cell, NK cells or tumour antigen-pulsed dendritic cells (Homey et al, 2002). This approach could be used to reverse inflammatory disorders, with the block of T and NK cellular infiltration combined with blockage of IL-1 or TNF, and may enable lower doses and hence toxic effects of such agents (Homey et al, 2002). They may therefore provide adjuvent benefit.

The different approaches in chemokine receptor manipulation are well illustrated in the treatment of HIV. Chemokine manipulation remains an area to be explored in IBD. However, limited study has been carried out in other diseases. CXCR4 and CCR5 are co-receptors with CD4 and human immunodeficiency virus-type 1 (HIV-1) infection (Simmons et al, 1997). Bicyclams are novel low molecular weight anti-HIV agents shown to be effective as potent and selective CXCR4 antagonists. They are highly potent and selective inhibitors of HIV-1 and HIV-2 replication (Scols et al, 1997). CXCR4 antagonist bicyclam derivatives were assessed in clinical trials and, although effective, were withdrawn from phase II trials in view of cardiac side effects (Scozzafava et al, 2002). Receptor internalisation and inhibition of receptor recycling has been identified as another potential area for therapeutic intervention against HIV infection (Mack et al, 1998). Finally, manipulation of CXCR4 improves stem cell mobilisation and could be useful in future stem cell therapeutic applications (Lapidot et al, 2002).

CCR5 is thought to be an ideal target site for the development of inhibitors to the HIV infection. This receptor is expressed by T cells and macrophages, and functions as the main co-receptor for macrophage (M) - tropic strains of HIV-1. Detailed analysis has revealed that there is a complicated pattern of a HIV-1 envelope glycoprotein gp120 to different regions of CCR5, but a relatively simple pattern for chemokine binding (Wu et al, 1997). Potent CCR5 antagonists from several classes of polycyclic derivatives have been identified. The oxime-piperisine derivative SCH-351125 has progressed to clinical evaluation (Scozzafava et al, 2002).

Blockade of CXCR3 and CCR5 may also be effective in the treatment of chronic autoimmune/inflammatory processes such as rheumatoid arthritis, autoimmune diabetes, chronic transplant rejection and MS (Balashov et al, 1999). Analysis of the expression of these receptors may also be of clinical use in the immunologic staging of multiple sclerosis (Balashov et al, 1999).

1.12 Outline of MD thesis

As chemokines and their receptors are important constituents of gastrointestinal epithelial immunity, study of these important immunological mediators may help to identify targets for the development and use of new therapeutic agents. IBD is an intestinal epithelial disease in an accessible organ that is therefore conducive to treatment.

This MD sets to answer the following questions:

1 Which chemokines and their receptors are likely to be central to the disease processes in IBD?
2 Expression patterns of individual chemokines have been previously investigated, but is there a particular coordinate response to inflammatory stimuli in IBD?
3 What is the effect of pro-inflammatory cytokines on the chemokines identified?
4 What is the potential for therapeutic intervention at a chemokine/chemokine receptor/pro-inflammatory cytokine level in IBD?

In this research, the expression of the entire chemokine family within colonic mucosa from IBD patients was compared to the expression in non-inflamed and inflamed controls. A microarray, representing every member of this superfamily and their cognate receptors, was constructed and hybridised with probes derived from colonoscopic biopsies. While expression levels of individual chemokines and their receptors have been measured in colon tissue previously, no one has attempted to analyse transcription levels of the entire chemokine superfamily in parallel. Advances in gene expression profiling technology enabled construction of a custom chemokine microarray containing all chemokines and receptors. Results were confirmed and extended by real-time quantitative polymerase chain reaction (PCR), immunohistochemistry and flow cytometric analysis of colonic tissue.

Fujiie et al (2001) previously demonstrated that human colon carcinoma cell lines express CCL20, which is up-regulated by either TNF-α or IL-1β depending on lineage. In order to further characterise chemokine expression by epithelial cells, the array was used to profile gene expression from cultured Caco-2 and HT29 cell lines. These colonic cancer epithelial cell lines were chosen for studying expression of chemokines and cytokines, due to the spontaneous differentiation exhibited. In the pre-confluent state these cells are relatively undifferentiated. After a several days post-confluency, these cells develop markers of a differentiated phenotype for absorptive enterocytes including the expression of digestive enzymes, tight junctions, a well-developed brush-border, and a polarised morphology. In the cellular differentiation there are therefore important morphological and functional changes. In this research, the cultured cells were harvested 48 hours post-confluence, when they express a predominantly colonic phenotype (Engle et al, 1998), and cultured with and without combinations of IL-1β, TNF-α and LPS. In order to investigate potential regulatory pathways previously implicated in epithelial CXC chemokine production IL-1β and TNF-α dual stimulations were also performed in the presence of TSA and benzamide in Caco-2 cells to determine any involvement of histone deacetylation and PARP1, respectively (Ashburner et al, 2001), (Nirodi et al, 2001). The

expression of multiple pro-inflammatory cytokines, including CXCL8, is inhibited by spontaneous differentiation of the Caco-2 colon cancer cell line by growth to a post-confluent state.

Enzyme-linked immunosorbent assays (ELISA) were performed on the supernatants of Caco-2 cells to confirm that protein expression is consistent with mRNA expression observed.

Although analysis data from cultured colonic carcinoma cell lines is of value, primary colonic epithelial cell culture provides a more reliable model, with closer approximation to *in vivo* conditions. The epithelium was stripped from surgically removed, normal colonic sections, incubated in varying combinations of IL-1β, TNF-α and LPS, and profiled with the chemokine microarray.

To determine whether non-mucosal epithelial cells expressed the same subset of chemokines as colonic cells in response to pro-inflammatory cytokine stimulation, primary keratinocytes were grown to confluence and stimulated with and without combinations of IL-1β, TNF-α and LPS, and profiled with the chemokine microarray.

The knowledge gained from this research was subsequently utilised to investigate NEC, using immunohistochemical staining. This condition has phenotypic and mechanistic similarities to IBD, making comparative chemokine expression studies highly relevant.

1.13 Microarray technology

Microarray technology represents a major advance in functional genomics, allowing systematic identification of large numbers of genes in parallel (Li et al, 2002)[2]. When applied to clinical samples, this technology allows detailed comparisons and assessments not previously possible. In general, two microarray technologies have been emerged. The first includes deposition of oligonucleotides onto a glass surface. Commercially available oligonucleotide arrays are termed "GeneChip®" (registered trademark by Affymetrix). These arrays are synthesised using photolithographic techniques, and represent up to 40 000 genes. However, the high cost, limited length of oligonucleotide chains (20-80 bases long), and the necessity to know the gene sequences limits its application and accuracy. The second technology incorporates cDNA fragments printed on a glass slide or nylon membrane. cDNA probes are made from RNA transcripts through reverse transcription. During the process, a label is incorporated into the probe which is hybridised to the microarray. In addition to the lower costs, this method provides greater flexibility and enables more highly focused study. Fewer genes are included in this type of array (500-5000 bases long). To overcome the problem of cross hybridisation due to sequence homology, the 3'-untranslated end of the target genes are printed onto the array to reduce the probability of hybridisation being affected by pre-termination of reverse transcriptase. Some short domain sequences present at high frequency in the total cDNA population are included in the hybridisation solution to block potential cross-hybridisation of repetitive sequences (Warner et al, 2002), (Li et al, 2002)[2].

Fluorescence or the use of radio-labelling is used to achieve the detection of hybridised genes in each spot. A digital image of the array is then obtained, which is analysed for the location of

individual spots on the slide, spot boundary and signal intensity compared to background, using pixilation. A quantitative threshold is incorporated to enhance accuracy. Data normalisation allows for differences in quality and quantity of initial RNA. Relative quantification is achieved by determinance of ratio to stably expressed reference 'housekeeping genes'. This is a group of genes coding for proteins whose activities are essential for maintenance of cell function, and whose expression is believed to be uniform (Li et al, 2002)[2]. Mathematical hierarchical clustering groups data points whose branch lengths represent similarities, thus clustering the genes (Orr et al, 2002). The measured data are colour-coded.

Chapter 2

Materials and Methods

2.1 Materials and buffers

2.1.1 Materials

2.1.2 Buffers

2.2 Methods

2.2.1 Patient inclusion, sample collection and preservation

2.2.2 Total cellular RNA preparation, cDNA probe synthesis, microarray hybridisation and analysis

2.2.2.1 Microarray construction

2.2.2.2 Preparation of total cellular RNA from colonic biopsies and RNA assay cultured cell lines

2.2.2.3 RNA quantification

2.2.2.4 cDNA probe synthesis

2.2.2.5 Microarray hybridisation and analysis

2.2.2.6 Real-time quantitative RT-PCR

2.2.3 Histopathological assessment of colonic tissue

2.2.4 Immunohistochemical localisation and quantification of chemokines using immunoperoxidase technique

2.2.4.1 The technique of immunohistochemistry

2.2.4.2 Preparation of sections and pre-treatment methods

2.2.4.3 Primary antibody application

2.2.4.4 Secondary antibody application

2.2.4.5 Application of DAB

2.2.5 Analysis of cell lines

2.2.5.1 Cell propagation

2.2.5.2 Cell count and viability assessment

2.2.5.3 Cell stimulation

2.2.6 Quantitative determination of chemokine protein concentrations in cell culture supernatants

2.2.6.1 The technique of ELISA

2.2.6.2 ELISA procedure

2.2.6.3 Optical densometry

2.2.7 Flow cytometric analysis of colonic biopsies

2.2.8 Stimulation of colonic epithelium in colonic biopsies

2.2.9 Primary colonic epithelial culture and stimulation

2.2.9.1 Epithelial cell separation

2.2.9.2 Epithelial cell propagation

2.2.9.3 Cell count and viability assessment

2.2.9.4 Cell pellet formation

2.2.9.5 RNA extraction

2.2.9.6 Microarray hybridisation and analysis

2.1 Materials and Buffers

2.1.1 Materials

18s and 28s ribosomal RNA standards	Sigma Aldrich Company Ltd, Dorset, UK
L-Glutamine	Sigma Aldrich Company Ltd, Dorset, UK
Sodium hydroxide	Merck, Poole, Dorset, UK
ABC kit for immunohistochemistry	Vector laboratories, Peterborough, UK
Absolute alcohol	Chemix, Wiggan, Lancashire, UK
Acid ethanol	Chemix, Wiggan, Lancashire, UK
Benzamide	Sigma Aldrich Company Ltd, Dorset, UK
Bio-Spin 6 Chromatography Columns	BIO-RAD, Hercules, CA, USA
Biotinylated rabbit anti-goat antibody	Vector laboratories, Peterborough, UK
Bovine foetal calf serum	Sigma Aldrich Company Ltd, Dorset, UK
Caco-2 cells	European Collection of Animal Cell Cultures, Porton Down, UK
Calcium chloride	Merck, Poole, Dorset, UK
Cell dissolution solution/EDTA	Sigma Aldrich Company Ltd, Dorset, UK
Chymotrypsin	Sigma Aldrich Company Ltd, Dorset, UK
α^{33}P-dCTP	NEN, Boston, MA, USA
DAB - 3,3'-diaminobenzidine substrate Kit for peroxidase,	Vector laboratories, Peterborough, UK
Deoxynucleotides (dATP, dGTP and dTTP)	Amersham, UK
DMEM (Dulbecco's modified eagle's medium)	Sigma Aldrich Company Ltd, Dorset, UK
DPX (distyrene, plasticizer, and xylene)	Merck, Poole, Dorset, UK
E.coli lipopolysaccharide	Sigma Aldrich Company Ltd, Dorset, UK
Epilife™medium	Cascade Biologics Inc, Portland, OR
ExpressHyb hybridisation solution	Clontech, Palo Alto, CA, USA
Foetal Calf Serum	Sigma Aldrich Company Ltd, Dorset, UK
L-Glutamine	Sigma Aldrich Company Ltd, Dorset, UK
Hanks buffered salt solution	Sigma Aldrich Company Ltd, Dorset, UK
HT29 cells	European Collection of Animal Cell Cultures, Porton Down, UK
Human Cot-1 DNA	Invitrogen, Paisley, UK
Human keratinocyte growth supplement	HKGS, Cascade Biologics Inc, Portland, OR, USA
Hydrogen peroxide	Sigma Aldrich Company Ltd, Dorset, UK
IL-1β	PeproTech, Rocky Hill, NJ, USA
Marvel milk powder	Tescos, London, UK
McCoy's 5A cell culture medium	Sigma Aldrich Company Ltd, Dorset, UK
Methanol	Merck, Poole, Dorset, UK
Monoclonal anti-human CCR-6 antibody	R and D Systems, Oxon, UK
Monoclonal anti-human CXCR-1 antibody	R and D Systems, Oxon, UK
Monoclonal anti-human CXCR-2 antibody	R and D Systems, Oxon, UK

Monoclonal anti-human CCL20 alpha antibody	R and D systems, Oxon, UK
Normal human primary epidermal keratinocytes	Cascade Biologics Inc , Portland, OR, USA
NCTC medium	Sigma Aldrich Company Ltd, Dorset, UK
Penicillin streptomycin antibiotics	Sigma Aldrich Company Ltd, Dorset, UK
Poly (dA)	Invitrogen, Paisley, UK
Poly (dT)	Invitrogen, Paisley, UK
RNA 6000 Nano Assay kit, used with Agilent 2100 bioanalyser	Agilent Technology, California, USA
RNeasy kit	Qiagen, Crawley, UK
RNA later	Ambion, Austin, Texas, USA
RNeasy Mini Kit (Containing buffers RLT,RW1 and RPE)	Qiagen, Crawley, UK
RPMI medium	Sigma, Poole, Uk
Salmon Testes DNA	Sigma, Poole, UK
Sodium dodecyl sulphate (SDS)	BIO-RAD, Hercules, CA, USA
Sodium bicarbonate	Sigma, Poole, Uk
0.1mmol sodium hydroxide pH 8	Merck, Poole, Dorset, UK
Sodium tetraborax	Merck, Poole, Dorset, UK
SUPER RNaseIn	Ambion, Austin, Texas, USA SuperScript II Invitrogen, Paisley, UK
Superscript II RNase H^- Reverse Transcriptase	Invitrogen, Paisley, UK
Taqman Gold RT-PCR Kit	Applied Biosystems, Warrington, UK
T84 cells	European Collection of Animal Cell Cultures, Porton Down, UK
TNF-α	PeproTech, Rocky Hill, NJ, USA
Trichostatin	Sigma Aldrich Company Ltd, Dorset, UK
Trypsin solution (0.05g trypsin + 0.05g chymotrypsin in 100ml 0.1% calcium chloride pH 7.8)	Sigma Aldrich Company Ltd, Dorset, UK
Trypsin/EDTA	Sigma Aldrich Company Ltd, Dorset, UK
Xylene	Chemix, Wiggan, Lancashire, UK

2.1.2 Buffers

Quanitkine ELISA wash buffer concentrate (20ml wash buffer diluted in 480ml distilled water)
R and D Systems, Oxon, UK

Ethylenediaminetetraacetic acid (EDTA) Merck, Poole, Dorset, UK
(Made just prior to use, 2 litres distilled water, 0.744g EDTA, adjusted to pH 8 with sodium hydroxide, concentration 0.1M)

Phosphate buffered saline (PBS)
Sigma Aldrich Company Ltd, Dorset, UK
(1 tablet dissolved in 200ml distilled water, 0.1M , pH 7.2)

RNA gel loading buffer
Eppendorf, Hamburg, Germany

SSC buffer
BIO-RAD, Hercules, CA, USA
(150mM sodium chloride, 17.5mM sodium citrate, pH 7.0)

Sodium citrate buffer
Merck, Poole, Dorset, UK
(25ml 2M sodium hydroxide, 21g citric acid, 10 litres distilled water, 0.01M, pH 6.0)

Tris buffered saline (TBS)
Merck, Poole, Dorset, UK
(87.5g sodium chloride, 6.6g Tris, 41.5ml 1M hydrochloric acid, pH 7.6)

2.2 Methods

2.2.1 Patient inclusion, sample collection and preservation

The study protocols and consent forms are included in appendix 1. The local research ethics committee approved the study protocol, and all patients gave informed written consent. All diagnoses of CD and UC had been previously verified according to the British Society of Gastroenterology guidelines, using a combination of clinical, endoscopic, histological and radiological findings (Jenkins et al, 1997). Patients selected for this study were in three cohorts. The first cohort consisted of four groups: CD, UC, a non-IBD control group of patients investigated for symptoms warranting colonoscopic examination, where the final diagnosis was not IBD and histology was normal or showed only minor abnormalities, and a non-IBD inflammatory control group where the patients had microbiologically confirmed infectious colitis. The patients recruited had colonoscopic examination for clinical indications, and consented to additional biopsies being taken for research purposes. Colonoscopic biopsies were taken at six sites along the colon from each patient resulting in the collection of 122 colon biopsies from 21 patients. Additional biopsies taken adjacent to these sites were formalin-fixed and used to assess histopathological abnormality. Serial colonic biopsies were collected using standard disposable biopsy forceps. The second cohort of patients was included who underwent colectomy for CD, UC, diverticulitis or colonic carcinoma. Colonic tissue was also obtained from consenting 16 patients who had undergone colectomy for IBD or for colonic carcinoma or diverticulitis (in the case of controls). Where patients underwent colectomy, full thickness bowel tissue was obtained from 3 areas corresponding to minimal/moderate/severe inflammation where relevant and possible. Patients with colonic carcinoma served as controls, whereby normal tissue was removed from near the resection margin. The third cohort constituted 3 patients with infective diarrhoea, who underwent sigmoidoscopic examination with rectal biopsies. A rigid sigmoidoscope was inserted via the anus, with air insufflation. The extent of examination was up to 20cm, and 6 rectal biopsies were taken from the anterior rectal area at 9cm.

Colonic tissue was immediately transferred to RNA later at room temperature and stored at +4°C. Adjacent specimens were formalin-fixed for histological and immunohistochemical assessment.

Where inflammatory blood results were available, these were included and correlated with inflammatory scores and microarray results.

2.2.2 Total cellular RNA preparation, cDNA probe synthesis and microarray hybridisation, and RT-PCR

2.2.2.1 Microarray construction

Sequences corresponding to 3'UTR's sequence for all known 41 human chemokines and 21 receptors, plus related receptors, a selected collection of G protein coupled receptors (GPCR's) and their ligands, and 40 suitable housekeeping proteins (for normalisation) (see table 3.2) were amplified by PCR from IMAGE clones. Amplification oligonucleotides were designed to produce an amplicon of approximately 500bp, the 3'-UTR sequence chosen for low homology to other

genes and repetitive sequences. Alternatively, the desired fragments cloned from Universal cDNA Library Microarrays were printed using GMS 417 Microarrayer with four 50μm pins. Approximately 100pg PCR products were printed in duplicate on Hybond N+ membranes. The printed membranes were denatured, neutralised and cross-linked according to manufacturers' instructions.

2.2.2.2 Preparation of total cellular RNA from colonic biopsies and cultured cell lines

RNA was extracted from both colonic biopsies and cells lines by use of a Qiagen RNeasy total RNA extraction kit, according to manufacturer's instructions. The biopsy samples or cell line samples were disrupted and homogenised in 600μl of RLT containing 6μl of β-mercaptoethanol (β-ME). The lysates were transferred to QIAshredder spin columns, to fragment high molecular weight lysis products, and were centrifuged for 2 minutes at 21,000 g, in a micro centrifuge. Supernatants were transferred to a fresh tube, and 600μl 70% ethanol added to precipitate the RNA. The contents were gently mixed by pipetting. The resulting solution was transferred to RNeasy mini columns, and centrifuged for 15 seconds at 21,000 g. The flow-through was discarded and 700μl buffer RW1 was added to each RNeasy column, which was centrifuged for 15 seconds at 21,000 g, to wash the column. The flow-throughs were discarded and 500μl buffer RPE was pipetted onto each RNeasy column. The tubes were centrifuged for 15 seconds at 21,000 g and the flow-throughs were discarded. This was repeated and the flow-throughs were again discarded. The columns were centrifuged again for 2 minutes at 21,000 g in order to remove any remaining wash buffer. The flow-throughs were discarded, and the columns placed into new collecting tubes and 50μl RNAse-free water was pipetted directly onto the RNeasy silica-gel membrane, and left to sand for 5 minutes. Total RNA was recovered by centrifugation for 2 minutes at 21,000 g, to elute. The eluted total-cellular RNA was stored at -70°C.

2.2.2.3 RNA quantification

An RNA 1.2% agarose formaldehyde electrophoresis gel was prepared as follows: 1.8g agarose was added to 15ml 10x formaldehyde gel buffer. The 10x formaldehyde gel buffer consisted of 200mM 3-(N-morpholino)propanesulfuric acid, 50mM sodium acetate, 10mM EDTA, pH 7.0. 100ml RNase-free water was added. The mixture was heated in a microwave oven to melt the agarose, and then cooled to 65°C in a water bath. 2.7ml of 37% (12.3M) formaldehyde and 4.5μl of a 10mg/ml ethidium bromide solution were added, the gel mixed thoroughly and poured onto gel casting tray. The gel was equilibrated by electrophoresis in 1 x FA gel running buffer at 70V for 30 minutes.

The RNA/gel-loading buffer mixtures were heat-denatured for 5 minutes at 68°C, placed on ice for 1 minute, and then loaded into the gel, in addition to 18s and 28s Ribosomal standards. The gel was run at 110V for 30 minutes to 2 hours to check the yield and quantity of the RNA obtained.

A second method of RNA assay was employed, using an RNA 6000 Nano assay kit with an Agilent 2100 bioanalyser. 400μl of RNA gel matrix was centrifuged at 1500g for 10 minutes in a spin filter. 130μl of the filtered RNA gel matrix was mixed thoroughly with 2μl of the RNA dye

concentrate in an RNase free micro centrifuge tube, protected from light and stored at +4°C. 9μl of gel-dye mix and 5μl of RNA 6000 Nano Markers were loaded into an RNA chip according to manufacturer's instructions. 1μl RNA ladder was pipetted into the ladder well. 1μl of the sample was added to each of the 12 sample wells, and the chip was vortexed for 1 minute. The chip was inserted into the Agilent 2100, and an electropherogram obtained.

2.2.2.4 cDNA probe synthesis

RNA was used to synthesise cDNA probes for microarray hybridisation by reverse transcription. Oligo dT was annealed to the total RNA template as follows: The annealing mix was made from 3μl RNase-free water and 2μl Oligo dT. This was incubated at +70°C for 10 minutes and then transferred to ice for 5 minutes.

The following components were added to each annealed RNA/oligo dT mixture: 1.5μl 20mM dATP/dTTP/dGTP, 3μl 0.1M dithiothreitol (DTT) 60μl, 3μl Super RNase in 6μl Superscript II buffer, 5μl [^{33}P]-dCTP and 1.5μl of superscript II RNAse H$^-$ Reverse Transcriptase. The reaction was mixed and incubated 42°C for 1 hour. A further 1.5μl of the superscript II RNase H$^-$ Reverse Transcriptase was added, and the reaction incubated at 42°C for a further hour.

RNA was hydrolysed by addition of 1.5μl 1% SDS, 1.5μl 0.5M EDTA, 4.5μl 3M NaOH and incubated at 68°C for 30 minutes. The reactions were neutralised with 15μl 1M Tris 7.5, 4.5μl 2N HCl. 15μl 1μg/ml COT-1 DNA was added to each sample and the volume made up to 100μl with the addition of 27μl RNase-free water.

Equilibrated Bio-spin 6 chromatography columns were centrifuged for 2 minutes at 1000 g. Reverse transcribed probes were added to these columns (without disturbing the column bed) and were centrifuged for a further 4 minutes at 1000 g. The flow through containing the purified probe was denatured at 95°C for 3 minutes, and then chilled on ice for 3 minutes before hybridising to the microarray.

2.2.2.5 Microarray hybridisation and analysis

Detection and quantitation of signal hybridised to the microarray provides a measure of the relative abundance of the transcript from a target gene. The resulting expression profile were analysed by hierarchical clustering, performed blind to cohort, biopsy site and histopathology scoring, samples being grouped together solely on the similarity between gene expression profiles.

Microarrays were pre-hybridised in 8ml hybridisation solution at +55°C for 2 hours in a Techne HB1 hybridisation oven. The hybridisation solution consisted of 8ml ExpressHyb, 20μl of 10mg/ml Salmon Testes DNA, 10μl 1mg/ml Poly (dA) per hybridisation reaction. After 30 minutes, the positions of the strips were checked, and altered where appropriate, so that there were no air-bubbles, and the strips were facing inside, adherent to the glass.

The denatured purified probe was added to the hybridisation tubes containing hybridisation solution and hybridised to the microarray for 14-20 hours at 55°C.

Following hybridisation the microarrays were washed in 20ml 0.1% SDS/0.2 x SSC for 1 hour at 55°C. The solution was discarded, and a further 20ml of the same solution replaced and washed again for 1 hour at 55°C. The solution was discarded, and a further 20ml replaced, washing performed for 1 hour at 65°C. The microarrays were air dried at room temperature.

Hybridised microarrays were exposed to Low Energy PhosphorImage Screens for periods up to 1 month, and scanned by Storm860 (Molecular Dynamics). Data was extracted using IMAGENE software (BioDiscovery, Los Angeles, CA) and normalised to the average expression level of the housekeeping gene panel, with final expression levels expressed as a percentage of average of this panel. Table 1.1 lists the housekeeping genes included in the microarray. These genes code for proteins whose activities are essential for the maintenance of cell function. The 40 chosen served as reference genes against which the expression levels of chemokine genes were normalised. This method enables reliable quantitative gene expression. Data manipulations were performed with Microsoft Excel. Hierarchical clustering was performed though use of GeneSpring microarray analysis software (Silicon Genetics, Redwood City, CA).

Table 2.1: Panel of housekeeping genes included in the microarray

Human mRNA for alpha-catenin complete cds
Human mRNA for platelet-type phosphofructokinase complete cds
Human lysosomal glycosylasparaginase (AGA) gene
Human ETS2 oncogene
Human capping protein alpha mRNA partial_cds
Human mRNA for mitochon
Human cytoplasmic beta-actin gene complete cds
Unknown est hits only
Human mitochondrial ADP/ADT translocator mRNA complete cds
Human superoxide dismutase (SOD-1) mRNA complete cds
Homo sapiens protein tyrosine kinase (Syk) mRNA complete cds
Lipoamide dehydrogenase (NAD)
Unknown ~20 est only
Human mRNA for lactate dehydrogenase-A (LDH-A EC 1.1.1.27)
Human glutamate receptor 2 (HBGR2) mRNA complete cds
Human alpha-2-macroglobulin mRNA complete cds
Human glyceraldehyde 3-phosphate dehydrogenase mRNA
DAD-1 pBS AS
SLUG-1 pBS AS
Actin 5' fragment
Actin Middle fragment
Actin 3' Fragment
Deoxyhypusine synthase mRNA
Eukaryotic initiation factor 2B-epsilon
90-kDa heat-shock protein gene
HKGB06 histone H2B.1 mRNA 3' end
ADP-ribosylation factor 1 gene
Enylyl cyclase-associated protein
Cytosolic malate dehydrogenase
Haperonin protein (Tcp20)
Glutamate dehydrogenase (GDH)
DNA repair helicase (ERCC3)
Endothelin-1 (EDN1) gene
(cytosin-5)-methyltransferase
Uroporphyrinogen III synthase mRNA
Calmodulin
MRL3 = mammalian ribosome L3
ADP/ATP translocase mRNA 3' end clone
Cytochrome bc-1 complex core protein II
HnRNP C2 protein mRNA

2.2.2.6 *Real-time quantitative RT-PCR*

cDNA was synthesised from ~0.5 μg total RNA using Taqman Gold RT-PCR Kit following manufacturer's protocol. Each reaction mix included 5μl RNA, 10μl 10x RT buffer, 22μl 25mM $MgCl_3$, 20μl dNTPs, 5μl primers (random hexamers), 2μl RNase inhibitor, 29.75μl RNase free distilled water and 6.24μl Multiscribe RT. This was placed to 25°C for 10 minutes, 37°C for 60 minutes and 95°C for 5 minutes. Expression levels of CXCL's 1-3, CXCR1 and CXCR2 were measured with TaqMan primers and probes designed using Primer Express v.2, and CCR6, CCL20, CXCL8 and rRNA with TaqMan Assay Reagents. Quantitative PCRs were performed using 5μl ABI7900 with TaqMan Universal PCR Master Mix using recommended protocol. Duplicate reactions were performed with ≥ 3 dilutions of each cDNA. Expression levels in each sample were normalised by comparison to the matching rRNA level. Final data were expressed as fold-up regulation relative to an average of all uninvolved IBD samples analysed (i.e. where the biopsies were taken from a macro- and microscopically normal area, from a patient with IBD).

The relative level of up regulated expression of these chemokines in inflamed IBD colon was expressed as a percentage of the average transcript copy number detected for the non-IBD cohort normalised to 18S rRNA copy number. This serves as a good internal control in relative RT-PCR as there is little variation in expression. The normalised data was compared to the histopathological score for inflammation.

2.2.3 Histopathological assessment of colonic tissue

Haematoxylin and eosin stain (H&E) was performed on the colonic sections by laboratory technicians in the department of histopathology, Royal Free Hospital. The sections were dewaxed, rinsed in alcohol followed by water, and then stained with Harris's haematoxylin for 10 minutes. The section were washed in running tap water, followed by differentiation in acid alcohol (1% hydrochloric acid in 70% alcohol) for 10 seconds and a further wash in running tap water for 5 minutes. They were then stained with eosin for 4 minutes, and washed in tap water. Finally, the sections were dehydrated in an alcohol gradient, immersed in xylene and mounted in DPX.

Histopathological assessment was performed by Professor Dhillon (consultant histopathologist) for chronic and acute inflammation and epithelial and glandular architecture change, according to table 2.2. All scoring was undertaken in a blinded fashion.

Table 2.2: Histopathology scoring method used on colonic tissue. This scoring method was devised by the Royal Free Hospital Professor of histopathology, Professor Dhillon, as there are no accepted internationally validated alternatives.

Score A: Acute inflammation No acute inflammation Occasional lamina propria polymorphs/eosinophils Moderate numbers of lamina propria polymorphs/eosinophils, Crypt abscesses Frank pus
Score C: Chronic inflammation (lymphocytes and plasma cells) No chronic inflammation Slight increase in lamina propria mononuclear cells Moderate increase in lamina propria mononuclear cells Marked increase with > 2 lymphoid aggregates/follicles per biopsy
Score D: Destructive epithelial change None Superficial erosions Apthoid ulceration Frank ulceration
Score R: Reactive/neoplastic glandular architectural change None Occasional bifid glands Glandular disarray and/or atrophy Dysplasia

2.2.4 Immunohistochemical localisation and quantification of chemokines using immunoperoxidase technique

2.2.4.1 The technique of immunohistochemistry

This technique is used to the study epitope-localisation within tissue sections using monoclonal antibodies and an indirect amplification system. Paraffin embedded formalin-fixed sections were used. Monoclonal antibodies raised to the antigen of interest were applied to tissue sections. In order to identify the localisation of binding, and amplify the signal so that it can be detected under a microscope, a number of indirect amplification techniques were employed. This involves a colour-reaction system with biotin and horseradish peroxidase (Bancroft and Gamble, 2002).

2.2.4.2 Preparation of sections and pre-treatment methods

At room temperature, 3μm sections of tissue were de-paraffinised by immersion for 10 minutes in 200ml xylene and then brief immersion in alcohol gradient from 100% to 70% before transfer to tris buffered saline (TBS). In order to block endogenous peroxidase activity, sections were immersed in a 2% solution of hydrogen peroxide in methanol for 10 minutes. Following this, the sections were washed in running water for 10 minutes.

The following conditions were used as pre-treatment, in order to establish the optimum pre-treatment:

- No treatment
- Trypsin 10 minutes (warmed to 37°C)
- Trypsin 20 minutes (warmed to 37°C)
- High-powered microwave treatment for 20 minutes in sodium citrate buffer, then in trypsin for 15 seconds (37°C)
- High-powered microwave treatment for 25 minutes in sodium citrate buffer
- Pressure cooker treatment in sodium citrate buffer for 1 minute 30 seconds pressure cooker treatment for 1 minute 30 seconds
- Pressure cooker treatment in ethylenediaminetetraacetic acid buffer (EDTA) for 1 minute 30 seconds
- Negative control

After the pre-treatment phase, the sections were encircled on the slides using a hydrophobic pen. They were then laid out in a humidity chamber and washed in TBS.

Following the blockade of endogenous peroxide activity, non-specific background immunoreactivity was blocked by incubation in 200μl/slide in either a 1% solution of normal horse serum (NHS), a 5% solution of foetal calf serum (FCS), or a 3% / 5% solution of milk powder, in TBS buffer. This solution was shaken off the slides after 20 minutes. Following incubation period, sections that were to be used as negative controls (i.e. with no primary antibody applied) did not have the NHS removed.

2.2.4.3 Primary antibody application

For each slide, 200µl of antibody was applied at a set dilution, in TBS buffer, containing 5% foetal calf serum where indicated in the text. The sections were incubated either for 1 hour at room temperature in a humidity chamber at room temperature, or overnight (approximately 18 hours) at +4°C in a humidity chamber.

After the primary antibody incubation, sections were washed in several changes TBS for 10 minutes.

2.2.4.4 Secondary antibody incubation

Link antibody incubation was then performed, using biotinylated rabbit-anti-mouse at a 2% dilution in TBS buffer containing 2% normal horse serum, or 5% foetal calf serum, for 40 minutes The sections were washed in TBS buffer for 10 minutes.

Following this, the next stage of the amplification signal was achieved using peroxidase conjugate complex (ABC). This was used at a dilution of 2% avidin biotin + 2% normal horse serum or 5% foetal calf serum in TBS buffer for 30 or 40 minutes, prepared 30 minutes in advance. The sections were again washed in TBS for 10 minutes.

2.2.4.5 Application of DAB

Bound peroxidase was visualised with di-amino-benzidine (DAB) solution, applied to each slide and washed off with TBS when staining was seen to be optimised using a light microscope. The slides were placed in a staining rack, in running tap water. This was immersed in haematoxylin for 4 minutes to counterstain the sections, then in running tap water. The sections were then dipped twice in acid alcohol, washed again in running tap water, then immersed in sodium tetraborax for 2 minutes to stain the haematoxylin nuclei blue. Following this, the sections were washed again in running tap water, then dehydrated by brief dips in 3 troughs containing absolute alcohol at increasing concentrations, finishing with immersion for a few seconds in 2 troughs containing xylene. The sections were mounted in DPX and viewed by light microscopy.

2.2.5 Analysis of Cell lines

2.2.5.1 Cell propagation

3 sets of different passage-number Caco-2 and HT29 cells were incubated at 37°C, in 2 x 75cm cell-culture flasks, containing 10ml of DME medium, supplemented with 10% FCS, 2mmol/l glutamine, 1% non-essential-amino-acids and 5ml antibiotics, or 10ml McCoy's 5A medium supplemented with 10% FCS, 2mmol/l glutamine and 1% non-essential amino acids, respectively. Growth and possible infection were monitored. When the cells had formed a confluent monolayer, with dome formation, the medium was aspirated, and the cells were washed with approximately 10ml room temperature-phosphate buffer solution (PBS) to remove the adherent medium. 3ml of trypsin were added to each flask, and incubated for 8 minutes, until the most of the cells were seen to be detached when viewed by light microscopy. The flasks were tapped firmly to detach remaining cells.

The trypsin/cell mixtures were centrifuged at 10,000g at room temperature 5 minutes. The supernatant was discarded and the cell pellet re-suspended gradually in 4ml medium, made up to a final volume of 20ml.

2.2.5.2 Cell Count and viability assessment

15µl of the cell suspension were added to 15µl of trypan blue 0.4%. This was mixed gently, added to a cytometer with a cover slip, and viewed under a light microscope. The viable cells were counted within 6 grids, and an average calculated. The dead cells were also counted within the same grids and the cell viability calculated by the standard grid equation total number of live cells x 10^4 x 2 /ml (dilution factor of 2).

2.2.5.3 Cell stimulation

20 x 10cm well plates were used. 1.5 x 10^6 cells were added to 10ml medium. The plates were incubated and medium changed every 3 days. At 3-days post confluence, combinations of 1µM benzamide, 10µM trichostatin, 10ng/ml TNF-α, 10ng/ml IL-1β and 10µg/ml *E.coli* lipopolysaccharide were applied to the Caco-2 cells, as detailed in table 2.3. At 3 days post confluence, the HT29 cells, combinations of 10ng/ml TNF-α, 10ng/ml IL-1β and 10µg/ml *E.coli* lipopolysaccharide were applied as detailed in table 2.3.

Table 2.3: Stimulation solutions applied to Caco-2 cells. The table details quantification of the additives.

Stimulation	**Solution added**
Nil	10ml medium
IL-1β	10µl of 10µg/ml Il-1β in 10ml medium (10ng/ml)
TNF-α	1µl of 0.1mg/ml TNF-α in 10ml medium (10ng/ml)
Benzamide (1µM)	100µl of 100mM benzamide in 10ml medium
Trichostatin A 10µM	100µl of 1mMol Trichostatin A in 10ml medium
E.coli LPS 10µg/ml	100µl of 1mg/ml of LPS in 10ml medium

At 2-, 4- and 18-hour time points, the supernatants were removed from the relevant plates and stored at -70°C.

5ml sterile phosphate buffered saline (PBS) was added to each of these plates, and rocked gently, to wash remaining FCS from the cells. The PBS was then aspirated and discarded. 3ml trypsin were added to each plate, and incubated at 37°C for approximately 8 minutes, to detach the cells. The trypsin/cultured cell mixes were centrifuged for 5 minutes at 10,000g. The supernatants were discarded, and the cell pellets re-suspended in 5 ml sterile PBS. The suspensions were again centrifuged for 5 minutes at 10,000 g. The supernatants were discarded, and the remaining pellets re-suspended in 1ml sterile PBS, and transferred to sterile eppendorfs. These were centrifuged at 10,000 g for 5 minutes, and the supernatants discarded. The resulting dry cell-pellets were frozen at -70°C.

2.2.6 Quantitative determination of chemokine protein concentrations in cell culture supernatants

2.2.6.1 The technique of ELISA

This assay incorporated the quantitative sandwich enzyme immunoassay technique. A monoclonal antibody specific for one of CCL20, CXCL8, CXCL1 or CCL5 had been pre-coated onto 4 microplates. When standards and samples were pipetted into the well, any antibody-specific chemokine present was bound by the immobilised antibody. After washing away any unbound substances, an enzyme-linked polyclonal antibody specific for the appropriate chemokine was added to the wells. Following a wash to remove any unbound antibody-enzyme reagent, a substrate solution was added to the wells and colour developed in proportion to the amount of chemokine bound in the initial step. The colour development was stopped and the optical densities determined.

The chemokine standards were reconstituted with distilled water according to the manufacturer's guidelines, to produce a stock which was diluted to form the recommended standards.

2.2.6.2 ELISA procedure

The sample or standards were added to the appropriate wells, diluted according to specific manufacturer's guidelines. The ELISA plate was covered, and incubated for the recommended length of time at room temperature.

Using an auto washer, each well was aspirated and washed the recommended number of times. This was programmed to deliver 400µl of wash buffer to each well during each cycle. All liquid was removed at each step, and after the last wash, the plate was inverted and blotted.

Chemokine conjugate was added to each well and incubated at room temperature for the recommended time (1-2.5 hours, depending on the antibody). The washing step was repeated, for recommended number of cycles (3-6). During the washing process, the substrate solution was prepared. Colour reagents A and B were mixed together in equal volumes, within 15 minutes of use. This was placed in darkness until the ELISA plate was ready. When the washing process was complete, 200µl of substrate solution were added to each well using an ELISA multi-pipette. This was incubated for 30 minutes at room temperature in the dark.

Details for CCL20 ELISA

The CCL20 standard was reconstituted with distilled water to produce a stock of 5000pg/ml. After 20 minutes of gentle agitation, this was diluted with the R and D standard calibrator dilutent RD6-21 to make 7 x 50% serial dilutions, of 500pg/ml, 250pg/ml, 125pg/ml, 62.5pg/ml, 31.2pg/ml, 15.6pg/ml, 7.8pg/ml. The calibrator diluent served as the zero standard (0pg/ml). 100µl of assay diluent RD1-57 was added to each well, followed by 100µl of standard or sample. The ELISA plate was covered, and incubated for 2 hours at room temperature. Each well was then aspirated and washed three times with the Quantikine ELISA wash buffer. 200µl of CCL20 conjugate was added to each well. The plate was covered, and incubated for 2 hours at room temperature. Following this, the washing step was repeated, for 3 cycles. 200µl of substrate solution were added to each well, and the procedure completed as described above.

Details for CXCL8 ELISA

The CXCL8 standard was reconstituted with 5ml calibrator standard Quantikine diluent RD5P to produce a stock of 2000pg/ml. After 20 minutes of gentle agitation, this was diluted with calibrator diluent RD5P (1X) to make 7 x 50% serial dilutions of 2000pg/ml (stock), 1000 pg/ml, 500pg/ml, 250pg/ml, 125pg/ml, 62.5pg/ml, and 31.2pg/ml. The calibrator diluent served as the zero standard (0mg/ml). 100µl of assay diluent RD1-8 was added to each well, followed by 50µl of standard or sample. 100µl of conjugate was added to each well, and the plate was agitated gently. The plate was covered and incubated for 2 hours at room temperature, and then washed in Quantikine wash buffer 6 times using the automated washer. 200µl of substrate solution was added to each well, and the ELISA was completed as described above.

Details for CXCL1 ELISA

The CXCL1 standard was reconstituted with 5ml Quantikine calibrator diluent RD5B produce a stock of 1000pg/ml. After 20 minutes of gentle agitation, this was diluted with calibrator diluent RD6-21 to make 6 x 50% standard concentrations of 1000pg/ml, 500pg/ml, 250pg/ml, 125pg/ml, 62.5pg/ml, 31.2pg/ml. The calibrator diluent alone served as the zero standard (0pg/ml). 200µl of the standard or sample were added to each well. The plate was covered and incubated for 1.5 hours at room temperature. Each well was aspirated and washed three times in Quantikine wash buffer. 200µl of CXCL1 conjugate was added to each well. The plate was covered and incubated for 1 hour. The washing step was repeated, again for 3 times. 200µl of substrate solution (prepared as described in section 2.2.4.2) were added to each well. This was incubated for 15 minutes at room temperature in the dark.

Details for CCL5 ELISA

The CCL5 standard was reconstituted with distilled water to produce a stock of 2000pg/ml. After 20 minutes of gentle agitation this was diluted to make 7 x 50% serial dilutions, of 2000pg/ml, 1000 pg/ml, 500pg/ml, 250pg/ml, 125pg/ml, 62.5pg/ml, 31.2pg/ml. The calibrator diluent served as the zero standard (0pg/ml). 100µl of assay diluent RD5H was added to each well, followed by 100µl of standard or sample. The ELISA plate was covered and incubated for 2 hours at room temperature. Each well was aspirated and washed three times in Quantikine wash buffer. 200µl of RANTES conjugate was added to each well. The plate was covered and incubated for 1 hour at room temperature. The washing step was repeated for 3 times. 200µl of substrate solution was added to each and incubated for 30 minutes at room temperature in the dark.

2.2.6.3 Optical densometry

50µl of the stop solution was then added to each well, and the optical density of each well was obtained using a microplate reader set to 450nm. The wavelength correction was set to 540nm. The duplicate readings for each standard and sample were averaged and subtracted from the average zero standard optical density.

2.2.7 Flow cytometric analysis of colonic biopsies

Colonic biopsies were obtained as described in section 2.2.1.1. They were placed directly into calcium and magnesium-free Hanks Balanced Salt Solution for 10-20 minutes at +37°C on a rocker, to strip the epithelial layer from the lamina propria. Mechanical disruption was then performed using a vortex. The fluid was retrieved. 2ml of the cell dissolution solution was added to the biopsy, and again rocked for 10-20 minutes 37°C. This was mechanically disrupted, and the process repeated a further 2 times. The remaining tissue was digested with collagenase 4 mg/ml for 2-3 hours. 1ml of 2μg/ml collagenase in RPMI medium with 10% FCS was added to the lamina propria. This was vortexed. Saline was added to both tubes to make up to 10ml. These were then centrifuged 15000g for 10 minutes. The supernatants were discarded, pellets re-suspended in 10ml saline, and re-spun at 15000rpm for a further 10 minutes. The tissue was washed twice with PBS 2ml/sample. The supernatants were discarded and the pellets resuspended in the drops of PBS remaining. 2ml PBS/albumin/paraformaldehyde per tube was added, and stored at +4°C.

A single-cell suspension was prepared from each compartment and stained with conjugated antibodies to CXCR1, CXCR2, CCR6 and CCL20 (R&D). Analysis was performed by 4-colour flow cytometry (Dako, UK) with lineage markers for T and B cells, monocytes, neutrophils, colonocytes and APC's (Coulter-Immunotech and Serotec UK). Isotype control reagents were used throughout.

2.2.8 Stimulation of colonic epithelium in colonic biopsies

9 biopsies were taken from each of 6 patients, from the rectosigmoid area using standard disposable biopsy forceps. The 1st was placed directly into RNA later, and the remaining 8 were placed into 4ml enriched diluted RPMI colonic epithelial cell culture medium (100ml RPMI, 100ml distilled water, 0.94g NCTC, 0.22g sodium bicarbonate, 10% foetal calf serum). These were then orientated on 5mm^2 sterile sponge squares with the help of a light microscope, with epithelium facing upwards. They were immersed in 4ml RPMI medium with the following additions, in 5cm petri dishes, and placed in an enclosed plastic container filled with 95% oxygen, and incubated at 37°C on a rocker, for 2 or 4 hours:

- Nil added
- 10ng/ml TNF-α
- 10ng/ml IL-1β
- 10ng/ml TNF-α + 10ng/ml IL-1β

At 2 and 4 hours the appropriate biopsies were retrieved and placed into RNA later at room temperature and stored at +4°C.

2.2.9 Primary colonic epithelial culture and stimulation

2.2.9.1 Epithelial cell separation

3 sets of 2cm^2 sections of normal colonic epithelium were placed directly into Cell Dissociation Solution. The tissue sections were obtained from 3 patients who underwent colectomy for colonic carcinoma, with consent and ethical approval. These were incubated at 37°C for 45 minutes, with mechanical agitation at 5-minute-intervals. The Cell Dissolution Solutions were

replaced twice. The lamina propria was placed in RNA later and stored and room temperature. The solutions containing the epithelium were centrifuged at 10, 000g at room temperature for 10 minutes, and the pellets were re-suspended in PBS twice to wash the cells.

2.2.9.2 Epithelial cell propagation

50μl of the cell pellets were re-suspended in 4ml of 50% RPMI medium containing 50% distilled water, 9.4g/litre NCTC, 13.1mmol sodium bicarbonate, 10%FCS and 2% antibiotics, with the addition of the following pro-inflammatory cytokines: nil, 10ng/ml TNF-α, 10ng/ml IL-1β or 10ng/ml TNF-α and 10ng ml IL-1β. These were incubated at 37°C for 2 hours.

2.2.9.3 Cell count and viability assessment

An assessment of the cell count and viability was performed as described in section 2.2.3.2.

2.2.9.4 Cell pellet formation

The enriched medium/cell mixes were centrifuged at 10 000g for 10 minutes, and the supernatant discarded. The pellets were washed twice in PBS and stored in RNA later.

2.2.9.5 RNA extraction

RNA was isolated as described in section 2.2.1.2.

2.2.9.6 Microarray hybridisation and analysis

Hybridisation and microarray analysis was performed as described in section 2.2.1.5

Chapter 3

Quantification of chemokine RNA in colonic tissue

3.1 Introduction

3.2 Microarray hybridisation analysis of total cellular RNA obtained from colonic tissue

- 3.2.1 Sample preparation
- 3.2.2 Array results
- 3.2.3 Discussion

3.3 Real time quantitative PCR (RT-PCR) on colonic tissue

- 3.3.1 Background
- 3.3.2 RT-PCR technique
- 3.3.3 Results
- 3.3.4 Conclusion

3.4 Discussion

3.1 Introduction

Recent advances in gene expression profiling technology have enabled construction of a custom cDNA microarray incorporating the entire chemokine superfamily and their receptors. Detection and quantisation of signal hybridised to the microarray provides a measurement of the relative abundance of target genes and included every known chemokine recognised in 2001 (Skelton et al, 2003). As chemokines determine the extent, type and duration of leukocyte infiltration, characterisation of the pattern of expression within normal, non-inflamed and inflamed IBD, and infectious colitis is likely to further understanding of disease process in IBD.

3.2 Microarray hybridisation analysis of total cellular RNA obtained from colonic tissue

3.2.1 Sample preparation

Patient and sample inclusion, methods for inflammatory scoring, RNA preparation, cDNA probe synthesis, microarray hybridisation and quantisation are detailed in section 2.2. Disease activity in patients with IBD ranged from focally normal to moderate/severe. An RNA assay was performed on each sample, as described in 2.2.3, using the Agilent bioanalyser. Graph 3.1 represents a sample electropherogram obtained. Figure 3.1 represents the pseudo-gel appearance with each lane corresponding to a different sample. The patient details for each lane represented are outlined in table 3.1. A conventional gel is picture in figure 5.1.

3.2.2 Array results

The expression profiles analysed by hierarchical clustering are illustrated in figure 3.2.
Table 3.2 indicates which genes were strongly, weakly expressed or not expressed at all. The array values for these chemokines are listed in table 3.3.

Graph 3.1: Electropherogram to illustrate the RNA assay from minimally diseased UC lamina propria (sample 139) and mildly diseased whole UC tissue (sample 141), including fluorescence (y-axis) and time in seconds (x-axis). 2 ribosomal peaks are visible, and 1 marker peak, demonstrating good RNA preparation.

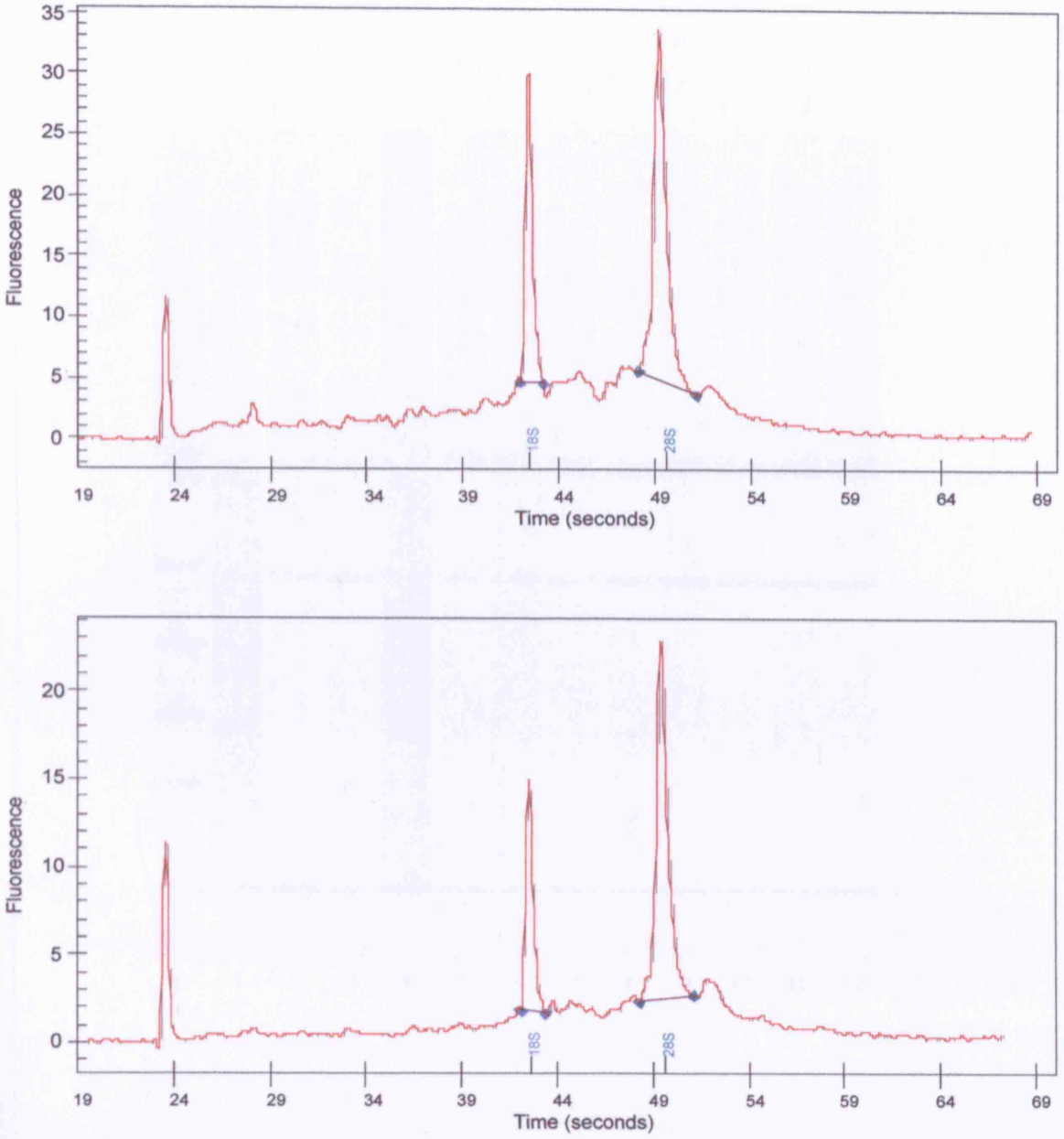

Figure 3.1: Pseudo-gel lanes to illustrate the RNA assay from samples listed in table 3.1. Two ribosomal peaks are visible, and one marker peak, demonstrating good RNA preparation. L=ladder.

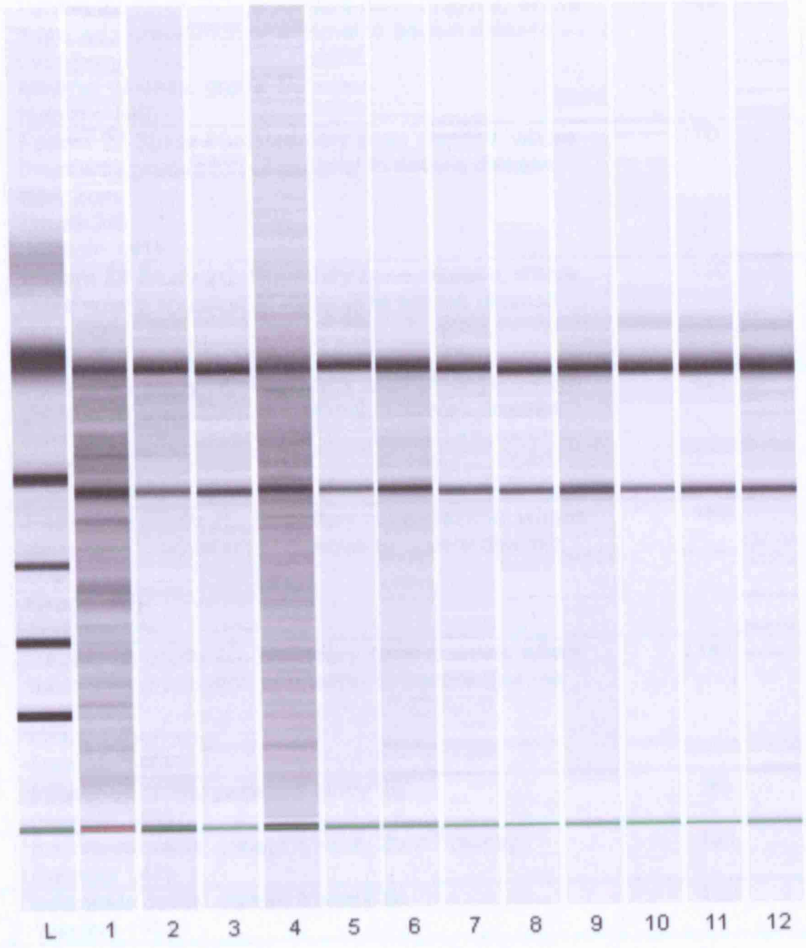

Table 3.1: Clinical details and corresponding semi-quantified RNA concentration (ng/μl) from samples included in graph and figure 3.1, assessed using the Agilent system.

Sample Peak	Sample description	RNA Concentration (ng/μl)	rRNA ratio 28S/18S
1	Patient 22 Study 2C Severe UC, stripped lamina propria (sample 137)	192	1.15
2	Patient 22 Study 2C Severe UC, stripped lamina propria (sample 138)	45	1.76
3	Patient 22 Study 2C Minimal diseased area in UC, stripped lamina propria (sample 139)	146	1.79
4	Patient 22 Study 2C. Boundary zone disease, where there was graduation of minimal to severe disease over 2cm. Minimal disease: grade 1/6 (sample 140)	43	1.22
5	Patient 22 Study 2C. Boundary zone disease, where there was graduation of minimal to severe disease over 2cm. Grade 2/6 (sample 141)	70	2.08
6	Patient 22 Study 2C. Boundary zone disease, where there was graduation of minimal to severe disease over 2cm. Grade 3/6 (sample 142)	150	1.59
7	Patient 22 Study 2C. Boundary zone disease, where there was graduation of minimal to severe disease over 2cm. Grade 4/6 (sample 143)	127	1.95
8	Patient 22 Study 2C. Boundary zone disease, where there was graduation of minimal to severe disease over 2cm. Grade 5/6 (sample 144)	192	1.85
9	Patient 22 Study 2C. Boundary zone disease, where there was graduation of minimal to severe disease over 2cm. Grade 6/6 (sample 145)	141	1.48
10	Infectious colitis: patient 4 study 2b (sample 146)	96	2.33
11	Infectious colitis: patient 4 study 2b 2nd biopsy (sample 147)	191	2.29
12	Infectious colitis: patient 5 study 2b (sample 148)	122	2.27

Figure 3.2

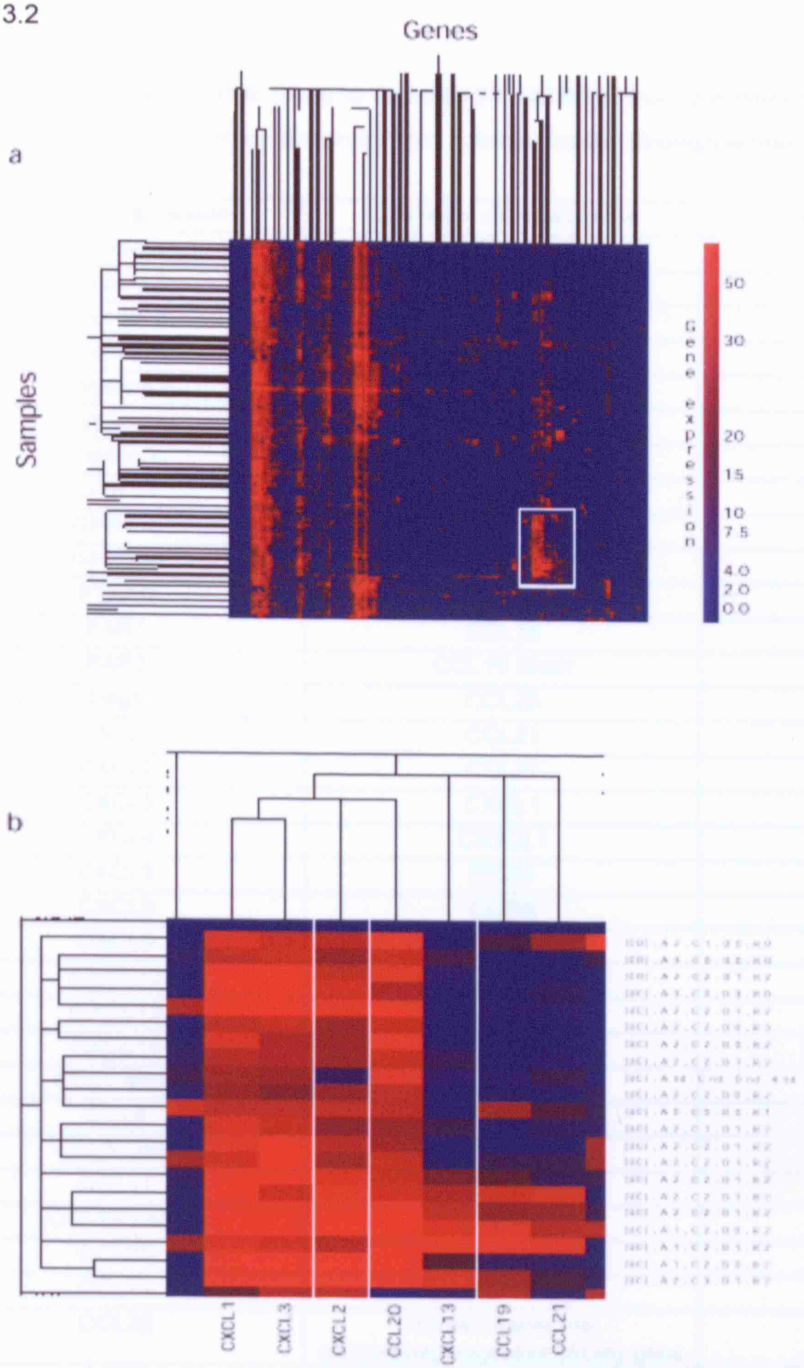

Hierarchical clustering of gene expression data from colonic biopsy tissue. Genes represented on the microarray are clustered along the horizontal axis, while colon biopsy samples (including from 13 IBD patients and 9 normal controls) are clustered along the vertical axis (a). The bar on the right hand side gives an indication of the level of gene expression: blue=low, red=high. Data are the relative amount of gene expression given as a percentage of the mean of the expression levels of a group of 40 housekeeping genes present on the array. Dendograms reveal up regulation of expression of a distinct subset of chemokines within a group of inflamed colon samples (white box). A cluster of 21 biopsies, taken from 5 UC and 1 CD patients, exhibited an expression profile clearly distinct from the other 101 profiles analysed. Within this exceptional cluster, much higher levels of gene expression were observed for a group of four chemokines: CXCL1, CXCL2, CXCL3, and CCL20, in comparison to other samples. An expanded view of this exceptional cluster of samples is shown in (b), which also shows histopathological scores on the right.

Table 3.2: Categories of level of gene expression, obtained from the semi-quantitative assessment of the microarray obtained from colonic tissue (strong/low/nil).

Strongly expression	Low level of expression	No expression
Trypsin 1	CCL1 long	Thrombin
Trypsin 2	CCL2	Elast 2B Short
Trypsin 3	CCL3	FPRL1
Trypsin 4	CCL5 Short	P2Y5
Tryptase a	SCYA3L	H963 short
Tryptase b	CCL8	P2Y9
Caldecrin	CCL13	EBI2
GPR16	CCL14	GPR34 short
GPR115	CCL15	GPR34 long
GPR128	CCL16	GPR38
PTAFR	CCL17 Long	GPR15
PAR1	CCL18	GPR31
PAR3	CCL19 Short	GPR32 long
Edg5	CCL25	CRTH2
CXCL1	CCL21	GPR44
CXCL2	CCL27	CNR2
CXCL3	CXCL1	P2Y2
CXCL4	CX3CL1	Edg2
CXCL5	CCR4	Edg3
CXCL8	CCR5	Edg8
CXCL9	CCR6	CB2
CXCL10	CCR7	EMR1
CXCL13	CCR11	CCL7 Short
CXCL14	CXCR3	CCL17 Short
CCL1 short	CXCR5	CCL22
CCL4	CCXCR1	CCL23
CCL5 Long	D6	CCR1
CCL11	DARC	CCR2
CCL19 Long	CCRL2	CCR3 Short
CCL20	hm74	CCR3 Long
CCL24	RDC1	CCR8 short
CCL26	Human lysosomal glycosylasparaginase (AGA) gene	CCR8 long
CCL28	Unknown ~20 est only	CCR9
CCR10	Eukaryotic initiation factor 2B-epsilon	CXCR1
CXCR4	Endothelin-1 (EDN1) gene	CXCR2
		CX3CR1
		TYMSTR
		Human glutamate receptor 2 (HBGR2) mRNA complete cds
		SLUG-1 pBS AS

Table 3.3: Relative expression levels of CCR6, CXCL1, CXCL2, CXCL3, CCL20 and actin, obtained by semi-quantitative assessment of the microarray result from colonic biopsy tissue, with inflammatory quotients. Where the level is less than 10-15, it is not significantly detected.

Disease	Patient number	Biopsy number	A+C	ESR	CRP	CXCL1	CXCL2	CXCL3	CCL20	CCR6	Actin
CD	8	1	2	3	1	12.8749	0.8470	3.1330	31.2816	0.7899	346.4544
CD	8	2	2	3	1	8.7457	2.9049	4.2431	6.7504	0.2778	336.1245
CD	8	3	0	3	1	22.5269	3.3604	17.8231	5.7147	0.6164	628.2627
CD	8	4	0	3	1	23.1730	9.6857	15.4482	10.7338	0.5346	449.4529
CD	8	5	X	3	1	21.8538	5.8944	5.6031	6.5003	0.3223	371.7373
CD	8	6	X	3	1	31.0232	8.3014	15.1541	22.2012	0.5130	365.7528
CD	10	1	1	7	1	20.0171	6.8922	15.3389	16.7883	5.1261	358.6358
CD	10	2	0	7	1	14.5013	3.5726	9.3770	14.5460	0.7404	355.0979
CD	10	3	0	7	1	22.0209	3.6033	7.9750	4.9603	4.3418	344.0808
CD	10	4	0	7	1	26.0775	-0.8020	2.9427	-1.4565	5.5940	453.9998
CD	10	5	2	7	1	3.6960	2.2128	-0.3772	7.6534	6.3451	362.0924
CD	10	6	1	7	1	10.8994	7.2273	12.6070	23.3377	2.2330	366.5142
CD	11	1	1	54	X	13.8694	14.7741	10.4023	26.1079	8.2763	343.8991
CD	11	2	3	54	X	60.8048	39.6568	51.2944	76.5898	1.3545	352.9199
CD	11	3	2	54	X	17.9911	0.2326	44.4122	66.7550	2.4710	546.4922
CD	11	4	3	54	X	44.7716	25.4855	47.4023	47.3764	3.5464	356.4390
CD	11	5	4	54	X	71.5410	42.8516	76.1840	69.2414	6.0468	436.5160
CD	11	6	1	54	X	9.7207	10.7988	17.8908	30.9975	0.4957	412.0918
CD	19	1	0	5	2	-1.9594	2.1085	-6.7021	3.6386	0.2642	369.7157
CD	19	2	1	5	2	0.1036	0.8530	1.9697	3.3976	3.0730	369.4977
CD	19	3	0	5	2	0.1036	0.8530	1.9697	3.3976	3.0730	369.4977
CD	19	4	0	5	2	-3.7685	-3.4466	-2.7605	0.2301	3.6173	343.5172
CD	19	5	0	5	2	-9.3031	4.2649	-3.2190	-1.1311	11.9557	388.4097
CD	19	6	0	5	2	3.8875	-2.9530	0.7016	9.0994	-1.4857	426.3173
CD	26	1	2	11	33	9.3098	-1.6388	18.4687	7.8416	2.7814	435.3324
CD	26	2	0	11	33	3.6251	1.5139	2.0994	-1.4244	1.1101	529.5197
CD	26	3	0	11	33	-23.6457	2.0445	-16.9478	6.4123	1.3075	397.5809
CD	26	4	2	11	33	-0.7637	-4.9232	6.2853	0.3028	1.9835	318.6884
CD	26	5	0	11	33	0.9197	-1.2976	-7.7278	15.2485	1.1668	367.2537
CD	26	6	0	11	33	4.1106	-2.0160	-4.8278	15.6759	0.7695	372.3677
CD	27	1	0	X	X	0.1730	-1.6189	4.1967	9.8823	1.7248	325.6347
CD	27	2	0	X	X	0.5518	-5.1628	13.3833	6.5200	1.7102	1038.4470
CD	27	3	0	X	X	-0.5074	5.2589	-4.3915	-0.2833	3.7082	381.5902
CD	27	4	0	X	X	11.3596	-0.9036	1.9010	-0.2783	3.2320	354.1940
CD	27	5	0	X	X	-4.6034	-3.0410	-24.1020	12.9208	5.1031	342.9209
CD	27	6	0	X	X	10.3938	7.5107	3.1070	11.7817	1.7255	330.0374
CD	27	7	X	X	X	13.2048	19.2750	1.1552	16.0979	5.1195	348.3253
CD	27	8	X	X	X	-24.8656	-8.7647	-18.1149	-1.6757	1.7446	357.0293
UC	14	1	3	X	2	76.3014	52.3859	73.2142	34.1510	6.7583	421.1785
UC	14	2	4	X	2	15.7516	14.8189	13.5579	59.1894	15.0781	429.9246
UC	14	3	4	X	2	43.8319	28.6012	46.8544	48.5583	7.8825	414.7547
UC	14	4	4	X	2	36.1315	27.1006	33.0975	47.5600	41.8447	406.2785
UC	14	5	4	X	2	27.2374	25.3038	22.4103	44.0568	7.9887	414.1393
UC	14	6	4	X	2	61.1366	27.5784	35.5777	90.5397	8.2764	483.1898
UC	15	1	0	6	1	-1.4729	0.0522	-2.1635	2.0368	1.7478	375.1228
UC	15	2	0	6	1	3.7115	-0.0440	3.5608	5.4699	7.3108	349.5528
UC	15	3	1	6	1	-4.0283	0.3721	2.6327	7.5898	11.6711	357.7953
UC	15	4	0	6	1	-0.2017	7.2293	5.6980	6.8256	1.5048	421.7919
UC	15	5	0	6	1	1.0720	2.2942	2.0967	7.8511	1.4603	406.0595
UC	15	6	0	6	1	42.3754	43.2141	46.6632	41.7457	2.8440	406.0476
UC	16	1	4	X	X	70.8922	64.3215	51.3471	57.2426	43.7738	412.1900
UC	16	2	4	X	X	103.0396	65.9267	82.6721	86.3766	21.9850	392.6150
UC	16	3	4	X	X	90.2338	71.0096	76.4090	97.4653	40.8783	451.3805
UC	16	4	3	X	X	118.6627	97.3310	79.9315	224.6048	7.1606	419.5867
UC	16	5	5	X	X	107.9886	88.8025	90.2766	204.2723	34.9361	434.2251
UC	16	6	3	X	X	105.3239	72.4221	76.8655	119.6691	39.4180	425.5767
UC	17	1	1	22	1	2.0338	7.0122	2.0232	8.6323	19.5953	410.7297
UC	17	2	0	22	1	9.0195	0.1902	12.9755	22.1977	22.0599	405.4407
UC	17	3	0	22	1	14.3768	2.0963	3.6602	16.5170	21.2405	411.5254
UC	17	4	0	22	1	13.9148	-3.6922	5.1116	21.5377	9.9284	465.5858
UC	17	5	X	22	1	32.3059	12.8348	27.3105	67.7673	18.8053	448.8158
UC	17	6	3	22	1	58.5755	37.2587	56.0680	105.5990	60.7511	419.5464
UC	20	1	0	26	8	5.7780	0.6282	-2.3852	1.3241	-1.4984	407.8900
UC	20	2	0	26	8	1.9752	1.2027	4.3116	10.3770	0.4773	360.9973

Disease	Patient number	Biopsy number	A+C	ESR	CRP	CXCL1	CXCL2	CXCL3	CCL20	CCR6	Actin
UC	20	3	1	26	8	5.4671	-0.0795	10.7542	10.1988	4.2818	363.2218
UC	20	4	1	26	8	12.2917	3.4961	6.4713	17.6947	-8.9472	395.4206
UC	20	5	1	26	8	25.1548	8.3146	17.5892	10.3820	3.7700	759.5252
UC	20	6	1	26	8	15.4865	7.9634	16.6067	42.8783	1.8183	410.3911
UC	22	3	0	X	1	19.4916	-1.0965	-8.0291	18.0899	-0.1894	385.0719
UC	22	4	0	X	1	6.6813	-1.3051	-2.8120	15.9631	-3.1205	343.7870
UC	22	5	0	X	1	-7.2783	13.3539	-0.8630	11.7424	1.2650	343.6040
UC	22	6	0	X	1	13.1488	0.3253	15.9135	41.7960	3.3527	460.6306
UC	24	1	3	4	1	62.7557	24.4343	50.2653	28.9280	-17.7794	410.3400
UC	24	2	4	4	1	64.9093	37.1050	88.2906	31.6147	-1.0429	427.5066
UC	24	3	4	4	1	56.1021	31.8826	81.8871	48.2678	7.2570	417.1119
UC	24	4	4	4	1	70.4182	60.5149	80.2583	48.2665	7.8329	416.2848
NC	2	1	0	X	X	-0.2190	3.8335	5.2834	12.6271	7.1537	421.4732
NC	2	2	0	X	X	-8.8135	-15.1013	10.1989	13.7289	1.3280	469.6950
NC	2	3	0	X	X	-2.8988	4.5627	0.3383	17.9112	6.8110	483.6956
NC	2	4	0	X	X	-0.6211	7.5623	3.1030	20.0274	5.5511	409.6362
NC	2	5	0	X	X	0.5005	11.4150	10.3127	3.8930	9.3200	548.0643
NC	2	6	0	X	X	13.9239	-3.7388	9.8499	22.8854	5.3488	411.0658
NC	3	1	0	20	1	11.0390	12.5244	6.4053	22.7139	61.8943	325.1905
NC	3	2	1	20	1	7.2339	11.9648	-0.4453	32.6213	31.1152	413.1063
NC	3	3	2	20	1	26.5854	18.9765	26.2818	40.4560	34.8796	437.0917
NC	3	4	1	20	1	15.6659	6.1117	11.3393	19.1784	8.9297	424.3180
NC	3	5	1	20	1	40.5344	26.2632	30.9687	39.0233	83.2575	344.8207
NC	3	6	1	20	1	23.9518	36.7326	16.9440	22.1064	23.6298	378.8347
NC	4	1	0	10	X	-4.1463	3.7218	9.4150	10.9594	0.7727	420.8719
NC	4	2	0	10	X	4.8784	4.7943	5.4958	12.2348	0.8596	427.6017
NC	4	3	0	10	X	5.9780	-3.7342	4.7105	6.5080	0.5364	415.4632
NC	4	4	0	10	X	5.5466	10.4986	7.9543	7.4960	0.6581	449.3612
NC	4	5	0	10	X	5.5864	0.6016	2.8163	11.5737	1.4473	434.6147
NC	4	6	0	10	X	10.1648	6.9588	23.1799	38.1919	3.2657	508.0801
NC	5	1	0	30	2	-13.6005	38.8622	-3.5160	3.8918	0.1839	430.2939
NC	5	2	0	30	2	-2.5468	12.5896	5.8248	13.2968	0.2484	414.9209
NC	5	3	0	30	2	5.4174	-0.7200	-14.6395	22.1980	0.2506	451.1165
NC	5	4	0	30	2	17.1942	6.0634	14.7182	21.8759	0.7066	448.9122
NC	5	5	0	30	2	-26.0016	24.1237	1.0105	20.2189	0.4409	398.8933
NC	5	6	0	30	2	19.2480	37.1556	33.3878	1.0000	1.0789	376.5103
NC	6	1	0	X	X	7.9354	0.2333	4.0395	4.4832	0.2256	433.8658
NC	6	2	0	X	X	-0.0980	0.9326	6.3528	6.6286	0.7707	474.2064
NC	6	3	0	X	X	1.6096	1.1078	-4.8241	0.4066	0.4113	548.9994
NC	6	4	0	X	X	10.9319	4.2401	5.7460	4.7119	0.6264	386.2401
NC	6	5	0	X	X	10.1150	1.5485	3.3874	13.1870	1.3097	395.9917
NC	6	6	0	X	X	12.6332	2.1200	5.2575	15.6482	0.7061	401.6341
NC	7	1	0	14	1	11.1686	10.2053	4.3032	28.6057	0.3873	315.4730
NC	7	2	0	14	1	-6.5940	4.3403	11.8628	26.4948	0.3388	364.2574
NC	7	3	1	14	1	11.9159	5.8418	11.6333	37.4177	0.1210	389.1010
NC	7	4	1	14	1	7.2894	4.1901	9.2669	12.9519	0.4329	400.6389
NC	7	5	0	14	1	0.5613	25.9713	25.2512	26.0664	0.2590	415.3815
NC	7	6	0	14	1	21.8615	29.9831	24.0653	21.6639	0.4569	395.2661
NC	9	1	0	X	X	5.7519	1.7493	4.5685	15.6118	0.2191	313.6221
NC	9	2	0	X	X	6.7942	-2.7744	8.8658	24.6999	0.3801	390.7842
NC	9	3	0	X	X	18.2866	3.5256	18.6544	28.0346	1.0151	361.7976
NC	9	4	0	X	X	17.2065	10.1838	28.3822	36.3086	0.3475	408.5482
NC	9	5	0	X	X	17.2388	4.8350	32.2560	26.6987	0.6148	345.3693
NC	9	6	0	X	X	12.5234	9.4645	9.9836	16.1377	0.5193	307.7266
NC	12	4	0	6	X	20.2124	19.5941	22.1473	39.3281	9.0037	354.0463
NC	12	5	X	6	X	9.9150	13.2802	18.8921	62.7797	-1.4224	424.9258
NC	12	6	1	6	X	15.5039	19.6422	25.8823	42.6748	0.4324	409.4057
NC	13	1	0	X	X	3.9450	1.9831	2.6849	15.8513	2.7795	357.0173
NC	13	2	0	X	X	9.6373	2.1302	1.7465	2.4384	2.5851	361.8945
NC	13	3	0	X	X	1.4192	-0.8072	0.8242	6.6552	0.9122	348.5861
NC	13	4	0	X	X	8.3447	11.5721	26.9656	18.1984	1.6846	326.5469
NC	13	5	0	X	X	7.6176	6.0608	9.6638	13.0144	1.1867	383.2233
NC	13	6	0	X	X	9.6438	3.0351	12.1918	12.8499	2.6780	365.6987
IC	3	1	1	20	1	2.8818	-0.0721	8.8835	16.3687	3.9696	511.8683
IC	3	1	1	20	1	3.5660	9.7493	8.3908	11.4326	-7.8936	461.2344
IC	4	1	1	10	X	40.0601	17.6262	45.6392	3.9862	35.2708	292.3201
IC	5	1	X	30	2	8.4829	7.8139	21.7840	31.2960	3.2860	418.1888

Table 3.4: Relative expression levels of CCR7, CCL19, CCL21, CXCL13 and CXCR5, obtained by semi-quantitative assessment of the microarray result from colonic biopsy tissue, with inflammatory quotients. Where the level is less than 10-15, it is not significantly detected.

Disease	Patient number	Biopsy	A+C	ESR	CRP	CCL19 short	CCL19 long	CCL21	CXCL13	CCR7	CXCR5	CXCL8
CD	8	1	2	3	1	7.6581	29.2088	28.9176	14.5287	10.8450	81.7277	-0.1819
CD	8	2	2	3	1	2.7346	11.2992	4.1284	-0.6900	16.4589	9.6061	4.8334
CD	8	3	0	3	1	209.0410	11.8893	58.7563	-4.7489	43.0671	10.1236	1.1732
CD	8	4	0	3	1	13.2684	19.2475	18.7204	11.0482	37.9545	17.2862	3.5394
CD	8	5	X	3	1	7.3449	13.9501	12.5040	7.9865	21.5871	9.2578	3.5390
CD	8	6	X	3	1	-3.0583	10.1948	6.1761	-0.9555	26.8163	12.8334	1.5808
CD	10	1	1	7	1	-0.8761	7.9946	11.2768	-1.7905	19.3999	6.2641	2.6167
CD	10	2	0	7	1	0.0976	10.7994	10.1213	6.1080	17.9285	9.5862	1.7082
CD	10	3	0	7	1	11.4965	21.4767	20.0390	7.7364	22.6354	7.1186	1.8931
CD	10	4	0	7	1	0.8461	5.1800	8.3065	2.8924	24.5054	6.2873	4.5789
CD	10	5	2	7	1	6.4503	4.4060	10.7450	-1.1166	4.2780	9.4003	0.0206
CD	10	6	1	7	1	3.1619	10.0532	13.4567	3.8653	10.7812	4.4354	2.7000
CD	11	1	1	54	X	3.0086	2.2213	12.6301	0.5462	20.7683	0.5445	13.5040
CD	11	2	3	54	X	-1.2965	15.5683	27.4084	8.3496	7.1200	9.2191	16.8727
CD	11	3	2	54	X	28.4447	32.9960	96.0469	17.0314	-2.3114	10.7802	18.2085
CD	11	4	3	54	X	3.7283	7.5096	6.9889	14.9440	7.0013	5.0862	19.5457
CD	11	5	4	54	X	0.9670	7.3360	8.9196	10.3291	5.9364	3.5415	59.8868
CD	11	6	1	54	X	0.1832	-0.6607	4.8776	-3.3372	3.3199	6.6745	3.9208
CD	19	1	0	5	2	3.3187	-7.1466	9.2631	-0.7019	6.5212	10.1022	-6.0164
CD	19	2	1	5	2	1.4921	14.0847	12.1638	-1.6701	9.1831	23.2061	1.6790
CD	19	3	0	5	2	1.4921	14.0847	12.1638	-1.6701	9.1831	23.2061	1.6790
CD	19	4	0	5	2	-4.6988	8.4206	7.5084	-2.5888	12.3966	9.2351	-4.3788
CD	19	5	0	5	2	-4.4922	7.4541	7.2124	-2.1790	-16.5177	-1.8619	-1.9305
CD	19	6	0	5	2	1.6137	21.8513	11.3711	-5.0340	2.9210	15.1517	-2.4679
CD	26	1	2	11	33	31.3665	60.1897	27.3112	5.7301	1.1894	12.7171	-2.0090
CD	26	2	0	11	33	-8.7378	5.9646	7.9664	-6.7465	4.0731	6.6842	23.9084
CD	26	3	0	11	33	-37.0787	1.4498	11.9805	-0.5556	-7.2235	6.7070	-2.7596
CD	26	4	2	11	33	1.6311	17.2077	20.1109	1.0019	-14.5687	3.0035	-38.6880
CD	26	5	0	11	33	9.4313	-1.9122	-0.9009	-7.1680	-14.2496	1.2181	-14.7967
CD	26	6	0	11	33	7.9726	15.6101	26.6885	8.7783	4.7347	13.8981	11.2733
CD	27	1	0	X	X	9.7631	10.5542	-11.0040	8.2011	0.4688	13.8591	0.6439
CD	27	2	0	X	X	31.1344	33.6573	-35.0917	26.1532	1.4951	44.1970	2.0534
CD	27	3	0	X	X	-4.1570	9.1017	12.8357	9.5212	-0.8316	7.0025	4.1978
CD	27	4	0	X	X	0.0425	6.5080	17.8134	10.5345	-9.5009	3.8199	12.7330
CD	27	5	0	X	X	-2.9595	14.3328	15.2978	-5.7541	-2.4500	-3.8697	-5.9125
CD	27	6	0	X	X	1.9984	11.0430	8.1336	-5.2033	-4.1619	11.9705	3.8767
CD	27	7	X	X	X	-12.6654	20.5955	12.4645	0.4112	2.1117	-1.9424	-8.0434
CD	27	8	X	X	X	-19.9827	-6.9545	6.1389	5.5546	-1.9828	5.1960	-5.7294
UC	14	1	3	X	2	12.8838	4.7847	11.6083	1.8787	8.6508	6.4955	13.6191
UC	14	2	4	X	2	-3.5283	80.2029	3.4903	-2.9167	3.7391	-1.9638	4.6304
UC	14	3	4	X	2	-1.6180	4.8091	3.1028	1.9747	1.8587	2.4761	6.9737
UC	14	4	4	X	2	1.7872	3.2716	9.9296	13.1798	3.0661	11.4435	8.8113
UC	14	5	4	X	2	0.3775	8.4917	7.2897	1.7714	6.4952	-3.5527	5.1588
UC	14	6	4	X	2	-4.8138	2.9504	5.3615	-0.4459	-1.7607	5.2091	5.4667
UC	15	1	0	6	1	0.5210	-0.1340	6.5862	5.0589	1.8926	1.6806	0.3478
UC	15	2	0	6	1	1.8272	4.4262	10.8671	-1.7412	4.4147	6.9705	4.2910
UC	15	3	1	6	1	-0.2943	3.7539	12.5093	3.5619	7.8079	2.7836	3.0939
UC	15	4	0	6	1	-1.1880	5.0040	8.9187	4.9855	3.6431	12.0449	-2.3053
UC	15	5	0	6	1	1.3974	4.8396	10.8582	-0.2338	7.6099	10.2486	7.6280
UC	15	6	0	6	1	19.5669	30.6941	17.4520	1.1224	7.5021	8.0306	6.0069
UC	16	1	4	X	X	36.9432	54.9627	59.3990	35.1498	2.7882	9.9558	13.2467
UC	16	2	4	X	X	3.2956	9.9494	9.5015	6.5135	3.4179	7.3107	9.7835
UC	16	3	4	X	X	10.1472	26.0315	29.1819	45.8887	15.7030	13.6140	11.9205
UC	16	4	3	X	X	2.4790	12.9980	10.8539	17.5342	8.8656	6.1149	20.0756
UC	16	5	5	X	X	11.2685	31.8955	15.7963	59.2312	11.3312	10.2872	15.2563
UC	16	6	3	X	X	47.1082	69.0461	38.5265	62.6923	18.7282	14.4698	17.2829
UC	17	1	1	22	1	7.3407	5.0736	8.1977	2.3441	12.3994	10.3353	-1.6825
UC	17	2	0	22	1	35.7244	41.9542	38.1714	21.6300	8.7141	11.6315	-3.2986
UC	17	3	0	22	1	6.4894	12.2391	13.0674	8.2545	23.6407	9.3071	-1.2612
UC	17	4	0	22	1	5.0388	8.8711	10.8017	5.9472	17.3592	1.7765	-2.1548
UC	17	5	X	22	1	1.2781	9.3549	14.8944	9.9485	13.6105	10.6372	5.1620
UC	17	6	3	22	1	88.2710	134.3733	69.4340	99.6166	28.8345	21.0437	2.1289

Disease	Patient number	Biopsy	A+C	ESR	CRP	CCL19 short	CCL19 long	CCL21	CXCL13	CCR7	CXCR5	CXCL8
UC	20	1	0	26	8	5.0084	19.4135	10.9561	-1.6759	1.4228	8.3414	-1.8178
UC	20	2	0	26	8	-0.4509	9.5686	11.8070	-5.0168	5.6925	9.9194	-0.5710
UC	20	3	1	26	8	0.9877	10.9630	17.2868	-2.0292	9.9104	12.4680	-0.8514
UC	20	4	1	26	8	4.4308	6.7246	3.6139	4.3999	3.7466	8.8405	-2.1269
UC	20	5	1	26	8	5.8725	13.7329	5.6941	1.4235	10.7152	11.8684	-2.6398
UC	20	6	1	26	8	3.8814	14.7841	17.3264	-1.5036	5.3017	7.5052	-5.8846
UC	22	3	0	X	1	1.7384	10.1790	10.5660	8.0127	16.9505	0.7957	-0.6030
UC	22	4	0	X	1	-4.2549	5.5911	20.2179	-1.8184	3.9343	6.4861	-5.9077
UC	22	5	0	X	1	0.2766	-2.3730	5.1754	-3.6308	9.2649	-3.6305	-1.7037
UC	22	6	0	X	1	3.0647	6.2282	8.1864	-2.2321	8.8406	0.2292	-4.8815
UC	24	1	3	4	1	2.2075	7.3644	11.1046	14.8181	5.3318	5.8116	0.7705
UC	24	2	4	4	1	0.1871	1.8169	6.6823	-1.0231	8.1877	-0.5225	13.4531
UC	24	3	4	4	1	2.2329	13.6567	14.4873	6.0288	4.1717	-2.5316	1.7076
UC	24	4	4	4	1	7.8019	19.3153	13.4334	21.0819	7.8002	-0.4840	37.6692
NC	2	1	0	X	X	3.5581	8.5048	9.8491	0.8969	12.1968	14.1511	-4.7694
NC	2	2	0	X	X	-7.8975	6.7777	2.3277	17.7092	5.5701	3.2277	-12.2402
NC	2	3	0	X	X	31.4751	21.4957	46.1526	19.6399	34.9106	27.2836	14.0265
NC	2	4	0	X	X	-7.6105	0.8107	6.1071	4.9509	3.9116	-3.4362	-5.5954
NC	2	5	0	X	X	19.0203	53.7535	37.0881	51.8065	3.3122	11.1621	5.3086
NC	2	6	0	X	X	-2.4631	6.6079	-8.8340	5.9300	22.5041	4.1707	-0.4959
NC	3	1	0	20	1	15.6914	38.2060	30.5783	12.9128	12.6706	13.3367	-2.1418
NC	3	2	1	20	1	5.6925	10.2639	13.8114	-3.0140	3.6981	16.3039	3.6653
NC	3	3	2	20	1	27.1241	49.2010	31.7655	15.3147	17.7188	8.7626	2.9741
NC	3	4	1	20	1	17.4636	20.0613	19.3559	10.6457	30.2603	5.5648	6.2912
NC	3	5	1	20	1	13.1248	17.3120	18.6057	0.9599	7.4777	16.6884	3.3314
NC	3	6	1	20	1	1.9407	16.4544	26.3330	2.5937	-4.2338	13.7842	-3.0538
NC	4	1	0	10	X	1.9229	5.1465	6.6557	2.2877	14.2748	10.2489	0.7698
NC	4	2	0	10	X	5.4008	1.3795	8.8734	2.7536	18.3080	9.7615	3.6875
NC	4	3	0	10	X	4.6348	6.1205	9.0752	-1.1446	16.9712	7.4117	0.1056
NC	4	4	0	10	X	7.9311	8.0614	11.6834	27.8008	15.0571	9.3106	-1.2664
NC	4	5	0	10	X	16.1057	25.7403	12.6617	8.5232	20.3600	12.3805	0.3611
NC	4	6	0	10	X	42.5884	50.7304	38.8753	30.9698	13.3283	14.9105	0.7099
NC	5	1	0	30	2	0.1789	7.0962	8.7325	2.9334	2.1497	6.3069	-6.1130
NC	5	2	0	30	2	2.0633	-2.1682	-8.3346	4.1179	18.6054	13.0402	-3.8090
NC	5	3	0	30	2	-7.3306	7.7019	9.9181	-5.3538	11.4509	26.4846	-0.2731
NC	5	4	0	30	2	1.8923	10.9343	19.6860	2.4224	13.4831	9.3148	1.7098
NC	5	5	0	30	2	1.3899	-21.9865	-4.0219	-15.2481	9.8971	22.5527	-14.1184
NC	5	6	0	30	2	3.1955	35.4591	11.7773	12.6391	367.0143	24.3462	-15.1666
NC	6	1	0	X	X	13.1030	7.5496	8.7489	-4.7393	10.6871	12.8758	9.5895
NC	6	2	0	X	X	1.1098	11.4558	5.8427	9.8245	6.8518	15.2700	-4.7680
NC	6	3	0	X	X	1.7524	1.5651	2.0339	-6.6688	5.9768	0.5578	-11.4182
NC	6	4	0	X	X	0.1256	14.7076	15.2024	2.9270	8.2903	14.2177	1.4508
NC	6	5	0	X	X	8.2528	23.5727	24.4094	-2.0329	8.3183	8.9493	1.9416
NC	6	6	0	X	X	2.4444	29.9691	17.1879	3.1797	12.4404	10.1869	3.6470
NC	7	1	0	14	1	17.0808	39.6253	30.9546	2.2243	4.8009	21.0702	-9.3324
NC	7	2	0	14	1	-5.3062	10.5144	5.8440	1.1078	1.5271	6.6097	-3.3164
NC	7	3	1	14	1	16.0274	38.7308	24.7255	9.5000	2.8103	8.3895	-5.6282
NC	7	4	1	14	1	4.1168	16.2114	11.5148	4.4228	6.8181	3.8885	-5.6635
NC	7	5	0	14	1	7.0067	44.7141	8.9021	12.0586	7.8501	5.2735	-0.1578
NC	7	6	0	14	1	0.9607	13.7405	33.5027	0.5714	5.1014	5.6152	-1.9661
NC	9	1	0	X	X	-0.6237	2.1657	4.2602	-0.9949	14.6228	1.1620	-2.2458
NC	9	2	0	X	X	4.7468	6.3981	12.8400	3.0555	13.3034	4.2095	-4.6635
NC	9	3	0	X	X	11.5569	17.1895	10.3323	-1.0014	18.6148	3.2712	-0.3492
NC	9	4	0	X	X	7.6883	9.3791	4.8633	0.5055	23.4021	3.3725	2.1493
NC	9	5	0	X	X	4.6625	11.1430	12.5488	0.0579	28.6400	5.7093	-8.6612
NC	9	6	0	X	X	7.4789	11.7408	24.1539	5.1806	17.4734	3.5281	-3.2698
NC	12	1	0	6	X	10.5100	23.9294	11.6897	-0.0663	15.3215	6.6667	3.1860
NC	12	2	X	6	X	6.5845	13.6571	8.3560	10.2589	2.0937	3.2265	0.8247
NC	12	3	1	6	X	19.1073	42.5240	15.0341	3.0582	1.9642	35.5199	2.1393
NC	13	1	0	X	X	8.7003	11.6789	17.3732	6.0980	3.3015	0.1839	-0.1994
NC	13	2	0	X	X	4.8109	11.2980	9.5787	4.0205	9.0082	2.0883	-0.5702
NC	13	3	0	X	X	3.7208	4.3525	15.8914	1.7759	5.6123	0.0771	-0.3258
NC	13	4	0	X	X	14.7825	17.7772	31.8412	4.5306	11.1243	11.5630	5.3570
NC	13	5	0	X	X	2.8245	4.3762	18.6069	5.1186	8.0976	3.7216	5.0515
NC	13	6	0	X	X	7.6005	5.5330	9.3008	4.9067	9.6400	2.4577	0.4661
IC	3	1	1	20	1	-1.9539	12.7037	25.4656	-4.9228	5.3993	6.9070	-1.4900
IC	3	1	1	20	1	2.6676	13.1229	9.9517	2.3246	1.1680	-2.3700	-4.0568

Disease	Patient number	Biopsy	A+C	CRP	ESR	CCL19 short	CCL19 long	CCL21	CXCL13	CCR7	CXCR5	CXCL8
IC	4	1	1	10	X	6.3302	30.9513	46.2831	1.3017	32.0367	17.9000	35.2708
IC	5	1	X	30	2	3.8937	26.0358	56.2811	6.8028	12.4964	8.1859	0.3478

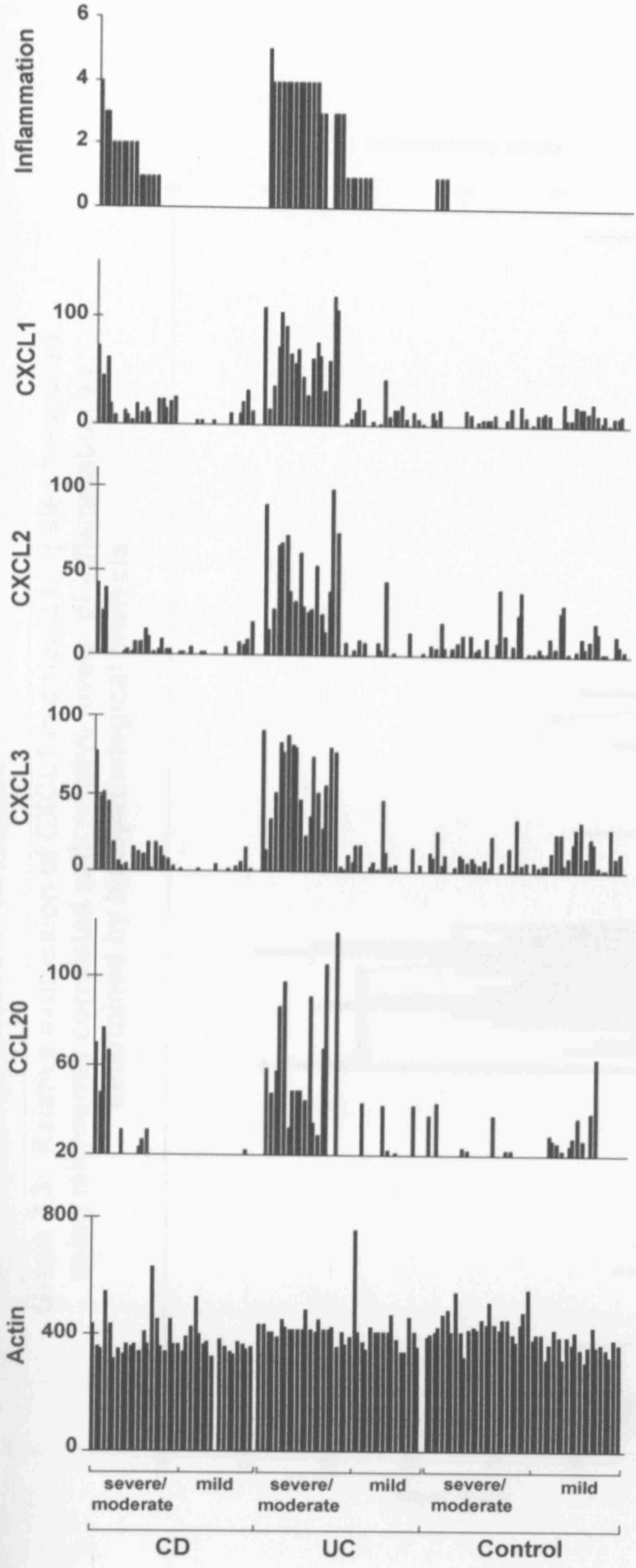

Graph 3.2: Data from colonic biopsy tissue. Relative expression levels of selected chemokines and actin measured by microarray analysis, in comparison to relative levels of inflammation as determined by histopathological analysis. Inflammation is given as a cumulative score for acute and chronic inflammation. Samples are grouped according to CD, UC or control cohort.

Graph 3.3: Relative expression of CXCL1 in colonic biopsies measured using microarray correlated with relative levels of inflammation as determined by histopathological analysis

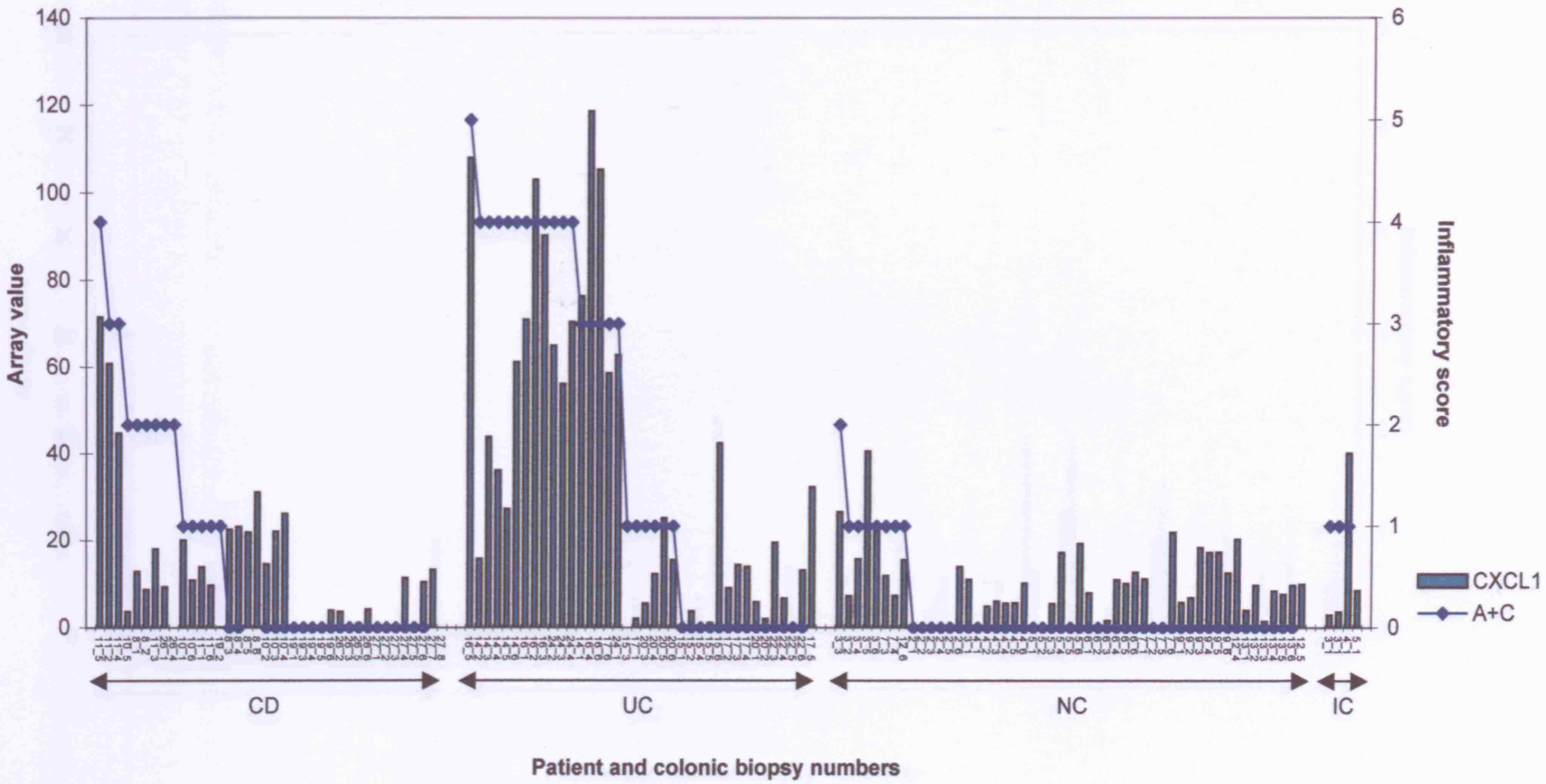

Patients are grouped according to disease, and chronologically placed according to inflammatory scores A+C (as defined in table 2.3). Patient and colonic biopsy details are outlined in appendix table 1. NC=normal control, IC=inflammatory control.

Graph 3.4: Relative expression of CXCL2 in colonic biopsies measured using microarray correlated with relative levels of inflammation as determined by histopathological analysis

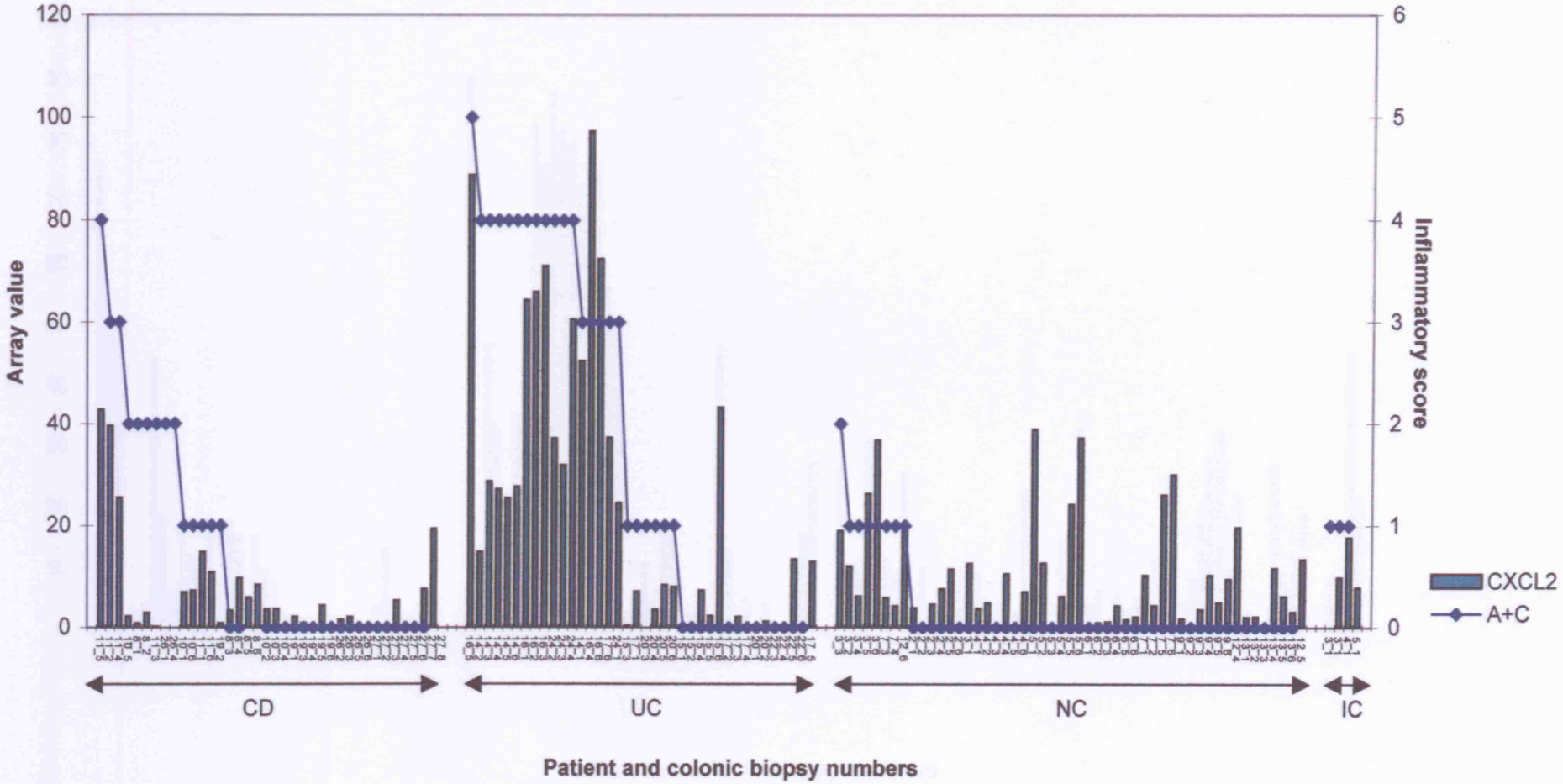

Patients are grouped according to disease, and chronologically placed according to inflammatory scores A+C (as defined in table 2.1). Patient and colonic biopsy details are outlined in appendix table 1. NC=normal control, IC=inflammatory control.

Graph 3.5: Relative expression of CXCL3 in colonic biopsies measured using microarray analysis correlated with relative levels of inflammation as determined by histopathological analysis

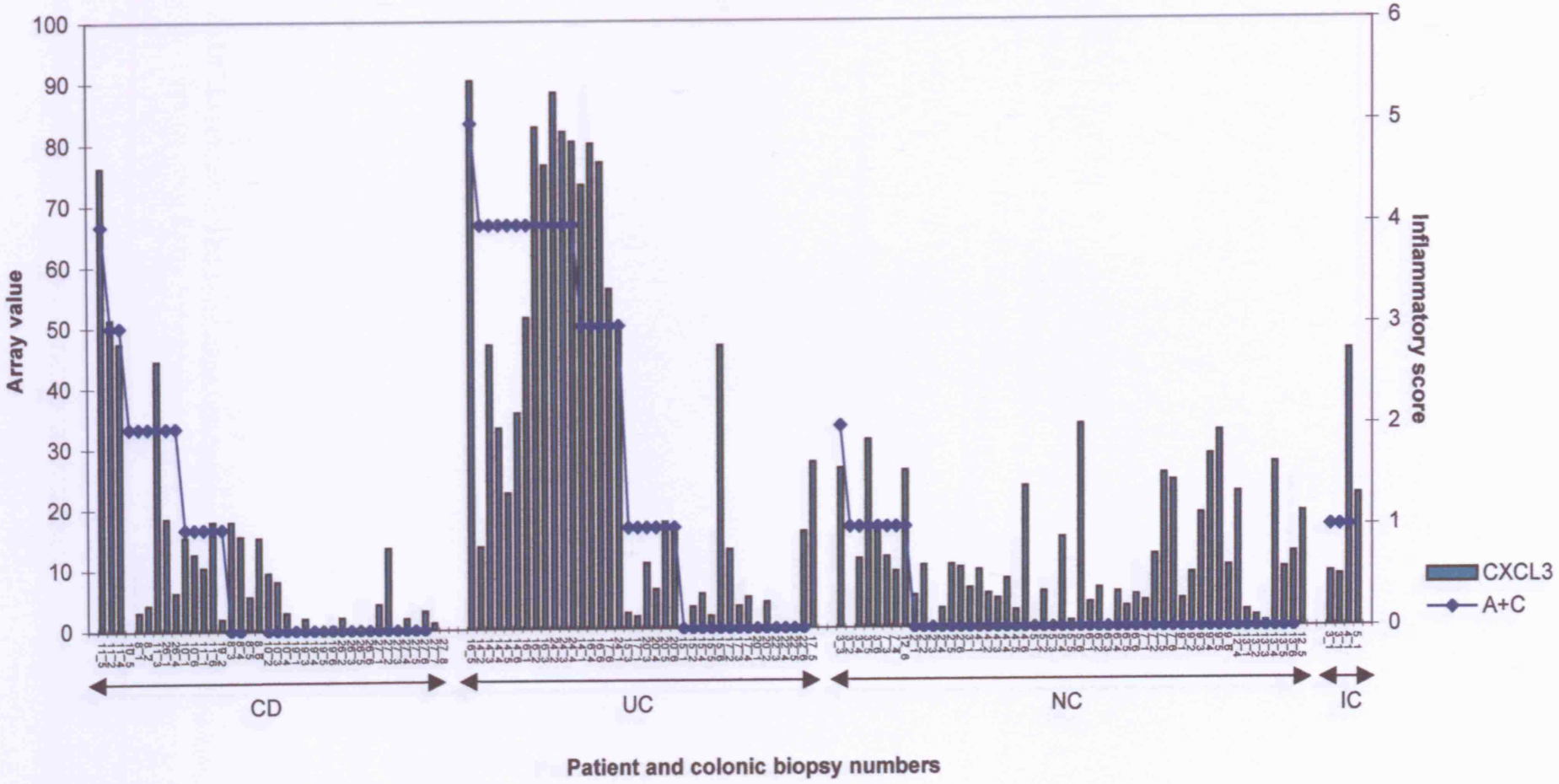

Patients are grouped according to disease, and chronologically placed according to inflammatory scores A+C (as defined in table 2.1). Patient and colonic biopsy details are outlined in appendix table 1. NC=normal control, IC=inflammatory control.

Graph 3.6: Relative expression of CCL20 in colonic biopsies measured using microarray correlated with relative levels of inflammation as determined by histopathological analysis

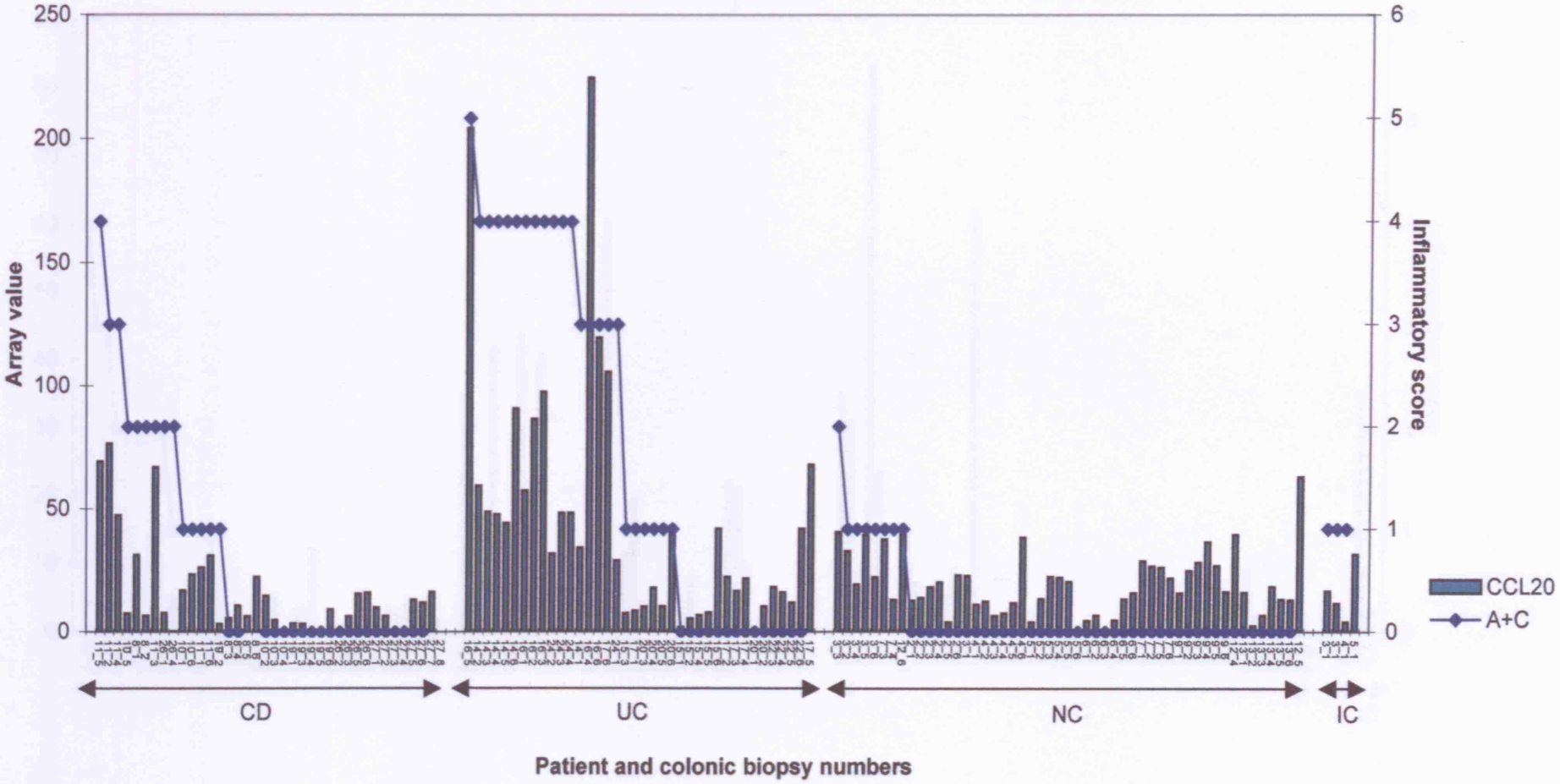

Patients are grouped according to disease, and chronologically placed according to inflammatory scores A+C (as defined in table 2.1). Patient and colonic biopsy details are outlined in appendix table 1. NC=normal control, IC=inflammatory control.

Graph 3.7: Relative expression of CCR6 in colonic biopsies measured using microarray correlated with relative levels of inflammation as determined by histopathological analysis

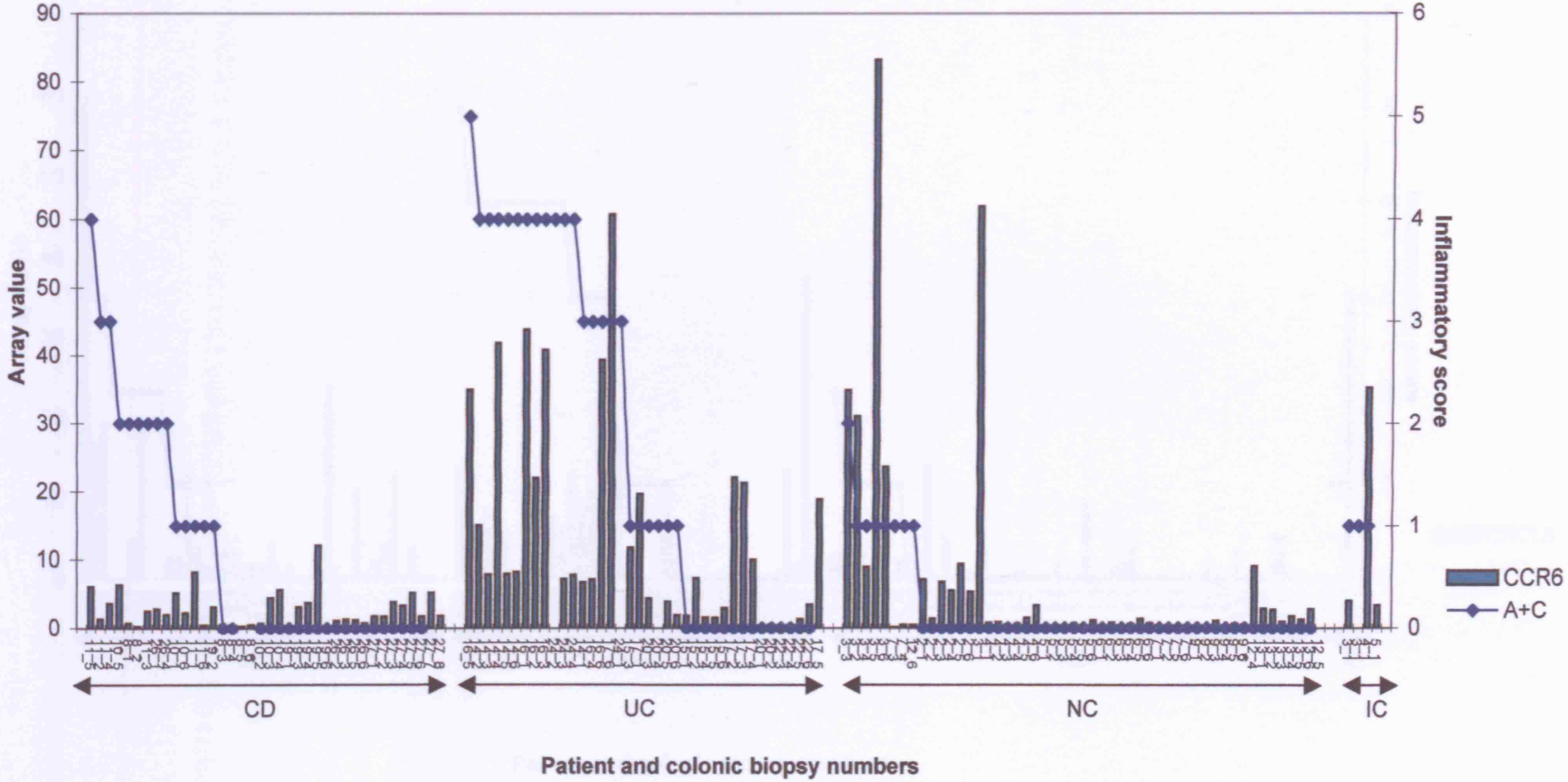

Patients are grouped according to disease, and chronologically placed according to inflammatory scores A+C (as defined in table 2.1). Patient and colonic biopsy details are outlined in appendix table 1. NC=normal control, IC=inflammatory control.

Graph 3.8: Relative expression of CXCL8 in colonic biopsies measured using microarray correlated with relative levels of inflammation as determined by histopathological analysis

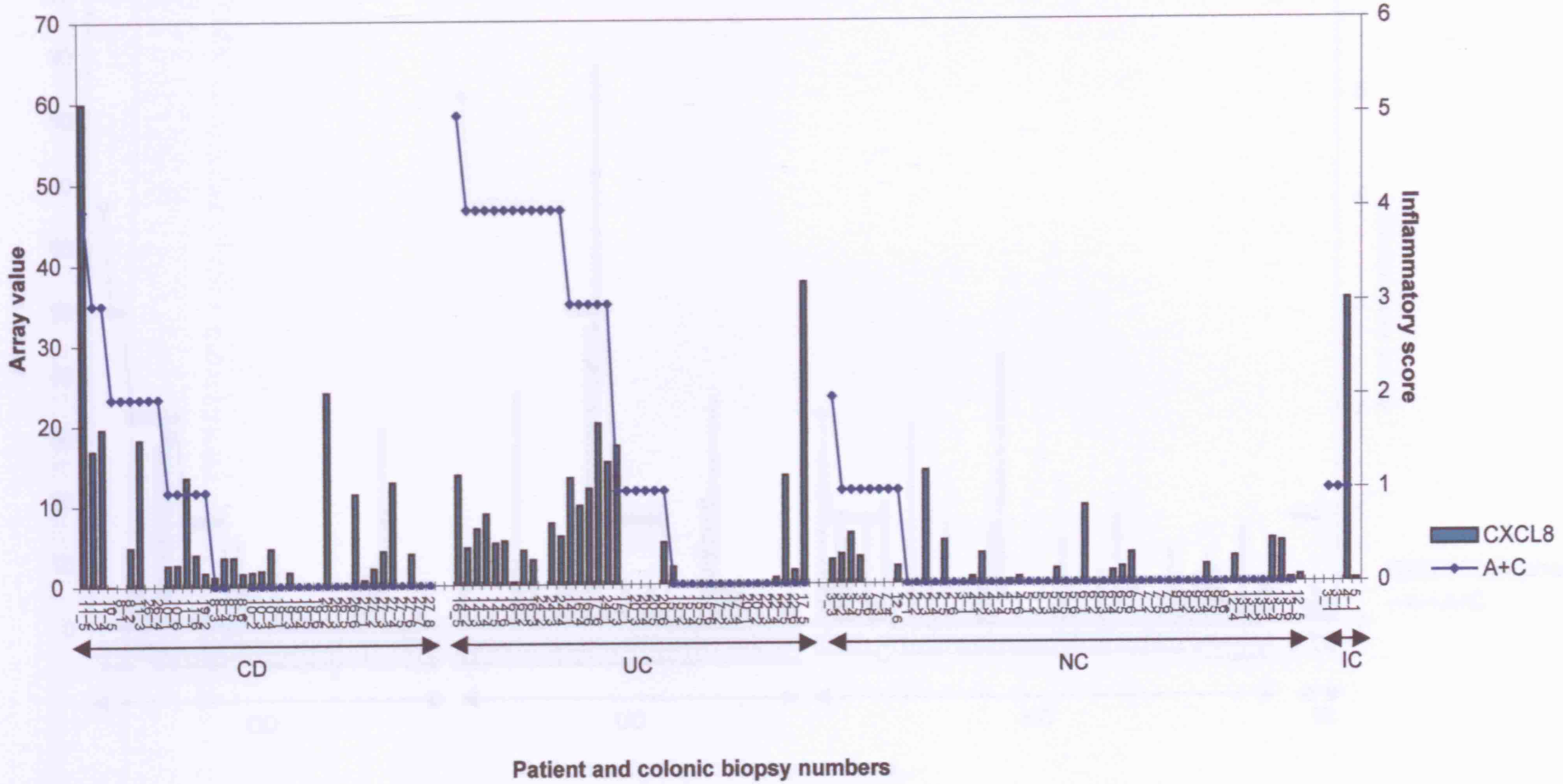

Patients are grouped according to disease, and chronologically placed according to inflammatory scores A+C (as defined in table 2.3). Patient and colonic biopsy details are outlined in appendix table 1. NC=normal control, IC=inflammatory control.

Graph 3.9: Relative expression of CCL19 (short arm) in colonic biopsies measured using microarray correlated with relative levels of inflammation as determined by histopathologocal analysis

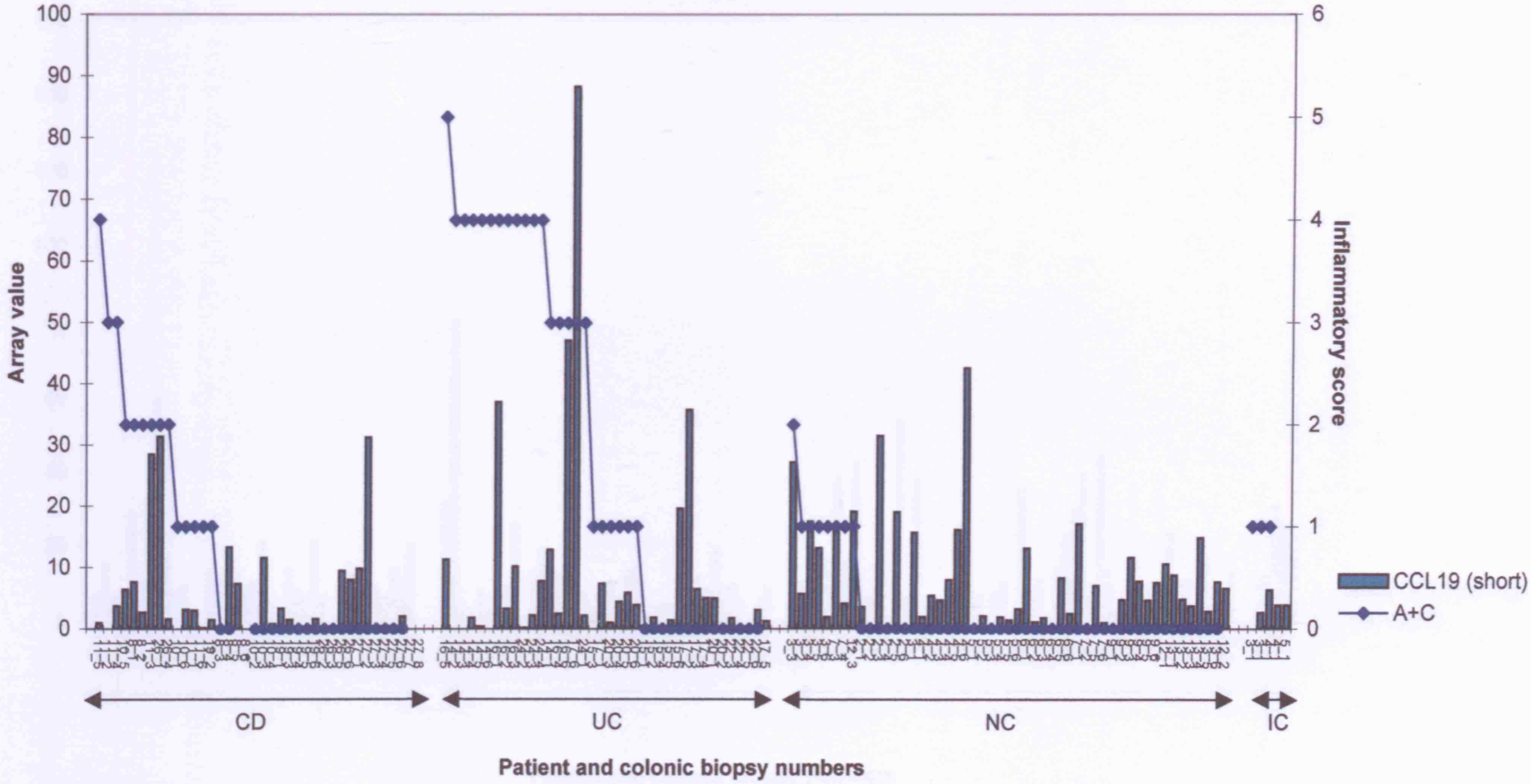

Patients are grouped according to disease, and chronologically placed according to inflammatory scores A+C (as defined in table 2.1). Patient and colonic biopsy details are outlined in appendix table 1. NC=normal control, IC=inflammatory control.

Graph 3.10: Relative expression of CCL19 (long arm) in colonic biopsies measured using microarray correlated with relative levels of inflammation as determined by histopathological analysis

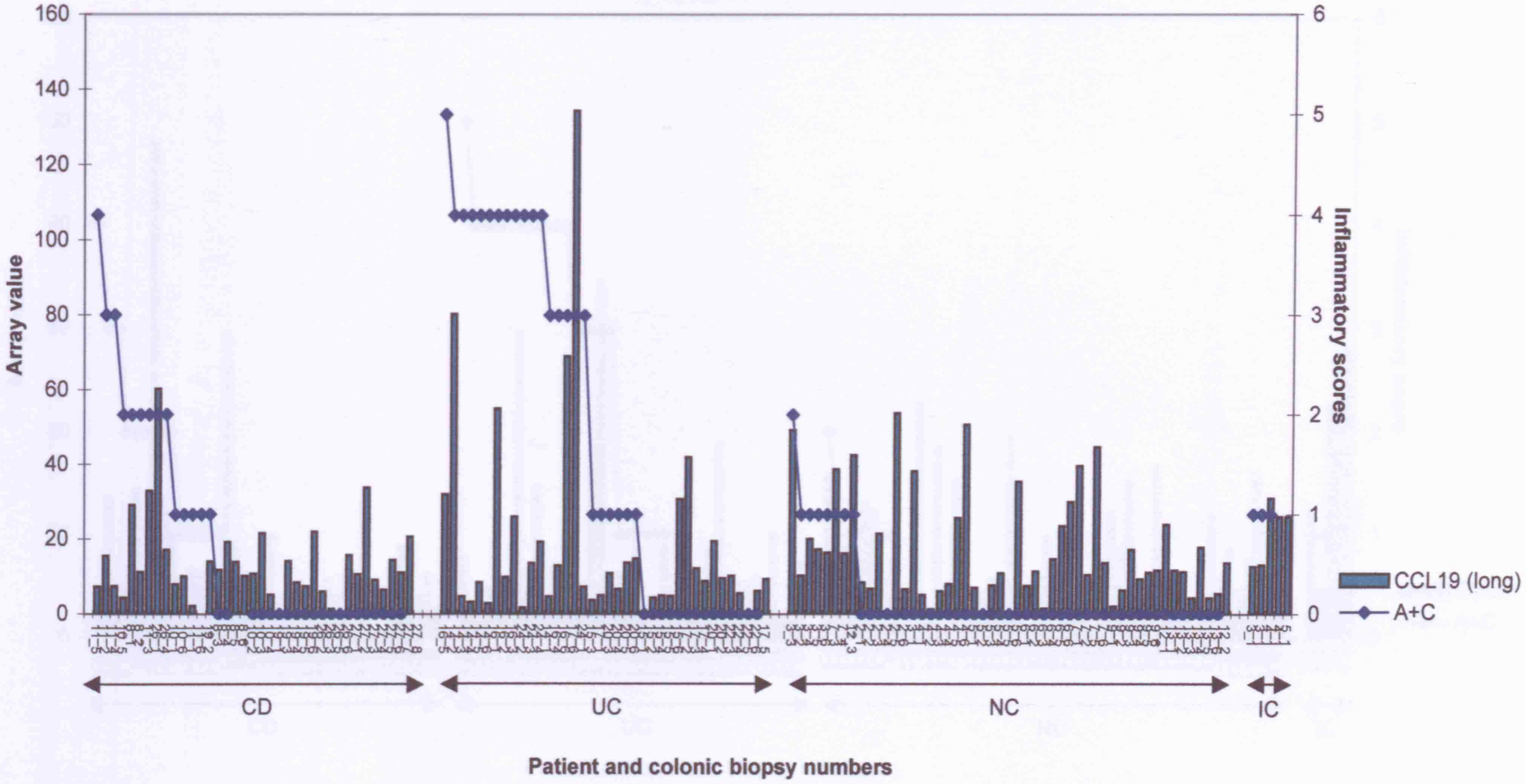

Patients are grouped according to disease, and chronologically placed according to inflammtory scores A+C (as defined in table 2.1). Patients and colonic biopsy details are outlined in appendix table 1. NC=normal control, IC=inflammatory control.

Graph 3.11: Relative expression of CCL21 in colonic biopsies measured using microarray correlated with relative levels of inflammation as determined by histopathological analysis

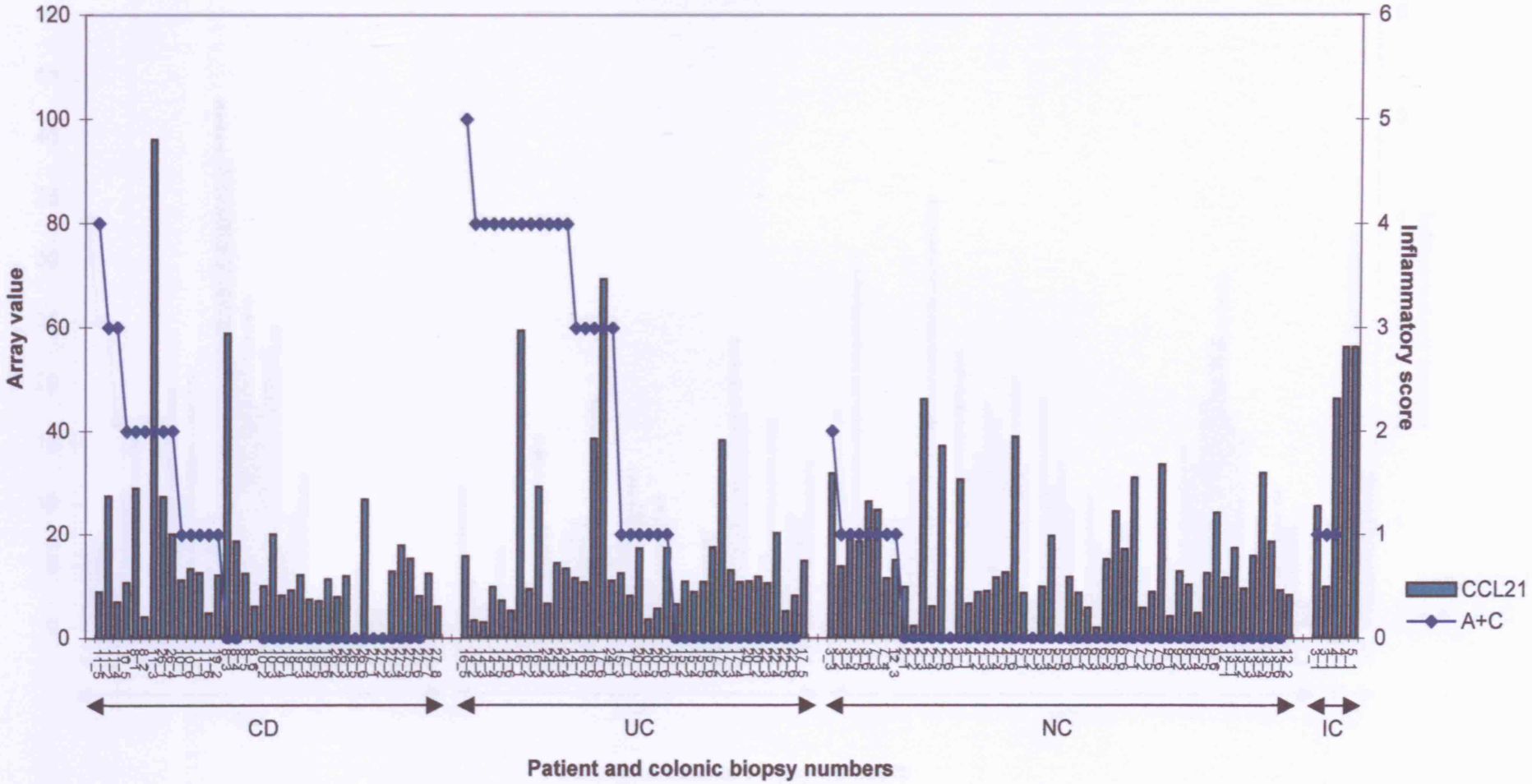

Patients are grouped according to disease, and chronologically placed according to inflammatory scores A+C (as defined in table 2.1). Patients and colonic biopsy details are outlined in appendix table 1. NC=normal control, IC=inflammatory control.

Graph 3.12: Relative expression of CCR7 in colonic biopsies measured using microarray correlated with relative levels of inflammation as determined by histopathological analysis

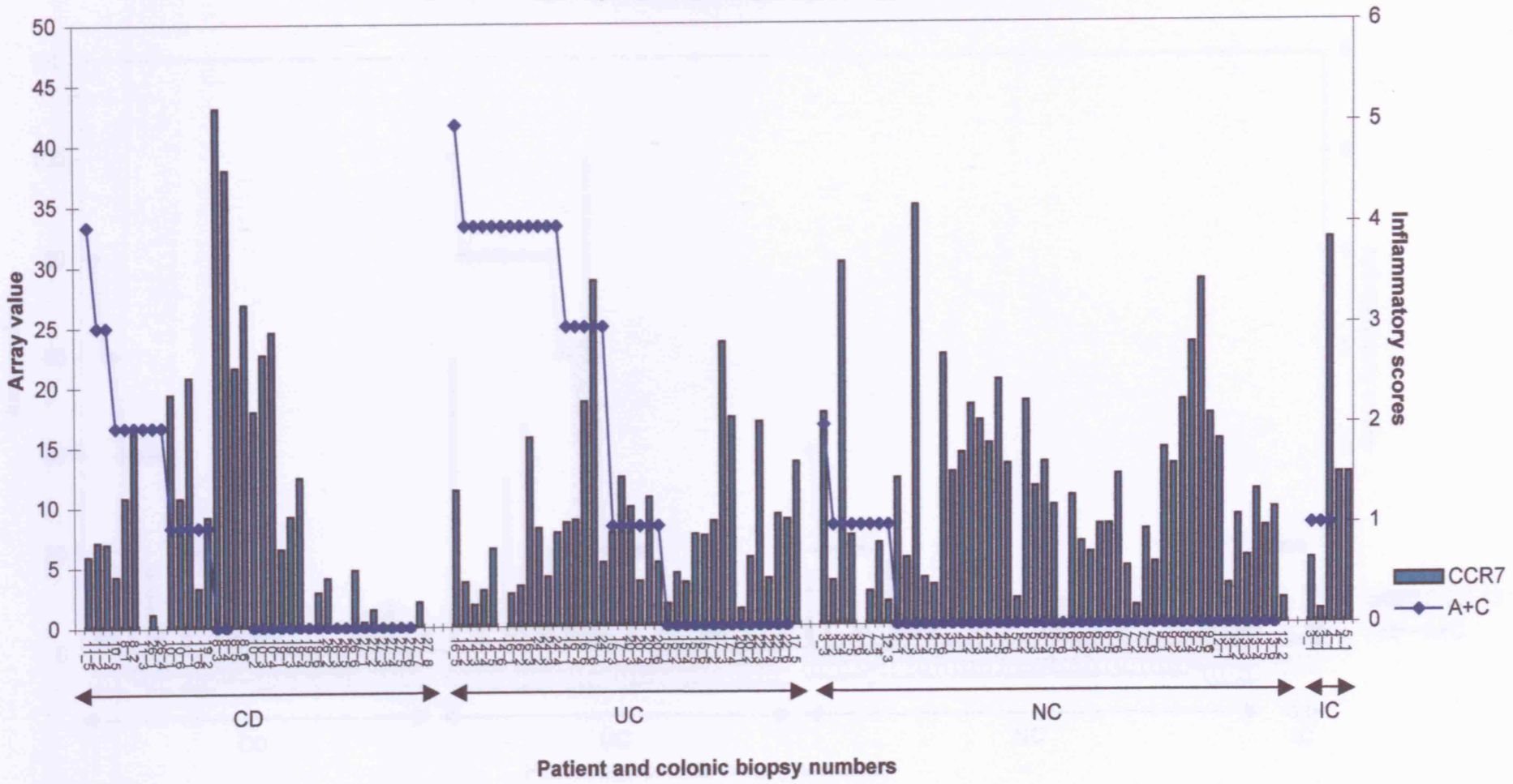

Patients are grouped according to disease, and chronologically placed according to inflammatory scores A+C (as defined in table 2.1). Patient and colonic biopsy details are outlined in appendix table 1. NC=normal control, IC=inflammatory control.

Graph 3.13: Relative expression of CXCL13 in colonic biopsies measured using microarray correlated with relative levels of inflammation as determined by histopathological analysis

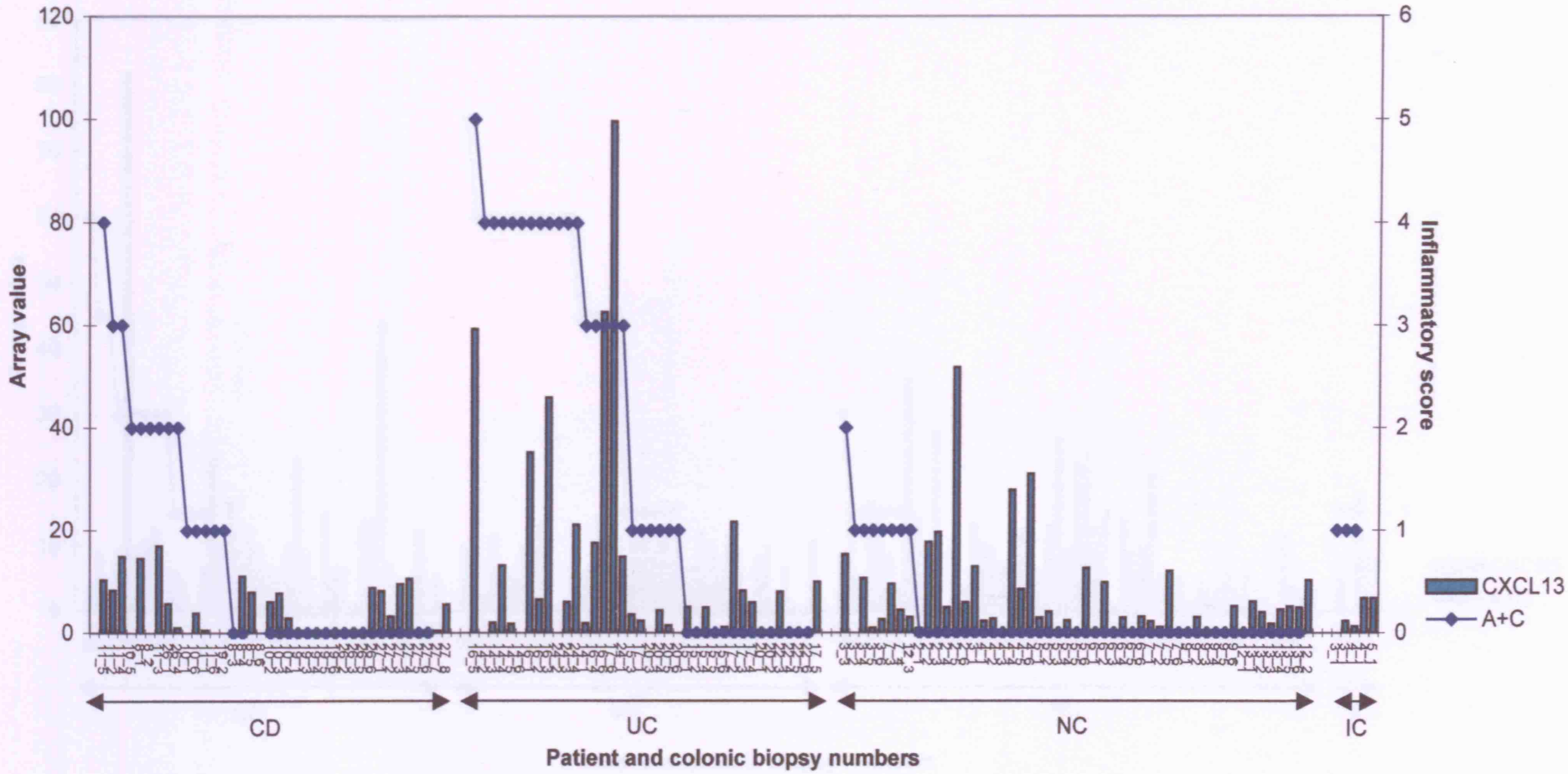

Patients are grouped according to disease, and chronologically placed according to inflammatory scores A+C (as defined in table 2.1). Patient and colonic biopsy details are outlined in appendix table 1. NC=normal control, IC=inflammatory control.

Graph 3.14: Relative expression of CXCR5 in colonic biopsies measured using microarray correlated with relative levels of inflammation as determined by histopathological analysis

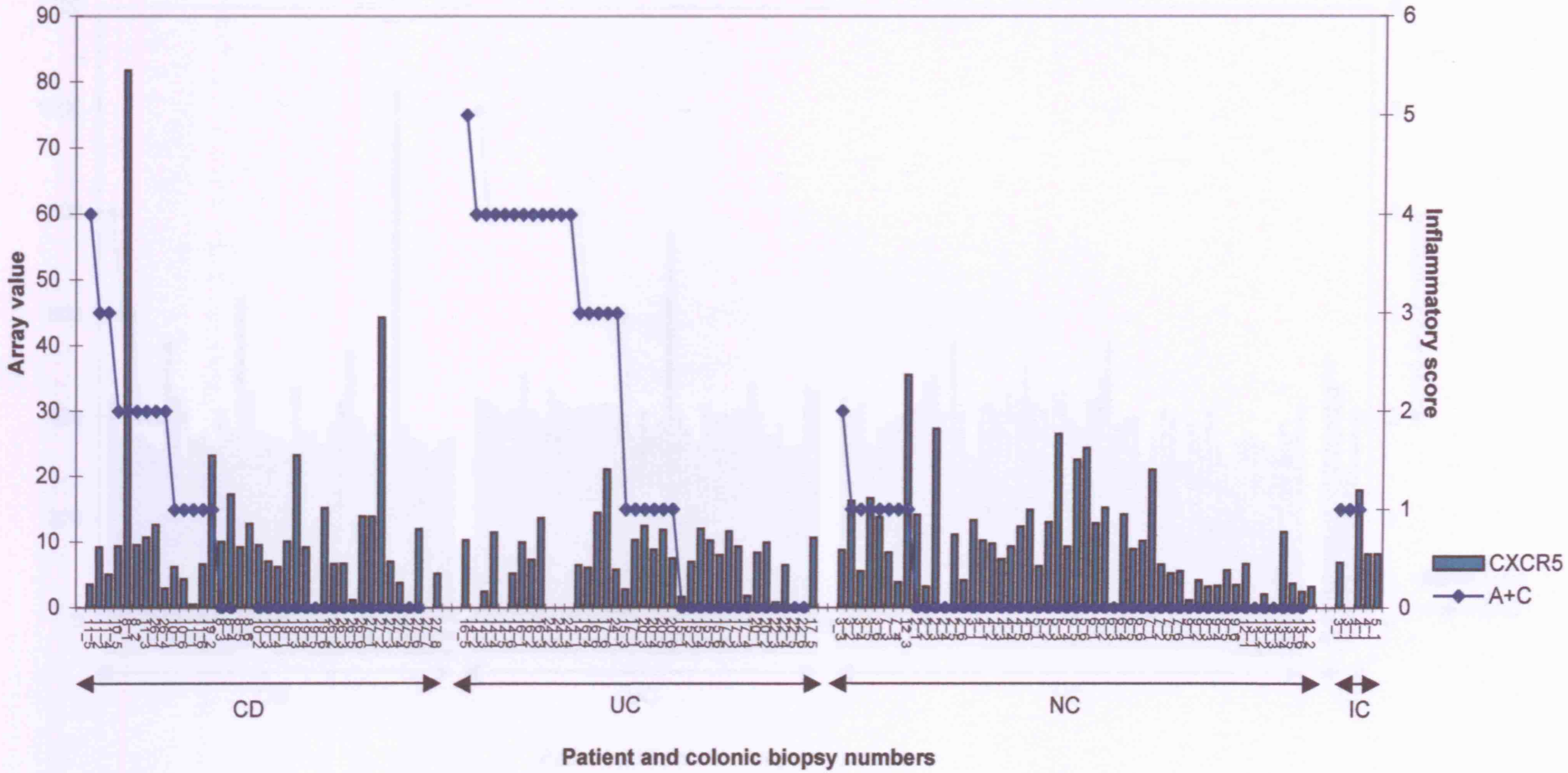

Patients are grouped according to disease, and chronologically placed according to inflammatory scores A+C (as defined in table 2.1). Patient and colonic biopsy details are outlined in appendix table 1. NC=normal control, IC=inflammatory control.

Graph 3.15: Relative expression of actin in colonic biopsies measured using microarray correlated with relative levels of inflammation as determined by histopathological analysis

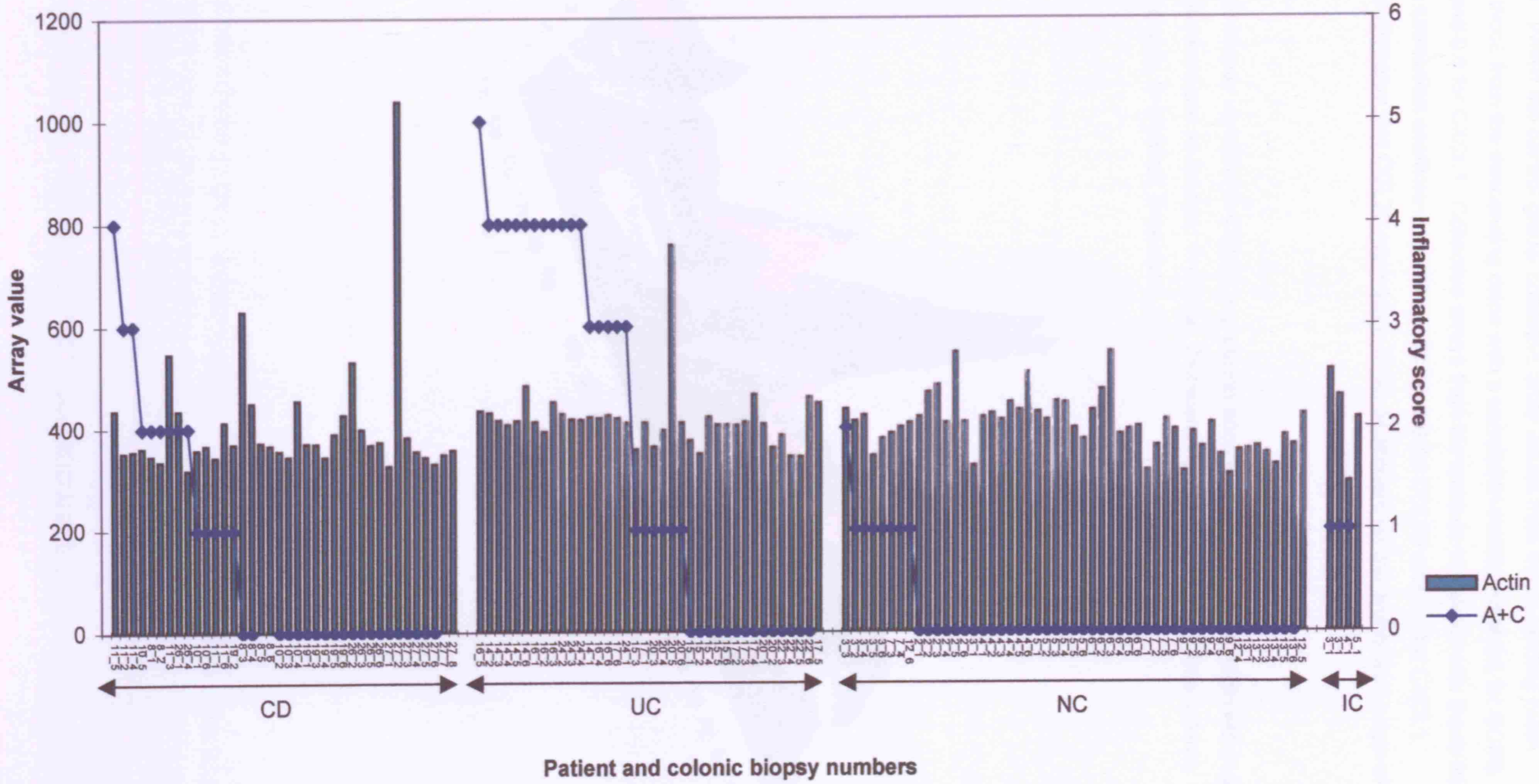

Patients are grouped according to disease, and chronologically placed accoprding to inflammatory scores A+C (as defined in table 2.1). Patients and colonic biopsy details are outlined in appendix table 1. NC=normal control, IC=inflammatory control.

Any variation in chemokine expression is not dependent on the anatomical origin of the biopsy within the colon. Within the control group, collective array values from the ascending colon correlated with those from the descending colon with a correlation coefficient of 0.9 for CCR6, 0.8 for CCL20 and 0.6 for CXCL1. Collective arrays from the caecum correlated with those from the rectum with correlation coefficients of 0.9 for CCR6, 0.3 for CCL20 and 0.2 for CXCL1. Graph 3.16 demonstrates that CCL20 expression is not dependent on the anatomical origin of the biopsy.

Graph 3.16: Inter-biopsy variation in CCL20 expression according to anatomical origin within the colon. Biopsy numbers are as follows: 1=caecal, 2=ascending colonic, 3=transverse colonic, 4=descending colonic, 5=sigmoid, 6=rectal.

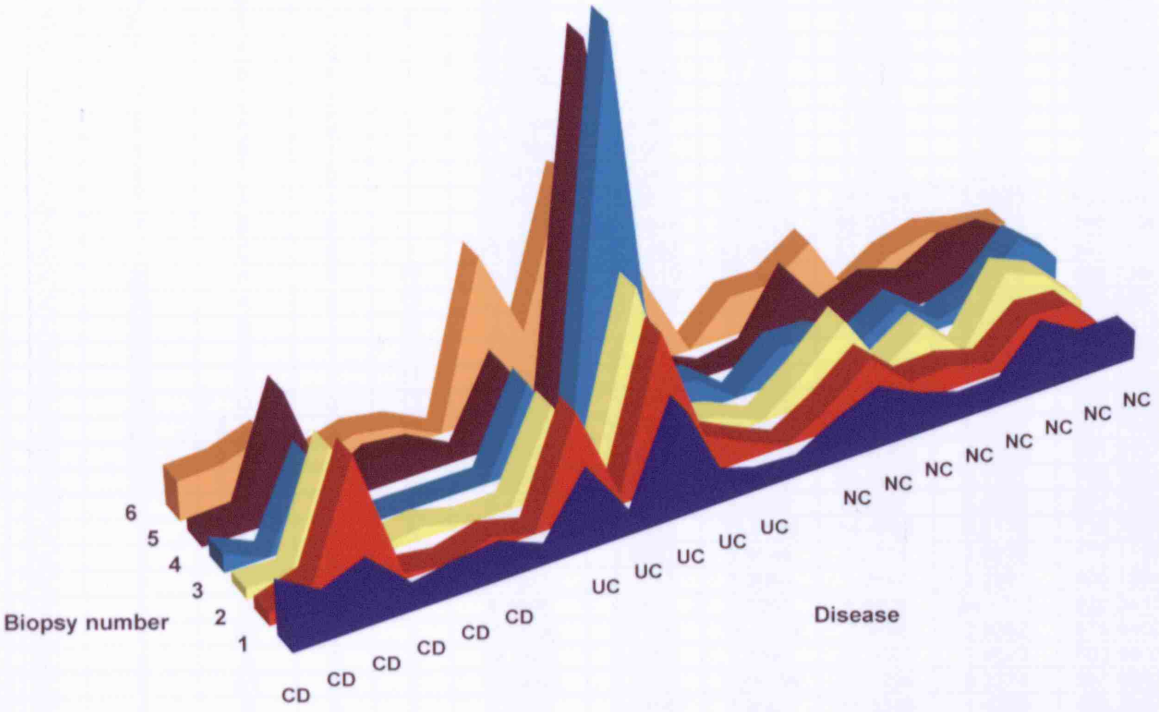

Table 3.5: Relative expression levels of CCR6, CXCL1, CXCL2, CXCL3, CCL20 and actin, obtained by semi-quantitative assessment of the microarray result from surgically obtained colonic tissue, with inflammatory quotients. Where the level is less than 10-15, the level is not significantly detected. NC=normal control, IC=inflammatory control, EP=epithelial, LP= lamina propria. The area corresponds to colonic area of tissue removed, as outlined in appendix 4.4.

Disease	Patient numb	Area	A+C	CRP	CXCL1	CXCL2	CXCL3	CCL20	CCR6	Actin
CD	2	A	4	41	100.8261	58.3924	79.0613	63.4849	5.8293	574.2011
CD	2	B	3	41	22.5390	22.1163	2.1148	13.5489	4.8289	683.0761
CD	2	C	4	41	107.2955	22.2024	-1.8996	2.3480	4.2019	695.259
CD	4	B	6	164	97.2476	33.4671	23.3156	24.3013	0.2930	697.1609
CD	4	C	5	164	68.1159	-18.0976	16.2214	63.1070	10.4685	528.7879
CD	9	A	4	14	11.5418	11.689	5.5921	11.0219	10.3578	641.2316
CD	10	A	0	5	35.6980	7.5072	5.4903	1.0903	4.1451	738.4473
CD	10	C	6	5	14.7531	5.8306	0.4484	46.9656	6.1984	397.0774
CD	11	A	5	X	9.9263	3.7272	-5.1632	0.0319	-3.1632	494.7478
CD	11	C	0	X	55.7554	25.0411	21.2332	9.4199	-0.7306	627.52
CD	12	A	1	X	36.0224	9.1794	7.6938	9.5805	11.9946	518.1672
CD	19	A		1	31.2437	3.3533	14.5116	5.6249	1.2018	572.6756
CD	19	B	0	1	4.8093	34.7166	-4.8903	13.2242	8.9279	343.7313
CD	19	C	1	1	5.8379	2.4358	0.3919	32.0534	8.7015	284.081
CD	21	B	1	4	9.6780	1.1254	4.3095	4.0694	7.4000	561.5011
UC	1	A	2	1	23.6965	8.1610	16.2988	10.0500	1.7653	542.6757
UC	1	B	4	1	25.0052	11.0644	17.643	16.7935	2.1352	517.3833
UC	1	C	3	1	0.0539	1.2330	3.0834	-0.231	-1.5436	383.1522
UC	6	A	0	1	21.1594	3.4587	10.9874	1.9034	3.7067	533.87
UC	6	B	1	1	21.1594	3.4587	10.9874	1.9034	3.7067	533.87
UC	6	C	0	1	6.3451	7.5340	5.3911	1.8873	1.6785	477.9281
UC	7	A	4	1	25.2699	16.9673	16.6468	24.6745	3.0525	553.8692
UC	7	B	6	1	89.1538	51.4646	53.5029	66.0324	3.4550	566.1126
UC	7	C	6	1	83.5015	42.1483	42.6756	41.3496	4.8529	593.7514
UC	20	A	5	17	46.6659	30.9410	27.0636	26.1417	0.3975	459.7350
UC	20	A	5	17	39.2749	10.3667	10.5086	39.5597	1.8959	609.6693
UC	20	B	1	17	-3.1721	7.0751	2.4309	4.74629	0.8818	603.3918
UC	20	B	1	17	4.0192	-0.1546	6.0834	-1.1481	-3.7148	567.0453
UC	20	C	1	17	2.7889	2.5092	4.7758	5.5220	3.2695	487.5164
UC	20	D	0	17	6.2281	3.3695	6.9976	-2.5232	-5.3301	616.3956
UC	20	A (EP)	5	17	62.7754	29.7871	34.8244	44.6003	4.5966	507.7942
UC	20	A (EP)	5	17	58.0784	39.9142	35.9316	52.8063	-0.9420	501.2137
UC	20	A (LP)	5	17	34.6882	9.6923	7.9720	24.0042	8.1191	742.1554
NC	3	A	0	X	9.4101	8.2383	5.6433	8.8987	6.4836	801.7334
NC	3	A1	0	X	15.8894	3.9952	13.8106	14.4696	0.5170	739.7801
NC	5	A	0	1	10.6296	3.8982	6.6046	5.2778	2.8939	777.1137
NC	5	A1	0	1	5.7871	3.3713	2.9664	1.2442	3.2931	800.1594
NC	5	B	0	1	8.3605	4.4631	6.5091	5.8905	24.7713	620.3415
NC	5	B1	0	1	19.7606	3.7176	16.4113	2.3696	2.9352	675.0402
NC	8	A	0	3	19.7805	8.8928	7.3591	31.9007	3.9523	603.5003
NC	8	A1	0	3	13.0460	6.1049	7.28756	27.1299	0.3374	597.9862
NC	8	B	0	3	8.0723	5.5309	3.8601	11.3358	1.4339	499.3367
NC	8	B1	0	3	16.8343	9.2220	13.1781	17.7758	3.0529	524.0433
NC	13	A	2	X	11.5418	11.689	5.5921	11.0219	10.3578	641.2316
NC	13	A1	2	X	10.8647	3.6845	0.6680	4.4457	2.2809	602.1659
NC	13	B	0	X	24.5121	10.3813	10.2689	12.2783	10.0292	675.4843
NC	13	B1	0	X	6.6954	6.5051	4.2162	2.5024	-0.8613	571.4995
NC	13	C	0	X	19.4091	8.1652	5.3375	5.4435	4.3749	587.9377
NC	13	C1	0	X	11.5038	4.7620	7.0025	3.3774	2.8527	630.1692
NC	14	A	0	X	-6.8175	0.1386	13.2673	4.5205	4.2090	729.3366
NC	17	A	2	X	9.1072	7.6558	16.0198	7.2121	-3.2358	530.773
NC	17	A	2	X	-0.6146	-0.9580	-2.8858	7.5801	-5.9784	531.8575
NC	17	A1	2	X	12.8702	7.5610	13.4896	5.74915	3.1080	569.6506
NC	17	B	2	X	6.8974	5.2349	8.4505	5.9500	2.0468	516.0421
NC	17	B1	2	X	10.2199	4.8911	2.5744	13.2360	-0.7707	502.1918
NC	17	C	2	X	11.5208	11.0391	17.5738	7.33237	3.6652	580.4735
NC	17	C1	2	X	20.2980	21.3493	12.3230	16.4396	3.3978	608.1404
IC	18	A	5	135	162.6139	30.1001	34.2105	59.3703	-0.2452	710.5713
IC	18	B	3	135	28.7168	23.7888	26.7610	46.6442	1.0456	490.4558
IC	18	C	1	135	4.7016	3.5173	-1.1868	10.7329	0.03867	528.7184
IC	18	D	1	135	4.5289	4.6158	12.5410	34.6338	1.4185	603.9584
IC	18	A	5	135	37.7656	30.4828	7.8781	4.0879	-0.3608	626.4506

Table 3.6: Relative expression levels of CCR7, CXCR5, CXCL13 and CCL19 obtained by semi-quantitative assessment of the microarray result from surgically obtained colonic tissue, with inflammatory quotients. Where the level is less than 10-15, the level is not significantly detected. NC=normal control, IC=inflammatory control, EP=epithelial, LP= lamina propria. The area corresponds to colonic area of tissue removed, as outlined in appendix 4.4.

Disease	Patient number	Area	A+C	CRP	CCL19 Short	CCL19 Long	CCL21	CCR7	CXCR5	CXCL13
CD	2	A	4	41	79.6076	87.9298	82.2570	23.5312	36.8905	5.7014
CD	2	B	3	41	157.3356	110.8881	48.0372	13.2821	24.0383	8.2274
CD	2	C	4	41	116.5953	115.3098	58.4547	14.6874	25.3977	28.1209
CD	4	B	6	164	87.844	117.5998	116.4881	7.5262	29.0717	8.5333
CD	4	C	5	164	114.9364	107.8265	127.1042	11.5760	46.3315	20.3391
CD	4	C	5	164	114.9364	107.8265	127.1042	11.5760	46.3315	20.3391
CD	4	C	5	164	114.9364	107.8265	127.1042	11.5760	46.3315	20.3391
CD	9	A	4	14	79.4142	74.2687	281.6056	21.9062	41.3949	17.2098
CD	10	A	0	5	38.1767	53.2136	130.3662	5.89218	29.0918	-3.6856
CD	10	C	6	5	-1.2583	-3.7106	22.8861	-2.3643	20.51969	-5.2855
CD	11	A	5	X	2.7920	2.7621	41.6278	-6.6714	13.7468	-9.5219
CD	11	C	0	X	69.8316	89.34	146.0917	23.0177	33.1898	10.2242
CD	12	A	1	X	24.2509	29.8648	90.2405	12.8028	36.0714	28.5893
CD	19	A	X	1	0.8324	29.4338	22.7735	11.9989	20.9184	-4.4769
CD	19	B	0	1	-0.0139	2.7383	28.1079	-10.1363	12.4370	-2.4621
CD	19	C	1	1	7.4914	15.3813	39.5029	-4.5773	18.3859	0.0371
CD	21	B	1	4	8.1257	8.3758	58.9448	8.6597	4.2631	-1.0291
UC	1	A	2	1	52.0797	58.2063	87.6864	17.9008	40.6108	11.4822
UC	1	B	4	1	57.3785	63.5078	69.9469	18.4408	15.0436	9.0774
UC	1	C	3	1	12.1891	15.6323	66.7882	5.0769	14.6020	-3.7275
UC	6	A	0	1	7.19724	14.9215	28.8104	17.7358	30.2089	-0.0491
UC	6	B	1	1	7.1972	14.9215	28.8104	17.7358	30.2089	-0.0491
UC	6	C	0	1	6.5710	11.8651	19.4039	7.0807	0.8421	36.2187
UC	7	A	4	1	22.8779	37.6508	63.3747	13.6075	9.6070	4.4297
UC	7	B	6	1	55.8069	67.0602	85.9114	19.6916	15.2223	20.0069
UC	7	C	6	1	95.6809	105.911	134.2061	33.1437	30.1117	62.9534
UC	20	A	5	17	1.4447	11.1472	21.8653	7.7929	16.0058	3.8284
UC	20	A	5	17	-2.4573	3.2409	23.6273	6.5793	4.4699	-1.5026
UC	20	A	5	17	16.8156	30.1119	51.1590	15.9279	8.7774	-0.8725
UC	20	B	1	17	-2.4573	3.2409	23.6273	6.5793	4.4699	-1.5026
UC	20	B	1	17	-3.9675	19.1262	11.1384	2.3234	-0.0230	0.3987
UC	20	C	1	17	1.0261	15.6229	15.8123	3.4027	2.8181	-0.1201
UC	20	D	0	17	0.2941	11.0784	25.2027	1.0159	4.9186	-1.4737
UC	20	A (EP)	5	17	2.5196	11.2187	14.6652	8.4751	9.0790	1.7819
UC	20	A (EP)	5	17	3.4018	17.8284	21.6351	6.3544	6.0928	-2.2900
UC	20	A (LP)	5	17	3.9473	11.4084	36.5619	15.3061	9.0501	0.1389
NC	3	A	0	X	10.7053	10.8216	64.3865	2.6711	11.4161	-1.4656
NC	3	A1	0	X	19.8447	16.8856	64.8887	7.8262	11.7413	-0.1869
NC	5	A	0	1	11.6900	13.4325	89.6825	10.3600	11.2747	1.8847
NC	5	A1	0	1	14.1269	19.8206	100.4257	4.1766	16.4743	4.0499
NC	5	B	0	1	6.6815	7.1791	55.9999	2.546	10.3285	-0.0519
NC	5	B1	0	1	8.6394	14.2334	85.1862	10.2746	13.9676	-0.6025
NC	8	A	0	3	25.8582	31.0827	119.8651	10.3998	16.4211	-1.7785
NC	8	A1	0	3	23.1084	24.8337	89.1413	12.6520	17.7790	4.5655
NC	8	B	0	3	24.3540	26.4488	82.4353	10.8883	13.4270	3.4567
NC	8	B1	0	3	26.7243	32.6031	94.5875	13.9008	16.2606	6.2325
NC	13	A	2	X	13.1443	6.9462	38.6306	2.3196	4.1983	1.7377
NC	13	A1	2	X	21.8937	20.6354	86.0148	10.1211	13.6930	3.7320
NC	13	B	0	X	18.1167	17.2681	70.2185	5.2243	8.3198	-0.0451
NC	13	B1	0	X	19.4763	18.2748	80.1671	6.0429	7.6139	1.6869
NC	13	C	0	X	11.4414	6.6519	39.6009	2.0411	0.2146	0.4057
NC	13	C1	0	X	21.6811	19.3194	97.0426	7.3300	12.4611	-0.3633
NC	14	A	0	X	-5.3386	4.6498	16.7036	5.9890	9.0353	1.2078
NC	17	A	2	X	-0.5628	2.1303	11.5426	6.6429	0.6414	-1.8869
NC	17	A	2	X	9.3184	11.0534	73.6477	5.4420	10.1458	3.0072
NC	17	A	2	X	-0.5628	2.1303	11.5426	6.6429	0.6414	-1.8869
NC	17	A1	2	X	13.2169	12.0681	75.9645	8.3283	15.0876	1.4482
NC	17	B	2	X	18.0074	12.8209	66.4561	6.9519	11.4248	1.0566
NC	17	B1	2	X	17.5325	13.7817	62.8344	1.7806	15.1809	1.4571
NC	17	C	X	X	8.4472	9.8749	66.1971	3.4593	13.6505	-0.1146

Disease	Patient number	Area	A+C	CRP	CCL19 Short	CCL19 Long	CCL21	CCR7	CXCR5	CXCL13
NC	17	C1	X	X	18.8871	16.0371	93.2074	6.1971	17.7915	1.9294
NC	18	A	5	135	-0.6801	8.1759	61.7679	2.5724	4.2004	-1.9115
IC	18	A	5	135	0.8099	10.8737	52.1892	-0.4255	18.5848	-5.4121
IC	18	B	3	135	-1.4111	7.2062	6.6712	8.9004	4.1830	-0.7881
IC	18	C	1	135	-4.2832	6.7041	11.9748	1.3051	2.9030	-1.7692
IC	18	D	1	135	-0.9684	4.1206	20.0188	16.6221	8.1196	3.0969

Table 3.7: Relative expression levels of CXCL8, CXCL9, CXCL10, CXCL11, CCL5 and CCR5 obtained by semi-quantitative assessment of the microarray result from surgically obtained colonic tissue, with inflammatory quotients. Where the level is less than 10-15, the level is not significantly detected. NC=normal control, IC=inflammatory control, EP=epithelial, LP= lamina propria. The area corresponds to colonic area of tissue removed, as outlined in appendix 4.4.

Diagnosis	Patient number	Area	A+C	CXCL8	CXCL9	CXCL10	CXCL11	CCL5 short	CCL5 long	CCR5
CD	2	A	4	5.1137	139.7526	53.2823	28.7791	76.2268	170.4330	12.4891
CD	2	B	3	-20.8134	109.6064	17.1207	20.5021	57.8243	172.0704	21.0579
CD	2	C	4	-1.1245	108.2494	33.4426	24.2733	68.8560	153.6119	27.6764
CD	4	B	6	32.4698	209.5981	89.5948	60.0737	43.2562	56.3139	27.7204
CD	4	C	5	-3.1325	172.3670	59.2163	79.0350	43.1809	184.8137	25.2824
CD	4	C	5	-3.1325	172.3670	59.2163	79.0350	43.1809	184.8137	25.2824
CD	4	C	5	-3.1325	172.3670	59.2163	79.0350	43.1809	184.8137	25.2824
CD	9	A	4	-6.0428	26.5097	0.7988	26.8672	63.0073	127.3206	8.4783
CD	10	A	X	2.6983	20.1228	5.7665	53.1985	33.1115	131.6294	2.1952
CD	10	C	6	-4.5829	11.1987	-2.6484	19.4009	23.6033	99.3887	-5.1738
CD	11	A	5	-15.1662	-5.7621	-10.5014	14.9834	5.0679	111.6167	-5.4539
CD	11	C	0	46.0796	83.0080	32.0517	70.3899	45.8378	85.1607	8.3507
CD	12	A	1	5.8381	10.5462	11.4429	50.4204	38.7271	162.3557	10.9860
CD	19	A	X	-0.1787	17.8978	17.2092	-0.1117	42.6440	98.9645	7.0884
CD	19	B	0	-11.1404	25.4330	2.5896	18.0503	16.6675	108.7396	12.8852
CD	19	C	1	-0.3421	16.8873	-3.1571	8.2982	33.3430	53.4101	-3.8644
CD	21	B	1	3.2776	-0.6379	-3.5479	1.1896	11.6279	119.1176	3.6182
UC	1	A	2	0.2125	24.5904	7.1398	30.9770	23.8651	78.9211	6.6988
UC	1	B	4	-0.3242	26.0065	11.3002	19.3977	27.4168	90.4866	9.8816
UC	1	C	3	-2.9516	42.2825	12.3159	3.3617	34.1194	213.8564	1.3304
UC	6	A	0	0.0864	-0.5409	-0.5473	14.3376	20.8288	99.1011	5.3279
UC	6	B	1	0.0864	-0.5409	-0.5473	14.3376	20.8288	99.1011	5.3279
UC	6	C	0	4.5715	-0.1626	0.9090	15.2000	12.2461	77.2761	3.7668
UC	7	A	4	5.2739	7.0601	5.1577	20.2598	24.1716	94.1087	4.9444
UC	7	B	6	26.0933	26.0800	19.7765	24.8659	21.9823	68.9394	13.3087
UC	7	C	6	16.9725	36.4729	26.2338	29.5633	24.8147	78.8936	16.3895
UC	20	A	5	5.0808	3.0221	6.1035	2.4857	14.9839	36.1348	1.8387
UC	20	A	5	-2.1357	-0.7264	-0.8959	4.1001	20.9748	67.0246	9.2060
UC	20	A	5	104.3876	12.8868	-1.5480	3.7184	38.9765	127.8926	6.3041
UC	20	B	1	-2.1357	-0.7264	-0.8959	4.1001	20.9748	67.0246	9.2060
UC	20	B	1	-5.3806	-8.7775	-8.0915	-2.3412	11.8429	36.9673	-1.8351
UC	20	C	1	-0.6640	1.4197	-0.6301	1.9215	7.7371	30.1087	0.9386
UC	20	D	0	2.6727	3.4846	0.1197	2.6303	66.6885	41.1736	-2.6627
UC	20	A(EP)	5	126.1982	5.8592	3.5968	-0.5979	14.8113	56.0558	4.1086
UC	20	A(EP)	5	151.7507	1.1738	1.8298	-1.6056	11.6198	36.8284	-0.3860
UC	20	A(LP)	5	-1.4620	2.4849	0.9029	-1.4941	10.7306	133.6877	0.1416
NC	3	A	0	-1.5524	4.6580	-0.2489	23.4785	7.0335	101.6972	8.6608
NC	3	A1	0	0.0367	2.7763	1.8325	19.1046	26.5283	124.4337	9.6773
NC	5	A	0	-2.4945	-0.9774	0.2889	12.4544	12.2128	102.5660	5.7874
NC	5	A1	0	0.8898	9.2412	2.8900	9.9244	15.4428	120.9531	3.3439
NC	5	B	0	-0.3083	6.4117	-0.7662	17.1780	8.9760	63.9936	5.2399
NC	5	B1	0	-0.5362	7.4501	-1.3398	23.8222	25.7757	80.9913	7.7646
NC	8	A	0	0.4049	3.5853	0.4268	20.6212	28.4833	86.4384	14.5312
NC	8	A1	0	0.1341	3.8618	2.2462	20.0075	34.5933	80.6139	10.0050
NC	8	B	0	-0.7455	2.6759	0.4406	11.4014	13.7557	96.1777	7.3186
NC	8	B1	0	-1.0535	6.7594	1.8704	19.7899	29.2378	100.9755	10.1213
NC	13	A	2	0.4287	13.7938	0.8976	27.6175	6.9255	64.7898	9.6589
NC	13	A1	2	4.2759	16.0863	10.3872	31.4496	11.9522	63.5402	16.5702
NC	13	B	0	1.7687	3.6386	-0.3241	15.8124	7.7003	86.1515	6.7404
NC	13	B1	0	16.1728	9.3637	3.9084	27.8924	16.2462	87.7114	6.5457
NC	13	C	0	-1.0836	39.7923	5.3861	28.7191	8.1328	69.7831	9.9314
NC	13	C1	0	-0.0453	56.4083	14.5962	38.0566	13.8350	69.1314	16.6738
NC	14	A	0	-5.1113	3.0273	-1.3804	-4.5567	29.9021	78.9379	1.1443
NC	17	A	2	2.7872	8.8108	7.5872	37.7588	25.0323	93.8290	14.1046
NC	17	A	2	-0.0337	3.2799	1.4620	-0.9985	8.0542	67.9628	1.2662
NC	17	A1	2	-0.2728	7.9738	4.4730	40.4502	18.2868	83.4760	11.5703
NC	17	B	2	-2.5514	7.0377	-0.6391	25.0308	23.1749	95.0651	12.5005
NC	17	B1	2	1.0233	5.8827	4.0077	22.3752	22.1949	55.2292	15.1780

Diagnosis	Patient number	Area	A+C	CXCL8	CXCL9	CXCL10	CXCL11	CCL5 short	CCL5 long	CCR5
NC	17	C	2	0.3495	3.3324	2.0050	35.4696	19.5423	93.0635	9.9286
NC	17	C1	2	3.2548	8.0132	5.6344	50.9765	29.4552	93.0309	17.1980
IC	18	A	5	2.4397	1.9883	4.7236	5.8708	22.9830	104.2279	6.8047
IC	18	A	5	21.3609	5.7512	3.9517	29.8322	4.1445	66.5106	-1.6043
IC	18	B	3	-0.1874	1.2508	1.4613	1.8252	11.0044	47.7474	6.8047
IC	18	C	1	-0.7218	1.5809	-1.7444	-2.4490	18.2912	58.6752	-2.9447
IC	18	D	1	-2.1165	-2.7329	1.0782	0.7918	30.4217	57.9696	-0.6332

Table 3.8: Relative expression levels of CCL2, CCL24, CXCR1, CXCR2, CXCR3, CCR3 and CCL3 obtained by semi-quantitative assessment of the microarray result from surgically obtained colonic tissue, with inflammatory quotients. Where the level is less than 10-15, the level is not significantly detected. NC=normal control, IC=inflammatory control, EP=epithelial, LP= lamina propria. The area corresponds to colonic area of tissue removed, as outlined in appendix 4.4.

Diagnosis	Patient number	Area	A+C	CCL2	CCL24	CXCR1	CXCR2	CXCR3	CCR3 short	CCR3 long	CCL3
CD	2	A	4	-0.1317	28.5522	1.6097	14.0617	5.7945	0.5413	9.6046	6.1043
CD	2	B	3	-4.8876	35.3853	0.6458	16.2971	4.4249	1.1068	6.1510	32.4196
CD	2	C	4	16.0683	46.7557	1.4109	8.0741	13.6459	-2.8727	7.4392	51.5953
CD	4	B	6	-0.3699	35.6756	-3.0868	18.1142	6.4328	-0.9389	-0.6973	75.8496
CD	4	C	5	9.6750	40.6805	3.6184	4.1684	13.5520	-2.6708	11.1771	36.0800
CD	4	C	5	9.6750	40.6805	3.6184	4.1684	13.5520	-2.6708	11.1771	36.0800
CD	4	C	5	9.6750	40.6805	3.6184	4.1684	13.5520	-2.6708	11.1771	36.0800
CD	9	A	4	2.2636	33.9425	21.1827	10.9644	6.8540	-5.8624	15.1816	20.5149
CD	10	A	X	0.1604	25.1947	1.7225	16.8975	3.8136	-3.8684	17.0180	16.4623
CD	10	C	6	-5.5817	45.5390	-4.0826	14.9594	-5.7126	-1.0803	21.8983	10.4844
CD	11	A	5	-13.5005	21.4387	-13.6464	-7.5406	-8.8191	-14.9940	-7.3989	-4.9154
CD	11	C	0	-3.6680	31.2998	-0.7157	20.0554	6.0880	-4.1294	8.6057	43.8182
CD	12	A	1	3.3924	42.4669	8.0541	20.1462	6.6175	1.4684	2.9019	15.9940
CD	19	A	X	3.9640	29.9350	0.7997	5.8582	50.3849	-1.9150	2.6068	1.3047
CD	19	B	0	-3.0242	42.5394	-1.5683	1.5982	-3.1853	0.4310	-8.0185	-3.7435
CD	19	C	1	-6.4555	87.9543	-9.8552	15.5614	4.5126	-7.9272	13.4457	-5.2624
CD	21	B	1	0.6454	30.8187	-1.8422	6.3450	21.3917	-1.7031	10.6177	8.1685
UC	1	A	2	1.2548	40.1682	-0.3824	2.9333	19.6929	-0.4289	2.6175	8.5380
UC	1	B	4	0.8454	46.0135	-0.7328	2.2467	27.0616	-2.7401	2.6732	9.5570
UC	1	C	3	-0.5648	13.4828	3.3268	1.4281	10.2467	-7.6993	0.0343	5.7140
UC	6	A	0	2.9122	46.4250	-0.9307	3.7486	31.6502	-1.8055	3.1357	3.1192
UC	6	B	1	2.9122	46.4250	-0.9307	3.7486	31.6502	-1.8055	3.1357	3.1192
UC	6	C	0	0.7242	52.0014	-0.3069	10.5898	14.2535	0.5656	2.0853	1.4292
UC	7	A	4	3.7937	36.2441	2.5767	10.5185	18.0470	-1.4208	2.0419	9.7901
UC	7	B	6	1.2295	54.0179	0.4033	14.0468	23.8031	-0.7616	3.8905	12.2340
UC	7	C	6	1.6617	69.3582	1.2783	11.7500	26.7966	5.3646	3.8678	16.4848
UC	20	A	5	-0.0686	45.1972	-0.0812	5.4863	22.2661	-0.9839	2.9526	4.7585
UC	20	A	5	4.5797	25.6403	-0.7706	6.6673	19.0350	-2.3667	1.6999	0.5156
UC	20	A	5	7.2767	30.8656	-0.7823	7.9058	26.5178	-2.1945	0.7957	45.1197
UC	20	B	1	4.5797	25.6403	-0.7706	6.6673	19.0350	-2.3667	1.6999	0.5156
UC	20	B	1	-5.3483	30.0628	-0.3326	-3.6410	17.3355	-5.0426	-9.9685	-2.0924
UC	20	C	1	2.4345	43.1761	-2.1635	1.6393	29.4969	-3.1848	4.2097	-1.8872
UC	20	D	0	3.2949	36.0338	3.9255	2.8700	22.3815	1.9397	-0.2770	4.0835
UC	20	A(EP)	5	4.4900	17.5263	2.8127	10.8238	35.9036	0.2047	0.0484	51.5262
UC	20	A(EP)	5	1.4672	38.3649	1.3474	7.6987	21.2224	6.7926	1.1022	45.3933
UC	20	A(LP)	5	-0.3312	9.6656	6.2483	2.1436	10.8727	-0.6456	2.4620	2.0134
NC	3	A	0	5.8078	8.1912	0.4401	9.3485	4.8829	1.6476	6.1249	0.9462
NC	3	A1	0	3.8086	25.3072	0.0165	3.4331	14.4737	0.9550	3.9006	6.9424
NC	5	A	0	8.3875	13.1118	3.0075	5.1024	1.6814	1.1132	3.2878	7.3213
NC	5	A1	0	5.3851	9.9175	1.0100	3.7635	3.9903	2.4912	-0.6934	4.8370
NC	5	B	0	2.2727	26.6144	1.2914	5.3314	5.0382	0.4951	0.2690	9.4550
NC	5	B1	0	3.1187	27.4073	1.7187	4.3924	16.4439	-0.4606	3.3441	5.6290
NC	8	A	0	7.6456	33.0384	1.1527	7.4469	9.6921	1.2906	1.4075	5.7008
NC	8	A1	0	5.7190	49.8864	3.1023	3.2620	7.9254	1.5165	4.3065	2.5165
NC	8	B	0	3.7011	54.1159	1.3371	2.1367	11.6952	1.6627	2.7013	2.3132
NC	8	B1	0	4.6682	34.5780	4.7181	7.8167	12.4210	1.1687	4.5817	8.1276
NC	13	A	2	2.6126	27.2019	1.0803	11.3008	0.7967	-1.0822	2.5442	4.5123
NC	13	A1	2	7.5689	19.6721	7.4317	16.6052	5.3611	1.2646	6.1390	8.8459
NC	13	B	0	2.7753	43.3773	1.4411	5.9742	1.8136	-2.5691	-3.2223	2.7079
NC	13	B1	0	3.2131	25.1952	1.0267	12.1783	6.7352	0.9986	3.6646	4.0946
NC	13	C	0	2.1972	31.0544	0.0021	10.5087	0.4720	-0.2335	0.4306	3.0183
NC	13	C1	0	0.8576	28.7928	0.0461	10.3613	7.5330	0.8707	2.0358	4.6066
NC	14	A	0	6.5568	24.6366	0.8666	-2.0723	20.9195	6.6131	-4.3220	5.1023
NC	17	A	2	5.4259	48.3374	1.4567	5.2721	14.2808	1.2989	2.7033	7.6278
NC	17	A	2	3.6975	23.2180	0.9730	4.4159	9.3116	-4.3856	2.9083	-4.4454
NC	17	A1	2	1.1519	47.2905	3.5051	7.6184	13.4593	0.6362	1.7535	6.8581

Diagnosis	Patient number	Area	A+C	CCL2	CCL24	CXCR1	CXCR2	CXCR3	CCR3 short	CCR3 long	CCL3
NC	17	B	2	3.1493	37.9473	1.2104	1.4453	2.9064	-1.1001	3.1075	8.4929
NC	17	B1	2	1.3981	32.1540	2.0818	5.3566	2.3717	3.0823	4.2050	7.1262
NC	17	C	2	5.9770	43.0216	1.0746	2.8630	12.0968	-0.9792	1.2131	5.7224
NC	17	C1	2	4.5841	28.2103	3.4434	6.0228	8.9977	0.6254	4.9360	9.1278
IC	18	A	5	6.8902	10.6389	4.6936	26.2920	16.6122	-5.0042	3.1419	36.4437
IC	18	A	5	1.7121	6.0317	-2.3541	6.4398	19.3612	-4.2787	-5.7134	15.4263
IC	18	B	3	-1.1031	41.6168	-4.5666	8.7155	31.2186	-0.6308	0.5836	4.5157
IC	18	C	1	-8.8491	32.6969	2.4415	-1.5774	16.4416	1.2228	-1.2822	5.9388
IC	18	D	1	-5.5611	49.7404	0.8551	-1.6489	39.8729	-1.7180	2.9493	-2.3614

Graph 3.17: Relative expression of CXCL1 in full thickness colonic tissue measured using microarray correlated with relative levels of inflammation as determined by histopathological analysis

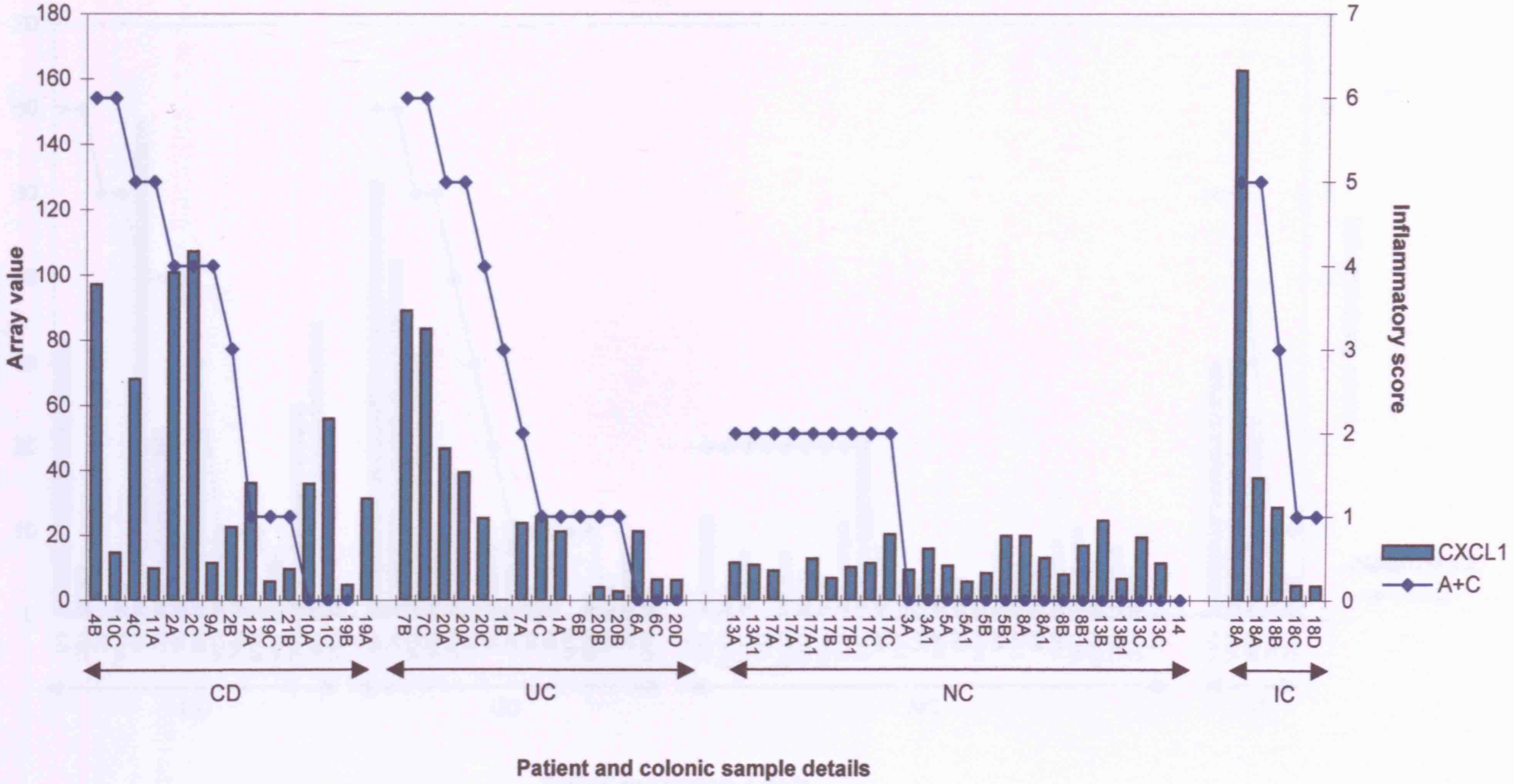

Patients are grouped according to disease, and chronologically placed according inflammatory scores A+C (as defined in table 2.3). Patient and sample details are outlined in appendix table 2. NC=normal control, IC=inflammatory control.

Graph 3.18: Relative expression levels of CXCL2 in full-thickness colonic tissue measured using microarray correlated with relative levels of inflammation as determined by histopathological analysis

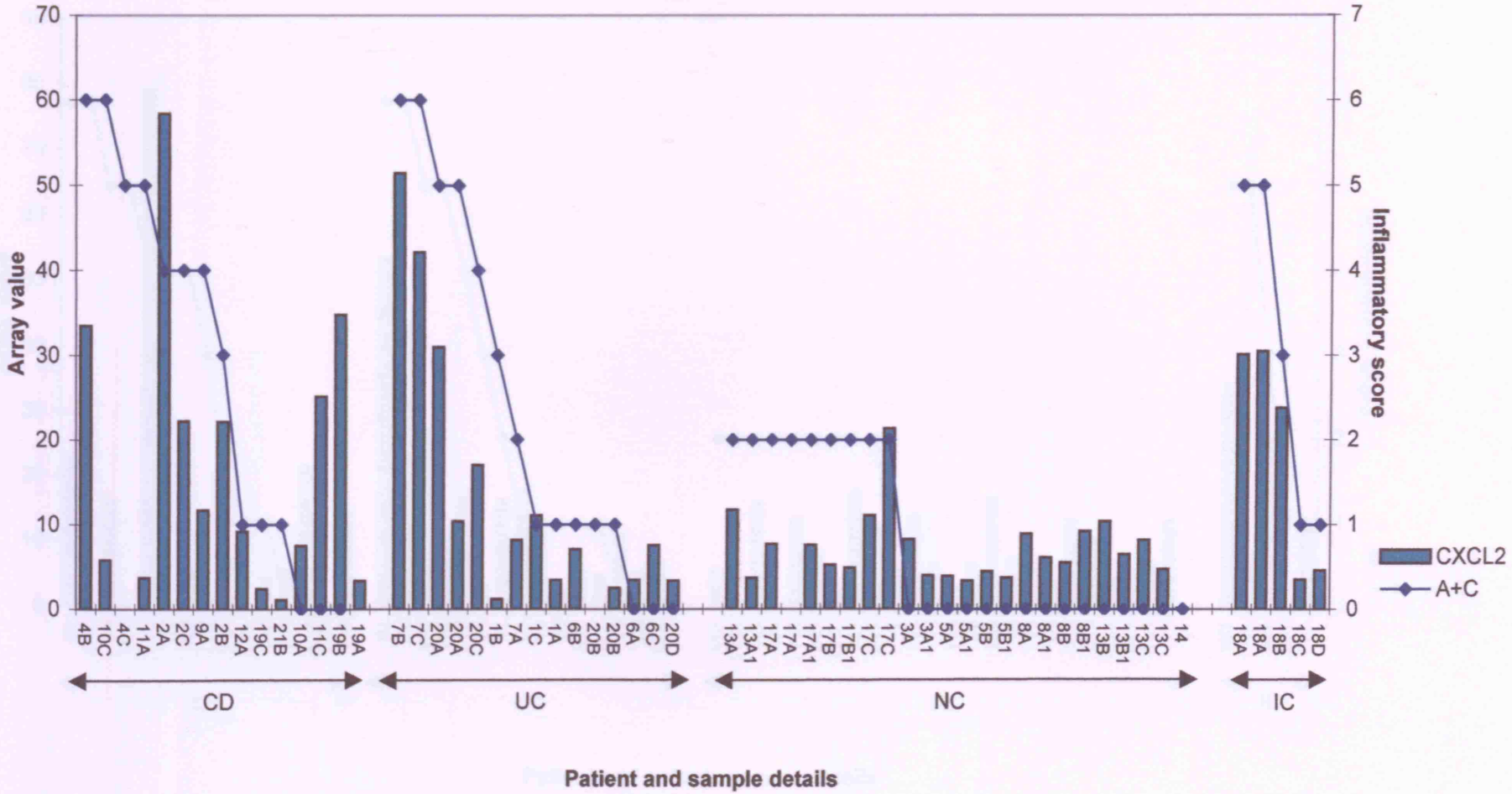

Patients are grouped according to disease, and chronologically placed according to inflammatory scores A+C (as defined in table 2.3). Patient and sample details are outlined in appendix table 2. NC=normal control, IC=inflammatory control.

Graph 3.19: Relative expression of CXCL3 in full thickness colonic tissue measured using microarray correlated with relative levels of inflammation as determined by histopathological analysis

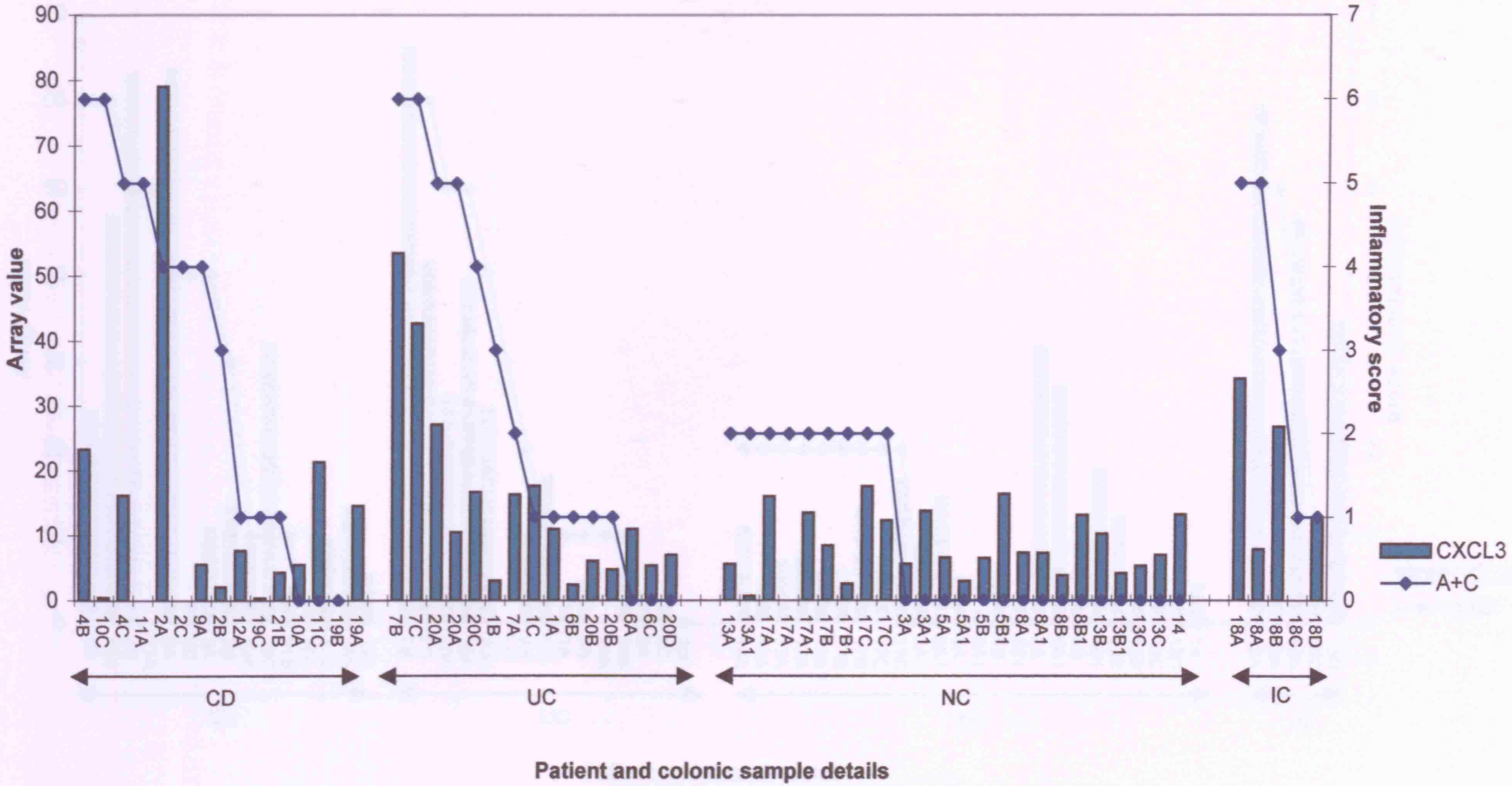

Patients are grouped according to disease, and chronologically placed according to inflammatory scores A+C (as defined in table 2.3). Patient and sample details are outlined in appendix table 2. NC=normal control, IC=inflmmatory control.

Graph 3.20: Relative expression levels of CCL20 in full-thickness colonic tissue measured using microarray correlated with relative levels of inflammation as determined by histopathological analysis

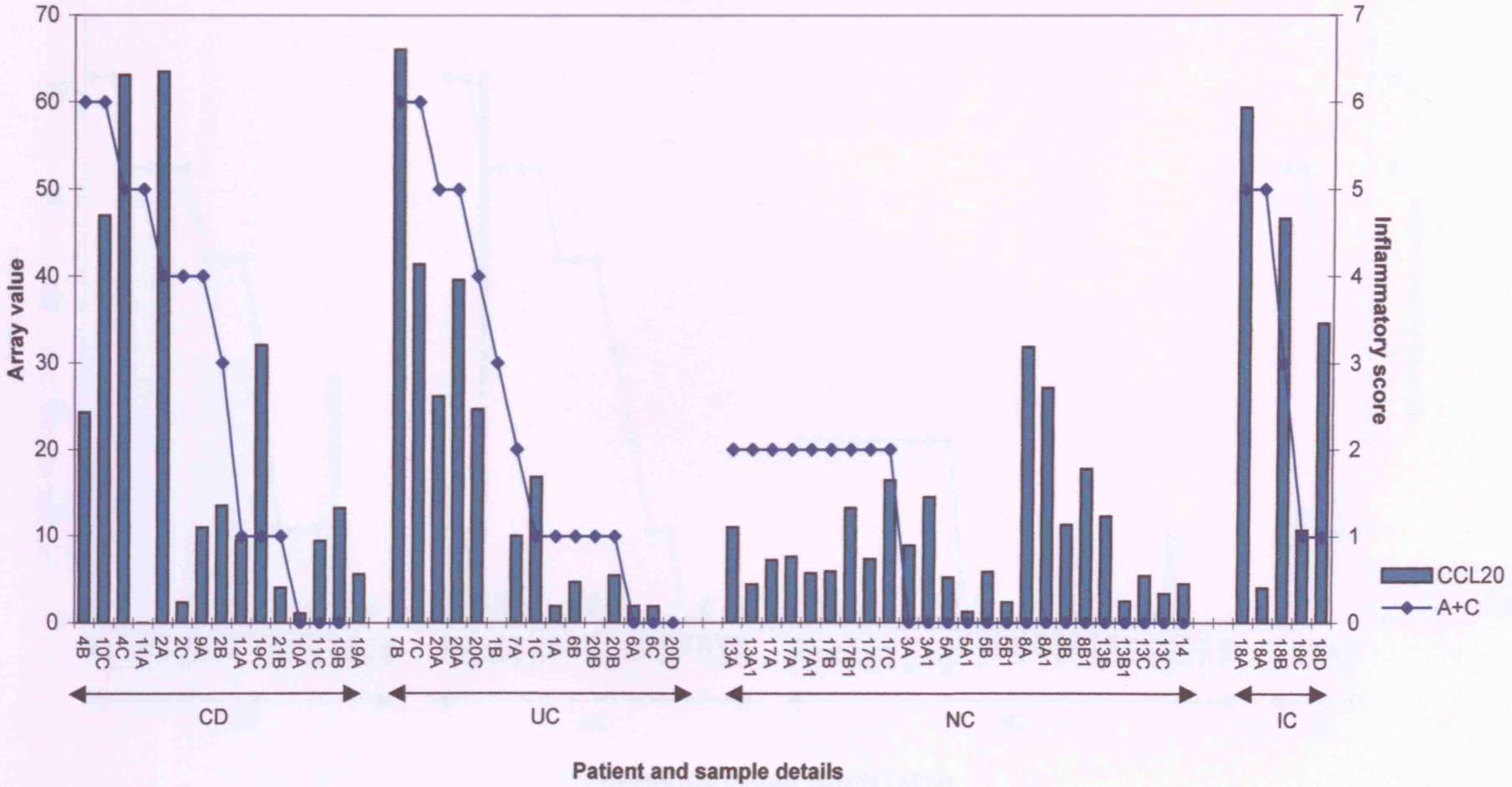

Patients are grouped according to disease, and chronologically placed according to inflammatory scores A+C (as defined in table 2.3). Patients and sample details are outlined in appendix 2. NC=normal control, IC=inflammtory control.

Graph 3.21: Relative expression of CXCL8 in full thickness colonic tissue measured using microarray correlated with relative levels of inflammation as determined by histopathological analysis

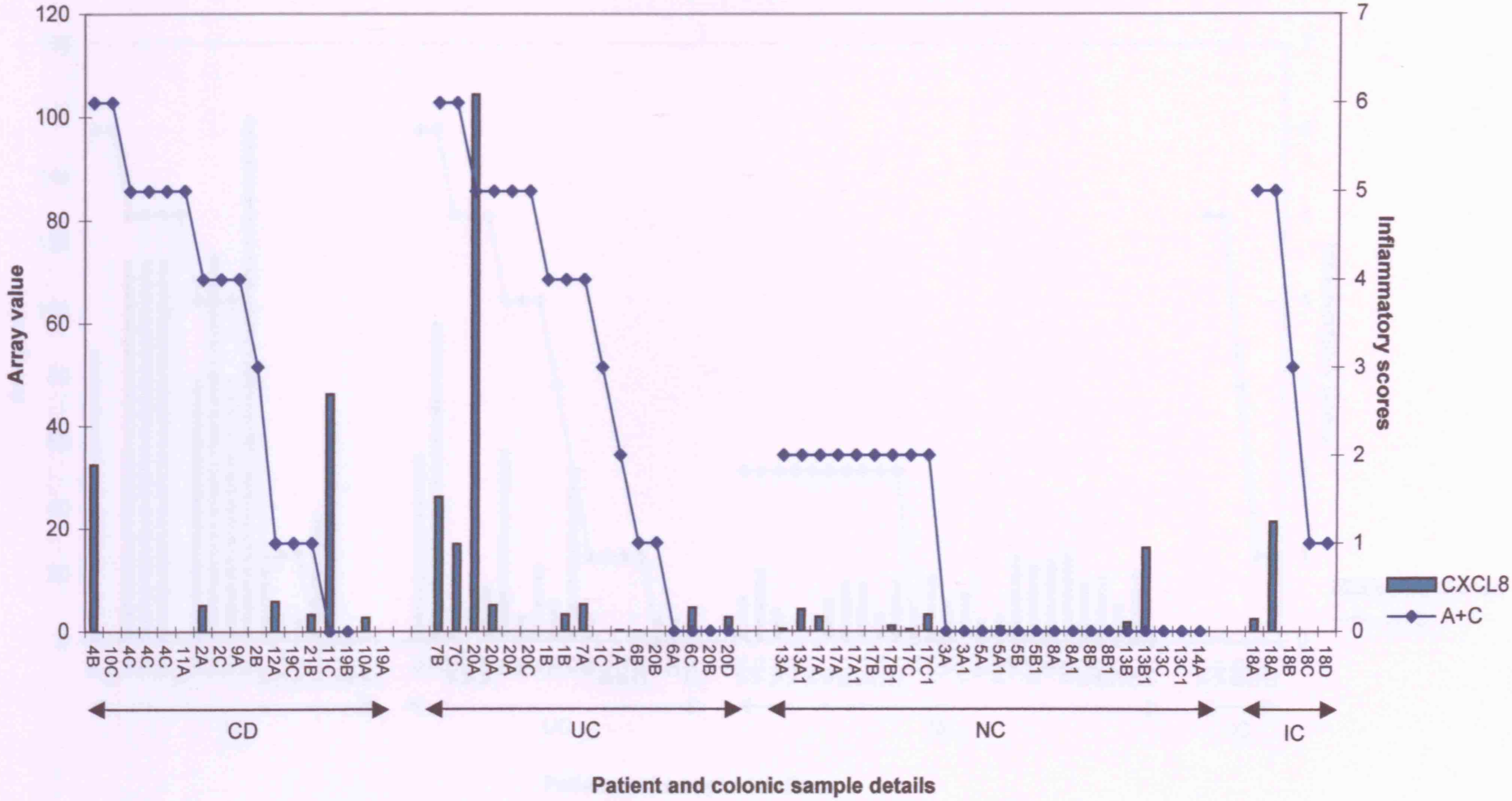

Patients are grouped according to disease, and chronologically placed according to infammatory scores A+C (as defined in table 2.3). Patient and sample details are outlined in appendix table 2. NC=normal control, IC=inflammatory control.

Graph 3.22: Relative expression levels of CCL19 (short arm) in full-thickness colonic tissue measured using microarray correlated with relative levels of inflammation as determined by histopathological analysis

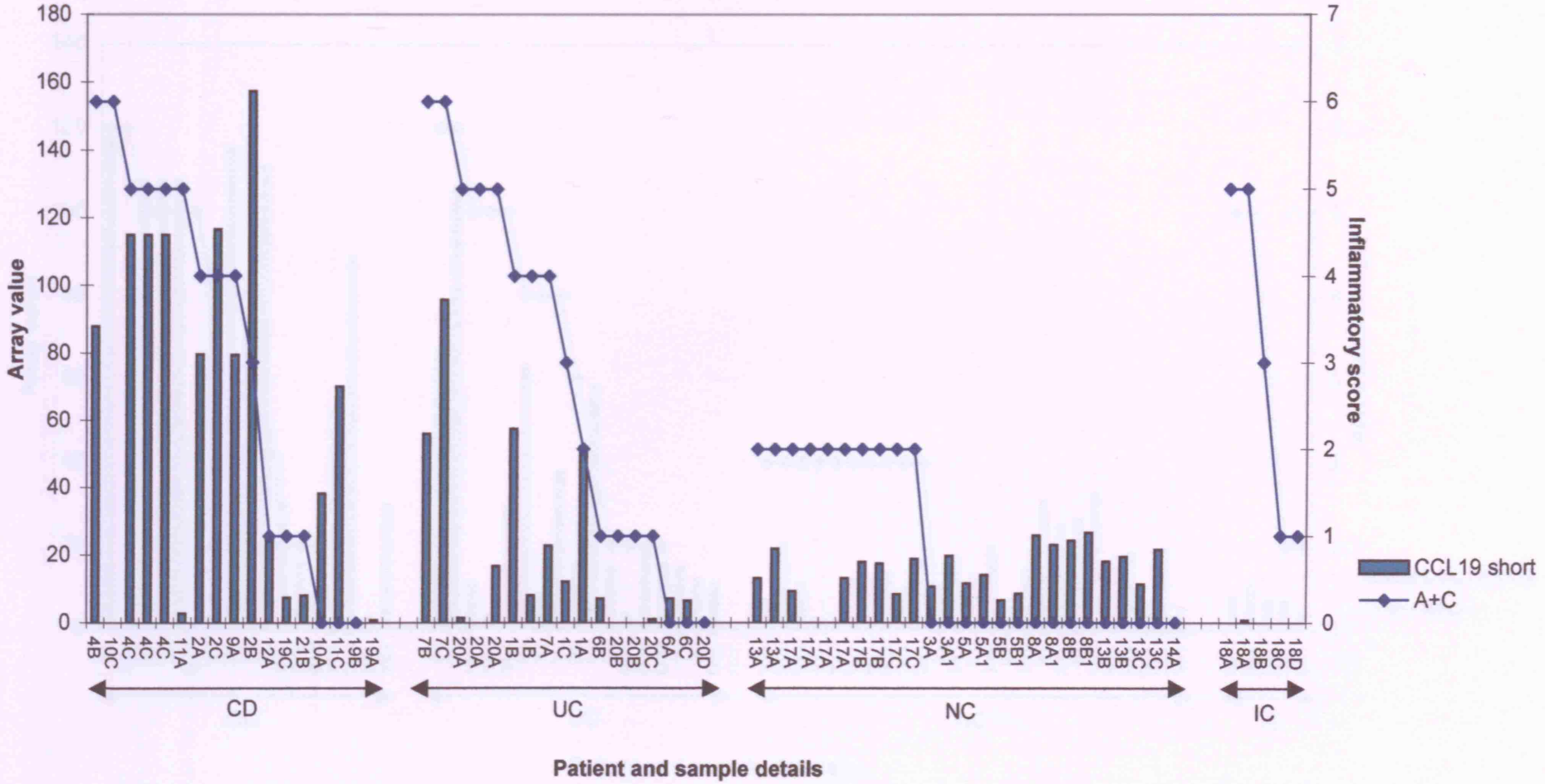

Patients are grouped according to disease and chronologically placed according to inflammatory scores A+C (as defined in table 2.3). Patient and sample details are outlined in appendix 2. NC=normal control IC=inflammatory control.

Graph 3.23: Relative expression levels of CCL19 (long arm) in full-thickness colonic tissue measured using microarray correlated with relative levels of inlammation as determined by histopathological analysis

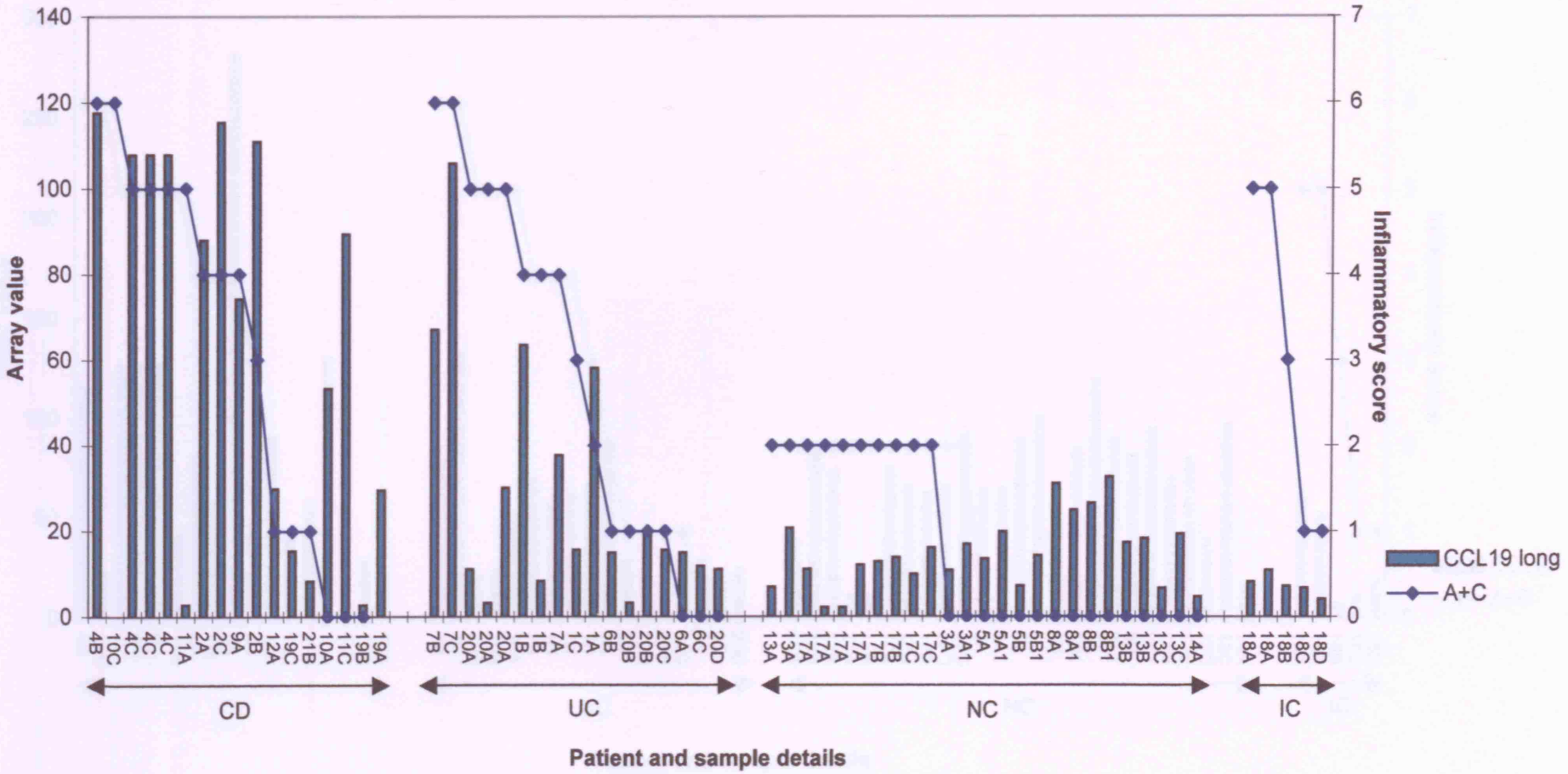

Patients are grouped according to disease, and chronologically placed according to inflammatory scores A+C (as defined in table 2.3). Patient and sample details are outlined in appendix table 2. NC=normal control, IC=inflammatory control.

Graph 3.24: Relative expression levels of CCL21 in full-thickness colonic tissue measured using microarray corelated with relative levels of inflammation as determined by histopathological analysis

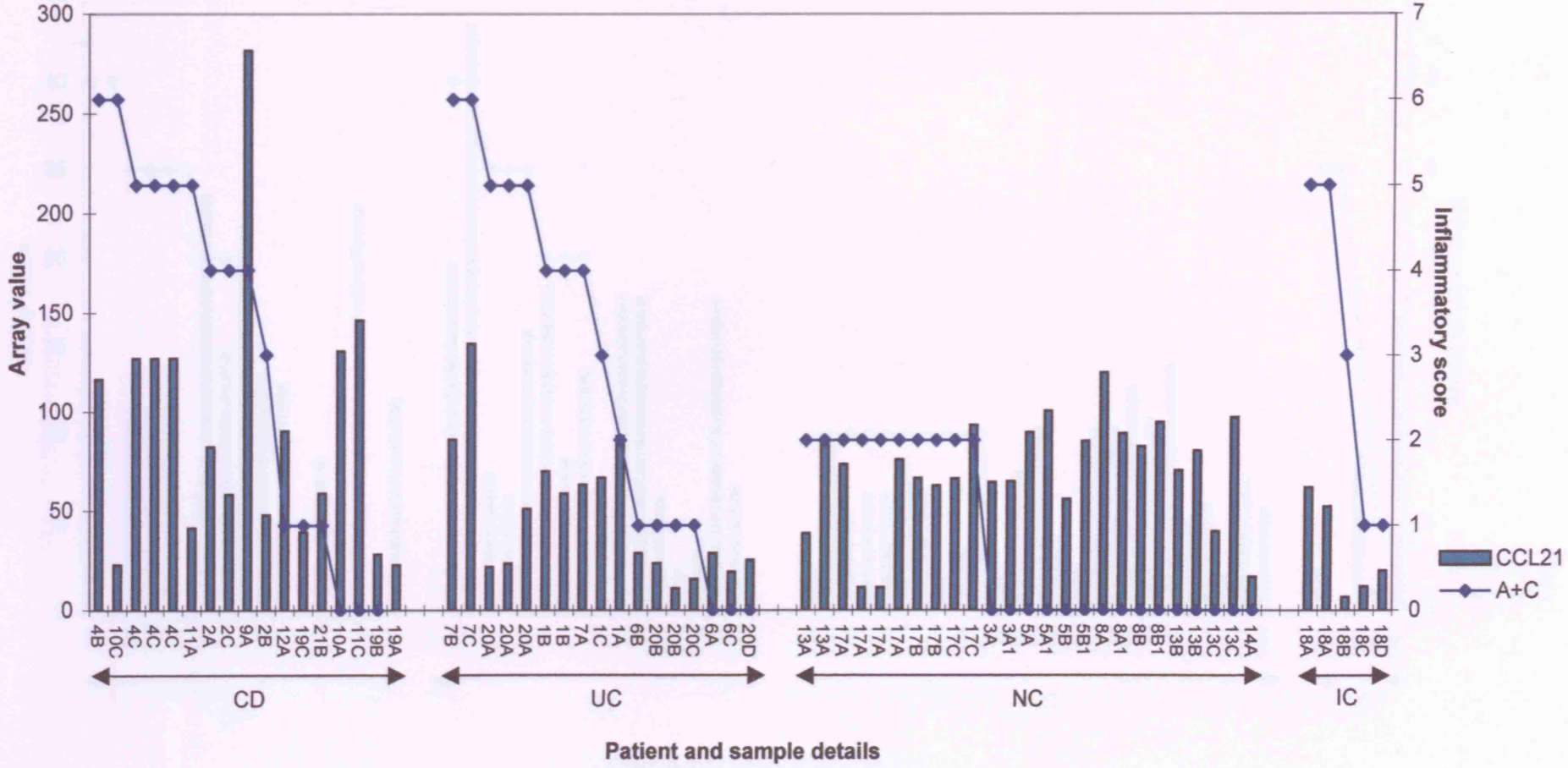

Patients are grouped according to disease, and chronologically placed according to inflammatory scores A+C (as defined in table 2.3). Patient and sample details are outlined in appendix 2. NC=normal control, IC=inflammatory control.

Graph 3.25: Relative expression of CCR7 in full-thickness colonic tissue measured using microarray correlated with relative levels of inflammation as determined by histopathological analysis

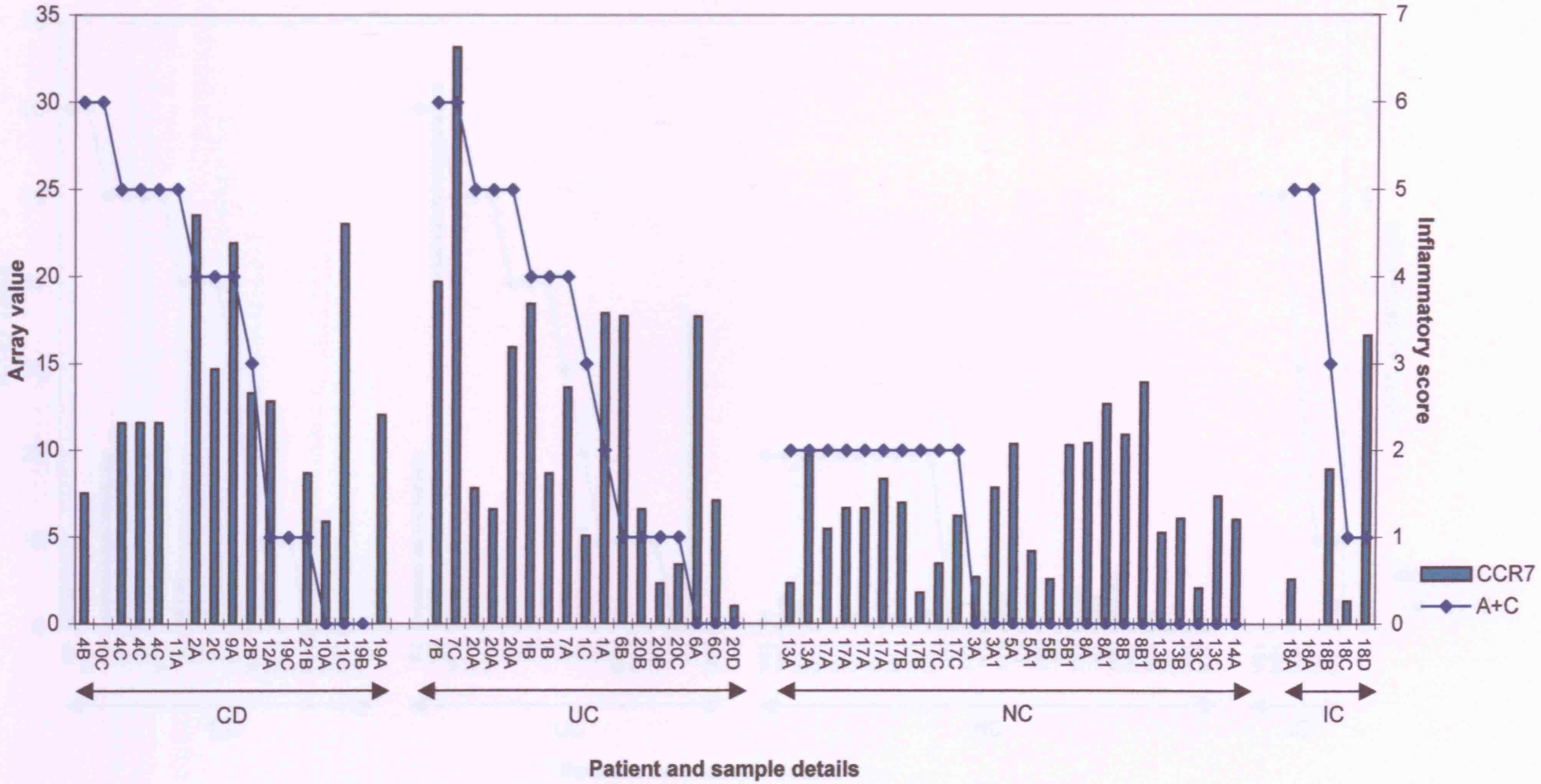

Patients are grouped according to disease, and chronologically placed according to inflammatory scores A+C (as defined in table 2.3). Patient and sample details are outlined in appendix 2. NC=normal control, IC=inflammatory control.

Graph 3.26: Relative expression levels of CXCL13 in full-thickness colonic tissue measured using miocroarray correlated with relative levels of inflammation as determined by histopathological analysis

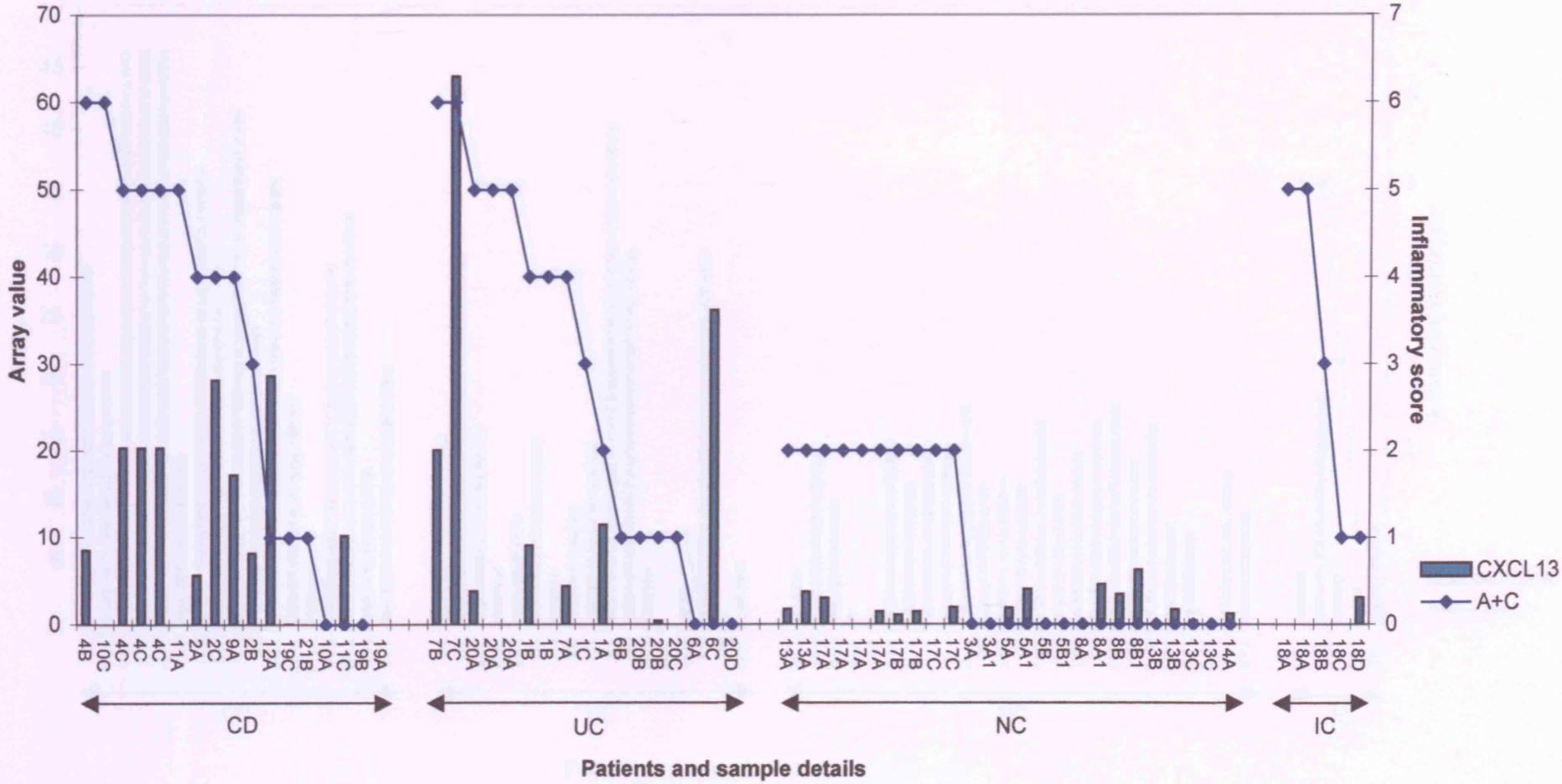

Patients are grouped according to disease, and chronologically placed according to inflammatory scores A+C (as defined in table 2.3). Patient and sample details are outlined in appendix 2. NC=normal control, IC=inflammatory control.

Grpah 3.27: Relative expression levels of CXCR5 in full-thickness colonic tissue measured using microararray correlated with relative levels of inflammation as determined by histopathological analysis

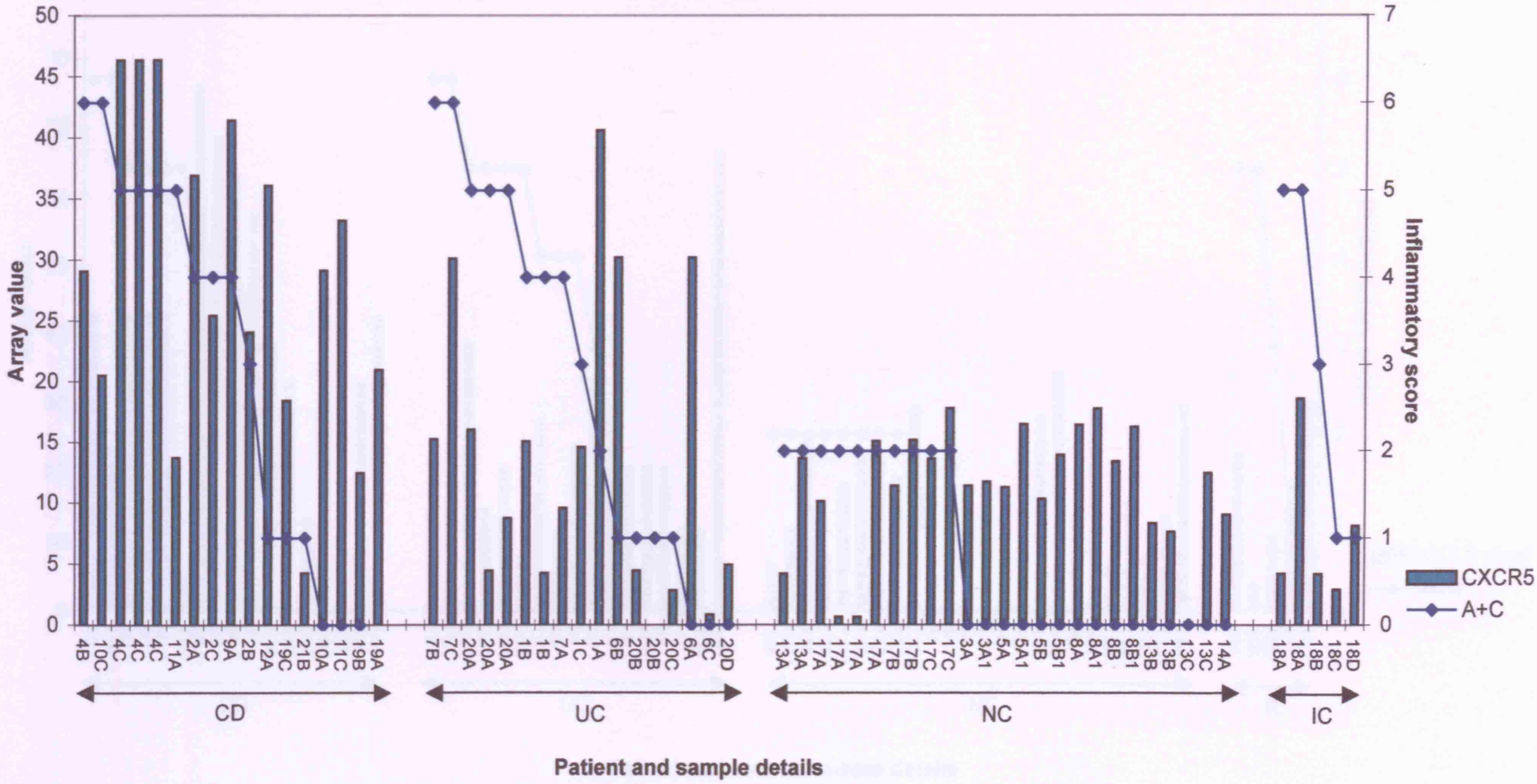

Patients are grouped according to disease, and chronologically placed according to inflammatory scores A+C (as defined in table 2.3). Patient and sample details are outlined in appendix 2. NC=normal control, IC=inflammtory control.

Grpah 3.28: Relative expression of CCL5 short arm in full thickness colonic tissue measured using microarray correlated with relative levels of inflammation as determined by histopathological analysis

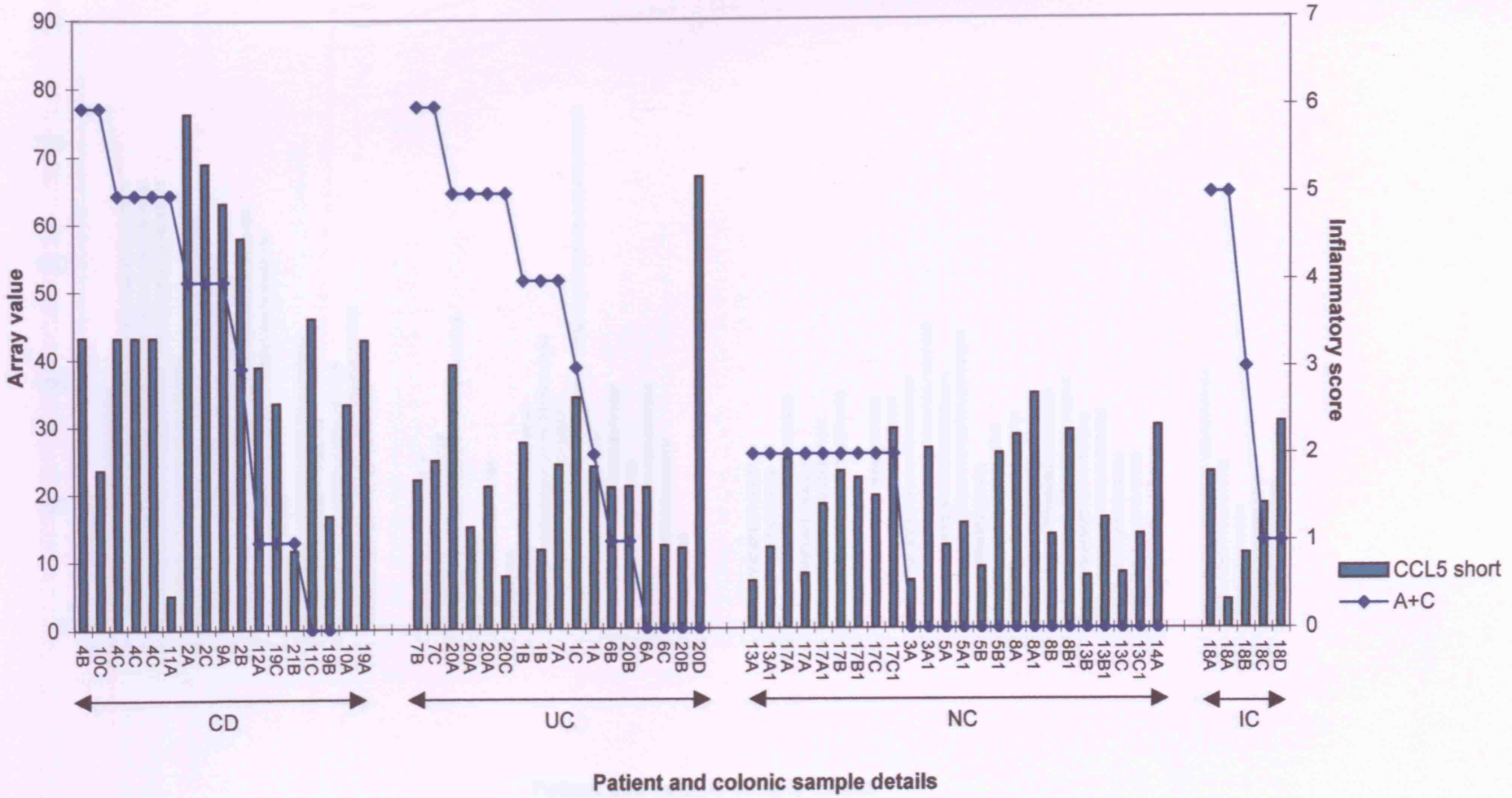

Patients are grouped according to disease, and chronologically placed according to inflammatory scores A+C (as defined in table 2.3). Patient and sample details are outlined in appendix table 2. NC=normal control, IC=inflammatory control.

Graph 3.29: Relative expression of CCL5L in full thickness colonic tissue measured using microarray correlated with relative levels of inflammation as determined by histopathological analysis

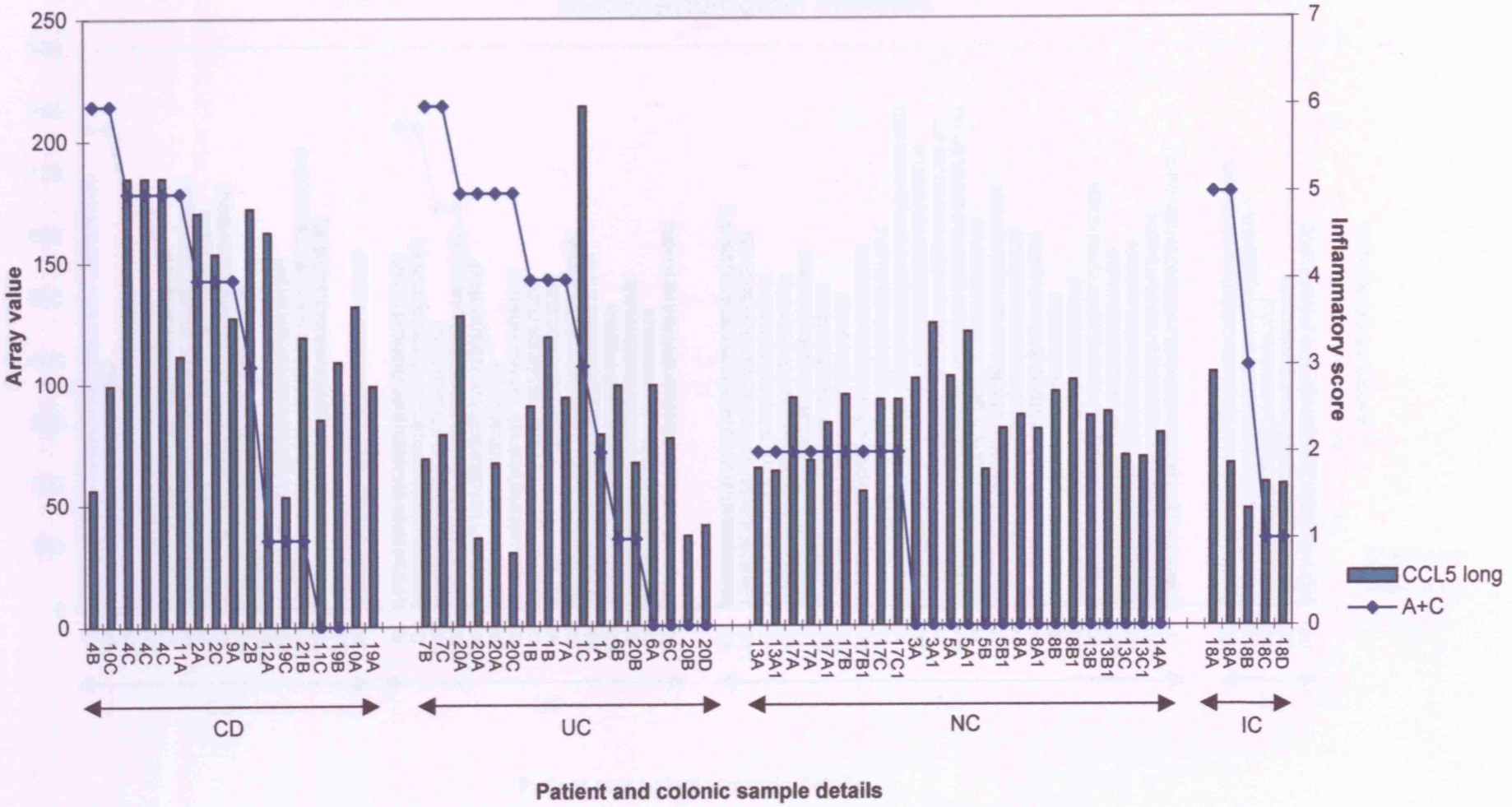

Patients are grouped according to disease, and chronologically placed according to inflammatory scores A+C (as defined in table 2.3). Patient and sample details are outlined in appendix table 2. NC=normal control IC=inflammatory control.

Graph 3.30: Relative expression of actin in full thickness colonic tissue measured using microarray correlated with relative levels of inflammation as determined by histopathological analysis

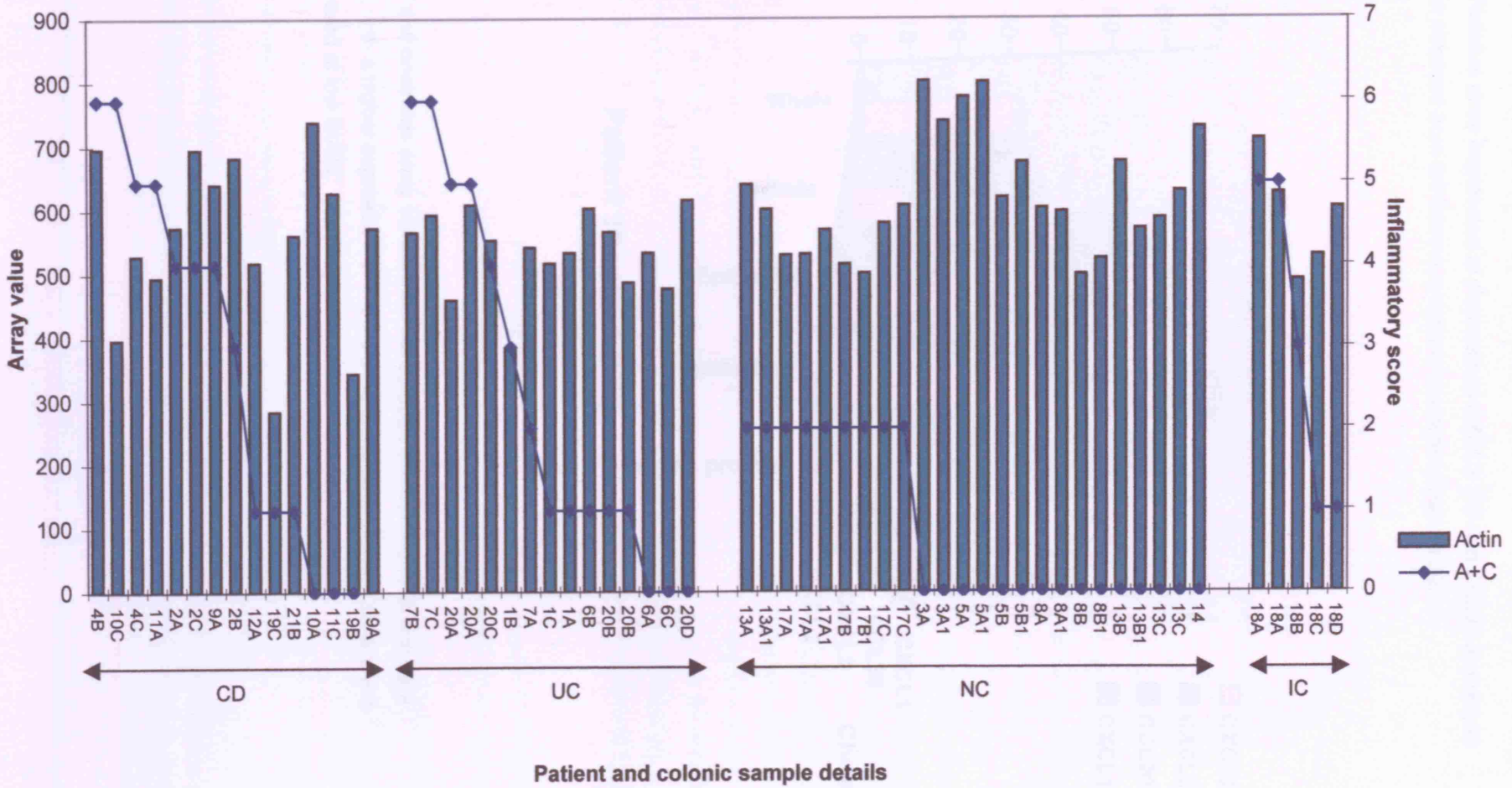

Patients are grouped according to disease, and chronologically placed according to inflammatory scores A+C (as defined in table 2.3). Patient and sample details are outlined in appendix table 2. NC=normal control, IC=inflammatory control.

Graph 3.31: Relative array expression of chemokines CXCL's 1-3 and CCL20 in stripped compartments obtained from full thickness colonic tissue from patient 20.

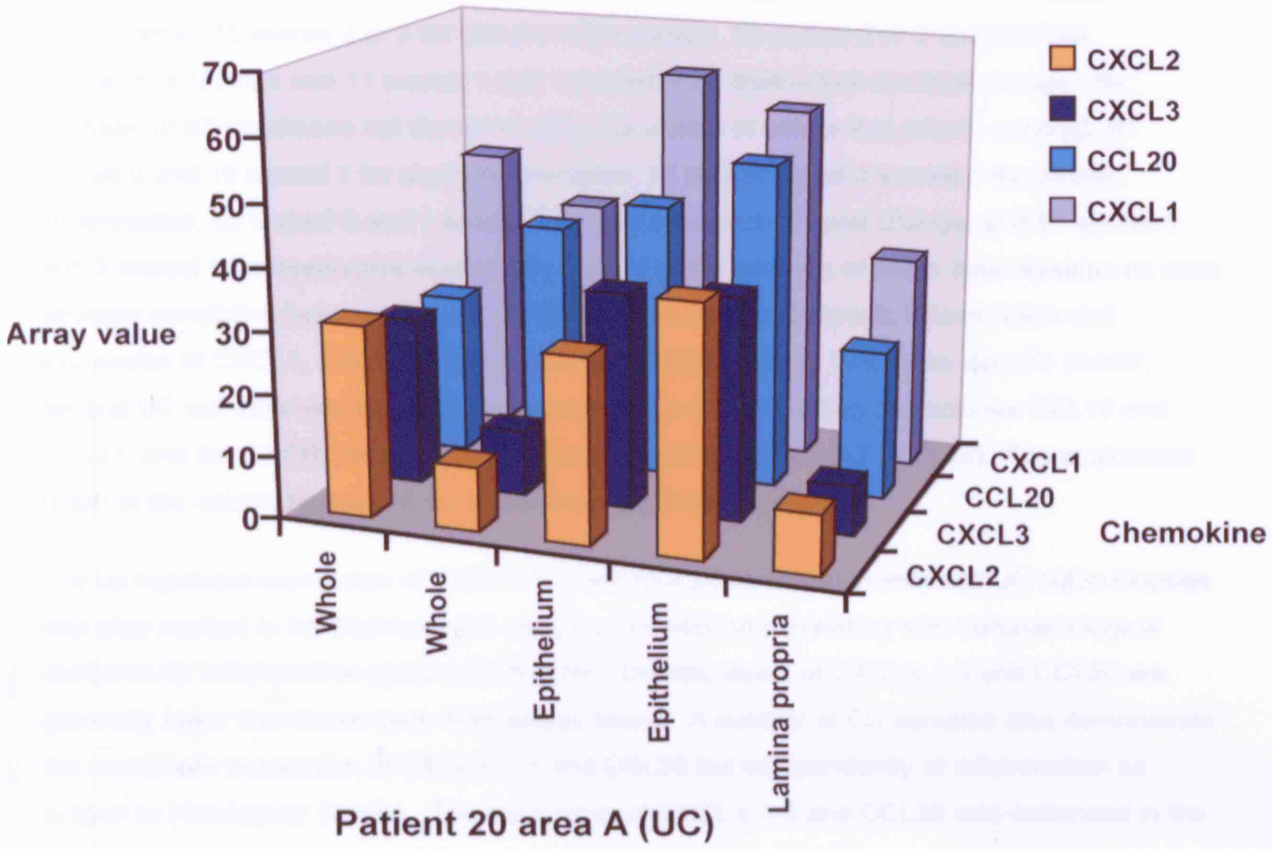

Graph 3.27 demonstrates array values from the stripped compartments in a severe case of UC, with a higher expression of chemokines in the epithelium. CCR6 levels were expressed at low levels.

3.2.3 Discussion

Of note, a cluster of 21 biopsies, taken from 5 UC and 1 CD patients, exhibited an expression profile clearly distinct from the other 101 profiles analysed. Within this exceptional cluster, much higher levels of gene expression were observed for a group of four chemokines, CXCL1, CXCL2, CXCL3, and CCL20, in comparison to other samples (graphs 3.3-3.6). The high histopathological quotients for inflammation, destructive mucosal change, and glandular architecture change assigned to these colon samples, further distinguishes this cluster. Of 20 specimens demonstrating this cluster (1 lost prior to scoring), 16 scored 2 or 3 for acute inflammation, 15 scored 2 or 3 for chronic inflammation, 16 scored 2 or 3 for glandular architecture change and 11 scored 1 and 1 scored 3 for destructive mucosal change. By contrast, of 97 specimens not demonstrating this cluster (4 others lost prior to scoring), 67 scored 0 and 19 scored 1 for acute inflammation, 91 scored 0 and 5 scored 1 for chronic inflammation, 95 scored 0 and 1 scored 1 for glandular architectural change, and 94 scored 0 and 3 scored 1 for destructive mucosal change. Further analysis of these data revealed an even stronger correlation between a cumulative score for acute and chronic inflammation and expression of CXCL1, CXCL2, CXCL3 and CCL20 (Graph 3.2). Within the specific cluster, several UC samples also exhibited expression of the CCR7 binding chemokines CCL19 and CCL21, and the CXCR5 binding chemokine, CXCL13 (graphs 3.9-3.11, 3.13). The anatomical origin of the colonic biopsy did not affect the chemokine expression.

The up regulated expression of CXCL's 1-3 and CCL20 observed in inflamed UC colon biopsies was also marked in full-thickness UC samples, expression correlating with histopathological quotients for inflammation (graphs 3.16-3.19). Overall, levels of CXCL's 1-3 and CCL20 are generally lower than those seen from biopsy tissue. A number of CD samples also demonstrate the coordinate expression of CXCL's 1-3 and CCL20 but independently of inflammation as judged by histological scoring. The expression of CXCL's 1-3 and CCL20 was enhanced in the full thickness specimens from CD patients in comparison to biopsies.

Interestingly, four specimens from a patient diagnosed with diverticulitis exhibited coordinated expression of CXCL's 1-3 and CCL20, expression levels correlating with inflammatory quotient.

Increased expression of CCL5 (RANTES) was observed in full thickness samples that was not detected at similar levels in any biopsy samples analysed in this study (graphs 3.27-3.28). CCL5 and CCR5 were expressed at generally higher levels in the CD cohort than the UC and control cohorts, while no significant difference was found between UC and control. Levels of chemokine expression did not correlate with inflammatory quotient.

Stripped epithelial analysis was limited to one patient who had severe UC. Expression of CXCL's 1-3 and CCL20 was higher in the epithelium than in the lamina propria (tables 3.5 and graph 3.30).

Formal statistical analysis of array data is not appropriate as they merely represent semi-quantisation. Such analysis is only appropriate for RT-PCR values.

Although ESR and CRP values were elevated in cases of inflamed compared to non-inflamed biopsy tissue, there was no reliable correlation between chemokine induction and inflammatory blood values. There was an overall tendency for CRP to be particularly elevated in CD and inflammatory colitis, and the ESR was higher in patients with UC. Results are included in appendix 2.3, 3.4 and 4.4. In full thickness tissue samples, there was some correlation between CRP and A+C, and therefore correlated with chemokine induction in a similar fashion.

3.3 Real time quantitative PCR (RT-PCR)

3.3.1 Background

In order to confirm and further quantify the microarray findings, real time quantitative reverse transcriptase coupled PCR (RT-PCR) was performed for CXCL's 1-3, 8-11, CCL's 3, 5, 20, 24, CCR's 5-6, CXCR's 1-3 on a subset of samples used for microarray analysis. The relative level of up regulated expression of these chemokines in inflamed IBD colon is expressed as a percentage of the average transcript copy number detected for the non-IBD cohort, normalised to 18S rRNA copy number. This data was compared to the histopathological quotient for inflammation.

3.3.2 RT-PCR technique

Quantitative reverse transcriptase polymerase chain reaction was performed as described in 2.2.2.6. The normalised data was compared to the histopathological quotients for inflammation.

3.3.3 Results

The data are listed in tables 3.9-11 and demonstrated in graphs 3.32-3.53.

Multiple non-paired t-test analyses of PCR results within colonic biopsy samples from CD/UC/normal control groups were performed on CXCR1, CXCR2, CXCL1, CXCL3, CXCL8, CCL20 and CCR6. There is a significant up regulation of the following in UC compared to normal control:

UC			
Chemokine	**Mean**	**Confidence interval**	**P value**
CXCL1	224.85	113.41 - 336.30	0.0003
CXCL3	122.72	63.77 - 181.68	0.0002
CXCL8	785.88	275.93 - 1295.83	0.004
CCL20	52.60	16.89 - 88.30	0.007
CXCR1	48.66	30.62 - 66.70	0.00001
CXCR2	41.17	24.75 - 57.59	0.00003
CCR6	19.66	11.03 - 28.29	0.0002

There is statistical up regulation of the same chemokines in CD compared to normal control only when CD samples were excluded where the corresponding biopsy assessed for histopathological inflammation had a quotient of A+C = 0.

CD			
Chemokine	**Mean**	**Confidence interval**	**P value**
CXCL1	21.96	3.36 - 40.56	0.009
CXCL3	12.09	3.01 - 21.17	0.004
CXCL8	222.19	0 - 457.45	0.017
CCL20	10.23	0.19 - 20.27	0.03
CXCR1	13.04	2.61 - 23.44	0.008
CXCR2	8.72	1.18 - 16.26	0.018

When a similar exclusion was applied to the UC subset, the statistical significance of up regulation increased, as listed below:

UC			
Chemokine	**Mean**	**Confidence interval**	**P value**
CXCL1	323.04	190.14 - 453.94	0.000001
CXCL3	176.25	106.83 - 245.67	0.000001
CXCL8	1138.66	458.72 - 1818.60	0.0003
CCL20	77.32	29.48 - 125.16	0.0005
CXCR1	66.63	47.53 - 85.53	0.000000004
CXCR2	58.06	40.74 - 75.38	0.000000009
CCR6	27.60	17.46 - 37.74	0.000001

Multiple non-paired t-test analyses were applied to the PCR values obtained from full-thickness colonic samples on chemokines CXCL1, CXCL9, CXCL10, CXCL11, CCL2, CCL3, CCL5, CCL20, CCL24, in addition to chemokine receptors CCR3, CCR5, CXCR1, CXCR2 and CXCR3. There is a significant up regulation of the following in IBD compared to normal control:

CD			
Chemokine	**Mean**	**Confidence interval**	**P value**
CCL5	12.33	8.06 - 16.60	0.0058
CCR5	39.25	25.62 - 52.88	0.009
CXCR3	2.98	1.90 - 4.06	0.023

Non-parametric analyses correlating inflammatory scores A+C with corresponding RT-PCR values for CCL20, CCR6, CXCR1 and CXCR2 indicated statistically significant-associations. Spearman's correlation coefficients were as follows: 0.66 ($p<0.005$) for CCL20, 0.48 ($p<0.005$) for CCR6, 0.68 ($p<0.005$) for CXCR1 and 0.66 ($p<0.005$).

Table 3.9: Relative expression levels of CXCR1, CXCR2, CXCL1, CXCL3, CXCL8, CCL20 and CCR6 in colonic biopsy tissue obtained by quantitative PCR, normalised as outlined in 2.2.2.6. NC=normal control.

Dx	Pnt numb	Bx numb	A+C	ESR	CRP	CXCR1	CXCR2	CXCL1	CXCL3	CXCL8	CCL20	CCR6
CD	11	5	4	54	X	43.4072	24.4499	90.7951	42.7262	1189.647	53.0164	6.0468
CD	11	2	3	54	X	7.8151	4.6059	25.2574	11.1964	144.2095	9.8499	1.3545
CD	11	4	3	54	X	22.0386	10.5349	49.1413	27.5074	251.8455	10.4393	3.5465
CD	8	1	2	3	1	1.0647	0.8853	0.8444	0.5282	0.452	0.5991	0.7899
CD	26	1	2	11	33	3.0904	2.1489	1.0351	0.8894	3.2057	0.7059	2.7814
CD	8	2	2	3	1	0.9533	0.7816	0.5617	0.4041	1.1768	0.1706	0.2778
CD	11	3	2	54	X	5.6193	4.2058	9.3655	4.3037	57.269	5.1778	2.471
CD	26	4	2	11	33	2.5549	3.1211	1.1105	1.2923	2.7826	0.8568	1.9835
CD	11	1	1	54	X	40.5692	35.6795	34.0532	22.2092	476.8756	14.8945	8.2764
CD	11	6	1	54	X	3.2654	0.7577	7.407	9.7936	94.4768	6.5892	0.4957
CD	26	2	0	11	33	1.548	2.6648	0.1715	0.6037	63.8706	0.9222	1.1101
CD	8	3	0	3	1	0.8329	1.0858	0.2198	0.1707	0.2395	0.1534	0.6165
CD	26	3	0	11	33	2.1496	1.2836	0.3572	0.6162	3.4933	0.8573	1.3075
CD	8	4	0	3	1	0.4748	0.2987	0.168	0.2462	0.328	0.1633	0.5346
CD	8	5	0	3	1	0.3419	0.2582	0.0895	0.0932	0.057	0.0818	0.3224
CD	26	5	0	11	33	1.9586	1.9622	0.5116	0.7392	9.6493	0.8056	1.1668
CD	8	6	0	3	1	1.3617	1.0581	2.9313	2.6168	4.5246	0.6597	0.5131
CD	26	6	0	11	33	1.1019	1.5611	0.2287	0.5792	14.3219	0.5274	0.7695
CD av			1.22	22.66		7.7860	5.4079	12.4583	7.0286	128.8013	5.9150	1.9091
CD SD			1.30	23.04		13.4185	9.4810	24.0312	11.9742	291.5387	12.5643	2.1492
CD n	18	18	18	18	18	18	18	18	18	18	18	18
UC	16	5	5	X	X	101.5053	92.6042	585.9974	279.8226	1334.642	178.6483	34.9361
UC	16	1	4	X	X	130.9626	73.5524	367.7222	243.8709	1552.894	44.3396	43.7738
UC	14	2	4	X	2	28.0724	29.9613	34.6181	27.3482	83.9659	31.7029	15.0781
UC	16	2	4	X	X	86.9238	81.8774	425.8368	287.0876	916.1558	43.906	21.985
UC	16	3	4	X	X	79.4736	101.6616	457.7403	314.3399	976.668	71.5493	40.8783
UC	14	4	4	X	2	39.08	22.9074	104.9622	67.5063	519.767	297.0134	41.8447
UC	14	5	4	X	2	43.4144	23.0686	68.3657	25.4539	167.9927	24.0062	7.9887
UC	14	6	4	X	2	80.5151	47.8666	622.1561	214.6887	4149.524	14.8945	8.2764
UC	14	1	3	X	2	31.5127	41.3334	200.1336	116.7114	357.4044	88.2035	58.1894
UC	16	4	3	X	X	79.3745	85.7694	413.8882	199.7674	1191.053	71.5423	7.1606
UC	16	6	3	X	X	70.8471	74.6479	591.9283	327.3522	2399.6	58.5017	39.418
UC	15	3	1	6	1	26.6817	21.5088	3.1437	11.0954	14.2157	3.4746	11.6711
UC	15	1	0	6	1	2.8931	2.0682	0.7329	0.7932	0.4632	0.642	1.7478
UC	15	2	0	6	1	14.4535	7.35	2.8459	4.8641	4.5871	2.0277	7.3108
UC	14	3	0	X	2	46.8497	25.7277	157.9176	69.7211	440.6242	11.7161	7.8825
UC	15	4	0	6	1	4.4619	0.8462	0.2968	0.8591	1.1496	0.7193	1.5048
UC	15	5	0	6	1	2.296	2.9271	1.2329	1.937	1.3505	0.594	1.4603
UC	15	6	0	6	1	6.4868	5.4187	7.8279	15.8112	33.7553	3.4649	2.844
UC av			2.38			48.6558	41.1720	224.8526	122.7239	785.8785	52.6081	19.6639
UC SD			1.91			38.2716	34.8243	236.4122	125.0640	1081.747	75.7778	18.3111
UC n	18	18	18	18	18	18	18	18	18	18	18	18
NC	7	3	1	14	1	0.3363	0.3685	1.1665	1.3263	0.7025	1.6176	0.121
NC	7	4	1	14	1	0.3195	0.516	1.2619	1.7449	1.892	2.2469	0.4329
NC	6	1	0	X	X	0.3897	0.2882	0.0856	0.2322	0.1816	0.0949	0.2256
NC	7	1	0	14	1	0.4318	0.2755	0.2592	0.4589	0.2088	0.5816	0.3873
NC	13	1	0	X	X	2.7844	3.406	2.1773	0.777	0.889	2.0523	2.7795
NC	6	2	0	X	X	0.5668	0.2176	0.228	0.3291	0.6692	0.6456	0.7707
NC	7	2	0	14	1	0.3957	0.8425	0.4752	0.5812	0.2683	0.6382	0.3388
NC	13	2	0	X	X	9.95	4.1387	2.2815	2.2802	0.397	0.9355	2.5851
NC	6	3	0	X	X	0.647	0.8114	0.2529	0.9102	0.4982	0.4783	0.4114
NC	13	3	0	X	X	1.5027	1.6556	1.1883	0.4931	1.9522	1.5163	0.9122
NC	2	4	0	X	X	3.6115	3.5275	0.6407	0.8101	1.9536	2.985	5.5511
NC	13	4	0	X	X	3.0017	3.3737	2.5861	1.5763	3.6865	2.0847	1.6846
NC	2	5	0	X	X	3.2734	3.3279	0.2629	0.3277	0.6303	2.339	9.32
NC	7	5	0	14	1	0.2356	0.2264	0.9062	0.9218	0.6889	1.4751	0.259
NC	13	5	0	X	X	2.4279	1.8549	3.2911	2.3047	9.8892	1.5608	1.1867
NC	2	6	0	X	X	1.0404	0.7306	1.0809	1.3299	0.7118	2.2488	5.3488
NC	7	6	0	14	1	0.2447	0.513	7.9768	7.5564	2.826	6.4104	0.4569
NC	13	6	0	X	X	1.772	3.0616	16.9026	2.9843	5.1777	1.3883	2.678
NC av			0.11			1.8295	1.6186	2.3902	1.4969	1.8457	1.7389	1.9694
NC SD			0.32			2.3416	1.4318	4.0671	1.7019	2.4221	1.4026	2.4815
NC n	18	18	18	18	18	18	18	18	18	18	18	18

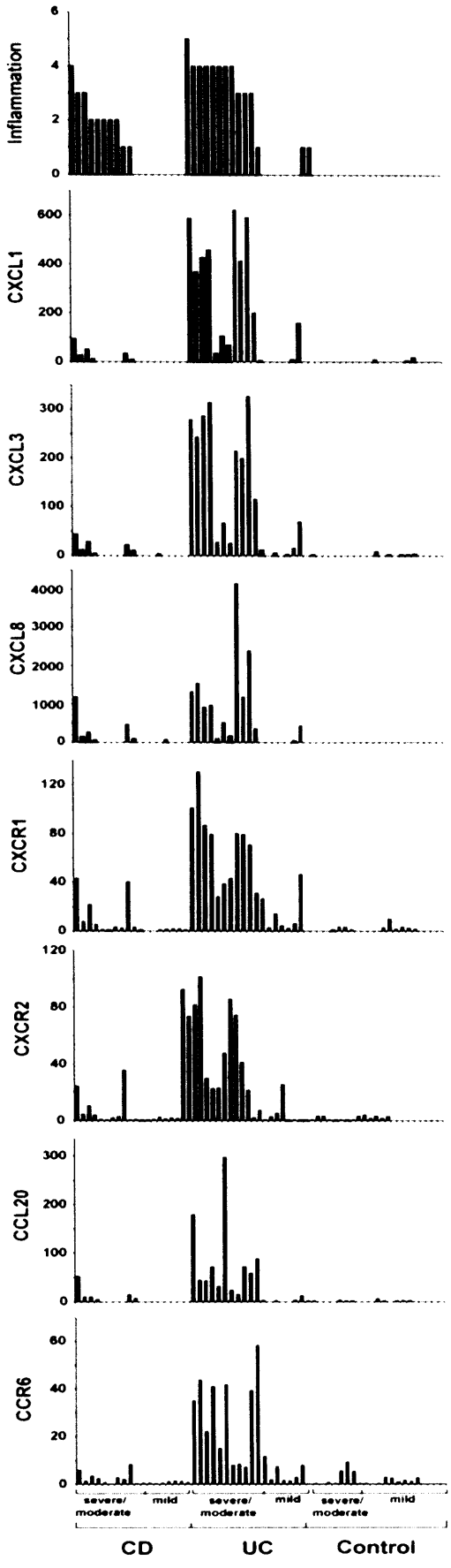

Graph 3.32: Taqman quantitative PCR analysis of chemokine and cognate receptor expression, in comparison to relative levels of inflammation as determined by histopathological analysis in colonic biopsy specimens. mRNA levels are expressed as fold-up-regulation compared to the average of the mRNA levels quantified for samples analysed from the control cohort.

Table 3.10: Taqman quantitative PCR analysis data of chemokine expression of CXCL1, 9, 10, 11, CCL3 and CCL5 from full thickness colonic tissue with inflammatory quotient, normalised as outlined in 2.2.2.6. Patient and sample area details are outlined in appendix table 1.

Patient number, area and diagnosis	A+C	CRP	CXCL1	CXCL9	CXCL10	CXCL11	CCL3	CCL5
10-C (CD)	6	5	17.229	656.11	606.77	125.53	6.3792	11.195
4-B (CD)	6	164	139.9	1427.7	5478.3	2463.8	29.63	11.011
11-A (CD)	5		3.8025	127.99	213.03	54.763	0.2258	0.7356
4-C (CD)	5	164	32.895	11376	13589	7819.7	7.216	13.737
2-A (CD)	4	41	40.699	273.9	716.91	391.03	0.6562	5.2238
2-C (CD)	4	41	6.7154	463.7	855.71	514.26	5.552	10.65
9 (CD)	4	14	5.8844	984.22	1271.9	433.81	8.8934	15.908
2-B (CD)	3	41	21.079	2174.8	1869.1	1725.1	3.9936	30.588
12-A (CD)	1		8.0707	696.03	1066	265.05	0.6036	7.6814
19-A (CD)	1	1	0.36	10.063	78.934	23.511	0.809	11.137
19-B (CD)	1	1	1.6264	238.07	635.17	298.95	0.2858	7.9073
19-C (CD)	1	1	6.4696	1202.2	2672.5	1477.3	1.1214	13.991
10-A (CD)	0	5	17.646	831.3	1387.8	302.43	3.6195	6.1457
CD av	2.92		22.3242	1666.5100	2375.4731	1216.7024	6.9710	12.3285
CD SD	2.20		35.8341	2907.7435	3519.0121	2034.7682	9.8082	7.9839
CD n	14	14	14	14	14	14	14	14
7-B (UC)	6	1	73.361	976.07	3577.6	2707.2	3.8931	5.7796
7-C (UC)	6	1	14.449	366.46	1080.1	1347.9	0.885	2.8999
20-A (UC)	5	17	12.936	134.33	545.08	1104.4	0.4987	2.3799
1-B (UC)	4	1	12.796	1836.7	2970.1	1647	0.9362	8.6154
1-B (UC)	4	1	0.9169	2.7907	8.2516	12.655	0.2721	2.1391
7-A (UC)	4	1	4.6465	105.55	462.23	186.6	1.9425	3.0837
1-C (UC)	3	1	4.6939	1042.7	2060.7	1293.6	1.3065	10.199
20-B (UC)	1	17	0.1137	0.9997	3.5853	6.1191	0.0283	1.3669
6-B (UC)	1	1	1.5486	31.381	107.63	17.636	0.4055	3.7753
6-A (UC)	0	1	0.8102	51.56	114.58	54.792	0.3806	3.0791
6-C (UC)	0	1	1.9874	51.958	83.93	59.688	0.3132	1.4425
UC av	3.09		11.6599	418.2272	1001.2534	767.0536	0.9874	4.0691
UC SD	2.25		21.1605	604.9115	1286.4226	912.2107	1.1091	2.9215
13-A (N)	2		6.6564	31.461	284.95	180.07	0.8084	2.502
17-A (N)	2		0.3479	5.714	59.346	7.9853	0.5708	3.5381
17-C (N)	2		1.2959	5.1218	27.301	13.153	1.0822	4.6995
13-C (N)	0		6.9012	111.66	308.96	582.94	0.6274	3.684
14 (N)	0		0.173	6.6991	26.665	26.273	0.068	2.407
3-A (N)	0		4.963	14.832	38.114	24.701	1.3565	4.6551
5-A (N)	0	1	2.6594	31.059	69.781	55.371	0.9457	1.5942
8-A (N)	0	3	2.5608	7.26	31.093	10.171	0.6144	4.5751
NC av	0.75		3.1947	26.7259	105.7763	112.5830	0.7592	3.4569
NC SD	1.0351		2.6827	36.0252	119.1704	198.4048	0.3873	1.1815
NC n	8	8	8	8	8	8	8	8
18-A (IC)	5	135	105.52	27.616	238.66	60.157	13.136	0.8534
18-B (IC)	3	135	11.987	1	1	1	1	1
18-C (IC)	1	135	1	3.1435	16.045	3.8202	1.1915	1.1454

Table 3.11: Taqman quantitative PCR analysis data of chemokines CCL20 and 24, chemokine receptor expression of CCR3, CCR5, CXCR3 from full thickness colonic tissue with inflammatory quotients A+C, normalised as outlined in 2.2.2.6. Patient and sample area details are outlined in appendix table 1.

Patient number, area and diagnosis	A+C	CRP	CCL20	CCL24	CCR3	CCR5	CXCR3
10-C (CD)	6	5	0.3181	9.5588	10.158	26.231	3.1268
4-B (CD)	6	164	0.5536	0.8017	4.1414	76.649	3.0866
11A (CD)	5		0.2496	1.0869	7.3605	6.0215	2.6992
4-C (CD)	5	164	3.0913	2.0909	17	94.1	7.8532
2-A (CD)	4	41	5.2631	1.3526	3.6717	19.534	1.3711
2-C (CD)	4	41	0.3863	0.5234	1.7752	20.469	2.1788
9 (CD)	4	14	1.4703	2.1842	17.071	47.781	3.1331
2-B (CD)	3	41	3.9134	2.7526	3.7831	56.923	6.8712
12-A (CD)	1		0.4413	1.7207	35.288	37.151	2.5142
19 (CD)	1	1	5.2225	0.2771	2.0194	8.2673	1.2271
19-B (CD)	1	1	0.4108	0.8033	10.302	22.614	0.7042
19C (CD)	1	1	1.0686	5.6666	35.878	53.708	2.2598
10-A (CD)	0	5	0.485	5.1696	10.411	49.908	3.0173
11-C (CD)	0		0.6757	1.135	10.606	30.109	1.6564
CD av			1.6821	2.5088	12.1046	39.2475	2.9785
CD SD			1.8649	2.5974	11.0874	25.5021	2.0191
CD n			14	14	14	14	14
7-B (UC)	6	1	9.9964	7.9487	32.326	79.666	5.465
7-C (UC)	6	1	1.216	2.9209	8.3987	12.206	1.7406
20-A (UC)	5	17	2.5531	4.8354	5.3844	10.617	2.9537
1-B (UC)	4	1	1.6274	4.107	17.108	30.844	2.6613
1-B (UC)	4	1	0.3948	0.4072	7.1037	4.1681	0.748
7-A (UC)	4	1	2.0353	1.0274	5.9349	11.225	1.1633
1-C (UC)	3	1	0.2797	4.3729	7.0456	12.447	2.3959
20-B (UC)	1	17	0.0911	0.578	0.4077	0.8414	0.4822
6-B (UC)	1	1	0.3726	0.4827	7.4556	4.1736	0.4923
6-A (UC)	0	1	0.0752	0.5641	7.9632	12.475	1.2608
6-C (UC)	0	1	0.2007	0.546	21.752	33.885	0.7456
UC av			1.7129	2.5264	10.9890	19.3225	1.8280
UC SD			2.8787	2.5155	9.1458	22.5233	1.4905
UC n			11	11	11	11	11
13-A (NC)	2		0.5818	0.9417	8.7417	15.994	0.7825
17-A (NC)	2		0.2495	1.2729	4.4123	13.737	0.6298
17-C (NC)	2		0.4266	2.8466	3.991	19.144	1.1739
13-C (NC)	0		0.7095	0.9705	7.2548	25.617	1.4648
14 (NC)	0		0.0141	0.0937	1.45	1.9853	1.1833
3-A (NC)	0		3.0118	2.0063	3.3749	8.6308	1.1396
5-A (NC)	0	1	0.5982	1.0192	2.0032	2.5954	1.4874
8-A (NC)	0	3	1.9287	0.9522	9.3807	12.903	1.6556
NC av			0.9400	1.2629	5.0760	12.5758	1.1896
NC SD			1.0118	0.8257	3.0193	8.0505	0.3512
NC n			8	8	8	8	8
18-A (IC)	5	135	12.792	0.7316	3.8188	5.715	0.562
18-B (IC)	3	135	4.3717	1	1	1	1
18-C (IC)	1	135	1	0.3691	1.1583	2.1805	0.3493

Graph 3.33: Relative expression of CXCL1 in colonic biopsies measured by RT-PCR corrrelated with relative levels of inflammation as determined by histopathological analysis

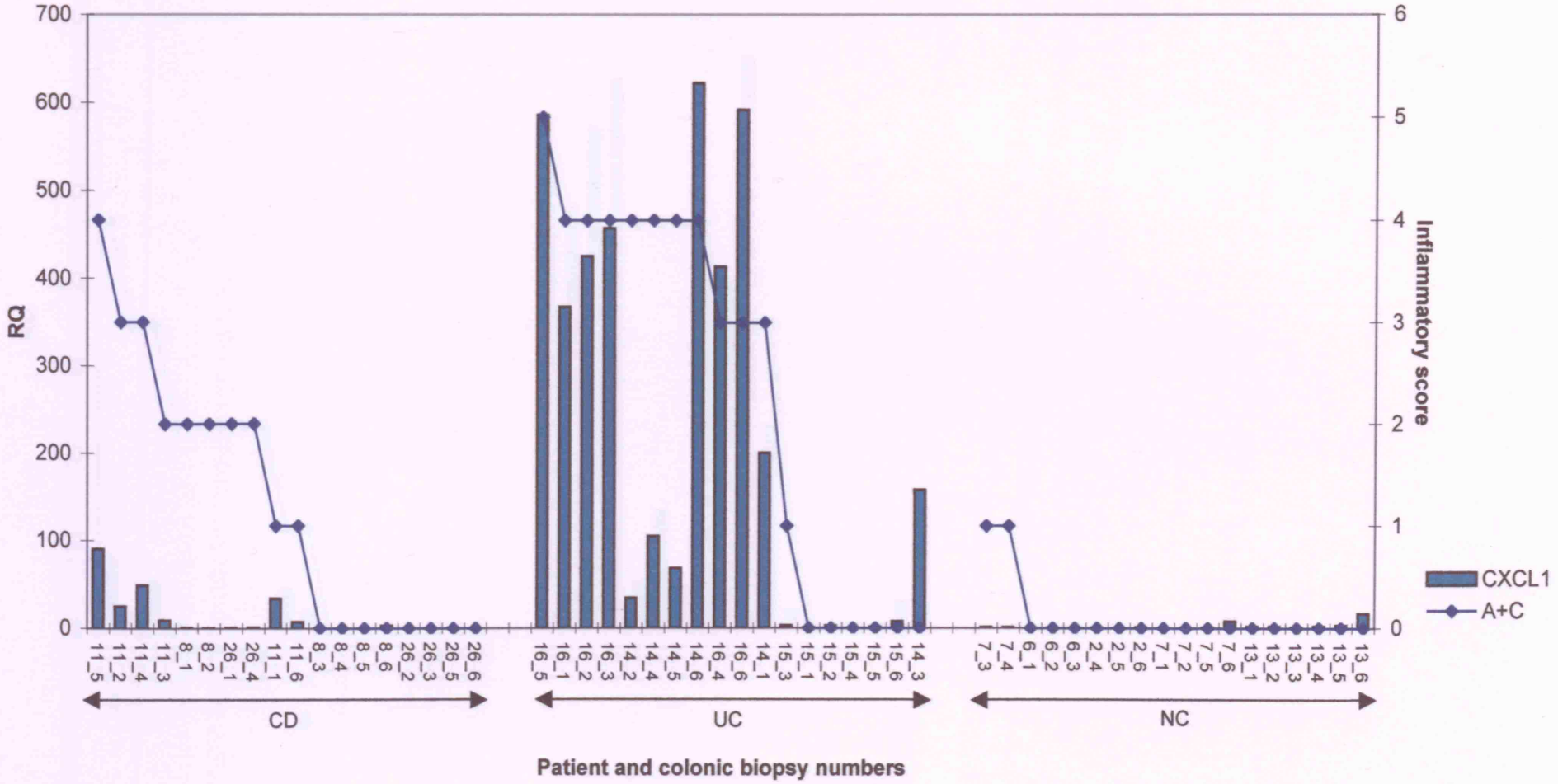

Patients are grouped according to disease, and chronologically placed according to inflammatory scores A+C (as defined in table 2.3). Patient and sample details are outlined in appendix table 2. NC=normal control, IC=inflammatory control.

Graph 3.34: Relative expression of CXCL3 in colonic biopsies measured by RT-PCR corrrelated with relative levels of inflammation as determined by histopathological analysis

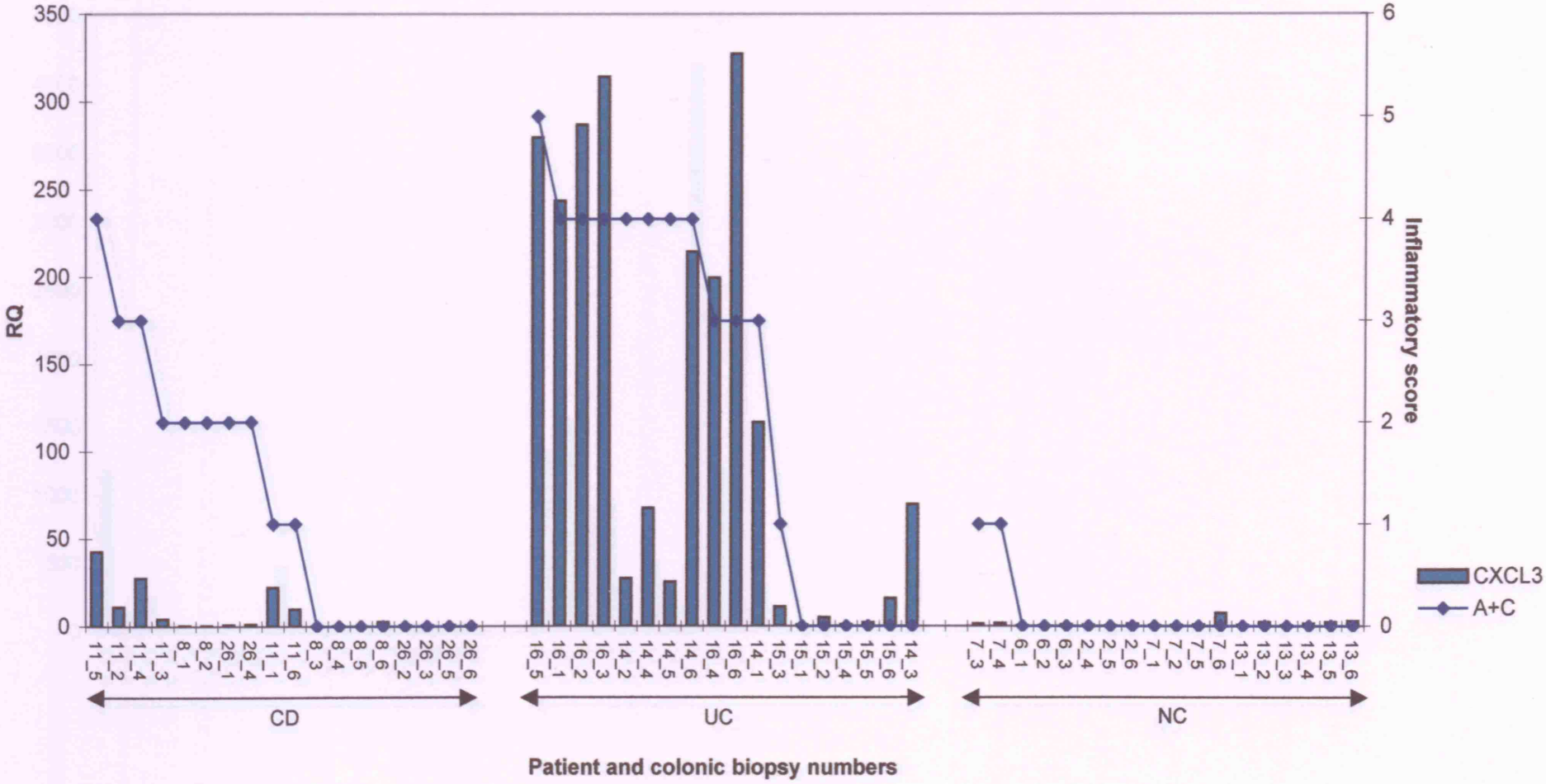

Patients are grouped according to disease, and chronologically placed according to inflammatory scores A+C (as defined in table 2.3). Patient and sample details are outlined in appendix table 2. NC=normal control, IC=inflammatory control.

Graph 3.35: Relative expression of CXCL8 in colonic biopsies measured by RT-PCR corrrelated with relative levels of inflammation as determined by histopathological analysis

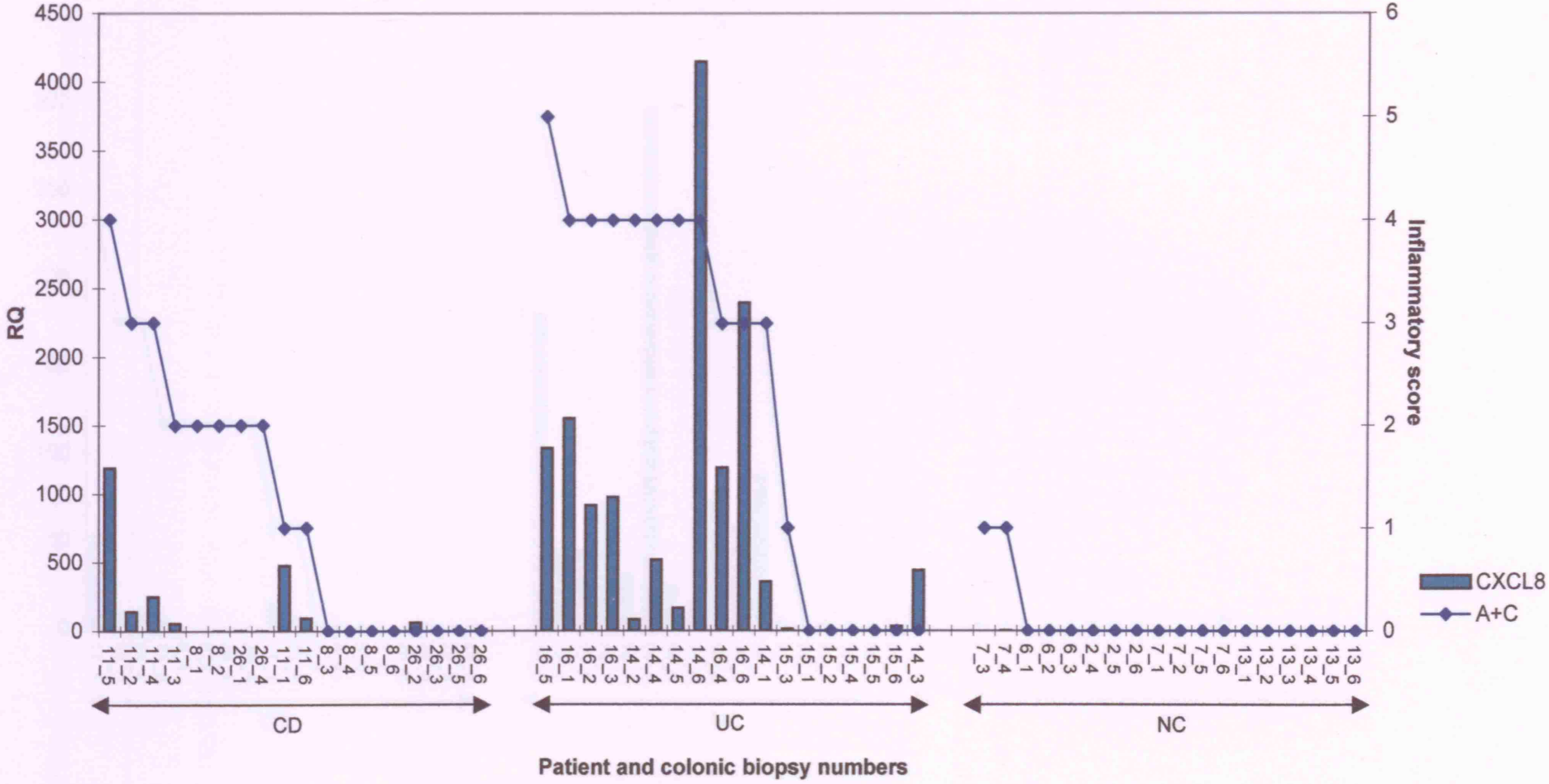

Patients are grouped accoridng to disease, and chronologically placed according to inflammatory scores A+C (as defined in table 2.3). Patient and sample details are ourlined in appendix table 2. NC=normal control, IC=inflammatory control.

Graph 3.36: Relative expression of CCL20 in colonic biopsies measured by RT-PCR corrrelated with relative levels of inflammation as determined by histopathological analysis

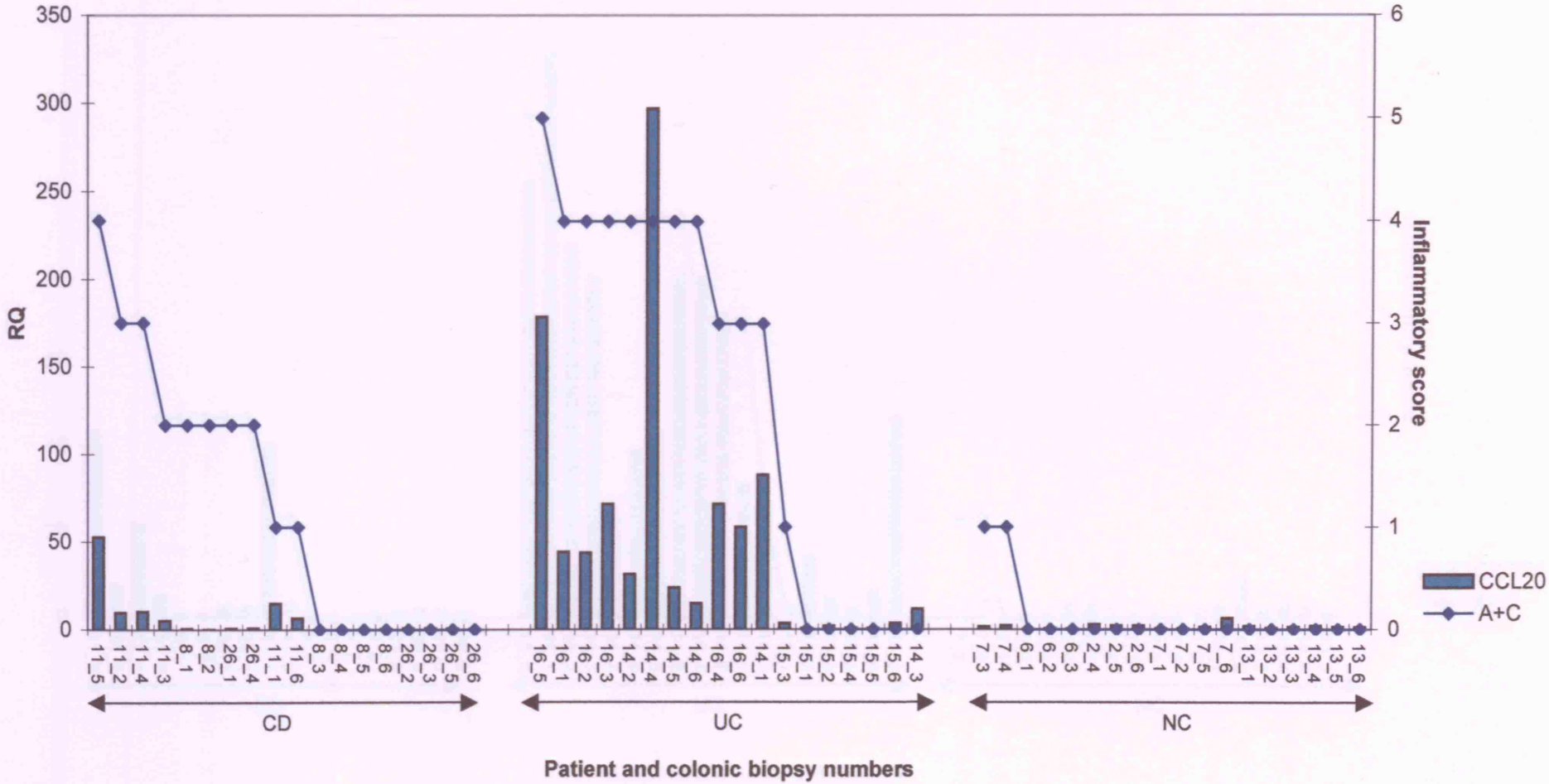

Patients are grouped according to disease, and chronologically placed according to inflammatory scores A+C (as defined in table 2.3). Patient and sample details are outlined in appendix table 2. NC=normal control, IC=inflammatory control.

Graph 3.37: Relative expression of CXCR1 in colonic biopsies measured by RT-PCR correlated with relative levels of inflammation as determined by histopathological analysis

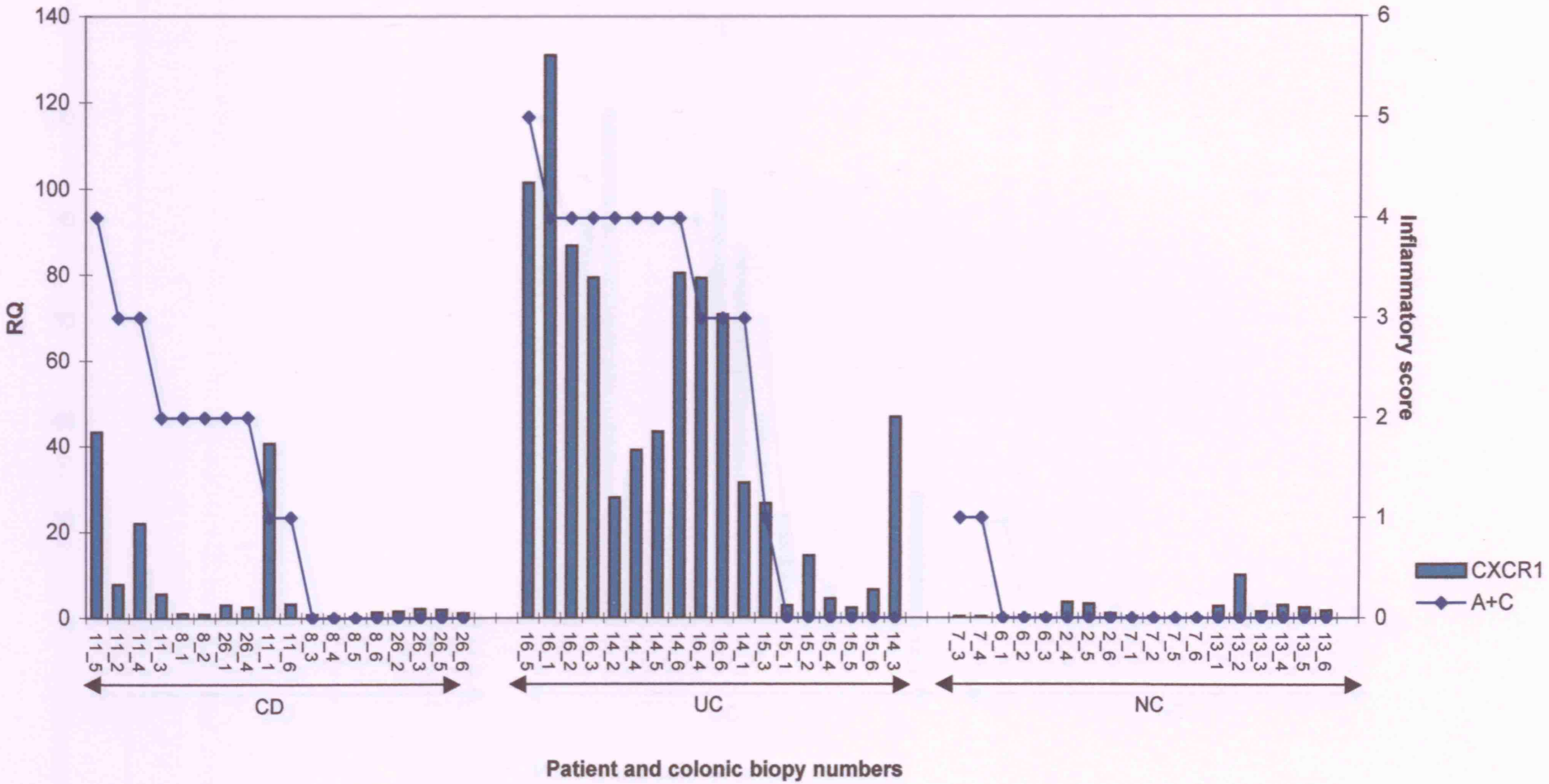

Patients are grouped according to disease, and chronologically placed according to inflammatory scores A+C (as defined in table 2.3). Patient and sample details are outlined in appendix 2. NC=normal control, IC=inflammatory control.

Graph 3.38: Relative expression of CXCR2 in colonic biopsies measured by RT-PCR corrrelated with relative levels of inflammation as determined by histopathological analysis

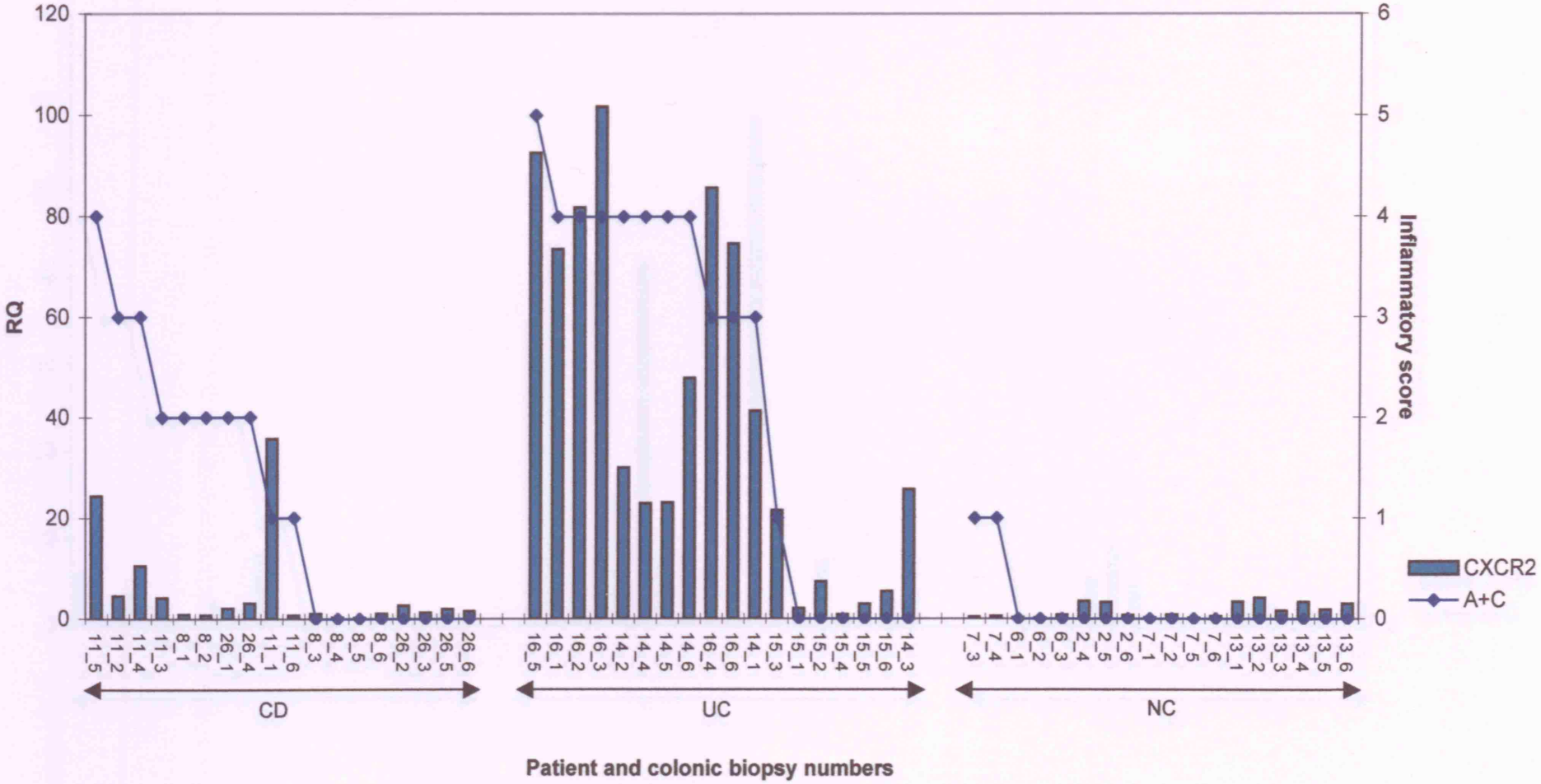

Patients are grouped according to disease, and chronologically placed according to inflammatory scores A+C (as defined in table 2.3). Patient and sample details are outlined in appendix 2. NC=normal control, IC=inflammatory control.

Graph 3.39: Relative expression of CCR6 in colonic biopsies measured by RT-PCR corrrelated with relative levels of inflammation as determined by histopathological analysis

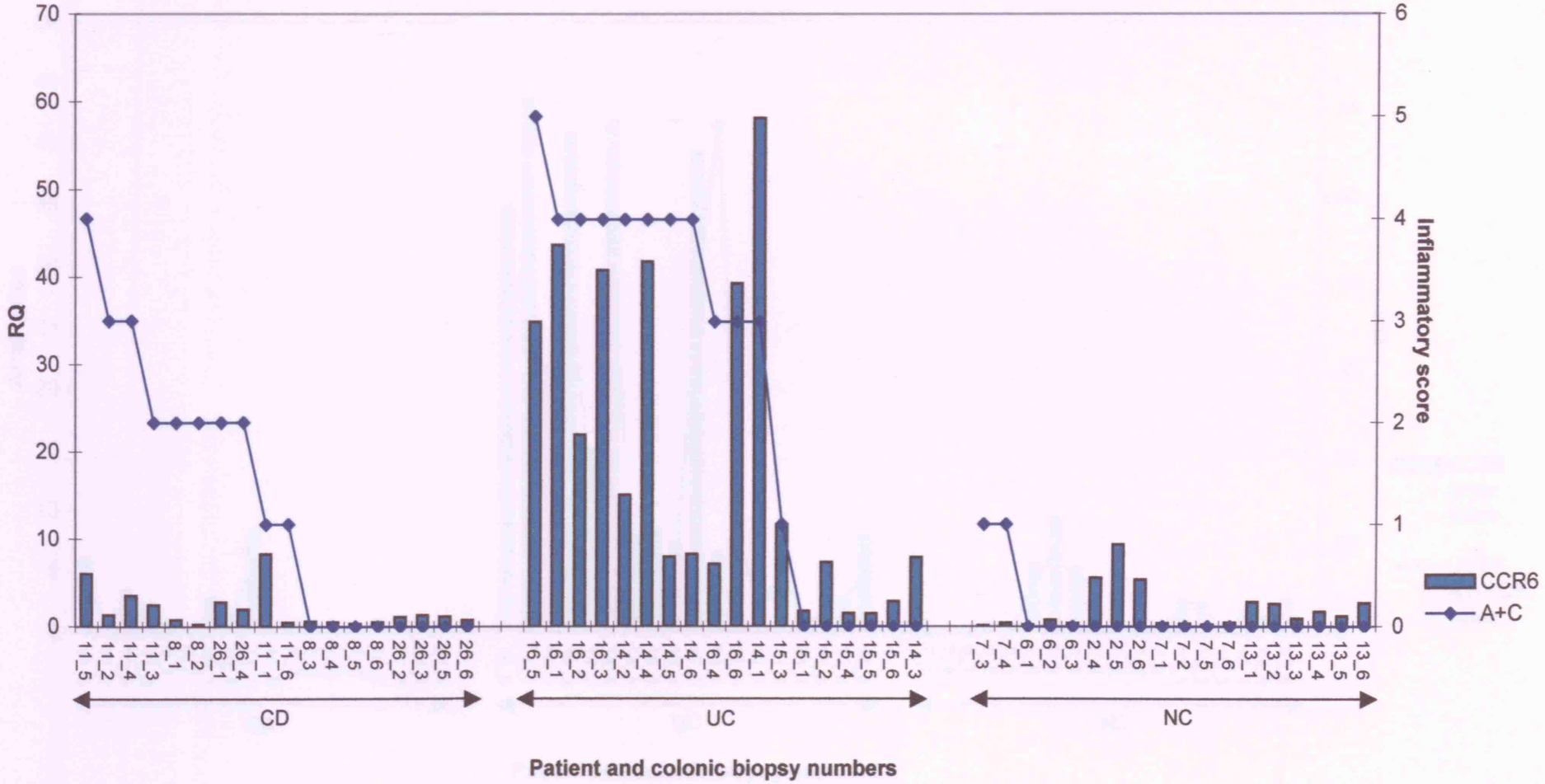

Patients are grouped according to disease, and chronologically placed according to inflammatory scores A+C (as defined in table 2.3). Patient and sample details are outlined in appendix table 2. NC=normal control, IC=inflammatory control.

Graph 3.40: Relative expression of CCR6 in colonic biopsies measured by microarray correlated with relative expression of CCR6 measured by RT-PCR

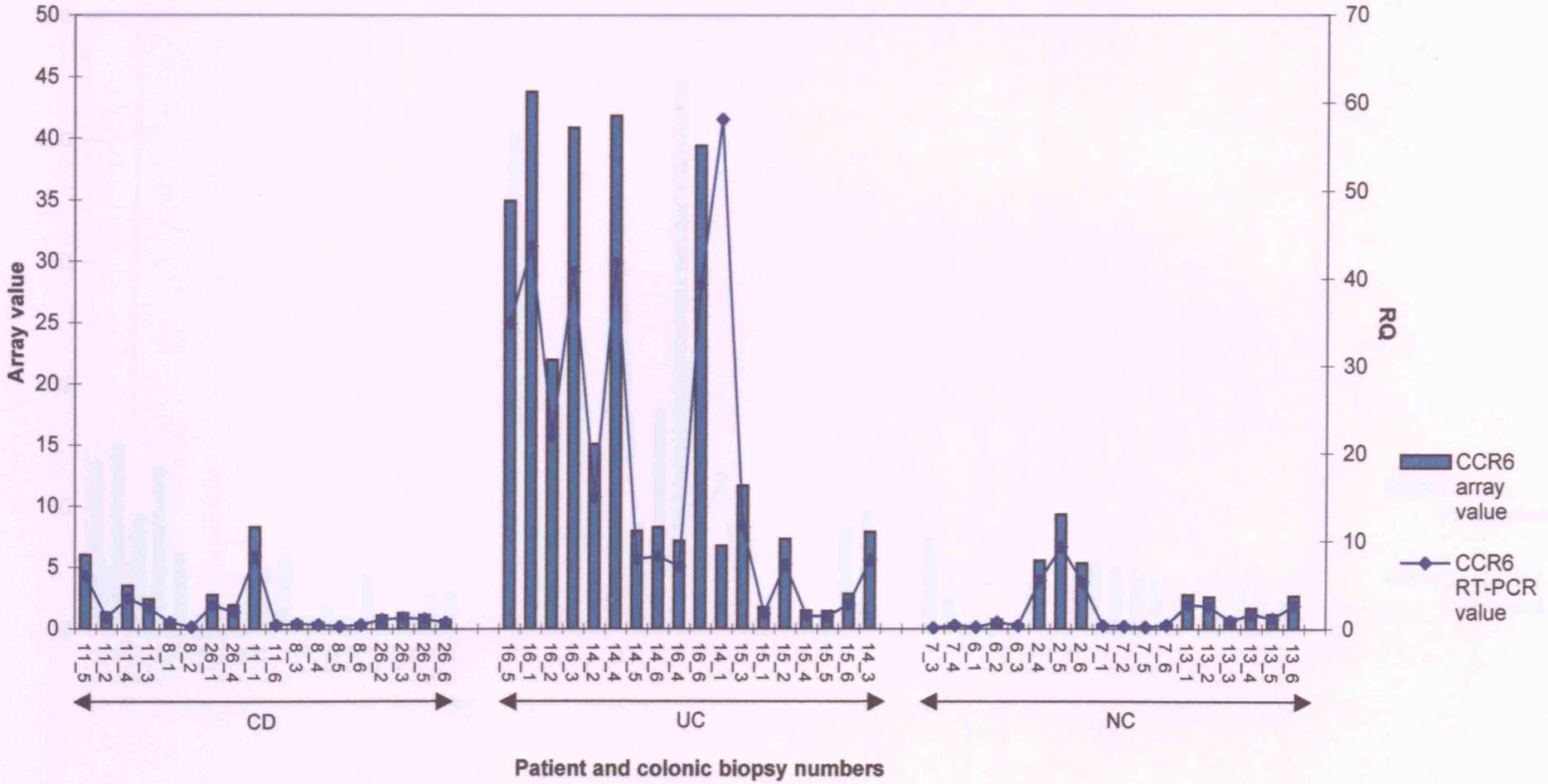

Patients are grouped according to disease, and chronologically placed according to inflammatory scores A+C (as defined in table 2.3). Patient and sample details are outlined in appendix table 2. NC=normal control, IC=inflammatory control.

Graph 3.41: Relative expression of CCL20 in colonic biopsies measured by microarray correlated with relative expression of CCL20 measured by RT-PCR-

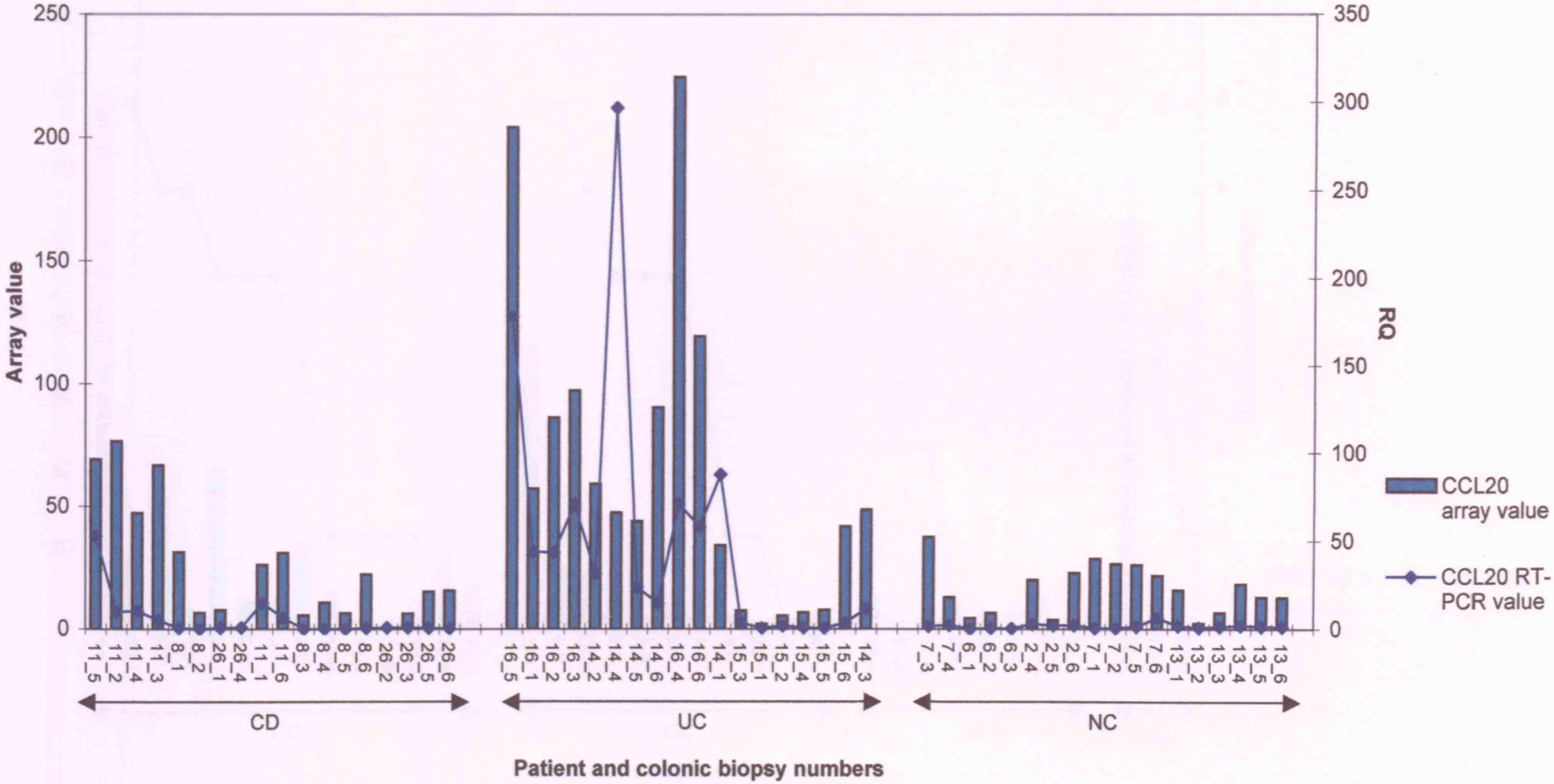

Patients are grouped according to disease, and chronologically placed according to inflammatory scores A+C (as defined in table 2.3). Patient and sample details are outlined in appendix table 2. NC=normal control, IC=inflammatory control.

Graph 3.42: Relative expression of CXCL1 in full thickness colonic tissue measured by RT-PCR corrrelated with relative levels of inflammation as determined by histopathological analysis

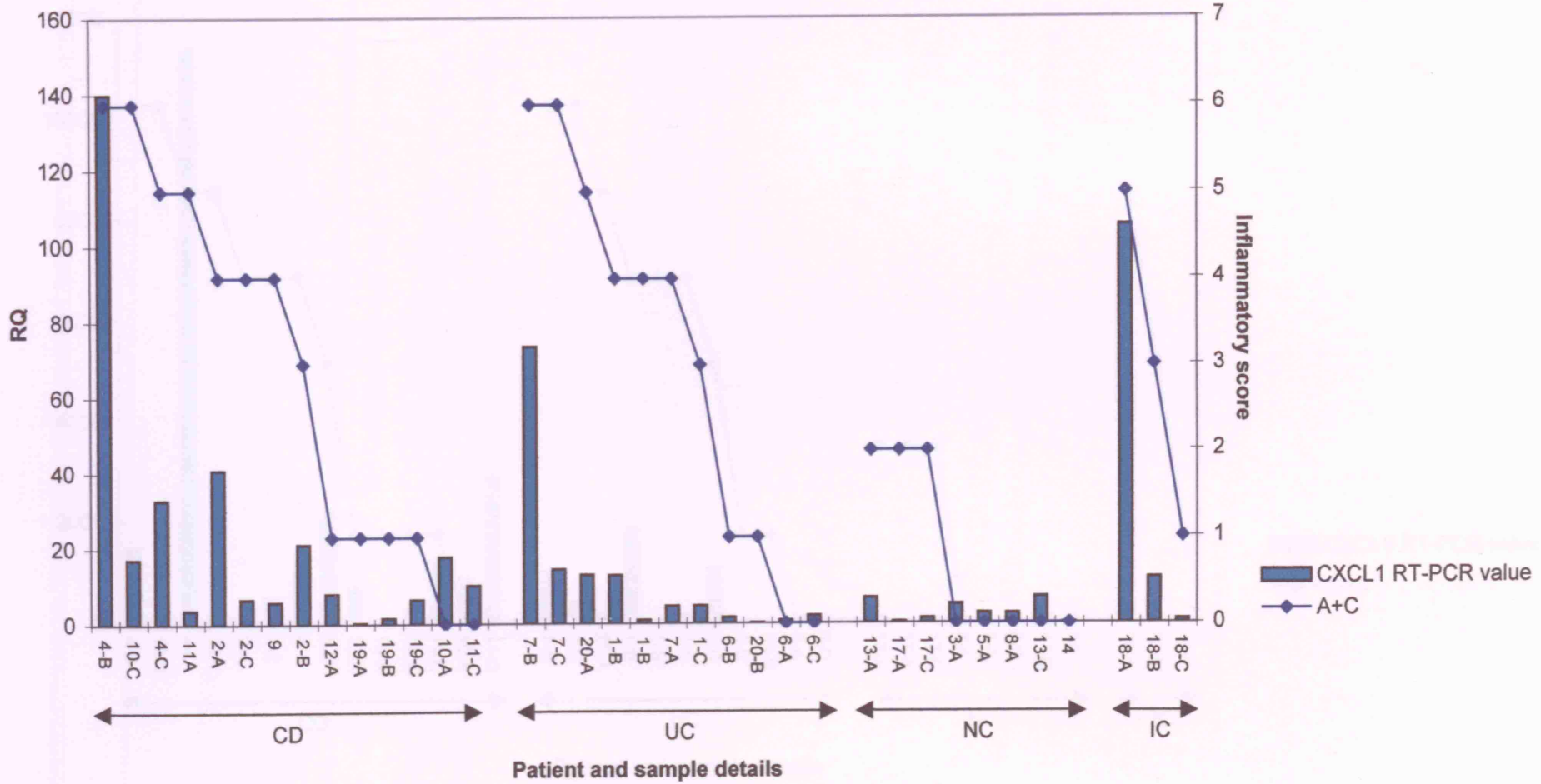

Patients are grouped according to disease, and chronologically placed according to inflammatory scores A+C (as defined in table 2.3). Patient and sample details are outlined in appendix table 2. NC=normal control, IC=inflammatory control.

Graph 3.43: Relative expression of CXCL9 in full thickness colonic tissue measured by RT-PCR corrrelated with relative levels of inflammation as determined by histopathological analysis

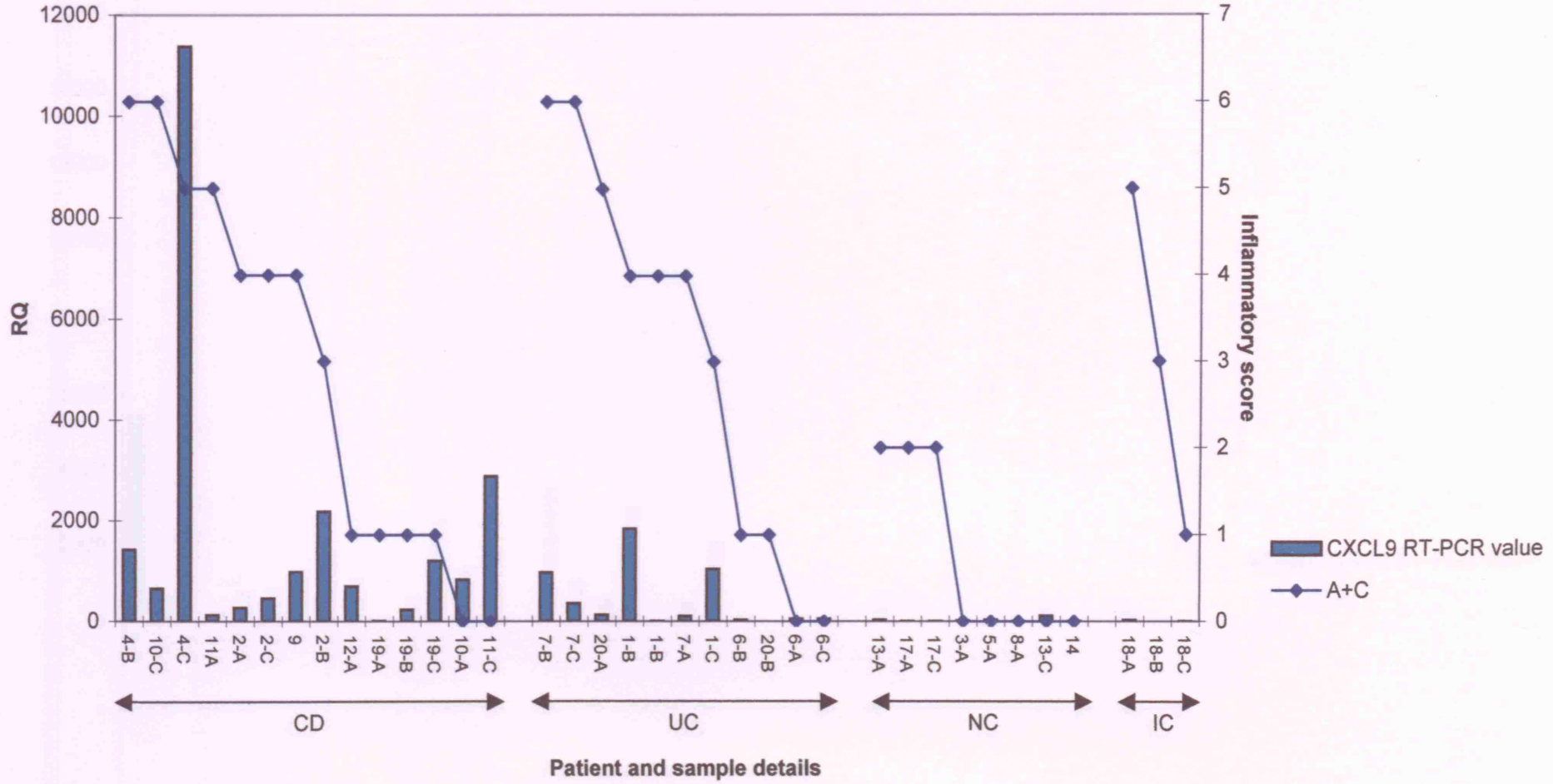

Patients are grouped according to disease, and chronologically placed according to inflammtory scores A+C (as defined in table 2.3). Patient and sample details are outlined in appendix table 2. NC=normal control, IC=inflammatory control.

Graph 3.44: Relative expression of CXCL10 in full thickness colonic tissue measured by RT-PCR corrrelated with relative levels of inflammation as determined by histopathological analysis

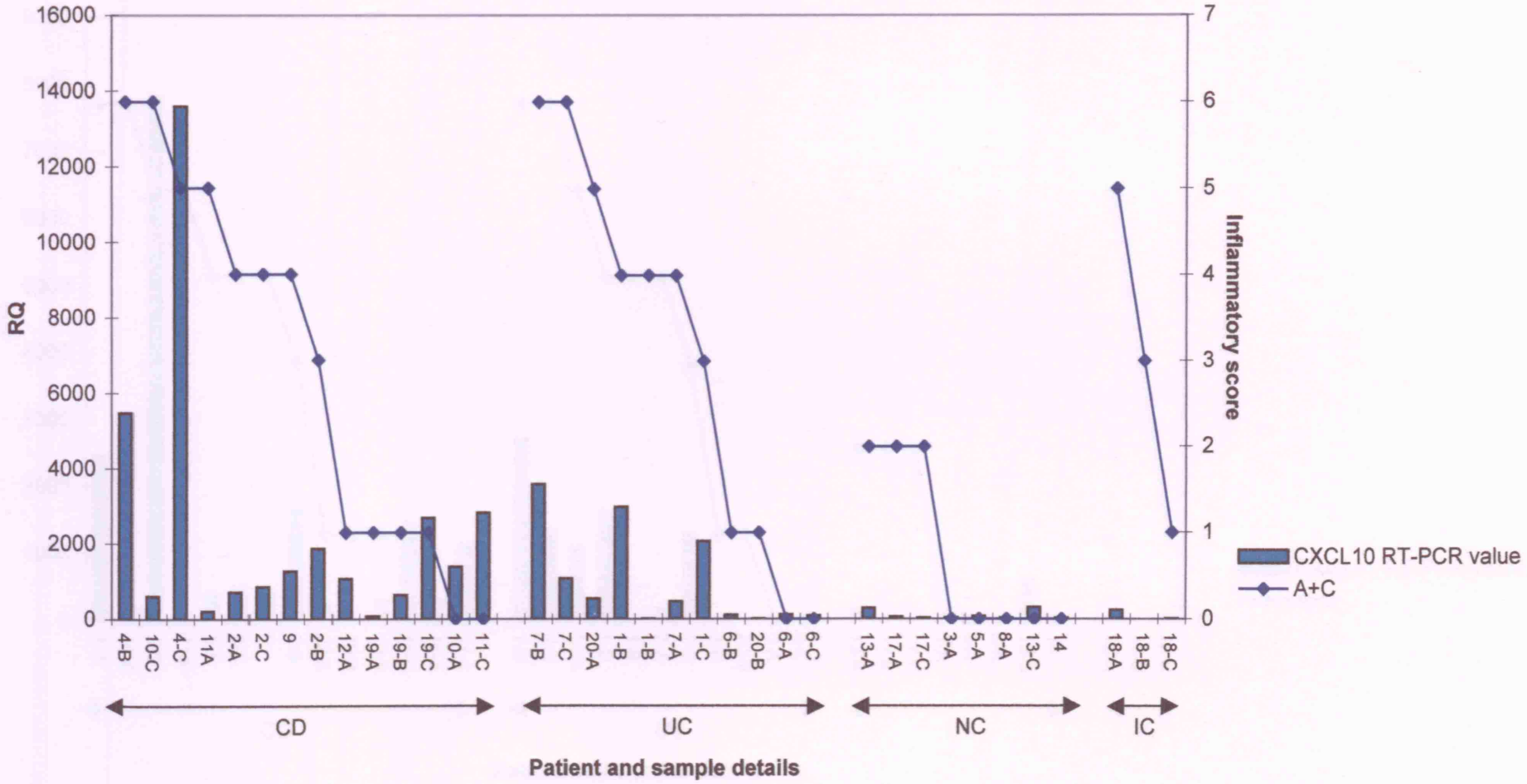

Patients are grouped according to disease, and chronologically placed according to inflammatory scores A+C (as defined in table 2.3). Patient and sample details are outined in appendix table 2.3. NC=normal control, IC=inflammtory control.

Graph 3.45: Relative expression of CXCL11 in full thickness colonic tissue measured by RT-PCR corrrelated with relative levels of inflammation as determined by histopathological analysis

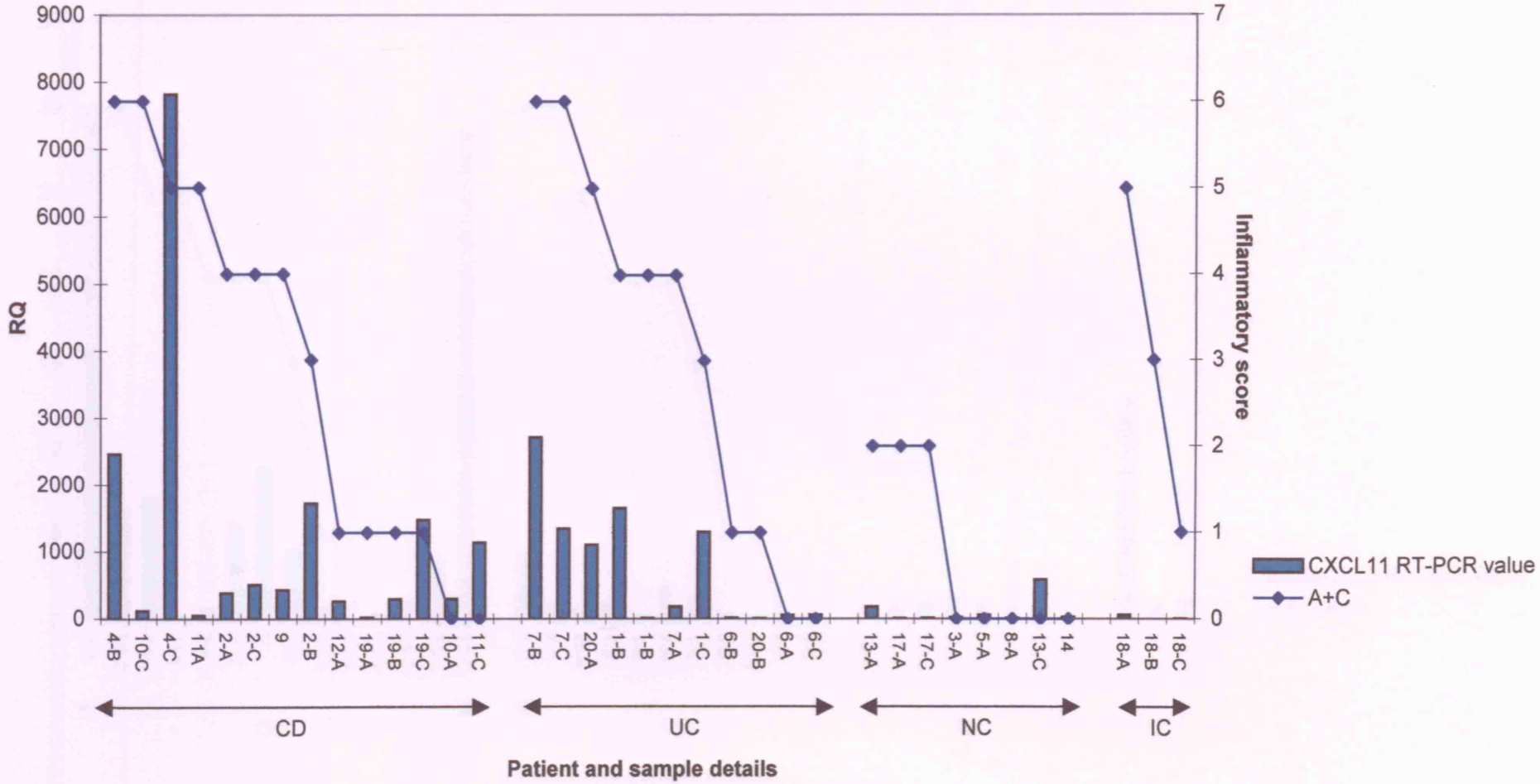

Patients are grouped according to disease, and chronologically placed according to inflammatory scores A=C (as defined in table 2.3). Patient and sample details are outlined in appendix table 2. NC=normal control, IC=inflammtory control.

Graph 3.46: Relative expression of CCL3 in full thickness colonic tissue measured by RT-PCR corrrelated with relative levels of inflammation as determined by histopathological analysis

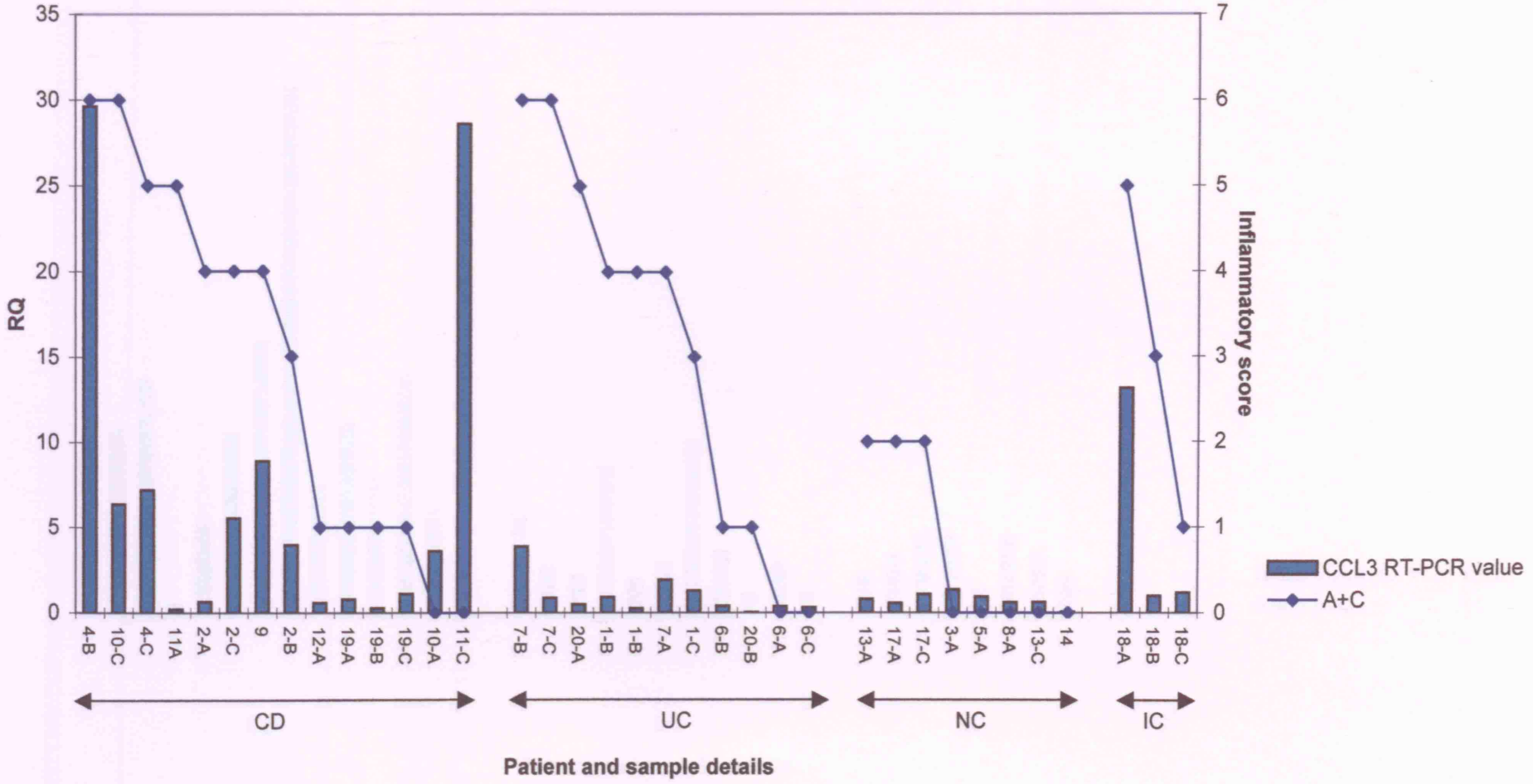

Patients are grouped according to disease, and chronologically placed according to inflammatory scores A+C (as defined in table 2.3). Patient and sample details are outlined in appendix table 2. NC=normal control, IC=inflammtory control.

Graph 3.47: Relative expression of CCL5 in full thickness colonic tissue measured by RT-PCR corrrelated with relative levels of inflammation as determined by histopathological analysis

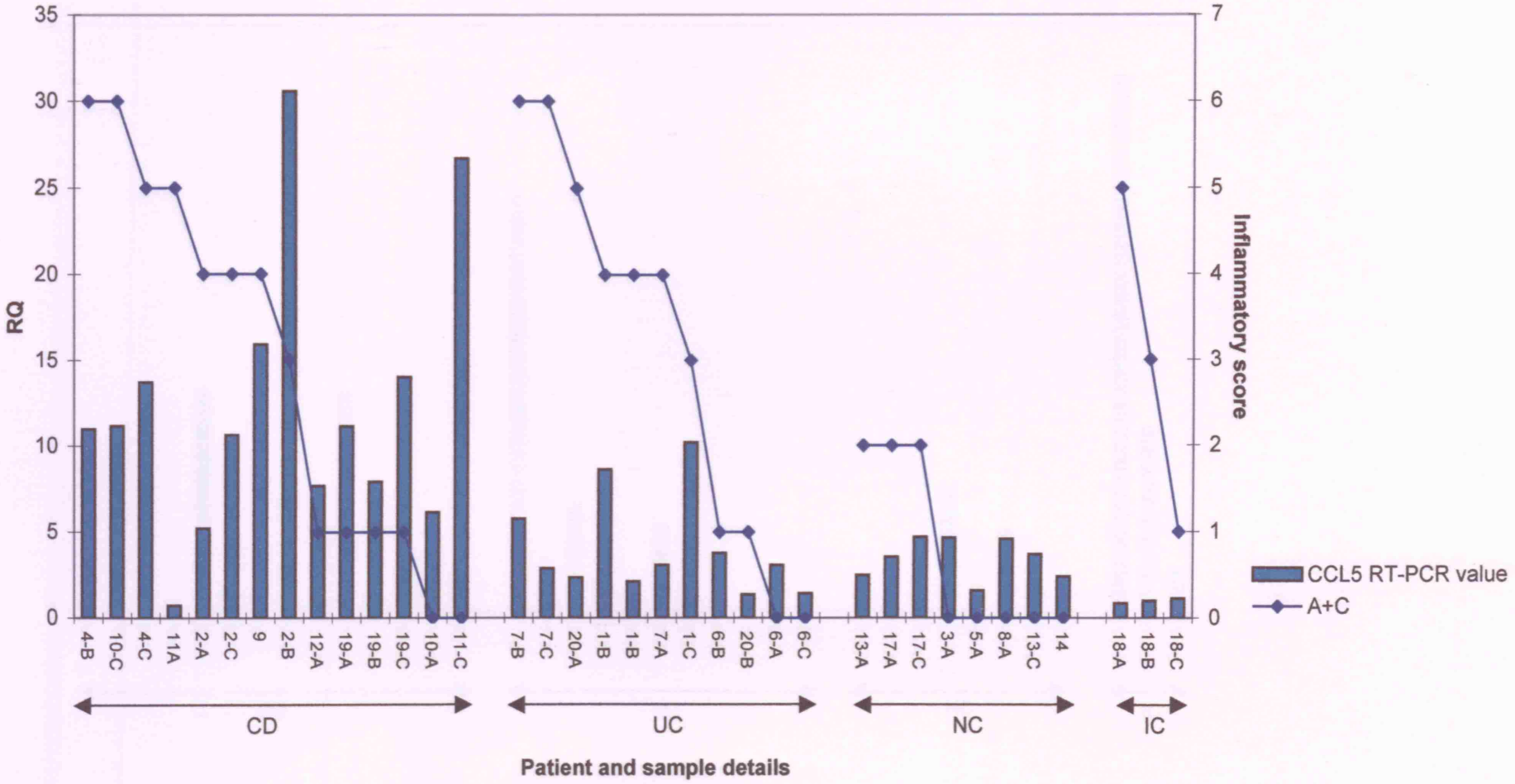

Patients are grouped according to disease, and chronologically placed according to inflammatory scores A+C (as defined in table 2.3). Patient and sample details are outlined in appendix table 2. NC=normal control, IC=inflammatory control.

Graph 3.48: Relative expression of CCL20 in full thickness colonic tissue measured by RT-PCR corrrelated with relative levels of inflammation as determined by histopathological analysis

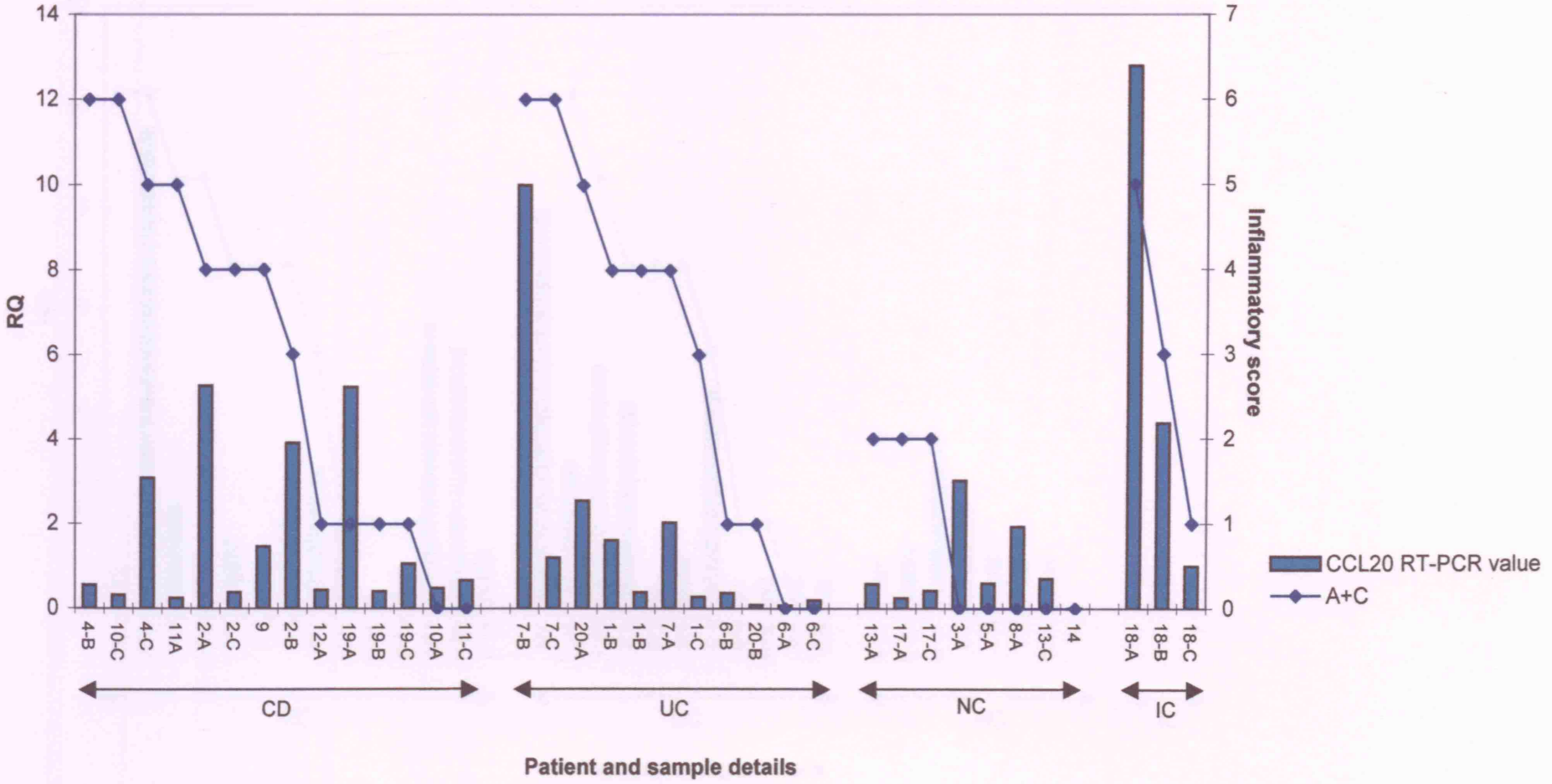

Patients are grouped according to disease, and chronologically placed according to inflammatory scores A+C (as defined in table 2.3). Patient and sample details are outlined in appendix table 2. NC=normal control, IC=inflammatory control.

Graph 3.49: Relative expression of CCL24 in full thickness colonic tissue measured by RT-PCR corrrelated with relative levels of inflammation as determined by histopathological analysis

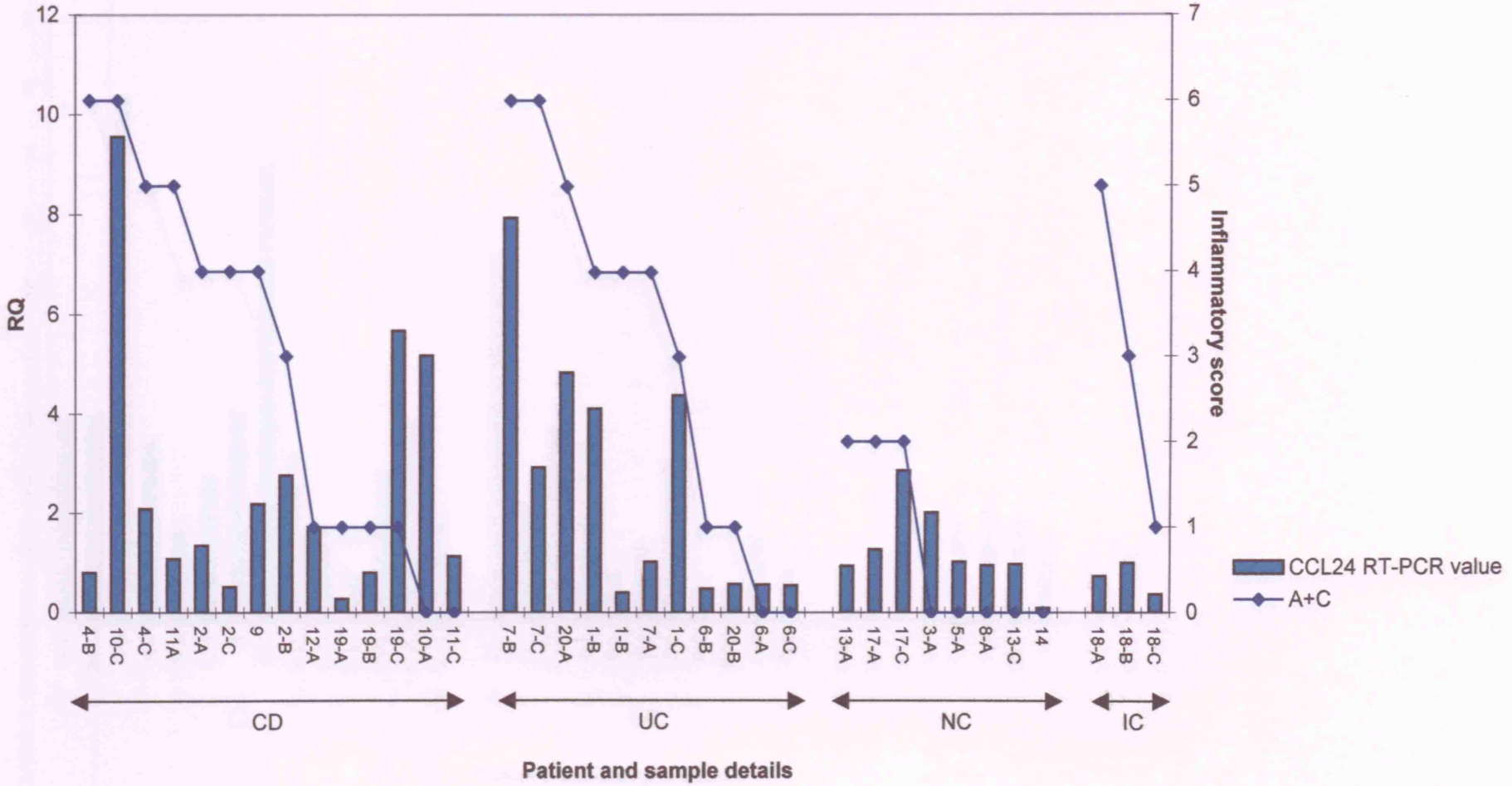

Patients are grouped according to disease, and chronologically placed according to inflammatory scores A+C (as defined in table 2.3). Patient and sample details are outlined in appendix table 2. NC=normal control, IC=inflammtory control.

Graph 3.50: Relative expression of CXCR3 in full thickness colonic tissue measured by RT-PCR corrrelated with relative levels of inflammation as determined by histopathological analysis

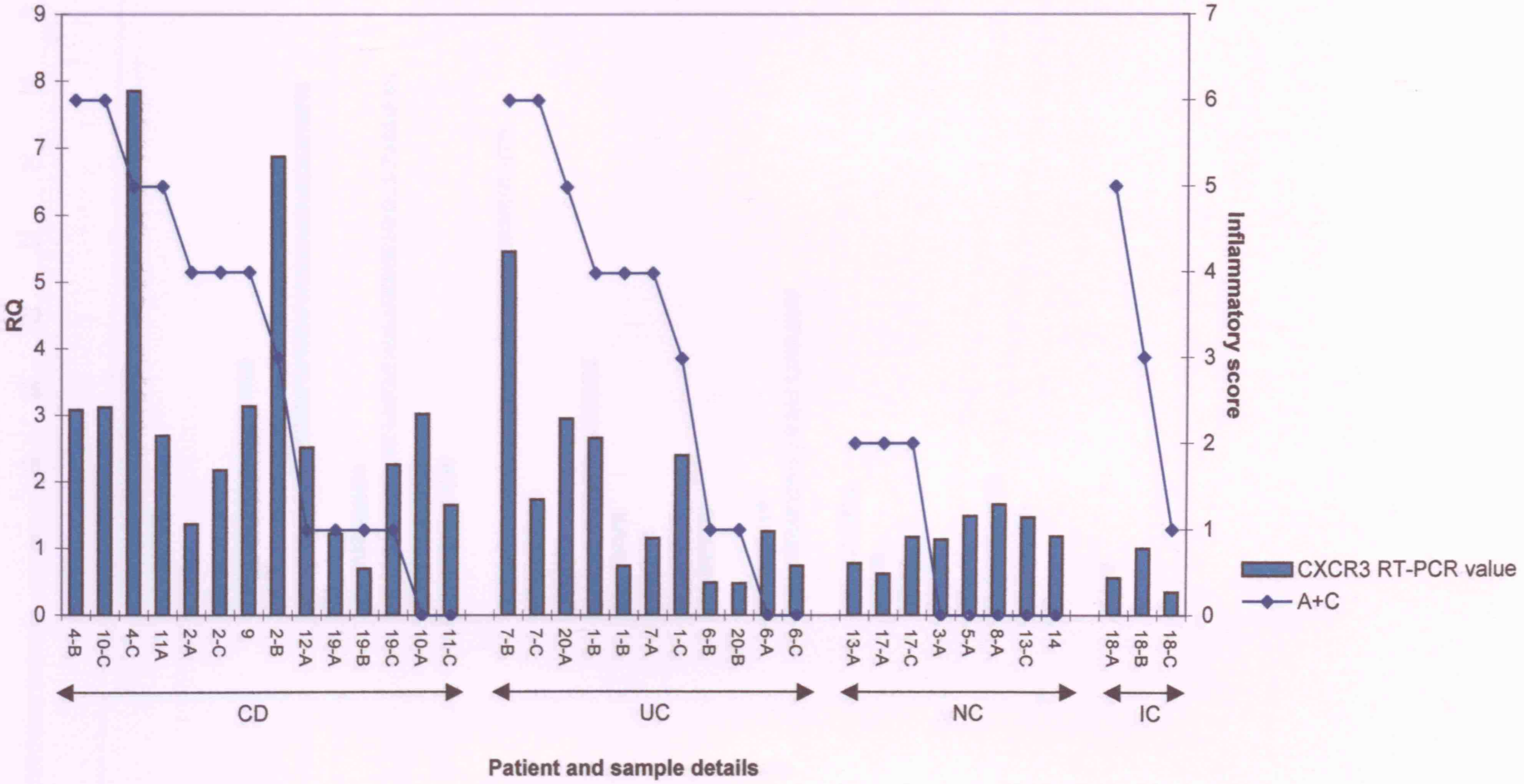

Patients are grouped according to disease, and chronologically placed according to inflammatory scores A+C (as defined in table 2.3). Patient and sample details are outlined in appendix table 2. NC=normal control, IC=inflammatory control.

Graph 3.51: Relative expression of CCR3 in full thickness colonic tissue measured by RT-PCR corrrelated with relative levels of inflammation as determined by histopathological analysis

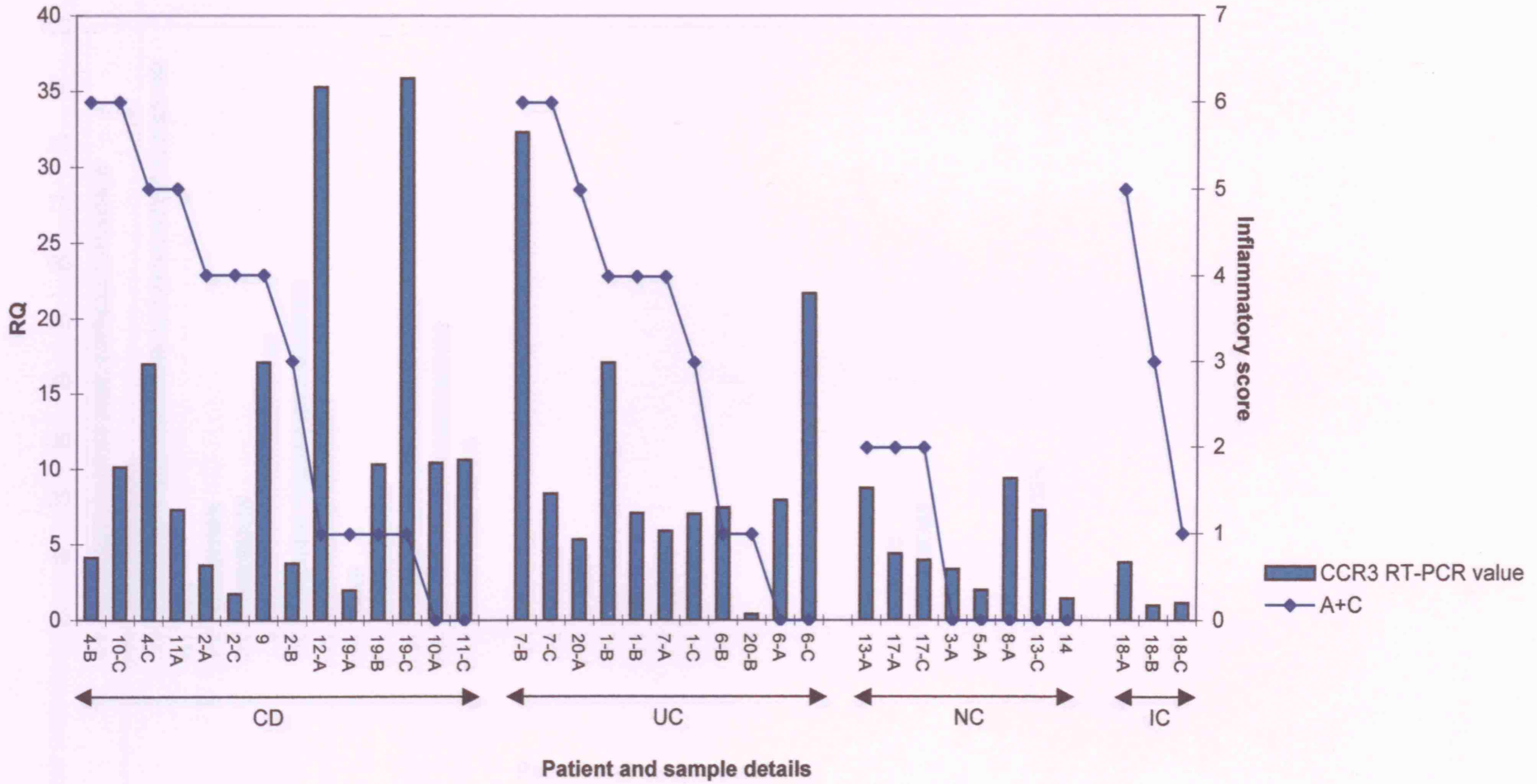

Patients are grouped according to disease, and chronologically placed according to inflammatory score A+C (as defined in table 2.3). Patient and sample details are outlined in appendix table 2. NC=normal control, IC=inflammatory control.

Graph 3.52: Relative expression of CCR5 in full thickness colonic tissue measured by RT-PCR corrrelated with relative levels of inflammation as determined by histopathological analysis

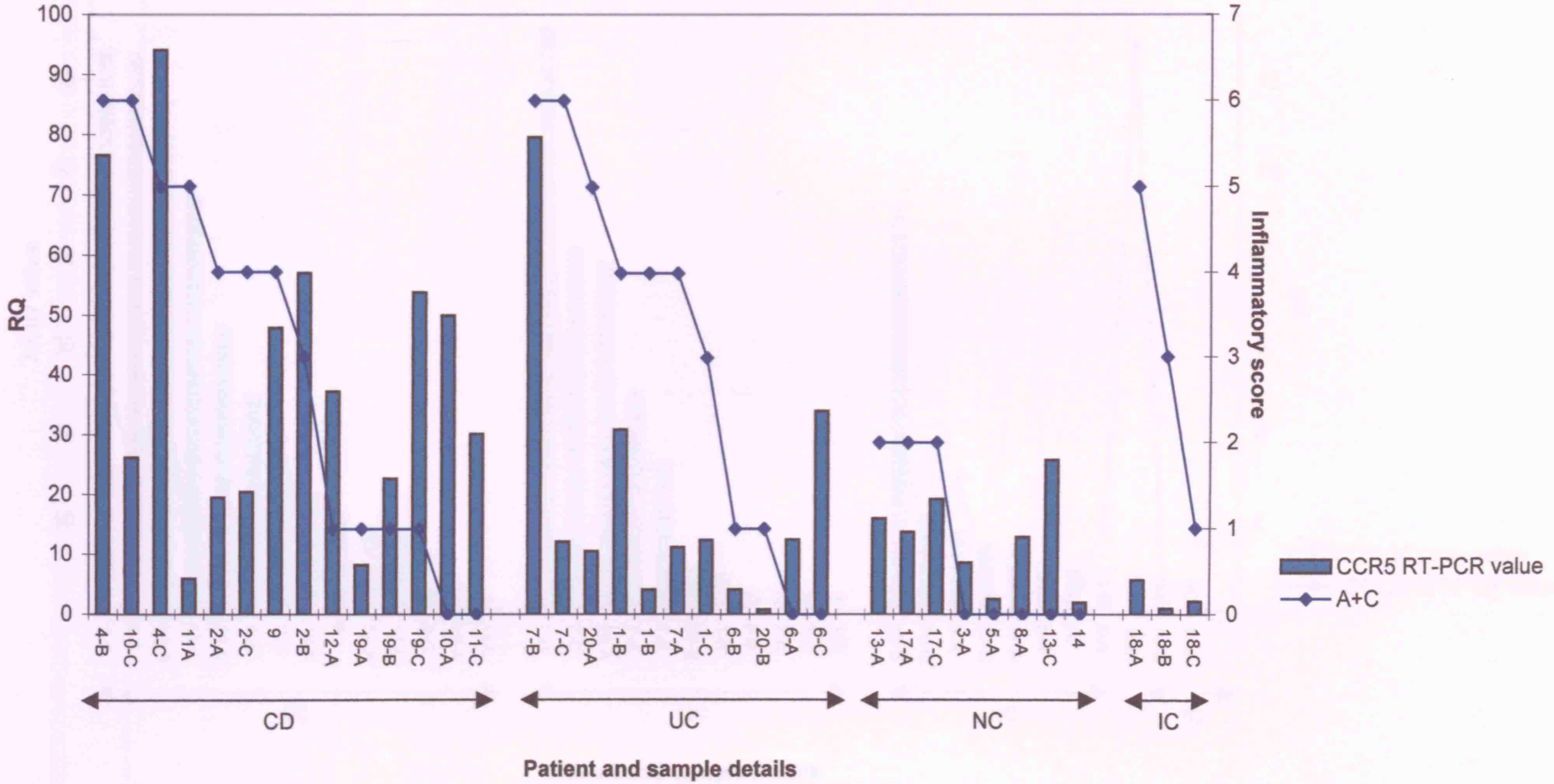

Patients are grouped according to disease, and chronologically placed according to inflammtory scores A+C (as defined in table 2.3). Patient and sample details are outlined in appendix table 2. NC=normal control, IC=inflammtory control.

Graph 3.53: Relative expression of CCL20 in full thickness colonic tissue measured by microarray corrrelated with relative expression of CCL20 measured by RT-PCR

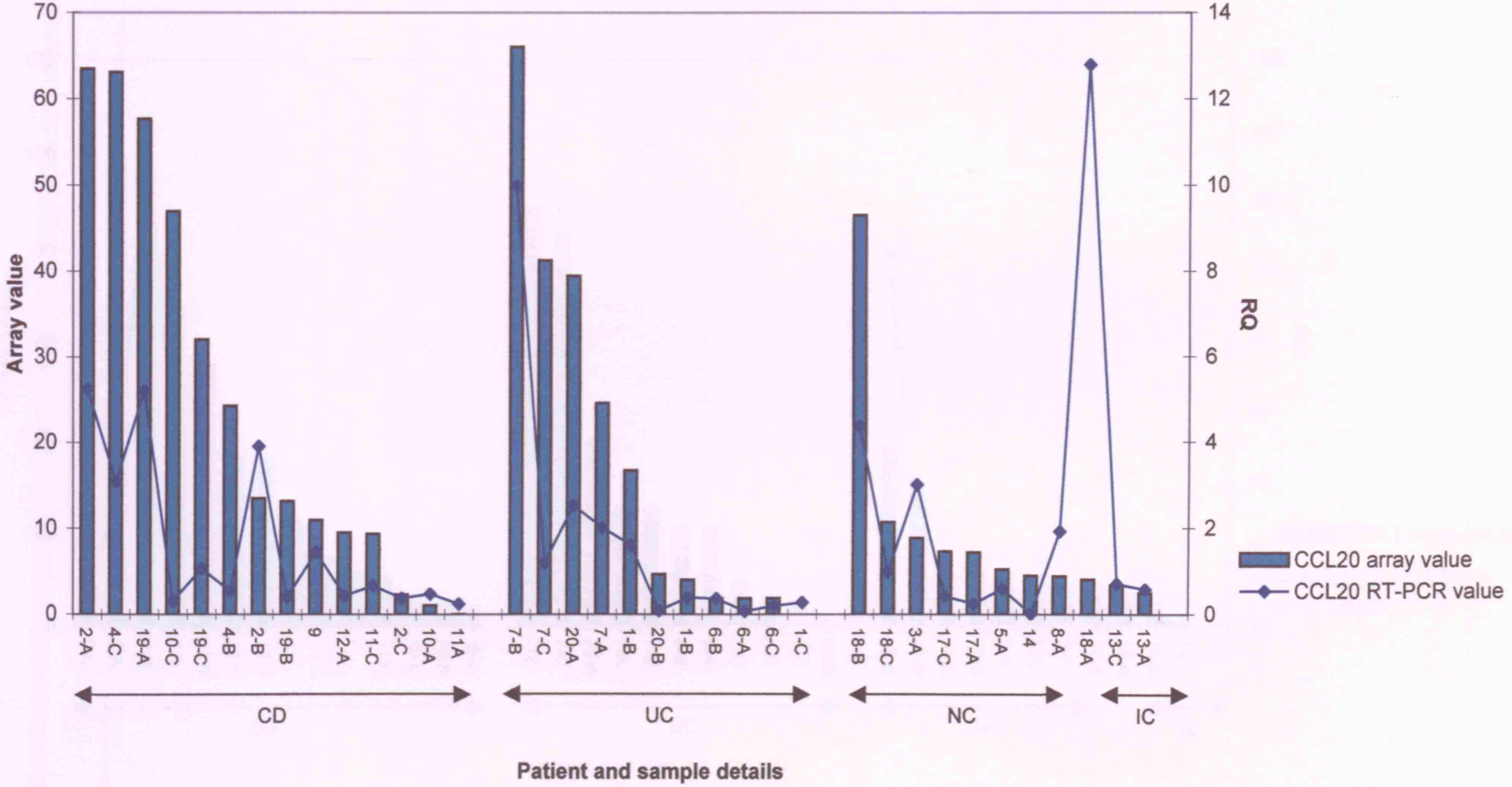

Patients are grouped according to disease, and chronologically placed according to inflammatory scores A+C (as defined in table 2.3). Patient and sample details are outlined in appendix table 2. NC=normal control, IC=inflammatory control.

Graph 3.54: Relative expression of CXCL1 in full thickness colonic tissue measured by microarray corrrelated with relative expression levels of CXCL1 measured by RT-PCR

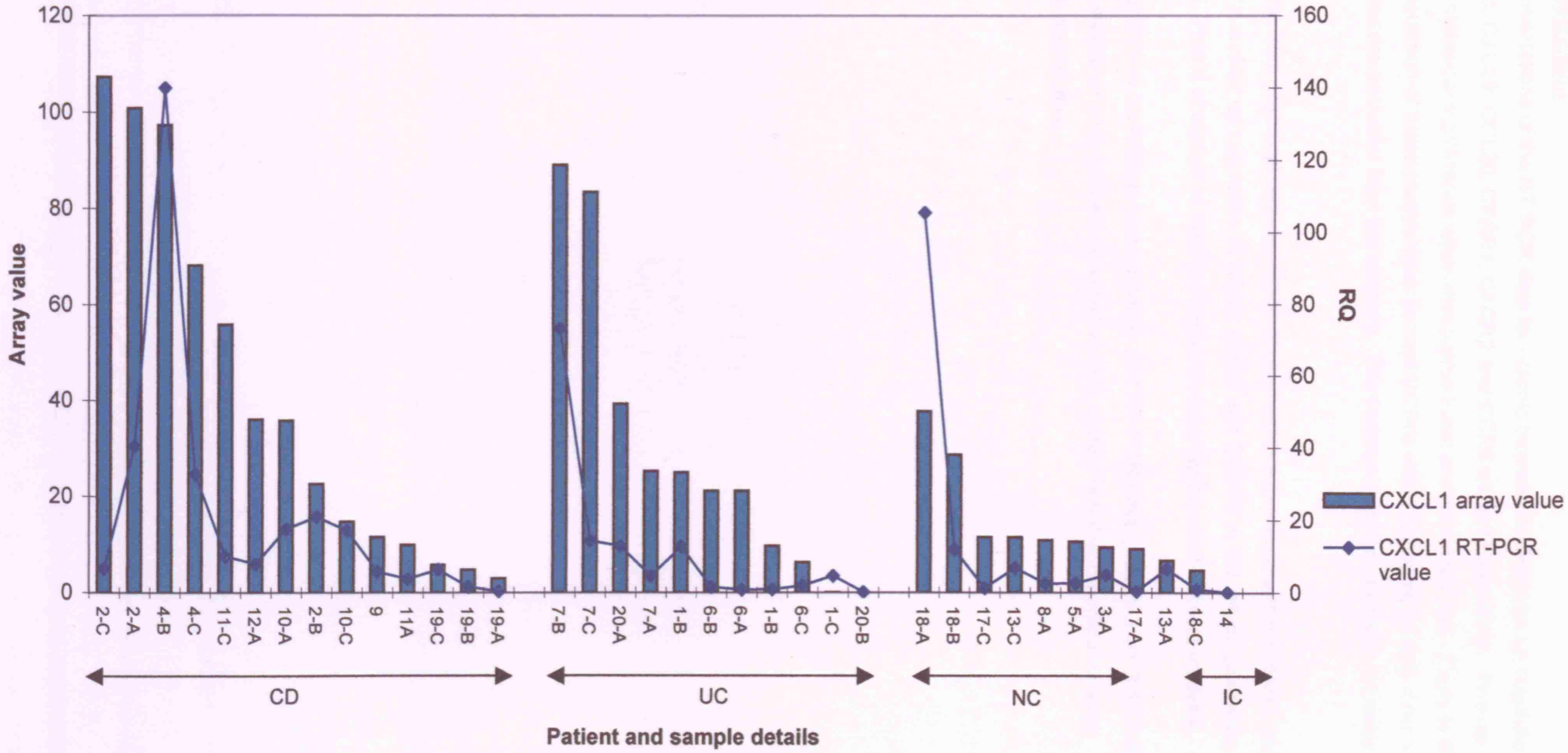

Patients are grouped according to disease, and chronologically placed according to inflammatory scores A+C (as defined in table 2.3). Patient and sample details are outlined in appendix table 2. NC=normal control, IC=inflammatory control.

3.3.4 Discussion

Graphical representations of the RT-PCR data for colonic biopsies implicate an up regulation of CXCL1, CXCL3, CXCL8, CCL20, CXCR1, CXCR2 and CCR6 within UC samples. This up regulation is of statistical significance when non-paired t-test analysis is applied. There is also statistical up regulation of these chemokines (except CCR6) within CD samples only if the non-inflamed samples are excluded from the analysis. The findings correlate well with the array data.

Of particular note from graphical representation of chemokine expression within full thickness samples, there is a clear up regulation of CCL5, CCR5 and CXCR3 in CD, which correlates well with array data. This is of statistical significance when applying non-paired t-test analysis.

There is good graphical correlation between array and RT-PCR data (graphs 3.40, 3.52-3.53), although direct statistical analysis between the two sets of data is not appropriate as array values are semi-quantitative.

3.3.4 Discussion

Graphical representations of the RT-PCR data for colonic biopsies implicate an up regulation of CXCL1, CXCL3, CXCL8, CCL20, CXCR1, CXCR2 and CCR6 within UC samples. This up regulation is of statistical significance when non-paired t-test analysis is applied. There is also statistical up regulation of these chemokines (except CCR6) within CD samples only if the non-inflamed samples are excluded from the analysis. The findings correlate well with the array data.

Of particular note from graphical representation of chemokine expression within full thickness samples, there is a clear up regulation of CCL5, CCR5 and CXCR3 in CD, which correlates well with array data. This is of statistical significance when applying non-paired t-test analysis.

There is good graphical correlation between array and RT-PCR data (graphs 3.40, 3.52-3.53), although direct statistical analysis between the two sets of data is not appropriate as array values are semi-quantitative.

3.4 Discussion

The technique of microarray profiling allows quantitative assessment of differential mRNA expression in situ, avoiding the amplification artefacts that may occur with RT-PCR studies. The effectiveness of the normalisation methodology is demonstrated by an even level of expression of the actin gene, independent of inflammation quotient (Graph 3.2). As the assessment is only semi-quantitative, confirmatory evidence from RT-PCR was necessary to validate the microarray data obtained. Quantitative RT-PCR generally confirms the correlation between transcriptional up regulation and level of inflammation observed in microarray experiments.

Overall the data provides a clear correlation between increasing expression of CXCL's1-3 and CCL20 with increasing acute and chronic inflammation quotient within the UC cohort, and to a lesser degree in the CD cohort. No samples in the non-IBD cohort exhibit significant up regulation of these chemokines. The variation in chemokine expression was not dependent on the anatomical origin of the biopsy. Real-time RT-PCR of colonic biopsy samples confirms the correlation between transcriptional up regulation and level of inflammation observed in microarray experiments. Statistical analysis from full thickness IBD sample RT-PCR data did not indicate a significant up regulation in CXCL's 1-3, CXCL8 and CCL20. This may well relate to drug treatment; the patients in the IBD biopsy cohort underwent colonoscopic examination for screening purposes, where as for the surgical resection cohort, the majority of patients had more active disease, and were almost all on some form of immunosuppressive agent. In the biopsy cohort, 1/8 UC and 2/6 CD patients were on immunosuppressive therapy, compared to 6/6 UC and 6/9 CD in the full thickness cohort (appendix 2.3 and 4.4).

CCL20 expression is of particular interest as this chemokine is specifically involved in mucosal immunity, particularly in human intestinal epithelium, where it induces local migration of dendritic cell subsets expressing the receptor CCR6. CXCL1 and its receptors CXCR1 and CXCR2 are thought to account for the initial destructive changes seen in UC, with a neutrophilic infiltration into the epithelium. The up regulated expression of CXCL's1-3 and CCL20 observed in inflamed UC colon biopsies was also noted in full-thickness UC samples, expression correlating with histopathological scoring for inflammation (graphs 3.23-3.35). However RT-PCR results for full thickness specimens did not reach levels of statistical significance. Overall, levels of CXCL's1-3 and CCL20 are generally lower than those seen from biopsy tissue which is likely to relate to a larger proportion of non-epithelial cells in comparison to biopsy samples, thus lowering the relative mRNA concentration of epithelial expressed genes. Data from array analysis of stripped epithelium and lamina propria is supportive of this, with higher expression of chemokines in the epithelial compartment, although direct conclusions are inappropriate on the basis of one patient.

Interestingly a number of CD samples also demonstrate the coordinated expression of CXCL's1-3 and CCL20 but independently of inflammation as judged by histological scoring. This is potentially due to the characteristically patchy nature of CD pathology, where even adjacent biopsies can show quite distinct focal inflammatory responses, and to the use of a histological

scoring index based on mucosal changes alone. The expression of CXCL's1-3 and CCL20 was enhanced in the full thickness specimens from CD patients in comparison to biopsies, suggesting origin within cells in the deeper layers.

Four specimens from a patient diagnosed with diverticulitis exhibited coordinated expression of CXCL's1-3 and CCL20, expression levels correlating with inflammatory quotient, suggesting that these are up regulated in gastrointestinal inflammation generally rather than IBD specimens.

Increased expression of CCL5 (RANTES) was observed in full thickness samples that was not detected at similar levels in any biopsy samples analysed in this study. These observations were confirmed using real-time quantitative RT-PCR and the analysis extended to the CCL5 receptor, CCR5. CCL5 and CCR5 are expressed at generally higher levels in the CD cohort than the UC and control cohorts, while no significant difference was found between UC and control. Levels of chemokine expression did not correlate with inflammatory quotient, again suggestive of the involvement of cells compartmentalised within the submucosa.

The levels of CXCL8 detected by the array were low in comparison to CXCL's 1-3, although there was an up regulation of this chemokine in inflamed UC and CD tissue. Both CXCR1 and CXCR2 act as receptors for the chemokines CXCL1 and CXCL8, whilst CXCR2 is also the receptor for CXCL2 and CXCL3 (Zlotnik et al, 2000). RT-PCR analysis did indicate an up regulation in each of these chemokines and receptors in inflamed IBD biopsy tissue.

Both CXCR1 and CXCR2 act as receptors for the chemokines CXCL1 and CXCL8, whilst CXCR2 is also the receptor for CXCL2 and CXCL3 (Zlotnik et al, 2000). CCR6 is a more unusual chemokine receptor in that it only binds a single chemokine, CCL20 (Yeung et al, 2000). As there was an observed up regulation in expression of CXCL's1-3, CXCL8 and CCL20, it is a reasonable assumption that cells expressing the cognate receptors for these ligands will be chemotactically recruited, resulting in a simultaneous detectable increase in receptor expression. Levels of transcript for these receptors were too low to be accurately detected by the array, so gene expression quantification by real-time RT-PCR was of value. In support of a functional role for this chemokine cluster in colonic IBD, the levels of expression for these receptors correlated well with both the expression of their cognate chemokines and scoring for inflammation in biopsy tissue. Within the specific cluster, several UC samples also exhibited expression of the CCR7 binding chemokines, CCL19 and the CXCR5 binding chemokine, CXCL13. CCR7 enable dendritic cells to be guided into draining lymph nodes by the lymphoid chemokine CCL21, the ligand for CCR7 (Nakayama et al, 2001). These antigen-presenting cells are crucial for the initiation of an immunological response, activating naïve T and B cells, which return to the site of inflammation. As homeostatic trafficking of B and T lymphocytes and dendritic cells into secondary lymphoid tissue is predominantly mediated by these chemokines, and organised lymphoid aggregates in the deep lamina propria are characteristic of UC, expression of these three chemokines presumably indicates the presence of lymphoid tissue within these particular biopsies (Baba et al, 1997), (Lindhout et al, 1999), (Yeung et al, 2000). However, this cannot be confirmed as histology was performed on adjacent biopsies. Taken together, these data lead to the proposal that gene expression of this defined chemokine subset consisting of CXCL1,

CXCL2, CXCL3, and CCL20 may be closely related to inflammatory events occurring in the colon of IBD subjects.

Chapter 4

Immunohistochemical localisation and quantification of CCR6, CCL20, CXCR1 and CXCR2, using the immunoperoxidase technique

4.1 Background

4.2 Immunohistochemical localisation CCL20 using the immunoperoxidase technique

- 4.2.1 Optimisation of pre-treatment method using appendix sections
- 4.2.2 Titration of primary antibody and finalisation of optimal pre-treatment method, using appendix and colonic surgical sections
- 4.2.3 Use of established immunohistochemistry technique on colonic biopsy sections
- 4.2.4 Titration of link antibody using colonic biopsy sections, and finalisation of pre-treatment method
- 4.2.5 Immunohistochemical localisation and scoring of CCL20 on colonic biopsy series

4.3 Immunohistochemical localisation CCR6 using the immunoperoxidase technique

- 4.3.1 Optimisation of pre-treatment method using appendix sections
- 4.3.2 Titration of primary antibody using appendix sections
- 4.3.3 Use of established immunohistochemistry technique on colonic sections
- 4.3.4 Titration of link antibody using colonic sections, and finalisation of pre-treatment method
- 4.3.5 Immunohistochemical localisation and scoring of CCR6 on colonic biopsy sections

4.4 Immunohistochemical localisation of CXCR1 using the immunoperoxidase technique

- 4.4.1 Optimisation of pre-treatment method using surgical colonic sections
- 4.4.2 Titration of primary antibodies using colonic biopsy sections
- 4.4.3 Further titration of link antibodies using colonic biopsy sections
- 4.4.4 Immunohistochemical localisation and scoring of CXCR1 on colonic biopsies

4.5 Immunohistochemical localisation of CXCR2 using the Immunoperoxidase technique

4.5.1 Optimisation of pre-treatment method using surgical colonic and appendix sections

4.5.2 Titration of primary antibodies using colonic biopsy sections

4.5.3 Immunohistochemical localisation and scoring of CXCR2 on colonic biopsies

4.6 Discussion

4.1 Background

Analysis of the microarray and PCR data indicated that a distinct subset of chemokines, consisting of CXCL's 1-3 and 8 and CCL20, was up regulated in active colonic IBD, compared to non-inflamed areas and tissue from controls. In order to confirm gene expression levels as determined by RNA analysis, immunohistochemical studies were undertaken to determine protein expression of CCL20, CCR6, CXCR1 and CXCR2 in adjacent biopsies. The immunoperoxidase technique used is described in section 2.2.4.

4.2 Immunohistochemical localisation of CCL20 using immunoperoxidase technique

The CCL20 antibody had not been previously tested for immunohistochemical studies on paraffin-embedded tissue, so a series of experiments were undertaken to determine optimal experimental conditions. The CCL20 antibody used was a goat antibody species, which necessitated use of a biotinylated rabbit anti-goat secondary antibody. In place of NHS, normal rabbit serum was used.

4.2.1 Optimisation of pre-treatment method using appendix sections

Aim: To establish the optimal link antibody pre-treatment method.

Tissue sections: 3μm sections of appendix tissue were used, prepared as standard.

Immunohistochemical staining: The sections were incubated 1 hour in the primary anti-CCL20 antibody at a dilution of 1/50 (2μg/ml), as recommended by the manufacturer.

Results: The 2 optimal pre-treatments methods were pressure cooker treatment with EDTA for 90 seconds and high-powered microwave treatment in citrate buffer for 25 minutes. There was immunohistochemical staining with CCL20 at 1/50 dilution (2μg/ml), although this was not clearly distinguishable from background staining. Furthermore, the genuine staining quite weak. Further work was required to elucidate optimal antibody dilution.

Conclusion: This initial experiment established 2 optimal pre-treatment preparations of the link conjugates for use in subsequent experiments, which were pressure cooker treatment in EDTA and high-powered microwave treatment in citrate buffer for 25 minutes. Due to inadequate genuine uptake with excessive background staining, primary antibody incubation was extended to overnight with the addition of a blocking agent.

4.2.2 Titration of link antibody and finalisation of optimal pre-treatment method, using appendix and colonic surgical sections

Aims: This experiment was designed to further optimise the pre-treatment method, the primary antibody dilution and application of a blocking agent. The pre-treatment methods used were those identified to be optimal in the previous experiment.

Methods: The tissue sections, blocking agents, pre-treatment methods and primary antibody dilutions are listed in table 4.1. The sections were incubated overnight (approximately 18 hours) at +4°C in a humidity chamber.

Results: The optimal pre-treatment method was pressure cooker treatment in EDTA for 90 seconds, at a dilution of 1/50 (2μg/ml), with inclusion of FCS as a blocking agent. Microwave treatment for 25 minutes in citrate buffer also gave similar staining, although not as strong.

Conclusion: The optimal pre-treatment, dilution and blocking agent had been established.

Table 4.1: List of sections, pre-treatments methods, primary antibody dilutions and blocking agents used in immunoperoxidase immunohistochemical optimisation for CCL20, as outlined in 4.2.2.

Surgical section	Pathology	Pre-treatment	Primary antibody dilution	Primary antibody solution	Blocking agent
Colon	UC	PC(EDTA)	Nil (control)	Nil	Nil
Colon	UC	PC(EDTA)	1/100 (1μg/ml)	2μl ab / 400μl TBS	Nil
Colon	UC	PC(EDTA)	1/100 (1μg/ml)	2μl ab + 20μl FCS/400μl TBS	FCS
Colon	UC	PC(EDTA)	1/90 (1.1μg/ml)	3μl ab + 13.5μl FCS / 270μl TBS	FCS
Colon	UC	PC(EDTA)	1/80 (1.25μg/ml)	3μl ab + 12μl FCS / 240μl TBS	FCS
Colon	UC	PC(EDTA)	1/75 (1.33μg/ml)	6μl ab + 22.5μl FCS / 450μl TBS	FCS
Colon	UC	PC(EDTA)	1/75 (1.33g/ml)	3μl ab + 11.25μl milk / 225μl TBS	Milk powder 5%
Colon	UC	PC(EDTA)	1/75 (1.33μg/ml)	3μl ab + 6.75μl milk / 225μl TBS	Milk powder 3%
Colon	CD	PC(EDTA)	Nil (control)	Nil	Nil
Colon	CD	PC(EDTA)	1/100 (1μg/ml)	2μl ab / 400μl TBS	Nil
Colon	CD	PC(EDTA)	1/100 (1μg/ml)	2μl ab + 20μl FCS / 400μl TBS	FCS
Colon	CD	PC(EDTA)	1/75 (1.33mg/ml)	As above	FCS
Colon	CD	PC(EDTA)	1/50 (0.002mg/ml)	20μl ab / 1000μl TBS	Nil
Colon	Control	PC(EDTA)	1/75 (1.33)	As above	FCS
Colon	UC	M25	Nil (control)	Nil	Nil
Colon	UC	M25	1/100 (1.33μg/ml	2μl ab / 400μl TBS	Nil
Colon	UC	M25	1/50 (2μg/ml)	20μl ab / 1000μl TBS	Nil
Colon	CD	M25	Nil (control)	Nil	Nil
Colon	CD	M25	1/50 (2μg/ml)	20μl ab / 1000μl TBS	Nil
Appendix	appendicitis	PC(EDTA)	1/50 (2μg/ml)	20μl ab / 1000μl TBS	Nil
Appendix	appendicitis	M25	1/50 (2μg/ml)	20μl ab / 1000μl TBS	Nil
Appendix	appendicitis	M25	Nil	Nil	Nil

4.2.3 Use of established immunohistochemical technique on colonic biopsy sections

Aims: The experiment was designed to use the CCL20 primary antibody at the established optimal dilution of 1/50 (2μg/ml), with the optimal pre-treatment method of pressure cooker EDTA or microwave cooking in citrate buffer, on colonic biopsy sections.

Methods: Tissue sections: 2 x 3μm paraffin embedded, formalin-fixed colonic biopsy tissue sections were used, from each of 3 patients: 1 with UC, 1 with CD, and 1 with no disease (control). In addition, 2 sections were used for control negative without primary antibody incubation. The sections were prepared as standard.

Immunohistochemistry technique: The pre-treatment method of 90 seconds of pressure-cooking treatment immersed in EDTA. Blockade of endogenous peroxide activity was achieved by of FCS in TBS buffer. The sections were incubated in the primary antibody overnight (approximately 18 hours) at +4°C in a humidity chamber, at a dilution of 1/50 (2μg/ml).

Results: Although the optimal dilution was found to be between 1/50 (2μg/ml) for surgical colonic sections, for these biopsy sections this dilution led to over-staining, with inadequate discernible difference between the cases.

Conclusion: A 1/50 dilution (2μg/ml) was too concentrated for colonic biopsy tissue.

4.2.4 Titration of link antibody using colonic biopsy sections, and finalisation of pre-treatment method

Aims: To optimise the primary antibody dilution in colonic biopsy tissue.

Methods: Tissue sections: 3μm paraffin embedded; formalin-fixed colonic biopsy tissue sections were used, from patients with UC and with no disease i.e. normal controls.

Immunohistochemistry technique: The 2 antigen retrieval methods used were microwave treatment 25 minutes in citrate buffer or pressure cooking treatment in EDTA. The primary antibody dilution was varied from1/65 (1.54μg/ml) to 1/100 (1μg/ml). FCS was used throughout as a blocking agent. The sections were incubated overnight (approximately 18 hours) at +4°C in a humidity chamber.

Results: The optimal pre-treatment condition was high-powered microwave treatment for 25 minutes in citrate buffer, at a primary antibody dilution of 1/65 (1.54μg/ml).

Conclusion: The optimal conditions have been established for staining of the CCL20 chemokine for colonic biopsies. These constitute high-powered microwave cooking in citrate buffer for 25 minutes, with an antibody dilution of 1/65, (1.54μg/ml) with a 5% FCS at the initial blocking step, primary antibody solutions, in addition to the secondary and tertiary dilutions.

4.2.5 Immunohistochemical localisation and scoring of CCL20 on colonic biopsy sections

Aims: Previous experiments had established the optimal conditions for staining of the CCL20 chemokine on colonic biopsies. These conditions were used on the study colonoscopic biopsies.

Methods: Tissue sections: 3μm paraffin-embedded, formalin-fixed colonic biopsy tissue sections used from the 10 patients: a total of 18 biopsies from patients with UC, 18 CD, 18 with no disease (normal control), from adjacent sites as those taken for microarray analysis. Sections were included from control patients 2, 6, 7, 13; from UC patients 14, 15, 16; and from CD patients 8, 11, 26, prepared as standard. The subset was chosen on the basis of the previous microarray data. Patient details are outlined in appendix table 2.3.

Immunohistochemistry technique: The optimal pre-treatment method of 25 minutes high-powered microwave was used. Blockade of endogenous peroxide activity was achieved by incubation in a 5% FCS solution in TBS buffer. 1/65 (1.5mg/ml) primary antibody in TBS buffer was applied, with 5% FCS. Sections were incubated overnight (18 hours approximately) at +4 °C in the primary ant-CCL20 antibody, in a humidity chamber.

Scoring: A semi-quantitative score from 0 (none) to 4 (dense confluent staining) was determined for epithelium, and percentage immunoreactive lamina propria cells determined (0=0%, 1= 25 %, 2=50%, 3=75%, 4=100%). The scoring was performed under blind conditions, whereby the slide identity was concealed, and all the slides were allocated a number randomly. Unblinding only took place when all the scoring was complete. The scores are listed in table 4.2. Once scoring reliability had been ensured statistically, the original scores were correlated with both microarray data and histopathology inflammation scores. For each biopsy, a corresponding biopsy from the

same area had been assessed by a consultant histopathologist, and scored on the basis of inflammation as detailed in appendix table 1.

Table 4.2: CCL20 immunohistochemistry scores for the colonic biopsy series, inflammatory scores and gene expression levels as determined by TaqMan real-time quantitative PCR values.

Patient	Biopsy number	Lamina propria	Surface epithelium	Crypt epithelium	Vascular	A+C histology	RT-PCR value
8 (CD)	1	3	1	1	3	2	0.599091
8 (CD)	2	2.5	1	1	1	2	0.17059
8 (CD)	3	3	3	3	2	0	0.153426
8 (CD)	4	2	1.5	1	3	0	0.163337
8 (CD)	5	1	2	2	2	X	0.081841
11(CD)	6	2.5	2	3	2	4	6.589219
11(CD)	3	3.5	3.5	3.5	2	3	5.177789
11(CD)	5	X	X	X	X	3	53.01643
11(CD)	4	2.5	2.5	2	X	2	10.43926
11(CD)	2	2.5	2	1	2	1	9.849935
11(CD)	7	3	2.5	3	2	1	X
11(CD)	1	0	1	1	0	0	14.89446
26(CD)	1	2	2	2	2	2	0.705906
26(CD)	4	1	2	1	2	2	0.8568
26(CD)	2	1.5	2.5	2	3	0	0.922163
26(CD)	3	2	1	1.5	2	0	0.857305
26(CD)	5	3	3	2.5	3	0	0.805637
26(CD)	6	2	0	3	2	0	0.527373
16(UC)	5	3	4	4	3	5	178.6483
14(UC)	3	2	1	3	2	4	11.71609
14(UC)	4	3	X	3	3	4	297.0134
14(UC)	5	3	3	4	3	4	24.00619
14(UC)	6	3	3	4	3	4	14.89446
14(UC)	7	3	3	4	4	4	X
14(UC)	2	3	4	4	3	3	31.70287
14(UC)	1	3	3	4	4	1	88.20348
15(UC)	7	2	2.5	2.5	2	2	X
15(UC)	3	3	1	1	2	X	3.474553
15(UC)	1	2.4	2	2	2	0	0.642036
15(UC)	2	2.5	1	1	2.5	0	2.027678
15(UC)	4	2.5	2.5	2.5	2.5	0	0.719282
15(UC)	5	1	0.5	0.5	0	0	0.594007
15(UC)	6	2	1	1	X	0	3.464931
16(UC)	3	2	2	2	3	4	71.54928
16(UC)	2	3	3	3	3	4	43.90597
16(UC)	4	3	3	3	3	3	71.54229
16(UC)	1	3	1.5	3	2.5	3	44.33963
16(UC)	6	3	3	4	4	3	58.5017
2 (Cont)	4	1	2	1	3	0	2.984966
2 (Cont)	5	2.5	1	1	1	0	2.338963
2 (Cont)	6	1.5	1	1.5	1	0	2.248837
6 (Cont)	1	2.5	2	2	2	0	0.094938
6 (Cont)	2	2	2	3	2.5	0	0.64559
6 (Cont)	3	3	3	3	2	0	0.478332
7 (Cont)	3	1	2.5	1	2	1	1.617588
7 (Cont)	4	1.5	1	1	2	1	2.246919
7 (Cont)	5	0	1	1	1	0	1.475071
7 (Cont)	6	1	1	1	0	0	6.410438
13(Cont)	1	1	1	1	X	0	2.052337
13(Cont)	2	X	X	X	X	0	0.93552
13(Cont)	3	2	1	1	1	0	1.516256
13(Cont)	4	1	1	2	2	0	2.084657
13(Cont)	5	2	1	1	1	0	1.560758
13(Cont)	6	1	0	1.5	2	0	1.388343

Statistical validation: As the scoring was semi-quantitative, it was important to statistically validate the scoring technique consistency and reliability. 11 slides were re-scored for all parameters, blind from the slide identity and the original score. Each value was paired with the initial scoring value. These pairs were incorporated into a student's t-test for paired parametric

data. Each of the first scores for 11 slides was paired with the corresponding second scores, as listed in table 4.3. This statistical test is useful for investigating a variable in two groups where there is a meaningful one-to-one correspondence between the data points in one group and those in the other. The null hypothesis states that there is no significant difference between the 2 groups.

Table 4.3: List of initial and repeat semi-quantitative immunohistochemistry scores for CCL20, to demonstrate reproducibility of scoring method.

Score number	Score 1 (X_a)	Score 2 (X_b)	$X_a - X_b$
1	3	2.5	0.5
2	2	2	0
3	1.5	1.5	0
4	1	1	0
5	3	3	0
6	3	3	0
7	2.5	2	0.5
8	2	2	0
9	1	1	0
10	2	2	0
11	1	1	0
12	2	2	0
13	2	2	0
14	2	1.5	0.5
15	2	2.5	-0.5
16	1.5	1.5	0
17	1	2	-1
18	1	1	0
19	2	2	0
20	3	3	0
21	2.5	2.5	0
22	2.5	2	0.5
23	2	2	0
24	2	2	0
25	2	2	0
26	0	0	0
27	2	1.5	0.5
28	2	2	0
29	3	3	0
30	3	3	0
31	3	3	0
32	2.5	2	0.5
33	3	3	0
34	4	4	0
35	2	2	0
36	2	2	0
37	2	2	0
38	2	2	0
39	1	1	0
40	2	2	0
41	2.5	2	0.5
42	1	1	0
43	1	1	0
44	1	1	0
45	3	3	0
46	1.5	1	0.5
47	2.5	2.5	0
48	2	2	0
49	3	3	0
50	3	3	0
51	2.5	2	0.5
52	2	2	0
53	2	2	0
54	2	2	0
55	2	2	0
56	1	1	0
57	2.5	2.5	0
58	2	2	0

Table 4.4: Values for statistical validation of CCL20 immunohistochemistry scores

Values	X_a	X_b	$X_a - X_b$
n	58	58	58
Sum	119.	116.5	3
Mean	2.0603	2.0086	0.0517
Sum_sq	277.75	264.25	3.5
SS	31.5388	30.2457	3.3448
Variance	0.5533	0.5306	0.0587
Standard Deviation	0.7838	0.7284	0.2422

$Mean_A - Mean_B = 0.0517$

$t = -1.63$, $df = 57$

Two-tailed $p = 0.109599$

On the basis of this $p>0.05$, the null hypothesis cannot be rejected, i.e. that there is no statistical difference between the original and repeat scoring values. Thus, the scoring reducibility is acceptable.

Results: The immunohistochemical scores are listed in table 4.2. There was no staining on the negative slides, where the primary antibody had been omitted (figure 4.1a). Weak epithelial staining is seen in control section, while stronger immunoreactivity is seen in both CD and UC, with increased density of subepithelial $CCL20^+$ cells (figures 4.1 b-d). Of 17 normal control *biopsies, 2 showed enhanced expression of CCL20 in crypt epithelium (score >2), compared to 11/16 UC and 6/15 CD specimens (4.1 c, g, h, I, j). Similar increase was seen in CCL20 expression in surface epithelium (1/17 control biopsies, 10/16 UC and 6/15 CD). There were some positive staining in sub-epithelial macrophages and intraepithelial lymphocytes. Lymphocytic staining was patchy. Occasional neutrophils stained, though not as strongly as for CCR6 (figures 4.1 k, l). $CCL20^+$ lamina propria cell density exceeded 50% of total cells in 2/17 controls, 12/16 UC and 12/15 CD (4.3 b, c, d, g, I, j).

Non-parametric correlation analyses between CCL20 immunohistochemical scores and corresponding RT-PCR values indicated a fair association. Spearman's correlation coefficients were as follows: 0.33* (p=0.023) for lamina propria, 0.31* (p=0.032) for surface epithelium, 0.38* (p=0.008) for crypt epithelium (illustrated below) and 0.38* (p=0.009) for vascular endothelium (* indicates statistical significance).

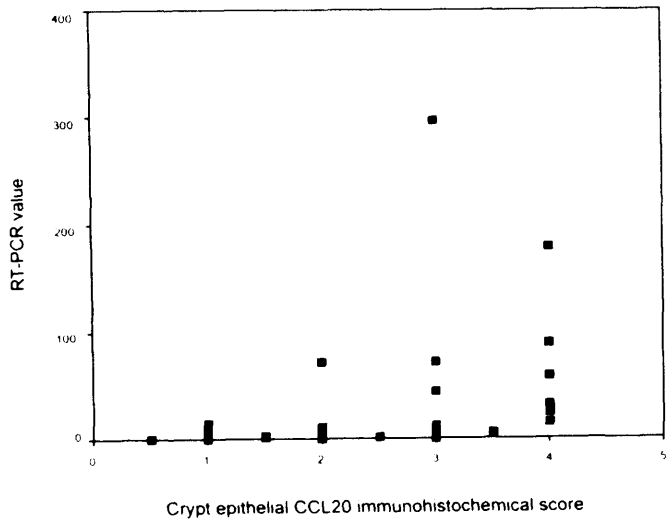

Figure 4.1: Colonic immunohistochemical staining for $CCL20^{+}$ cells using the immunoperoxidase technique. 4.1(a): Negative i.e. no primary antibody added, original magnification x10. 4.1(b): Normal control, original magnification x40. 4,1(c), (d), (e): UC, original magnification x 20 (c), x40 (d), (e).

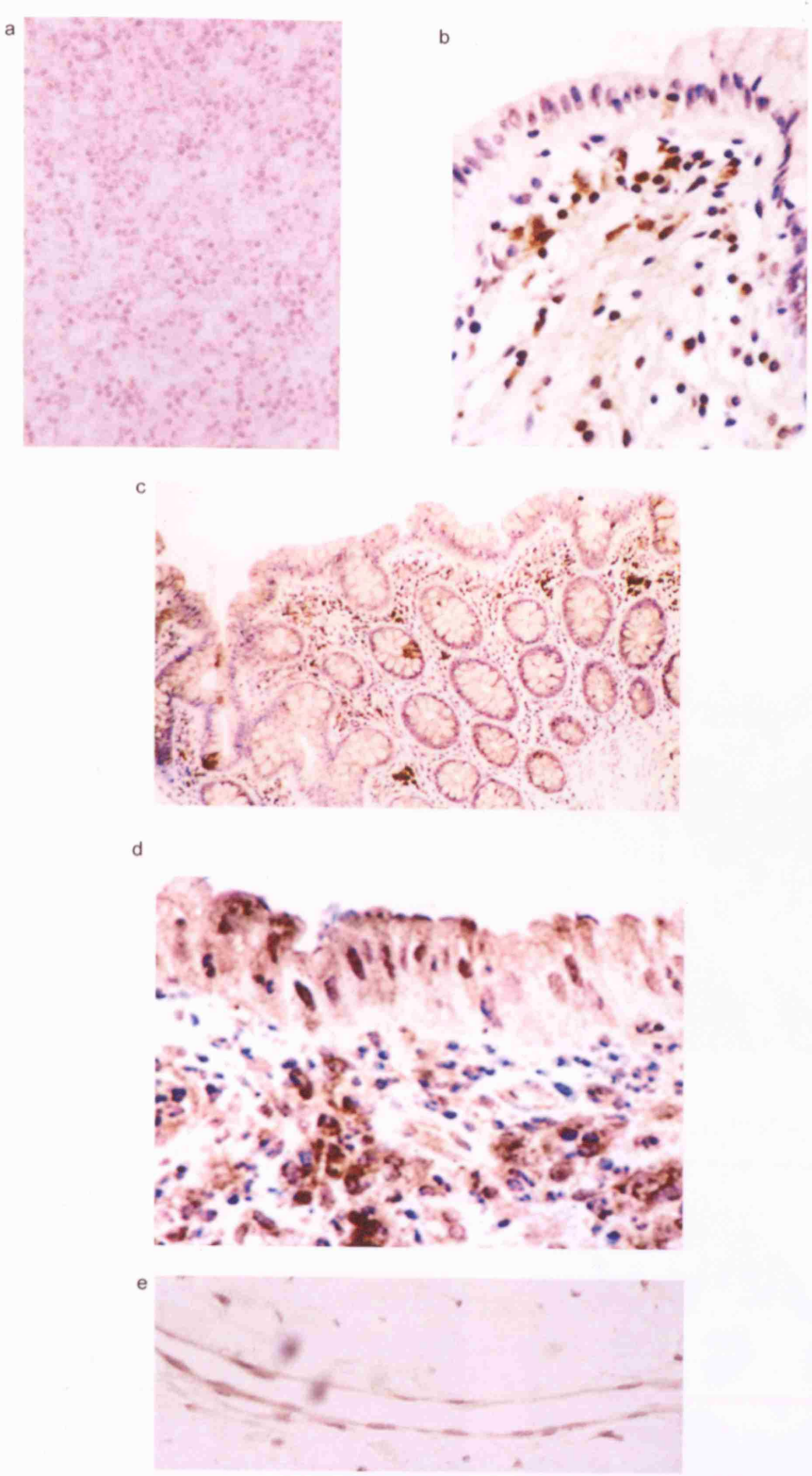

Figure 4.1: Colonic immunohistochemical staining for $CCL20^{+}$ cells in CD, using the immunoperoxidase technique. Original magnification x40 for (i), (j), (l) x20 for (f), (h), (k), x10 for (g). Neutrophilic staining is demonstrated in (k) and (l).

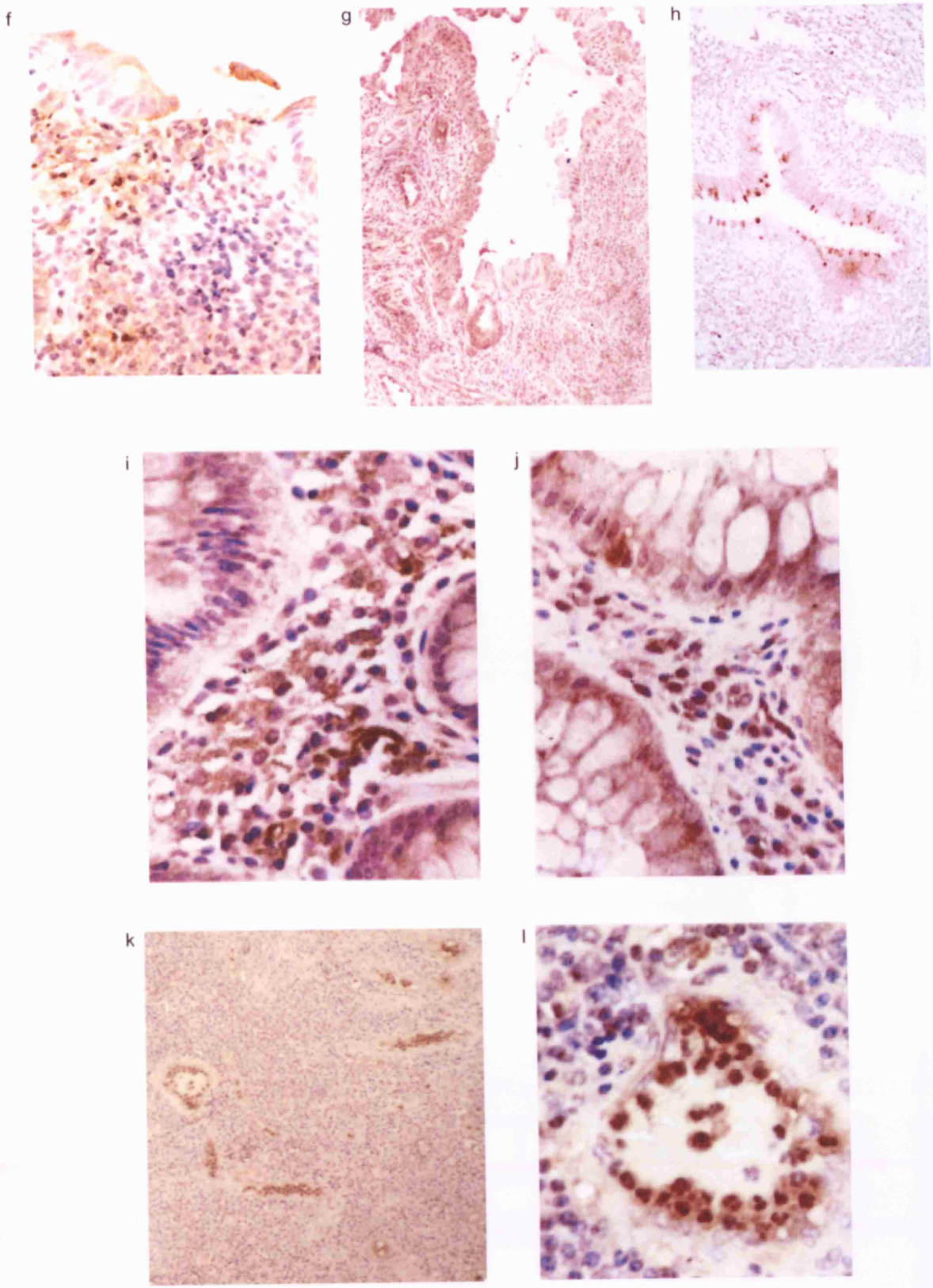

Graph 4.1: Colonic biopsy CCL20 immunohistochemical scores of surface epithelium correlated with corresponding histopathological inflammatory scores

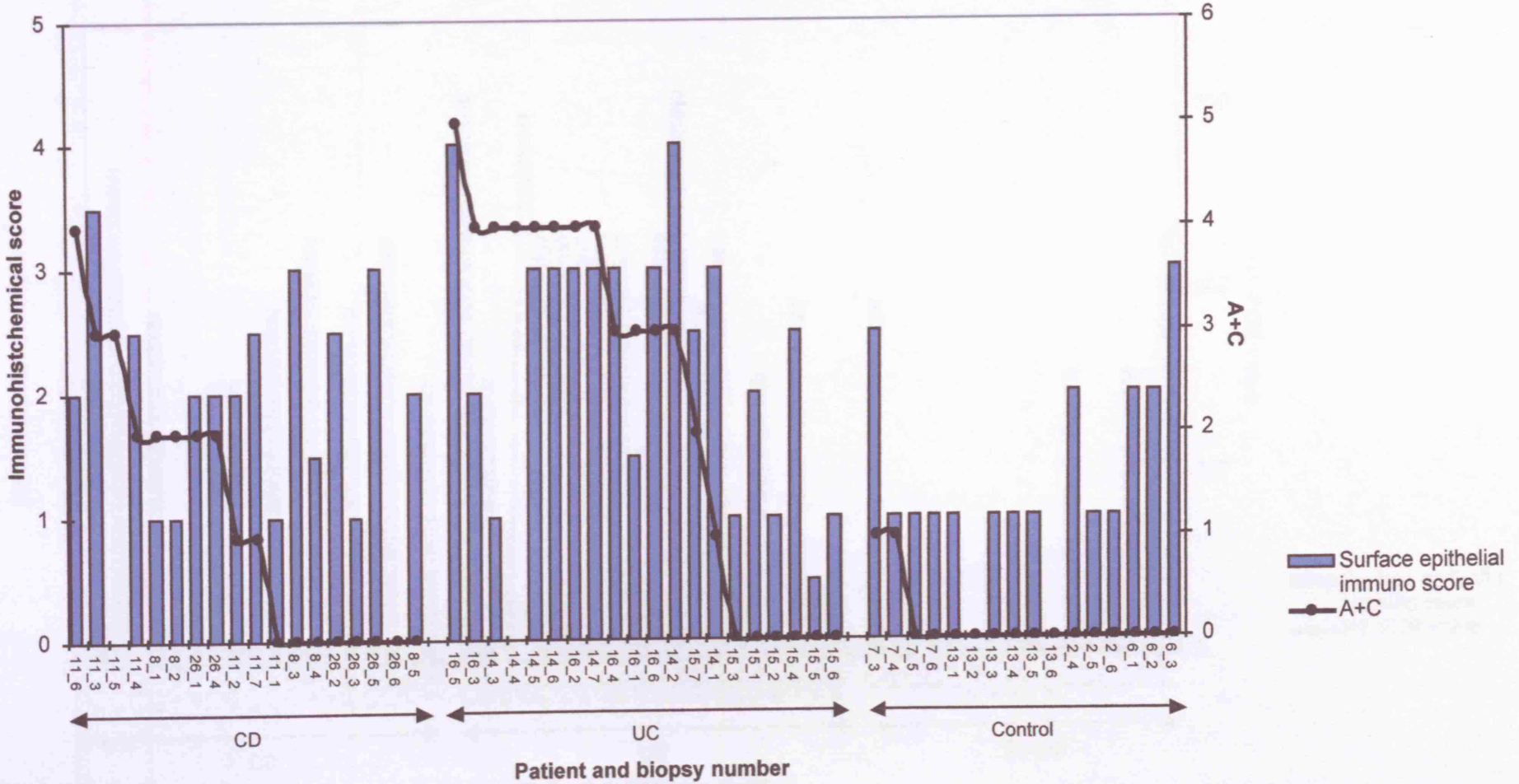

Patients are grouped according to disease, and chronologically placed according to inflammatory scres A+C. Patient and sample details are outlined in appendix table 2.3, and immunohistochemical scores are listed in table 4.2.

Graph 4.2: Colonic biopsy CCL20 immunohistochemical scores of surface epithelium correlated with corresponding RT-PCR taqman values

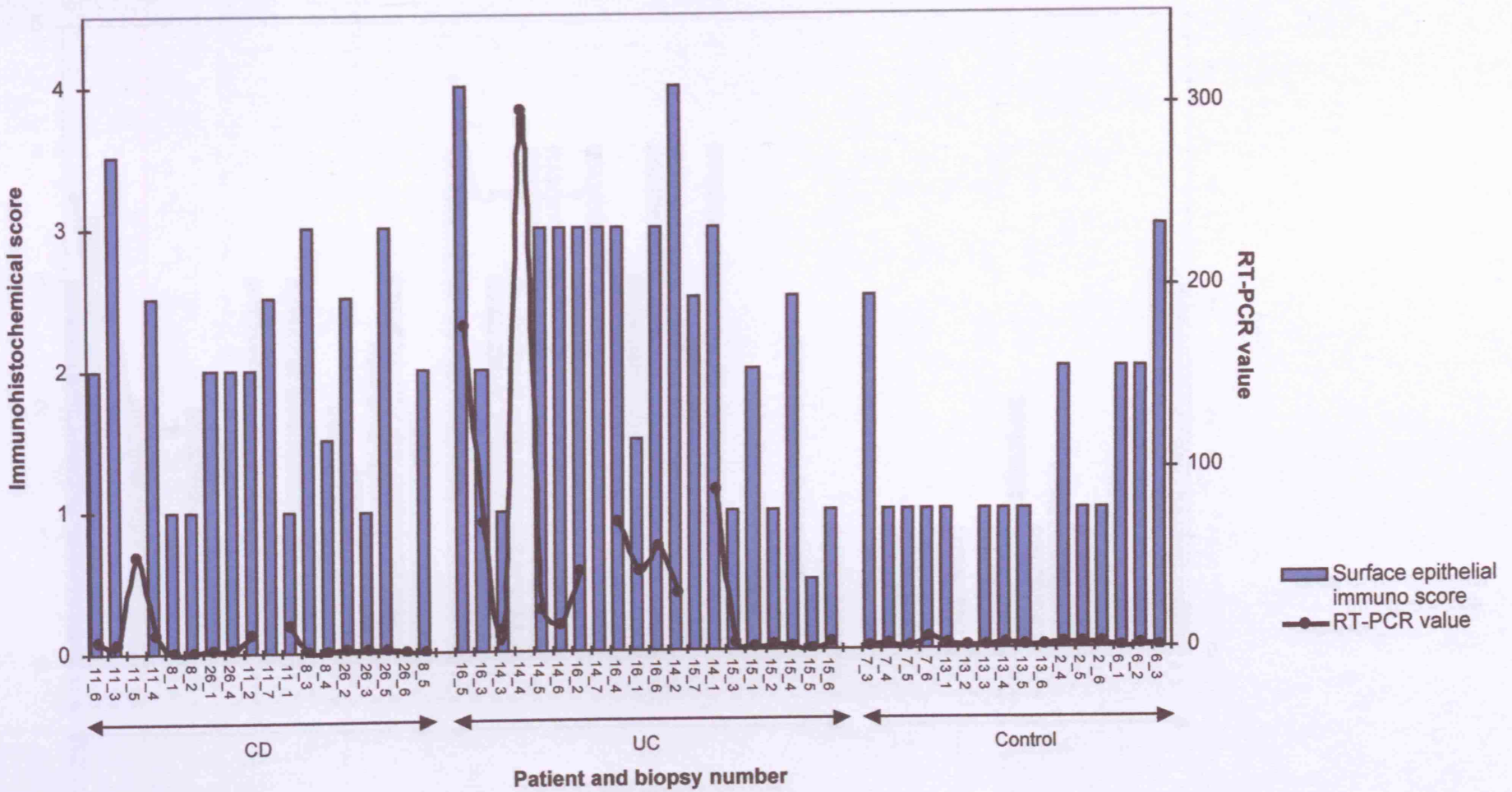

Patients are grouped according to disease. Patient and sample details are outlined in appendix table 2.3. Imunohistochemical scores are listed in table 4.2, and RT-PCR values in table 3.8.

Graph 4.3: Colonic biopsy CCL20 immunohistochemical scores of crypt epithelium correlated with corresponding histopathological inflammatory scores

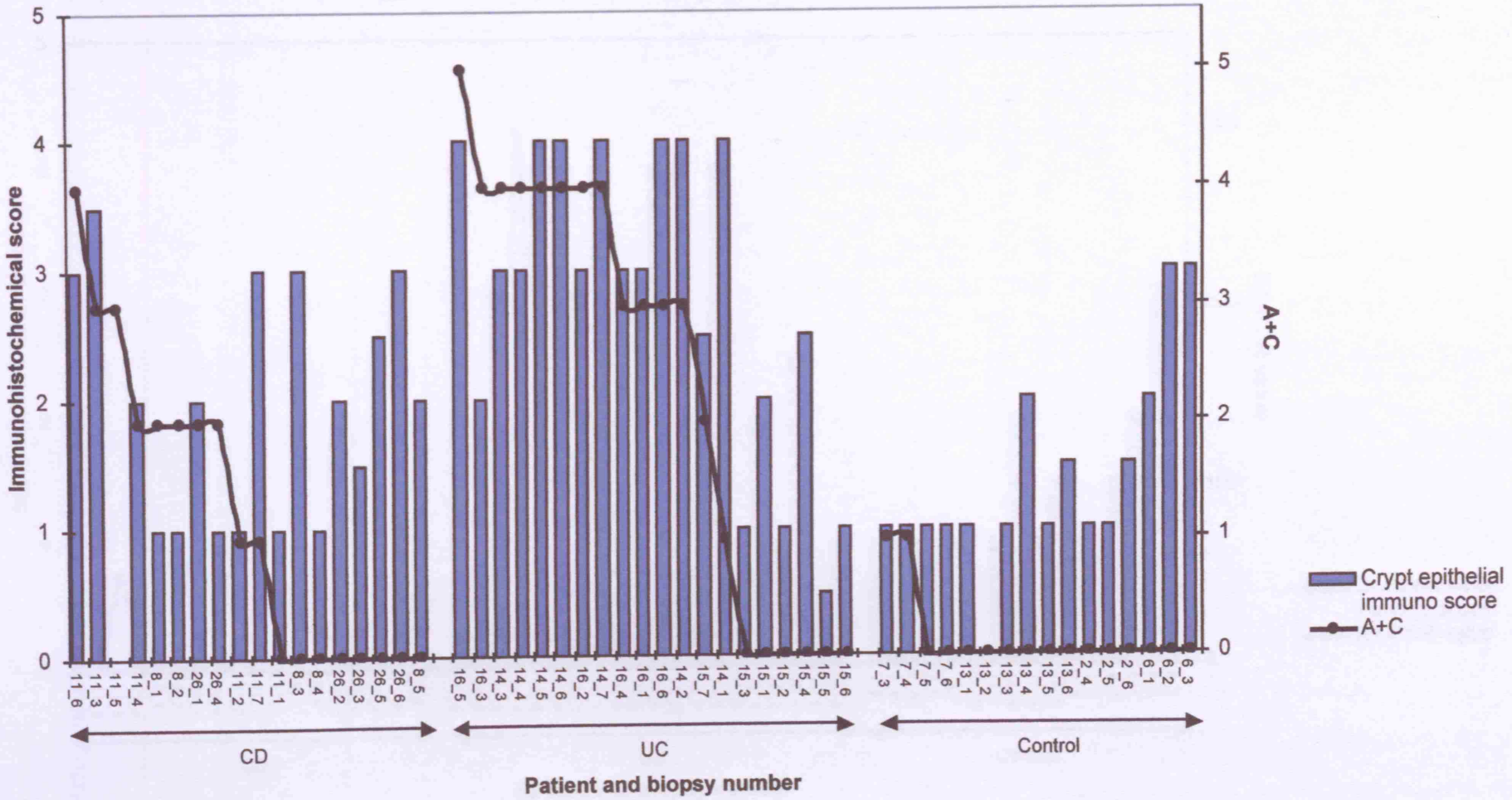

Patients are grouped according to disease and chronologically placed according to inflammatory scores A+C. Patient and sample details are outlined in appendix table 2.3, and immunohistochemical scores in table 4.2.

Graph 4.4: Colonic biopsy CCL20 immunohistochemical scores of crypt epithelium correlated with corresponding RT- PCR taqman values

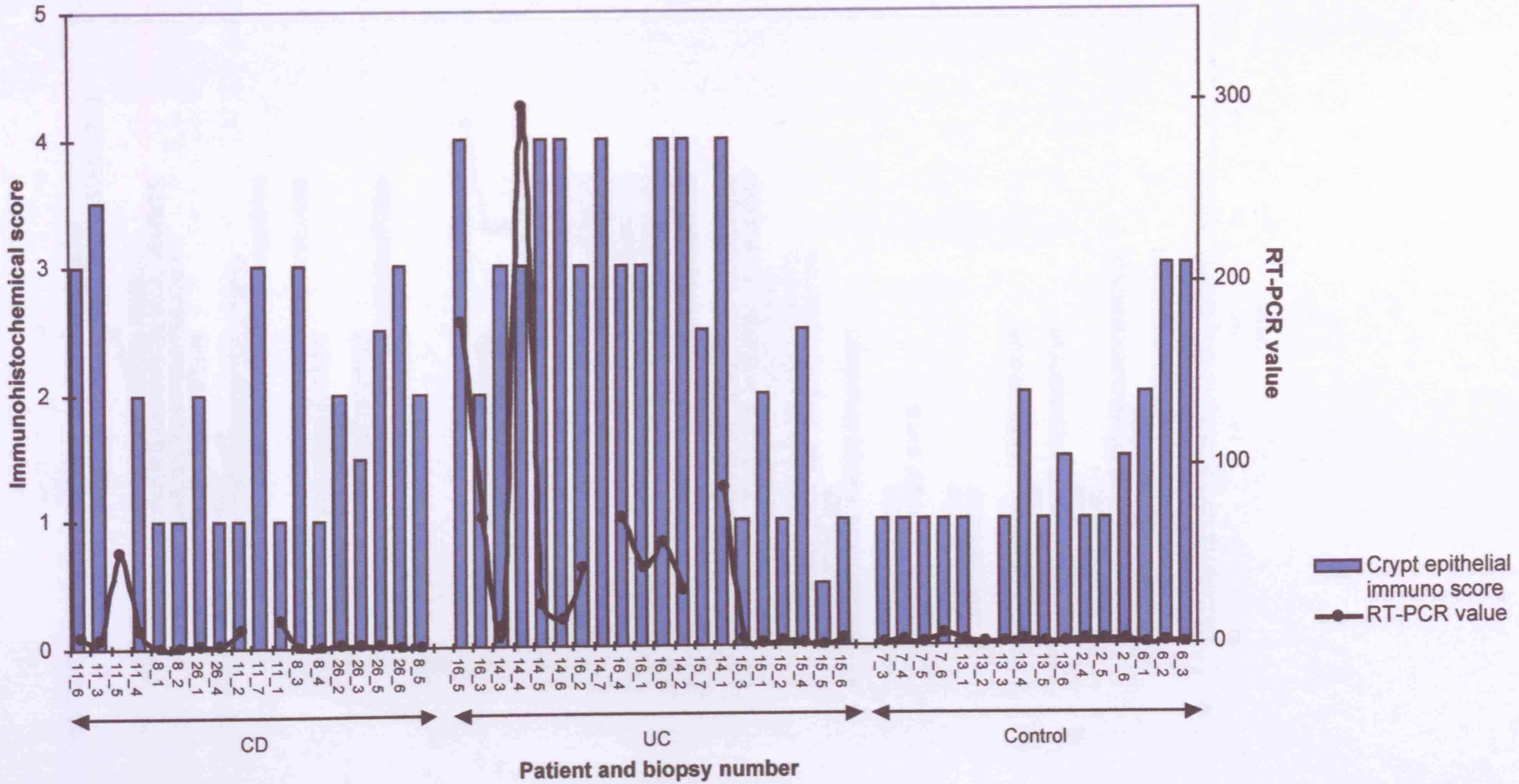

Patients are grouped according to disease. Patient and sample details are outlined in appendix table 2.3. Immunohistochemical scores are listed in table 4.2, and RT-PCR values in table 3.8.

Graph 4.5: Colonic biopsy CCL20 immunohistochemical scores of lamina propria correlated with corresponding histopathological inflammatory scores

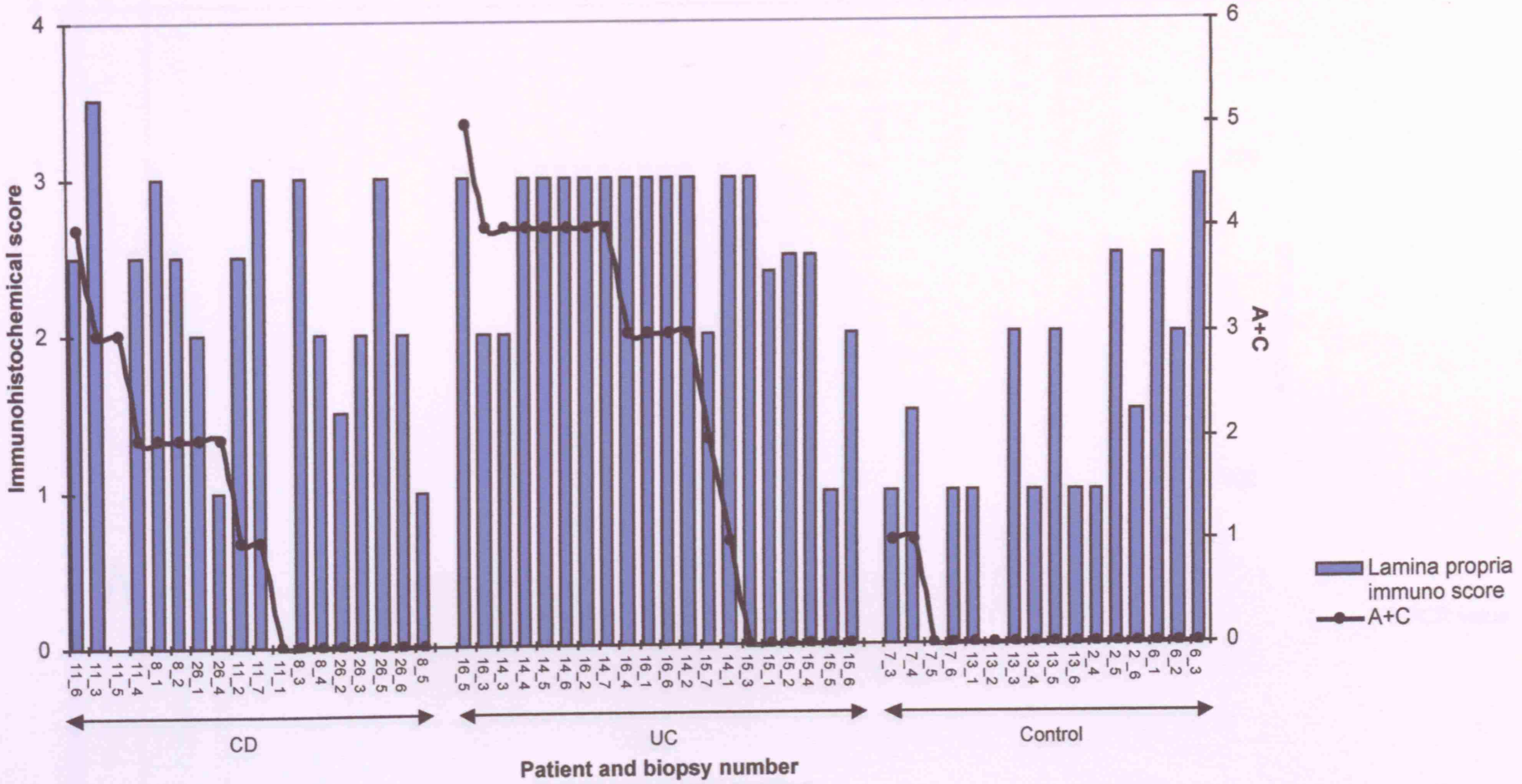

Patients are grouped according to disease, and chronologically placed according to inflammatory scores A+C. Patient and sample details are outlined in appendix table 2.3, and immunohistochemical scores in table 4.2.

Graph 4.6: Colonic biopsy CCL20 immunohistochemical scores of lamina propria correlated with corresponding RT-PCR taqman values

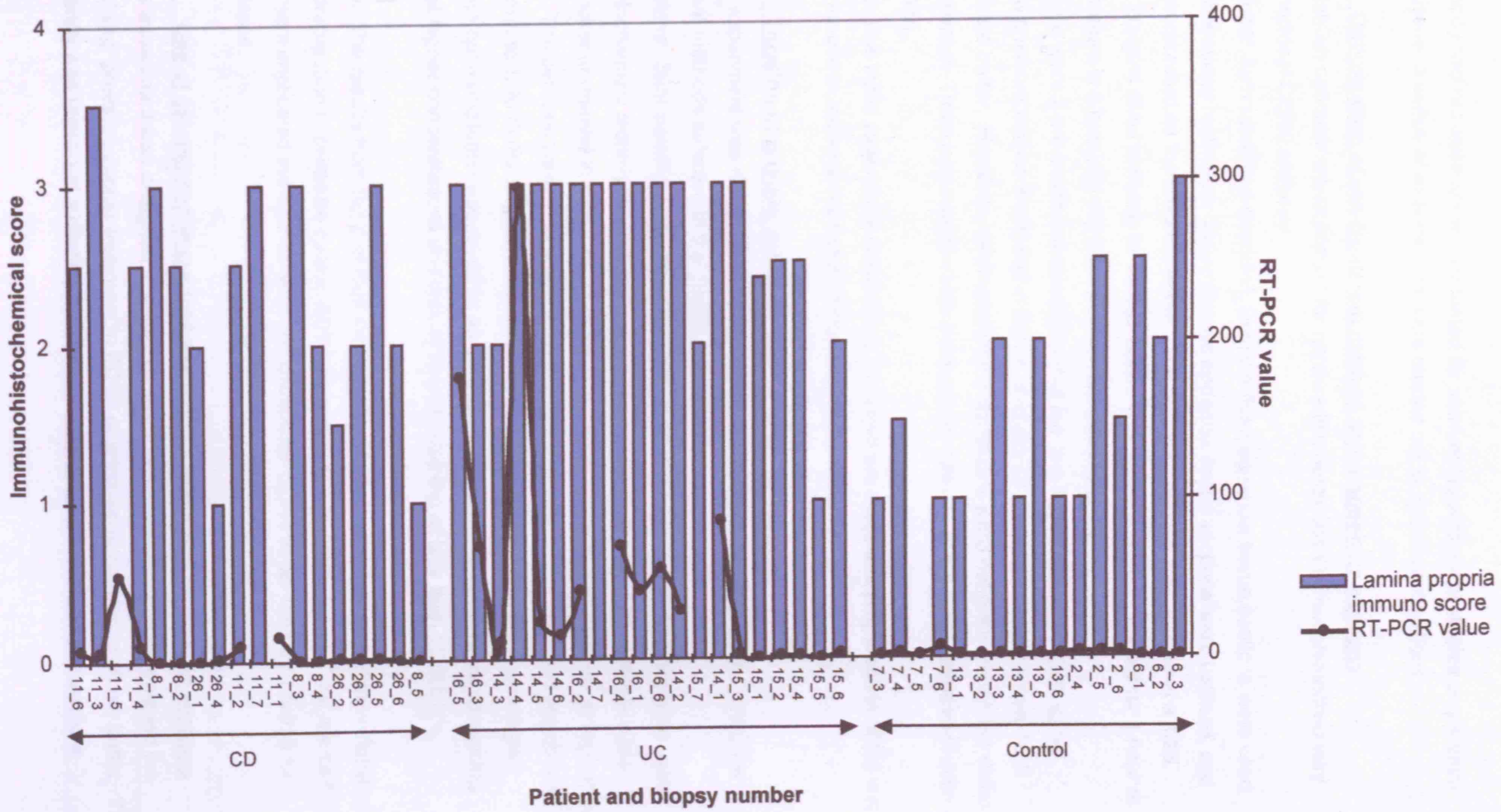

Patients are grouped according to disease. Patient and sample details are outlined in appendix table 2.3. Immunohistochemical scores are listed in table 4.2, and RT-PCR values in table 3.8.

4.3 Immunohistochemical localisation of CCR6 using the immunoperoxidase technique

As this antibody had not been previously tested for immunohistochemical studies on paraffin-embedded tissue, a series of experiments were carried out to optimise conditions.

4.3.1 Optimisation of pre-treatment method using appendix sections

Aim: To establish optimum pre-treatment for horseradish peroxidase immunohistochemistry using a monoclonal CCR6 antibody.

Tissue sections: 3μm paraffin-embedded, formalin-fixed appendix tissue sections were used.

Immunohistochemical technique: Non-inflamed appendix tissue sections were ustilised, and NHS was incorporated as the blocking agent. The primary antibody was applied at a 1/25 dilution, i.e. 20μg/ml (64μl antibody in 1600μl TBS). The sections were incubated for 1 hour at room temperature in a humidity chamber at room temperature.

Results: There were 2 pre-treatment conditions that led to a higher quality of staining; 90 seconds in a pressure cooker immersed in EDTA, and the 25 minutes in a microwave (high power) in citrate buffer. However, although these 2 conditions were definably better, the slides were over stained. There was considerable background staining at the recommended dilution of 1/25 (20μg/ml).

Conclusion: This initial experiment established 2 optimal pre-treatment preparations of the link conjugates for use in subsequent experiments.

4.3.2 Titration of primary antibody using appendix sections

Aims: This experiment was designed to optimise the link CCR6 antibody dilution, using the pre-treatment methods selected in the previous experiment.

Tissue sections: 3μm paraffin-embedded, formalin-fixed appendix tissue sections were used.

Immunohistochemical technique: The optimal pre-treatment methods of 90 seconds in the pressure cooker immersed in EDTA or 25 minutes in citrate buffer in a microwave on high power were used. The sections were incubated in the primary antibody, at the dilutions ranging from 1/100 (5μg/ml) to 1/8000 (62.5ng/ml). The ensuing conditions were otherwise unchanged.

Results: The optimal dilution was found to be 1/1000 i.e. 0.5μg/ml, with background staining increased at higher concentrations and loss of specific staining at less than 1/2000 (i.e. 0.25μg/ml).

Conclusion: The results from the previous experiment enabled establishment of the optimal pre-treatment preparation of pressure cooker EDTA or microwave in citrate buffer. The results from this experiment implicated the optimal antibody dilution for CCR6 to be 1/1000 (0.5μ/ml) for appendix tissue.

4.3.3 Use of established immunohistochemical technique on colonic sections

Aims: This experiment was designed to establish which pre-treatment method enabled the optimal staining: pressure cooker treatment in EDTA or microwave cooking in citrate buffer. The CCR6 antibody was utilised at a dilution of 1/1000 (0.5μg/ml), on colonic biopsy sections.

Methods: Tissue sections: 2 x 3μm paraffin embedded, formalin-fixed colonic biopsy tissue sections used, from each of 3 patients: 1 with UC, 1 with CD, and 1 with no disease (control). In addition 2 slides were used as control negative, with no primary antibody.
Results: Although the optimal dilution was found to be between 1/1000 (0.5μg/ml) with surgical appendix sections, with these colonic sections there was over-staining, and little discernible difference between the cases, with marked over staining.
Conclusion: Previous experiments established the optimal pre-treatment preparation of pressure cooker treatment in EDTA or microwave 25 minutes, of the link conjugates for use in subsequent experiments, at a dilution of 1/1000 (0.5μg/ml) for appendix tissue. This experiment indicated that the optimal dilution for CCR6 staining was less this for colonic tissue, and further studies were needed.

4.3.4 Titration of link antibody using colonic sections, and finalisation of pre-treatment method

Aims: This experiment was designed to establish the optimal pre-treatment method and CCR6 antibody dilution specifically for colonic biopsies. Results from previous experiments indicated that the 2 optimal pre-treatment methods were pressure cooker in EDTA or high-powered microwave treatment for 25 minutes in citrate buffer. Analysis of results from experiment 4.3.3 also indicated that a dilution of less than 1/1000 (0.5μg/ml) was appropriate.
Tissue sections: 3μm paraffin embedded, formalin-fixed colonic biopsy tissue sections from patients with UC/control (i.e. no disease) were used. Appendix and splenic sections were also included.
Immunohistochemical technique: The optimal pre-treatment methods of 90 seconds in the pressure cooker immersed in EDTA or microwave treatment in citrate buffer on high power for 25 minutes were used. The blocking agent used was NHS, milk powder or FCS. The primary antibody dilution used varied from 1/2000 (0.25μg/ml) to 1/4000 (0.125μg/ml).
Results: The optimal pre-treatment method was high-powered microwave treatment in citrate buffer, with a primary antibody dilution of 1/3000 i.e. 0.167μg/ml.
Conclusion: The optimum conditions have been established for staining of the CCR6 chemokine for colonic biopsies i.e. high-powered microwave treatment in citrate buffer for 25 minutes. The optimal primary antibody dilution was 1/3000 (0.167μg/ml), with a 5% FCS at the initial blocking step, primary antibody solutions, in addition to the secondary and tertiary dilutions.

4.3.5 Immunohistochemical localisation and scoring of CCR6 on colonic biopsies

Aims: Previous experiments had established the optimum conditions for staining of the CCR6 chemokine on colonic biopsies, i.e. high-powered microwave cooking in citrate buffer for 25 minutes. The optimal antibody dilution was found to be 1/3000 (0.17μg/ml), with a 5% FCS at the initial blocking step, primary antibody solutions, in addition to the secondary and tertiary dilutions. This technique was used on a subset of colonic biopsy series, chosen on the basis of the previous microarray data.
Tissue sections: 3μm paraffin embedded, formalin-fixed colonic biopsy tissue sections used from the 10 patients, from control patients 2, 6, 7; 13; from UC patients 14, 15, 16; and from CD

8, 11, 26. In addition, 2 negative controls were included. Patient details are outlined in appendix table 2.3.

Immunohistochemical technique: The optimal pre-treatment method of high-powered microwave cooking for 25 minutes was used.

Scoring: A semi-quantitative score from 0 (none) to 4 (dense confluent staining) was determined for epithelium, and percentage immunoreactive lamina propria cells determined (0 = 0%, 4 = 100%). The scoring was performed under blind conditions, whereby the slide identity was concealed, and all the slides were allocated a number randomly. Unblinding only took place when all the scoring was complete. In some slides, the blood vessels could not be identified clearly, so this score was omitted where necessary. The scores obtained are listed in table 4.5. Once scoring reliability had been ensured statistically, the original scores were correlated with both microarray data and histopathology inflammation scores. For each biopsy, a corresponding biopsy from the same area had been assessed by a consultant histopathologist, and scored on the basis of inflammation as detailed in table 2.2.

Table 4.5: CCR6 immunohistochemistry semi-quantitative assessment scores for the colonic biopsy series, with histopathological inflammatory scores and gene expression levels as determined by taqman real-time quantitative RT-PCR values.

Patient	Biopsy number	Lamina propria	Lymphoid	Surface epithelium	Crypt epithelium	Vascular	A+C	RT-PCR value
8 (CD)	1	3.5	X	3	2	3	2	0.789946
8 (CD)	2	3	X	3	3	3	2	0.277835
8 (CD)	3	3.5	X	4	4	3	0	0.616488
8 (CD)	4	3.5	X	3	3	X	0	0.5346
8 (CD)	5	2	X	3	3	3	X	0.322371
11(CD)	6	3	X	4	3	2	4	0.49571
11(CD)	3	2	X	4	3	3	3	2.471008
11(CD)	5	2	X	4	4	X	3	6.046842
11(CD)	4	2.5	X	3.5	3.5	2	2	3.546451
11(CD)	2	3	X	2	3	3	1	1.354527
11(CD)	7	3	X	4	4	3	1	X
11(CD)	1	2	X	2.5	2.5	3	0	8.276393
26(CD)	1	3	X	3	4	3	2	2.781361
26(CD)	4	3	X	4	4	3	2	1.983527
26(CD)	2	2	X	4	4	X	0	1.110116
26(CD)	3	3	X	4	4	3	0	1.307485
26(CD)	5	3	X	4	4	3	0	1.166769
26(CD)	6	4	X	4	4	3	0	0.769538
14(UC)	3	3	3.5	X	4	4	4	7.882462
14(UC)	4	4	4	4	4	3	4	41.84468
14(UC)	5	3	X	4	4	3	4	7.988732
14(UC)	6	3	X	4	4	3	4	8.276393
14(UC)	7	2	X	3	2	3	4	X
14(UC)	2	3	X	3	2	3	3	15.07809
14(UC)	1	1	X	1	1	2	1	58.18939
15(UC)	7	3	4	4	4	X	2	X
15(UC)	3	3	X	4	4	3	1	11.67106
15(UC)	1	4	X	4	4	3	0	1.747792
15(UC)	2	3	X	4	4	2	0	7.310757
15(UC)	4	3	X	4	4	3	0	1.504779
15(UC)	5	2	X	3	3	2	0	1.460329
15(UC)	6	3	X	4	4	3	0	2.843975
16(UC)	3	3	X	4	3	3	4	40.87831
16(UC)	2	3	X	3	2	3	4	21.98496
16(UC)	4	2	4	2	2	3	3	7.16059
16(UC)	5	3	X	2	2	X	5	34.93608
16(UC)	6	3	X	4	3	3	3	39.41799
2 (Cont)	4	1	X	3	2	2	0	5.551059
2 (Cont)	5	2.5	X	4	3	3	0	9.319959
2 (Cont)	6	2.5	4	3	2	3	0	5.348756
6 (Cont)	1	2	X	3	2	3	0	0.225641
6 (Cont)	2	2	X	3	3	1	0	0.770736
7 (Cont)	3	2	4	4	3	3	1	0.12103
7 (Cont)	4	3	X	4	4	3	1	0.432922
7 (Cont)	5	2	X	3	2	3	0	0.259028
7 (Cont)	6	2	4	4	2	3	0	0.456853
13(Cont)	1	1	X	X	4	2	0	2.77946
13(Cont)	2	1	X	2	1	2	0	2.585078
13(Cont)	3	2.5	X	4	3	3	0	0.91217
13(Cont)	4	2	X	3	3	2	0	1.684642
13(Cont)	5	2	X	4	4	2	0	1.186685
13(Cont)	6	2	X	4	4	3	0	2.677956

Statistical validation: As the scoring was semi-quantitative, it was important to statistically validate the scoring technique consistency and reliability. 11 slides were re-scored for all parameters, blind from the slide identity and the original score. Each value was paired with the initial scoring value. These pairs were incorporated into a student's t-test for paired parametric data. Each of the first scores for 11 slides was paired with the corresponding second scores, as listed in table 4.6. This statistical test is useful for investigating a variable in two groups where there is a meaningful one-to-one correspondence between the data points in one group and

those in the other. The null hypothesis states that there is no significant difference between the 2 groups.

Table 4.6: List of initial and repeat semi-quantitative immunohistochemistry scores for CCR6, to demonstrate reproducibility of scoring method.

Score number	Score 1 (X_a)	Score 2 (X_b)	$X_a - X_b$
1	4	4	0
2	3	3	0
3	4	4	0
4	4	4	0
5	3.5	4	-0.5
6	3.5	4	-0.5
7	3.5	4	-0.5
8	4	4	0
9	4	4	0
10	4	4	0
11	4	4	0
12	2.5	3	-0.5
13	2	2	0
14	3.5	4	-0.5
15	2	2	0
16	4	4	0
17	3.5	4	-0.5
18	3	2	1
19	3	2	1
20	3	3	0
21	3	3	0
22	4	4	0
23	4	4	0
24	1	1	0
25	1	1	0
26	4	4	0
27	4	3	1
28	3	2.5	0.5
29	4	4	0
30	4	4	0
31	3	4	-1
32	4	4	0
33	3	3	0
34	3	3	0
35	3	2.5	0.5
36	3	3	0
37	2	2.5	-0.5
38	3	3	0
39	4	3.5	0.5
40	3	3	0
41	3	3	0
42	2.5	2.5	0
43	3	3	0
44	2	2.5	-0.5
45	3	3	0
46	3	2.5	0.5
47	1	2	-1
48	2	2.5	-0.5
49	2	2.5	-0.5
50	3	4	-1
51	1	2	-1
52	3	2	1
53	2	3	-1
54	3	3	0
55	2	3	-1
56	3	3.5	-0.5
57	3	3	0
58	3	3	0
59	3	3	0
60	3	3	0
61	3	3	0
62	2	3	-1
63	3	2	1

Table 4.7: Statistical validation table of CCR6 semi-quantitative immunohistochemistry scores.

Values	X_a	X_b	$X_a - X_b$
n	63	63	63
Sum	189.5	195	-5.5
Mean	3.0079	3.0952	-0.0873
Sum_sq	612.75	642.5	15.75
SS	42.746	38.9286	15.2698
Variance	0.6895	0.6279	0.2463
Standard Deviation	0.8303	0.7924	0.4963

$Mean_A - Mean_B = -0.873$

$t = -1.4$

$df = 62$

Two-tailed $p = 0.167619$

On the basis of this $p>0.05$, the null hypothesis cannot be rejected, i.e. that there is no statistical difference between the original and repeat scoring values. The scoring reducibility is therefore not un-acceptable statistically.

Results: There was no staining in the control negative slides, where no primary antibody had been applied, demonstrated in figure 4.2a. In areas of inflammation a population of lymphocytes stained in the pericellular area (figure 4.2 e,f). More lymphocytic $CCR6^+$ staining was evident in IBD cases. Lymphoid areas were consistently strongly stained, corresponding primarily to the T-areas (4.2b). Neutrophils stained strongly, corresponding to inflammatory areas (figure 4.2 g, h, i,). There was moderate vascular staining and variable surface and crypt epithelial staining, particularly on the basolateral layer. Generally, control immunoreactivity was more pronounced on the surface than crypt epithelium. Both UC and CD showed stronger immunoreactivity of both surface and crypt epithelium. The $CCR6^+$ cells were more dense in the upper third of the lamina propria, and subjacent to the epithelium (figure 4.2 c,d). Clear differences were apparent in the deeper lamina propria area between cases of IBD and control, although the differences were subtler in the subepithelial area, with $CCR6^+$ cells extending to the deeper lamina propria (figure 4.2c, d, f). An occasional dendritic cell was evident in the subepithelial area. Muscular tissue was consistently unstained.

Formal quantisation of the staining is listed in table 4.5, and graphically represented in figure 4.4. Slides from patients with IBD had higher deeper-lamina propria scores than the control group, with lymphocytes staining particularly. There were more than 50% of total cells $CCR6^+$ in 1/17 controls, 13/16 UC and 12/15 CD. The scoring correlated with the histological inflammatory score as described before, and with mRNA expression from array data.

Non-parametric correlation analyses between CCR6 immunohistochemical scores and corresponding RT-PCR did not indicate an association. Spearman's correlation coefficients were as follows: 0.11 (p=0.43) for lamina propria, -0.039 (p=0.79) for surface epithelium, 0.020 (p=0.89) for crypt epithelium and 0.018 (p=0.91) for vascular endothelium.

Figure 4.2a-f: Colonic immunohistochemical staining of $CCR6^{+}$ cells using the immunoperoxidase technique. Original magnification x10 for (a) and (b), x20 for (c), (d), and (f) x40 for (e). A control negative is demonstrated in (a) where no primary antibody was applied. Appendiceal section immunostaining is demonstrated in (b). Control tissue immunostaining is demonstrated in (c), CD tissue in (d), and UC tissue in (e) and (f).

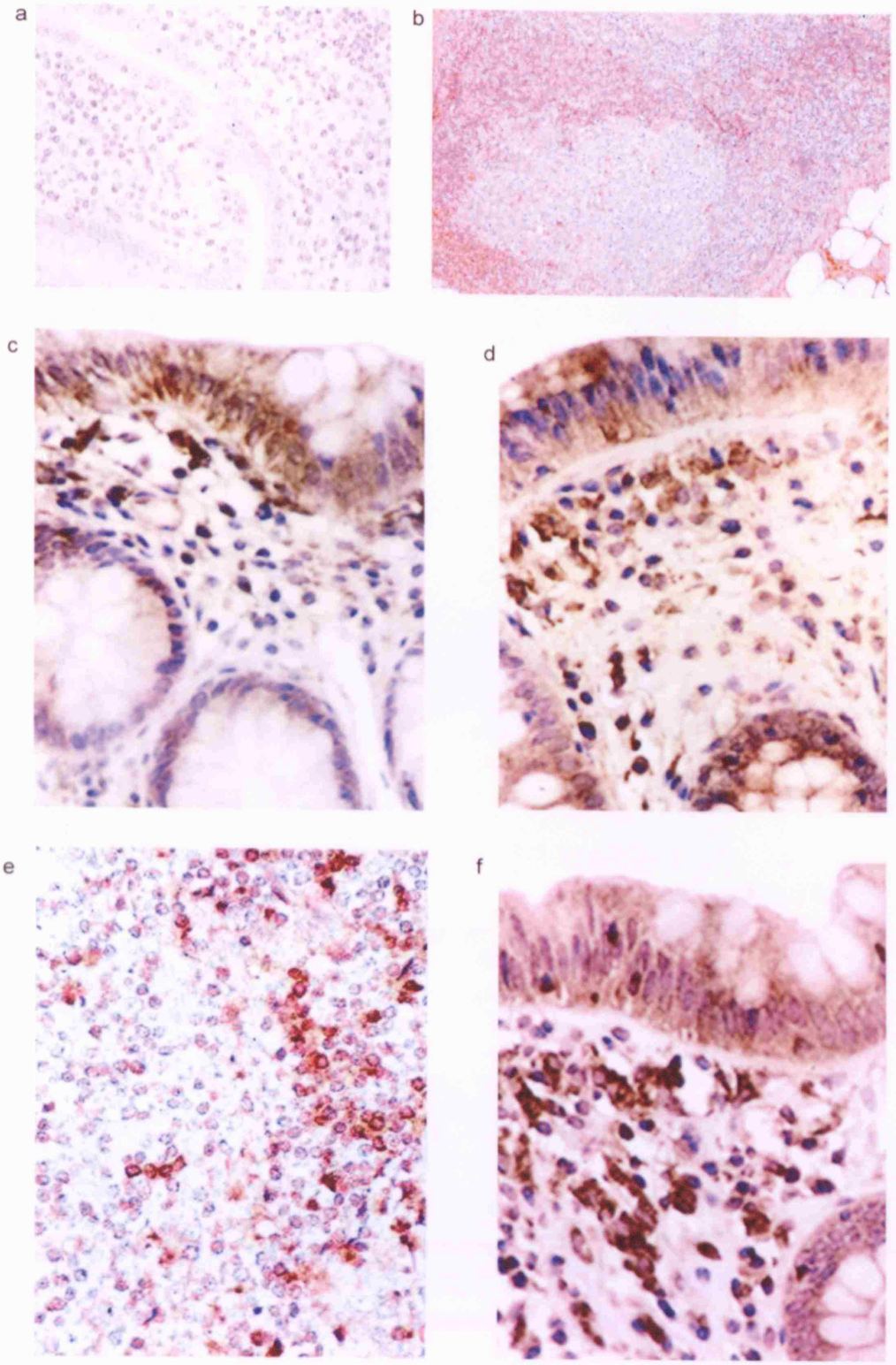

Figure 4.2g-l: Colonic immunohistochemical staining of $CCR6^+$ cells in CD, using the immunoperoxidase technique, original magnification x40. Neutrophilic staining is demonstrated.

g

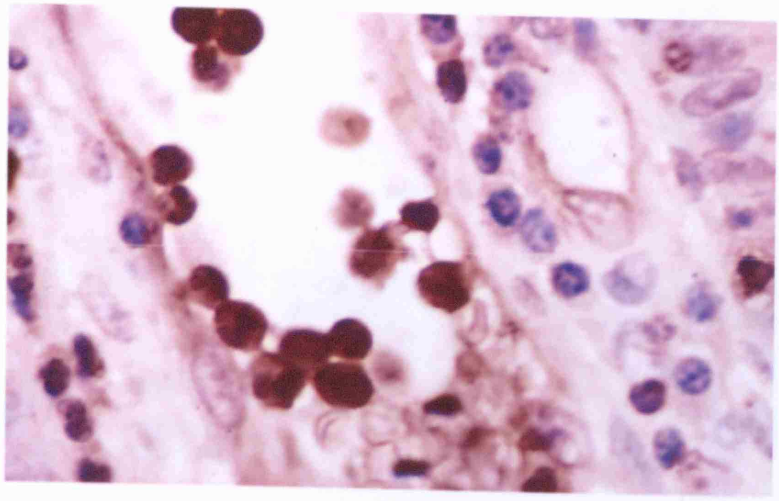

h

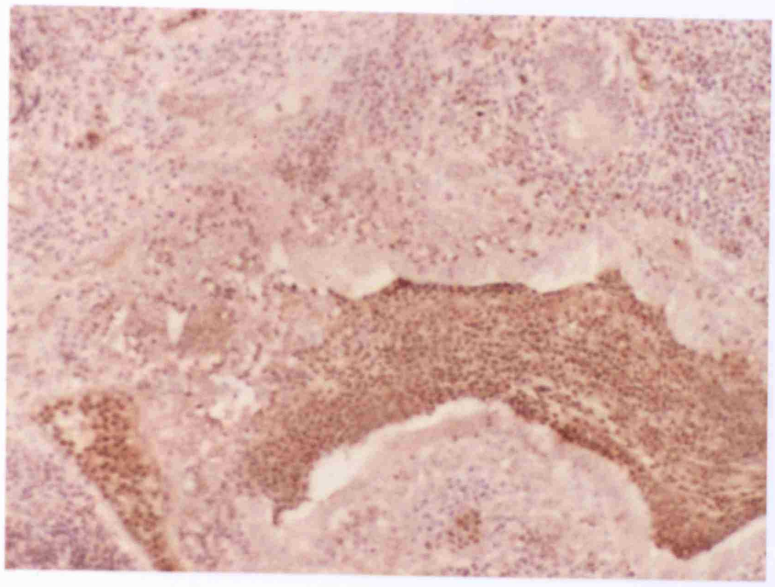

i

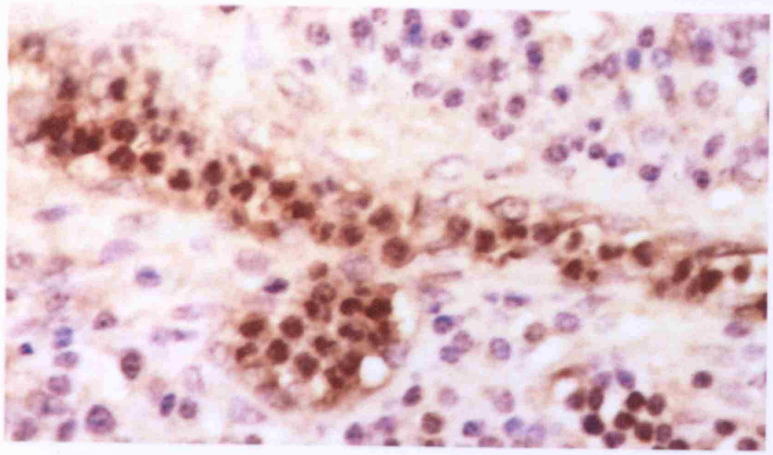

Graph 4.7: Colonic biopsy CCR6 immunohistochemical scores of surface epithelium correlated with corresponding histopathological inflammatory scores

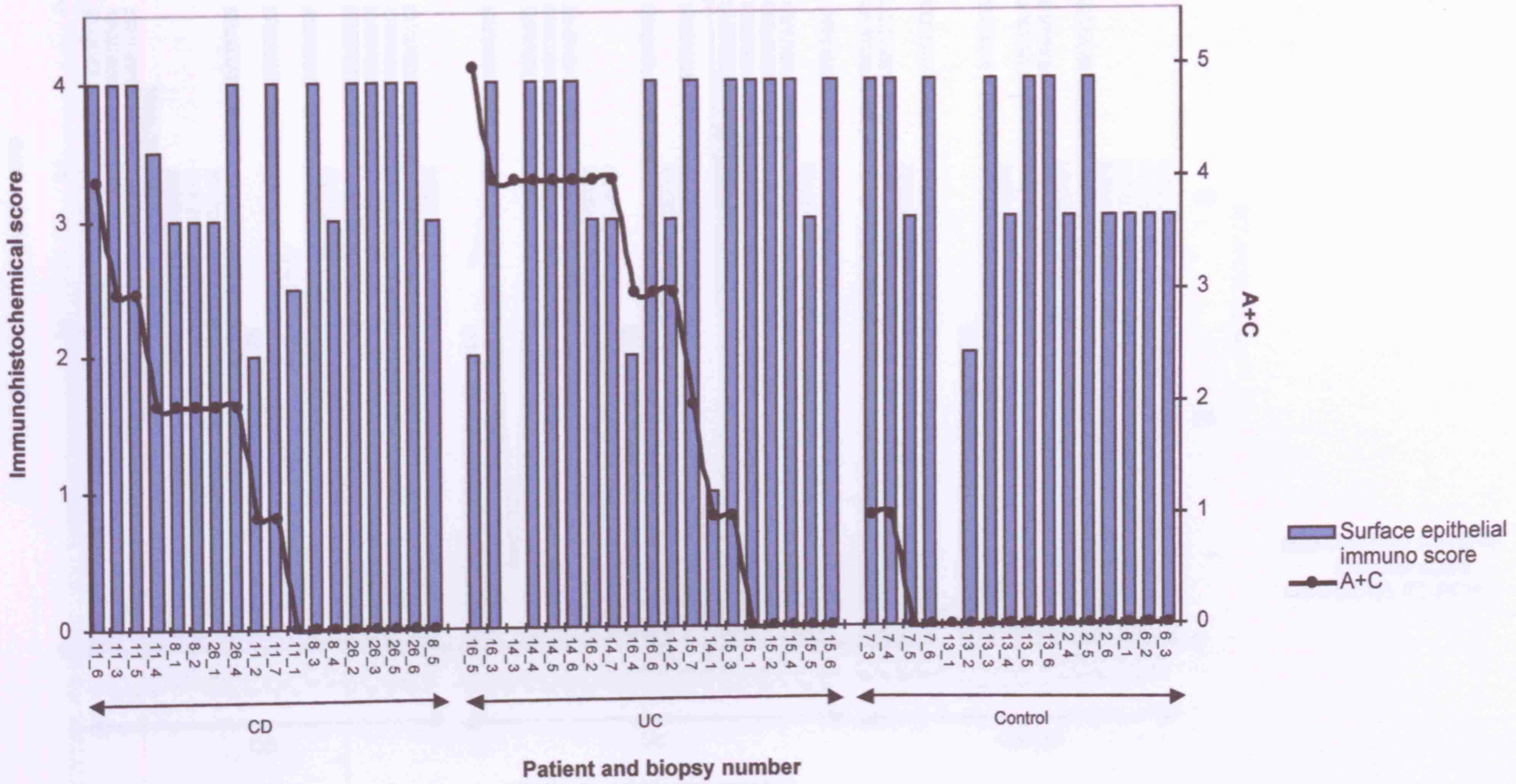

Patients are grouped according to disease, and chronologically placed according to inflammatory scores A+C. Patient and sample details are outlined in appendix table 2.3, and immunohistochemical scores in table 3.8.

Graph 4.8: Colonic biopsy CCR6 immunohistochemical scores of surface epithelium correlated with corresponding RT- PCR taqman values

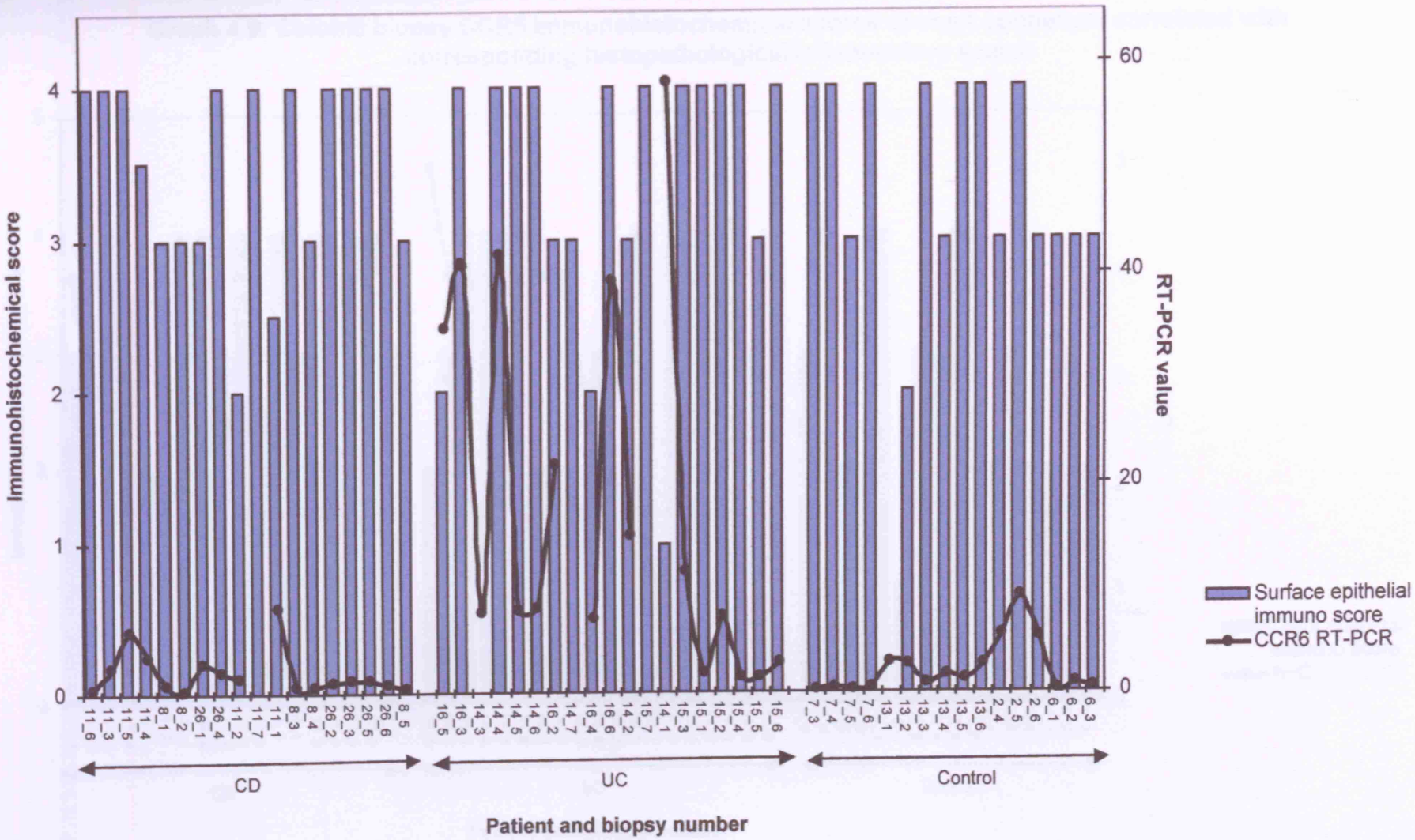

Patients are grouped according to disease. Patient and sample details are outlined in appendix table 2.3. Immunohistochemical scores are listed in table 4.5, and RT-PCR values in table 3.8.

Graph 4.9: Colonic biopsy CCR6 immunohistochemical scores of crypt epithelium correlated with corresponding histopathological inflammatory scores

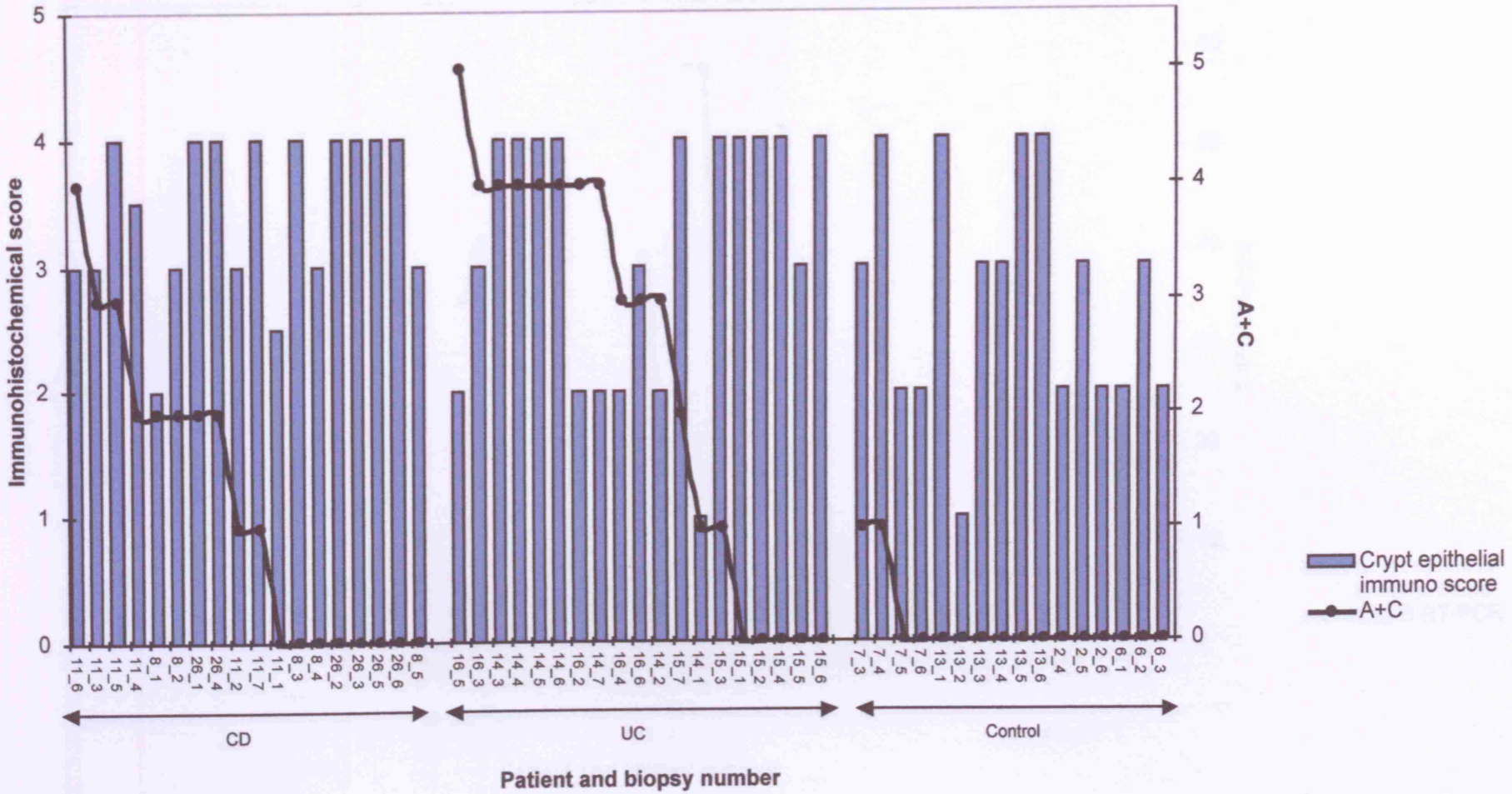

Patients are grouped according to disease, and chronologically placed according to inflammatory scores A+C. Patient and sample details are outlined in appendix table 2.3, and immunohistochemical scores in table 4.5.

Graph 4.10: Colonic biopsy CCR6 immunohistochemical scores of crypt epithelium correlated with corresponding RT-PCR taqman values

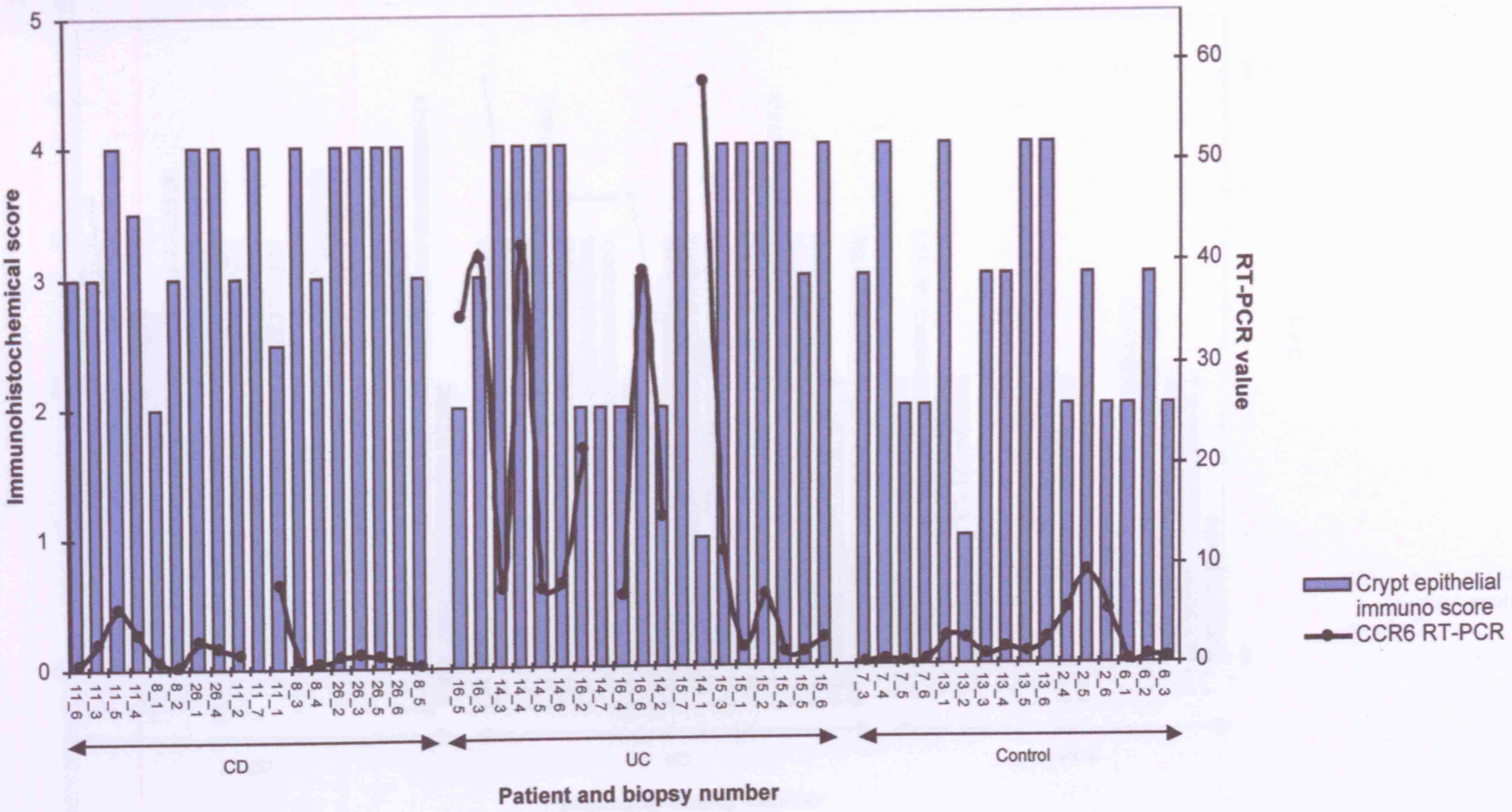

Patients are grouped according to disease. Patient and sample details are outlined in appendix table 2.3. Immunohistochemical scores are listed in table 4.5, and RT-PCR values in table 3.8.

Graph 4.11: Colonic biopsy CCR6 immunohistochemical scores of lamina propria correlated with corresponding histopathological inflammatory scores

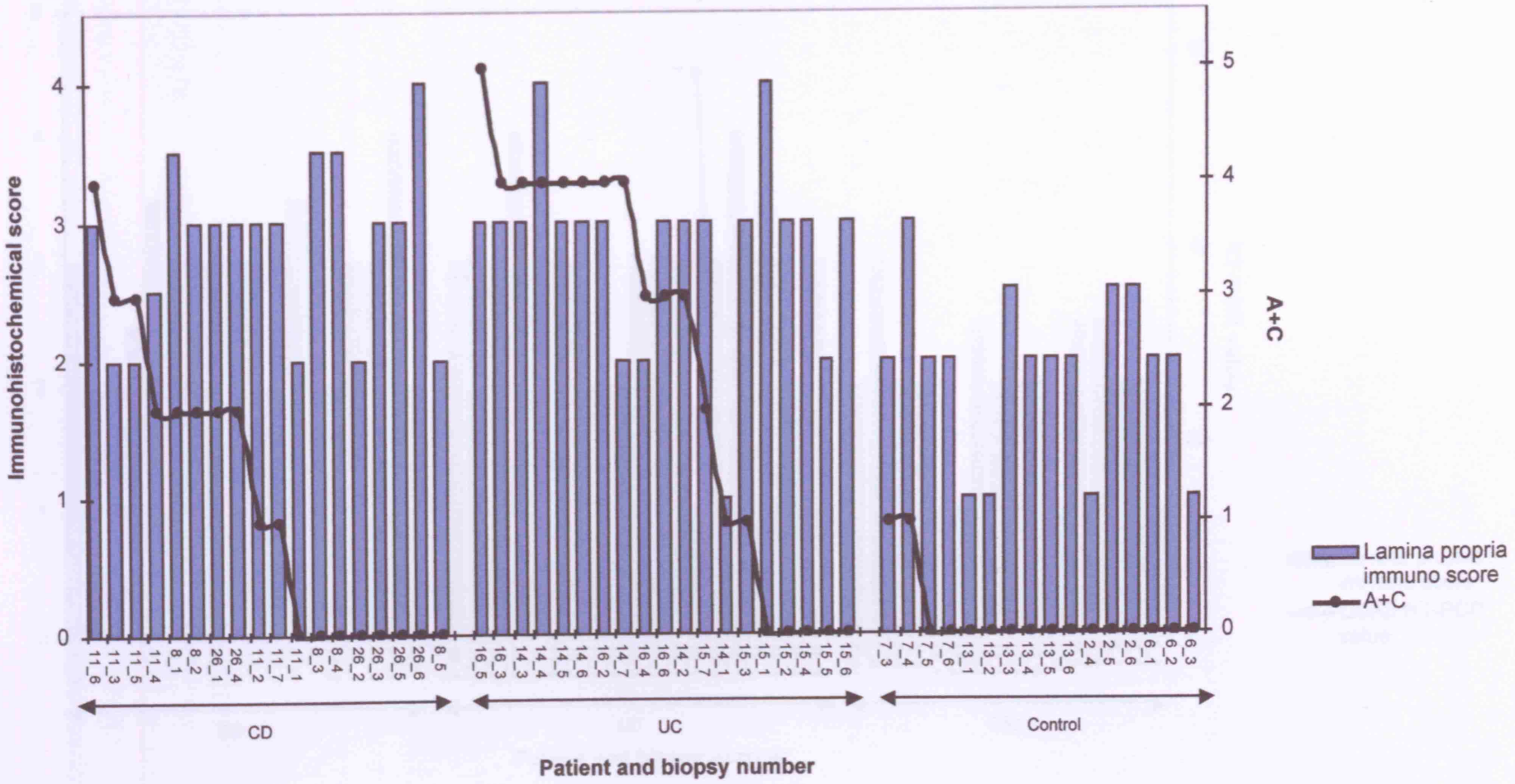

Patients are grouped according to disease, and chronologically placed according to inflammatory scores A+C. Patient and sample details are outlined in appendix table 2.3, and immunohistochemical scores in table 3.8.

Graph 4.12: Colonic biopsy CCR6 immunohistochemical scores of lamina propria correlated with corresponding RT-PCR taqman values

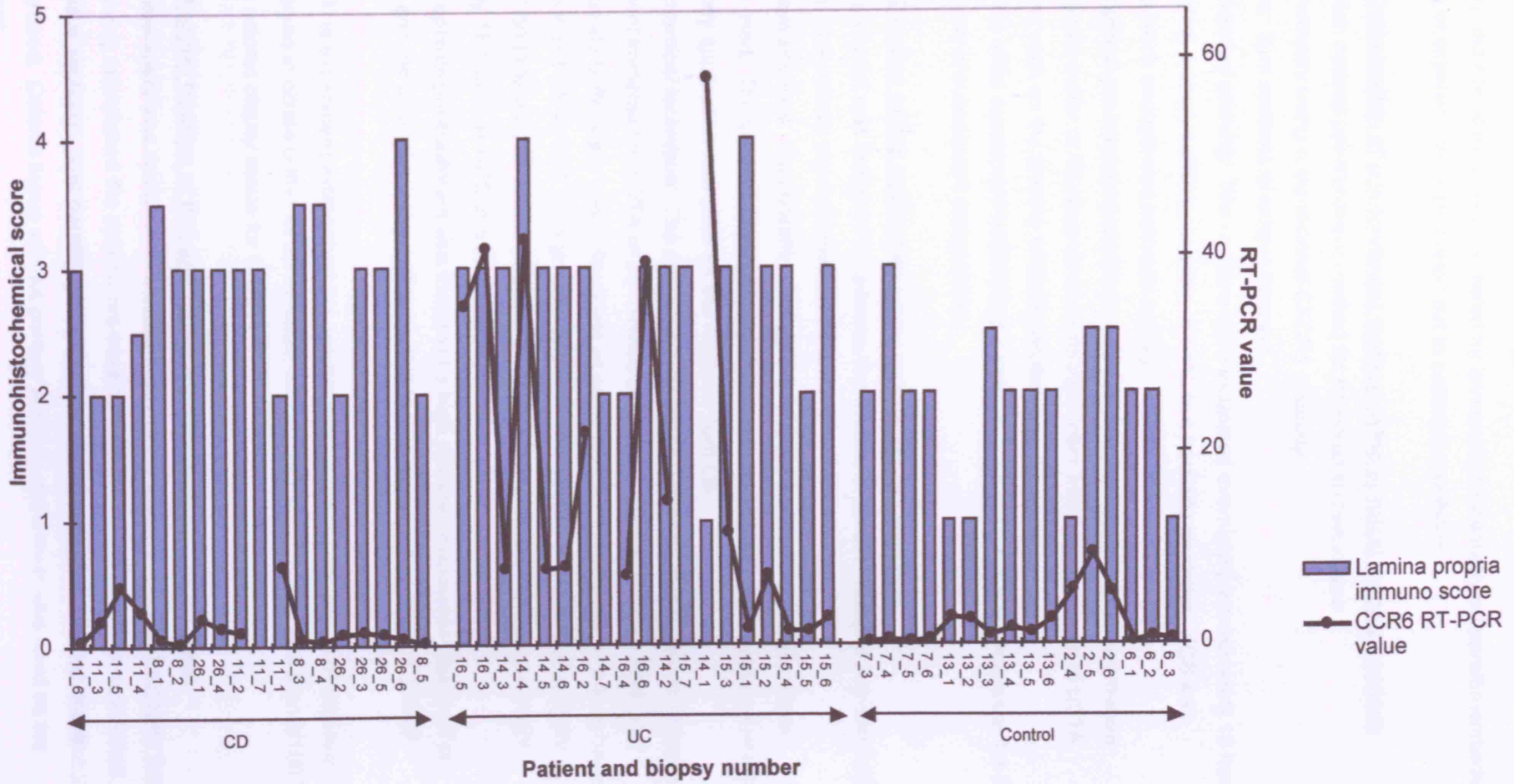

Patients are grouped according to disease. Patient and sample details are outlined in appendix table 2.3. Immunohistochemical scores are listed in table 4.5, and RT-PCR values in table 3.8.

4.4 Immunohistochemical localisation of CXCR1 using the immunoperoxidase technique

As this antibody had not been previously tested for immunohistochemistry on paraffin-embedded tissue, a series of experiments were carried out to optimise conditions.

4.4.1 Optimisation of pre-treatment method using surgical colonic sections

Aim: To establish optimal pre-treatment method for horseradish peroxidase immunohistochemistry using a monoclonal CXCR1 antibody.

Tissue sections: 3μm sections of colonic biopsies.

Immunohistochemical staining: The sections were incubated overnight (approximately 18 hours) in a 1/50 (10μg/ml) primary antibody solution at +4°C in a humidity chamber. FCS was incorporated to block endogenous peroxide activity.

Results: The optimal pre-treatment conditions were 25 minutes high-powered microwave treatement in citrate buffer or 90 seconds of pressure-cooker treatmet immersed in EDTA. However, further work on the primary antibody dilution was necessary.

Conclusion: This initial experiment established 2 optimal pre-treatments preparations of the link conjugates for use in subsequent experiments.

4.4.2 Titration of link antibodies using colonic biopsy sections

Aims: This experiment was designed to optimise the dilution of CXCR1 receptor link antibodies, and to establish the optimal pre-treatment method.

Methods: Tissue sections: 3μm paraffin embedded, formalin-fixed colonic biopsy tissue sections were used. The sections were obtained from patients with UC. Colonic tissue without primary antibody application was used for the negative controls.

Immunohistochemical technique: The optimal pre-treatment methods of 90 seconds of pressure cooker treatment immersed in EDTA or 25 minutes of high powered-microwave treatment immersed in citrate buffer were used. Blockade of endogenous peroxide activity was achieved by a 5% solution of FCS in TBS. The primary antibody was applied at the following dilutions varying from 1/50 (10μg/ml) to 1/1000 (0.5μg/ml). The sections were incubated overnight (approximately 18 hours) at +4°C in a humidity chamber.

Results: The optimal pre-treatment was found to be high powered microwave-treatment in citrate buffer, and the optimal primary antibody dilution was found to be less than 1/1000 (0.5μg/ml).

Conclusion: This experiment established the optimal pre-treatment preparation of microwave cooking immersed in citrate buffer for 25 minutes, with an optimal dilution of less than 1/1000 (0.5μg/ml) for colonic biopsy tissue for CXCR1.

4.4.3 Further titration of link antibodies using colonic biopsy sections

Aims: This experiment was designed to establish the optimal dilution of CXCR1 receptor link antibodies, having established the optimal pre-treatment method in the previous experiment.

Methods: Tissue sections: 3μm paraffin embedded, formalin-fixed colonic biopsy tissue sections were used. Colonic tissue without primary antibody application was used as the negative control.

Immunohistochemical technique: The optimal pre-treatment technique of 25 minutes in citrate buffer in a microwave on high power was used. Blockade of endogenous peroxide activity, was achieved by of a 5% solution of FCS in TBS. The primary antibody was applied at dilutions varying from 1/1000 (0.5μg/ml) to 1/1400 (0.357μg/ml). The sections were incubated overnight (approximately 18 hours) at +4°C in a humidity chamber.

Results: The optimal primary antibody dilution was found to be 1/1400, corresponding to a protein concentration of 3.3μg/ml.

Conclusion: This experiment established the optimal dilution of CXCR1 antibodies for immunohistochemistry on colonic biopsies as 1/1400 (3.3μg/ml) with the use of FCS as a blocking agent, with high-powered microwave cooking immersed in citrate buffer for 25 minutes as the optimal pre-treatment method.

4.4.4 Immunohistochemical localisation and scoring of CXCR1 on colonic biopsies

Aims: Previous experiments had established the optimum conditions for staining of the CXCR1 chemokine on colonic biopsies. These include high-powered microwave cooking in citrate buffer for 25 minutes, with an antibody dilution of 1/1400 (0.357μg/ml), with a 5% FCS at the initial blocking step, primary antibody solutions, in addition to the secondary and tertiary dilutions. This technique was used on colonic biopsy series from 10 patients, obtained during colonoscopic examination.

Tissue sections: 3μm paraffin embedded, formalin-fixed colonic biopsy tissue sections used from the 10 patients: a total of 18 biopsies from 3 patients with UC, 18 biopsies from 3 patients with CD, 18 biopsies from 4 patients with no disease (control). Sections were used from control patients 2, 6, 7, 13; from UC patients 14, 15, 16; and from CD 8, 11, 26. In addition, 2 negative controls were included. Patient details are outlined in appendix table 2.3.

Immunohistochemical technique: The optimal pre-treatment method of high-powered microwave cooking was used. Blockade of endogenous peroxide activity was achieved by incubation in a 5% FCS. Sections were incubated overnight (18 hours approximately) at +4 °C in the primary anti-CCR6 antibody, in a humidity chamber at a dilution of 1/1400 (0.357μg/ml).

Scoring: A semi-quantitative score from 0 (none) to 4 (dense confluent staining) was determined for epithelium, and percentage immunoreactive lamina propria cells determined. The scoring was performed under blind conditions, whereby the slide identity was concealed, and all the slides were allocated a number randomly. Unblinding only took place when all the scoring was complete. In some slides, the blood vessels could not be identified clearly, so this score was omitted where necessary. The immunohistochemical scores are detailed in table 4.8. Once scoring reliability had been ensured statistically, the original scores were correlated with both microarray data and histopathology inflammation scores. For each biopsy, a corresponding biopsy from the same area had been assessed by a consultant histopathologist, and scored on the basis of inflammation as detailed in appendix table 1.

Table 4.8: CXCR1 immunohistochemistry semi-quantitative assessment scores for the colonic biopsy series, with histopathological inflammatory scores, CXCR1 gene array expression levels and CXCL1 taqman real-time quantitative RT-PCR values.

Patient number	Biopsy number	Lamina propria	Surface epithelium	Crypt epithelium	Endothelium	A+C	RT- PCR taqman data	CXCL1 array data
8 (CD)	1	3.5	2	2.5	3	2	1.06473	12.8749
8 (CD)	2	2	2	2	X	2	0.953326	8.745721
8 (CD)	3	4	4	4	3.5	0	0.832874	22.52686
8 (CD)	4	3	2.5	3	3	0	0.47482	23.17299
8 (CD)	5	2	1	1	X	X	0.341853	21.8538
11 (CD)	5	3.5	3	3	3	4	43.40723	71.54096
11 (CD)	2	3	3.5	3	3	3	7.81508	60.80482
11 (CD)	4	3.5	4	4	X	3	22.03855	44.77158
11 (CD)	3	3	3	3	3	2	5.619342	17.9911
11 (CD)	1	4	3	3	3	1	40.56923	13.86936
11 (CD)	6	2	4	3	3	1	3.265394	26.0775
26 (CD)	1	3	3	2	3	2	3.090364	9.309776
26 (CD)	4	4	3	4	4	2	2.55489	-0.763714
26 (CD)	2	2	1	1	X	0	1.548028	3.625055
26 (CD)	3	2.5	4	2	2	0	2.149553	-23.64567
26 (CD)	5	4	4	4	3.5	0	1.958634	0.919665
26 (CD)	6	2.5	4	4	2.5	0	1.101944	4.110564
14 (UC)	2	3	3.5	3.5	3	4	28.07241	15.75156
14 (UC)	4	3	3	3	3	4	39.08003	36.13151
14 (UC)	5	2.5	2.5	2	3	4	43.41444	27.23739
14 (UC)	6	3	3	2	3	4	80.5151	61.13659
14 (UC)	3	3.5	2	2.5	3	4	X	43.83194
15 (UC)	3	3	2	3	3	X	26.68166	-4.0283
15 (UC)	1	4	3	3.5	X	0	2.893119	-1.472942
15 (UC)	2	2.5	3	3	3	0	14.45353	3.711542
15 (UC)	4	3	3	3	3	0	4.461921	-0.201736
15 (UC)	5	4	4	4	3.5	0	2.296038	1.071995
15 (UC)	6	3	3.5	4	3	0	6.486833	42.37537
16 (UC)	1	3	3	3	3	3	130.9626	70.89221
16 (UC)	2	3	X	3	3	4	86.92375	103.0396
16 (UC)	3	3	2.5	3	3	4	79.47363	90.23378
16 (UC)	4	2	2	2	3.5	3	79.37453	118.6627
16 (UC)	5	3.5	2.5	2	X	5	101.5053	107.9886
16 (UC)	6	3	4	2	3	3	70.84712	105.3239
2 (Cont)	4	X	X	X	X	0	3.611473	-0.621108
2 (Cont)	5	2	2.5	2	3.5	0	3.273393	0.500493
2 (Cont)	6	2.5	2	2	3	0	1.040369	13.92387
6- (Cont)	2	2	3.5	3	3	0	0.566802	-0.098042
6 (Cont)	1	2	2.5	2	3	0	0.389738	7.935384
6 (Cont)	3	2.5	3.5	3.5	3	0	0.646964	1.609613
7 (Cont)	3	2	2.5	2	2	1	0.336266	11.91588
7 (Cont)	4	3	4	4	3	1	0.319501	7.289379
7 (Cont)	5	3.5	2	2	3.5	0	0.235615	0.56133
7 (Cont)	6	2	2	2.5	3	0	0.244664	21.86151
13 (Cont)	1	2	2.5	2	3	0	2.784345	3.945038
13 (Cont)	2	3	2.5	2.5	3	0	9.949971	9.637292
13 (Cont)	3	2.5	2	2	3	0	1.502744	1.419159
13 (Cont)	4	2.5	3	3	X	0	3.00168	8.344731
13 (Cont)	5	3	2	2	3	0	2.427908	7.617582
13 (Cont)	6	2	2	2	2	0	1.77196	9.643832

Statistical Validation of Established Scoring Method

As the scoring was semi-quantitative, it was important to statistically validate the scoring technique consistency and reliability. 11 slides were re-scored for all parameters, blind from the slide identity and the original score. Each value was paired with the initial scoring value. These pairs were incorporated into a student's t-test for paired parametric data. Each of the first scores for 11 slides was paired with the corresponding second scores, as listed in table 4.9. This statistical test is useful for investigating a variable in two groups where there is a meaningful

one-to-one correspondence between the data points in one group and those in the other. The null hypothesis states that there is no significant difference between the 2 groups.

Table 4.9: List of initial and repeat semi-quantitative immunohistochemistry scores for CXCR1, to demonstrate reproducibility of scoring method.

Score number	Score 1 (X_a)	Score 2 (X_b)	$X_a - X_b$
1	3.5	3	0.5
2	3.5	3	0.5
3	3	3	0
4	3	3	0
5	3	3	0
6	3.5	4	-0.5
7	3.5	4	-0.5
8	4	4	0
9	4	4	0
10	3	3	0
11	2	2	0
12	4	4	0
13	3.5	3	0.5
14	4	4	0
15	3	3	0
16	3.5	3.5	0
17	4	4	0
18	3	3	0
19	4	3.5	0.5
20	3	3	0
21	3	4	-1
22	3	3	0
23	3	3	0
24	2	2	0
25	4	4	0
26	4	3.5	0.5
27	3	3	0
28	2	2.5	-0.5
29	3	3	0
30	3	3	0
31	4	4	0
32	4	4	0
33	4	4	0
34	4	4	0
35	3	3	0
36	2.5	2	0.5
37	2.5	3	-0.5
38	2	2	0
39	3	3	0
40	3	3	0
41	2	2	0
42	2.5	2.5	0
43	2	2	0
44	3	3	0
45	3.5	3.5	0
46	3	3	0
47	3.5	3.5	0
48	3	3	0
49	3	3	0
50	4	3.5	0.5
51	3	3	0
52	3	2.5	0.5
53	0.5	0.5	0
54	2	2	1
55	3	3	0

Table 4.10: Values for statistical validation of CXCR1 immunohistochemistry scores

Values	X_a	X_b	$X_a - X_b$
n	54	54	54
Sum	171.5	169.5	2
Mean	3.1759	3.1389	0.037
Sum_sq	564.75	553.25	5
SS	20.0787	21.2083	4.9259
Variance	0.3788	0.4002	0.0929
Standard Deviation	0.6155	0.6326	0.3049

$Mean_A - Mean_B = 0.037$

$t = 0.89$

$df = 53$

Two-tailed $p = 0.376504$

On the basis of this $p>0.05$, the null hypothesis cannot be rejected, i.e. there is no statistical difference between the original and repeat scoring values. The scoring reducibility is therefore not un-acceptable statistically.

Results: Where the primary antibody incubation had been omitted, there was no staining (figure 4.3a). CXCR1 immunoreactivity is seen to be widespread, on a number of cell types, including plasma cells, macrophages, dendritic cells, neutrophils, goblet cells, myofibroblasts. The normal controls showed no epithelial immunoreactivity (figures 4.3b). The $CXCR1^+$ lamina propria cell population was distributed differently to CCL20 and CCR6, with little staining of subepithelial cells in controls, but there was clear staining of small round cells within the deeper lamina propria (figures 4.3b). Both CD and UC specimens showed an upward extension of $CXCR1^+$ cells (figure 4.3c-f). There was strong vascular endothelial staining.

Non-parametric correlation analyses between CXCR1 immunohistochemical scores and corresponding RT-PCR values indicated no association. Spearman's correlation coefficients were as follows: 0.30 (p=0.034) for lamina propria, 0.14 (p=0.36) for surface epithelium, 0.067 (p=65) for crypt epithelium and 0.035 (p=0.83) for vascular endothelium.

Figure 4.3a, b: Colonic immunohistochemical staining of $CXCR1^+$ cells using the immunoperoxidase technique. Original magnification x10 (a), x40 (b). A negative control is demonstrated in (a). Control tissue staining is demonstrated in (b).

a

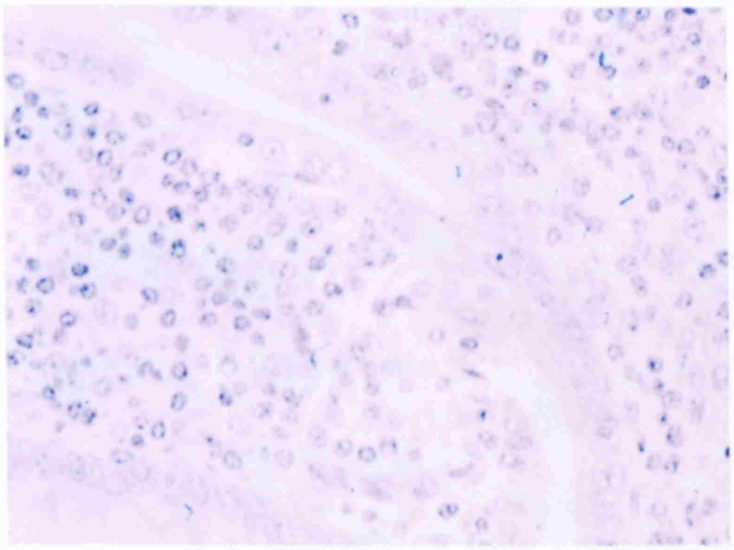

b

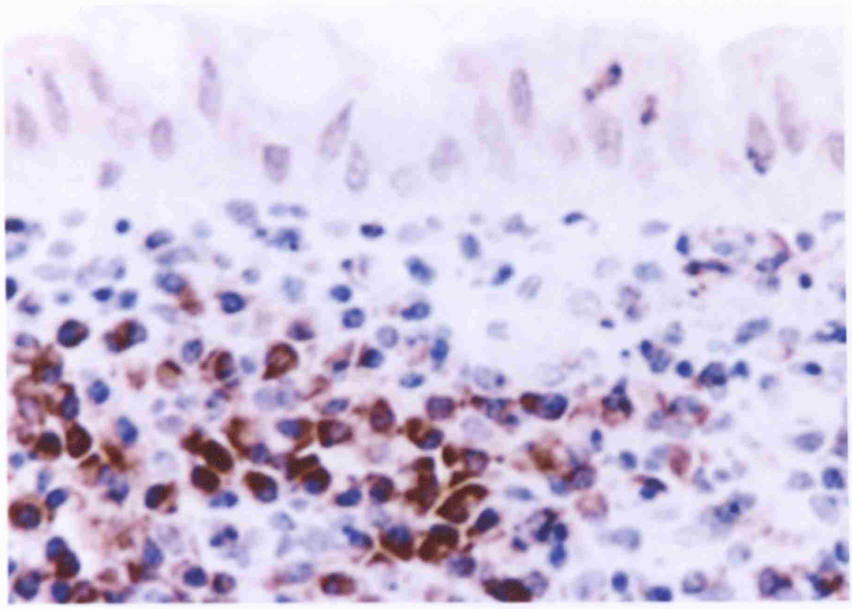

Figure 4.3c, d: Colonic immunohistochemical staining of $CXCR1^+$ cells in UC, using the immunoperoxidase technique, original magnification x40.

c

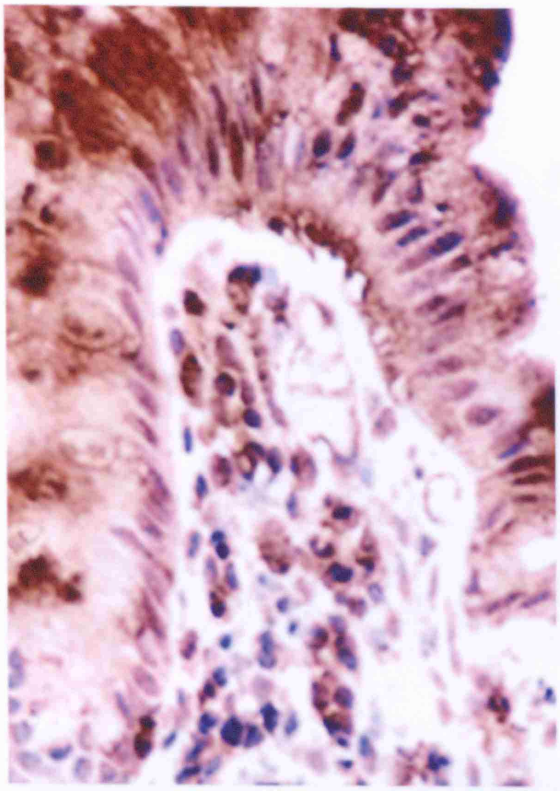

d

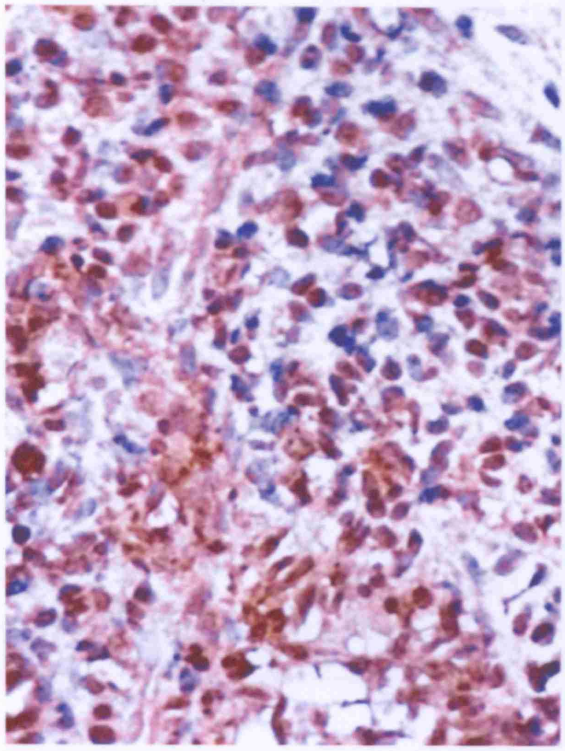

Figure 4.3e, f: Colonic immunohistochemical staining of $CXCR1^+$ cells in CD, using the immunoperoxidase technique. Original magnification x40.

e

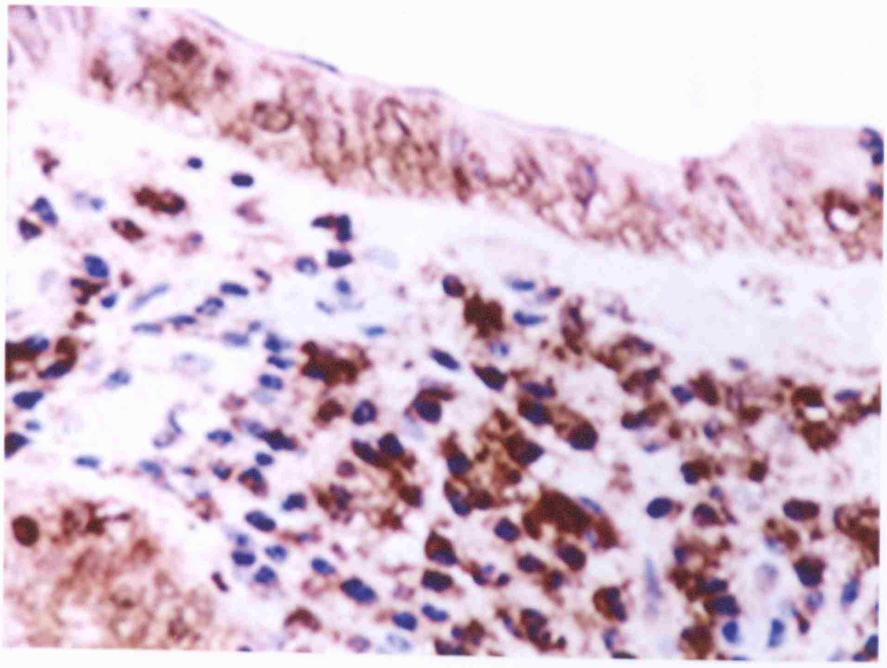

f

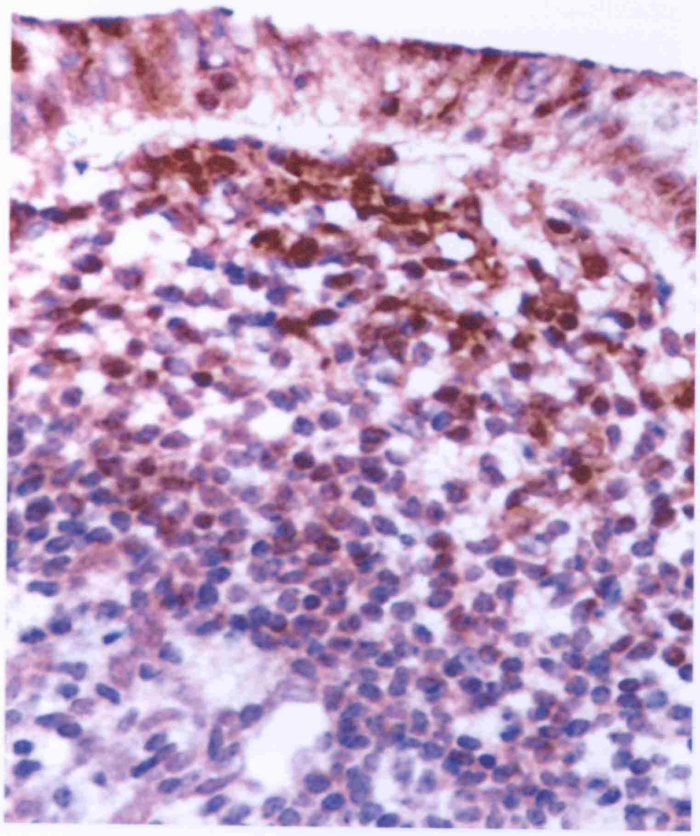

Graph 4.13: Colonic biopsy CXCR1 immunohistochemical scores of surface epithelial correlated with corresponding histopathological inflammatory scores

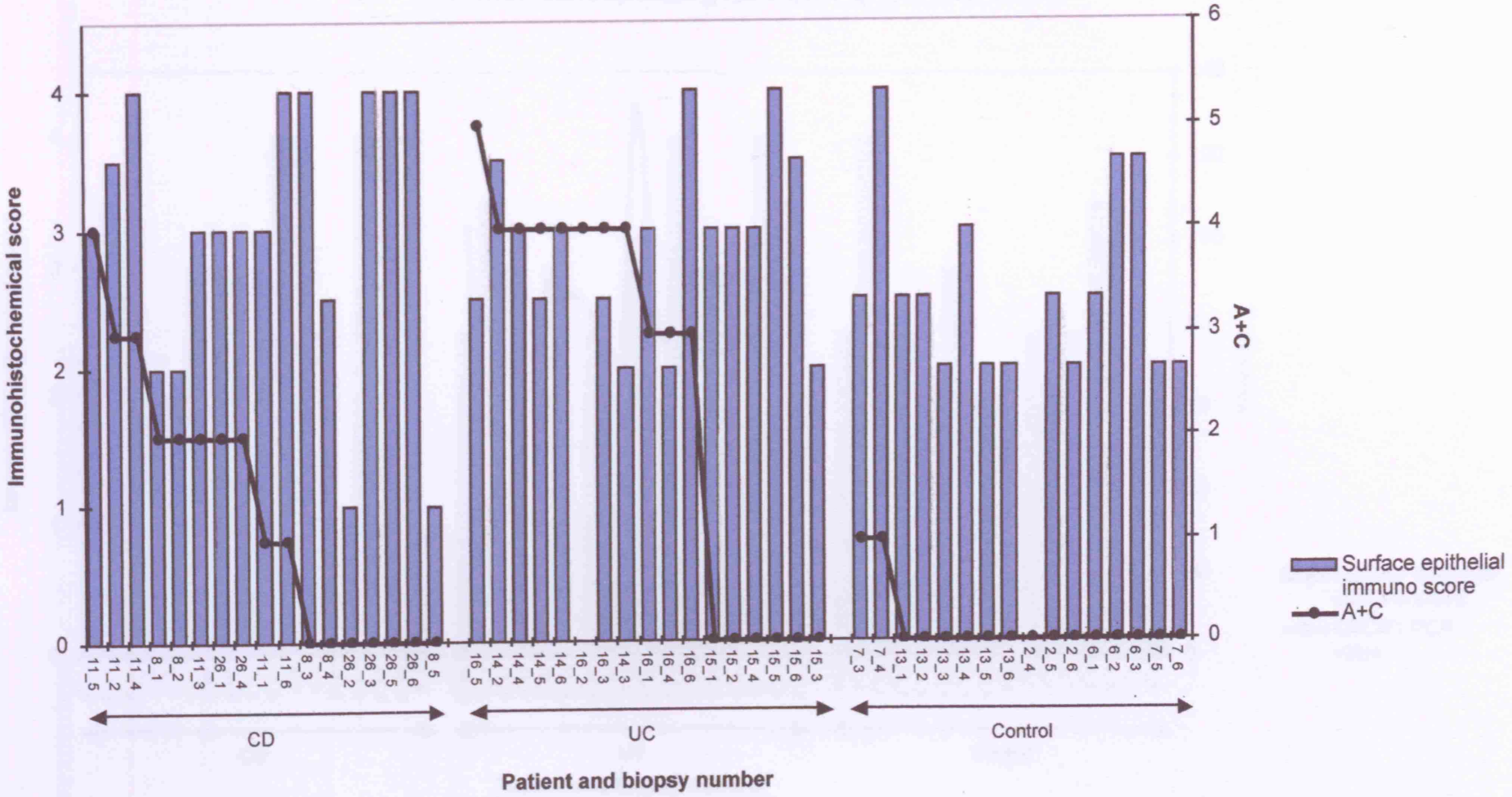

Patients are grouped according to disease, and chronolically placed according to inflammatory scores A+C. Patient and sample details are outlined in appendix table 2.3, and immunohistochemical scores in table 4.8.

Graph 4.14: Colonic biopsy CXCR1 immunohistochemical scores of surface epithelium correlated with corresponding RT-PCR taqman values

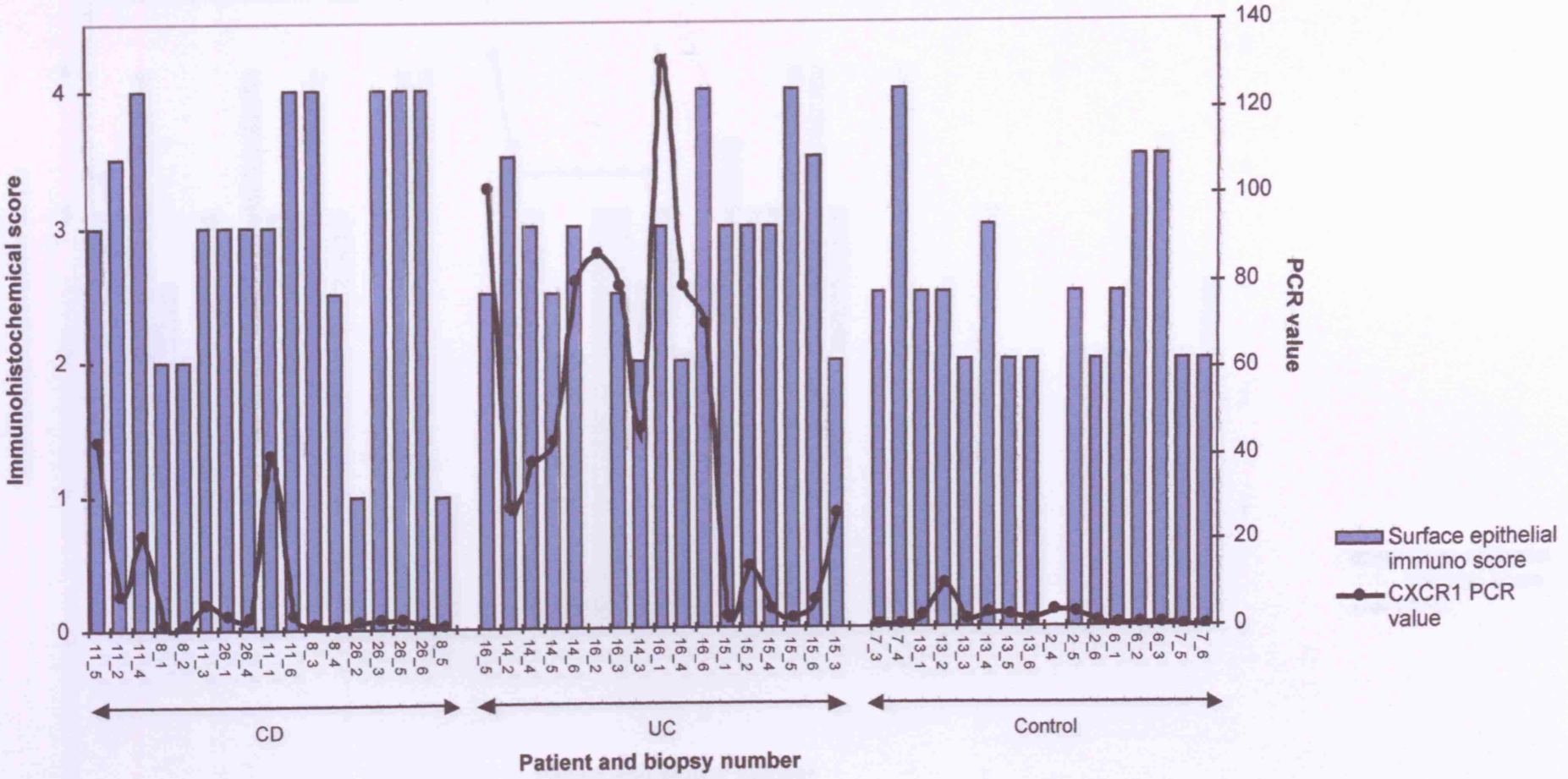

Patients are grouped according to disease. Patient and sample details are outlined in appendix table 2.3. Immunohistochemical scores are listed in table 4.8 and RT-PCR values in table 3.8.

Graph 4.15: Colonic biopsy CXCR1 immunohistochemical scores of crypt epithelium correlated with coresponding histopathological inflammatory scores

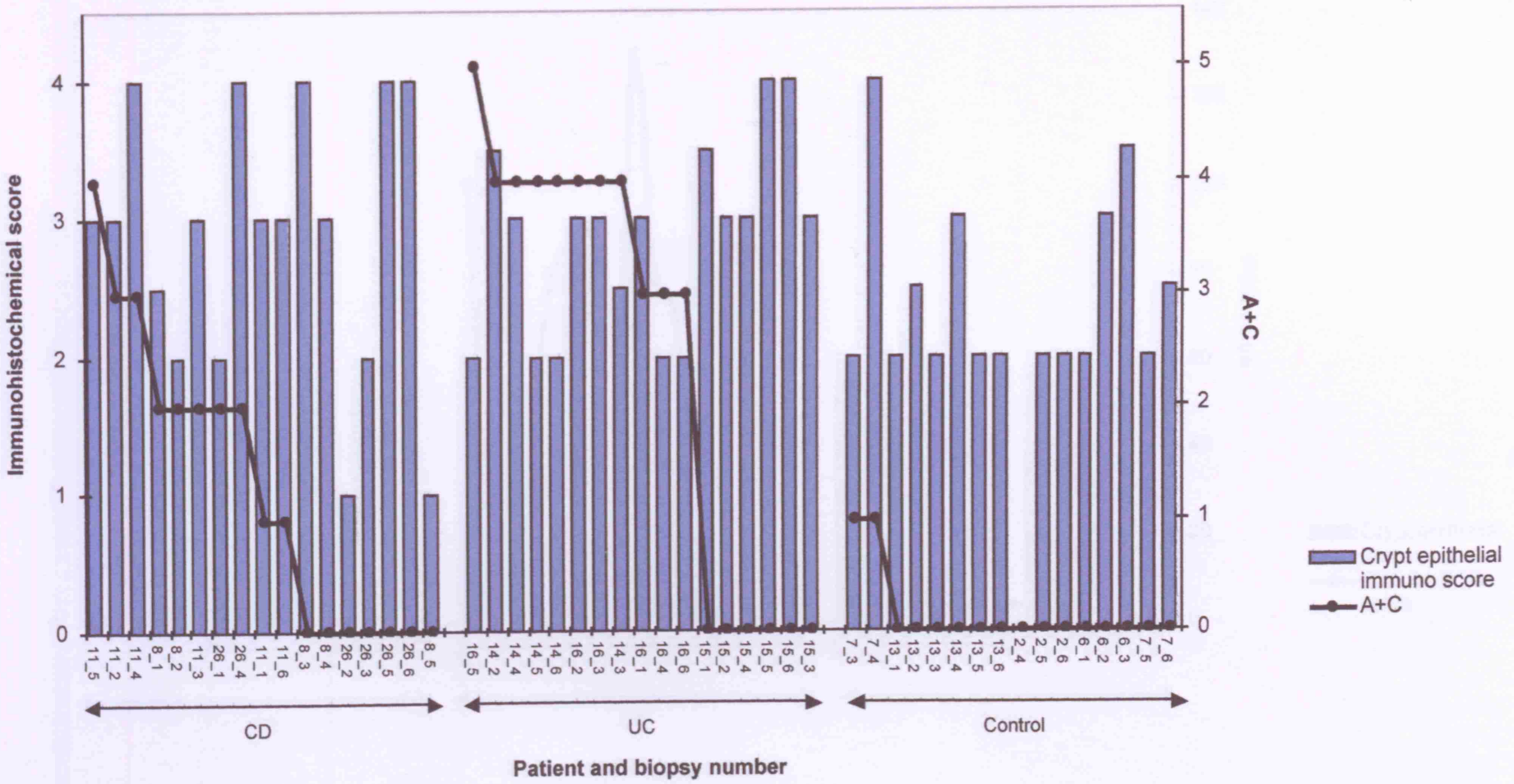

Patients are grouped according to disease. Patient and sample details are outlined in appendix table 2.3. Immunohistochemical scores are listed in table 4.8, and RT-PCR values in table 3.8.

Graph 4.16: Colonic biopsy CXCR1 immunohistochemical scores of crypt epithelium correlated with corresponding RT- PCR taqman values

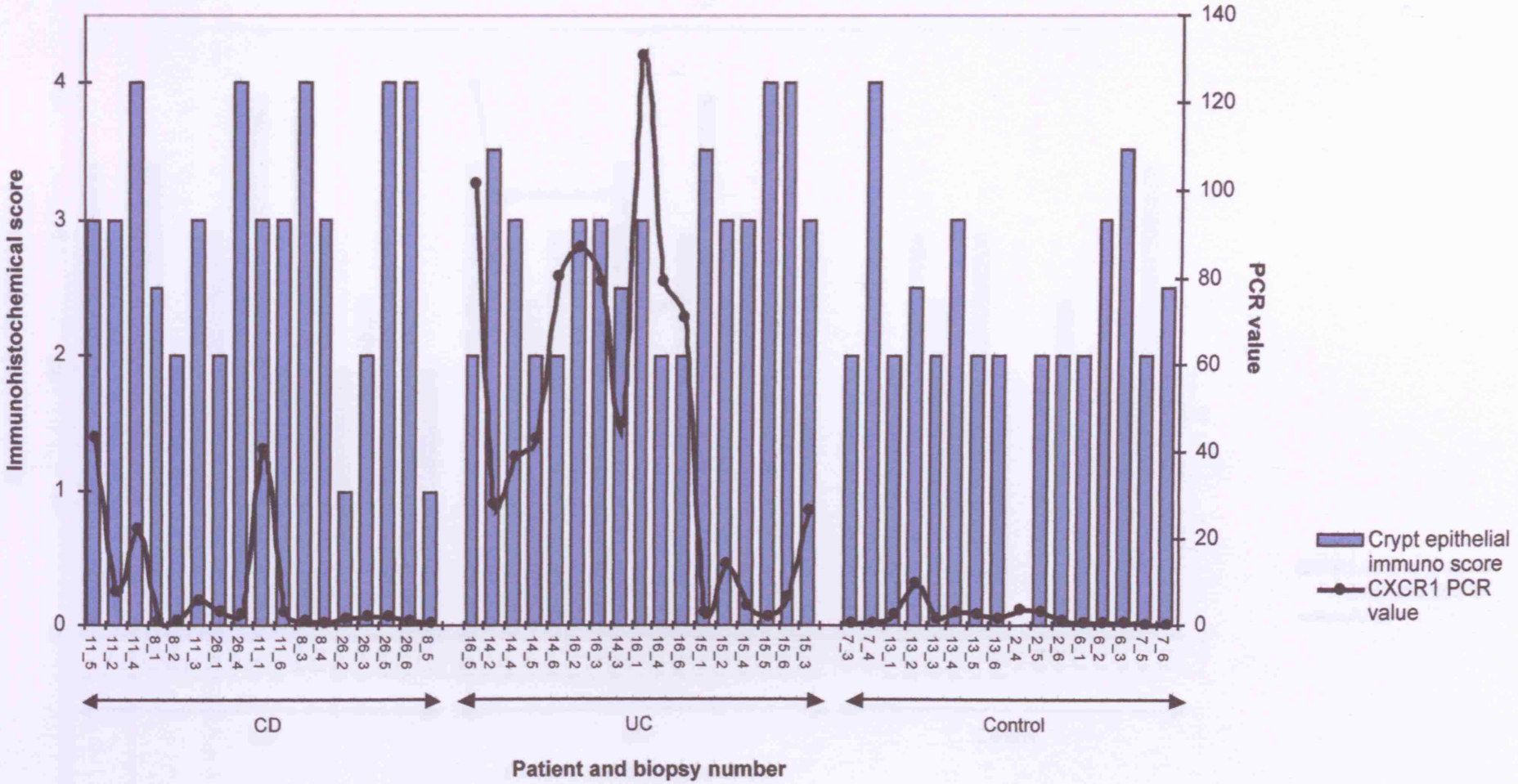

Patients are grouped according to disease, and chronologically placed according to inflammatory scores A+C. Patient and sample details are outlined in appendix table 2.3, and immunohistochemical scores in table 4.8.

Graph 4.17: Colonic biopsy CXCR1 immunohistochemical scores of lamina propria correlated with corresponding histopathological inflammatory scores

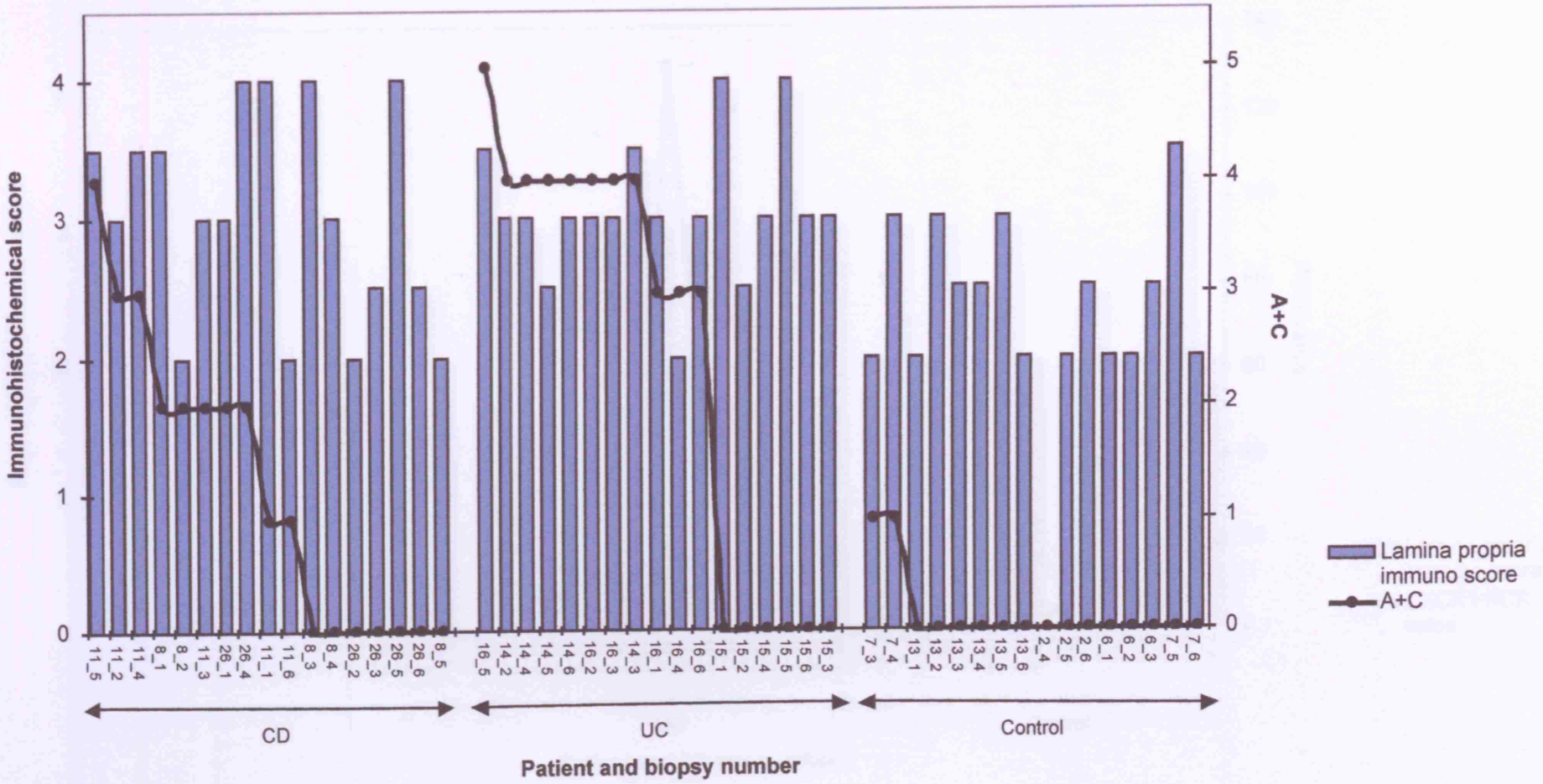

Patients are grouped according to disease and chronologically placed according to inflammatory scores A+C. Patient and sample details are outlined in appendix table 2.3, and immunohistochemical scores in table 4.8.

Graph 4.18: Colonic biopsy CXCR1 immunohistochemical scores of lamina propria correlated with correponding RT-PCR taqman values

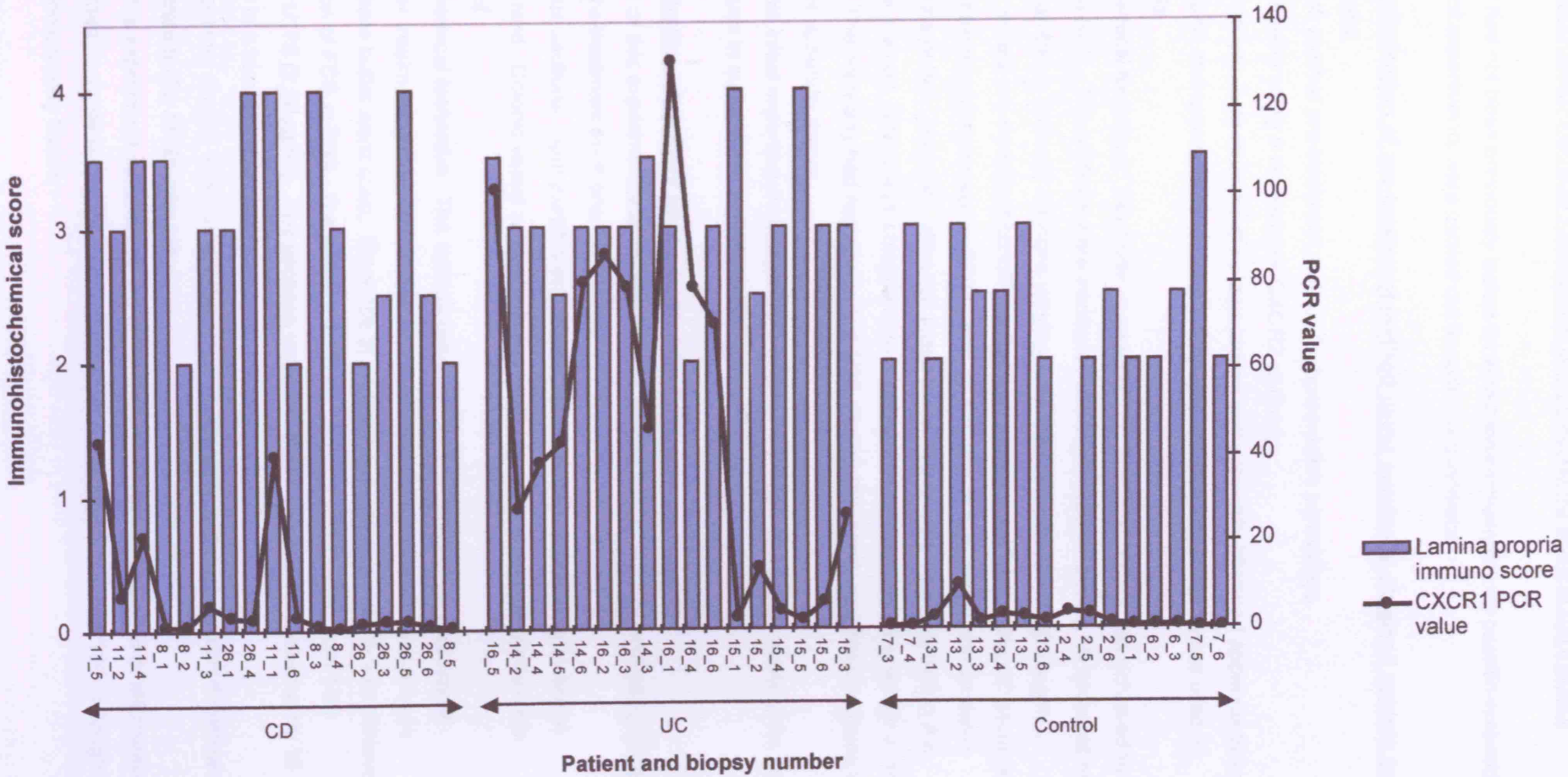

Patients are grouped according to disease. Patient and sample details are outlined in appendix table 2.3. Immunohistochemical scores are listed in table 4.8, and RT-PCR values in table 3.8.

4.5 Immunohistochemical localisation of CXCR2 using immunoperoxidase technique

As this antibody had not been previously tested for immunohistochemistry on paraffin-embedded tissue, a series of experiments were carried out to optimise conditions.

4.5.1 Optimisation of pre-treatment method using surgically-obtained colonic and appendix sections

Aim: To establish optimal pre-treatment method for horseradish peroxidase immunohistochemistry using a monoclonal CXCR2 antibody.

Preparation of section: 3μm sections of colonic biopsy and surgically-obtained appendix tissue were used. Colonic and appendix tissue without primary antibody application were used as negative controls.

Immunohistochemical technique: Blockade of endogenous peroxide activity was achieved by incubation in 1% NHS. The sections were incubated overnight (approximately 18 hours) at +4°C in a humidity chamber in antibody dilutions varying from 1/50 (10μg/ml) to 1/100 (5μg/ml).

Results: There were 2 pre-treatment conditions that led to higher quality staining; 90 seconds of pressure cooker treatment immersed in EDTA, and 25 minutes of high powered-microwave treatment in citrate buffer. However, although these 2 conditions were definably better, the slides were over stained. There was considerable background staining, including on the control negative slide. The company had recommended 1/25 dilution (20μg/ml), and this was found to be too strong for appendix tissue.

Conclusion: This initial experiment established 2 optimal pre-treatment preparations of the link conjugates for use in subsequent experiments.

4.5.2 Titration of primary antibody on colonic biopsy sections

Aims: The aim of this experiment was to optimise the dilution of CXCR2 link antibodies using the 2 optimal pre-treatment methods.

Methods: Tissue sections: 3μm paraffin-embedded, formalin-fixed colonic biopsy tissue sections were used. Colonic tissue without primary antibody application was used as the negative control.

Immunohistochemical technique: The optimal pre-treatment methods of 90 seconds of pressure cooker treatment immersed in EDTA or 25 minutes of high-powered microwave treatment in citrate buffer were used. Blockade of endogenous peroxide activity was achieved by a 5% solution of FCS in TBS. The primary antibody dilutions used varied from 1/80 (6.25μg/ml) to 1/175 (2.86μg/ml). The sections were incubated overnight (approximately 18 hours) at +4°C in a humidity chamber.

Results: The optimal dilution was found to be 1/150 (0.36μg/ml), with high-powered microwave treatment in citrate buffer for 25 minutes.

Conclusion: This experiment established the optimal pre-treatment preparation of microwave cooking immersed in citrate buffer for 25 minutes, with an optimal dilution of 1/150 (3.33μg/ml) CXCR2 for colonic biopsy tissue.

4.5.3 Immunohistochemical localisation and scoring of CXCR2 on colonic biopsies

Aims: Previous experiments had established the optimum conditions for staining of the CXCR2 chemokine receptor on colonic biopsies. These include high-powered microwave cooking in citrate buffer for 25 minutes, with an antibody dilution of 1/150, with a 5% FCS at the initial blocking step, primary antibody solutions, in addition to the secondary and tertiary dilutions. This technique was used on colonic biopsy series from 10 patients, obtained during colonscopic examination.

Tissue sections: 3μm paraffin embedded, formalin-fixed colonic biopsy tissue sections used from the 10 patients: a total of 18 biopsies from 3 patients with UC, 18 biopsies from 3 patients with CD, 18 biopsies from 4 patients with no disease (control). In addition, 2 negative controls were included. The subset was chosen on the basis of the previous microarray data. Sections were used from control patients 2, 6, 7,13; from UC patients 14, 15, 16; and from CD patients 8, 11, 26. Patient details are outlined in appendix table 2.3.

Immunohistochemical technique: The optimal pre-treatment method of high-powered microwave cooking was used. Blockade of endogenous peroxide activity was achieved by incubation in a 5% FCS. Sections were incubated overnight (18 hours approximately) at +4 °C in the primary anti-CXCR2 antibody, in a humidity chamber, at a dilution of 1/150 (3.33μg/ml).

Scoring: A semi-quantitative score from 0 (none) to 4 (dense confluent staining) was determined for epithelium, and percentage immunoreactive lamina propria cells determined. The scoring was performed under blind conditions, whereby the slide identity was concealed, and all the slides were allocated a number randomly. Unblinding only took place when all the scoring was complete. In some slides, the blood vessels could not be identified clearly, so this score was omitted where necessary. The scores are listed in table 4.11.

Table 4.11: CXCR2 immunohistochemistry semi-quantitative assessment scores for the colonic biopsy series, with histopathological inflammatory scores, CXCR2 gene expression levels and CXCR2 TaqMan real-time quantitative RT-PCR values.

Patient number	Biopsy number	Lamina propria scores	Surface epithelial scores	Crypt epithelial scores	Vascular endothelium	Histopathology scores A+C	RT- PCR values	CXCL2 array data
8 (CD)	1	X	3	2	3	2	0.885285	0.846998
8 (CD)	2	4	1	1	3	2	0.781561	2.904937
8 (CD)	3	3	3	2	3	0	1.085761	3.360362
8 (CD)	4	3	3	2	3	0	0.298653	9.685717
8 (CD)	5	2	2	1	2	X	0.258249	5.894358
11 (CD)	5	3	3	3	3	4	24.44986	42.85161
11 (CD)	2	1	1	1	2	3	4.605901	39.65675
11 (CD)	4	X	X	X	X	3	10.53489	25.4855
11 (CD)	3	3	3	3	3	2	4.205781	0.232571
11 (CD)	1	3	1	1	2.5	1	35.6795	14.77413
11 (CD)	6	3	4	3	4	1	0.757672	-0.80196
26 (CD)	1	3	1	1	3	2	2.148863	-1.63881
26 (CD)	4	4	3.5	3.5	3.5	2	3.121054	-4.92316
26 (CD)	2	3	3	2	X	0	2.664798	1.513861
26 (CD)	3	4	3	3	2.5	0	1.283612	2.044539
26 (CD)	5	4	4	4	4	0	1.962163	-1.29762
26 (CD)	6	3	2	2.5	3	0	1.561064	-2.01602
14 (UC)	2	3	3	3	3	4	29.96129	14.81894
14 (UC)	4	3.5	3	3	2.5	4	22.90739	27.10058
14 (UC)	5	3.5	3.5	2	3	4	23.06857	25.30382
14 (UC)	6	4	1	1	X	4	47.86656	27.57841
14 (UC)	3	4	4	4	X	4	25.72771	28.6012
15 (UC)	3	4	4	4	4	1	21.50884	0.372091
15 (UC)	1	4	3.5	3.5	3	0	2.068177	0.052245
15 (UC)	2	3	3	2	3	0	7.349962	-0.044
15 (UC)	4	3	4	2.5	3	0	0.846214	7.229328
15 (UC)	5	2.5	2.5	2	X	0	2.927088	2.294234
15 (UC)	6	4	4	4	3.5	0	5.418718	43.21405
16 (UC)	2	3	2	1	3	4	81.87736	65.9267
16 (UC)	3	3	2	1	3	4	101.6616	71.00955
16 (UC)	1	3	1	1	X	3	73.5524	64.3215
16 (UC)	4	3	2.5	1	3	3	85.7694	97.331
16 (UC)	5	2.5	2.5	2	3	5	92.60424	88.80252
16 (UC)	6	3	1	1	3	3	74.64788	72.42212
2 (Cont)	4	2	1	1	2	0	3.527501	7.562334
2 (Cont)	5	2	3	2	2.5	0	3.327847	11.41498
2 (Cont)	6	X	2	2	2.5	0	0.730619	-3.73882
6 (Cont)	1	2	2.5	2.5	3	0	0.288146	0.233335
6 (Cont)	2	2	4	2	3	0	0.217637	0.932586
6 (Cont)	3	2	3	1	2	0	0.811372	1.107795
7 (Cont)	3	2	3	3	4	1	0.368528	5.84179
7 (Cont)	4	3	4	2	3	1	0.515986	4.190136
7 (Cont)	5	3	2	1	3	0	0.226369	25.97125
7 (Cont)	6	X	3	2	3	0	0.512955	29.98309
13 (Cont)	1	2.5	2.5	2.5	X	0	3.406032	1.983139
13 (Cont)	2	2	2.5	1	3	0	4.138684	2.130209
13 (Cont)	3	2	2	2	2	0	1.655632	-0.80715
13 (Cont)	4	2	3	1	X	0	3.373664	11.57205
13 (Cont)	5	3	3	3	3	0	1.854911	6.060763
13 (Cont)	6	3	3	2	3	0	3.061608	3.03505

Statistical validation: As the scoring was semi-quantitative, it was important to statistically validate the scoring technique consistency and reliability. 11 slides were re-scored for all parameters, blind from the slide identity and the original score. Each value was paired with the initial scoring value. These pairs were incorporated into a student's t-test for paired parametric data. Each of the first scores for 11 slides was paired with the corresponding second scores, as listed in table 4.12. This statistical test is useful for investigating a variable in two groups where there is a meaningful one-to-one correspondence between the data points in one group and

those in the other. The null hypothesis states that there is no significant difference between the 2 groups.

Table 4.12: List of initial and repeat semi-quantitative immunohistochemistry scores for CXCR2, to demonstrate reproducibility of scoring method.

Score number	Score 1 (X_a)	Score 2 (X_b)	$X_a - X_b$
1	3	3	0
2	2	2.5	-0.5
3	2.5	2.5	0
4	2.5	2	0.5
5	3	3	0
6	4	4	0
7	3	3	0
8	3	3	0
9	3	3	0
10	3	3	0
11	2	2	0
12	2	2	0
13	1	1	0
14	1	1	0
15	2	2	0
16	3	3	0
17	3	3	0
18	1	1	0
19	1	1	0
20	2.5	2	0.5
21	3	3	0
22	3	3	0
23	3	3	0
24	2	2.5	-0.5
25	3	3	0
26	2.5	2	0.5
27	2	2	0
28	2	1.5	0.5
29	1	1	0
30	2	2	0
31	3	3	0
32	2	3	-1
33	3	3.5	-0.5
34	1	1.5	-0.5
35	2	2	0
36	3	3	0
37	3	3	0
38	2	2	0
39	1	1	0
40	3	3	0
41	2	2	0
42	2.5	2.5	0
43	1	1	0
44	3	3	0
45	3	3	0
46	3	3	0
47	3	3	0
48	3	3	0
49	2	2.5	-0.5
50	2.5	3	-0.5
51	3	3	0
52	4	4	0
53	4	4	0
54	4	4	0
55	3	3	0
56	3	3	0

Table 4.13: Statistical validation table of CXCR2 semi-quantitative immunohistochemistry scores.

Values	X_a	X_b	$X_a - X_b$
n	56	56	56
Sum	140	142	-2
Mean	2.5	2.5357	-0.0357
Sum_sq	386.5	397	3.5
SS	36.5	36.9286	3.4286
Variance	0.6636	0.6714	0.0623
Standard Deviation	0.8146	0.8194	0.2497

$Mean_A - Mean_B = -0.0357$

$t = -1.07$

$df = 55$

Two-tailed $p = 0.1446445$

On the basis of this $p>0.05$, the null hypothesis cannot be rejected, i.e. that there is no statistical difference between the original and repeat scoring values. The scoring reducibility is therefore not unacceptable statistically.

Results: Where the primary antibody incubation had been omitted, there was no staining (figure 4.4a). The density of $CXCR2^+$ cells were higher, with >75% of cells $CXCR2^+$ in 2/17 controls, 10/17 UC and 10/15 CD specimens. Patchy immunoreactivity is seen on surface epithelium in all groups, with no overall increase in IBD (figures 4.4b-d, g, i). The lamina propria infiltrate is denser in both CD and UC specimens, with most cells $CXCR2^+$ in the upper lamina propria (4.4c, d, g). Purulent exudate is almost totally $CXCR2^+$(figure 4.4f).

Non-parametric correlation analyses between CXCR2 immunohistochemical scores and corresponding RT-PCR values indicated no association. Spearman's correlation coefficients were as follows: 0.19 (p=0.20) for lamina propria, -0.22 (p=0.13) for surface epithelium, -0.11 (p=0.44) for crypt epithelium and 0.01 (p=0.95) for vascular endothelium.

Figure 4.4a-b: Colonic immunohistochemical staining of $CXCR2^+$ cells in a control sections, using the immunoperoxidase technique, original magnification x10 (a) x40 (b). A negative control is demonstrated in (a).

a

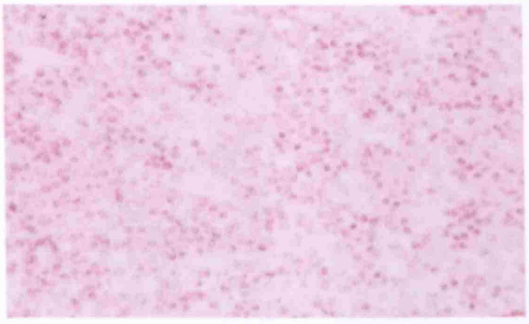

b

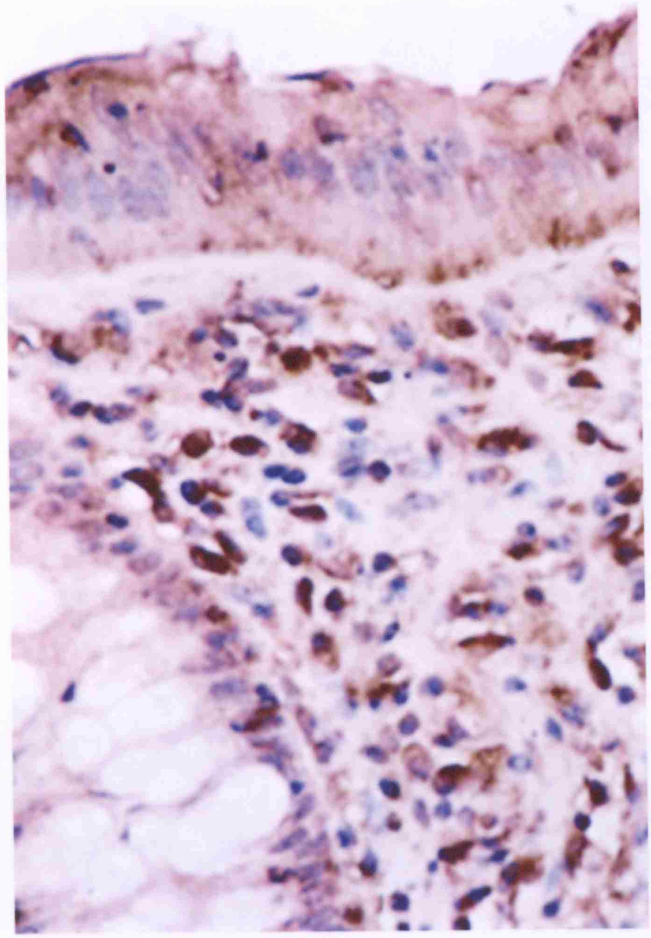

Figure 4.4c-h: Colonic immunohistochemical staining of $CXCR2^+$ cells in UC, using the immunoperoxidase technique, original magnification x40 (c)-(e), (g), (h), x10 (f). A thombosed vessel is demonstrated in (g).

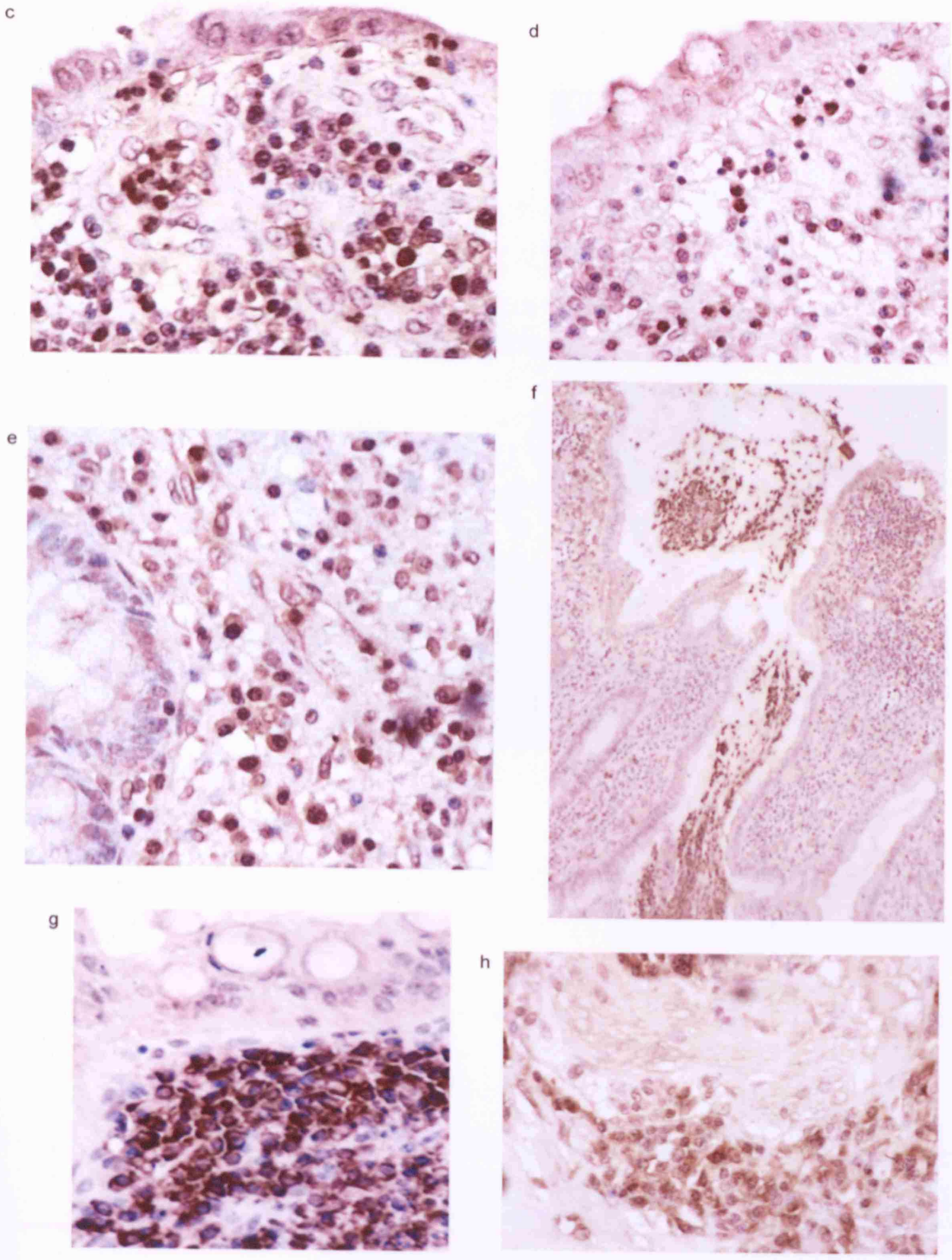

Figure 4.4i: Colonic immunohistochemical staining of CXCR2 in CD, using the immunoperoxidase technique, original magnification x40.

i

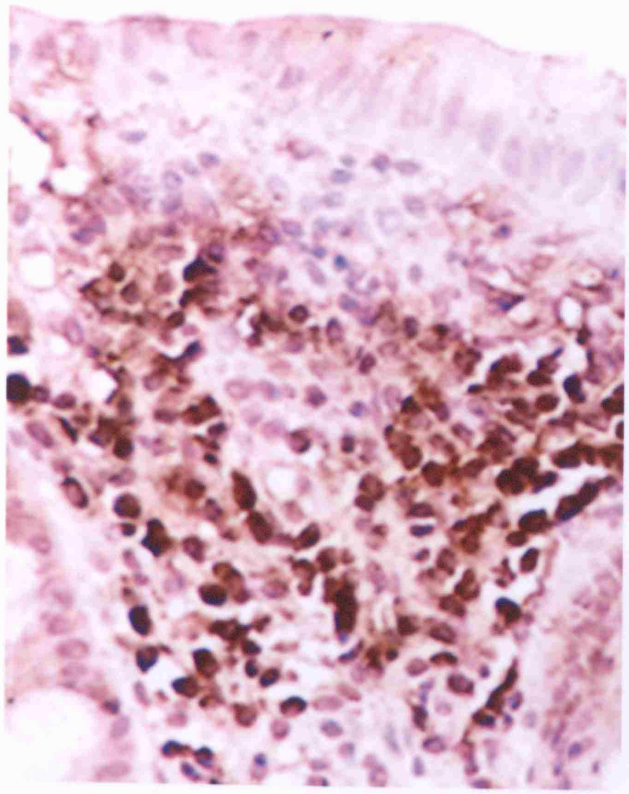

Graph 4.19: Colonic biopsy CXCR2 immunohistochemical scores of surface epithelium correlated with corresponding histopathological inflammatory scores

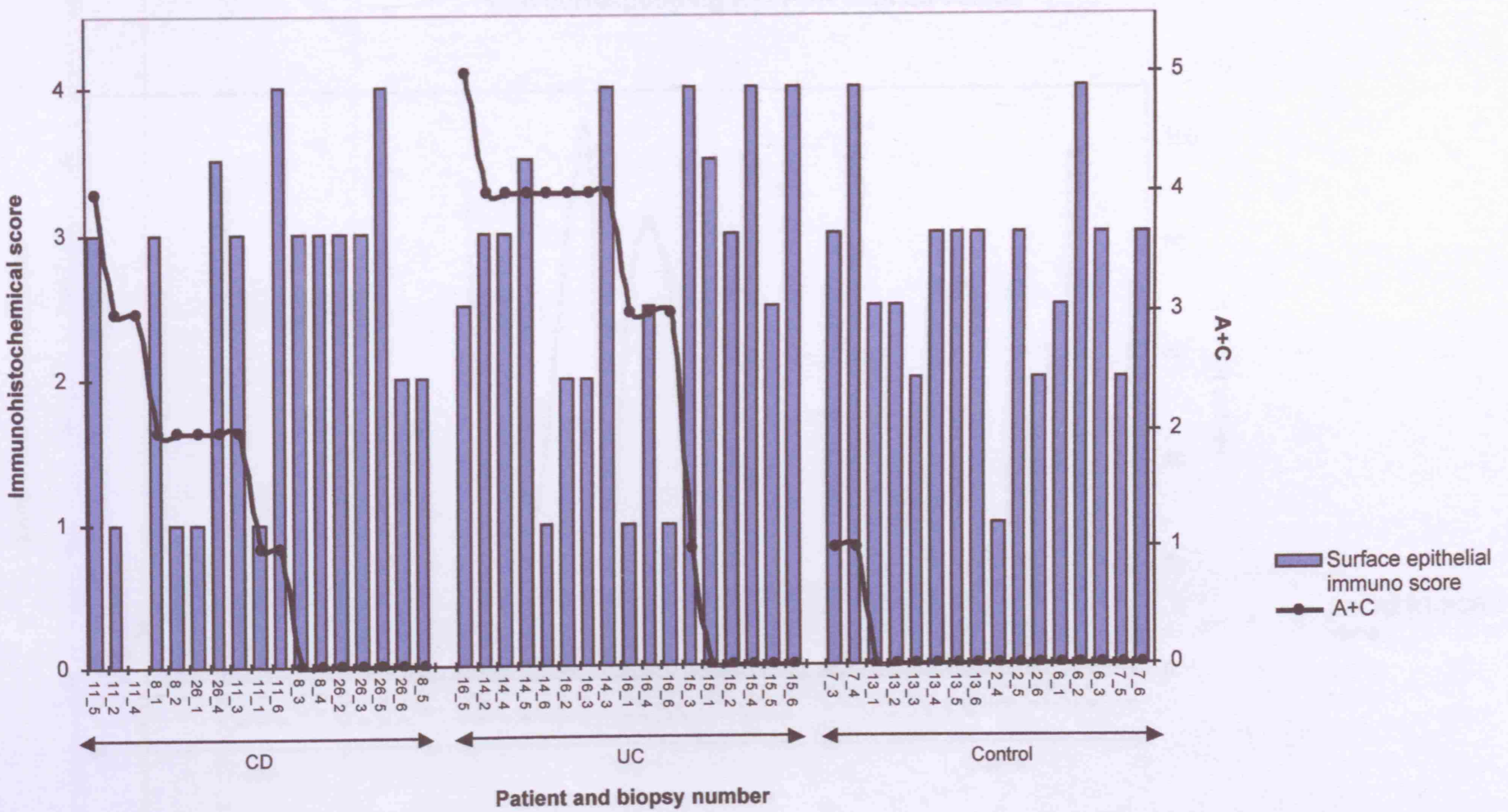

Patients are grouped according to disease, and chronologically placed according to inflammatory scores A+C. Patient and sample details are outlined in appendix table 2.3, and immunohistochemical scores in table 4.11.

Graph 4.20: Colonic biopsy CXCR2 immunohistochemical scores of surface epithelium correlated with corresponding RT- PCR taqman values

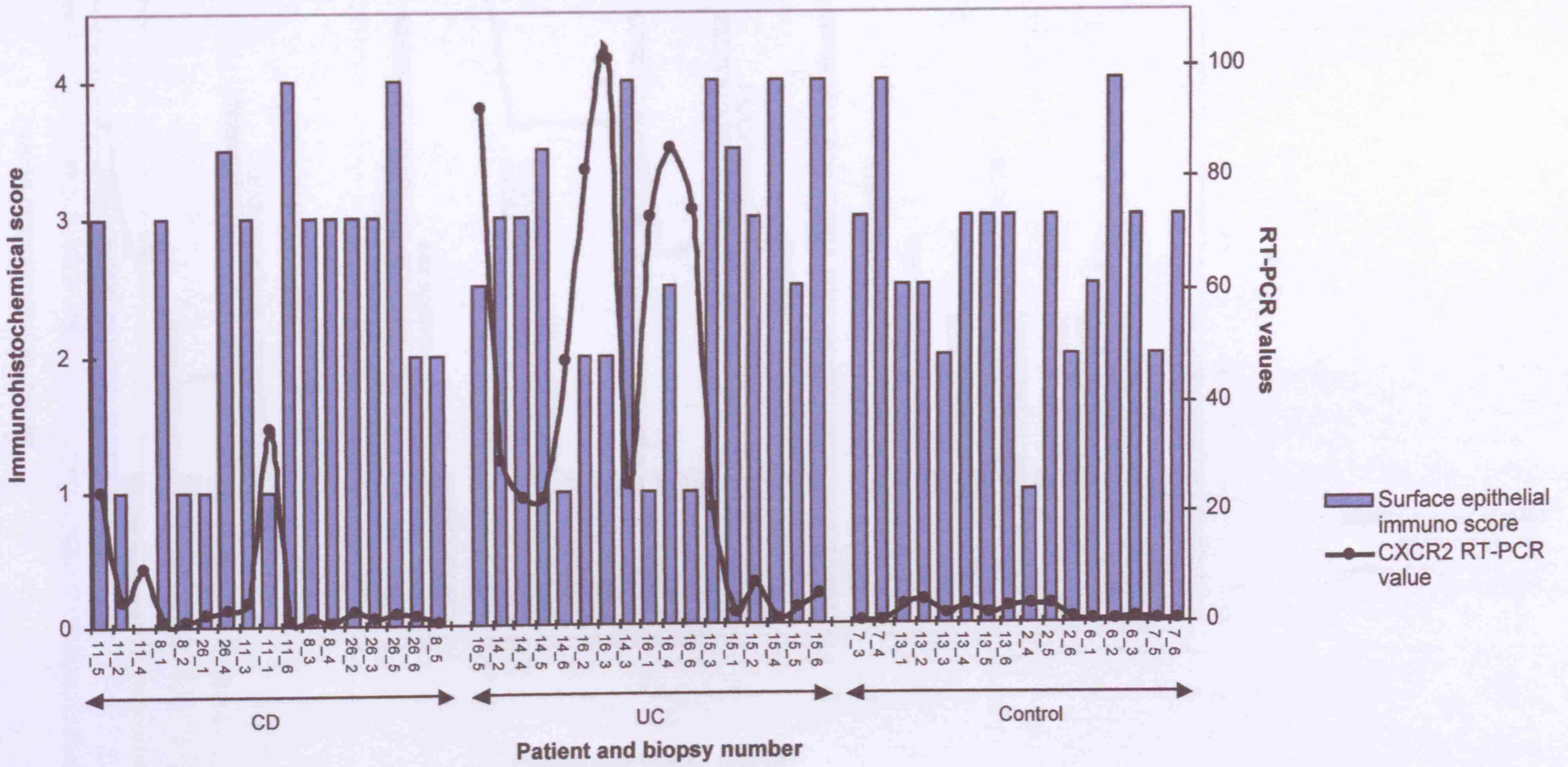

Patients are grouped according to disease. Patient and sample details are outlined in table 2.3. Immunohistochemical scores are listed in table 4.11, and RT-PCR values in table 3.6.

Graph 4.21: Colonic biopsy CXCR2 immunohistochemistry scores of crypt epithelium correlated with corresponding histopathological inflammatory scores

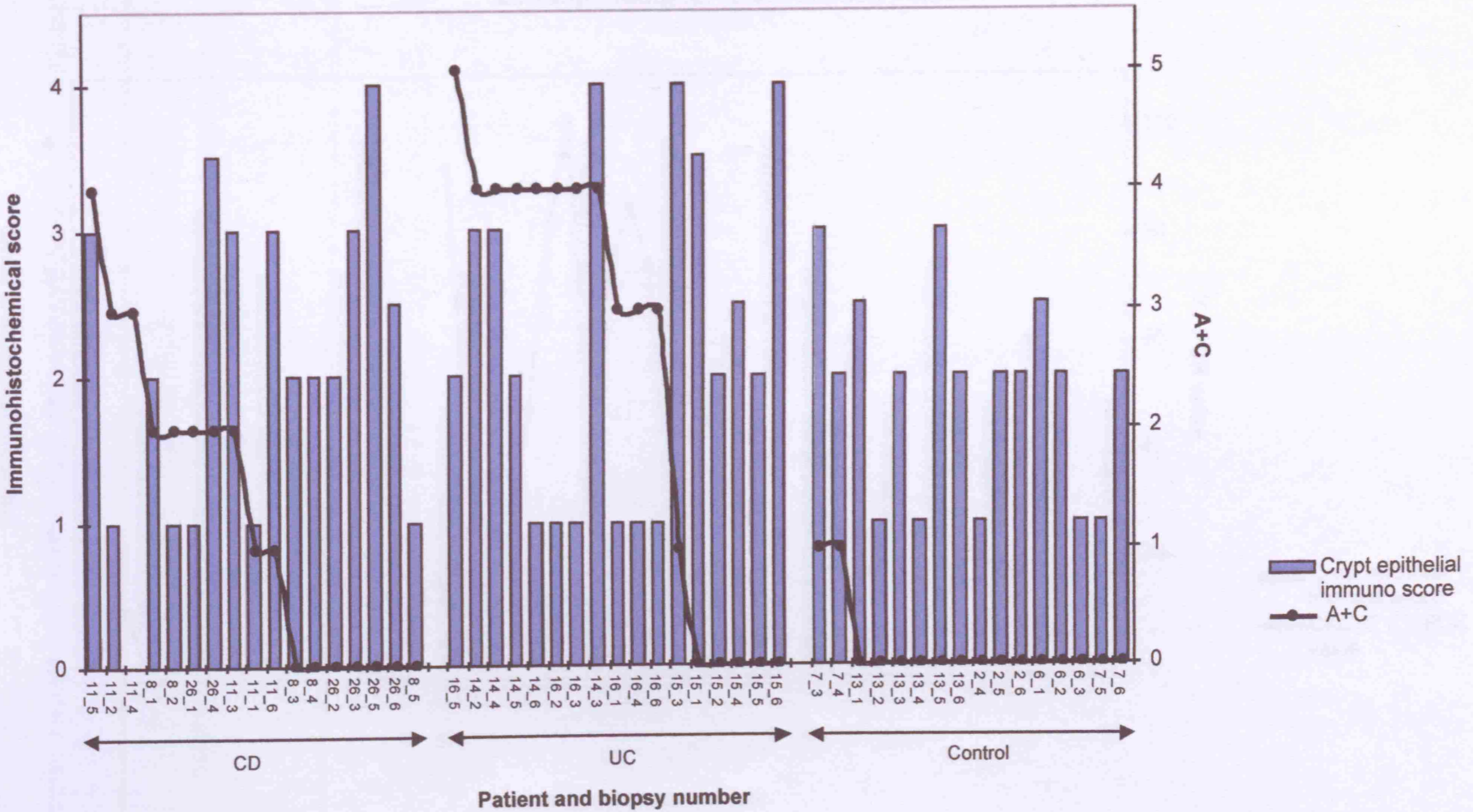

Patients are grouped according to disease and chronologically placed according to inflammatory scores A+C. Patient and sample details are outlined in appendix table 2.3, and immunohistochemical scores in table 4.11.

Graph 4.22: Colonic biopsy CXCR2 immunohistochemical scores of crypt epithelium correlated with corresponding RT- PCR taqman values

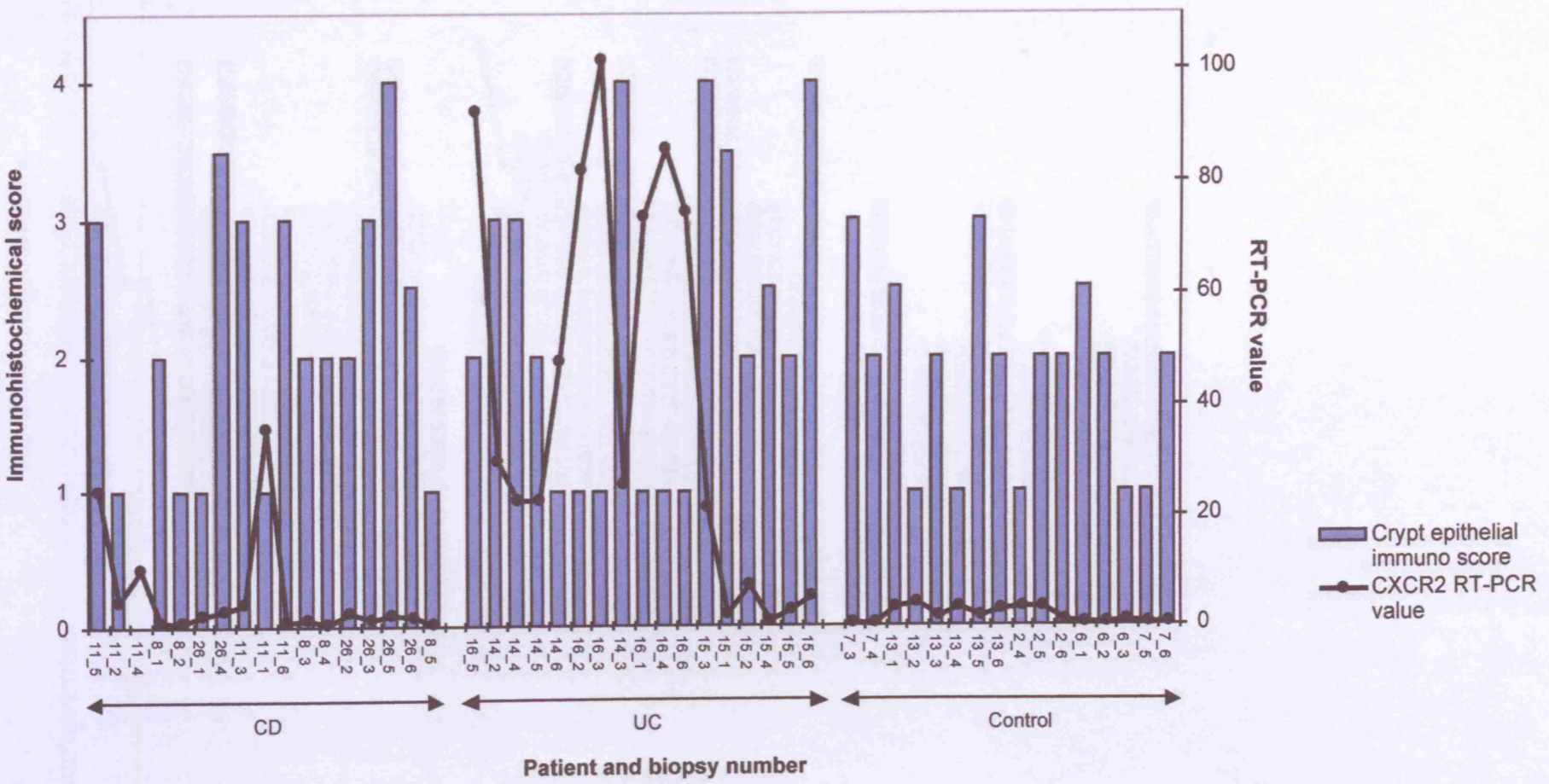

Patients are grouped according to disease. Patient and sample details are outlined in table 2.3. Immunohistochemical scores are listed in table 4.11, and RT-PCR values in table 3.6.

Graph 4.23: Colonic biopsy CXCR2 immunohistochemical scores of lamina propria correlated with corresponding histopathological inflammatory scores

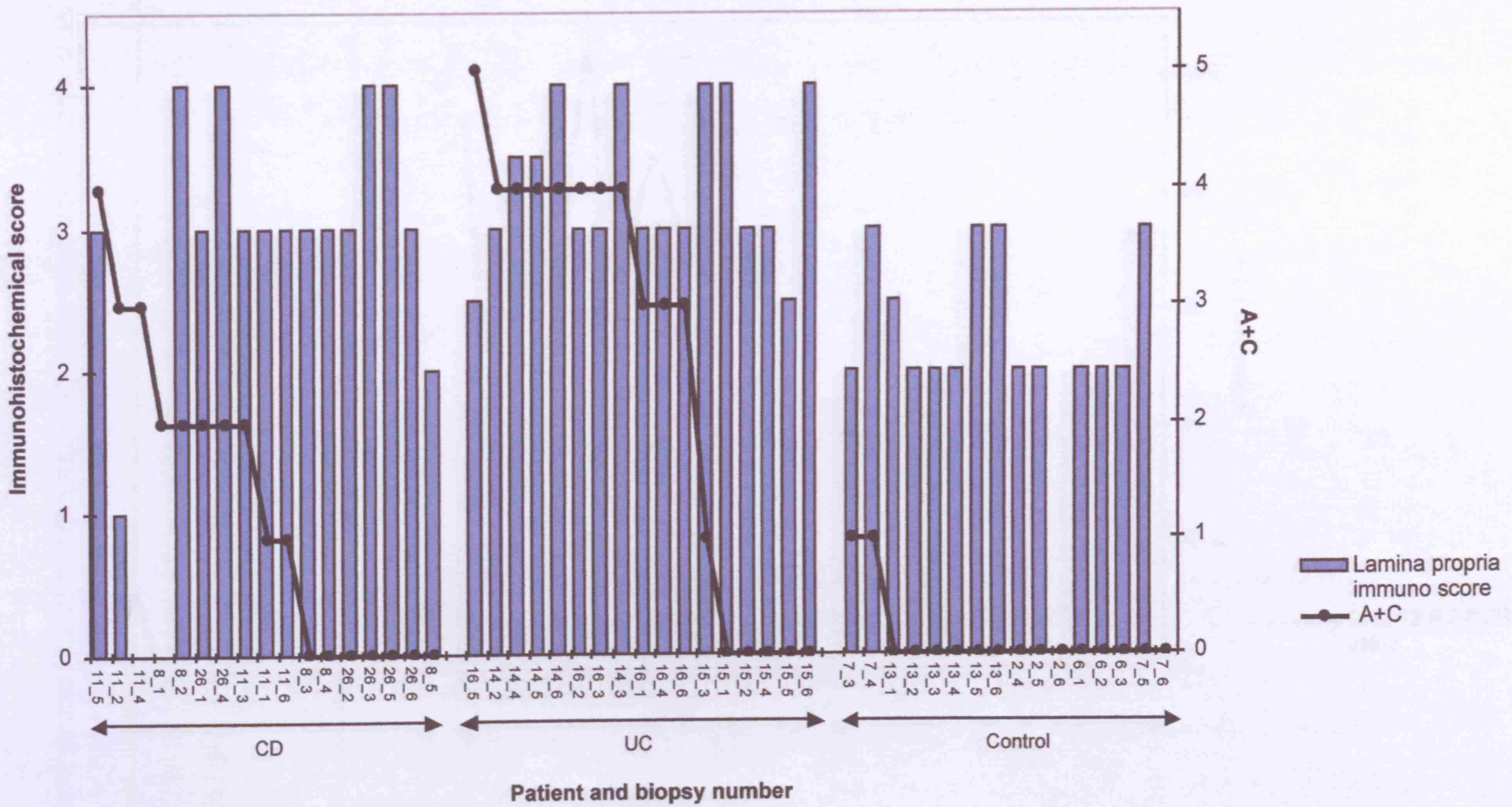

Patients are grouped according to disease and chronologically placed according to inflammatory scores A+C. Patient and sample details are outlined in appendix table 2.3., and immunohistochemical scores in table 4.11.

Graph 4.24: Colonic biopsy CXCR2 immunohistochemical scores of lamina propria correlated with corresponding RT-PCR taqman values

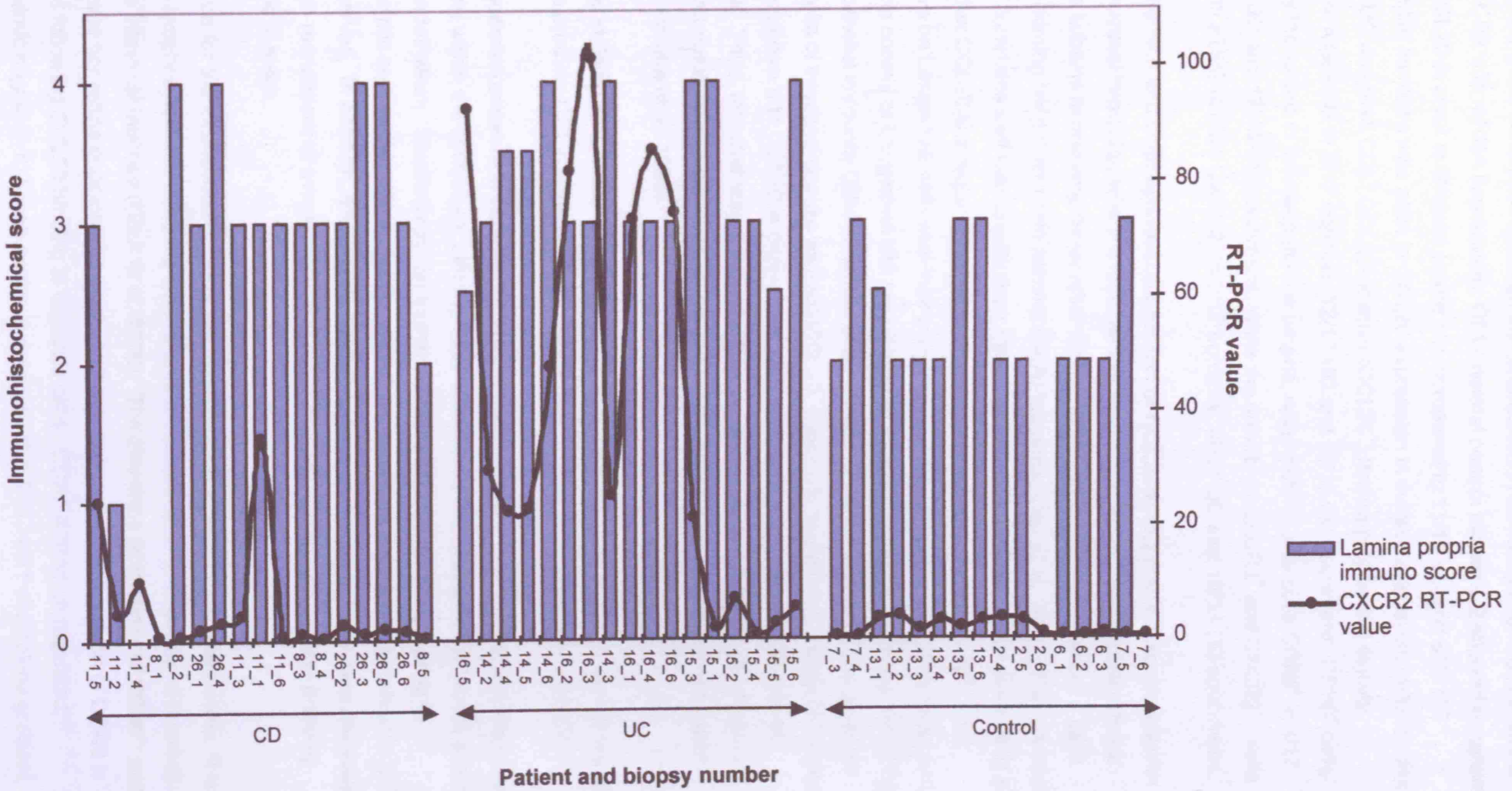

Patients are grouped according to disease. Patient and sample details are outlined in table 2.3. Immunohistochemical scores are listed in table 4.11, and RT-PCR values in table 3.6.

4.6 Discussion

There was generally good correlation between immunohistochemical scores for CCL20, CCR6, CXCR1 and CXCR2 with mRNA expression. Of 17 normal control biopsies, 2 showed enhanced expression of CCL20 in crypt epithelium (score >2), compared to 11/16 UC and 6/15 CD specimens. Similar increase was seen in CCL20 expression in surface epithelium (1/17 control biopsies, 10/16 UC and 6/15 CD). CCL20-positive ($CCL20^+$) lamina propria cell density exceeded 50% of total cells in 2/17 controls, 12/16 UC and 12/15 CD specimens. $CCR6^+$ cells were particularly increased in the deep lamina propria, with >50% of total cells $CCR6^+$ in 1/17 controls, 13/16 UC and 12/15 CD specimens, while the density of $CXCR1^+$ and $CXCR2^+$ cells were higher, with >75% of cells $CXCR2^+$ in 2/17 controls, 10/17 UC and 10/15 CD specimens.

The increased surface and crypt epithelial expression of CCL20 in IBD tissue is consistent with its function in mucosal immunity, where it induces the local migration of dendritic cell subsets and lymphocyte subsets expressing its receptor CCR6, including B cells and memory T cells expressing gut-homing ($\alpha4\beta7$) and skin homing (CLA) Integrins (Liao et al, 1999), (Nakayama et al, 2001). This correlates well with results from other centres. For example, Dieu-Nosjean et al demonstrated that CCL20 is a major chemokine produced by activated epithelial cells, and selectively active on Langerhan cells and their precursors. This implicates CCL20 to be a pivotal chemokine in the control of Langerhan cell recruitment at inflamed epithelial surfaces and in the regulation of epithelial immunity (Dieu-Nosjean et al, 2000). *In situ* hybridisation has revealed that epithelial cells of intestinal tissues express CCL20, especially those lining lymphoid follicles. It has also been shown that CCL20 is chemotactic for memory T-cells and naïve B cells in Peyer's patches. Thus, this chemokine may well be physiologically involved in formation and function of the mucosal lymphoid tissues by attracting lymphocytes and dendritic cells toward epithelial cells (Tanaka et al. 1999).

The neutrophilic staining for CCL20 correlates well with a study by Scapini, which demonstrated that neutrophils produce CCL20 when cultured with either LPS or TNF-α (Scapini et al, 2001).

There was a moderate correlation between CCR6 mRNA expression and immunohistochemical receptor staining within the epithelium, although this association was weak for the lamina propria and vascular endothelium. Qualitatively, an increased expression in the lamina propria, occasional dendritic cell, vascular endothelium, lymphocyte subsets and crypt epithelium in IBD cases was observed. In addition, neutrophils exhibited staining, indicating these cells are likely to be involved in recruitment of lymphocytes and dendritic cells. Lymphoid staining primarily corresponded to T-areas.

CCR6 is required for the localisation of immature dendritic cells to the sub-epithelial zone. It is chemotactic to lymphocytes and dendritic cells, and is a mucosa-specific regulator of humoral immunity in the intestinal mucosa (Cook et al, 2000). The presence or absence of $CCR6^+$ cells does not implicate nor refute ongoing immunological activation, as the expression of CCR6 is down regulated following CCL20 binding to dendritic cells. CCR7 is then up regulated, facilitating dendritic migration to lymph nodes in response to a CCL19/21 chemokine gradient.

There was a predominance of $CCR6^+$ cells within the deeper lamina propria in IBD cases. Although it is difficult to be sure of the immunological significance, this pattern may well be part of CCR6 down regulation following dendritic cell activation.

There was weak correlation between mRNA expression and immunohistochemical staining for CXCR1. Specific interpretation of the staining was made difficult by widespread staining in a variety of cell types, as previously noted (Williams et al, 2000). CXCR1 immunoreactivity was noted on a variety of cell types including plasma cells, macrophages, dendritic cells, neutrophils, goblet cells and myofibroblasts within the lamina propria. There was also strong vascular endothelial immunoreactivity. $CXCR1^+$cells were broadly absent from the subepithelial cells in control tissue, with a clear staining within the deeper lamina propria. There was an upward extension in IBD, with $CXCR1^+$ cells prominent throughout the lamina propria including in the subepithelial area.

CXCR1 was seen to be up regulated in a sub-population of macrophages deep to the epithelium in UC, confirming William's et al paper, who also noted an up regulation of B and T cells outside the germinal centre areas in UC. However, they also noted a similar pattern in acute appendicitis, indicating that this may be not specific to IBD. Finally, this group demonstrated an intense up regulation of CXCR1 by the luminal epithelium in UC but not in acute appendicitis, so this may be specific to IBD.

There was moderate association between CXCR2 RT-PCR values and the epithelial immunohistochemical scores for corresponding biopsies although the association within the lamina propria and vascular endothelium was weak. There was patchy immunoreactivity on surface epithelium in all groups with no overall increase in IBD. Purulent exudate was almost totally $CXCR2^+$. The pattern of immunohistochemical staining for CXCR2 differed from that demonstrated in William's et al paper, with more widespread lamina propria staining in IBD tissue, particularly in the upper lamina propria. This CXCL8 receptor may have a role in mediating the immune response in the gastrointestinal tract. Further characterisation is necessary.

Chapter 5

Coordinate chemokine response in stimulated human colon cancer cells

5.1 Introduction

5.2 Coordinate chemokine response in stimulated Caco-2 cells

5.2.1 Caco-2 cell count and viability assessment

5.2.2 RNA gel electrophoresis

5.2.3 Microarray results

5.2.4 Quantitative determination of chemokine protein concentrations in stimulated Caco-2 cell supernatants

5.2.4.1 Quantitative determination of CCL20 protein expression

5.2.4.2 Quantitative determination of CXCL8 protein expression

5.2.4.3 Quantitative determination of CXCL1 protein expression

5.5.4.4 Quantitative determination of CCL5 protein expression

5.3 Coordinate chemokine response in stimulated HT29 cells

5.3.1 HT29 count and viability assessment

5.3.2 RNA assay

5.3.3 Microarray results

5.3.4 RT-PCR results

5.4 Coordinate chemokine response in stimulated primary colonic epithelial cells

5.4.1 Primary colonic epithelial microarray results

5.5 Coordinate chemokine response in stimulated keratinocyte cells and primary lung epithelial cells

5.6 Discussion

5.1 Introduction

From the microarray data, a specific subset of chemokines was up regulated in inflamed IBD colon, consisting of CXCL's1-3, CXCL8 and CCL20. To characterise epithelial cell chemokine production further, *in vitro* study was undertaken using immortalised epithelial cell lines. The effect of pro-inflammatory stimulation on epithelial chemokine expression was assessed. A consistent pattern of chemokine production by Caco-2 and HT29 cells would provide further evidence for an epithelial cell chemokine response. The method of cell culture used is described in 2.2.5. Two cell lines were included to ensure the results were not merely anomalous to one cell line.

The human epithelial colon carcinoma cell lines Caco-2 and HT29 cells were chosen for studying expression of chemokines and cytokines, due to the spontaneous differentiation exhibited. In the pre-confluent state these cells are relatively undifferentiated. Several days post-confluency, these cells develop markers of a differentiated phenotype for absorptive enterocytes including the expression of digestive enzymes, tight junctions, a well developed brush-border, and a polarised morphology. For this reason, they were harvested at 48 hours post confluency, when they express a predominantly colonic phenotype so as to simulate in-vivo conditions as closely as possible, and allow correlation of data with those obtained from colonic biopsies (Engle et al 1998), (Ashburner et al, 2001). Study of Caco-2 cell lines is of particular relevance as they exhibit a similar pattern of inflammatory responsiveness to isolated colonocytes, more so than other colon cancer cell lines. Finally, primary epithelial cell culture was attempted using surgically obtained epithelial cells, to give a closer approximation to *in vivo* conditions.

Fujiie et al (2001) previously demonstrated human colon carcinoma cell lines express CCL20, up regulated by either TNF-α or IL-1β depending on lineage. In order to determine whether IL-1β and TNF-α were also capable of inducing human colon carcinoma cell lines to express the other chemokines identified as coordinately up regulated in inflamed IBD colon (CXCL's1-3 and CXCL8), the human chemokine array was used to profile gene expression of Caco-2 and HT-29 cells cultured with and without IL-1β, TNF-α, LPS, or IL-1β and TNF-α together. In order to investigate potential regulatory pathways previously implicated in epithelial CXC chemokine production, Caco-2 IL-1β and TNF-α dual stimulations were also performed in the presence of Trichostatin A (TSA) and benzamide to determine any involvement of histone deacetylation and poly (ADP-ribose) polymerase (PARP1) respectively (Wood et al, 1995), (Fusunyan et al, 1999), (Kawai et al, 2001), (Nirodi et al, 2001).

Many regulatory pathways, such as the transactivation of NF-κB have been implicated in epithelial CXC chemokine production (Wood et al, 1995), (Fusunyan et al, 1999), (Ashburner et al, 2001).

Validation of the measured chemokine response was undertaken at the protein level using ELISA on the supernatants collected from the stimulated Caco-2 cell culture plates at 2, 4 and

18 hours. These had been stored frozen at -70°C, and thawed at room temperature. The method used is described in 2.2.6.

5.2 Coordinate chemokine response in stimulated Caco-2 cells

5.2.1 Caco-2 cell count and viability assessment

Cell counts for passage number 4:

Live cell counts: 171, 203, 175, 185, 167, 158 (i.e. viable cells / standard grid sub-division)

Total live cell count in 6 grids = 1065, average = 176.5

Dead cell counts: 2, 0, 1, 2, 1, 0

Total dead cell counts in 6 grids = 6, average = 1

Number of live cells / total number cells x 100 = 99.44% viability

The cell count per volume was calculated using the following equation:

Total number of live cells x 10^4 x 2 (dilution factor) / ml = 3.53 x 10^6 cells/ml

In order to have 1.5 x 10^6 cells, 425 µl was added to 20 x 10cm petri dishes containing 10ml medium.

Cell counts for passage number 22:

Live cell counts: 94, 104, 112, 88, 138, 97, 88

Total live cell count in 6 grids = 633, average = 105.5

Dead cell counts: 4, 3, 6, 2, 4, 5

Total dead cell counts in 6 grids = 24, average = 4

Number of live cells / total number cells x 100= 96.35% viability

The cell count per volume was calculated using the following equation:

Total number of live cells x 10^4 x 2 (dilution factor) / ml = 2.11 x 10^6 cells/ml

In order to have 1.5 x 10^6 cells, 710.9µl were added to 30 x 10cm Petri dishes containing 10ml medium.

Cell counts for passage number 24:

Live cell counts: 203, 172, 202, 180, 149, 145

Total live cell count in 6 grids = 1051, average = 175.1666

Dead cell counts: 2, 3, 4, 1, 3, 6

Total dead cell counts in 6 grids = 19, average = 3.1666

Number of live cells / total number cells x 100 = 98.22% viability

The cell count per volume was calculated using the following equation:

Total number of live cells x 10^4 x 2 (dilution factor) /ml = 3.503 x 10^6 cells/ml

In order to have 1.5 x 10^6 cells, 428.20µl was added to 20 x 10cm petri dishes containing 10ml medium.

5.2.2 RNA gel electrophoresis

The 18 and 28S ribosomal bands were clearly visible (figure 5.1).

Figure 5.1: Agarose gel electrophoresis for RNA extracted from Caco-2 cells. RNA was extracted from Caco-2 cells from passage numbers 4. This was loaded into an agarose gel, and run at 110V for 30 minutes. The 18 and 28S ribosomal bands are indicated.

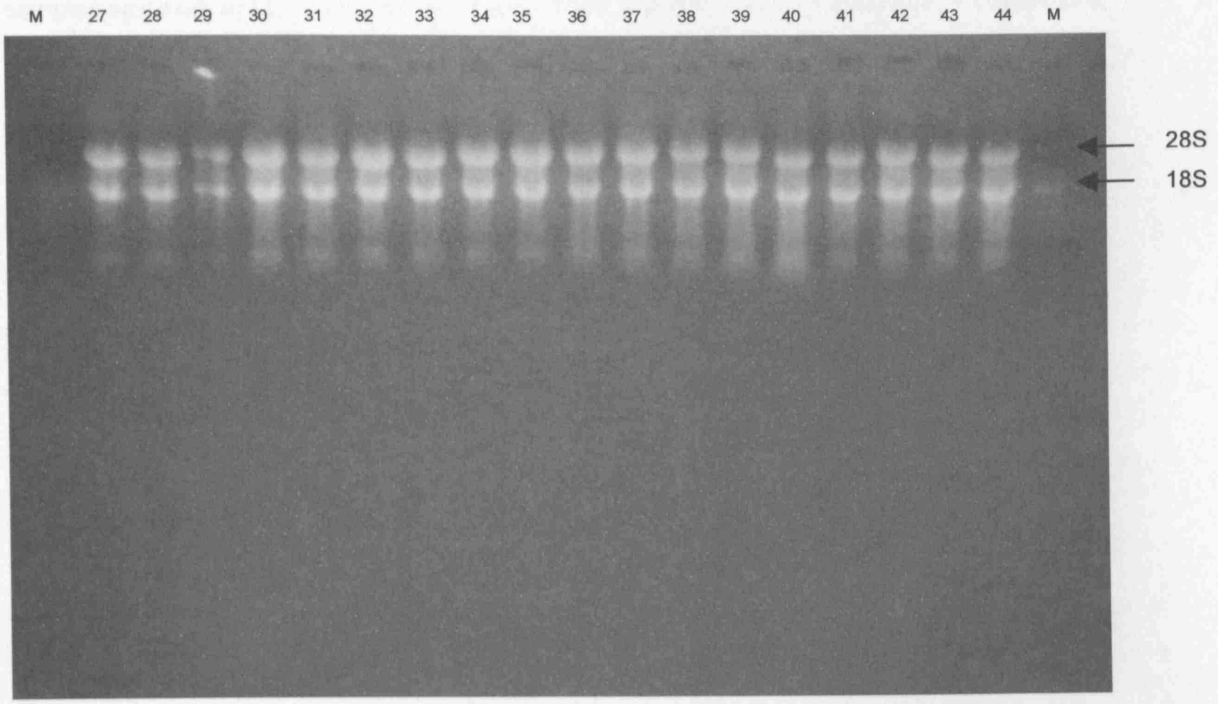

5.2.3 Microarray results

The Microarray hybridised with cDNA probes derived from Caco-2 cells are represented in figure 5.2. with arrows demonstrating the spots for CCL20 pre- and post-stimulation with combinations of IL-1β, TNF-α, and LPS. Chromographic representation of hierarchical gene clustering is demonstrated in figure 5.3. The semi-quantitative results from the Caco-2 hierarchical clustering data are listed in table 5.1 and 5.2. As the chemokines were up regulated at 2 hours, the 4-hour samples were not analysed to conserve the limited number of arrays available. Furthermore, passage number 22 was not analysed.

Graphs 5.1-5.4 demonstrate the relative expression levels of selected chemokines by Caco-2 cells following 2 and 18 hours exposure to various stimuli, as measured by microarray analysis. Minimal expression was detected at 18 hours post-stimulation.

Figure 5.2: Hybridised genes for Caco-2 analysis, detected by radio labelling, with arrows demonstrating the spots corresponding to CCL20 pre- and post-stimulation with combinations of IL-1β, TNF-α and LPS.

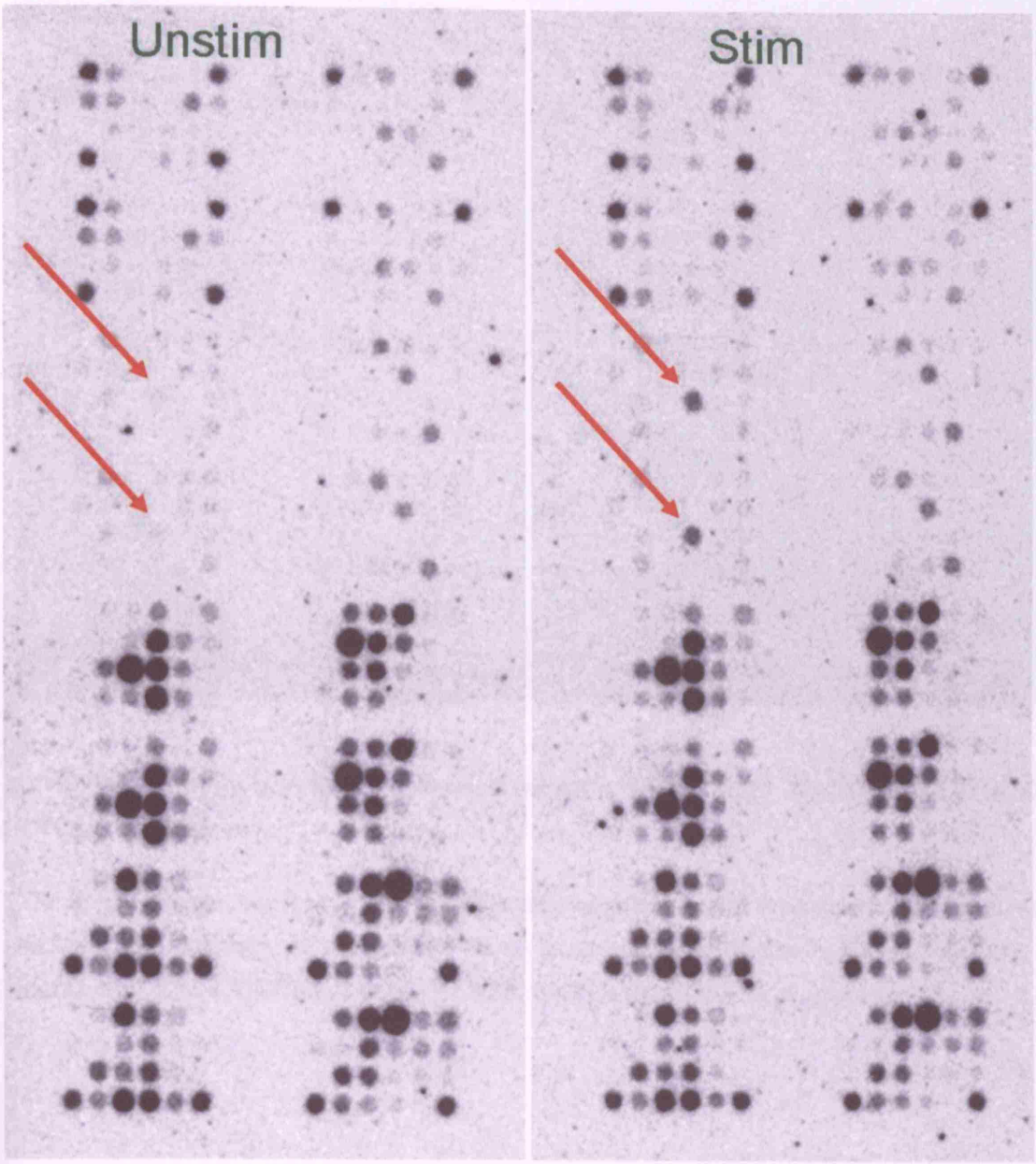

Figure 5.3: Hierarchical cluster of Caco-2 expression data at 2 hours

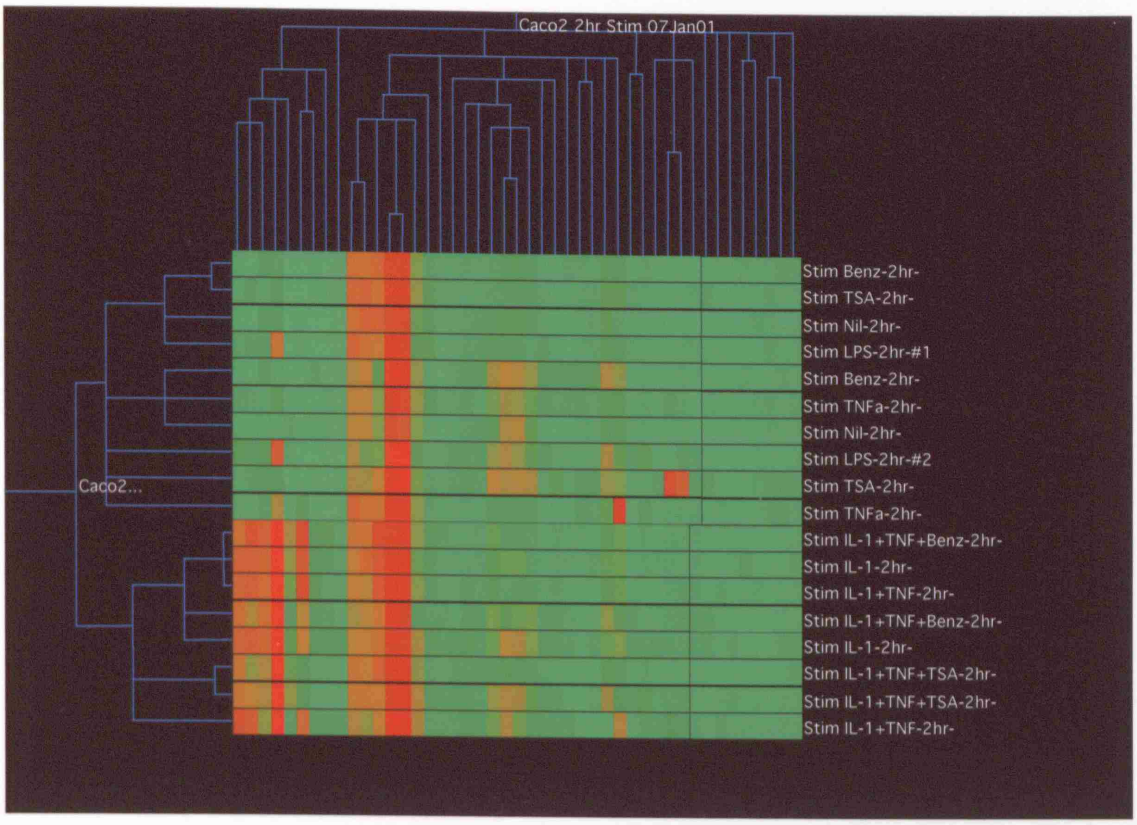

Chemokines are represented in columns from left to right: CXCL1, CXCL3, CXCL2, CCL20, CXCL8, CXCL10 etc.

The levels of gene expression are colour-coded whereby green represents a low level, and red represents a high level of expression. All IL-1β-stimulated cells cluster together due to increased CXCL1, CXCL3, CXCL2, CCL20, CXCL8 and CXCL10 expression.

Table 5.1: 2-hour normalised chemokine expression levels of CXCL1, 2, 3, 8, 10, CCL20 and actin from microarray analysis for Caco-2 cells stimulated with nil/IL-1β/ TNF-α/IL-1β + TNF-α/IL-1β +TSA/IL-1β + TNF-α + benzamide/TSA/LPS.

	Nil Passage 4	Nil Passage 22	IL-1β Passage 4	IL-1β Passage 22	TNF-α Passage 4	TNF-α Passage 22	IL-1β + TNF-α Passage 4	IL-1α + TNF-α Passage 22	IL-1β + TNF-α + TSA Passage 4
CXCL1	-1.33659	-0.76154	53.773677	55.66477	-0.54776267	5.89106253	51.79726054	67.87799969	43.99932685
CXCL2	9.764078	2.029387	51.515065	52.019625	7.31841113	2.21048079	47.44653819	28.23968497	33.21792813
CXCL3	-1.20058	-5.77764	56.562495	59.489627	-3.63688997	6.08268258	58.42978744	58.86321193	28.58370801
CXCL8	-1.13787	4.453102	28.678778	19.366339	-5.04537611	-1.71659524	24.15973389	4.132609002	21.84301985
CXCL10	0.90638	-1.72908	63.080533	41.980744	16.9932006	1.04788216	79.06230749	49.14949367	16.49383707
CCL20	12.73041	0.384668	222.96995	188.49878	32.858326	16.4380466	213.6822055	183.4424122	377.7967088
Actin 5' fragment	21.77957	53.4738	29.742599	51.015121	24.7218811	54.9262986	20.14261763	58.98347478	17.99925327
Actin middle fragment	94.74223	88.01166	97.938445	88.139338	63.203487	84.1655748	56.01119737	68.79029947	88.01928424
Actin 3' fragment	442.9086	435.6609	460.01517	467.75327	509.186388	438.257335	487.0165698	464.985421	501.4303954

	IL-1β + TNF-α + TSA Passage 22	IL-1β + TNF-α + benzamide Passage 4	IL-1β + TNF-α + benzamide Passage 22	Benzamide Passage 4	Benzamide Passage 22	TSA Passage 4	TSA Passage 22	LPS Passage 4	LPS Passage 22
CXCL1	44.23832487	45.39715908	49.24758228	1.64416601	0.39111718	1.29845367	-1.4163975	2.59767822	17.2442347
CXCL2	33.37554064	55.21223162	50.43634762	10.0427253	8.95001524	1.04075745	10.6787706	11.0161206	16.3635385
CXCL3	39.76689767	66.55163937	35.0314542	-1.72961451	-1.07262585	11.5259407	6.70402216	8.42242257	10.0014434
CXCL8	28.81000345	32.87765519	8.068895792	-4.9026487	-1.89703628	-1.1988034	-1.182087	-3.4750402	3.03524874
CXCL10	14.76398255	77.06841561	36.7610434	-6.11310429	-2.54934333	0.40953542	-0.9752284	2.08472387	-0.834093
CCL20	309.2236159	213.2551775	175.9428224	9.52923077	2.21295191	14.6229774	10.4781463	44.9338071	64.8705368
Actin 5' fragment	62.05054915	33.01908927	59.1245535	18.3389642	51.7973991	30.9416221	56.0293903	38.3033148	79.0901046
Actin middle fragment	94.11084098	86.7974407	110.3725957	44.6160305	88.1937549	53.2103811	115.256413	49.0162588	110.454662
Actin 3' fragment	456.6958857	505.2553417	465.9915827	471.03092	430.084966	477.675433	496.432403	509.420048	448.157528

Table 5.2: 18-hour normalised chemokine expression levels of CXCL1, 2, 3, 8, 10, CCL20, and actin from microarray analysis for Caco-2 cells stimulated with nil/IL-1β/ TNF-α/IL-1β + TNF-αIL-1β +TSA/IL-1β + TNF-α + benzamide/TSA/LPS

	Nil Passage 4	Nil Passage 22	IL-1β Passage 4	IL-1β Passage 22	TNF-α Passage 4	TNF-α Passage 22	IL-1β + TNF-α Passage 4	IL-1β + TNF-α Passage 22	IL-1β + TNF-α + TSA Passage 4
CXCL1	1.0504011	4.8995496	7.05089919	15.9433987	3.265983701	-4.219060403	7.826463565	17.59769311	14.54607609
CXCL2	1.8979855	18.401751	9.47763122	44.9046848	4.445401228	0.686771135	5.626651084	36.81897225	0.05988548
CXCL3	9.6387231	2.2929458	13.3231735	24.1723727	9.066227121	-1.254071001	15.4437359	27.59619372	7.650465994
CXCL8	0.2551618	2.5061614	0.67946764	1.17725593	-1.841271524	-7.576237625	1.060075175	0.580444058	-1.307528178
CXCL10	-2.020052	-1.076941	-0.41497937	-1.58035588	1.226209094	-5.086127421	4.626567407	3.858595607	-0.925198508
CCL20	4.9970903	18.433616	42.396648	44.0997437	5.231582025	10.49231315	26.86404607	44.73673705	182.4316044
Actin 5' fragment	33.838313	39.061383	27.2580256	35.2864773	31.37036751	50.72970733	22.93897698	48.27786821	26.75215326
Actin middle fragment	46.88996	69.420642	53.96172	59.583285	57.22883023	96.31997441	34.00028059	61.33554578	60.06733148
Actin 3' fragment	424.26573	439.16045	433.455256	442.116136	437.5793461	325.6121409	450.1761375	436.5482343	464.6879536

	IL-1β + TNF-α + TSA Passage 22	IL-1β + TNF-α + benzamide Passage 4	IL-1β + TNF-α + benzamide Passage 22	Benzamide Passage 4	Benzamide Passage 22	TSA Passage 4	TSA Passage 22	LPS Passage 4	LPS Passage 22
CXCL1	8.805273757	17.46906953	15.25513712	-0.62360456	-3.57724488	7.07731844	-4.2190604	9.42650034	10.4877099
CXCL2	3.690322753	40.84283418	24.71885379	11.82695694	5.218727426	6.93879152	0.68677114	14.1807132	23.2582603
CXCL3	2.964417108	31.4431998	19.22967296	16.12953709	2.168101055	7.96439411	-1.254071	18.0020248	7.4891691
CXCL8	3.685483382	1.05910398	5.016381269	-1.52446566	-0.59541019	-1.80136306	-7.57623763	-1.08610605	-1.35393859
CXCL10	0.163198104	7.187519647	1.653251103	3.68314614	-0.14764425	0.95034809	-5.08612742	-1.74714932	-0.6015837
CCL20	250.9144512	35.25064584	37.42555892	4.345286203	1.402398996	25.4906697	10.4923131	12.3475911	11.3541149
Actin 5' fragment	49.63402901	22.13000757	66.54554644	29.87842781	45.02479171	29.0662919	50.7297073	23.30604	48.3911307
Actin middle fragment	97.84688757	44.75068429	112.27624	72.91768292	79.13525199	91.2960432	96.3199744	67.2496538	69.8010921
Actin 3' fragment	437.541398	441.7090975	425.6156306	447.2457439	421.3165526	387.418124	325.612141	477.104186	439.970105

Graph 5.1: 2-hour chemokine expression levels from microarray analysis of Caco-2 cells post pro-inflammatory stimulation (passage 4).

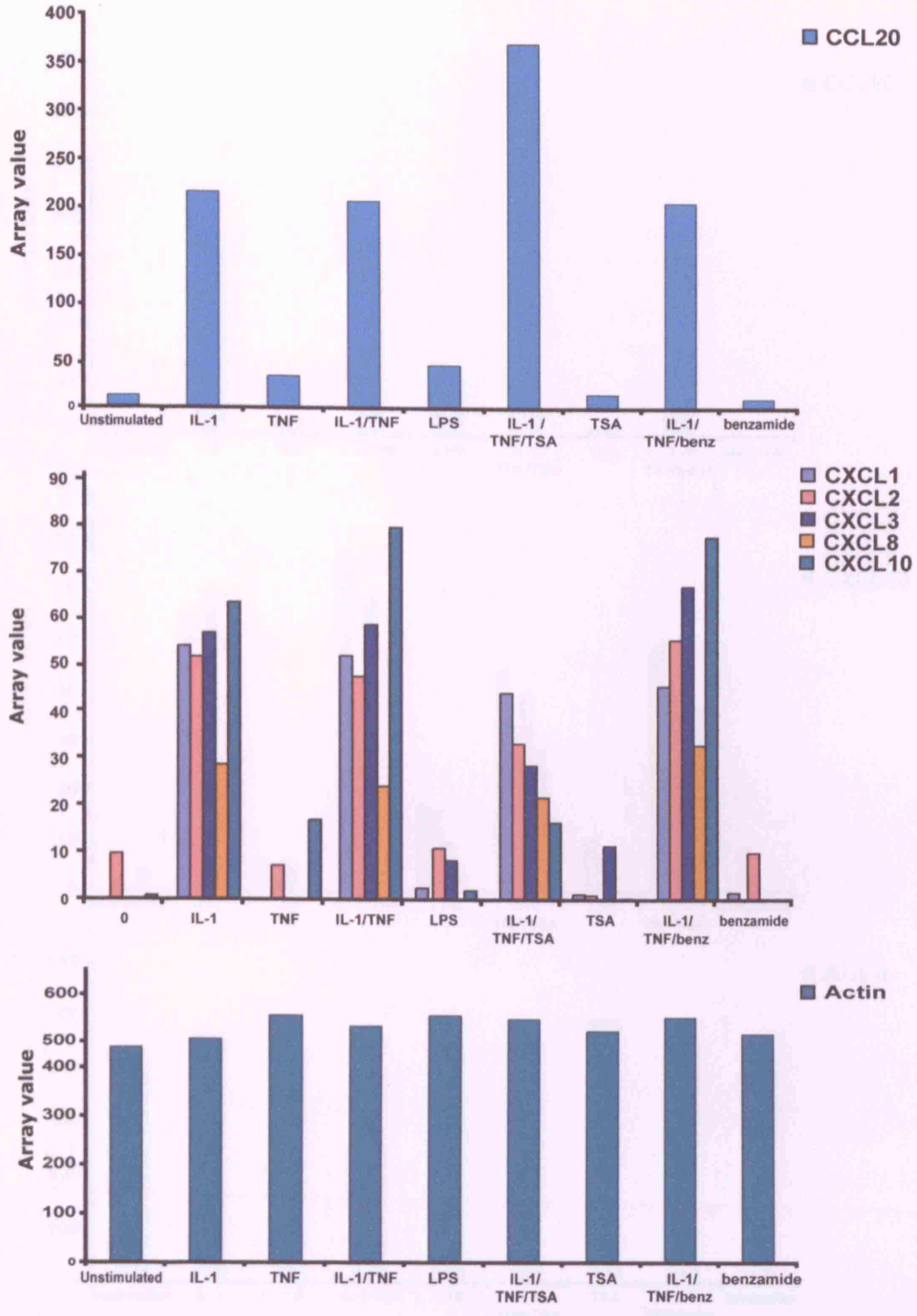

Graph 5.1 demonstrates chemokine induction following pro-inflammatory stimulation at 2 hours as measured by microarray analysis. Caco-2 cellular expression of CCL20, CXCL's1-3 and CXCL8 are primarily up regulated by IL-1β, without synergism by TNF-α. There is a consistent hybridisation signal for actin in all 2-hour samples analysed.

Graph 5.2: 2-hour chemokine expression levels from microarray analysis of Caco-2 cells post pro-inflammatory stimulation (passage 22).

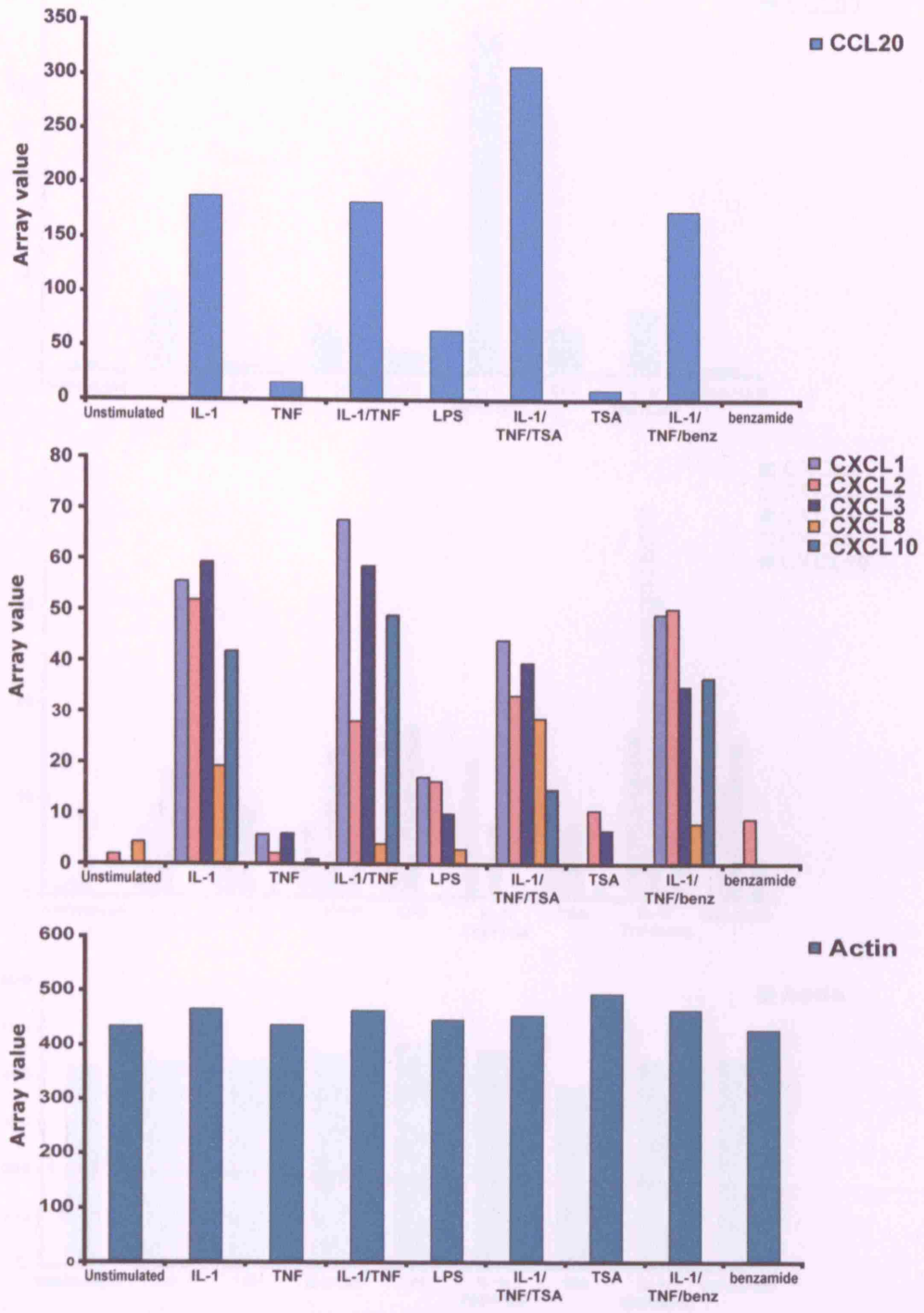

Graph 5.2 demonstrates chemokine induction following pro-inflammatory stimulation at 2 hours as measured by microarray analysis. Caco-2 cellular expression of CCL20, CXCL1-3's and CXCL8 are primarily up regulated by IL-1β, without synergism by TNF-α. There is a consistent hybridisation signal for actin in all 2-hour samples analysed.

Graph 5.3: 18-hour chemokine expression levels from microarray analysis of Caco-2 cells post pro-inflammatory stimulation (passage 4).

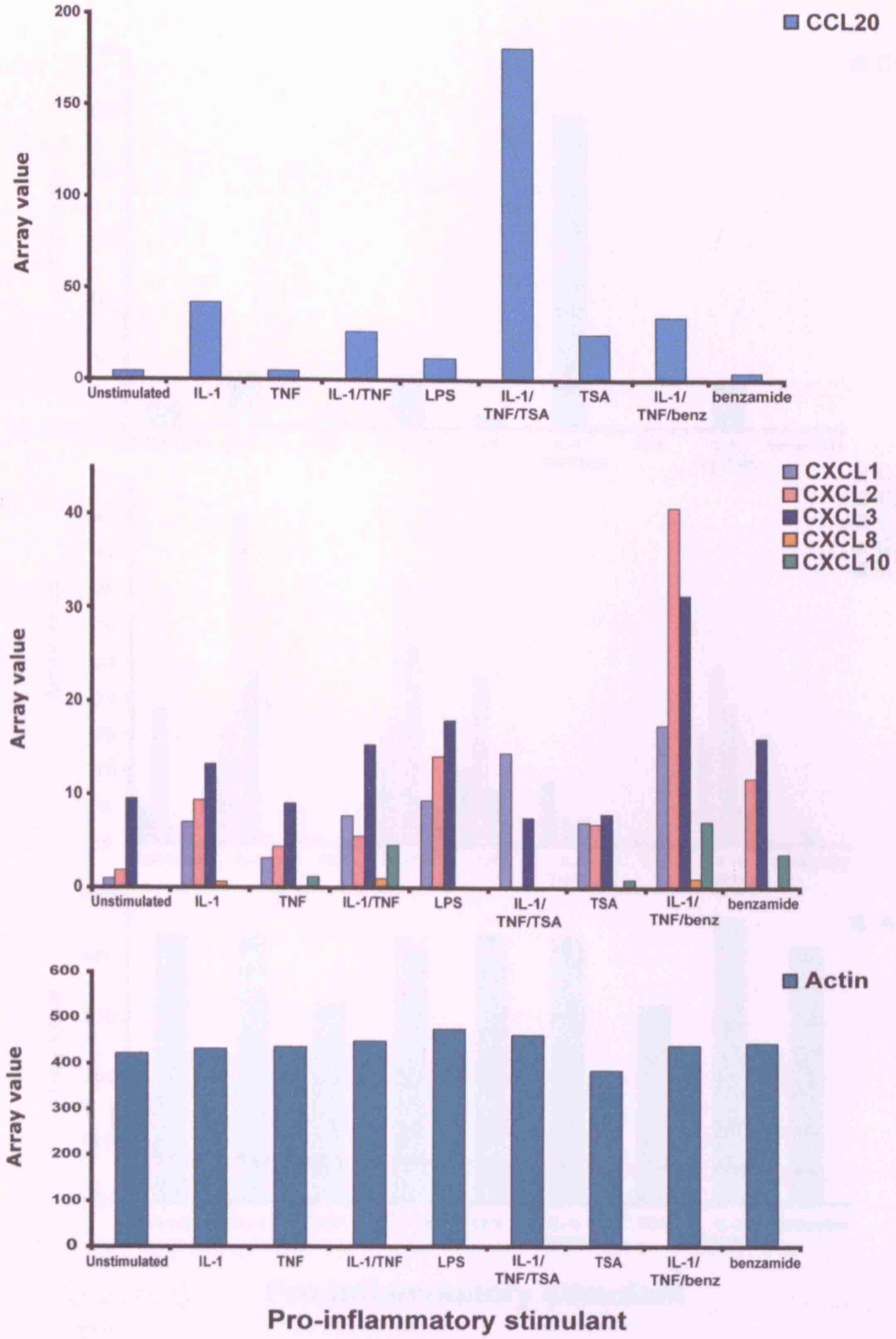

Graph 5.3 demonstrates chemokine induction following pro-inflammatory stimulation at 18 hours as measured by microarray analysis. Caco-2 cellular expression of CCL20, CXCL1-3's and CXCL8 are primarily up regulated by IL-1β, without synergism by TNF-α. There is a consistent hybridisation signal for actin in all 18-hour samples analysed.

Graph 5.4: 18-hour chemokine expression levels from microarray analysis of Caco-2 cells post pro-inflammatory stimulation (passage 22).

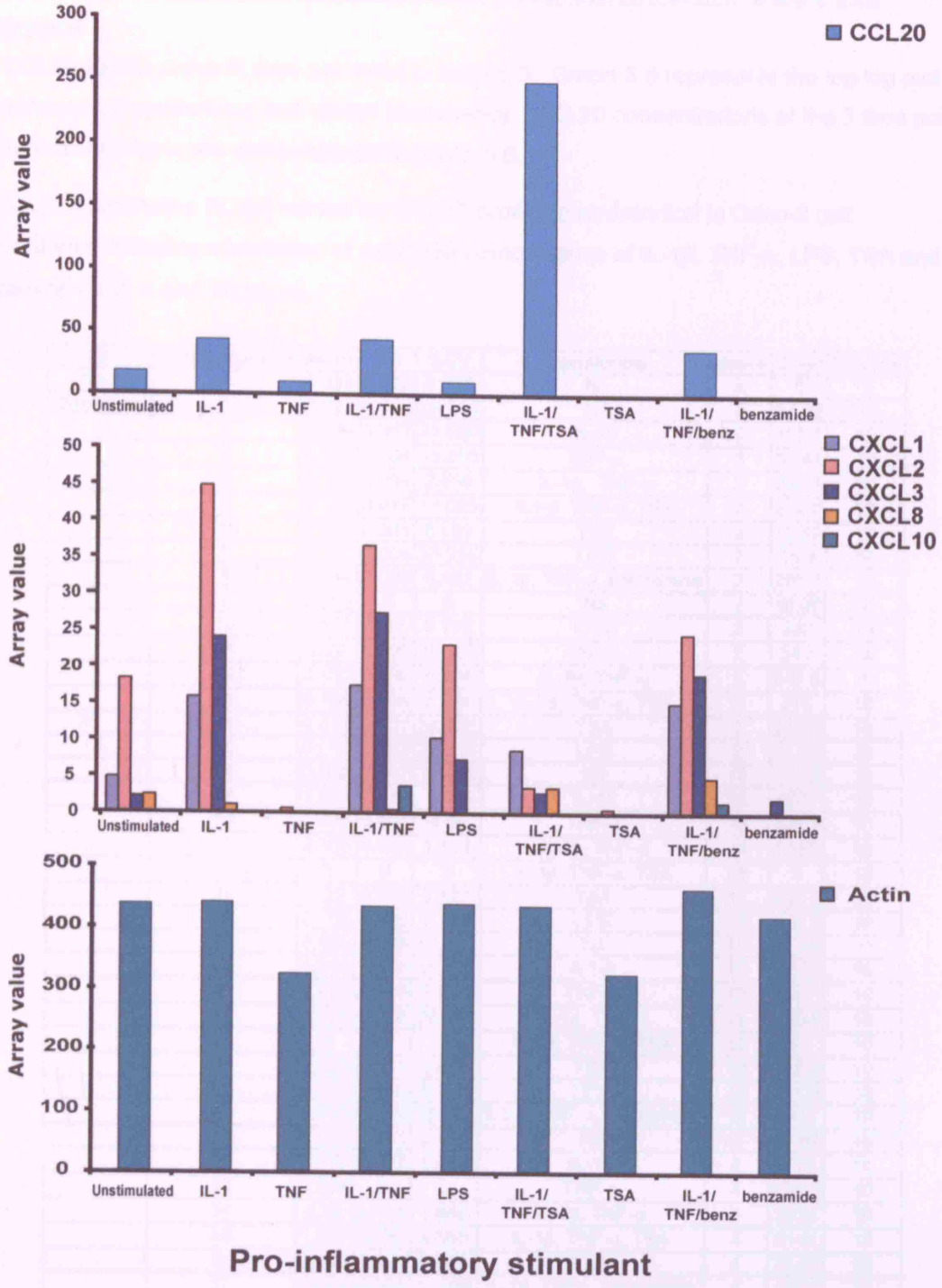

Graph 5.4 demonstrates chemokine induction following pro-inflammatory stimulation at 18 hours as measured by microarray analysis. Caco-2 cellular expression of CCL20, CXCL1-3's and CXCL8 are primarily up regulated by IL-1β, without synergism by TNF-α. There is a consistent hybridisation signal for actin in all 18-hour samples analysed.

5.2.4 Quantitative determination of chemokine protein concentrations in stimulated Caco-2 cell supernatants

ELISA was performed on Caco-2 supernatants, as outlined in 2.2.5.

5.2.4.1 Quantitative determination of CCL20 protein concentration in Caco-2 cells supernatant

The CCL20 ELISA curve fit data are listed in table 5.3. Graph 5.5 represents the log-log plot of the standard concentrations and optical absorbency. CCL20 concentrations at the 3 time points in different conditions are demonstrated in graph 5.6.

Table 5.3: Quantitative ELISA values for CCL20 protein concentration in Caco-2 cell supernatants, following stimulation of cells with combinations of IL-1β, TNF-α, LPS, TSA and benzamide for 2, 4 and 18 hours.

ID	Group Number	Mean	SD	%CV	Conditions	Hours	Conc	Dilution
Blank	0	0.022	0.002	9.867	Nil	X	0	1
Samples	1	0.022	0.006	26.311	Nil	2	37.52	10
	2	0.194	0.042	21.505	IL-1β	2	405.1	10
	3	0.023	0.004	18.856	TNF-α	2	39.41	10
	4	0.133	0.004	2.658	IL-1β, TNF-α	2	269.3	10
	5	0.113	0.017	15.085	IL1-β, TNF-α, TSA	2	224.7	10
	6	0.008	0.001	8.839	TSA	2	12.88	10
	7	0.01	0.004	35.355	LPS	2	16.4	10
	8	0.144	0.008	5.402	IL-1β, TNF-α, benzamide	2	293.4	10
	9	0.012	0	0	Nil	2	19.07	10
	10	0.121	0.01	8.215	IL-1β	2	242	10
	11	0.02	0.009	45.962	TNF-α	2	34.7	10
	12	0.123	0.006	5.174	IL-1β, TNF-α	2	247.5	10
	13	0.108	0.004	3.274	IL-1β, TNF-α, TSA	2	215	10
	14	0.019	0.007	38.222	TSA	2	31.89	10
	15	0.011	0.003	26.937	LPS	2	17.29	10
	16	0.062	0.007	11.498	Nil	18	116.9	10
	17	1.826	0.019	1.046	IL-1β	18	4577	10
	18	0.095	0.004	4.49	TNF-α	18	186.1	10
	19	2.195	0.033	1.514	IL-1β, TNF-α	18	5585	10
	20	0	0	0	IL-1β, TNF-α, TSA	18	X	10
	21	0.22	0.006	2.577	TSA	18	462.9	10
	22	0.106	0.008	7.338	LPS	18	210.7	10
	23	0.029	0.005	17.068	Nil	18	51.86	10
	24	1.341	0.004	0.264	IL1-β	18	3278	10
	25	0.076	0.005	6.513	TNF-α	18	147	10
	26	2.056	0.585	28.442	IL-1β, TNF-α	18	5204	10
	27	0	0	0	IL1-β, TNF-α, TSA	18	X	10
	28	0.154	0.001	0.459	TSA	18	315.5	10
	29	0.142	0.01	6.996	LPS	18	287.9	10
	30	1.202	0.202	16.832	IL1-β, TNF-α, benzamide	18	2911	10
	31	0.029	0.001	2.438	Nil	4	51.86	10
	32	0.76	0.037	4.841	IL-1β	4	1772	10
	33	0.037	0	0	TNF-α	4	269.3	10
	34	0.88	0.016	1.848	IL-1β, TNF-α	4	2078	10
	35	1.291	0.06	4.656	IL-1β, TNF-α, TSA	4	3146	10
	36	0.043	0.004	9.983	TSA	4	78.41	10
	37	0.633	0.088	13.963	IL-1β, TNFα, benzamide	4	1455	10
	38	0.211	0	0	TNF-α	18	442.4	10
	39	2.519	0	0	IL-1β, TNF-α	18	6480	10
	40	0	0	0	IL-1β, TNF-α, TSA	18	X	10
	41	2.131	0	0	IL-1β, TNF-α, benzamide	18	5408	10
	42	0.428	0	0	TSA	18	952	10
	43	0.211	0	0	IL1-β	2	442.4	10
Standards	1	1.815	0.025	1.403	X	X	500	1
	2	1.111	0.001	0.064	X	X	250	1
	3	0.585	0.003	0.484	X	X	125	1
	4	0.283	0.019	6.746	X	X	62.5	1

5.2.4 Quantitative determination of chemokine protein concentrations in stimulated Caco-2 cell supernatants

ELISA was performed on Caco-2 supernatants, as outlined in 2.2.5.

5.2.4.1 Quantitative determination of CCL20 protein concentration in Caco-2 cells supernatant

The CCL20 ELISA curve fit data are listed in table 5.3. Graph 5.5 represents the log-log plot of the standard concentrations and optical absorbency. CCL20 concentrations at the 3 time points in different conditions are demonstrated in graph 5.6.

Table 5.3: Quantitative ELISA values for CCL20 protein concentration in Caco-2 cell supernatants, following stimulation of cells with combinations of IL-1β, TNF-α, LPS, TSA and benzamide for 2, 4 and 18 hours.

ID	Group Number	Mean	SD	%CV	Conditions	Hours	Conc	Dilution
Blank	0	0.022	0.002	9.867	Nil	X	0	1
Samples	1	0.022	0.006	26.311	Nil	2	37.52	10
	2	0.194	0.042	21.505	IL-1β	2	405.1	10
	3	0.023	0.004	18.856	TNF-α	2	39.41	10
	4	0.133	0.004	2.658	IL-1β, TNF-α	2	269.3	10
	5	0.113	0.017	15.085	IL1-β, TNF-α, TSA	2	224.7	10
	6	0.008	0.001	8.839	TSA	2	12.88	10
	7	0.01	0.004	35.355	LPS	2	16.4	10
	8	0.144	0.008	5.402	IL-1β, TNF-α, benzamide	2	293.4	10
	9	0.012	0	0	Nil	2	19.07	10
	10	0.121	0.01	8.215	IL-1β	2	242	10
	11	0.02	0.009	45.962	TNF-α	2	34.7	10
	12	0.123	0.006	5.174	IL-1β, TNF-α	2	247.5	10
	13	0.108	0.004	3.274	IL-1β, TNF-α, TSA	2	215	10
	14	0.019	0.007	38.222	TSA	2	31.89	10
	15	0.011	0.003	26.937	LPS	2	17.29	10
	16	0.062	0.007	11.498	Nil	18	116.9	10
	17	1.826	0.019	1.046	IL-1β	18	4577	10
	18	0.095	0.004	4.49	TNF-α	18	186.1	10
	19	2.195	0.033	1.514	IL-1β, TNF-α	18	5585	10
	20	0	0	0	IL-1β, TNF-α, TSA	18	X	10
	21	0.22	0.006	2.577	TSA	18	462.9	10
	22	0.106	0.008	7.338	LPS	18	210.7	10
	23	0.029	0.005	17.068	Nil	18	51.86	10
	24	1.341	0.004	0.264	IL1-β	18	3278	10
	25	0.076	0.005	6.513	TNF-α	18	147	10
	26	2.056	0.585	28.442	IL-1β, TNF-α	18	5204	10
	27	0	0	0	IL1-β, TNF-α, TSA	18	X	10
	28	0.154	0.001	0.459	TSA	18	315.5	10
	29	0.142	0.01	6.996	LPS	18	287.9	10
	30	1.202	0.202	16.832	IL1-β, TNF-α, benzamide	18	2911	10
	31	0.029	0.001	2.438	Nil	4	51.86	10
	32	0.76	0.037	4.841	IL-1β	4	1772	10
	33	0.037	0	0	TNF-α	4	269.3	10
	34	0.88	0.016	1.848	IL-1β, TNF-α	4	2078	10
	35	1.291	0.06	4.656	IL-1β, TNF-α, TSA	4	3146	10
	36	0.043	0.004	9.983	TSA	4	78.41	10
	37	0.633	0.088	13.963	IL-1β, TNFα, benzamide	4	1455	10
	38	0.211	0	0	TNF-α	18	442.4	10
	39	2.519	0	0	IL-1β, TNF-α	18	6480	10
	40	0	0	0	IL-1β, TNF-α, TSA	18	X	10
	41	2.131	0	0	IL-1β, TNF-α, benzamide	18	5408	10
	42	0.428	0	0	TSA	18	952	10
	43	0.211	0	0	IL1-β	2	442.4	10
Standards	1	1.815	0.025	1.403	X	X	500	1
	2	1.111	0.001	0.064	X	X	250	1
	3	0.585	0.003	0.484	X	X	125	1
	4	0.283	0.019	6.746	X	X	62.5	1

ID	Group Number	Mean	SD	%CV	Conditions	Hours	Conc	Dilution
	5	0.158	0.022	13.874	X	X	31.2	1
	6	0.078	0.005	6.346	X	X	15.6	1
	7	0.042	0.011	27.262	X	X	7.8	1

Graph 5.5: Log-log plot of CCL20 standard concentrations and optical absorbency

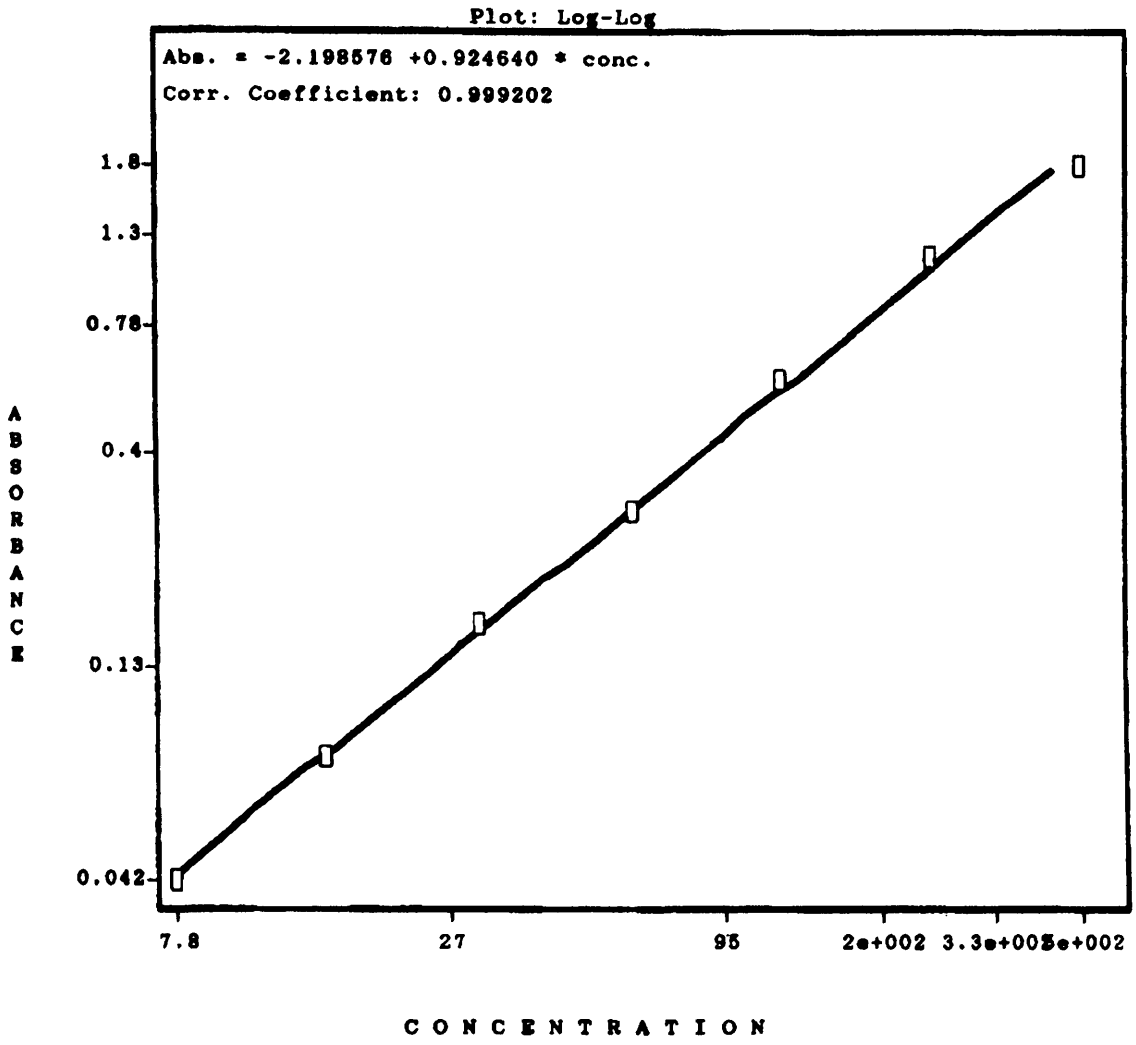

Graph 5.6: Concentrations of CCL20 protein in the supernatants of stimulated Caco-2 cells at 2, 4 and 18 hours

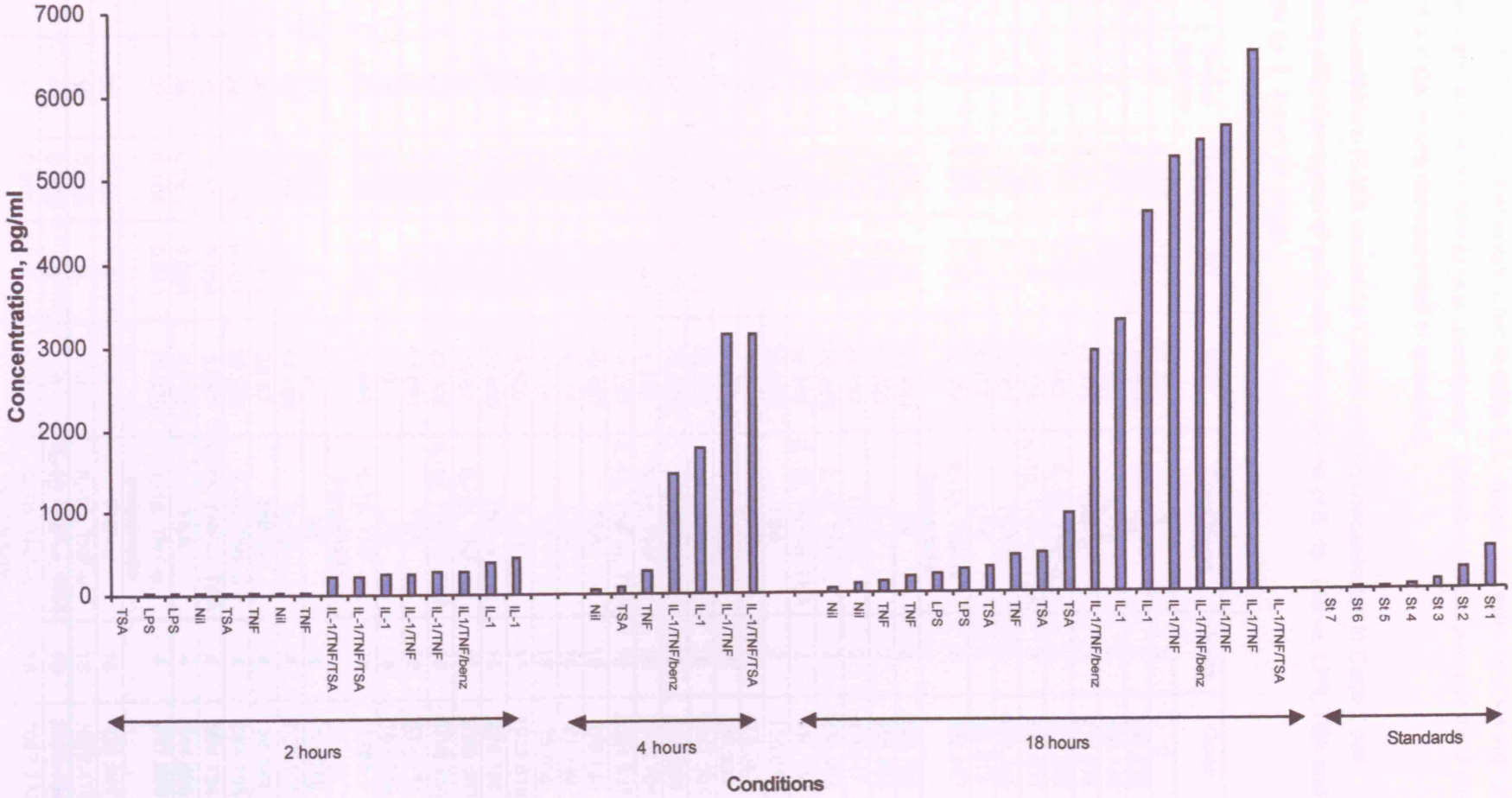

Graph 5.8 demonstrates CCL20 induction is primarily stimulated by IL-1 with little synergy from TNF

5.2.4.2 Quantitative determination of CXCL8 protein concentration in Caco-2 cell supernatant

The CXCL8 ELISA curve fit data are listed in table 5.4. Graph 5.7 represents the log-log plot of the standard concentrations and optical absorbency. CXCL8 concentrations at the 3 time points in different conditions are demonstrated in graph 5.8.

Table 5.4: Quantitative ELISA values for CXCL8 protein concentration in Caco-2 cell supernatants after stimulation of cells with combinations of IL-1β, TNF-α, LPS, TSA and benzamide for 2, 4 and 18 hours.

ID	Group number	Mean	SD	%CV	Conditions	Hours	Conc	Dilution
Blank	0	0.056	0.017	30.305	X	X	0	1
Samples	1	0.092	0.128	139.876	Nil	2	493.822	10
	2	0.074	0.008	10.583	IL-1β	2	390.746	10
	3	0.071	0.066	93.278	TNF-α	2	373.974	10
	4	0.124	0.009	7.443	IL-1β, TNF-α	2	687.395	10
	5	0.107	0.03	27.756	IL-1β, TNF-α, TSA	2	585.937	10
	6	0.089	0.041	46.081	TSA	2	479.255	10
	7	0.015	0.001	4.877	LPS	2	80.613	10
	8	0.069	0.011	15.484	IL-1β, TNF-α, benzamide	2	362.857	10
	9	0.053	0.06	114.484	Nil	2	275.765	10
	10	0.086	0.016	19.022	IL-β	2	458.998	10
	11	0.009	0.002	24.957	TNF-α	2	50.317	10
	12	0.044	0.045	102.852	IL-1β, TNF-α	2	230.804	10
	13	0.06	0.034	56.569	IL-1β, TNF-α, TSA	2	316.183	10
	14	0.03	0.011	35.955	TSA	2	156.051	10
	15	0.013	0	0	LPS	2	73.087	10
	16	0.007	0.009	141.421	Nil	18	39.999	10
	17	0.178	0.076	42.903	IL-1β	18	1047.201	10
	18	0.035	0.026	75.835	TNF-α	18	181.569	10
	19	0.277	0.004	1.532	IL-1β, TNF-α	18	1796.701	10
	20	0.342	0.049	14.287	IL-1β, TNF-α, TSA	18	2351.537	10
	21	0.06	0.03	49.497	TSA	18	316.183	10
	22	0.003	0.001	47.14	LPS	18	21.149	10
	23	0.007	0.005	76.15	Nil	18	39.999	10
	24	0.294	0.019	6.505	IL-1β	18	1933.618	10
	25	0.044	0.013	30.885	TNF-α	18	228.186	10
	26	0.417	0.082	19.67	IL-1β, TNF-α	18	3068.597	10
	27	0.487	0.102	20.908	IL-1β, TNF-α, TSA	18	3799.939	10
	28	0.098	0.047	48.591	TSA	18	529.111	10
	29	0.019	0	0	LPS	18	103.149	10
	30	0.274	0.016	5.946	IL-1β, TNF-α, benzamide	18	1768.1	10
	31	0.011	0	0	Nil	4	63.015	10
	32	0.098	0.042	42.789	IL-1β	4	529.111	10
	33	0.018	0.004	23.57	TNF-α	4	98.141	10
	34	0.154	0.031	20.203	IL-1β, TNF-α	4	884.105	10
	35	0.11	0.004	3.857	IL-1β, TNF-α, TSA	4	604.124	10
	36	0.083	0.004	5.112	TSA	4	444.625	10
	37	0.104	0.011	10.879	IL-1β, TNF-α, benzamide	4	567.866	10
	38	0.024	0	0	TNF-α	18	128.247	10
	39	0.293	0	0	IL-1β, TNF-α	18	1929.419	10
	40	0.302	0	0	IL-1β, TNF-α, TSA	18	2005.494	10
	41	0.261	0	0	IL-1β, TNF-α, benzamide	18	1667.213	10
	42	0	0	0	TSA	18	0	10

ID	Group number	Mean	SD	%CV	Conditions	Hours	Conc	Dilution
43	0.069	0	0	IL-1β	2	365.632	10	
Standards	1	1.257	0.232	18.451	X	X	2000	1
	2	1.063	0.021	1.93	X	X	1000	1
	3	0.611	0.057	9.258	X	X	500	1
	4	0.352	0.085	24.106	X	X	250	1
	5	0.197	0.018	9.332	X	X	125	1
	6	0.104	0.011	10.879	X	X	62.5	1
	7	0.064	0.006	8.839	X	X	31.2	1

Graph 5.7: Log-log plot of CXCL8 standard concentrations and optical absorbency

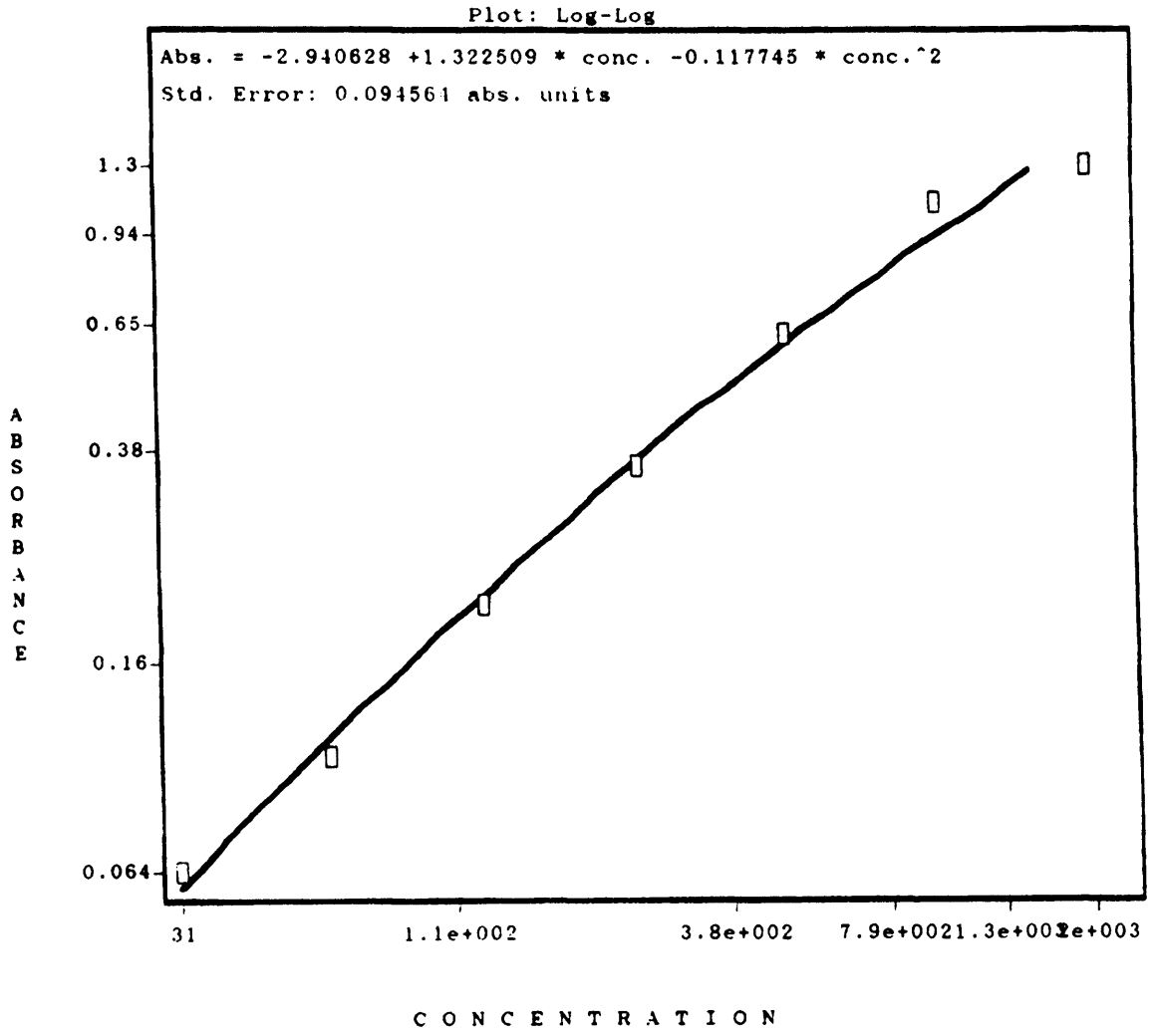

Graph 5.8: Concentrations of CXCL8 protein in supernatants of stimulated Caco-2 cells at 2, 4 and 18 hours

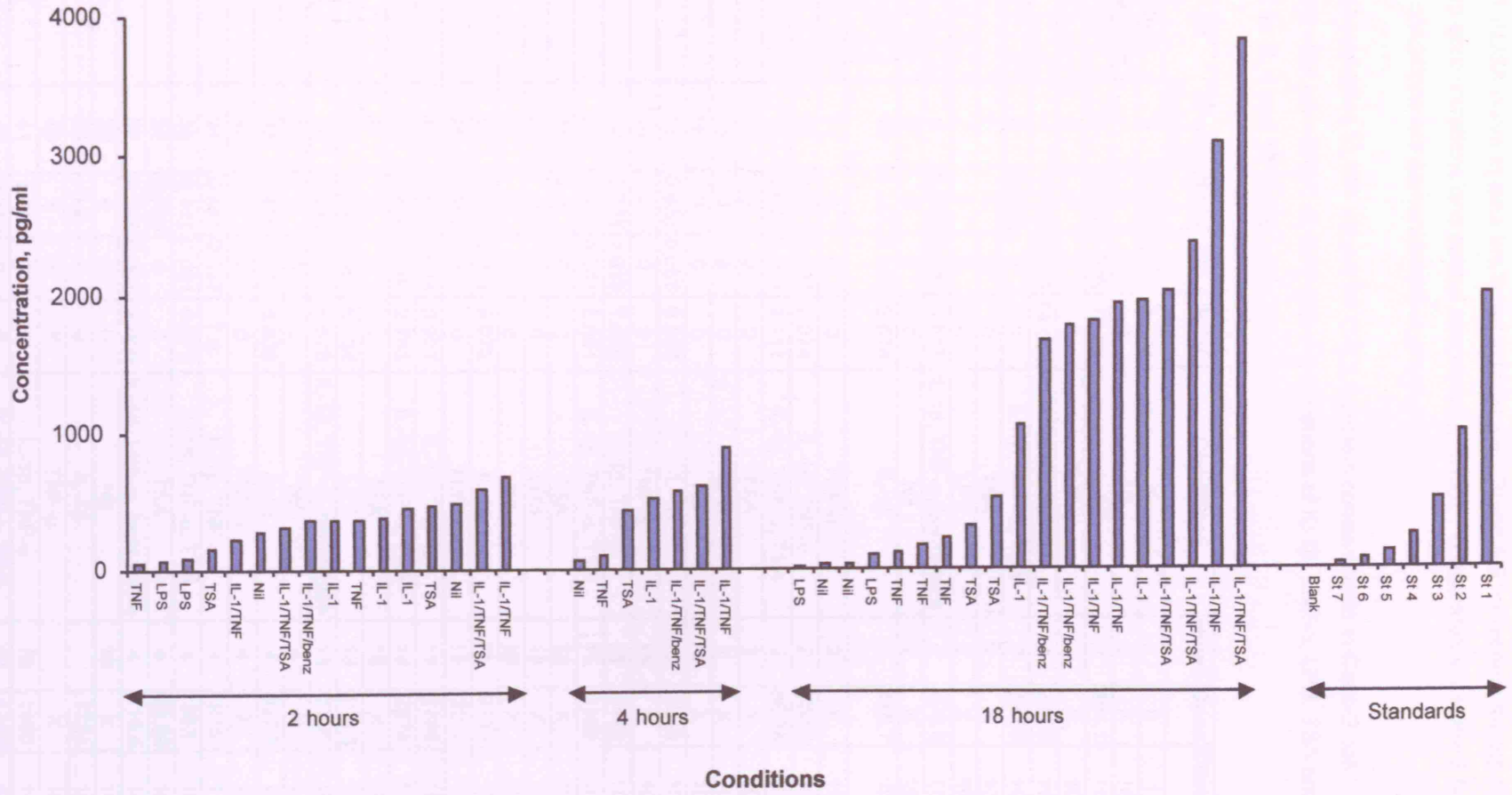

Graph 5.8 demonstrates that CXCL8 is primarily induced by IL-1 with little synergy from TNF. There is further induction with the addition of TSA.

5.2.4.3 Quantitative determination of CXCL1 protein concentration in Caco-2 cell supernatant

The CXCL1 ELISA curve fit data are listed in table 5.5. Graph 5.9 represents the log-log plot of the standard concentrations and optical absorbency. CXCL1 concentrations at the 3 time points in different conditions are demonstrated in graph 5.10.

Table 5.5: Quantitative ELISA values for CXCL1 protein concentration in Caco-2 cell supernatants after stimulation of cells with combinations of IL-1β, TNF-α, LPS, TSA and benzamide for 2, 4 and 18 hours.

ID	Group number	Mean	SD	%CV	Conditions	Hours	Conc	Dilution
Blank	0	0.038	0.001	3.722	X	X	0	1
Samples	1	0	0	0	Nil	2	X	10
	2	0.129	0.025	19.26	IL-1β	2	294.1	10
	3	0	0	0	TNF-α	2	X	10
	4	0.095	0.013	14.068	IL-1β, TNF-α	2	224.6	10
	5	0.008	0	0	IL-1β, TNF-α, TSA	2	23.59	10
	6	0	0	0	TSA	2	X	10
	7	0	0	0	LPS	2	X	10
	8	0.086	0.001	0.817	IL-1β, TNF-α, benzamide	2	205.3	10
	9	0	0	0	Nil	2	X	10
	10	0.154	0.015	9.674	IL-1β	2	345.7	10
	11	0	0	0	TNF-α	2	X	10
	12	0.171	0.004	2.074	IL-1β, TNF-α	2	380.3	10
	13	0.034	0.001	2.111	IL-1β, TNF-α, TSA	2	86.68	10
	14	0	0	0	TSA	2	X	10
	15	0	0	0	LPS	2	X	10
	16	0	0	0	Nil	18	X	10
	17	0.653	0.057	8.663	IL-1β	18	1288	10
	18	0	0	0	TNF-α	18	X	10
	19	0.755	0.013	1.686	IL-1β, TNF-α	18	1470	10
	20	0.603	0.041	6.801	IL-1β, TNF-α, TSA	18	1198	10
	21	0	0	0	TSA	18	X	10
	22	0	0	0	LPS	18	X	10
	23	0	0	0	Nil	18	X	10
	24	1.148	0.093	8.072	IL-1β	18	2150	10
	25	0.007	0	0	TNF-α	18	20.9	10
	26	1.526	0.014	0.927	IL-1β, TNF-α	18	2786	10
	27	1.459	0.04	2.763	IL-1β, TNF-α, TSA	18	2674	10
	28	0	0	0	TSA	18	X	10
	29	0.042	0.003	6.734	LPS	18	106.5	10
	30	1.843	0.123	6.676	IL-1β, TNF-α, benzamide	18	3308	10
	31	0	0	0	Nil	4	X	10
	32	0.455	0.031	6.838	IL-1β	4	927.8	10
	33	0	0	0	TNF-α	4	X	10
	34	0.481	0.037	7.8	IL-1β, TNF-α	4	975	10
	35	0.162	0.001	0.873	IL-1β, TNF-α, TSA	4	363	10
	36	0.008	0	0	TSA	4	23.59	10
	37	0.344	0.007	2.056	IL-1β, TNF-α, benzamide	4	719.6	10
	38	0	0	0	Nil	18	X	10
	39	0.9	0	0	IL-1β		1724	10
	40	X	X	X	TNF-α		X	10
	41	1.048	0	0	IL-1β, TNF-α	18	1980	10
	42	0.913	0	0	IL-1β, TNF-α, TSA	18	1747	10
	43	0.668	0	0	IL-1β, TNF-α, benzamide	18	1315	10
	44	0	0	0	TSA	18	X	10
	45	0.159	0	0	IL-1β	2	356.9	10

ID	Group number	Mean	SD	%CV	Conditions	Hours	Conc	Dilution
Standards	1	X	X	X	X	X	x	1
	2	2.52	0.037	1.459	X	X	500	1
	3	1.537	0.041	2.668	X	X	250	1
	4	0.706	0.017	2.404	X	X	125	1
	5	0.285	0.004	1.243	X	X	62.5	1
	6	0.129	0.003	2.193	X	X	31.2	1

Graph 5.9: Log-log plot of CXCL1 standard concentrations and optical absorbency

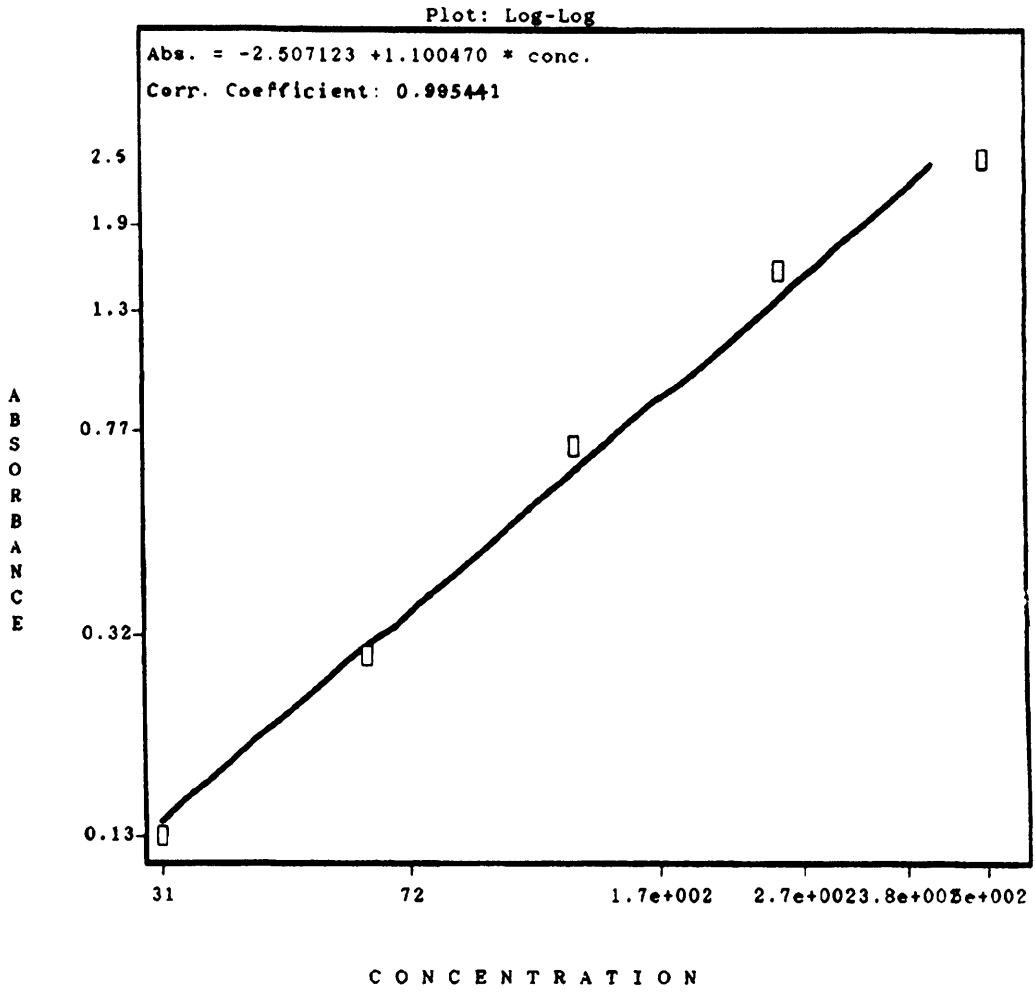

Graph 5.10: Concentrations of CXCL1 protein in supernatants of stimulated Caco-2 cells at 2, 4 and 18 hours

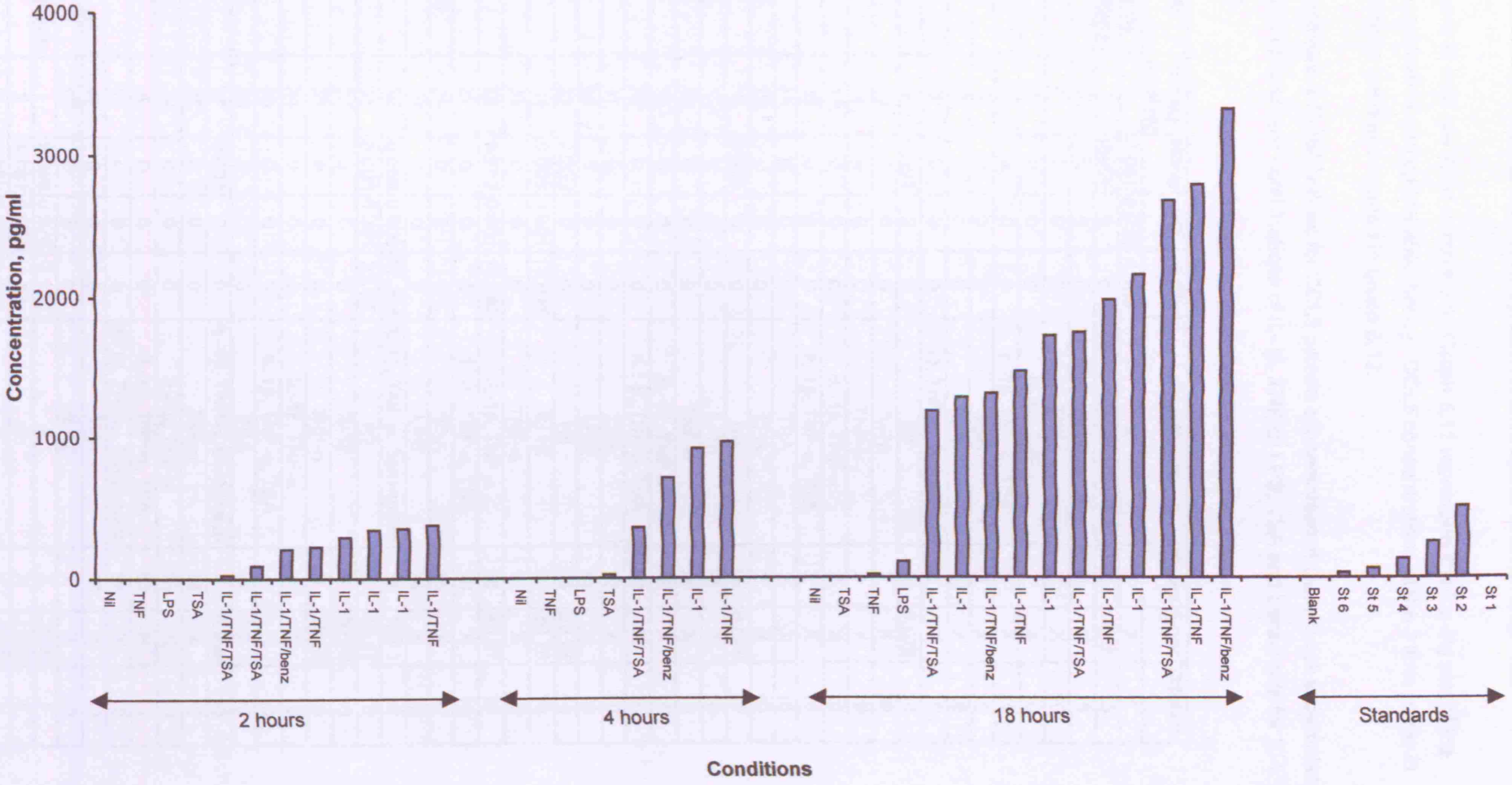

Graph 5.10 demonstrates that CXCL1 is primarily induced by IL-1.

5.2.4.4 Quantitative determination of CCL5 protein concentration in Caco-2 cell supernatant

The CCL5 curve fit data are listed in table 5.6. Graph 5.11 represents the log-log plot of the standard concentrations and optical absorbency. CCL5 concentrations at the 3 time points in different conditions are demonstrated in graph 5.12.

Table 5.6: Quantitative ELISA values for CCL5 protein concentration in Caco-2 cell supernatants after stimulation of cells with combinations of IL-1β, TNF-α, LPS, TSA and benzamide for 2, 4 and 18 hours.

ID	Group number	Mean	SD	%CV	Conditions	Hours	Conc	Dilution
Blanks	0	0.068	0.003	4.159	X	X	X	1
Samples	1	0.004	0	0	Nil	2	19.2	10
	2	0	0	0	IL-1β	2	X	10
	3	0	0	0	TNF-α	2	X	10
	4	0	0	0	IL-1β, TNF-α	2	X	10
	5	0	0	0	IL-1β, TNF-α, TSA	2	X	10
	6	0	0	0	TSA	2	X	10
	7	0	0	0	LPS	2	X	10
	8	0	0	0	IL-1β, TNF-α, benzamide	2	X	10
	9	0.001	0	0	Nil	2	8.026	10
	10	0	0	0	IL-1β	2	X	10
	11	0	0	0	TNF-α	2	X	10
	12	0	0	0	IL-1β, TNF-α	2	X	10
	13	0	0	0	IL-1β, TNF-α, TSA	2	X	10
	14	0	0	0	TSA	2	X	10
	15	0	0	0	LPS	2	X	10
	16	0.001	0	0	Nil	18	8.026	10
	17	0	0	0	IL-1β	18	X	10
	18	0	0	0	TNF-α	18	X	10
	19	0	0	0	IL-1β, TNF-α	18	X	10
	20	0	0	0	IL1-β, TNF-α, TSA	18	X	10
	21	0	0	0	TSA	18	X	10
	22	0	0	0	LPS	18	X	10
	23	0.005	0	0	Nil	18	22.28	10
	24	0.008	0.001	17.678	IL-1β	18	30.73	10
	25	0	0	0	TNF-α	18	X	10
	26	0.012	0.001	11.785	IL-1β, TNF-α	18	40.97	10
	27	0	0	0	IL-1β, TNF-α, TSA	18	X	10
O:	28	0	0	0	TSA	18	X	10
	29	0	0	0	LPS	18	X	10
	30	0.056	0.006	11.264	IL-1β, TNF-α, benzamide	18	137.3	10
	31	0.006	0.001	23.57	Nil	4	40.97	10
	32	0	0	0	IL-1β	4	30.73	10
	33	0	0	0	TNF-α	4	22.28	10
	34	0	0	0	IL-1β, TNF-α	4	X	10
	35	0	0	0	IL-1β, TNF-α, TSA	4	X	10
	36	0	0	0	TSA	4	X	10
	37	0.001	0	0	IL-1β, TNF-α, benzamide	4	8.026	10
	38	0	0	0	TNF-α	18	X	10
	39	0	0	0	IL-1β, TNF-α	18	X	10
	40	0	0	0	IL-1β, TNF-α, TSA	18	X	10
	41	0	0	0	IL-1β, TNF-α, benzamide	18	X	10
	42	0	0	0	TSA	18	X	10
	43	0	0	0	IL-1β	2	X	10
Standards	1	2.398	0.075	3.126	X	X	2000	1
	2	1.801	0.029	1.61	X	X	1000	1
	3	1.327	0.003	0.213	X	X	500	1

ID	Group number	Mean	SD	%CV	Conditions	Hours	Conc	Dilution
	4	0.833	0.013	1.614	X	X	250	1
	5	0.495	0.002	0.429	X	X	125	1
	6	0.28	0.01	3.536	X	X	62.5	1
	7	0.14	0.003	2.02	X	X	31.2	1

Graph 5.11: Log-log plot of CCL5 standard concentrations and optical absorbency

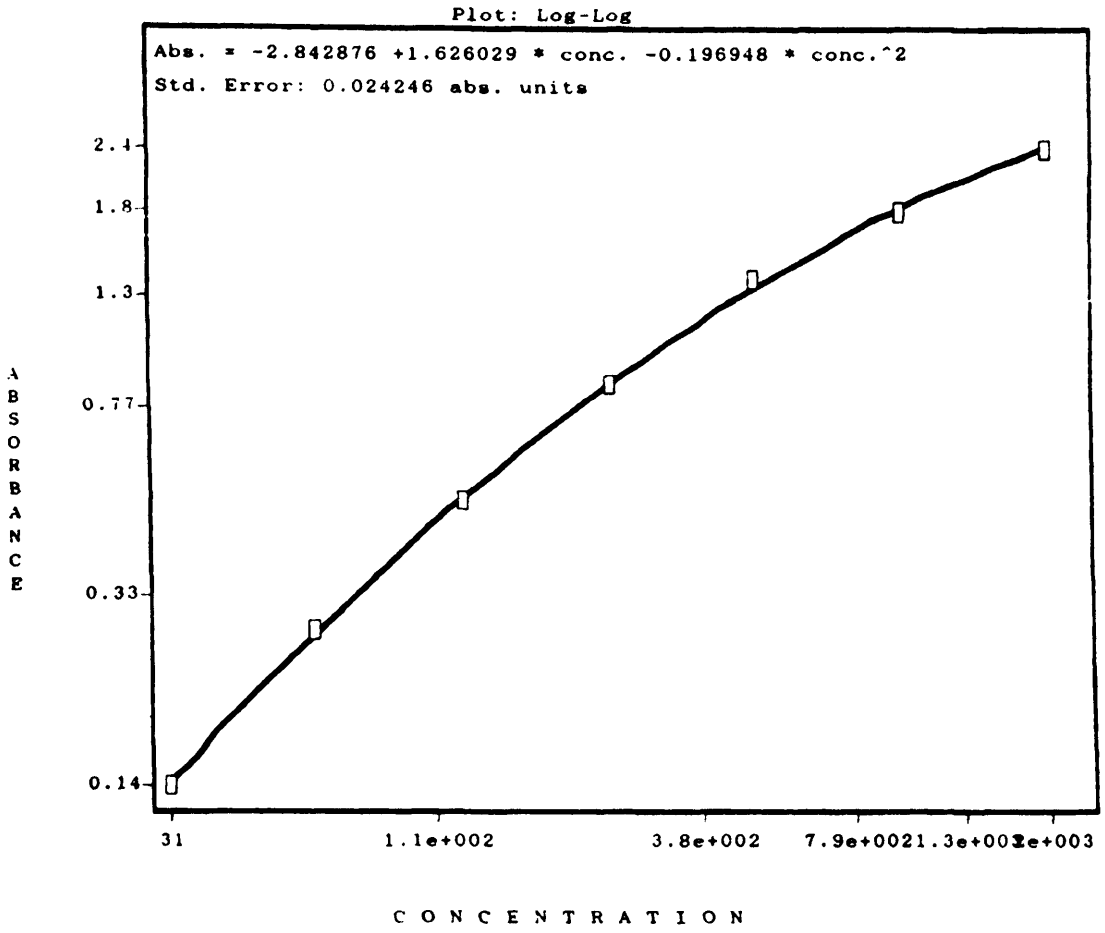

Graph 5.12: Concentrations of CCL5 protein in supernatants of stimulated Caco-2 cells at 2, 4 and 18 hours

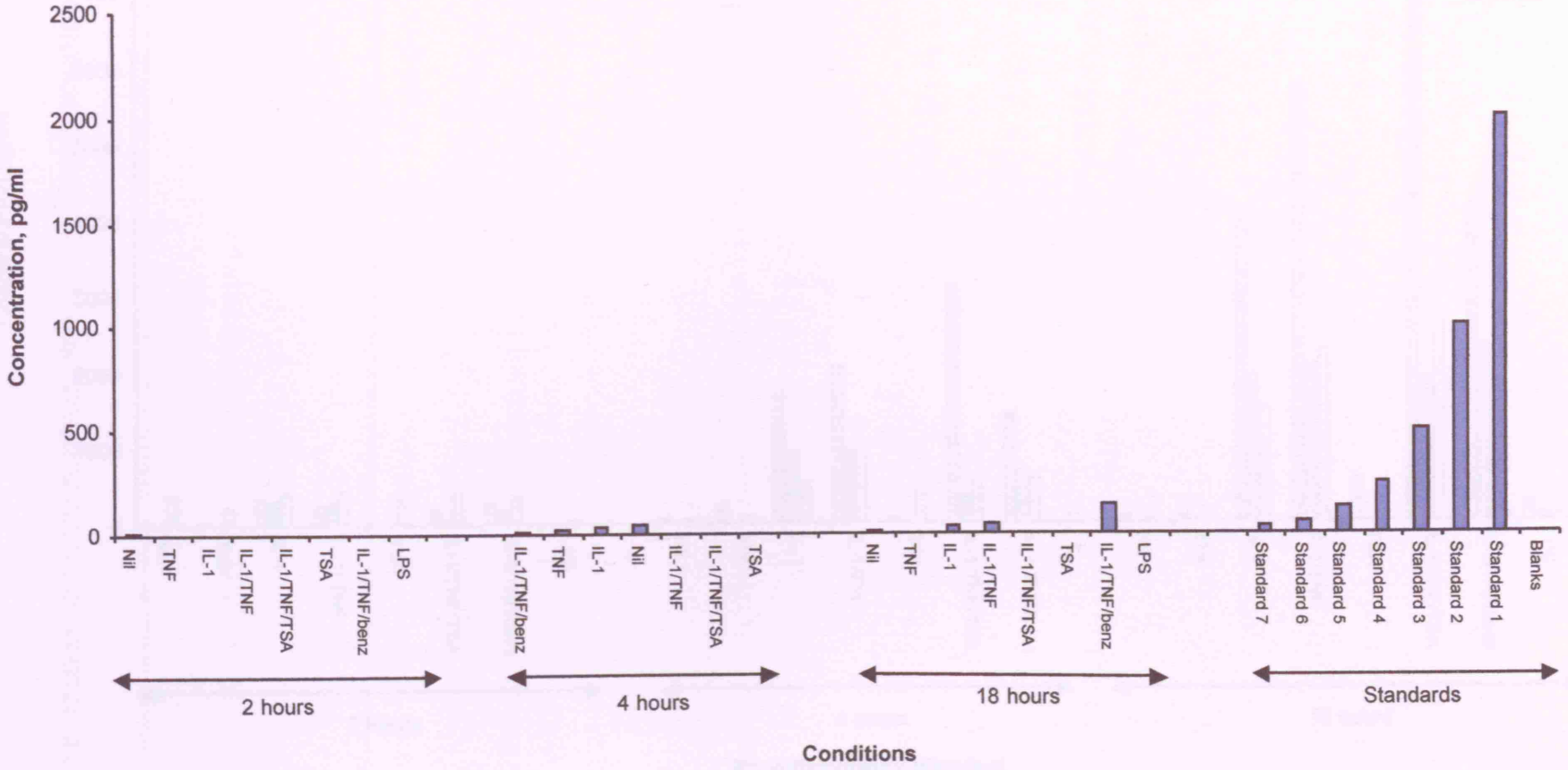

Graph 5.12 demonstrates no significant increase of CCL5 follwing pro-inflammatory stimulation.

Graph 5.13: Quantitative CCL20, CXCL1, CXCL8 and CCL5 protein concentration in stimulated Caco-2 cell supernatants at 2, 4, 18 hours

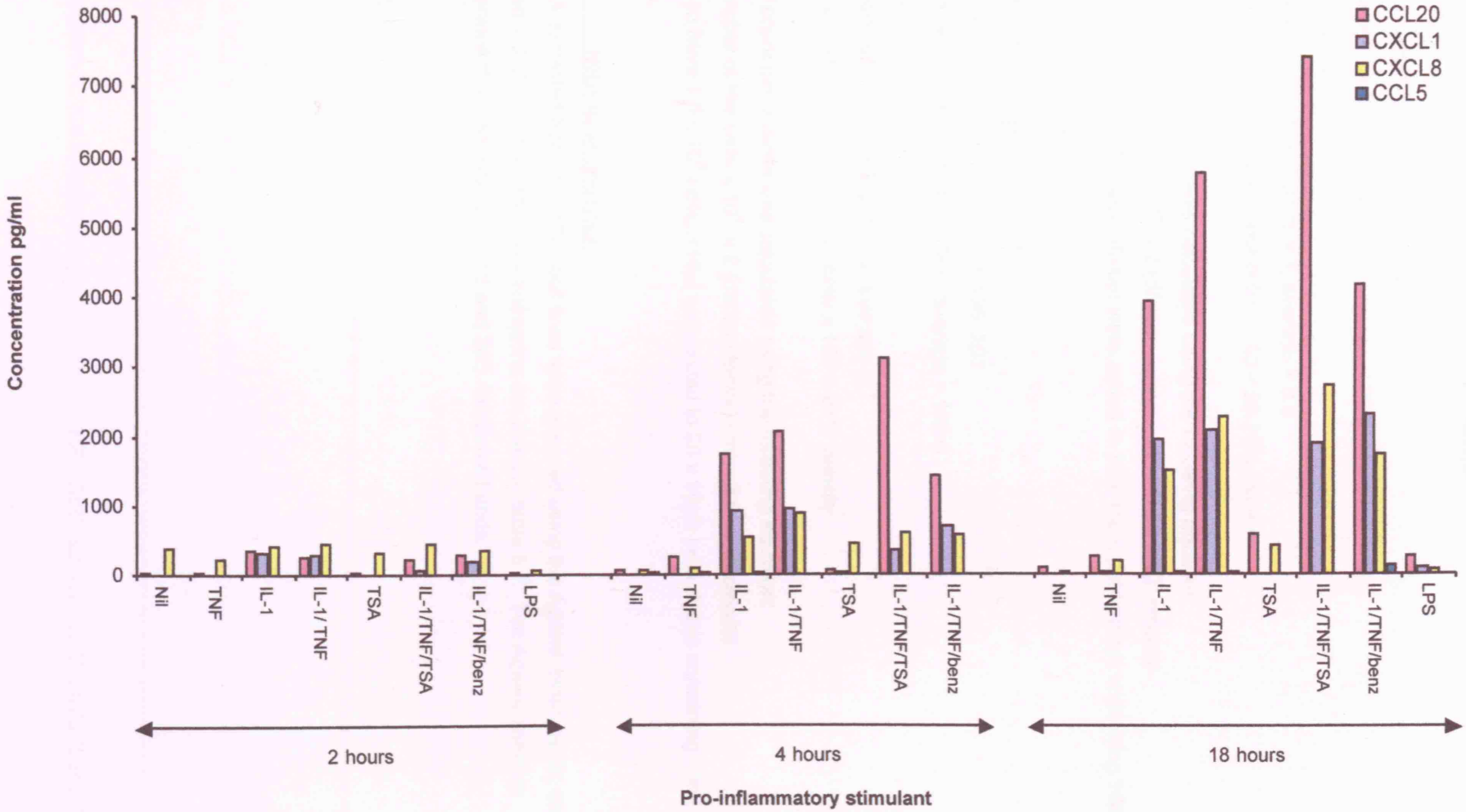

Graph 5.13 demonstrates that there is some synergy between IL-1 and TNF, althogh TNF alone had little chemokine stimulatory effect. TSA increases the induction of CCL20 and CXCL8. The ELISA data are consistent with the array data.

5.3 Coordinate chemokine response in stimulated HT29 cells

5.3.1 HT29 cell count and viability assessment

Cell counts for passage number 4:

Live cell counts: 71, 54, 77, 91, 72, 92

Total live cell count in 6 grids = 457, average = 76.2

Dead cell counts: 0, 0, 1, 1, 0, 1

Total dead cell counts in 6 grids = 3, average = 0.5

Number of live cells / total number cells x 100 = 99.25% viability

The cell count per volume was calculated using the following equation:

Total number of live cells x 10^4 x 2 (dilution factor) / ml = 1.523 x 10^6 cells/ml

In order to have 1.5 x 10^6 cells, 1000µl were added to 30 x 10cm petri dishes containing 10ml medium.

Cell counts for passage number 6:

Live cell counts: 193, 175, 170, 149, 196, 201

Total live cell count in 6 grids = 1084, average = 180.6

Dead cell counts: 2, 3, 3, 1, 6, 7

Total dead cell counts in 6 grids: 22, average 3.7

Number of live cells / total number cells x 100 = 98% viability

The cell count per volume was calculated using the following equation:

Total number of live cells x 10^4 x 2 (dilution factor) / ml = 3.6 x 10^6 cells/ml

In order to have 1.5 x 10^6 cells, 416µl was added to 20 x 10cm petri dishes containing 10ml medium.

5.3.2 RNA quantification

The RNA extracted from the HT29 cell lines were assayed using the Agilent bioanalyser, as described in 2.2.1.4. The RNA concentrations are listed in table 5.7. The Agilent analysis demonstrated the presence of the 18 and 28S ribosomal bands.

Table 5.7: Details of stimulatory conditions used in HT29 cell culture, corresponding with semi-quantified RNA concentrations (ng/μl) obtained via the Agilent bioanalyser.

Sample description	RNA Concentration (ng/μl)	rRNA ratio 28S/18S
Nil added, 2 hours	797.33	1.63
IL-1β added, 2hours	433.27	1.67
TNF-α added, 2 hours	1,630.55	1.54
IL-1β, TNF-α added, 2 hours	681.23	1.41
LPS added, 2 hours	835.04	1.53
IL-1β, TNF-α, LPS added, 2 hours	328.89	1.51
Nil added, 4 hours	628.22	1.55
IL-1β added, 4 hours	769.86	1.61
TNF-α added, 4 hours	1,115.40	1.47
IL-1β, TNF-α added, 4 hours	506.63	1.58
LPS added, 4 hours	683.45	1.56
IL-1β, TNF-α, LPS added, 4 hours	250.77	1.95
Nil added, 18 hours	250.77	1.85
IL-1β added, 18 hours	X	X
TNF-α added, 18 hours	374.57	1.83
IL-1β, TNF-α added, 18 hours	232.90	1.93
LPS added, 18 hours	418.25	1.78
IL-1β, TNF-α, LPS added, 18 hours	386.80	1.87

5.3.3 Microarray results

The semi-quantitative analysis of the hierarchical clustering data from the HT29 cells are listed in tables 5.8, and graph 5.14.

Table 5.8: 2-hour normalised chemokine expression levels of CXCL1, CXCL2, CXCL3, CXCL8, CXCL10, CCL20, actin from microarray analysis for HT29 cells stimulated with nil/IL-1β/ TNF-α/IL-1β + TNF-α/LPS

	Nil	IL-1β	TNF-α	IL-1β+ TNF-α	LPS
CXCL1	1.586165	49.95328	60.86593	75.93112	5.223268
CXCL2	2.871952	19.36857	33.51507	39.72311	3.486292
CXCL3	7.193405	19.60596	24.98065	49.98253	6.544003
CXCL8	-0.51834	10.85645	32.43581	32.48083	0.968629
CXCL10	0.628569	0.435182	4.89832	2.499823	3.929242
CCL20	2.314982	97.61907	71.88467	158.6681	2.840066
CCR6	4.577627	2.302553	1.2653346	-0.2269311	2.9717740
CXCR1	2.391939	5.3045107	2.680465	0.8087426	2.1499309
CXCR2	6.610192	13.163802	14.721554	5.9364542	39.030951
Actin 5' fragment	14.55392	32.01606	24.58444	31.50936	23.83024
Actin middle fragment	57.45671	62.58956	57.84549	50.97982	63.14721
Actin 3' fragment	601.1454	468.7162	504.2211	452.5112	536.5452

Graph 5.14: 2-hour chemokine expression levels from microarray analysis of HT29 cells post pro-inflammatory stimulation.

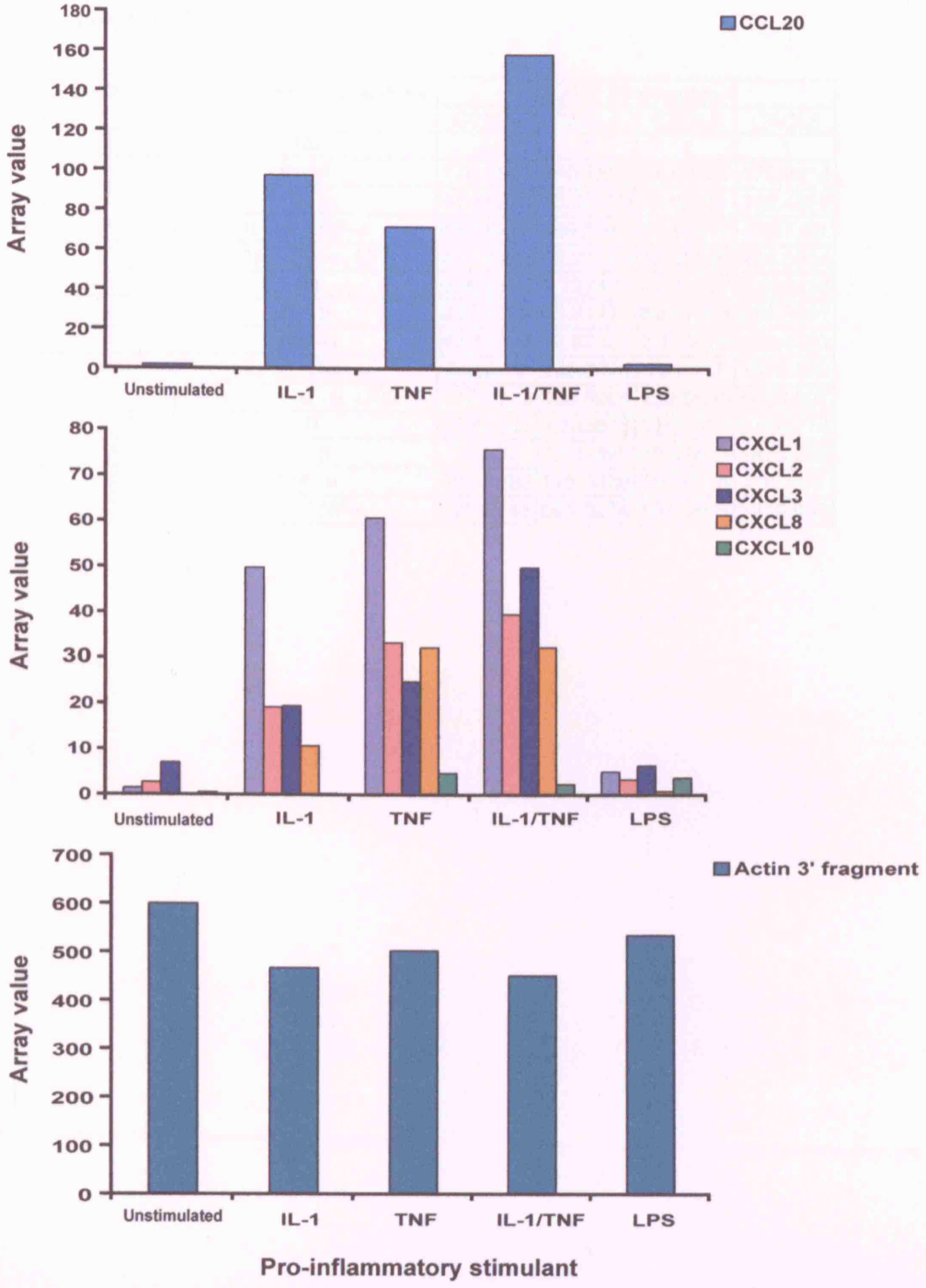

Graph 5.14 demonstrates HT29 CCL20, CXCL's1-3 and CXCL8 induction following pro-inflammatory stimulation with IL-1β or TNF-α at 2 hours as measured by microarray analysis.

5.3.4 RT-PCR results

RT-PCR was performed on the RNA extracted from HT29 cell lines, as outlined in 2.2.1.7. The normalised values are listed in table 5.9, and demonstrated in graphs 5.15-5.17.

Table 5.9: Normalised fold-up regulation RT-PCR values for CXCL1, CXCL3, CXCL8 and CCL20, expression in HT29.

Time course	Pro-inflammatory additive	RQ HT 29 passage 4			
		CCL20	CXCL1	CXCL3	CXCL8
2	Nil	1	1	1	1
2	IL-1β	174.5525	140.7896	14.00031	175.9414
2	TNF-α	47.56226	15.29799	5.48763	132.4978
2	IL-1β, TNF-α	683.8243	459.5944	95.86977	1267.09
2	IL-1β, TNF-α, LPS	411.7935	82.21789	12.56896	409.5934
4	Nil	0.895598	1.727407	0.851827	2.665434
4	IL-1β	229.2799	66.21771	89.47376	346.3661
4	TNF-α	49.52568	12.82535	2.193829	130.4483
4	IL-1β, TNF-α	2443.75	356.8128	70.2847	1668.959
4	IL-1β, TNF-α, LPS	1472.313	993.5055	239.5635	5680.307
18	Nil	11.91361	3.563675	3.051507	6.652774
18	IL-1β	303.37	223.068	89.67823	1476.205
18	TNF-α	195.1292	178.5325	35.08116	265.049
18	IL-1β, TNF-α	1024.741	591.3274	59.55605	1216.633

Graph 5.15: Line graphs to demonstrate correlation between RT-PCR and array expression values by HT29 cells after 2 hours of pro-inflammatory stimulation.

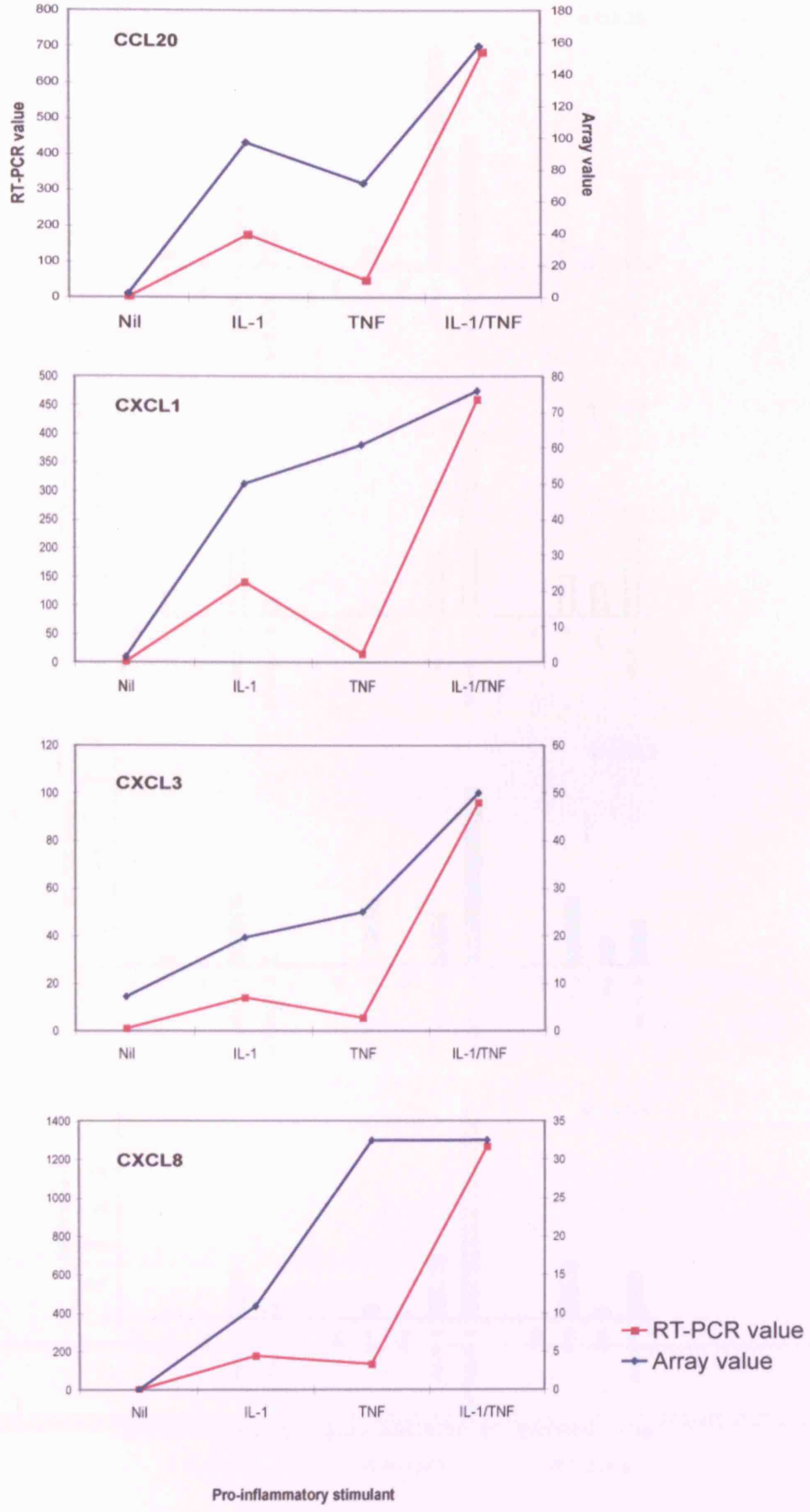

Graph 5.16: RT-PCR values of stimulated HT29 cells at 2, 4 and 18 hours.

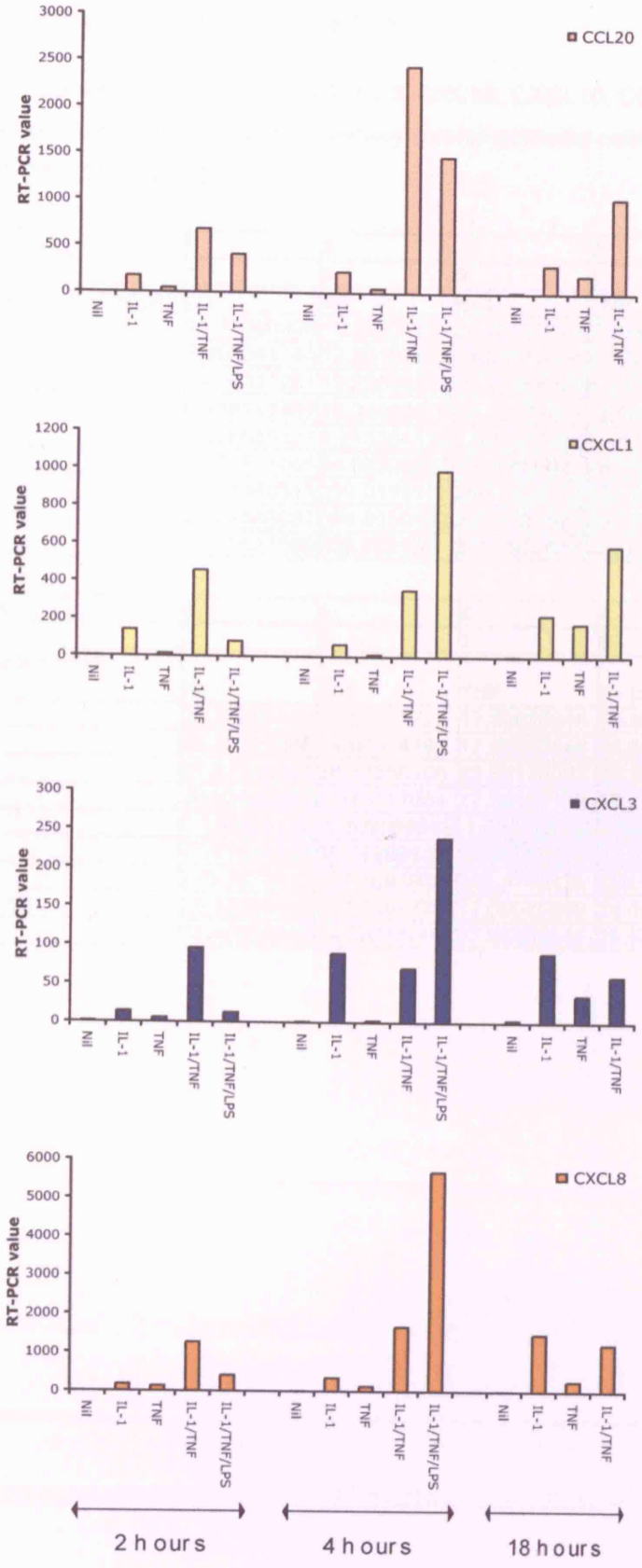

5.4 Coordinate chemokine response in stimulated primary colonic epithelial cells

5.4.1 Primary colonic epithelial microarray results

Primary colonic epithelial cells were stimulated as described in 2.2.8. The biopsies were obtained from patient 28-colonoscopy study 1. This patient had UC. The results are listed in table 5.10, and graphically represented in figure 5.18.

Table 5.10: 2-hour and 4-hour normalised CXCL's1-3, CXCL8, CXCL10, CCL20, actin expression levels from microarray analysis of primary colonic epithelial cells stimulated with nil/IL-1β/ TNF-α/IL-1β + TNF-α/LPS.

Time course/hours	0	2	2	2	2
Biopsy number	1	5	2	3	4
Pro-inflammatory stimulant added	Nil	Nil	IL-1	TNF	IL-1/TNF
CXCL1	11.71390996	16.25237251	26.88815023	7.998500368	13.41094027
CXCL2	7.452844743	12.26187669	34.23578404	9.072440884	12.86589912
CXCL3	14.56311281	13.23806823	25.70468803	6.467506899	18.65201113
CXCL8	0.736112437	15.34952078	20.70173331	-2.664901219	5.002822336
CXCL10	1.136656327	6.215564139	1.307367892	1.461915862	3.443612944
CCL20	50.07526005	54.62903667	62.4685502	26.57708272	45.30303621
Actin 5' fragment	221.4446311	319.3115157	266.1336972	303.4974205	293.7554165
Actin middle fragment	256.2545051	369.0150482	325.6331561	357.9816398	359.7262166
Actin 3' fragment	314.6521668	335.602133	321.7952687	305.0357647	328.1022808

Time course/hours	4	4	4	4
Biopsy number	5	6	7	8
Pro-inflammatory stimulant added	Nil	IL-1	TNF	IL-1/TNF
CXCL1	23.33895449	23.54861723	17.59025845	29.5593433
CXCL2	28.40928845	34.90314893	17.66992548	25.53070113
CXCL3	27.57243911	28.32888108	22.50170083	28.38968061
CXCL8	20.53198263	5.070117084	17.30169169	17.27517926
CXCL10	0.176854122	-1.309059842	-1.523826708	3.594699642
CCL20	77.81640803	98.79999832	69.99520015	91.9989934
Actin 5' fragment	276.3873915	287.4694929	342.4749435	329.1820721
Actin middle fragment	23.33895449	23.54861723	17.59025845	29.5593433
Actin 3' fragment	28.40928845	34.90314893	17.66992548	25.53070113

Graph 5.17: 2-hour and 4-hour chemokine expression levels from microarray analysis of primary colonic epithelial cells post pro-inflammatory stimulation.

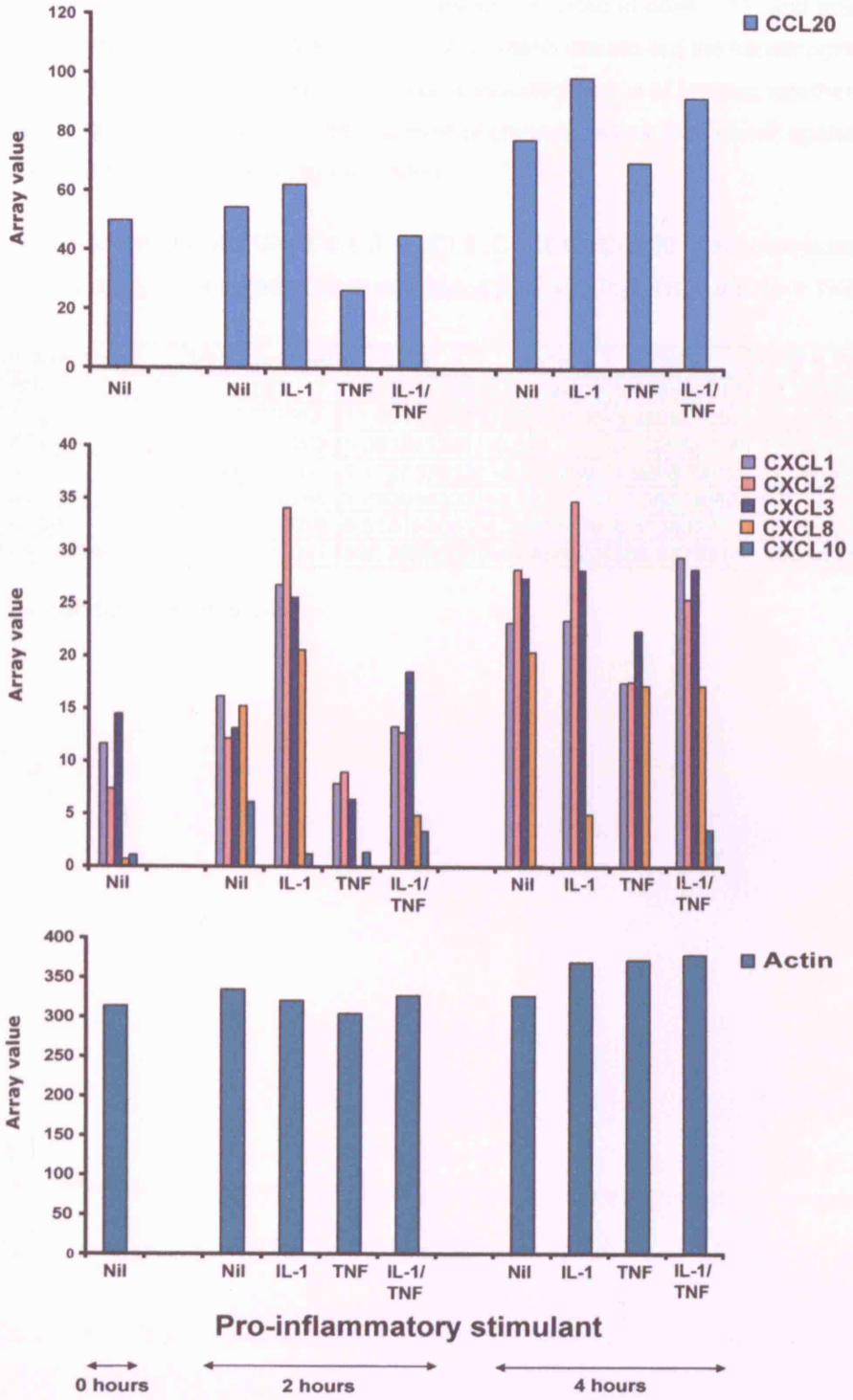

Graph 5.17 demonstrates induction of CCL20, CXCL's1-3 and CXCL8 in cultured primary colonic epithelial cells following stimulation with IL-1β or TNF-α. The results are of limited value as one set of biopsies were included in this study.

5.5 Coordinate chemokine response in stimulated keratinocytes and lung primary epithelial cells

Celltech group members found synergy between IL-1β and TNF-α for induction of CCL20, CXCL's 1-3 and CXCL8 in keratinocytes. The results are listed in table 5.11, and graphically represented in graph 5.19. Mr S Makh, at Slough Celltech carried out the keratinocyte cell culture (Platt et al, unpublished data). The data is included as it is of interest whether non-mucosal epithelial cells express the same subset of chemokines as the colonic epithelial cell lines in response to pro-inflammatory stimulation.

Table 5.11: 2-hour normalised CXCL's 1-3, CXCL8, CXCL10, CCL20, actin expression levels from microarray analysis of keratinocytes stimulated with nil/IL-1β/ TNF-α/IL-1β + TNF-α/LPS.

Keratinocytes	Unstimulated	LPS	IL-1β	TNF-α	IL-1β & TNF-α
CXCL1	1.244027117	8.418674185	0.80908809	3.903138313	27.33329233
CXCL2	2.42829663	11.46111481	0.58774196	3.388029297	16.49064534
CXCL3	4.072773202	5.361941931	-0.8211723	3.732954206	16.68859998
CXCL8	0.989548067	1.172053913	-0.983759	4.966839603	17.79189287
CXCL10	1.508698286	3.683946333	16.7870079	-2.56374663	1.072285562
CCL20	4.913642616	5.510163051	4.34605426	6.313833754	59.78933866
Actin 3' fragment	404.2506811	332.2600006	444.488623	388.6879314	408.931877

(18-hour data not available)

Graph; 5.18: 2-hour chemokine expression levels from microarray analysis of stimulated keratinocytes.

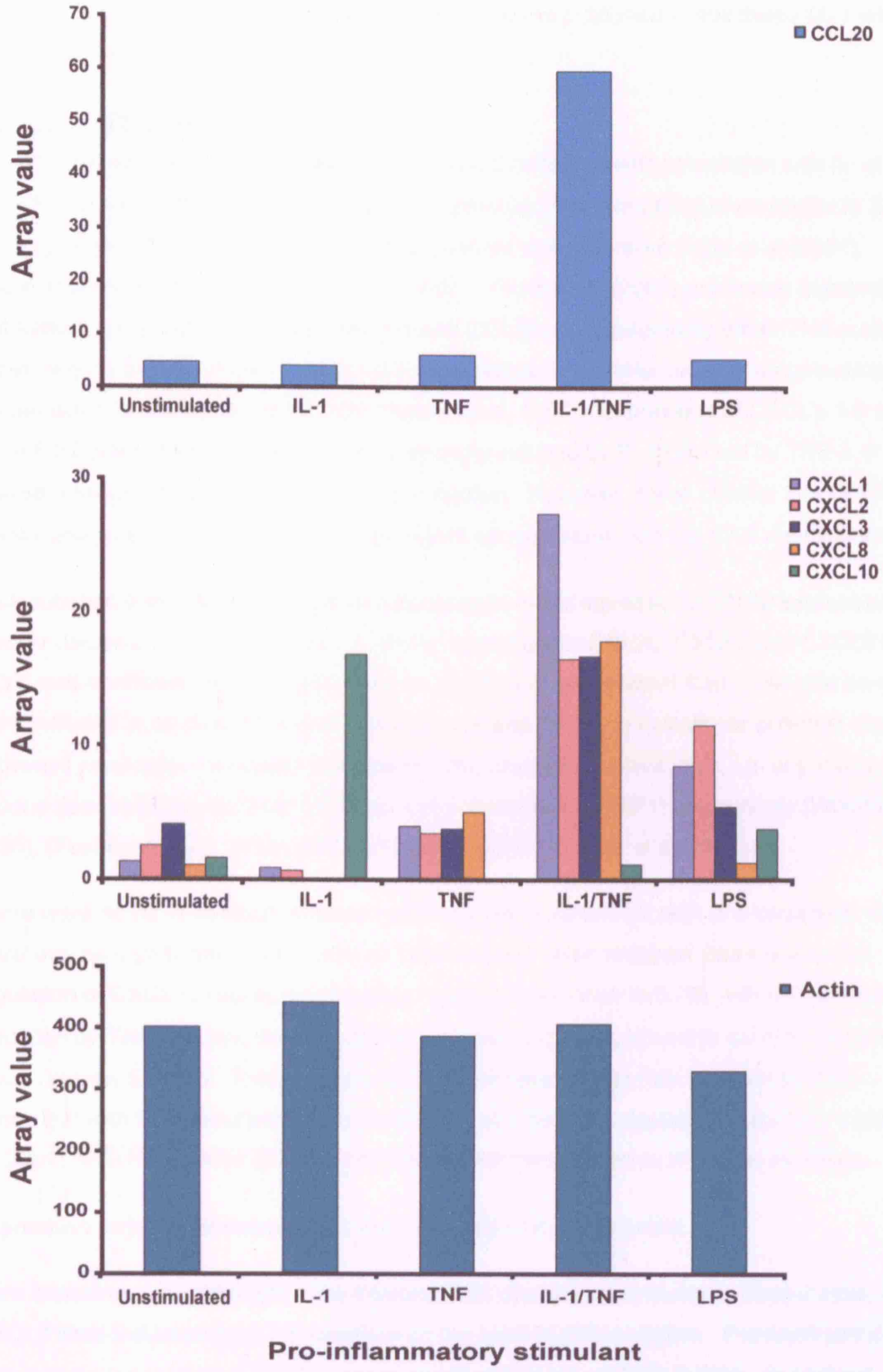

Graph 5.18 demonstrates synergy between IL-1β and TNF-α for induction of CCL20, CXCL's1-3 and CXCL8 in keratinocytes. The actin array levels were consistent.

Celltech group members found the same coordinated chemokine response following combined IL-1β and TNF-α stimulation of a lung epithelial primary cell line, human bronchial epithelium. This data is subject to company confidentiality, so is not published in this thesis (A. Platt et al, unpublished, personal communication).

5.6 Discussion

CCL20 expression was strongly induced in Caco-2 cells following stimulation with IL-1β but not by TNF-α or LPS, while levels of expression following dual stimulation were similar to IL-1β alone (graphs 5.1-5.4, 5.6, 5.13). This is consistent with data from Fujiie et al (2001), Izadapanah et al (2001), and Kwon et al (2002). Fujiie et al, (2001) previously demonstrated that human colon carcinoma cell lines express CCL20, up regulated by either TNF-α or IL-1β depending on lineage. Caco-2 cells secrete cytokines in a similar order of magnitude to that of normal isolated colonic epithelial cells (Huang et al, 1997). Expression of CXCL's 1-3 and CXCL8 followed the same pattern, being strongly induced by IL-1β but not by TNF-α or LPS, dual stimulation being equivalent to IL-1β induction. However, it was notable that CCL20 mRNA and protein showed substantially higher up regulation than the CXC chemokines.

Co-incubation with TSA resulted in an approximate 2-fold increase in CCL20 expression and a modest decrease in CXCL3 levels. A similar response for CCL20, CXCL1 and CXCL8 but not CCL5 was confirmed at the protein level on analysis of supernatant fluid. TSA and benzamide were included in co incubation studies with IL-1β and TNF-α to investigate potential regulatory pathways previously implicated in epithelial CXC chemokine production, i.e. any involvement of histone deacetylation and poly (ADP-ribose) polymerase (PARP1) respectively (Wood et al, 1995), (Fusunyan et al, 1999), (Ashburner et al, 2001), (Nirodi et al, 2001).

There were no other obvious induction of chemokine expression, with one exception: although there was no significant up regulation in inflamed IBD colon biopsies, there was an up regulation of CXCL10 expression by Caco-2 cells in response to IL-1β, with only a small induction by TNF-α alone, the dual stimulation resulting in a cumulative expression level at 18 hours (graphs 5.1-5.4). This induced CXCL10 expression was fully inhibited by TSA, consistent with its distinct pathway of induction via interferon regulatory factor (IRF)-3 (Kawai et al, 2001), which regulates gene expression by histone acetylation (Panja et al, 1998).

Expression levels of all chemokines were unaffected by benzamide.

Care should be taken though in the interpretation of expression levels in Caco-2 cells, as CXCL8 level induction by IL-1β depends on the level of differentiation. Pre-confluent Caco-2 cells can be induced by IL-1β to express significant levels of CXCL8 RNA. In contrast, differentiated post-confluent cells express much less CXCL8 mRNA in response to IL-1β (Huang et al, 1997). In order to ensure that the results were not merely anomalous to Caco-2 cells, HT29 cells study was important. The inflammatory response in Caco-2 cells, as in

isolated colonocytes, can be initiated by Il-1β but not TNF-α. This is in contrast to most other colon cancer cell lines, which respond to stimulation with either IL-1β or TNF-α.

In contrast to Caco-2 cells, stimulation of HT-29 cells with TNF-α resulted in a significant induction of CCL20 expression (graph 5.14) consistent with previous observations (Izadapanah et al, 2001), (Kwon et al, 2002). IL-1β and IL-1β+TNF-α stimulation also resulted in a significant up regulation of CCL20, although dual stimulation was not synergistic. Expression of CXCL's 1-3 and CXCL8 was significantly induced following treatment with either IL-1β, TNF-α, or IL-1β and TNF-α together. No other chemokine was observed to significantly up regulated following treatment with IL-1β and/or TNF-α.

The primary colonic epithelial cell cultures results were of limited value, as biopsies were only included from one patient. This was undertaken as a pilot study rather than for purposes of scientific conclusions.

Keratinocyte cell culture studies were undertaken to determine if non-mucosal epithelial cells expressed the same subset of chemokines as stimulated Caco-2 and HT-29 cells. In contrast to the Caco-2 cells, IL-1β alone did not stimulate significant levels of expression of CXCL's1-3, CXCL8 and CCL20 in primary keratinocytes, but simultaneous stimulation with TNF-α did induce the coordinated chemokine response. This is consistent with Nakayama et al (2001), who demonstrated greatly increased levels of CCL20 expression when keratinocytes were stimulated with IL-1β and TNF-α in concert.

The same coordinated chemokine response was seen following combined IL-1β and TNF-α stimulation of a lung epithelial primary cell line, human bronchial epithelium (A. Platt et al, unpublished, personal communication).

Graph 5.17: 2-hour and 4-hour chemokine expression levels from microarray analysis of primary colonic epithelial cells post pro-inflammatory stimulation.

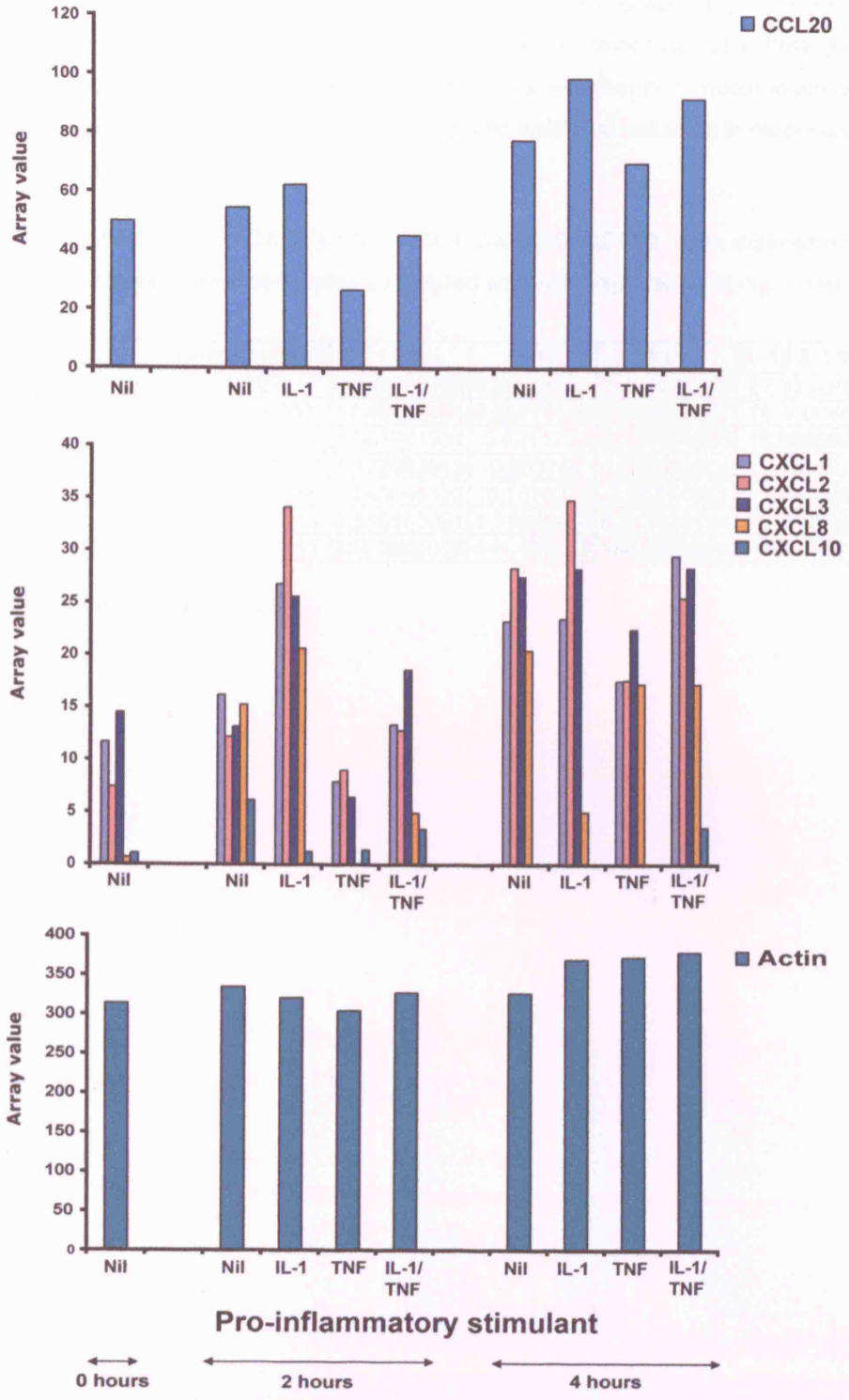

Graph 5.17 demonstrates induction of CCL20, CXCL's1-3 and CXCL8 in cultured primary colonic epithelial cells following stimulation with IL-1β or TNF-α. The results are of limited value as one set of biopsies were included in this study.

5.5 Coordinate chemokine response in stimulated keratinocytes and lung primary epithelial cells

Celltech group members found synergy between IL-1β and TNF-α for induction of CCL20, CXCL's1-3 and CXCL8. The results are listed in table 5.11, and graphically represented in graph 5.19. Mr S Makh, at Slough Celltech carried out the keratinocyte cell culture (Platt et al, unpublished data). The data is included as it is of interest whether non-mucosal epithelial cells express the same subset of chemokines as the colonic epithelial cell lines in response to pro-inflammatory stimulation.

Table 5.11: 2-hour normalised CXCL's1-3, CXCL8, CXCL10, CCL20, actin expression levels from microarray analysis of keratinocytes stimulated with nil/IL-1β/ TNF-α/IL-1β + TNF-α/LPS.

Keratinocytes	Unstimulated	LPS	IL-1β	TNF-α	IL-1β & TNF-α
CXCL1	1.244027117	8.418674185	0.80908809	3.903138313	27.33329233
CXCL2	2.42829663	11.46111481	0.58774196	3.388029297	16.49064534
CXCL3	4.072773202	5.361941931	-0.8211723	3.732954206	16.68859998
CXCL8	0.989548067	1.172053913	-0.983759	4.966839603	17.79189287
CXCL10	1.508698286	3.683946333	16.7870079	-2.56374663	1.072285562
CCL20	4.913642616	5.510163051	4.34605426	6.313833754	59.78933866
Actin 3' fragment	404.2506811	332.2600006	444.488623	388.6879314	408.931877

(18-hour data not available)

Graph; 5.18: 2-hour chemokine expression levels from microarray analysis of stimulated keratinocytes.

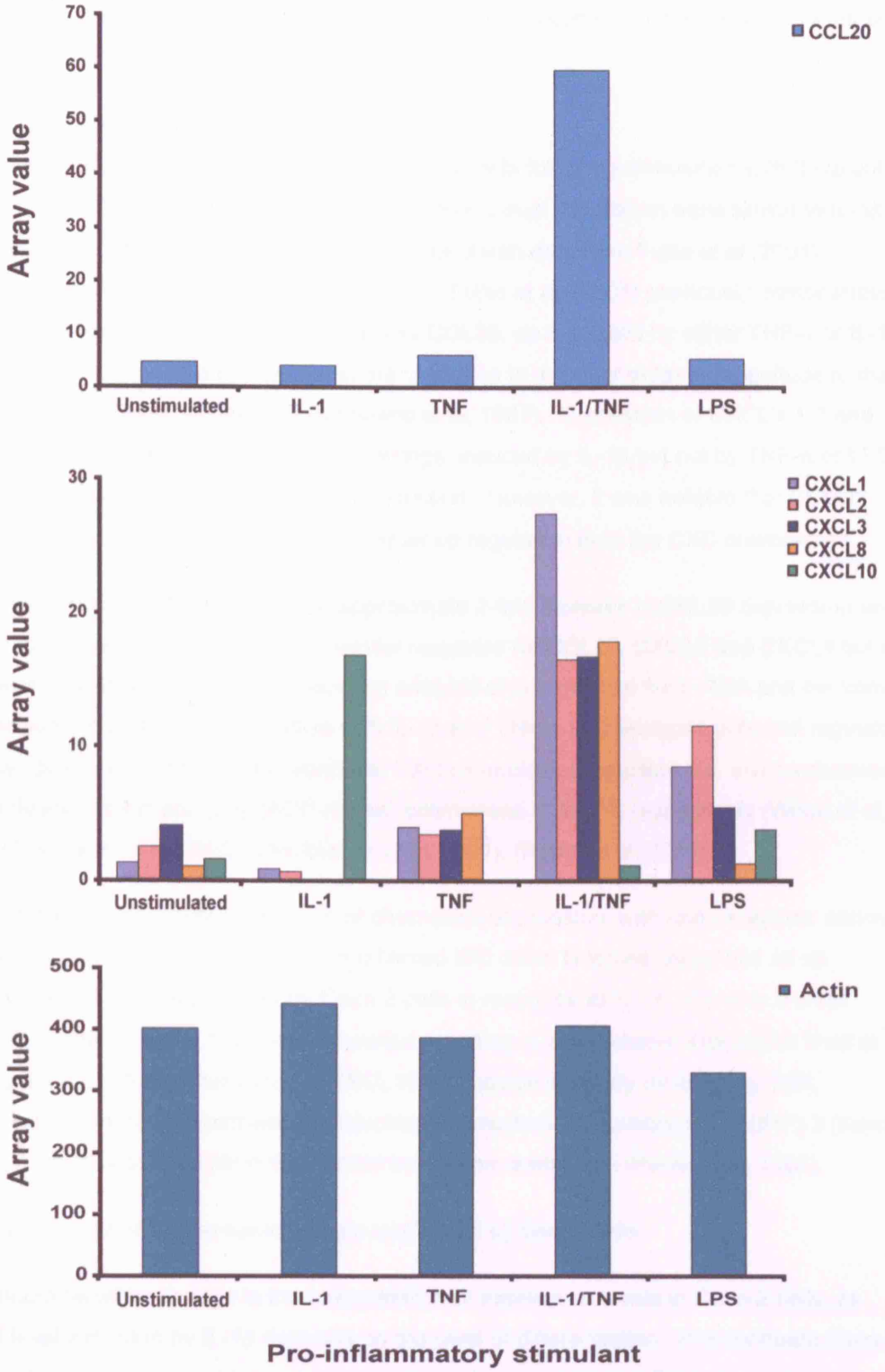

Graph 5.18 demonstrates synergy between IL-1β and TNF-α for induction of CCL20, CXCL's1-3 and CXCL8 in keratinocytes. The actin array levels were consistent.

Celltech group members found the same coordinated chemokine response following combined IL-1β and TNF-α stimulation of a lung epithelial primary cell line, human bronchial epithelium. This data is subject to company confidentiality, so is not published in this thesis (A . Platt et al, unpublished, personal communication).

5.6 Discussion

CCL20 expression was strongly induced in Caco-2 cells following stimulation with IL-1β but not by TNF-α or LPS, while levels of expression following dual stimulation were similar to IL-1β alone (graphs 5.1-5.4, 5.6, 5.13). This is consistent with data from Fujiie et al (2001), Izadapanah et al (2001), and Kwon et al (2002). Fujiie et al, (2001) previously demonstrated that human colon carcinoma cell lines express CCL20, up regulated by either TNF-α or IL-1β depending on lineage. Caco-2 cells secrete cytokines in a similar order of magnitude to that of normal isolated colonic epithelial cells (Huang et al, 1997). Expression of CXCL's 1-3 and CXCL8 followed the same pattern, being strongly induced by IL-1β but not by TNF-α or LPS, dual stimulation being equivalent to IL-1β induction. However, it was notable that CCL20 mRNA and protein showed substantially higher up regulation than the CXC chemokines.

Co-incubation with TSA resulted in an approximate 2-fold increase in CCL20 expression and a modest decrease in CXCL3 levels. A similar response for CCL20, CXCL1 and CXCL8 but not CCL5 was confirmed at the protein level on analysis of supernatant fluid. TSA and benzamide were included in co incubation studies with IL-1β and TNF-α to investigate potential regulatory pathways previously implicated in epithelial CXC chemokine production, i.e. any involvement of histone deacetylation and poly (ADP-ribose) polymerase (PARP1) respectively (Wood et al, 1995), (Fusunyan et al, 1999), (Ashburner et al, 2001), (Nirodi et al, 2001).

There were no other obvious induction of chemokine expression, with one exception: although there was no significant up regulation in inflamed IBD colon biopsies, there was an up regulation of CXCL10 expression by Caco-2 cells in response to IL-1β, with only a small induction by TNF-α alone, the dual stimulation resulting in a cumulative expression level at 18 hours (graphs 5.1-5.4). This induced CXCL10 expression was fully inhibited by TSA, consistent with its distinct pathway of induction via interferon regulatory factor (IRF)-3 (Kawai et al, 2001), which regulates gene expression by histone acetylation (Panja et al, 1998).

Expression levels of all chemokines were unaffected by benzamide.

Care should be taken though in the interpretation of expression levels in Caco-2 cells, as CXCL8 level induction by IL-1β depends on the level of differentiation. Pre-confluent Caco-2 cells can be induced by IL-1β to express significant levels of CXCL8 RNA. In contrast, differentiated post-confluent cells express much less CXCL8 mRNA in response to IL-1β (Huang et al, 1997). In order to ensure that the results were not merely anomalous to Caco-2 cells, HT29 cells study was important. The inflammatory response in Caco-2 cells, as in

isolated colonocytes, can be initiated by Il-1β but not TNF-α. This is in contrast to most other colon cancer cell lines, which respond to stimulation with either IL-1β or TNF-α.

In contrast to Caco-2 cells, stimulation of HT-29 cells with TNF-α resulted in a significant induction of CCL20 expression (graph 5.14) consistent with previous observations (Izadapanah et al, 2001), (Kwon et al, 2002). IL-1β and IL-1β+TNF-α stimulation also resulted in a significant up regulation of CCL20, although dual stimulation was not synergistic. Expression of CXCL's 1-3 and CXCL8 was significantly induced following treatment with either IL-1β, TNF-α, or IL-1β and TNF-α together. No other chemokine was observed to significantly up regulated following treatment with IL-1β and/or TNF-α.

The primary colonic epithelial cell cultures results were of limited value, as biopsies were only included from one patient. This was undertaken as a pilot study rather than for purposes of scientific conclusions.

Keratinocyte cell culture studies were undertaken to determine if non-mucosal epithelial cells expressed the same subset of chemokines as stimulated Caco-2 and HT-29 cells. In contrast to the Caco-2 cells, IL-1β alone did not stimulate significant levels of expression of CXCL's1-3, CXCL8 and CCL20 in primary keratinocytes, but simultaneous stimulation with TNF-α did induce the coordinated chemokine response. This is consistent with Nakayama et al (2001), who demonstrated greatly increased levels of CCL20 expression when keratinocytes were stimulated with IL-1β and TNF-α in concert.

The same coordinated chemokine response was seen following combined IL-1β and TNF-α stimulation of a lung epithelial primary cell line, human bronchial epithelium (A. Platt et al, unpublished, personal communication).

Chapter 6

Flow cytometric analysis on mucosally derived cells

6.1 Background

6.2 Results

6.3 Discussion

6.1 Background

Tissue was taken from surgically removed colon, from patients with IBD or colonic carcinoma. In the former, 2 square cm of tissue were taken from 3 separate areas. In the latter, 1 square cm was taken from 1 normal area. This was done with full consent of the patients, and with full ethical approval.

Flow cytometric analysis was performed on mucosally derived cells extracted from 3 colectomy specimens (1 uninflamed control, requiring resection for colon carcinoma, 1 with UC and 1 with CD). The method used is described in 2.2.5. Several sites were examined from each specimen, including both severely inflamed and mildly inflamed areas from both IBD specimens.

6.2 Results

Separate examination of both lamina propria and epithelial compartments showed widespread expression of the cognate chemokine receptors in both inflamed and control tissue, involving antigen presenting cells, B and T lymphocytes and monocytes. The intensity of CCL20 expression on epithelial cells was enhanced in IBD specimens, particularly in severe disease (graph. 6.1A). Increased percentages of $CCR6^+$ CD14 cells, and $CXCR1^+$ and $CXCR2^+$ cells of all lineages were detected. In addition to $CD45^+$ leukocytes (graph 6.1 B, C, D), CXCR's 1 and 2 were expressed on CD3, CD4 and CD8 T cells, CD19 B cells, and CD138 plasma cells, in addition to CD14 monocytes and cells expressing Fcγ receptors I and II (CD16, CD32) and CD86. The proportion of $CCR6^+$ cells was lower, except amongst antigen presenting cells, but $CCR6^+$ cells were identified in both T and B cells compartments and monocytes.

6.3 Discussion

The cognate receptors for the chemokine subset, CXCR1, CXCR2 and CCR6, were up regulated on T and B lymphocytes, macrophages, polymorph neutrophils and antigen presenting cells.

Graph 6.1: Flow cytometric analysis of chemokine and ligand expression in normal colon compared to CD (mildly inflamed and severe) and UC (mildly inflamed and severe), including CCL20, CCR6, CXCR1, CXCR2.

A. CCL20 in cytokeratin$^+$ colonocytes. Compared to normal colonocytes, there is substantially increased frequency of CCL20$^+$ cells in active IBD, with further increase in severely inflamed tissue.

B. CCR6 expression in lamina propria CD14$^+$ cells, showing increase in severe UC.

C. CXCR1 expression is increased on CD45$^+$ lamina propria cells in active disease.

D. CXCR2 expression shows similar increase amongst CD45$^+$ lamina propria cells in active disease.

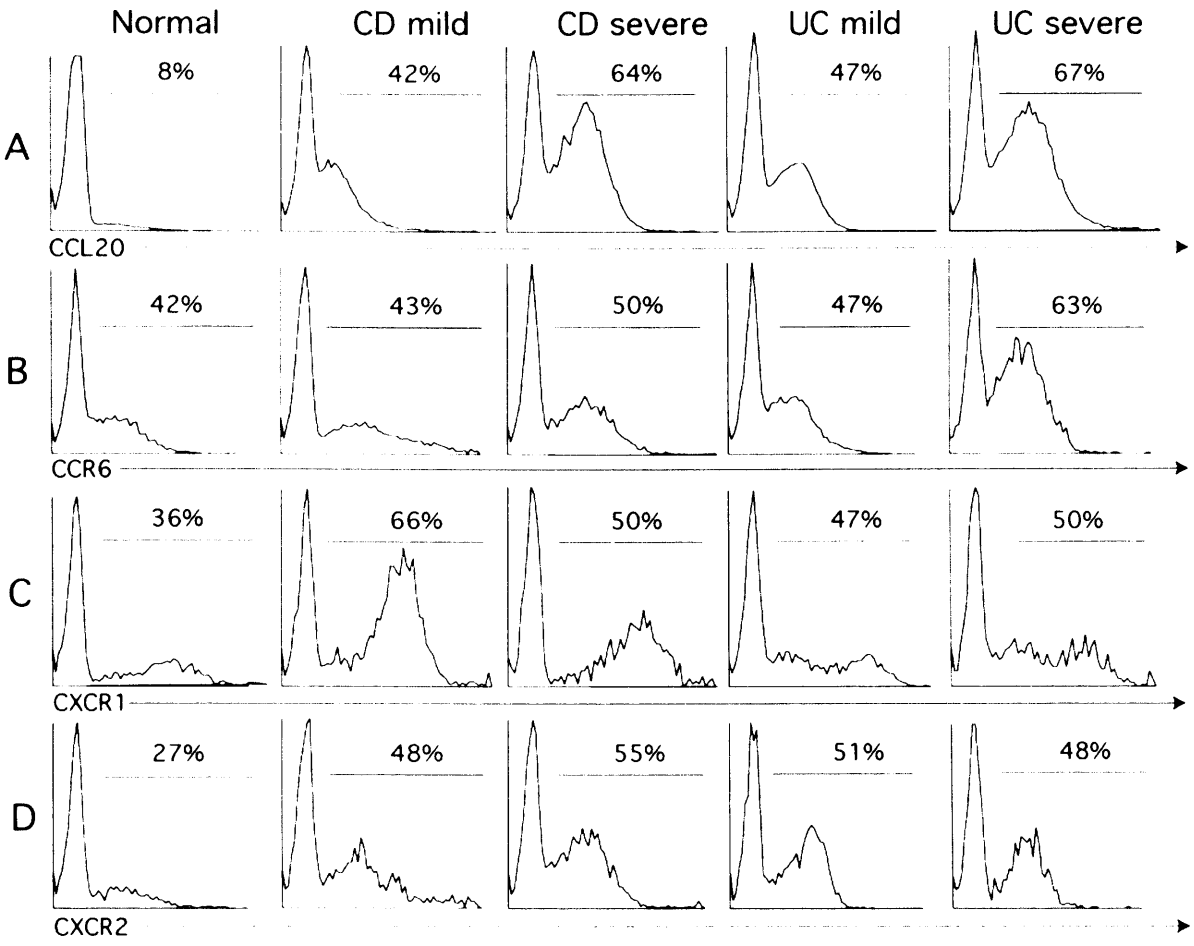

Chapter 7

Immunohistochemical localisation and quantification of CCL20 and CCR6 in necrotising enterocolitis, using the immunoperoxidase technique

7.1 Background

7.2 H&E and immunohistochemical staining of NEC and control tissue to investigate potential immune-neural interactions

7.3 Results

7.4 Discussion

7.1 Background

Necrotising enterocolitis (NEC) is a necrotic ulcerative bowel disorder in neonates. Approximately 50% of babies developing NEC require surgery, and the mortality rate of NEC is 20-40%. Of those who survive, approximately 25% develop long term sequelae. Research into this condition is therefore of great importance.

The aetiology is unknown, although predisposing factors include: extreme prematurity, formula feeds, dysmotility, reduced mesenteric blood flow, dysbiosis. Ninety percent of babies with NEC are pre-term.

Several groups are currently investigating the fundamental centrality of ganglionic nerve plexus pathology as a potential primary cause of the disorder. NEC-like lesions have been induced experimentally by targeted deletion of enteric glial cells in transgenic mice (Bush et al, 1998). Two groups have found a characteristic loss of nerve cells within the plexus, with absence of vasoactive intestinal polypeptide and nitric oxide synthetase (Sigge et al, 1998), (Wedel et al, 1998).

There are a number of features in common with IBD, such as the characteristic mucosal ulceration. As the receptor/ligand pair CCL20/CCR6 are of pivotal importance in IBD, their expression in necrotising enterocolitis is of great interest.

7.2 H&E and immunohistochemical staining of NEC and control tissue to investigate potential immune-neural interactions

The paediatric gastroenterology group at the Royal Free Hospital have been studying potential immune-neural interactions, including lymphocyte infiltrate, neural structures, and glial cells using immunohistochemical staining of the following:

- *Immunological:* CD3 (T cell marker), HLA-DR (Class II MHC), IL-12 (Th1-assocaited cytokine, TGF-β (regulatory cytokine)
- *Neural / glial:* Glial Fibrillary Acidic Protein (GFAP), Nerve Growth Factor Receptor (NGFR), Neural Fibrillary Protein (NFP), Neuron Specific Enolase (NSE)

The method used is as described in 2.2.3, by a member of the paediatric research group, Dr Fagbemi. The study cohort included 20 infants with NEC, (mean gestation 29 weeks (25-33), body weight 1050g (500-2340), surgery at 17 days (3-41); 11 small bowel, 8 ileocaecal, 1 colonic resection, and follow-up specimens at ileostomy closure in 8. The non-NEC controls included 13 pre-term infants (33-38 weeks gestation, 2000-2980g) who required intestinal resection (1-60 days); 6 with small bowel atresia, 4 with perforation, 2 with mesenteric infarction and 1 with bowel stenosis. In view of the demonstrated mucosal significance of CCL20/CCR6 in IBD, the sections were also stained for CCL20 and CCR6 using the methods described in 2.2.3.

7.3 Results

Microscopic examination of H&E stained bowel sections, and immunohistochemically-stained sections for neural fibrillary protein and neural growth factor (NGFR) enabled identification of a number of differences between NEC and control sections, as demonstrated in figure 7.1-7.3. The myenteric and submucous plexi were intact in all controls, although there was neural disruption observed in NEC cases, with intact innervation in 8/20, loss of submucus plexi and mucosal nerves in 10/20, patchy loss in 2/20. In NEC, there was submucosal neural disruption associated with loss of glial cells in myenteric plexus, and a focal lymphocyte infiltration seen in myenteric plexi. Neural disruption was not related to disease severity seen even if inflammation was apparently limited to mucosa. The neural disruption was strongly associated with myenteric plexus abnormalities.

Immunohistochemical staining of CCR6 and CCL20 demonstrated expression in NEC (figure 7.4, tables 7.1, 7.2). Follow-up at ileostomy closure demonstrated normal innervation pattern in 6/8. There was persistent disruption in 2/8, with a complex course with recurrent NEC and persistent glial CCL20 expression (negative in the other 6 cases).

7.4 Discussion

There was perineural T cell infiltration and glial disruption occurred in the myenteric plexus of 12/20 infants with NEC. This response was focal, associated with disruption of the submucosal plexi and mucosal nerves. Glial cells were immunoreactive for effector cytokines and chemokines: CCL20 is a potential cause of T cell infiltration. These changes may contribute to dysmotility and inflammation in NEC. Experimental data suggests that glial loss alone may induce NEC-like lesion, and raises the possibility of primary neural pathology in some cases. The cause for the focal glial CCL20 expression and T cell infiltration remain uncertain, though viral infection more likely than bacterial translocation. Chronic cases may be autoimmune related.

Figure 7.1: Histological examination of H&E stained bowel sections, demonstrating a lymphocyte infiltrate in myenteric plexus in NEC.

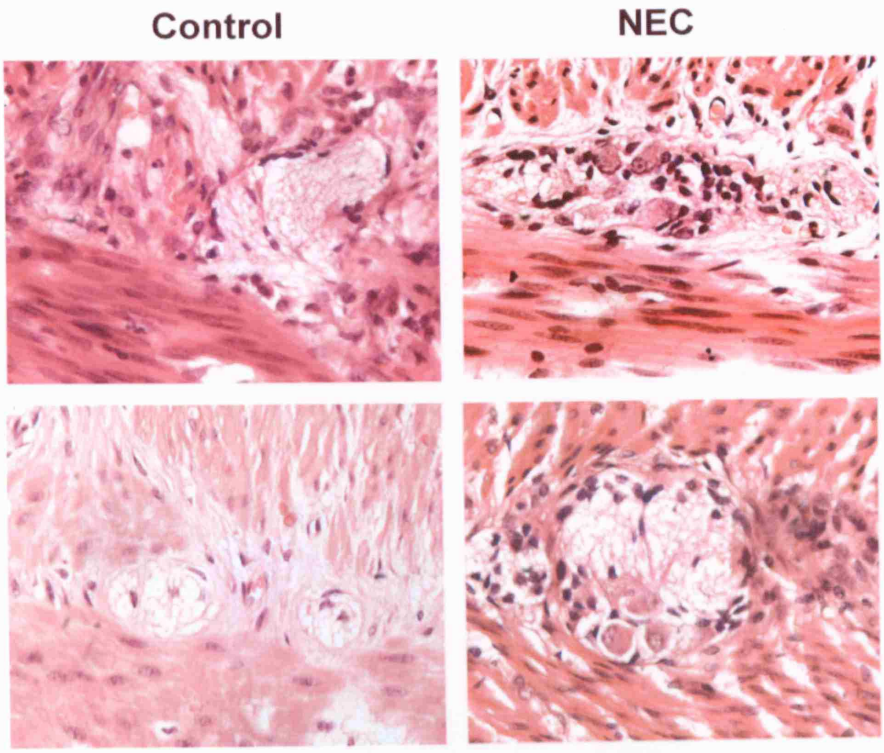

Figure 7.2: Immunohistochemical staining of neural fibrillary protein demonstrating normal innervation in a control patient.

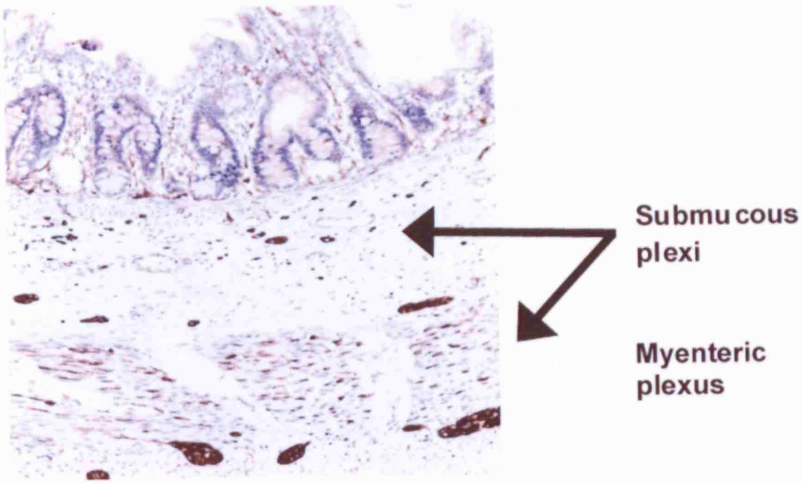

Figure 7.3: Immunohistochemical staining demonstrating neural disruption strongly associated with myenteric plexus abnormalities.

Control: NGFR staining

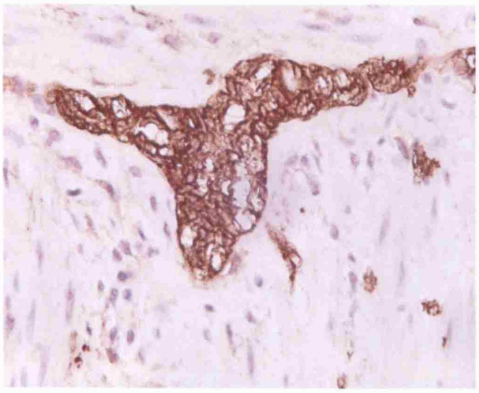

NEC – intact innervation

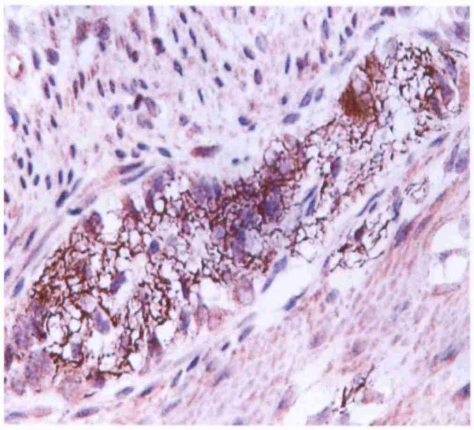

NEC –disrupted innervation

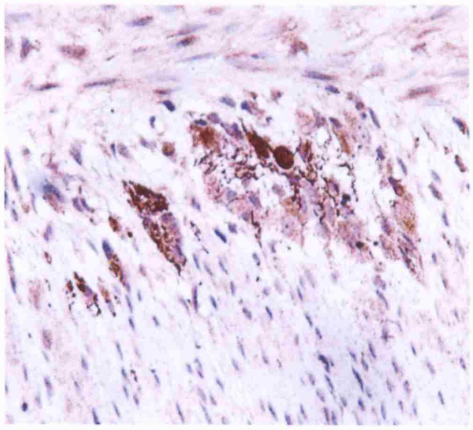

Figure 7.4: Immunohistochemical straining demonstrating constitutive CCR6 and CCL20 expression in NEC.

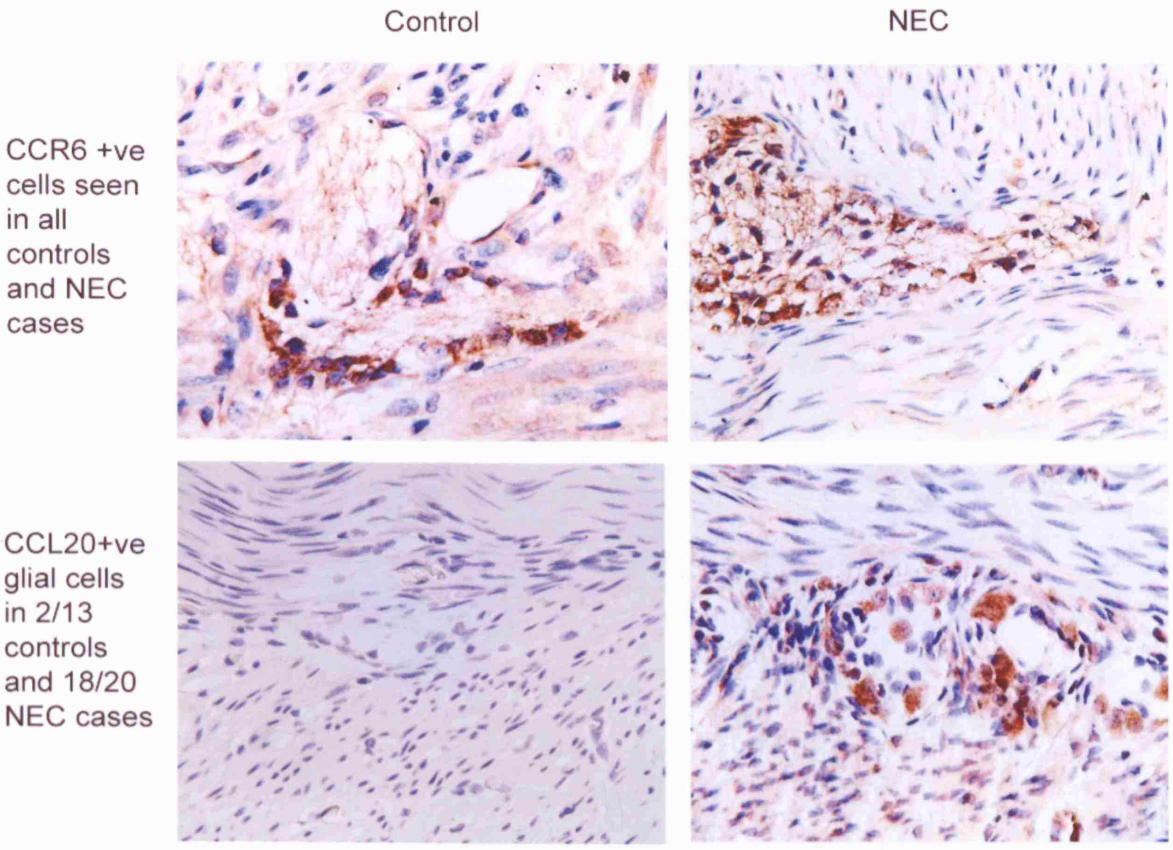

Table 7.1: CCL20 immunohistochemical scores of NEC and control samples.

Patient number	Diagnosis	Sample details	Surface epithelium	Crypt epithelium	Microglial intensity	Number of +ve cells in plexus	% plexi +ve	Superficial lamina propria	Deep lamina propria
1	NEC	NEC, small bowel resection, day 0	3	3	2.5	8	60	3	2
2	NEC		3	3	3	8	70	2.5	2.5
3	NEC		X	X	2	8	50	3	3
4	NEC	NEC, day 7 colon biopsy	X	X	X	X	X	X	X
5	NEC	NEC, ileum	3	2	3	8	85	3	3
6	NEC	NEC, small bowel	2	2	2	7	25	2	2.5
7	NEC	NEC, small bowel	2	2	2	6	30	2	2
8	NEC	NEC, small bowel	2	2	3	12	70	3	3
9	NEC		2	2	2.5	12	65	2	2
10	NEC	NEC, ileum and caecum	3	3	2.5	9	65	3	2
11	NEC		3	2	2	8	30	3	2
12	NEC	NEC, terminal ileum	X	2	2	5	50	3	2
13	NEC	NEC, small bowel	2.5	2.5	2.5	9	80	2.5	2.5
14	NEC	NEC, large bowel	X	X	X	X	X	X	X
15	NEC Day 0	NEC, small bowel resection, day 0	X	X	3	10	80	X	X
1	NEC Day 0	NEC, small bowel resection, day 0	X	X	X	X	X	X	X
16	NEC Day 0	NEC, small bowel resection	2	2	2.5	10	75	3	2
16	NEC Day 0	NEC, Large bowel resection	2.5	2.5	3	10	40	3	2.5
17	NEC Day 4	NEC, small bowel resection	3	3	X	X		3	3
18	NEC closure	NEC, small bowel resection, closure	3	2	3	14	70	3	2.5
19	NEC closure	NEC, closure, small bowel resection, closure	3	2	2.5	7	30	3	2
20	NEC closure	NEC, small bowel resection, closure	X	X	X	X	X	X	X
17	NEC closure	NEC, small bowel resection, closure	X	X	X	X	X	X	X
17	NEC closure	NEC, small bowel resection, closure	X	X	X	X	X	X	X
1	NEC closure	NEC, small bowel resection, day 0 closure	2	2	1	0	2	2	2
21	Control	Isolated caecal perforation, normal small bowel	1	2	1	0	2	1	1
22	Control	Small bowel atresia	3	3	1	0	2	1	1
22	Control	Small bowel atresia	X	X	X	X	X	X	X
23	Control	Small bowel infarction	2	2	1	3	5	2.5	1
24	Control	Jejunal stenosis	1	1	2	7	15	2	2
25	Control	Intestinal atresia type iv	1	1	2	5	5	2	1
26	Control	Jejunal atresia	4	3	2	9	45	3	2.5
26	Control	Jejunal atresia	1	1	1	0	2	1	1
27	Control	Small bowel infarction	2	1	1	3	5	1	1
28	Control		3	3	3	6	20	3	3
29	Control		3	3	2	8	10	2	2
30	Control		3	3	2	7	10	3	3
	CD	Large bowel	X	X	X	X	X	X	X
	CD	Large bowel	3	3	3	10	70	2	2
	CD	Large bowel	3	3	3	14	80	4	3
	UC	Large bowel	2.5	3	3	15	40	2	2
	UC	Large bowel	X	X	X	X	X	X	X
	UC	Large bowel	3	3	10	70	2	2	UC

Table 7.2: CCR6 immunohistochemical scores of NEC and control samples.

Patient number	Diagnosis	Sample details	Surface epithelium	Crypt epithelium	Microglial intensity	Number of +ve cells in plexus	% plexi +ve	Superficial lamina propria	Deep lamina propria
1	NEC	NEC, small bowel resection, day 0	X	X	X	X	X	X	X
2	NEC		X	X	X	X	X	X	X
3	NEC		X	X	X	X	X	X	X
4	NEC	NEC, day 7 colon biopsy	3	2	3	5	60	2.5	3
5	NEC	NEC, ileum	2	2	4	15	90	3	3
6	NEC	NEC, small bowel	No epithelium	No epithelium	2	8	50	3	3
7	NEC	NEC, small bowel	1	2	4	20	70	2	3
8	NEC	NEC, small bowel	2	2	4	20	80	3	3
9	NEC		2	2	3	8	60	3	3
10	NEC	NEC, ileum and caecum	2	2	3	17	70	2	2
11	NEC		2	2	3	12	85	2	3
12	NEC	NEC, terminal ileum	3	3	3	12	20	3	2
13	NEC	NEC, small bowel	2	2	4	35	95	3	3
14	NEC	NEC, large bowel	No epithelium	3	3	25	90	3	3
15	NEC Day 0	NEC, small bowel resection, day 0	No epithelium	No epithelium	3	8	80	2	3
1	NEC Day 0	NEC, small bowel resection, day 0	2	2	3	24	70	2	2
16	NEC Day 0	NEC, small bowel resection	4	3	3	23	70	4	4
16	NEC Day 0	NEC, Large bowel resection	4	3	3	15	70	3	3
17	NEC Day 4	NEC, small bowel resection	No epithelium	1	3	19	40	3	3
18	NEC closure	NEC, small bowel resection, closure	X	X	X	X	X	X	X
19	NEC closure	NEC, closure, small bowel resection, closure	X	X	X	X	X	X	X
20	NEC closure	NEC, small bowel resection, closure	3	3	2	3	5	3	4
17	NEC closure	NEC, small bowel resection, closure	2	2	3	12	40	2.5	2
17	NEC closure	NEC, small bowel resection, closure	4	4	3	10	30	3	3
1	NEC closure	NEC, small bowel resection, day 0 closure	3	2	3	6	40	3	3
21	Control	Isolated caecal perforation, normal small bowel	2	1	2	5	10	2	3
22	Control	Small bowel atresia	3	2	2.5	10	30	2	3
22	Control	Small bowel atresia	4	3	2	4	15	2	3
23	Control	Small bowel infarction	No epithelium	No epithelium	2	4	20	X	X
24	Control	Jejunal stenosis	3	3	2.5	15	35	2	2.5
25	Control	Intestinal atresia type iv	3	2	3	17	45	2	2
26	Control	Jejunal atresia	3	3	4	15	50	2	2
26	Control	Jejunal atresia	2	2	3	14	80	2	3
27	Control	Small bowel infarction	1	1	2	4	10	1	1
28	Control		X	X	X	X	X	X	X
29	Control		X	X	X	X	X	X	X
30	Control		X	X	X	X	X	X	X
	CD	Large bowel	X	X	X	X	X	X	X
	CD	Large bowel	3	2	3	5	60	2.5	3
	CD	Large bowel	2	2	4	15	90	3	3
	UC	Large bowel	No epithelium	No epithelium	2	8	50	3	3
	UC	Large bowel	1	2	4	20	70	2	3
	UC	Large bowel	2	2	4	20	80	3	3

Graph 7.1: CCL20 and CCR6 immunohistochemical scores of neural plexi (a), and percentage of plexi staining positve (b).

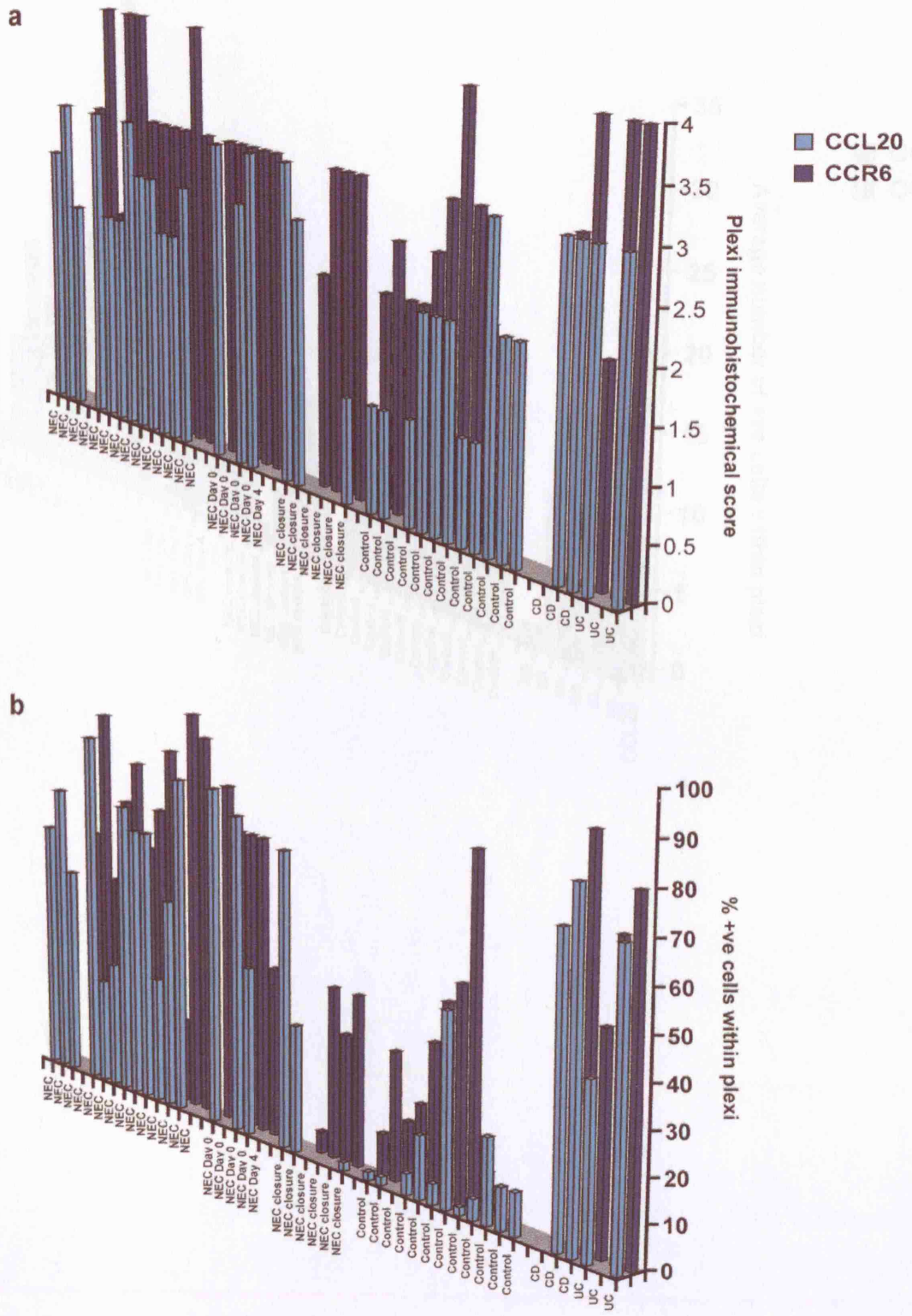

Graph 7.2: Percentage of cells immunohistochemically staining for CCL20 and CCR6 within enteric neural plexi.

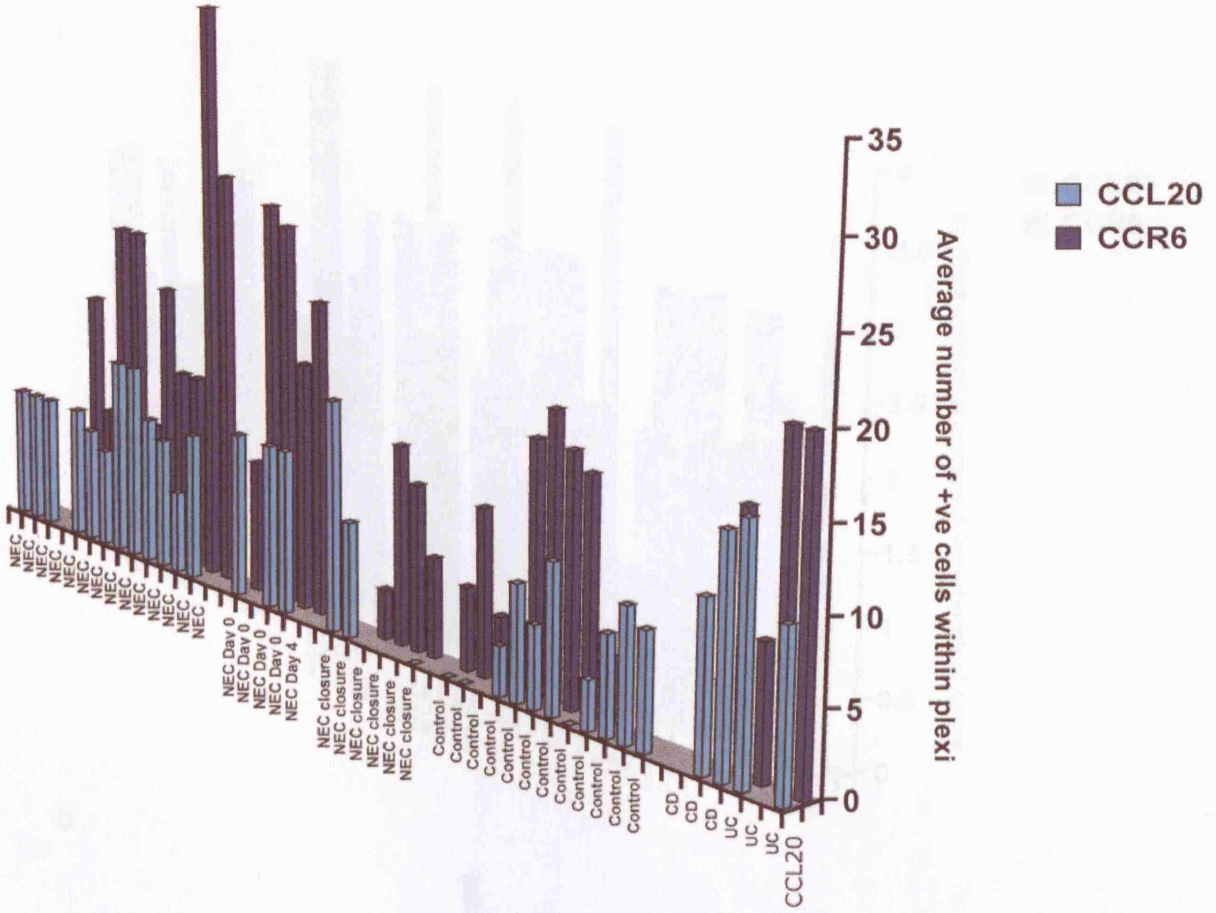

Graph 7.3: CCL20 and CCR6 immunohistochemical scores of surface (a) and crypt (b) epithelium from NEC and control samples.

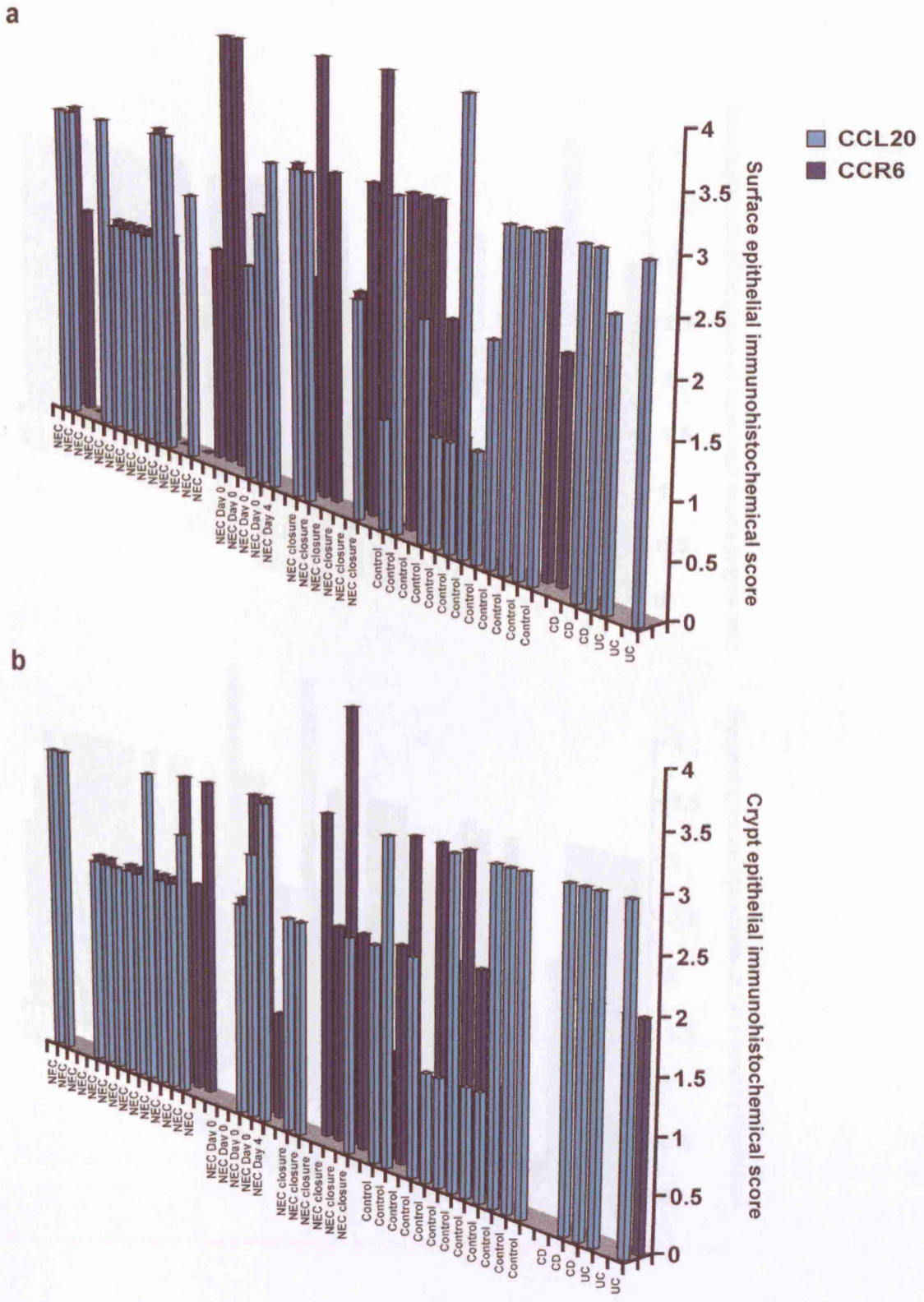

Graph 7.4: CCL20 and CCR6 immunohistochemical staining within the superficial (a) and deep (b) lamina propria area.

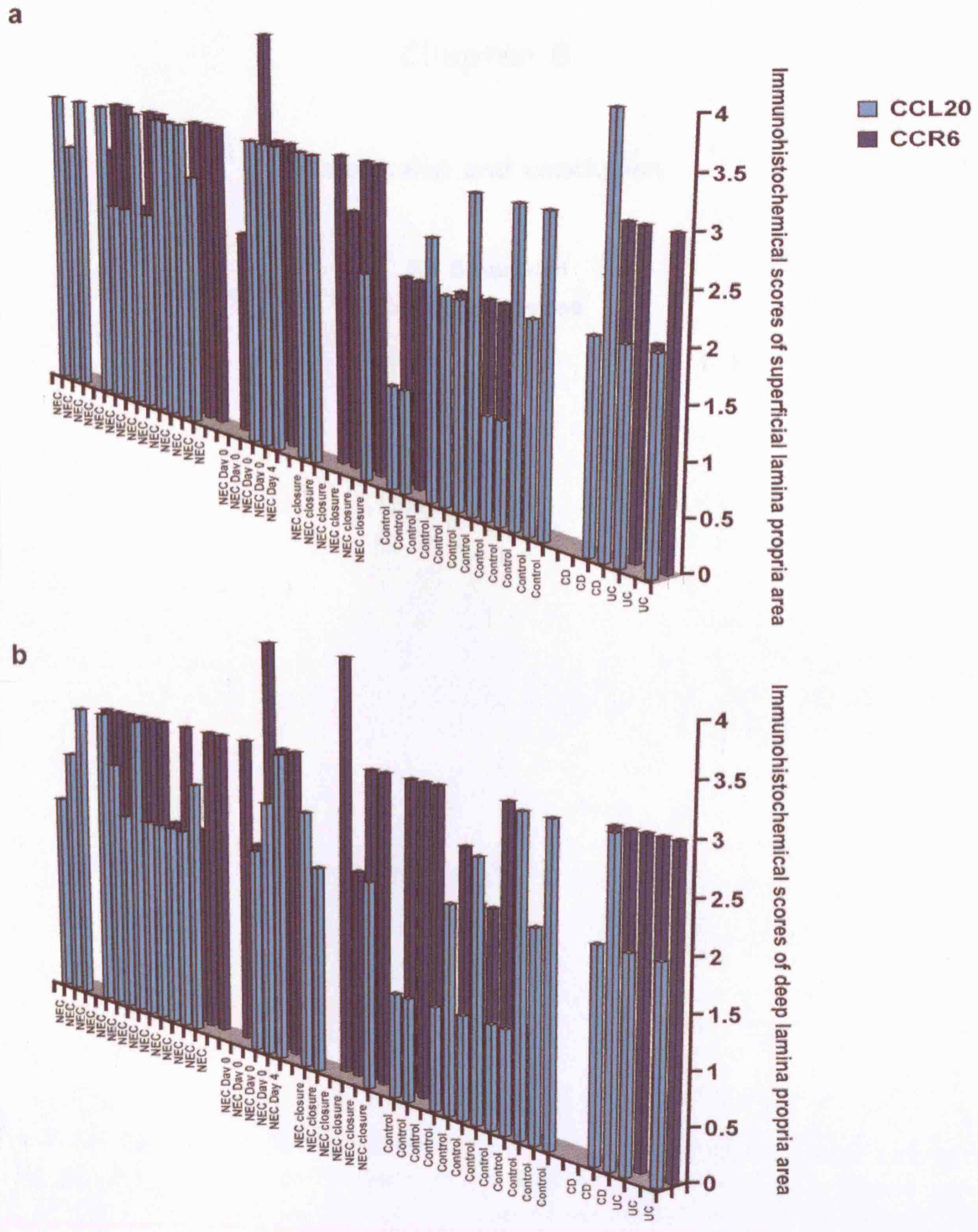

Chapter 8

Discussion and conclusion

8.1 Discussion
8.2 Conclusions

8.1 Discussion

Collective data from the research presented, incorporating colonic tissue microarray and RT-PCR, immunohistochemistry, cultured cell lines from colon, skin, and lung epithelia, and flow cytometry demonstrate a previously unrecognised coordinated epithelial chemokine response in active IBD, including CXCL's 1-3, CXCL8 and CCL20. This is the first report of coordinated expression of a distinct subset of the chemokine superfamily within human tissue. The four major CXC chemokines from the 4q.12 cluster, CXCL's 1-3 and 8 are up regulated together with the CC chemokine CCL20, with inducing stimulus varying with cell lineage. Chemokine receptors CXCR's 1 and 2 and CCR6, were also up regulated, primarily on T and B lymphocytes, macrophages, polymorph neutrophils and antigen presenting cells.

The proposed pathogenic mechanism for IBD incorporates an excessive immune response to environmental factors such as intestinal pathogens involving the chemokine subset described, in genetically susceptible individuals. Evidence indicates that rather than a specific pathogenic organism, the inflammatory process is likely to relate at least in part to an interaction between intestinal flora and the mucosa (Macpherson et al, 1996), (Martin et al, 2000), (Leiper et al, 2001).

The chemokine subset described dominates the total mucosal response in moderate to severe colitis, with expression stronger in colon biopsies from the UC than CD cohort, at similar degrees of mucosal inflammation. The concordance with inflammation was particularly notable for UC, with non-inflamed areas correlating with non-inflamed controls. Chemokine expression was independent of the anatomical origin of colonic biopsies, with array values statistically correlating between anatomical sites within normal control patients. Expression levels were higher in full thickness CD samples than CD biopsies, suggesting origin in deeper layers. Statistical analysis of RT-PCR data from full thickness IBD samples did not indicate a significant up regulation in CXCL's 1-3, CXCL8 and CCL20. This may well relate to drug treatment; the patients in the IBD biopsy cohort underwent colonoscopic examination for screening purposes, where the majority of patients in the surgical resection cohort had more active disease, and were almost all on some form of immunosuppressive agent. In the biopsy cohort, 1/8 UC and 2/6 CD patients were on immunosuppressive therapy, compared to 6/6 UC and 6/9 CD in the full thickness cohort (appendix 2.3 and 4.4). This presents a recruitment challenge for further similar research projects of this nature involving full thickness colonic samples in IBD cohorts if all patients on immunosuppressive therapy are to be excluded.

Analysis of inflamed full thickness sections taken from a single diverticulitis patient also demonstrates expression of the same chemokine subset, while colon biopsies from two infectious colitis patients were inconclusive given the low histopathological scoring for inflammation. Study of larger numbers of patients of defined genotype will be required both to determine whether subgroups of patients with CD may show similar elevation of these chemokines, and also to determine whether or not the coordinated chemokine expression pattern can be distinguished from that of non-IBD patients with acute colitis. It is likely that the coordinated chemokine response described will be invoked transiently in infectious colitis, and

further studies will be required to elucidate the role of this response in other mucosal inflammatory states.

These findings are compatible with other published data. In an early microarray analysis of three specimens of CD mucosa, CXCL3 was found to be elevated (Heller et al, 1997), and analysis of a small number of full thickness IBD and normal colon specimens indicates up regulation of CCL20 expression in CD but not UC (Kwon et al, 2002). Banks et al (2003) demonstrated up regulated chemokine expression correlated with disease activity, suggesting that the degree of tissue damage in IBD is dependent on the local expression of specific chemokines within IBD tissue. Previous research has also demonstrated that chemokines secreted by epithelial cells directly regulate the inflammatory intestinal response (Ohtsuka et al, 2001).

CCL20 up regulation is of particular importance, as this chemokine is specifically involved in mucosal immunity, especially in the human intestinal epithelium, where it induces local migration of dendritic cell subsets expressing the receptor CCR6 (Liao et al, 1999), (Dieu-Nosjean et al, 2000), (Nakayama et al, 2001), (Kwon et al, 2002), (Kaser et al, 2004). Presented data for epithelial expression of CCL20 have been collated from several different experimental modalities, including microarray, immunohistochemistry and flow cytometry. CCL20 is widely expressed by human intestinal epithelium, particularly in Peyer's patches, and the findings are compatible with this chemokine being a vital constituent of epithelial immunity. The absence of dendritic cells in Peyer's' patches in CCR6-deficient mice implicates a central role of CCL20 in the regulation of organised mucosa-associated lymphoid tissue (MALT) (Cook et al, 2000).

Immunohistochemical staining undertaken within this research demonstrates stronger CCL20 and CCR6 epithelial staining in IBD samples compared to controls. Furthermore, there are differential patterns of cellular density and locality within the lamina propria. For CCR6, in addition to the subepithelial locality seen in controls, $CCR6^{+}$ cells extend deep into the lamina propria in IBD cases. Conversely, $CC20^{+}$ cells are notable in the same subepithelial area as controls, although in greater numbers. This may well be crucial to dendritic cell activation during inflammation. While infiltrating leukocytes will contribute to the total chemokine response, undoubtedly including members of this coordinate response, the very modest up regulation of other known leukocyte chemokines seen in active UC suggests that a major contribution to the mucosal response is likely to be epithelial. Such epithelial dominance is consistent with the concept that epithelial activation may be a central determinant of colonic inflammation (Fiocchi et al, 1997), (Shao et al, 2001). Chemokine up regulation in epidermal cells occurs in response to external assault, and is thought to relate to an attempt to counteract potential antigenic invasion during the period of impaired barrier function, which is, not surprisingly, concordant with the proposed intestinal mucosal mechanism (Schmuth et al, 2002).

After binding of CCL20 to dendritic cells, the expression of CCR6 is down regulated, and CCR7 is up regulated. The change in expression levels of CCR6 and CCR7 contributes to the functional changes that are characteristic of dendritic maturation (Dieu et al 1998). Within the specific chemokine cluster identified, several UC samples also exhibited expression of the

CCR7-binding chemokines, CCL19 and CCL21, and the CXCR5 binding chemokine, CXCL13. CCR7 is a chemokine receptor of pivotal immunological importance, as it enables antigen-loaded mature dendritic cells to be guided into draining T cell-rich areas of lymph nodes by CCL19 and CCL21 (Nakayama et al, 2001), (Caux et al, 2002). These antigen-presenting cells are crucial for the initiation, continuation and regulation of an immunological response, activating naïve T and B cells, which subsequently return to the site of inflammation. After taking up antigen, dendritic cells become unresponsive to inflammatory chemokines and concomitantly acquire CCR7 expression. Maturing dendritic cells enter the lymph stream under the guidance of CCL19 and CCL21, which are expressed on lymphatic vessels (Caux et al, 2002), (Cravens et al, 2002). They therefore leave the inflamed tissue and enter draining lymph nodes. Concomitantly, CCR7-expressing naïve T cells enter lymph nodes in response to the production of CCL21 by HEVs, located primarily in the T-zone. Few HEV segments pass through the B-zones in lymph nodes (Campbell et al, 2003). CCR7 ligands are widely distributed in T-zone. Furthermore, the newly arriving dendritic cells may themselves be sources of CCL19 and CCL21, thus facilitating further amplification. Most of these pathways are uncharacterised, and the published data vary. However, the fact that these two chemokines can attract both dendritic cells and lymphocytes clearly implicates their role in the essential encounter between antigen-loaded dendritic cells and antigen-specific T cells. In mice lacking these two chemokines, or with B cells that lack CCR7, antigen engagement fails to cause movement to the T zone (Reif et al, 2002). There seems to be a carefully maintained chemokine balance within the lymphoid zones to facilitate appropriate cellular positioning within these two separate but adjacent zones. Following this encounter, dendritic cells produce many chemokines facilitating $CD4^+$ T cell interaction with $CD8^+$ T cells and B cells (Caux et al, 2002). Dendritic cells are also crucial to tolerisation (McColl et al, 2002). One possible pathogenic mechanism in IBD is a lack of T cell tolerisation which could lead to an over-active immune response with CCR7/CCL21/CCL19 potentially central to the ensuing inflammatory response.

As homeostatic trafficking of B and T lymphocytes and dendritic cells into secondary lymphoid tissue is predominantly mediated by CCL19 and CCL21, and organised lymphoid aggregates in the deep lamina propria are characteristic of UC, expression of these three chemokines presumably indicates the presence of lymphoid tissue within these particular biopsies (Yeung et al, 2000). However, this cannot be confirmed as histology was performed on adjacent biopsies.

CCR6 may well be pivotal for entry into lymphoid tissue, via HEV's. It is interesting to note that within lymphoid tissue, $CCR6^+$ immunoreactive cells are primarily limited to T cell areas. This is consistent with other research that has demonstrated CCR6 to be absent from germinal centre B cells of secondary lymphoid organs, although it is present in bone marrow- and peripheral blood-derived naïve and /or memory B cells (Krzysiek et al, 2000). CCR6 is down regulated following B cell antigen triggering, and is only up regulated after the clonal expansion into immunoglobulin -secreting plasma cells, at the post-germinal centre memory cell stage (Krzysiek et al, 2000). Thus, CCR6 is essentially restricted within the B cell compartment to B cells capable of antigenic challenge. Restricted CCR6 expression is likely to be central to the B cell maturation process.

Immunohistochemical staining of CXCR1 and CXCR2 demonstrates a clear upwards extension of immunoreactive cells towards the epithelium in IBD compared to controls, although there is no significant change in epithelial immunoreactivity. Although this cellular distribution has not yet been fully characterised, cellular positioning within the mucosa is likely to be of importance. *In vitro* studies using epithelial cell lines have demonstrated the capacity of lymphocyte and macrophage derived peptide factors to induce intestinal epithelial cell restitution (Mahida et al, 1997). Furthermore, following removal of surface epithelium, large numbers of lymphocytes, macrophages and eosinophils migrate out of the intestinal lamina propria. The migration occurs via tunnels in the extracellular matrix and is likely to be part of the host defence elicited following epithelial injury (McAlindon et al, 1998). The increased density of CCL20-, CXCR1- and CXCR2-staining cells in the subepithelial lamina propria is consistent with this, and chemokines are likely to direct the repositioning of cells during such inflammation.

The receptors CXCR1 and CXCR2 in conjunction with two of their cognate chemokines CXCL1 and CXCL8, are thought to account for the initial destructive changes seen in UC, with a neutrophilic infiltration into the epithelium (Williams et al, 2000). CXCR2 is also the receptor for CXCL2 and CXCL3 (Zlotnik et al, 2000). CXCL8 is known to attract neutrophils, macrophages and T lymphocytes and may well be pivotal in IBD inflammation. It activates CXCR1 and CXCR2 on microvascular endothelial cells using different signal transduction, which may contribute to the increased vascular permeability and leukocyte adhesiveness observed in acute inflammation (Schraufstatter et al, 2001). The precise role of CXCL8 is yet to be ascertained; although CXCL8 has previously been shown to be elevated in IBD tissue, with elevated levels also in quiescent IBD compared to control (Banks et al, 2003). This is not substantiated by the results from this thesis, which indicate that non-inflamed UC tissue has the same chemokine expression generally as control tissue. Up regulation in CD tissue did not however correlate with inflammation.

In previous research, CXCL8 levels have been found in *Helicobacter pylori* mediated gastritis in association with CXCL5, CXCL8, CXCL10 and CXCL13. Furthermore, an increased expression of CXCL8 and CCL3 was found in association with peptic ulceration. Eradication of *Helicobacter pylori* was demonstrated to reduce such chemokine expression (Ajuebor et al, 2002)[2]. The role for CXCL8 in the intestine is therefore not limited to the colon.

A further notable result from the research presented is increased expression of CCL5 and CCR5 in full thickness CD tissue that did not correlate with inflammation. However, colonic epithelial cell culture study did not indicate an induction of CCL5 following stimulation with pro-inflammatory cytokines. Qin et al (1997) suggested that CCR5 marks subsets of lymphocytes with a capacity for migration to inflammatory sites, or else that CCR5 is induced following inflammatory cytokine stimulation. Although this thesis does support the latter, other published data indicate up regulation of CCR5 by IL-2 (Baggioloni et al, 1998), which was not tested in this research, but may be a valuable experiment for future investigative study. The elevated levels of CCR5 and CCL5 in full thickness CD tissue remains uncharacterised, but these results are consistent with previous suggestions that CD is a Th1 disease, as CCR5 is expressed primarily

by Th1 cells (Baggioloni et al, 1998), (Sallusto et al, 1998)[1], (Monteleone et al, 2002). CCR5 is also expressed by immature dendritic cells (Sallusto et al, 1998)[2]. Several years ago, the second extracellular loop of CCR5 was identified as an ideal target for the development of inhibitors, as the chemokine pattern of binding is relatively simple. Furthermore, CCR5 functions as the principal co receptor for macrophage strains of HIV-1 (Wu et al, 1997).

Previously, it has been shown that CCL20 can be up regulated by stimulation by pro-inflammatory cytokines (Izadpanah et al, 2001). Furthermore, colonic epithelial cells freshly isolated from IBD patients and normal controls show strong expression of receptors for IL-1β but not TNF-α, and respond only to IL-1β. Cell culture results presented here is confirmatory of this. Data from stimulated gut-derived Caco-2 cells demonstrate that IL-1β up regulates CXCL's 1-3, CXCL8 and CCL20, while both IL-1β and TNF-α induce expression from HT-29 cells. Previous research has indicated that both IL-1β and TNF-α together are required to induce this group of chemokines in epithelial cells derived from the skin. This group substantially dominates the epithelial response by orders of magnitude over any other chemokines. In addition, the anti-inflammatory chemokine CXCL10 was induced in Caco-2 cells following pro-inflammatory stimulation with IL-1β and to a lesser extent TNF-α. IL-1β and TNF-α together led to a cumulative induction, which is consistent with published data (Parekh et al, 1999).

Results from cultured epithelial cell line chemokine response have to be interpreted with some caution, as Caco-2 cells are not always predictive for the response *in vivo*. They are differentiated tumour cells, which do not entirely respond as intestinal epithelial cells do. Experimentation using cell culture lines is complicated by the dynamic nature in cellular maturation in surface villous epithelial cells. The migration from the crypt base to the surface of the colon is accompanied by cellular differentiation that leads to important morphological and functional changes. Cellular differentiation of HT29 cells selectively impairs the IL-1β signalling pathway inhibiting NF-κB activity in response to IL-1β. This may result from an increased expression of the decoy IL-1RII, which does not transduce signal. Published research indicates that LPS- and IL-1β-induced CXCL8 secretion are impaired in differentiated cells which is contrary to the findings from this research, where CXCL8 levels were induced by IL-1β. Other published data indicate there is loss of IL-1β induced CXCL8 production in both HT-29 and Caco-2 cells on differentiation towards a small intestinal phenotype (Huang et al, 1997), (Bocker et al, 2000). To optimise the conditions of the cultured Caco-2 and HT29 cell lines, the cells were harvested just post-confluence, when they retain colonic phenotype rather than small intestinal (Engle et al, 1998) and appear to represent a physiologically relevant model of human colonocytes in respect of TNF-α and IL-1β responses (Fujiie et al, 2001), (Yang et al, 1997). This relative unresponsiveness to IL-1β following cellular differentiation may represent an important regulatory mechanism of differentiated intestinal epithelial cells (Bocker et al, 2000). TNF-α mediated NF-κB activity is unaffected by cellular differentiation. Although TNF-α and IL-1β transduce many of their shared pro-inflammatory responses through a common pathway of NF-κB induction, there are differences in their proximal signal pathways. There is also evidence from monocyte lines that they use differential regulatory steps in IκB kinase induction and IκBα

degradation (Nashuhara et al, 1999), (Hong et al, 2001). Further analysis of the differential response to IL-1β and TNF-α in gut-derived cell lines may give insight into the signalling pathways that differentiate colonic from small bowel IBD. In this initial investigative study, the cell lines included do provide initial valuable evidence that provide a basis for further primary epithelial study.

The transcription factor NF-κB is of great importance in the gastrointestinal tract, being a key regulator of gene expression involved with gastrointestinal immunity and inflammation. It regulates chemokines including CCL20, acute phase proteins, cytokines and growth factors in the inflamed mucosa of IBD patients (Fujie et al, 2001), (Izadapanah et al, 2001), and is essential for cell growth, oncogenesis and escape from apoptosis (Dhawan et al, 2002). Once released from an inactive cytoplasmic complex, NF-κB dimers translocate to the nucleus and bind to specific sequences to promote transcription (Dijkastra et al, 2002). Many of the drugs utilised for IBD are beneficial in part from their inhibition of NF-κB, such as mesalazine and steroids. Mesalasine prevents the IL-1 induced phosphorylation of the p65 subunit of NF-κB. Steroids maintain the NF-κB in the inactive cytoplasmic form (Dijkastra et al, 2002). IL-10 also inhibits NF-κB activation. Dysregulation of this transcription factor leads to constitutive expression of chemokines and cytokines. Several other cofactors and repressors are involved in chemokine regulation such as PARP. Identification of specific NF-κB inhibitors may be of great therapeutic benefit. The Caco-2 cell culture data presented indicates that TSA enhanced CCL20 production two-fold in conjunction with IL-1β, and fully inhibited IL-1β induction of CXCL10. This is consistent with a TSA distinct pathway of induction via reduction of histone deacetylase co-repressor proteins. Since acetylation of the histone tail induces transcription through chromatin remodelling, a reduction in deacetylation promotes chemokine production. Specific inhibitors of NF-κB may well be of therapeutic benefit in many diseases including IBD. Selective agents such as antisense p65 are likely to be more effective and less toxic that current therapeutic agents.

Primary epithelial cell culture is a more appropriate model than colonic carcinoma cell lines, and further research in this area is warranted. The pilot primary epithelial cell culture study yielded interesting results, with induction of CXCL' s1-3, CXCL8 and CCL20 following stimulation with IL-1β or TNF-α, which is concordant with other published data (Kwon et al, 2002). Kwon et al also found that colonic epithelial cells are an important source of CCL20 and postulated that increased production may be important in recruitment of $CD4^+$ T lymphocytes and immature dendritic cells to the epithelial layer in IBD. However, the greatest value of this small study was in establishing the viability of primary colonic cell culture in this manner, and further research is required.

Immunostaining of NEC sections for CCL20 and CCR6 illustrates the potential application of this technique to other diseases apart from IBD. Perineural T cell infiltration, glial disruption and $CCL20^+$ infiltration into the myenteric plexus have been demonstrated. Delineation of cause and effect is not possible from this research, although as CCL20 becomes increasingly characterised with time, its relevance in NEC should become more apparent. Furthermore, this provides a

potential target for therapeutic intervention, for example via CCR6 blockade. Furthermore, immunohistochemical examination of myenteric infiltration with CCL20/CCR6^{+} cells in IBD patients would be a valuable study. Double immunostaining of full thickness intestinal sections for CCL20 and CCR6 would probably yield interesting results and may help characterise these pathways. This was infact attempted towards the end of the research period, although as the CCR6 antibody was a mouse antibody species and the CCL20 a goat antibody species, results were unsatisfactory and further work is required. A primary entero-neural pathological process is unlikely to be causal of IBD, but may explain the associated dysmotility (Vrees et al, 2002). Previous research has established that enteric glia play an essential role in maintaining the integrity of the bowel, and their loss or dysfunction may contribute to the cellular mechanisms of IBD (Bush et al, 1998), (Bush, 2002). Disruption of the enteric glial network has also been hypothesised to contribute to the enhanced mucosal permeability and vascular dysfunction in IBD (Cabarrocas et al, 2003). IL-1β has been shown to suppress enteric glial proliferation and enhance further pro-inflammatory cytokine production (Cabarrocas et al, 2003). These glial cells therefore are clearly able to respond to inflammatory stimuli.

As chemokines and pro-inflammatory cytokines determine the intensity of the inflammatory response, therapeutic inhibition of the coordinate epithelial chemokine response is likely to provide significant clinical benefit in UC. Although manipulation of chemokine expression for therapeutic benefit has been accomplished for years with corticosteroids, cyclosporin A, etc., the production of more specific agents acting at individual cytokine levels remains an attractive and increasingly plausible option in the treatment of chronic inflammatory disorders.

The focal expression of CCL20 makes its interaction with CCR6 an attractive target for therapy, as this is unlikely to affect systemic immune responses. A further feature of the CCR6 receptor that makes it an ideal potential therapeutic target is the lack of promiscuity, with binding only to two ligands; CCL20 and β-defensin (Yeung et al, 2000). Blockade of this receptor may well be an effective and specific agent with minimal toxicity, not only in IBD but in other inflammatory epithelial conditions. Other possible targets include CCR5 in CD, which has previously been identified as potential target in other diseases including MS (Balashov et al, 1999).

The data presented here suggest that therapeutic inhibition of the interaction between IL-1β and colonic epithelium may remove one of the pro-inflammatory drivers in moderate/severe UC. Effective IL-1β inhibitory therapy may mediate a specific and effective anti-inflammatory response in UC. The evidence that different intestinal epithelial lines have distinct responses to IL-1β and TNF-α in the induction of members of this coordinate chemokine response suggests that IL-1β may be an important therapeutic target in its own right, particularly in UC (Bocker et al, 2000), (Fujiie et al, 2001), (Wen et al, 2001).

Multiple independent lines of evidence support the pivotal role of IL-1β: IL-1 receptor antagonist therapy is extremely effective in experimental colitis in rabbits (Cominelli et al, 1990), mice with targeted deletion of IL-1β converting enzyme are highly protected from colitis (Siegmund et al, 2001), polymorphism of both the IL-1β promoter and IL-1 receptor antagonist are associated

with IBD and may influence severity (Nemetz et al, 1999), (Carter et al, 2001), and significant reduction of the IL-1 receptor antagonist: IL-1 ratio occurs in active disease (Andus et al, 1997). Cominelli's study demonstrated that administration of the antagonist decreases IL-1 levels; specific blockade of IL-1 receptors reduces the inflammatory responses associated with experimental colitis (Cominelli et al, 1990). IL-1 gene expression and synthesis occur early in the course of immune complex-induced colitis, with tissue levels of IL-1 correlating with the degree of tissue inflammation.

Reducing the biological activities of IL-1 and TNF may be accomplished by several different, but highly specific strategies, including neutralising antibodies, soluble receptors, receptor antagonist, and inhibitors of proteases that convert inactive precursors to active, mature molecules. Blocking IL-1 and TNF has been highly successful in patients with rheumatoid arthritis and graft-versus-host disease but has not been successful in humans with sepsis (Deon et al, 2001). Clearly TNF-α is an important therapeutic target in CD, as TNF-α monoclonal antibodies have induced substantial clinical responses in previously resistant disease (Baert et al, 1999). Inhibition of IL-1β-converting enzyme (ICE) is a further anti-inflammatory strategy for IBD as it is a key contributor in intestinal inflammation. This enzyme is the intracellular protease that cleaves the precursors of IL-1β and IL-18 into active cytokines. Its naturally occurring inhibitor, IL-1Ra maintains an effective balance. Mice deficient in IL-1Ra develop spontaneous rheumatoid arthritis and lethal arteritis, but IL-1Ra administration reduces disease severity.

8.2 Conclusions

These data identify a previously unrecognised coordinated epithelial chemokine response in active IBD, including CXCL's 1-3, CXCL8 and CCL20. IL-1β appears to be the pivotal mediator of an epithelial response that dominates the chemokine environment in UC. Several new therapeutic targets have been identified that may well enable new specific non-toxic agents to be developed in the treatment of active IBD. The focal expression of CCL20 makes its interaction with CCR6 an attractive target for therapy, as this is unlikely to affect systemic immune responses. IL-1 receptor antagonism is also of potential therapeutic benefit in IBD.

Furthermore, the use of microarray hybridisation has been applied to IBD. DNA Microarray analysis represents one of the major recent advances in functional genomics, enabling the study of many genes within an investigative clinical setting.

References

Aderem A, Ulevitch RJ. Toll-like receptors in the induction of the innate immune response. Nature 2000; 406: 782-7.

Ai LS, Liao F. Mutating the four extracellular cysteines in the chemokine receptor CCR6 reveals their differing roles in receptor trafficking, ligand binding, and signaling. Biochemistry 2002; 41: 8332-41.

Ajuebor MN[1], Swain MG. Role of chemokines and chemokine receptors in the gastrointestinal tract. Immunology 2002; 105: 137-43.

Ajuebor MN[2], Swain MG, Perretti M. Chemokines as novel therapeutic targets in inflammatory diseases. Biochem Pharmacol 2002; 63: 1191-6.

Alon R, Grabovsky V, Feigelson S. Chemokine induction of integrin adhesiveness on rolling and arrested leukocytes local signaling events or global stepwise activation? Microcirculation 2003; 10: 297-311.

Andus T, Daig R, Vogl D, Aschenbrenner E, Lock G, Hollerbach S, Kollinger M, Scholmerich J, Gross V. Imbalance of the interleukin 1 system in colonic mucosa-association with intestinal inflammation and interleukin 1 receptor antagonist genotype 2. Gut 1997; 41: 651-657.

Ardite E, Panes J, Miranda M, Salas A, Elizalde JI, Sans M, Arce Y, Bordas JM, Fernandez-Checa JC, Pique JM. Effects of steroid treatment on activation of nuclear factor kappaB in patients with inflammatory bowel disease. Br J Pharmacol 1998; 124: 431-3.

Ashburner BP, Westerheide SD, Baldwin AS Jr. The p65 (RelA) subunit of NF-kappaB interacts with the histone deacetylase (HDAC) corepressors HDAC1 and HDAC2 to negatively regulate gene expression. Mol Cell Biol 2001; 21: 7065-7077.

Atreya R, Mudter J, Finotto S, Mullberg J, Jostock T, Wirtz S, Schutz M, Bartsch B, Holtmann M, Becker C, Strand D, Czaja J, Schlaak JF, Lehr HA, Autschbach F, Schurmann G, Nishimoto N, Yoshizaki K, Ito H, Kishimoto T, Galle PR, Rose-John S, Neurath MF. Blockade of interleukin 6 trans signaling suppresses T-cell resistance against apoptosis in chronic intestinal inflammation: evidence in crohn disease and experimental colitis in vivo. Nat Med 2000; 6: 583-8.

Baba M, Imai T, Nishimura M, Kakizaki M, Takagi S, Hieshima K, Nomiyama H and Yoshie O. Identification of CCR6, the specific receptor for a novel lymphocyte-directed CC chemokine LARC. J Biol Chem 1997; 272: 14893-14898.

Baert FJ, D'Haens GR, Peeters M, Hiele MI, Schaible TF, Shealy D, Geboes K, Rutgeerts PJ. Tumor necrosis factor α antibody (infliximab) therapy profoundly down-regulates the inflammation in Crohn's ileocolitis. Gastroenterol 1999; 116: 22–28.

Baggiolini M. Chemokines and leukocyte traffic. Nature 1998; 392: 565-8.

Baggiolini M, Dewald B, Moser B. Human chemokines: an update. Annu Rev Immunol 1997; 15: 675–705.

Bajetto A, Bonavia R, Barbero S, Schettini G. Characterization of chemokines and their receptors in the central nervous system: physiopathological implications. J Neurochem 2002; 6: 1311-29.

Balashov KE, Rottman JB, Weiner HL, Hancock WW. CCR5(+) and CXCR3(+) T cells are increased in multiple sclerosis and their ligands MIP1alpha and IP-10 are expressed in demyelinating brain lesions. Proc Natl Acad Sci USA 1999; 96: 6873–78.

Bancroft and Gamble, Churchhill Livingstone. Theory and practice of histological techniques. Chapter 20 page 421, edited 2002, edition 5.

Banks C, Bateman A, Payne R, Johnson P, Sheron N. Chemokine expression in IBD. Mucosal chemokine expression is unselectively increased in both ulcerative colitis and Crohn's disease. J Pathol 2003; 199: 28-35.

Bariol C, Meagher AP, Vickers CR, Byrnes DJ, Edwards PD, Hing M, Wettstein AR, Field A. Early studies on the safety and efficacy of thalidomide for symptomatic inflammatory bowel disease. J Gastroenterol Hepatol 2002; 17: 135-9.

Basset C, Holton J. Inflammatory bowel disease: is the intestine a Trojan horse? Sci Prog 2002; 85: 33-56.

Bauditz J, Wedel S, Lochs H. Thalidomide reduces tumour necrosis factor alpha and interleukin-12 production in patients with chronic active Crohn's disease. Gut 2002; 50: 196-200.

Beltinger J, McKaig BC, Makh S, Stack WA, Hawkey CJ, Mahida YR. Human colonic subepithelial myofibroblasts modulate transepithelial resistance and secretory response. Am J Physiol 1999; 277: C271-9.

Benjamin D, Wormsley S, Dower SK. Heterogeneity in interleukin IL-1 receptors expressed on human B cell lines. Differences in the molecular properties of IL-1 alpha and IL-1 beta binding sites. J Biol Chem 1990; 265: 9943-51.

Benoni C, Prytz H. Effects of smoking on the urine excretion of oral 51Cr EDTA in ulcerative colitis. Gut 1998; 42: 656-8.

Bernstein CN, Blanchard JF, Kliewer E, Wajda A. Cancer risk in patients with inflammatory bowel disease: a population-based study. Cancer 2001; 91: 854-62.

Berrebi D, Maudinas R, Hugot JP, Chamaillard M, Chareyre F, De Lagausie P, Yang

C, Desreumaux P, Giovannini M, Cezard JP, Zouali H, Emilie D, Peuchmaur M. Card15 gene overexpression in mononuclear and epithelial cells of the inflamed Crohn's disease colon. Gut 2003; 52: 840-6.

Bhatti M, Haskard DO, Hodgson HJ. Effects of nicotine on E-selectin expression in intestinal tissue biopsies in inflammatory bowel disease patients and controls. Gut 1997; 40 (supplement 1): F295.

Binder V, Orholm M. Familial occurrence and inheritance studies in inflammatory bowel disease. Neth J Med 1996; 48: 53-6.

Bocker U, Schottelius A, Watson JM, Holt L, Licato LL, Brenner DA, Sartor RB, Jobin C. Cellular differentiation causes a selective down-regulation of interleukin (IL)-1β-mediated NF-κB activation and IL-8 gene expression in intestinal epithelial cells. J Biol Chem 2000; 275: 12207-12213.

Bone-Larson CL, Simpson KJ, Colletti LM, Lukacs NW, Chen SC, Lira S, Kunkel SL, Hogaboam CM. The role of chemokines in the immunopathology of the liver. Immunol Rev 2000; 177: 8-20.

Bonen DK, Cho JH. The genetics of inflammatory bowel disease. Gastroenterol 2003; 124: 521-36.

Bonacchi A, Petrai I, Defranco RM, Lazzeri E, Annunziato F, Efsen E, Cosmi L, Romagnani P, Milani S, Failli P, Batignani G, Liotta F, Laffi G, Pinzani M, Gentilini P, Marra F. The chemokine CCL21 modulates lymphocyte recruitment and fibrosis in chronic hepatitis C. Gastroenterol 2003; 125: 1060-76.

Boone DL, Ma A. Connecting the dots from Toll-like receptors to innate immune cells and inflammatory bowel disease. J Clin Invest 2003; 111: 1284-6.

Bowman EP, Campbell JJ, Soler D, Dong Z, Manlongat N, Picarella D, Hardy RR, Butcher EC. Developmental switches in chemokine response profiles during B cell differentiation and maturation. J Exp Med 2000; 191: 1303-18.

Braat H, Peppelenbosch MP, Hommes DW. Interleukin-10-based therapy for inflammatory bowel disease. Expert Opin Biol Ther 2003; 3: 725-31.

Bush TG. An upstream target for induction of necrotizing enterocolitis and Crohn's disease? Bioessays 2002; 24: 130-40.

Bush TG, Savidge TC, Freeman TC, Cox HJ, Campbell EA, Mucke L, Johnson MH, Sofroniew MV. Fulminant jejuno-ileitis following ablation of enteric glia in adult transgenic mice. Cell 1998 17;93: 189-201.

Cabarrocas J, Savidge TC, Liblau RS. Role of enteric glial cells in inflammatory bowel disease. Glia 2003; 41: 81-93.

Calkins BM. A meta-analysis of the role of smoking in inflammatory bowel disease. Dig Dis Sci 1989; 34: 1841-54.

Cambridge G, Rampton DS, Stevens TR, McCarthy DA, Kamm M, Leaker B. Anti-neutrophil antibodies in inflammatory bowel disease: prevalence and diagnostic role. Gut 1992; 33: 668-74.

Campbell DJ, Kim CH, Butcher EC. Chemokines in the systemic organization of immunity. Immunol Rev 2003; 195: 58-71.

Campbell JD, HayGlass KT. T cell chemokine receptor expression in human Th1- and Th2-associated diseases. Arch Immunol Ther Exp (Warsz) 2000; 48: 451-6.

Campbell JJ, Hedrick J, Zlotnik A, Siani MA, Thompson DA, Butcher EC. Chemokines and the arrest of lymphocytes rolling under flow conditions. Science 1998; 279: 381-4.

Carlsen HS, Baekkevold ES, Johansen FE, Haraldsen G, Brandtzaeg P. B cell attracting chemokine 1 (CXCL13) and its receptor CXCR5 are expressed in normal and aberrant gut associated lymphoid tissue. Gut 2002; 51: 364-71.

Carramolino L, Kremer L, Goya I, Varona R, Buesa JM, Gutierrez J, Zaballos A, Martinez AC, Marquez G. Down-regulation of the beta-chemokine receptor CCR6 in dendritic cells mediated by TNF-alpha and IL-4. J Leukoc Biol 1999; 66: 837-44.

Carter MJ, di Giovine FS, Jones S, Mee J, Camp NJ, Lobo AJ, Duff GW. Association of the interleukin 1 receptor antagonist gene with ulcerative colitis in Northern European Caucasians. Gut 2001; 48: 461–467.

Carty E, Rampton DS, Schneider H, Rutgeerts P, Wright JP. Lack of efficacy of ridogrel, a thromboxane synthase inhibitor, in a placebo-controlled, double-blind, multi-centre clinical trial in active Crohn's disease. Aliment Pharmacol Ther. 2001; 15: 1323-9.

Caux C, Vanbervliet B, Massacrier C, Ait-Yahia S, Vaure C, Chemin K, Dieu-Nosjean, MC, Vicari A. Regulation of dendritic cell recruitment by chemokines. Transplantation 2002; 73: S7-11.

Cella M, Salio M, Sakakibara Y, Langen H, Julkunen I, Lanzavecchia A. Maturation, activation, and protection of dendritic cells induced by doublestranded RNA. J Exp Med 1999; 189: 821–29.

Charbonnier AS, Kohrgruber N, Kriehuber E, Stingl G, Rot A, Maurer D. Macrophage inflammatory protein 3alpha is involved in the constitutive trafficking of epidermal langerhans cells. J Exp Med 1999; 190: 1755-68.

Charles P, Elliott MJ, Davis D, Potter A, Kalden JR, Antoni C, Breedveld FC, Smolen JS, Eberl G, deWoody K, Feldmann M, Maini RN. Regulation of cytokines, cytokine inhibitors, and acute-phase proteins following anti-TNF-alpha therapy in rheumatoid arthritis. J Immunol 1999; 163: 1521-8.

Chigaev A, Zwartz G, Graves SW, Dwyer DC, Tsuji H, Foutz TD, Edwards BS, Prossnitz ER, Larson RS, Sklar LA. Alpha4beta1 integrin affinity changes govern cell adhesion. J Biol Chem. 2003; 278: 38174-82.

Cho C, Miller RJ. Chemokine receptors and neural function. J Neurovirol 2002; 8: 573-84.

Choy EH, Hazleman B, Smith M, Moss K, Lisi L, Scott DG, Patel J, Sopwith M. Efficacy of a novel PEGylated humanized anti-TNF fragment (CDP870) in patients with rheumatoid arthritis: a phase II double-blinded, randomized, dose-escalating trial. Rheumatology (Oxford) 2002; 41: 1133-7.

Choy MY, Walker-Smith JA, Williams CB, MacDonald TT. Differential expression of CD25 (interleukin-2 receptor) on lamina propria T cells and macrophages in the intestinal lesions in Crohn's disease and ulcerative colitis. Gut 1990; 31: 1365-70.

Collins CE, Cahill MR, Newland AC, Rampton DS. Platelets circulate in an activated state in inflammatory bowel disease. Gastroenterol 1994; 106: 840-5.

Cominelli F, Nast CC, Clark BD, Schindler R, Lierena R, Eysselein VE, Thompson RC, Dinarello CA. Interleukin 1 (IL-1) gene expression, synthesis, and effect of specific IL-1 receptor blockade in rabbit immune complex colitis. J Clin Invest 1990; 86: 972-80.

Cominelli F, Pizarro TT. Interleukin-1 and interleukin-1 receptor antagonist in inflammatory bowel disease. Aliment Pharmacol Ther 1996; 10 Suppl 2:49-53.

Cominelli F, Pizarro TT. Interleukin-1 receptor antagonist: a "novel" acute phase protein with antiinflammatory activities. J Clin Invest 1997; 99: 2813.

Cook DN, Prosser DM, Forster R, Zhang J, Kuklin NA, Abbondanzo SJ, Niu XD, Chen SC, Manfra DJ, Wiekowski MT, Sullivan LM, Smith SR, Greenberg HB, Narula SK, Lipp M, Lira SA. CCR6 mediates dendritic cell localization, lymphocyte homeostasis, and immune responses in mucosal tissue. Immunity 2000; 12: 495-503.

Cravens PD, Lipsky PE. Dendritic cells, chemokine receptors and autoimmune inflammatory diseases. Immunol Cell Biol 2002; 80: 497-505.

Creed TJ, Norman MR, Probert CS, Harvey RF, Shaw IS, Smithson J, Anderson J,

Moorghen M, Gupta J, Shepherd NA, Dayan CM, Hearing SD. Basiliximab (anti-CD25) in combination with steroids may be an effective new treatment for steroid-resistant ulcerative colitis. Aliment Pharmacol Ther 2003; 18: 65-75.

Daaka Y, Luttrell LM, Ahn S, Della Rocca, GJ, Ferguson SS, Caron MG, Lefkowitz RJ. Essential role for G protein-coupled receptor endocytosis in the activation of mitogen-activated protein kinase. J Biol Chem 1998; 273: 685–88.

Dellacasagrande J, Schreurs OJ, Hofgaard PO, Omholt H, Steinsvoll S, Schenck K, Bogen B, Dembic Z. Liver metastasis of cancer facilitated by chemokine receptor CCR6. Scand J Immunol 2003; 57: 534-44.

Deon D, Ahmed S, Tai K, Scaletta N, Herrero C, Lee IH, Krause A, Ivashkiv LB. Cross-talk between IL-1 and IL-6 signaling pathways in rheumatoid arthritis synovial fibroblasts. J Immunol 2001; 167: 5395-403.

D'Haens G, Swijsen C, Noman M, Lemmens L, Ceuppens J, Agbahiwe H, Geboes K, Rutgeerts P. Etanercept in the treatment of active refractory Crohn's disease: a single-center pilot trial. Am J Gastroenterol 2001; 96: 2564-8.

Dhawan P, Richmond A. Role of CXCL1 in tumorigenesis of melanoma. J Leukoc Biol 2002; 72: 9-18.

Dieu MC, Vanbervliet B, Vicari A, Bridon JM, Oldham E, Ait-Yahia S, Briere F, Zlotnik A, Lebecque S, Caux C. Selective recruitment of mature and immature dendritic cells by distinct chemokines expressed in different anatomic sites. J Exp Med 1998; 188: 373-386.

Dieu-Nosjean MC, Massacrier C, Homey B, Vanbervliet B, Pin JJ, Vicari A, Lebecque S, Dezutter-Dambuyant C, Schmitt D, Zlotnik A, Caux C. Macrophage inflammatory protein 3α is expressed at inflamed epithelial surfaces and is the most potent chemokine known in attracting Langerhans cell precursors. J Exp Med 2000; 192: 705-717.

Dijkstra G, Moshage H, Jansen PL. Blockade of NF-kappaB activation and donation of nitric oxide: new treatment options in inflammatory bowel disease? Scand J Gastroenterol Suppl 2002: 37-41.

Dinarello CA. Interleukin-1. Cytokine Growth Factor Rev 1997; 8: 253-65.

Dinarello CA[1]. Interleukin-18, a proinflammatory cytokine. Eur Cytokine Netw 2000; 11: 483-6.

Dinarello CA[2]. Proinflammatory cytokines. Chest 2000; 118: 503-8.

Dionne S, D'Agata ID, Hiscott J, Vanounou T, Seidman EG. Colonic explant production of IL-1and its receptor antagonist is imbalanced in inflammatory bowel disease (IBD). Clin Exp Immunol 1998; 112: 435-42.

Duerr RH. The genetics of inflammatory bowel disease. Gastroenterol Clin North Am 2002; 31: 63-76.

Dwinell MB, Johanesen PA, Smith JM. Immunobiology of epithelial chemokines in the intestinal mucosa. Surgery 2003; 133: 601-7.

Ebert LM, McColl SR. Up-regulation of CCR5 and CCR6 on distinct subpopulations of antigen-activated CD4+ T lymphocytes. J Immunol 2002; 168: 65-72.

Einerhand AW, Renes IB, Makkink MK, van der Sluis M, Buller HA, Dekker J. Role of mucins in inflammatory bowel disease: important lessons from experimental models. Eur J Gastroenterol Hepatol 2002; 14: 757-65.

Elliott S, Cawston T. The clinical potential of matrix metalloproteinase inhibitors in the rheumatic disorders. Drugs Aging 2001; 18: 87-99.

Engle MJ, Goetz GS, Alpers DH. Caco-2 cells express a combination of colonocyte and enterocyte phenotypes. J Cell Physiol 1998; 174: 362-369.

Evans RC, Wong VS, Morris AI, Rhodes JM. Treatment of corticosteroid-resistant ulcerative colitis with heparin - a report of 16 cases. Aliment Pharmacol Ther 1997; 11: 1037-40.

Feehally J, Burden AC, Mayberry JF, Probert CS, Roshan M, Samanta AK, Woods KL. Disease variations in Asians in Leicester. Q J Med 1993; 86: 263-9.

Fernandez EJ, Lolis E. Structure, function, and inhibition of chemokines. Annu Rev Pharmacol Toxicol 2002; 42: 469-99.

Finnie IA, Campbell BJ, Taylor BA, Milton JD, Sadek SK, Yu LG, Rhodes JM. Stimulation of colonic mucin synthesis by corticosteroids and nicotine. Clin Sci (Lond) 1996; 91: 359-64.

Fiocchi C. Intestinal inflammation: a complex interplay of immune and non-immune cell interactions. Am J Physiol 1997; 273: G769–G775.

Fitzhugh DJ, Naik S, Caughman SW, Hwang ST. C-C chemokine receptor 6 is essential for arrest of a subset of memory T cells on activated dermal microvascular endothelial cells under physiologic flow conditions in vitro. J Immunol 2000; 15: 165:6677-81.

Foxman EF, Campbell JJ, Butcher EC. Multistep navigation and the combinatorial control of leukocyte chemotaxis. J Cell Biol 1997; 139: 1349–60.

Fujiie S, Hieshima K, Izawa D, Nakayama T, Fujisawa R, Ohyanagi H, Yoshie O. Pro-inflammatory cytokines induce liver and activation-regulated chemokine/ macrophage inflammatory protein-3α/ CCL20 in mucosal cells through NF-κB. Internat Immunol 2001; 13: 1255-1263.

Fusunyan RD, Quinn JJ, Fujimoto M, MacDermott RP, Sanderson IR. Butyrate switches the pattern of chemokine secretion by intestinal epithelial cells through histone acetylation. Mol Med. 1999; 5: 631-640.

Fusunyan RD, Quinn JJ, Ohno Y, MacDermott RP, Sanderson IR. Butyrate enhances interleukin (IL)-8 secretion by intestinal epithelial cells in response to IL-1beta and lipopolysaccharide. Pediatr Res 1998; 43: 84-90.

Gaffney PR, Doyle CT, Gaffney A, Hogan J, Hayes DP, Annis P. Paradoxical response to heparin in 10 patients with ulcerative colitis. Am J Gastroenterol 1995; 90: 220-3.

Gan H, Ouyang Q, Jia D, Xia Q. Activation of nuclear factor-kappaB and its relationship with cytokine gene expression in colonic mucosa of ulcerative colitis patients. Zhonghua Nei Ke Za Zhi. 2002; 41: 252-5.

Gautam N, Olofsson AM, Herwald H, Iversen LF, Lundgren-Akerlund E, Hedqvist P, Arfors KE, Flodgaard H, Lindbom L. Heparin-binding protein (HBP/CAP37): a missing link in neutrophil-evoked alteration of vascular permeability. Nat Med 2001; 7: 1123-7.

Gear AR, Camerini D. Platelet chemokines and chemokine receptors: linking hemostasis, inflammation, and host defense. Microcirculation. 2003; 10: 335-50.

Geerling BJ, Dagnelie PC, Badart-Smook A, Russel MG, Stockbrugger RW, Brummer RJ. Diet as a risk factor for the development of ulcerative colitis. Am J Gastroenterol 2000; 95: 1008-13.

Gertner DJ, Rampton DS, Madden MV, Talbot IC, Nicholls RJ, Lennard-Jones JE. Increased leukotriene B4 release from ileal pouch mucosa in ulcerative colitis compared with familial adenomatous polyposis. Gut 1994; 35: 1429-32.

Ghosh S, May MJ, Kopp EB. NF-kappa B and Rel proteins: evolutionarily conserved mediators of immune responses. Annu Rev Immunol 1998; 16: 225-60.

Gibejova A, Mrazek F, Subrtova D, Sekerova V, Szotkowska J, Kolek V, du Bois RM, Petrek M. Expression of macrophage inflammatory protein-3 beta/CCL19 in pulmonary sarcoidosis. Am J Respir Crit Care Med 2003; 167: 1695-703.

Girardin SE, Boneca IG, Carneiro LA, Antignac A, Jehanno M, Viala J, Tedin K, Taha MK, Labigne A, Zathringer U, Coyle AJ, DiStefano PS, Bertin J, Sansonetti PJ, Philpott DJ. Nod1 detects a unique muropeptide from gram-negative bacterial peptidoglycan. Science 2003; 300: 1584-7.

Gong JH, Uguccioni M, Dewald B, Baggiolini M, Clark-Lewis I. RANTES and MCP-3 antagonists bind multiple chemokine receptors. J Biol Chem 1996; 271: 10521–27.

Gordon FH, Lai CW, Hamilton MI, Allison MC, Srivastava ED, Fouweather MG, Donoghue S, Greenlees C, Subhani J, Amlot PL, Pounder RE. A randomized placebo-controlled trial of a humanized monoclonal antibody to alpha4 integrin in active Crohn's disease. Gastroenterol 2001; 121: 268-74.

Grimaldi JC, Yu NX, Grunig G, Seymour BW, Cottrez F, Robinson DS, Hosken N, Ferlin WG, Wu X, Soto H, O'Garra A, Howard MC, Coffman RL. Depletion of eosinophils in mice through the use of antibodies specific for C-C chemokine receptor 3 (CCR3). J Leukocyte Biol 1999; 65: 846–53.

Grisham MB, Pavlick KP, Laroux FS, Hoffman J, Bharwani S, Wolf RE. Nitric oxide and chronic gut inflammation: controversies in inflammatory bowel disease. J Investig Med 2002; 50: 272-83.

Hacker UT, Gomolka M, Keller E, Eigler A, Folwaczny C, Fricke H, Albert E, Loeschke K, Endres S. Lack of association between an interleukin-1 receptor antagonist gene polymorphism and ulcerative colitis. Gut 1997; 40: 623-7.

Hampe J, Cuthbert A, Croucher PJ, Mirza MM, Mascheretti S, Fisher S, Frenzel H, King K, Hasselmeyer A, MacPherson AJ, Bridger S, van Deventer S, Forbes A, Nikolaus S, Lennard-Jones JE, Foelsch UR, Krawczak M, Lewis C, Schreiber S, Mathew CG. Association between insertion mutation in NOD2 gene and Crohn's disease in German and British populations. Lancet 2001; 357: 1925-8.

Hampson SJ, Parker MC, Saverymuttu SH, Joseph AE, McFadden JJ, Hermon-Taylor J. Quadruple antimycobacterial chemotherapy in Crohn's disease: results at 9 months of a pilot study in 20 patients. Aliment Pharmacol Ther 1989; 3: 343-52.

Hata K, Andoh A, Shimada M, Fujino S, Bamba S, Araki Y, Okuno T, Fujiyama Y, Bamba T. IL-17 stimulates inflammatory responses via NF-kappaB and MAP kinase pathways in human colonic myofibroblasts. Am J Physiol Gastrointest Liver Physiol 2002; 282: G1035-44.

Heath H, Qin S, Rao P, Wu L, LaRosa G, Kassam N, Ponath PD, Mackay CR. Chemokine receptor usage by human eosinophils. The importance of CCR3 demonstrated using an antagonistic monoclonal antibody. J Clin Invest 1997; 99: 178–84.

Heller RA, Schena M, Chai A, Shalon D, Bedilion T, Gilmore J, Woolley DE, Davis RW. Discovery and analysis of inflammatory disease-related genes using cDNA microarrays. Proc Natl Acad Sci U S A 1997; 94: 2150-5.

Heresbach D, Semana G, Gosselin M, Bretagne MG. An immunomodulation strategy targeted towards immunocompetent cells or cytokines in inflammatory bowel diseases (IBD). Eur Cytokine Netw 1999; 10: 7-15.

Herfarth H, Scholmerich J. IL-10 therapy in Crohn's disease: at the crossroads. Treatment of Crohn's disease with the anti-inflammatory cytokine interleukin 10. Gut 2002; 50: 146-7.

Heuschkel RB, MacDonald TT, Monteleone G, Bajaj-Elliott M, Smith JA, Pender SL. Imbalance of stromelysin-1 and TIMP-1 in the mucosal lesions of children with inflammatory bowel disease. Gut 2000; 47: 57-62.

Hieshima K, Yoshie O. Chemokine receptors and HIV-1 infection Nippon Rinsho 2002; 60: 681-7.

Hildebrand H, Brydolf M, Holmquist L, Krantz I, Kristiansson B. Incidence and prevalence of inflammatory bowel disease in children in south-western Sweden. Acta Paediatr 1994; 83: 640-5.

Hirano T. Interleukin 6 and its receptor: ten years later. Int Rev Immunol 1998; 16: 249-84.

Ho CY, Wong CK, Li EK, Tam LS, Lam CW. Suppressive effect of combination treatment of leflunomide and methotrexate on chemokine expression in patients with rheumatoid arthritis. Clin Exp Immunol 2003; 133: 132-8.

Homey B, Dieu-Nosjean MC, Wiesenborn A, Massacrier C, Pin JJ, Oldham E, Catron D, Buchanan ME, Muller A, deWaal Malefyt R, Deng G, Orozco R, Ruzicka T, Lehmann P, Lebecque S, Caux C, Zlotnik A. Up-regulation of macrophage inflammatory protein-3 alpha/CCL20 and CC chemokine receptor 6 in psoriasis. J Immunol 2000; 164: 6621-32.

Homey B, Muller A, Zlotnik A. Chemokines: agents for the immunotherapy of cancer? Nat Rev Immunol 2002; 2: 175-84.

Homey B, Zlotnik A. Chemokines in allergy. Curr Opin Immunol 1999; 11: 626-34.

Hong X, Xu LG, Li X, Zhai Z, Shu HB. CSN3 interacts with IκKγ and inhibits TNF- but not IL-1-induced NF-κB activation. FEBS Letters 2001; 499: 133-136.

Hoover DM, Boulegue C, Yang D, Oppenheim JJ, Tucker K, Lu W, Lubkowski J. The structure of human macrophage inflammatory protein-3alpha /CCL20. Linking antimicrobial and CC chemokine receptor-6-binding activities with human beta-defensins. J Biol Chem 2002; 277: 37647-54.

Horuk R. Chemokine receptors. Cytokine Growth Factor Rev 2001; 12: 313-35.

Horuk R, Martin AW, Wang Z, Schweitzer L, Gerassimides A, Guo H, Lu Z, Hesselgesser J, Perez HD, Kim J, Parker J, Hadley TJ, Peiper SC. Expression of chemokine receptors by subsets of neurons in the central nervous system. J Immunol 1997; 158: 2882-90.

Huang N, Katz JP, Martin DR, Wu GD. Inhibition of IL-8 gene expression in Caco-2 cells by compounds which induce histone hyperacetylation. Cytokine 1997; 9: 27-36.

Hugot JP, Chamaillard M, Zouali H, Lesage S, Cezard JP, Belaiche J, Almer S, Tysk C, O'Morain CA, Gassull M, Binder V, Finkel Y, Cortot A, Modigliani R, Laurent-Puig P, Gower-Rousseau C, Macry J, Colombel JF, Sahbatou M, Thomas G. Association of NOD2 leucine-rich repeat variants with susceptibility to Crohn's disease. Nature 2001; 411: 599-603.

Hugot JP, Laurent-Puig P, Gower-Rousseau C, Olson JM, Lee JC, Beaugerie L, Naom I, Dupas JL, Van Gossum A, Orholm M, Bonaiti-Pellie C, Weissenbach J, Mathew CG, Lennard-Jones JE, Cortot A, Colombel JF, Thomas G. Mapping of a susceptibility locus for Crohn's disease on chromosome 16. Nature 1996; 379: 821-3.

Hugot JP, Zouali H, Lesage S. Lessons to be learned from the NOD2 gene in Crohn's disease. Eur J Gastroenterol Hepatol 2003; 15: 593-7.

Hull J, Rowlands K, Lockhart E, Moore C, Sharland M, Kwiatkowski D. Variants of the chemokine receptor CCR5 are associated with severe bronchiolitis caused by respiratory syncytial virus. J Infect Dis 2003; 188: 904-7.

Ina K, Kusugami K, Shimada M, Tsuzuki T, Nishio Y, Binion DG, Imada A, Ando T. Suppressive effects of cyclosporine A on neutrophils and T cells may be related to therapeutic benefits in patients with steroid-resistant ulcerative colitis. Inflamm Bowel Dis 2002; 8: 1-9.

Ishihara K[1], Hirano T. IL-6 in autoimmune disease and chronic inflammatory proliferative disease. Cytokine Growth Factor Rev 2002; 13: 357.

Ishihara K[2], Hirano T. Molecular basis of the cell specificity of cytokine action. Biochim Biophys Acta 2002; 1592: 281-96.

Ishizuka K, Sugimura K, Homma T, Matsuzawa J, Mochizuki T, Kobayashi M, Suzuki K, Otsuka K, Tashiro K, Yamaguchi O, Asakura H. Influence of interleukin-10 on the interleukin-1 receptor antagonist/interleukin-1 beta ratio in the colonic mucosa of ulcerative colitis. Digestion 2001; 63 Suppl 1:22-7.

Iwasaki A, Kelsall BL. Localization of distinct Peyer's patch dendritic cell subsets and their recruitment by chemokines macrophage inflammatory protein (MIP)-3α, MIP-3β and secondary lymphoid organ chemokine. J Exp Med 2000; 191: 1381-1393.

Izadpanah A, Dwinell MB, Eckmann L, Varki NM, Kagnoff MF. Regulated MIP-3α/CCL20 production by human intestinal epithelium: mechanism for modulating mucosal immunity. Am J Physiol Gastrointest Liver Physiol 2001; 280: G710-G719.

Jenkins D, Balsitis M, Gallivan S, Dixon MF, Gilmour HM, Shepherd NA, Theodossi A, Williams GT. Guidelines for the initial biopsy diagnosis of suspected chronic idiopathic inflammatory bowel disease. The British Society of Gastroenterology Initiative. J Clin Pathol 1997; Feb; 50: 93-105.

Jing H, Vassiliou E, Ganea D. Prostaglandin E2 inhibits production of the inflammatory chemokines CCL3 and CCL4 in dendritic cells. J Leukoc Biol. 2003; 74: 868-79.

Jones BW, Heldwein KA, Means TK, Saukkonen JJ, Fenton MJ. Differential roles of Toll-like receptors in the elicitation of proinflammatory responses by macrophages. Ann Rheum Dis 2001; 60 Suppl 3: iii 6-12.

Jones SC, Crabtree JE, Rembacken BJ, Dixon MF, Trejdosiewicz LK, Whicher JT, Axon AT. Mucosal interleukin-6 secretion in ulcerative colitis. Effects of anti-inflammatory drugs and T-cell stimulation. Scand J Gastroenterol 1994; 29: 722-8.

Jones SC, Trejdosiewicz LK, Banks RE, Howdle PD, Axon AT, Dixon MF, Whicher JT. Expression of interleukin-6 by intestinal enterocytes. J Clin Pathol 1993; 46: 1097–1100.

Juliano RL. Signal transduction by cell adhesion receptors and the cytoskeleton: functions of integrins, cadherins, selectins, and immunoglobulin-superfamily members. Annu Rev Pharmacol Toxicol 2002; 42: 283-323.

Kaser A, Ludwiczek O, Holzmann S, Moschen AR, Weiss G, Enrich B, Graziadei I, Dunzendorfer S, Wiedermann CJ, Murzl E, Grasl E, Jasarevic Z, Romani N, Offner FA, Tilg H. Increased expression of CCL20 in human inflammatory bowel disease. J Clin Immunol 2004; 24: 74-85.

Kashyap A, Forman SJ. Autologous bone marrow transplantation for non-Hodgkin's lymphoma resulting in long-term remission of coincidental Crohn's disease. Br J Haematol 1998; 103: 651-2.

Kawai T, Takeuchi O, Fujita T, Inoue J, Muhlradt PF, Sato S, Hoshino K, Akira S. Lipopolysaccharide stimulates the MyD88-independent pathway and results in activation of IFN-regulatory factor 3 and the expression of a subset of lipopolysaccharide-inducible genes. J Immunol 2001; 167: 5887–5894.

Keshavarzian A, Banan A, Farhadi A, Komanduri S, Mutlu E, Zhang Y, Fields JZ. Increases in free radicals and cytoskeletal protein oxidation and nitration in the colon of patients with inflammatory bowel disease. Gut 2003; 52: 720-8.

Krishnan A, Korzenik JR. Inflammatory bowel disease and environmental influences. Gastroenterol Clin North Am 2002; 31: 21-39.

Kruidenier L, Kuiper I, Van Duijn W, Mieremet-Ooms MA, van Hogezand RA, Lamers CB, Verspaget HW. Imbalanced secondary mucosal antioxidant response in inflammatory bowel disease. J Pathol 2003; 201: 17-27.

Krzysiek R, Lefevre EA, Bernard J, Foussat A, Galanaud P, Louache F, Richard Y. Regulation of CCR6 chemokine receptor expression and responsiveness to macrophage inflammatory protein-3alpha/CCL20 in human B cells. Blood 2000; 96: 2338-45.

Kuboyama S. Increased circulating levels of interleukin-1 receptor antagonist in patients with inflammatory bowel disease. Kurume Med J 1998; 45: 33-7.

Kucharzik T, Hudson JT 3rd, Waikel RL, Martin WD, Williams IR. CCR6 expression distinguishes mouse myeloid and lymphoid dendritic cell subsets: demonstration using a CCR6 EGFP knock-in mouse. Eur J Immunol 2002; 32: 104-12.

Kucharzik T, Stoll R, Lugering N, Domschke W. Circulating antiinflammatory cytokine IL-10 in patients with inflammatory bowel disease (IBD). Clin Exp Immunol 1995; 100: 452-6.

Kuhn R, Lohler J, Rennick D, Rajewsky K, Muller W. Interleukin-10-deficient mice develop chronic enterocolitis. Cell 1993; 75: 263-74.

Kunkel EJ, Butcher EC. Chemokines and the tissue-specific migration of lymphocytes. Immunity 2002; 16: 1-4.

Kunkel EJ, Campbell DJ, Butcher EC. Chemokines in lymphocyte trafficking and intestinal immunity. Microcirculation 2003; 10: 313-23.

Kunkel EJ, Dunne JL, Ley K. Leukocyte arrest during cytokine-dependent inflammation in vivo. J Immunol 2000; 164: 3301-8.

Kwon JH, Keates S, Bassani L, Mayer LF, Keates AC. Colonic epithelial cells are a major site of macrophage inflammatory protein 3alpha (MIP-3alpha) production in normal colon and inflammatory bowel disease. Gut 2002; 51: 818-26.

Lahav M, Levite M, Bassani L, Lang A, Fidder H, Tal R, Bar-Meir S, Mayer L, Chowers Y. Lidocaine inhibits secretion of IL-8 and IL-1beta and stimulates secretion of IL-1 receptor antagonist by epithelial cells. Clin Exp Immunol 2002; 127: 226-33.

Langmead L, Dawson C, Hawkins C, Banna N, Loo S, Rampton DS. Antioxidant effects of herbal therapies used by patients with inflammatory bowel disease: an in vitro study. Aliment Pharmacol Ther 2002; 16: 197-205.

Lapidot T, Petit I. Current understanding of stem cell mobilization: the roles of chemokines, proteolytic enzymes, adhesion molecules, cytokines, and stromal cells. Exp Hematol 2002; 30: 973-81.

Leiper K, Campbell BJ, Jenkinson MD, Milton J, Yu LG, Democratis J, Rhodes JM. Interaction between bacterial peptides, neutrophils and goblet cells: a possible mechanism for neutrophil recruitment and goblet cell depletion in colitis. Clin Sci 2001; 101: 395-402.

Lewin J, Dhillon AP, Sim R, Mazure G, Pounder RE, Wakefield AJ. Persistent measles virus infection of the intestine: confirmation by immunogold electron microscopy. Gut 1995; 36: 564-9.

Ley K. Arrest chemokines. Microcirculation 2003; 10: 289-95.

Ley K. Integration of inflammatory signals by rolling neutrophils. Immunol Rev 2002; 186:8-18.

Li Xinmin[1], Stark GR. NFkappaB-dependent signaling pathways. Exp Hematol 2002; 30: 285-96.

Li Xinmin[2], Gu W, Mohan S, Baylink DJ. DNA microarrays: their use and misuse. Microcirculation 2002; 9: 13-22.

Liao F, Rabin RL, Smith CS, Sharma G, Nutman TB, Farber JM. CC-chemokine receptor 6 is expressed on diverse memory subsets of T-cells and determines responsiveness to macrophage inflammatory protein 3α. J Immunol 1999; 162: 186-194.

Liao F, Shirakawa AK, Foley JF, Rabin RL, Farber JM. Human B cells become highly responsive to macrophage-inflammatory protein-3 alpha/CC chemokine ligand-20 after cellular activation without changes in CCR6 expression or ligand binding. J Immunol 2002; 168: 4871-80.

Ligumsky M, Karmeli F, Sharon P, Zor U, Cohen F, Rachmilewitz D. Enhanced thromboxane A2 and prostacyclin production by cultured rectal mucosa in ulcerative colitis and its inhibition by steroids and sulfasalazine. Gastroenterol 1981; 81: 444-9.

Lin TJ, Maher LH, Gomi K, McCurdy JD, Garduno R, Marshall JS. Selective Early Production of CCL20, or Macrophage Inflammatory Protein 3alpha, by Human Mast Cells in Response to Pseudomonas aeruginosa. Infect Immun 2003; 71: 365-73.

Lin ZQ, Kondo T, Ishida Y, Takayasu T, Mukaida N. Essential involvement of IL-6 in the skin wound-healing process as evidenced by delayed wound healing in IL-6-deficient mice. J Leukoc Biol 2003; 73: 713-21.

Lindhout E, van Eijk M, van Pel M, Lindeman J, Dinant HJ & de Groot C. Fibroblast-like synoviocytes from rheumatoid arthritis patients have intrinsic properties of follicular dendritic cells. J Immunol 1999; 162: 5949-56.

Loftus EV Jr, Sandborn WJ. Epidemiology of inflammatory bowel disease. Gastroenterol Clin North Am 2002; 31: 1-20.

Lopez-Cubero SO, Sullivan KM, McDonald GB. Course of Crohn's disease after allogeneic marrow transplantation. Gastroenterol 1998; 114: 433-40.

Louis E, Satsangi J, Roussomoustakaki M, Parkes M, Fanning G, Welsh K, Jewell D. Cytokine gene polymorphisms in inflammatory bowel disease. Gut 1996; 39: 705-10.

Louis E, Ribbens C, Godon A, Franchimont D, De Groote D, Hardy N, Boniver J, Belaiche J, Malaise M. Increased production of matrix metalloproteinase-3 and tissue inhibitor of metalloproteinase-1 by inflamed mucosa in inflammatory bowel disease. Clin Exp Immunol 2000; 120: 241-6.

Lukacs NW, Prosser DM, Wiekowski M, Lira SA, Cook DN. Requirement for the chemokine receptor CCR6 in allergic pulmonary inflammation. J Exp Med 2001; 20: 194: 551-5.

Luster AD. The role of chemokines in linking innate and adaptive immunity. Curr Opin Immunol 2002; 14: 129-35.

MacDonald KP, Pettit AR, Quinn C, Thomas GJ, Thomas R. Resistance of rheumatoid synovial dendritic cells to the immunosuppressive effects of IL-10. J Immunol 1999; 163: 5599-607.

MacDonald TT, Murch SH. The aetiology and pathogenesis of chronic inflammatory bowel disease. Baillière's Clin Gastroenterol 1994; 8: 1-34.

Mack M, Luckow B, Nelson PJ, Cihak J, Simmons G, Clapham PR, Signoret N, Marsh M, Stangassinger M, Borlat F, Wells TN, Schlondorff D, Proudfoot AE. Aminooxypentane-RANTES induces CCR5 internalization but inhibits recycling: a novel inhibitory mechanism of HIV infectivity. J Exp Med 1998; 187: 1215-24.

Macpherson A, Khoo UY, Forgacs I, Philpott-Howard J, Bjarnason I. Mucosal antibodies in inflammatory bowel disease are directed against intestinal bacteria. Gut 1996; 38: 365-75.

Madsen K. Combining T cells and IL-10: a new therapy for Crohn's disease? Gastroenterol 2002; 123: 1877-88.

Mahida YR. The key role of macrophages in the immunopathogenesis of inflammatory bowel disease. Inflamm Bowel Dis 2000; 6: 21-33.

Mahler M, Leiter EH. Genetic and environmental context determines the course of colitis developing in IL-10-deficient mice. Inflamm Bowel Dis 2002; 8: 347-55 .

Marek A, Brodzicki J, Liberek A, Korzon M. TGF-beta (transforming growth factor-beta) in chronic inflammatory conditions - a new diagnostic and prognostic marker? Med Sci Monit 2002; 8: RA145-51.

Martin C, Burdon PC, Bridger G, Gutierrez-Ramos JC, Williams TJ, Rankin SM. Chemokines acting via CXCR2 and CXCR4 control the release of neutrophils from the bone marrow and their return following senescence. Immunity 2003; 19: 583-93.

Martin HM, Rhodes JM. Bacteria and inflammatory bowel disease. Curr Opin Infect Dis 2000; 13: 503-509.

Matsui T, Akahoshi T, Namai R, Hashimoto A, Kurihara Y, Rana M, Nishimura A, Endo H, Kitasato H, Kawai S, Takagishi K, Kondo H. Selective recruitment of CCR6-expressing cells by increased production of MIP-3 alpha in rheumatoid arthritis. Clin Exp Immunol 2001; 125:155-61.

Matsukawa A, Hogaboam CM, Lukacs NW, Kunkel SL. Chemokines and innate immunity. Rev Immunogenet. 2000; 2: 339-58.

McAlindon ME, Gray T, Galvin A, Sewell HF, Podolsky DK, Mahida YR. Differential lamina propria cell migration via basement membrane pores of inflammatory bowel disease mucosa. Gastroenterology 1998; 115: 841-8.

McCartney SA, Mitchell JA, Fairclough PD, Farthing MJ, Warner TD. Selective COX-2 inhibitors and human inflammatory bowel disease. Aliment Pharmacol Ther 1999; 13: 1115-7.

McColl SR. Chemokines and dendritic cells: a crucial alliance. Immunol Cell Biol 2002; 80: 489-96.

Miceli-Richard C, Lesage S, Rybojad M, Prieur AM, Manouvrier-Hanu S, Hafner R, Chamaillard M, Zouali H, Thomas G, Hugot JP. CARD15 mutations in Blau syndrome. Nat Genet 2001; 29: 19-20.

Mir A, Minguez M, Tatay J, Pascual I, Pena A, Sanchiz V, Almela P, Mora F, Benages A. Elevated serum eotaxin levels in patients with inflammatory bowel disease. Am J Gastroenterol 2002; 97: 1452-7.

Mizoguchi A, Mizoguchi E, Chiba C, Bhan AK. Role of appendix in the development of inflammatory bowel disease in TCR-α mutant mice. J Exp Med 1996; 184: 707-715.

Monteleone I, Vavassori P, Biancone L, Monteleone G, Pallone F. Immunoregulation in the gut: success and failures in human disease. Gut 2002; 50 Suppl 3:III 60-4.

Montgomery SM, Morris DL, Thompson NP, Subhani J, Pounder RE, Wakefield AJ. Prevalence of inflammatory bowel disease in British 26 year olds: national longitudinal birth cohort. BMJ 1998; 316, 1058–1059.

Mowat AM, Viney JL. The anatomical basis of intestinal immunity. Immunol Rev 1997; 156: 145-66.

Muller G, Lipp M. Shaping up adaptive immunity: the impact of CCR7 and CXCR5 on lymphocyte trafficking. Microcirculation 2003; 10: 325-34.

Murakami T, Nakajima T, Koyanagi Y, Tachibana K, Fujii N, Tamamura H, Yoshida N, Waki M, Matsumoto A, Yoshie O, Kishimoto T, Yamamoto N, Nagasawa T. A small molecule CXCR4 inhibitor that blocks T cell linetropic HIV-1 infection. J Exp Med 1997; 186: 1389–93.

Murch SH. Local and systemic effects of macrophage cytokines in intestinal inflammation. Nutrition 1998; 14: 780-3.

Murphy PM. Neutrophil receptors for interleukin-8 and related CXC chemokines. Semin Hematol 1997; 34: 311-8.

Mwantembe O, Gaillard MC, Barkhuizen M, Pillay V, Berry SD, Dewar JB, Song E. Ethnic differences in allelic associations of the interleukin-1 gene cluster in South African patients with inflammatory bowel disease (IBD) and in control individuals. Immunogenetics 2001; 52: 249-54.

Nagata K, Tanaka K, Ogawa K, Kemmotsu K, Imai T, Yoshie O, Abe H, Tada K, Nakamura M, Sugamura K, Takano S. Selective expression of a novel surface molecule by human Th2 cells in vivo. J Immunol 1999; 162: 1278–86.

Nakayama T, Fujisawa R, Yamada H, Horikawa T, Kawasaki H, Hieshima K, Izawa D, Fujiie S, Tezuka T, Yoshie O. Inducible expression of a CC chemokine liver- and activation-regulated chemokine (LARC)/ macrophage inflammatory protein (MIP)-3α/ CCL20 by epidermal keratinocytes and its role in atopic dermatitis. Internat Immunol 2001; 13: 95-103.

Nanki T, Lipsky PE. Cytokine, activation marker, and chemokine receptor expression by individual CD4(+) memory T cells in rheumatoid arthritis synovium. Arthritis Res 2000; 2: 415-23.

Nasuhara Y, Adcock IM, Catley M, Barnes PJ, Newton R. Differential IκB kinase activation and IkBa degradation by interleukin-1β and tumor necrosis factor-α in human U937 monocytic cells. J Biol Chem 1999; 274: 19965-19972.

Nemetz A, Nosti-Escanilla MP, Molnar T, Kope A, Kovacs A, Feher J, Tulassay Z, Nagy F, Garcia-Gonzalez MA, Pena AS. IL1β gene polymorphisms influence the course and severity of inflammatory bowel disease. Immunogenetics 1999; 49: 527-531.

Nemetz A, Toth M, Garcia-Gonzalez MA, Zagoni T, Feher J, Pena AS, Tulassay Z. Allelic variation at the interleukin 1beta gene is associated with decreased bone mass in patients with inflammatory bowel diseases. Gut 2001; 49: 644-9.

Ness TL, Hogaboam CM, Strieter RM, Kunkel SL. Immunomodulatory role of CXCR2 during experimental septic peritonitis. J Immunol 2003; 171: 3775-84.

Neurath MF, Becker C, Barbulescu K. Role of NF-kappaB in immune and inflammatory responses in the gut. Gut 1998; 43: 856-60.

Neurath MF, Fuss I, Kelsall BL, Stuber E, Strober W. Antibodies to interleukin 12 abrogate established experimental colitis in mice. J Exp Med 1995; 182: 1281-90.

Neurath MF, Weigmann B, Finotto S, Glickman J, Nieuwenhuis E, Iijima H, Mizoguchi A, Mizoguchi E, Mudter J, Galle PR, Bhan A, Autschbach F, Sullivan BM, Szabo SJ, Glimcher LH, Blumberg RS. The transcription factor T-bet regulates mucosal T cell activation in experimental colitis and Crohn's disease. J Exp Med 2002; 195: 1129-43.

Nirodi C, NagDas S, Gygi SP, Olson G, Aebersold R, Richmond A. A role for poly(ADP-ribose) polymerase in the transcriptional regulation of the melanoma growth stimulatory activity (CXCL1) gene expression. J Biol Chem 2001; 276: 9366-9374.

Ogilvie P, Paoletti S, Clark-Lewis I, Uguccioni M. Eotaxin-3 is a natural antagonist for CCR2 and exerts a repulsive effect on human monocytes. Blood 2003; 102: 789-94.

Ogura Y, Bonen DK, Inohara N, Nicolae DL, Chen FF, Ramos R, Britton H, Moran T, Karaliuskas R, Duerr RH, Achkar JP, Brant SR, Bayless TM, Kirschner BS, Hanauer SB, Nunez G, Cho JH. A frameshift mutation in NOD2 associated with susceptibility to Crohn's disease. Nature 2001 31; 411: 603-6.

Ohtsuka Y, Lee J, Stamm DS, Sanderson IR. MIP-2 secreted by epithelial cells increases neutrophil and lymphocyte recruitment in the mouse intestine. Gut 2001; 49: 526-33.

Olson TS, Ley K. Chemokines and chemokine receptors in leukocyte trafficking. Am J Physiol Regul Integr Comp Physiol 2002; 283: R7-28.

Ono SJ, Nakamura T, Miyazaki D, Ohbayashi M, Dawson M, Toda M. Chemokines: roles in leukocyte development, trafficking, and effector function. J Allergy Clin Immunol 2003; 111: 1185-99.

Onuffer JJ, Horuk R. Chemokines, chemokine receptors and small-molecule antagonists: recent developments. Trends Pharmacol Sci 2002; 23: 459-67.

Orholm M, Binder V, Sorensen TI, Rasmussen LP, Kyvik KO. Concordance of inflammatory bowel disease among Danish twins. Results of a nationwide study. Scand J Gastroenterol 2000; 35: 1075-81.

Orr MS, Scherf U. Large-scale gene expression analysis in molecular target discovery. Leukemia 2002; 16: 473-7.

Oshima T, Pavlick KP, Laroux FS, Verma SK, Jordan P, Grisham MB, Williams L, Alexander JS. Regulation and distribution of MAdCAM-1 in endothelial cells in vitro. Am J Physiol Cell Physiol 2001; 281: C1096-105 .

Otte JM, Rosenberg IM, Podolsky DK. Intestinal myofibroblasts in innate immune responses of the intestine. Gastroenterol 2003; 124: 1866-78.

Panja A, Goldberg S, Eckmann L, Krishen P, Mayer L. The regulation and functional consequence of proinflammatory cytokine binding on human intestinal epithelial cells. J Immunol 1998; 161: 3675-3684.

Papadakis KA. Chemokines in inflammatory bowel disease. Curr Allergy Asthma Rep 2004; 4: 83-9.

Papadakis KA, Targan SR. The role of chemokines and chemokine receptors in mucosal inflammation. Inflamm Bowel Dis 2000; 6: 303-313.

Parekh BS, Maniatis T. Virus infection leads to localized hyperacetylation of histones H3 and H4 at the IFN-β promoter. Mol Cell 1999; 3: 125-129.

Patel KD, Cuvelier SL, Wiehler S. Selectins: critical mediators of leukocyte recruitment. Semin Immunol 2002; 14: 73-81.

Pavlick KP, Laroux FS, Fuseler J, Wolf RE, Gray L, Hoffman J, Grisham MB. Role of reactive metabolites of oxygen and nitrogen in inflammatory bowel disease. Free Radic Biol Med 2002; 33: 311-22.

Pender SL, Tickle SP, Docherty AJ, Howie D, Wathen NC, MacDonald TT. A major role for matrix metalloproteinases in T cell injury in the gut. J Immunol 1997; 158: 1582-90.

Pender SL, Quinn JJ, Sanderson IR, MacDonald TT. Butyrate upregulates stromelysin-1 production by intestinal mesenchymal cells. Am J Physiol Gastrointest Liver Physiol 2000; 279: G918-24 .

Perez-Canadillas JM, Zaballos A, Gutierrez J, Varona R, Roncal F, Albar JP, Marquez G, Bruix M. NMR solution structure of murine CCL20/MIP-3alpha, a chemokine that specifically chemoattracts immature dendritic cells and lymphocytes through its highly specific interaction with the beta-chemokine receptor CCR6. J Biol Chem 2001; 27; 276: 28372-9.

Porreca E, Reale M, Di Febbo C, Di Gioacchino M, Barbacane RC, Castellani ML. Down-regulation of cyclooxygenase-2 (COX-2) by interleukin-1 receptor antagonist in human monocytes. Immunology 1996; 89: 424-9.

Powell JJ, Harvey RS, Ashwood P, Wolstencroft R, Gershwin ME, Thompson RP. Immune potentiation of ultrafine dietary particles in normal subjects and patients with inflammatory bowel disease. J Autoimmun 2000; 14: 99-105.

Power CA, Meyer A, Nemeth K, Bacon KB, Hoogewerf AJ, Proudfoot AE, Wells TN. Molecular 7cloning and functional expression of a novel CC chemokine receptor cDNA from a human basophilic cell line. J Biol Chem 1995; 270: 19495-500.

Premont RT, Inglese J, Lefkowitz RJ. Protein kinases that phosphorylate activated G protein-coupled receptors. Faseb J 1995; 9: 175–82.

Propst A, Propst T, Herold M, Vogel W, Judmaier G. Interleukin-1 receptor antagonist in differential diagnosis of inflammatory bowel diseases. Eur J Gastroenterol Hepatol 1995; 7: 1031-6.

Proudfoot AE. Chemokine receptors: multifaceted therapeutic targets. Nat Rev Immunol 2002; 2: 106-15.

Qin S, Rottman JB, Myers P, Kassam N, Weinblatt M, Loetscher M, Koch AE, Moser B, Mackay CR. The chemokine receptors CXCR3 and CCR5 mark subsets of T cells associated with certain inflammatory reactions. J Clin Invest 1997; 101: 746–54.

Ragozzino D. CXC chemokine receptors in the central nervous system: Role in cerebellar neuromodulation and development. J Neurovirol 2002; 8: 559-72.

Rajarathnam K. Designing decoys for chemokine-chemokine receptor interaction. Curr Pharm Des 2002; 8: 2159-69.

Rampton DS, Sladen GE, Youlten LJ. Rectal mucosal prostaglandin E2 release and its relation to disease activity, electrical potential difference, and treatment in ulcerative colitis. Gut 1980; 21: 591-6.

Rampton DS, Stott RB. Crohn's disease in monozygotic twins. Postgrad Med J 1986; 62: 1047-9.

Randolph GJ, Beaulieu S, Lebecque S, Steinman RM, Muller WA. Differentiation of monocytes into dendritic cells in a model of transendothelial trafficking. Science 1998; 282: 480–83.

Reif K, Ekland EH, Ohl L, Nakano H, Lipp M, Forster R and Cyster JG. Balanced responsiveness to chemoattractants from adjacent zones determines B-cell position. Nature 2002; 416: 94-99.

Reimund JM, Wittersheim C, Dumont S, Muller CD, Kenney JS, Baumann R, Poindron P, Duclos B. Increased production of tumour necrosis factor-alpha interleukin-1 beta, and interleukin-6 by morphologically normal intestinal biopsies from patients with Crohn's disease. Gut 1996; 39: 684-9.

Reiss Y, Proudfoot AE, Power CA, Campbell JJ, Butcher EC. CC chemokine receptor (CCR)4 and the CCR10 ligand cutaneous T cell-attracting chemokine (CTACK) in lymphocyte trafficking to inflamed skin. J Exp Med 2001; 194: 1541-7.

Reuter BK, Asfaha S, Buret A, Sharkey KA, Wallace JL. Exacerbation of inflammation-associated colonic injury in rat through inhibition of cyclooxygenase-2. J Clin Invest 1996; 98: 2076-85.

Rhodes JM. Surveillance for colitis-associated cancer: we cannot stop now. Dig Liver Dis 2002; 34: 319-21. Dig Liver Dis 2002; 34: 339-42.

Richmond A. Nf-kappa B, chemokine gene transcription and tumour growth. Nat Rev Immunol 2002; 2: 664-74.

Robertson MJ. Role of chemokines in the biology of natural killer cells. J Leukoc Biol 2002; 71: 173-83.

Rollins BJ. Chemokines. Blood 1997; 90: 909-28.

Rose-John S, Schooltink H. CDP-870. Celltech/Pfizer. Curr Opin Investig Drugs 2003; 45: 588-92.

Rossi D, Zlotnik A. The biology of chemokines and their receptors. Annu Rev Immunol Annu Rev Immunol 2000; 18: 217-42.

Rowbotham DS, Mapstone NP, Trejdosiewicz LK, Howdle PD, Quirke P. Mycobacterium paratuberculosis DNA not detected in Crohn's disease tissue by fluorescent polymerase chain reaction. Gut 1995; 37: 660-7.

Ruschpler P, Lorenz P, Eichler W, Koczan D, Hanel C, Scholz R, Melzer C, Thiesen HJ, Stiehl P. High CXCR3 expression in synovial mast cells associated with CXCL9 and CXCL10 expression in inflammatory synovial tissues of patients with rheumatoid arthritis. Arthritis Res Ther 2003; 5: R241-52.

Rutgeerts P, Van Deventer S, Schreiber S. Review article: the expanding role of biological agents in the treatment of inflammatory bowel disease - focus on selective adhesion molecule inhibition. Aliment Pharmacol Ther 2003; 17: 1435-50.

Ryan P, Kelly RG, Lee G, Collins JK, O'Sullivan GC, O'Connell J, Shanahan F. Bacterial DNA within granulomas of patients with Crohn's disease - detection by laser capture microdissection and PCR. Am J Gastroenterol. 2004; 99: 1539-43.

Sadlack B, Merz H, Schorle H, Schimpl A, Feller AC, Horak I. Ulcerative colitis-like disease in mice with a disrupted interleukin-2 gene. Cell 1993; 75: 253-61.

Sallusto F, Lanzavecchia A. Efficient presentation of soluble antigen by cultured human dendritic cells is maintained by granulocyte/macrophage colony-stimulating factor plus interleukin 4 and downregulated by tumor necrosis factor alpha. J Exp Med 1994; 179: 1109-18.

Sallusto F[1], Lanzavecchia A, Mackay CR. Chemokines and chemokine receptors in T-cell priming and Th1/Th2-mediated responses. Immunol Today 1998; 19: 568–74.

Sallusto F[2], Lenig D, Mackay Cr, Lanzavecchia A. Flexible programs of chemokine receptor expression on human polarized T helper 1 and 2 lymphocytes. J Exp Med 1998; 187: 875–83.

Sallusto F, Mackay CR, Lanzavecchia A. The Role of Chemokine Receptors in Primary, Effector, and Memory Immune Responses. Annu Rev Immunol 2000; 18: 593-620.

Sallusto F[3], Schaerli P, Loetscher P, Schaniel C, Lenig D, Mackay CR, Qin S, Lanzavecchia A. Rapid and coordinated switch in chemokine receptor expression during dendritic cell maturation. Eur J Immunol 1998; 28: 2760–69.

Samson M, Soularue P, Vassart G, Parmentier M. The genes encoding the human CC-chemokine receptors CC-CKR1 to CC-CKR5 (CMKBR1-CMKBR5) are clustered in the p21.3-p24 region of chromosome 3. Genomics 1996; 36: 522-6.

Sandborn WJ. Optimizing anti-tumor necrosis factor strategies in inflammatory bowel disease. Curr Gastroenterol Rep 2003; 5: 501-5.

Sandborn WJ, Targan SR. Biologic therapy of inflammatory bowel disease. Gastroenterol 2002; 122: 1592-608.

Sanderson JD, Moss MT, Tizard ML, Hermon-Taylor J. Mycobacterium paratuberculosis DNA in Crohn's disease tissue. Gut 1992; 33: 890-6.

Sarsfield P, Rinne A, Jones DB, Johnson P, Wright DH. Accessory cells in physiological lymphoid tissue from the intestine: an immunohistochemical study. Histopathology 1996; 28: 205-11.

Sato K, Kawasaki H, Nagayama H, Enomoto M, Morimoto C, Tadokoro K, Juji T, Takahashi T. TGF-beta 1 reciprocally controls chemotaxis of human peripheral blood monocyte-derived dendritic cells via chemokine receptors. J Immunol 2000; 164: 2285-95.

Scapini P, Laudanna C, Pinardi C, Allavena P, Mantovani A, Sozzani S, Cassatella MA. Neutrophils produce biologically active macrophage inflammatory protein-3alpha (MIP-3alpha)/CCL20 and MIP-3beta/CCL19. Eur J Immunol 2001; 31: 1981-8.

Schaufelberger HD, Uhr MR, McGuckin C, Logan RP, Misiewicz JJ, Gordon-Smith EC, Beglinger C. Platelets in ulcerative colitis and Crohn's disease express functional interleukin-1 and interleukin-8 receptors. Eur J Clin Invest 1994; 24: 656-63.

Scheerens H, Hessel E, Waal-Malefyt R, Leach MW, Rennick D. Characterisation of chemokines and chemokine receptors in two murine models of inflammatory bowel disease: IL-

10 $^{-/-}$ mice and Rag-2 $^{-/-}$ mice reconstituted with CD4 $^{+}$CD45RB ^{high} T cells. Euro J Immunol 2001; 31: 1465-1474.

Schmuth M, Neyer S, Rainer C, Grassegger A, Fritsch P, Romani N, Heufler C. Expression of the C-C chemokine MIP-3 alpha/CCL20 in human epidermis with impaired permeability barrier function. Exp Dermatol 2002; 11: 135-42.

Schols D, Struyf S, Van Damme J, Este JA, Henson G, De Clercq E. Inhibition of T-tropic HIV strains by selective antagonization of the chemokine receptor CXCR4. J Exp Med 1997; 186: 1383–88.

Schraufstatter IU, Chung J, Burger M. IL-8 activates endothelial cell CXCR1 and CXCR2 through Rho and Rac signaling pathways. Am J Physiol Lung Cell Mol Physiol 2001; 280: L1094-103.

Schreiber S[1]. Experimental immunomodulatory therapy of inflammatory bowel disease. Neth J Med 1998; 53: S24-31.

Schreiber S, Heinig T, Thiele HG, Raedler A. Immunoregulatory role of interleukin 10 in patients with inflammatory bowel disease. Gastroenterol 1995; 108: 1434-44.

Schreiber S[2], Nikolaus S, Hampe J. Activation of nuclear factor kappa B inflammatory bowel disease. Gut 1998; 42: 477-84.

Schreiber S, Nikolaus S, Hampe J, Hamling J, Koop I, Groessner B, Lochs H, Raedler A. Tumour necrosis factor alpha and interleukin-1 beta in relapse of Crohn's disease. Lancet 1999; 353: 459-61.

Schutyser E, Struyf S, Menten P, Lenaerts JP, Conings R, Put W, Wuyts A, Proost P, Van Damme J. Regulated production and molecular diversity of human liver and activation-regulated chemokine/macrophage inflammatory protein-3 alpha from normal and transformed cells. J Immunol 2000; 165: 4470-7.

Schutyser E, Struyf S, Van Damme J. The CC chemokine CCL20 and its receptor CCR6. Cytokine Growth Factor Rev 2003; 14: 409-26.

Scozzafava A, Mastrolorenzo A, Supuran CT. Non-peptidic chemokine receptors antagonists as emerging anti-HIV agents. J Enzyme Inhib Med Chem 2002; 17: 69-76.

Sellebjerg F, Sorensen TL. Chemokines and matrix metalloproteinase-9 in leukocyte recruitment to the central nervous system. Brain Res Bull 2003; 61: 347-55.

Shanahan F. Crohn's disease. Lancet 2002; 359: 62-9.

Shao L, Serrano D, Mayer L. The role of epithelial cells in immune regulation in the gut. Sem Immunol 2001; 13: 163-175.

Sharan R, Schoen RE. Cancer in inflammatory bowel disease. An evidence-based analysis and guide for physicians and patients. Gastroenterol Clin North Am 2002; 31: 237-54.

Shigematsu S. Therapeutic potential of interleukin-1 receptor antagonist in inflammatory bowel disease. Kurume Med J 1998; 45: 175-9.

Shimizu Y, Murata H, Kashii Y, Hirano K, Kunitani H, Higuchi K, Watanabe A. CC-chemokine receptor 6 and its ligand macrophage inflammatory protein 3alpha might be involved in the amplification of local necroinflammatory response in the liver. Hepatology 2001; 34: 311-9.

Shiokawa D, Maruta H, Tanuma S. Inhibitors of poly(ADP-ribose) polymerase suppress nuclear fragmentation and apoptotic-body formation during apoptosis in HL-60 cells. FEBS Lett 1997; 413: 99-103.

Shirachi A. Therapeutic implications of interleukin-10 in inflammatory bowel disease. Kurume Med J 1998; 45: 63-7.

Shirazi T, Longman RJ, Corfield AP, Probert CS. Mucins and inflammatory bowel disease. Postgrad Med J 2000; 76: 473-8.

Siegmund B. Interleukin-1beta converting enzyme (caspase-1) in intestinal inflammation. Biochem Pharmacol 2002; 64: 1-8.

Siegmund B, Lehr HA, Fantuzzi G, Dinarello CA. IL-1 β-converting enzyme (caspase-1) in intestinal inflammation. Proc Natl Acad Sci U S A 2001; 6; 98:13249-54.

Simmonds NJ, Millar AD, Blake DR, Rampton DS. Antioxidant effects of aminosalicylates and potential new drugs for inflammatory bowel disease: assessment in cell-free systems and inflamed human colorectal biopsies. Aliment Pharmacol Ther 1999; 13: 363-72.

Simmons G, Clapham PR, Picard L, Offord RE, Rosenkilde MM, Schwartz TW, Buser R, Wells TNC, Proudfoot AE. Potent inhibition of HIV-1 infectivity in macrophages and lymphocytes by a novel CCR5 antagonist. Science 1997; 276: 276–79.

Sims TN, Dustin ML. The immunological synapse: integrins take the stage. Immunol Rev 2002; 186: 100-17.

Siveke JT, Hamann A. T helper 1 and T helper 2 cells respond differentially to chemokines. J Immunol 1998; 15: 160:550-4.

Skelton L, Cooper M, Murphy M, Platt A. Human immature monocyte-derived dendritic cells express the G protein-coupled receptor GPR105 (KIAA0001, P2Y14) and increase intracellular calcium in response to its agonist, uridine diphosphoglucose. J Immunol 2003; 171: 1941-9.

Stadnyk AW. Intestinal epithelial cells as a source of inflammatory cytokines and chemokines. Can J Gastroenterol 2002; 16: 241-6.

Stamenkovic I. Extracellular matrix remodelling: the role of matrix metalloproteinases. J Pathol. 2003; 200: 448-64.

Stassen M, Hultner L, Muller C, Schmitt E. Mast cells and inflammation. Arch Immunol Ther Exp (Warsz) 2002; 50: 179-85.

Steidler L, Hans W, Schotte L, Neirynck S, Obermeier F, Falk W, Fiers W, Remaut E. Treatment of murine colitis by Lactococcus lactis secreting interleukin-10. Science 2000; 289: 1352-5.

Stein JV, Rot A, Luo Y, Narasimhaswamy M, Nakano H, Gunn MD, Matsuzawa A, Quackenbush EJ, Dorf ME, von Andrian UH. The CC chemokine thymus-derived chemotactic agent 4 (TCA-4, secondary lymphoid tissue chemokine, 6Ckine, exodus-2) triggers lymphocyte function-associated antigen 1-mediated arrest of rolling T lymphocytes in peripheral lymph node high endothelial venules. J Exp Med 2000; 191: 61-76.

Stokkers PC, van Aken BE, Basoski N, Reitsma PH, Tytgat GN, Van Deventer SJ. Five genetic markers in the interleukin 1 family in relation to inflammatory bowel disease. Gut 1998; 43: 33-9.

Sugita S, Kohno T, Yamamoto K, Imaizumi Y, Nakajima H, Ishimaru T, Matsuyama T. Induction of macrophage-inflammatory protein-3alpha gene expression by TNF-dependent NF-kappaB activation. J Immunol 2002; 168: 5621-8.

Sullivan SK, McGrath DA, Liao F, Boehme SA, Farber JM, Bacon KB. MIP-3alpha induces human eosinophil migration and activation of the mitogen-activated protein kinases (p42/p44 MAPK). J Leukoc Biol 1999; 66: 674-82.

Sykes AP, Bhogal R, Brampton C, Chander C, Whelan C, Parsons ME, Bird J. The effect of an inhibitor of matrix metalloproteinases on colonic inflammation in a trinitrobenzenesulphonic acid rat model of inflammatory bowel disease. Aliment Pharmacol Ther 1999; 13: 1535-42.

Talbot DC, Montes A, Teh WL, Nandi A, Powles RL. Remission of Crohn's disease following allogeneic bone marrow transplant for acute leukaemia. Hosp Med 1998; 59: 580-1.

Tanaka Y, Imai T, Baba M, Ishikawa I, Uehira M, Nomiyama H, Yoshie O. Selective expression of liver and activation-related chemokine (LARC) in intestinal epithelium in mice and humans. Eur J Immunol 1999; 29: 633-642.

Thompson NP, Driscoll R, Pounder RE, Wakefield AJ. Genetics versus environment in inflammatory bowel disease: results of a British twin study. BMJ 1996; 312: 95-6.

Thompson NP, Montgomery SM, Wadsworth ME, Pounder RE, Wakefield AJ. Early determinants of inflammatory bowel disease: use of two national longitudinal birth cohorts. Eur J Gastroenterol Hepatol 2000; 12: 25-30.

Tohyama M, Shirakara Y, Yamasaki K, Sayama K, Hashimoto K. Differentiated keratinocytes are responsible for TNF-alpha regulated production of macrophage inflammatory protein 3alpha/CCL20, a potent chemokine for Langerhans cells. J Dermatol Sci 2001; 27: 130-9.

Trinchard-Lugan I, Ho-Nguyen Q, Bilham WM, Buraglio M, Ythier A, Munafo A. Safety, pharmacokinetics and pharmacodynamics of recombinant human tumour necrosis factor-binding protein-1 (Onercept) injected by intravenous, intramuscular and subcutaneous routes into healthy volunteers. Eur Cytokine Netw 2001; 12: 391-8.

Tysk C, Lindberg E, Jarnerot G, Floderus-Myrhed B. Ulcerative colitis and Crohn's disease in an unselected population of monozygotic and dizygotic twins. A study of heritability and the influence of smoking. Gut 1988; 29: 990-6.

Van Assche G, Rutgeerts P. Anti-TNF agents in Crohn's disease. Expert Opin Investig Drugs 2000; 9: 103-11.

Vanbervliet B, Homey B, Durand I, Massacrier C, Ait-Yahia S, de Bouteiller O, Vicari A, Caux C. Sequential involvement of CCR2 and CCR6 ligands for immature dendritic cell recruitment: possible role at inflamed epithelial surfaces. Eur J Immunol 2002; 32: 231-42.

Van Deventer SJ. Review article: Chemokine production by intestinal epithelial cells: a therapeutic target in inflammatory bowel disease? Aliment Pharmacol Ther 1997; 11 Suppl 3: 116-20.

Van Kemseke C, Belaiche J, Louis E. Frequently relapsing Crohn's disease is characterized by persistent elevation in interleukin-6 and soluble interleukin-2 receptor serum levels during remission. Int J Colorectal Dis 2000; 15: 206–210.

Van Tol EA, Verspaget HW, Pena AS, Lamers CB. Normal inflammatory bowel disease mucosa conceals alterations in natural killer cell activity. Scand J Gastroenterol 1992; 27: 999-1005.

Varona R, Cadenas V, Flores J, Martinez-A C, Marquez G. CCR6 has a non-redundant role in the development of inflammatory bowel disease. Eur J Immunol 2003; 33: 2937-46.

Varona R, Villares R, Carramolino L, Goya I, Zaballos A, Gutierrez J, Torres M, Martinez-A C, Marquez G. CCR6-deficient mice have impaired leukocyte homeostasis and altered contact hypersensitivity and delayed type hypersensitivity reactions. J Clin Invest 2001; 07: R37-45.

Virag L, Szabo C. The therapeutic potential of poly(ADP-Ribose) polymerase inhibitors. Pharmacol Rev 2002; 54: 375-429.

Vrees MD, Pricolo VE, Potenti FM, Cao W. Abnormal motility in patients with ulcerative colitis: the role of inflammatory cytokines. Arch Surg. 2002; 137: 439-45.

Wakefield AJ, Sawyerr AM, Dhillon AP, Pittilo RM, Rowles PM, Lewis AA, Pounder RE. Pathogenesis of Crohn's disease: multifocal gastrointestinal infarction. Lancet 1989; 2: 1057-62.

Wang L, Walia B, Evans J, Gewirtz AT, Merlin D, Sitaraman SV. IL-6 induces NF-kappaB activation in the intestinal epithelia. J Immunol 2003; 171: 3194-201.

Warner EE, Dieckgraefe BK. Application of genome-wide gene expression profiling by high-density DNA arrays to the treatment and study of inflammatory bowel disease. Inflamm Bowel Dis 2002; 8: 140-57.

Watts DA, Satsangi J. The genetic jigsaw of inflammatory bowel disease. Gut 2002; 50 Suppl 3: III31-6.

Webb LM, Ehrengruber MU, ClarkLewis I, Baggiolini M, Rot A. Binding to heparan sulfate or heparin enhances neutrophil responses to interleukin 8. Proc Natl Acad Sci USA 1993; 90: 7158–62.

Weigmann B, Neurath MF. T-bet and mucosal Th1 responses in the gastrointestinal tract. Gut 2002; 51: 301-3.

Wen X, Wu GD. Evidence for epigenetic mechanisms that silence both basal and immune-stimulated transcription of the IL-8 gene. J Immunol 2001; 166: 7290-7299.

Williams EJ, Haque S, Banks C, Johnson P, Sarsfield P, Sheron N. Distribution of the interleukin-8 receptors, CXCR1 and CXCR2, in inflamed gut tissue. J Pathol 2000; 192: 533-9.

Wood LD, Richmond A. Constitutive and cytokine-induced expression of the melanoma growth stimulatory activity/ GROα gene requires both NF-κB and novel constitutive factors. J Biol Chem 1995; 270: 30619-30626.

Woywodt A, Ludwig D, Neustock P, Kruse A, Schwarting K, Jantschek G, Kirchner H, Stange EF. Mucosal cytokine expression, cellular markers and adhesion molecules in inflammatory bowel disease. Eur J Gastroenterol Hepatol 1999; 11: 267-76.

Wu L, LaRosa G, Kassam N, Gordon CJ, Heath H, Ruffing N, Chen H, Humblias J, Samson M, Parmentier M, Moore JP, Mackay CR. Interaction of chemokine receptor CCR5 with its ligands: multiple domains for HIV-1 gp120 binding and a single domain for chemokine binding. J Exp Med 1997; 186: 1373–81.

Xanthou G, Duchesnes CE, Williams TJ, Pease JE. CCR3 functional responses are regulated by both CXCR3 and its ligands CXCL9, CXCL10 and CXCL11. Eur J Immunol 2003;3 3: 2241-50.

Yang D, Chen Q, Hoover DM, Staley P, Tucker KD, Lubkowski J, Oppenheim JJ. Many chemokines including CCL20/MIP-3alpha display antimicrobial activity. J Leukoc Biol 2003; 74: 448-55.

Yang SK, Choi MS, Kim OH, Myung SJ, Jung HY, Hong WS, Kim JH, Min YI. The increased expression of an array of C-X-C and C-C chemokines in the colonic mucosa of patients with ulcerative colitis: regulation by corticosteroids. Am J Gastroenterol 2002; 97: 126-32.

Yang SK, Eckmann L, Panja A & Kagnoff MF. Differential and regulated expression of C-X-C, C-C, and C-chemokines by human colon epithelial cells 1997; Gastroenterol 113,1214-1223.

Yeung MM, Melgar S, Baranov V, Oberg A, Danielsson A, Hammarstrom S and Hammarstrom ML. Characterisation of mucosal lymphoid aggregates in ulcerative colitis: immune cell phenotype and TcR-gammadelta expression. Gut 2000; 47: 215-227.

Yoshie O, Imai T, Nomiyama H. Chemokines in immunity. Adv Immunol 2001; 78: 57-110.

Zboril V. Anti-cytokines in the treatment of idiopathic intestinal inflammations-theory and practice. Vnitr Lek 2002; 48: 583-6.

Zhelev DV, Alteraifi A. Signaling in the motility responses of the human neutrophil. Ann Biomed Eng 2002; 30: 356-70.

Zlotnik A, Yoshie O. Chemokines: a new classification system and their role in immunity. Immunity 2000; 12: 121-7.